GEOLOGICAL SURVEY RESEARCH 1965

Chapter C

GEOLOGICAL SURVEY PROFESSIONAL PAPER 525-C

GEOLOGICAL SURVEY RESEARCH 1965

Chapter C

*Scientific notes and summaries
of investigations by members of
the Conservation, Geologic, and
Water Resources Divisions in
geology, hydrology, and related
fields*

UNITED STATES DEPARTMENT OF THE INTERIOR

STEWART L. UDALL, Secretary

GEOLOGICAL SURVEY

Thomas B. Nolan, Director

CONTENTS

GEOLOGIC STUDIES

CONTENTS

GEOLOGICAL SURVEY RESEARCH 1965

This collection of 44 short papers is the second published chapter of Geological Survey Research 1965. The papers report on scientific and economic results of current work by members of the Conservation, Geologic, and Water Resources Divisions of the U.S. Geological Survey.

Chapter A, to be published later in the year, will present a summary of significant results of work done during the present fiscal year, together with lists of investigations in progress, reports published, cooperating agencies, and Geological Survey offices.

Geological Survey Research 1965 is the sixth volume of the annual series Geological Survey Research. The five volumes already published are listed below, with their series designations.

Geological Survey Research 1960—Prof. Paper 400

Geological Survey Research 1961—Prof. Paper 424

Geological Survey Research 1962—Prof. Paper 450

Geological Survey Research 1963—Prof. Paper 475

Geological Survey Research 1964—Prof. Paper 501

STRATIGRAPHIC DATA BEARING ON INFERRED PULL-APART ORIGIN OF GEM VALLEY, IDAHO

By STEVEN S. ORIEL, DON R. MABEY, and FRANK C. ARMSTRONG, Denver, Colo.

Abstract.—The possible origin of some filled basin-range valleys as pull-aparts or tensional rifts on the back edge of a thrust plate was mentioned by Rubey and Hubbert in 1959. The concept was subsequently applied to Gem Valley, mainly as an interpretation of gravity and other data in the northern part of the valley. New stratigraphic information indicates that Paleozoic units on opposite sides of the valley contrast markedly in thickness and facies. Original sites of deposition, therefore, probably were not closer together than the 7 to 12 miles now separating the exposures.

THE PULL-APART CONCEPT

The development of pull-apart gaps on the back edges of thrust plates has been suggested as a probable corollary of the hypothesis of overthrusting by gravitational sliding not accompanied by regional compression (Rubey and Hubbert, 1959, p. 194). The manner in which a pull-apart or tensional rift may form has been illustrated by Rubey and Hubbert (1959, fig. 9) as shown on figure 1. A thick plate of rock starts moving down the flank of a geosyncline
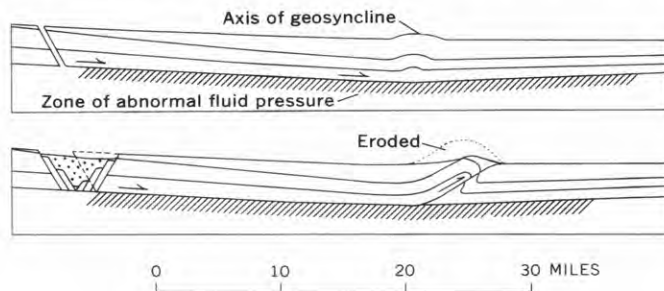
FIGURE 1.—Development of a pull-apart rift under the gravitational-sliding hypothesis. An incipient bedding-plane glide surface develops in a zone of abnormal fluid pressure on the flank of a geosyncline and breaks through a fold formed along the forward edge of the thrust plate. A tensional rift forms along the belt of parting at the back edge of the plate. (After Rubey and Hubbert, 1959, p. 194.)

toward the axis; and the rocks buckle along the forward edge of the plate. The major bedding-plane glide surface probably lies in a zone of abnormal fluid pressure. The forward edge of the bedding plane fault develops near the axial plane of an asymmetrical anticline, cuts across bedding, and breaks through to the surface (fig. 1). The back edge breaks loose along a normal fault or faults, as the plate slides into the geosynclinal trough. Under the gravitational-sliding hypothesis, ". . . gaps left in the rear by the pulling away of thrust plates would express themselves later either as intermontane valleys filled with younger sediments or as uplifts denuded tectonically of the rocks that have slipped off to the side" (Rubey and Hubbert, 1959, p. 194).

Several attempts have been made to recognize pull-apart gaps in southeastern Idaho. Although such mountain ranges as the Bear River and the Portneuf, about 60 miles west of the east front of the Wyoming overthrust belt, have been mentioned as possibly having been tectonically denuded by the younger rocks sliding eastward, nearby long intermontane valleys are regarded as more likely pull-apart rifts (Rubey and Hubbert, 1959, p. 197). The early history of these valleys is not known, but very recent high-angle faults are known to cut Tertiary to Recent sediments and the valleys have most often been interpreted as graben.

APPLICATION OF PULL-APART CONCEPT TO GEM VALLEY

Three gravity profiles were prepared across the Idaho-Wyoming thrust belt, at the suggestion of W. W. Rubey, to aid tectonic reconstructions. These profiles revealed large negative gravity anomalies over several intermontane valleys, consonant with a tensional origin of the valleys. Subsequently, one of

these valleys, Gem Valley in Caribou County, Idaho, (fig. 2) was surveyed in more detail (Mabey and Armstrong, 1962).

Gem Valley includes both Portneuf Valley and the north end of Gentile Valley and is about 7 miles wide and 35 miles long. It is bounded on the west by the Portneuf and Fish Creek Ranges and on the east by the Chesterfield and Bear River Ranges and the intervening Soda Springs Hills. The ranges rise as much as 4,000 feet above the generally level floor of the valley. Basalt flows cover much of the floor of the valley and overlie, and are interbedded with, Cenozoic sediments. Part of the basalt came from vents within the valley and part from the Blackfoot lava field to the northeast.

The gravity survey defined a low in the northern part of Gem Valley of about 40 milligals (fig. 2), which is interpreted as indicating a nearly flat bot-
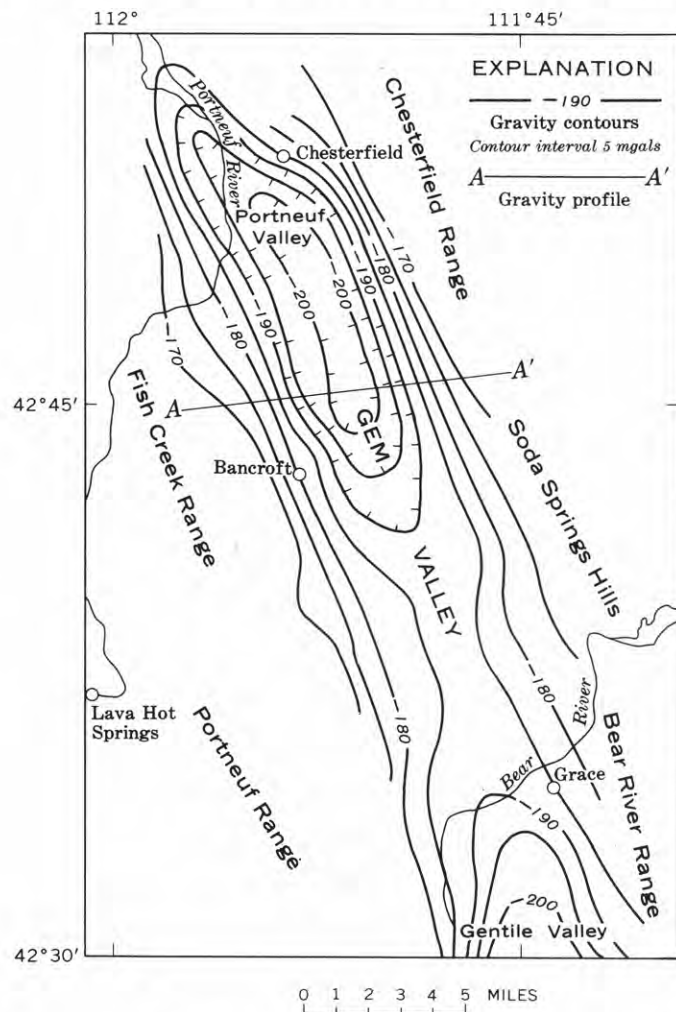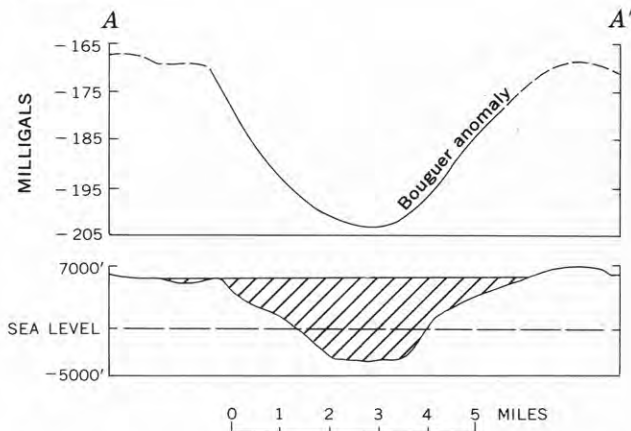
FIGURE 3.—Interpretation of the Gem Valley gravity low. The density of material (shaded) in the gravity low along section $A–A'$ on figure 2 is 0.5 g per cm³ lower than that of the enclosing Paleozoic rock. (From Mabey and Armstrong, 1962, p. D74.)

tomed trough 9,000 feet deep, containing material 0.5 grams per cubic centimeter less dense, on the average, than the enclosing rock (fig. 3). In the north end of Gem Valley the axis of this trough roughly parallels folds in Paleozoic and lower Mesozoic rock of the Chesterfield Range (Mansfield, 1929, pl. 1). The trough terminates northward by convergence of the sides. Trough flanks inferred from the anomaly do not coincide with the range fronts at most places, suggesting either step faulting or, less likely, erosional retreat of range fronts. On the west side of the north end of Gem Valley, exposed Cambrian and Ordovician rocks dip mainly eastward; on the east side, middle and upper Paleozoic rocks are folded but dip eastward near the valley margin. These data were used to infer that Gem Valley could have originated from late Cenozoic block faulting or from tensional rifting at the back of a thrust plate (Mabey, 1963) in late Mesozoic or earliest Cenozoic time.

No deep holes have been drilled in Gem Valley, and the age of the lowest sediment fill is not known. If the beginning of formation of the trough could be dated it would be helpful in choosing between alternative origins.

PERTINENT STRATIGRAPHIC INFORMATION

Stratigraphic information on rocks older than the thrusting bears on the genesis of Gem Valley. If the valley formed by the pulling away of a thrust plate, then rocks at the edges of the gap should match—or nearly match, if allowance is made for some breakage along the edges, as shown on figure 1.

New, unpublished stratigraphic information on the Paleozoic rocks of the Portneuf and Fish Creek

FIGURE 2.—Bouguer gravity-anomaly map of Gem Valley. A Bouguer-anomaly profile and inferred configuration of post-Paleozoic rocks of section $A–A'$ are given on figure 3. (After Mabey and Armstrong, 1962, p. D73.)

Ranges indicates that the rocks do not match. Marked contrasts in units on both sides of Gem Valley make it unlikely that present exposures were ever closer to one another than the 7 to 12 miles now separating them. Several of the units are more than twice as thick on the west side of the valley as on the east, and a few differ notably in facies. Differences in units have been observed thus far only along the central and southern parts of the valley. The contrasts are summarized in the paragraphs that follow.

The oldest unit shared by the flanking ranges is the Brigham Quartzite of Precambrian and Cambrian age. Its thickness is not known, for its base is not exposed in these ranges. The upper 2,500 feet has been subdivided into 3 mappable lithologic units west of the valley (Oriel, 1965). These units are recognizable along strike in other parts of the Portneuf Range but not in exposures examined east of the valley. This contrast probably reflects lateral facies differences.

Cambrian rocks above the Brigham Quartzite are more than 5,900 feet thick in the Portneuf Range, whereas they are 5,100 feet thick in the Bear River Range. Composition of some of the formations differs markedly from one side of Gem Valley to the other. This may not be useful, however, in determining gross palinspastic relations because marked local facies changes are also evident within Cambrian units in the Bear River Range (Armstrong, 1965). One of the units of regional extent probably not affected by local facies relations is the arkosic Worm Creek Quartzite Member of the St. Charles Limestone. The member is 914 feet thick in the Portneuf Range and 695 feet thick in the Bear River Range.

Ordovician rocks are 3,550 feet thick west of Gem Valley and 2,420 feet thick on the east in the Soda Springs Hills. The Garden City Formation is 1,350 feet thick on the west and 1,160 feet on the east; the Swan Peak Quartzite, 1,200 feet and 600 feet, respectively; the Fish Haven Dolomite, 1,000 feet and 660 feet. Moreover, thin units such as limestone and fossiliferous strata found within the Swan Peak Quartzite in the Soda Springs Hills have not been seen in the Portneuf Range.

The Silurian Laketown Dolomite is 1,040 feet thick in the Portneuf Range and less than 500 feet thick in the Soda Springs Hills.

Contrasts in Devonian rocks on opposite sides of Gem Valley are even more marked. Devonian strata assigned to the Jefferson Formation are about 3 times thicker in the Fish Creek Range, where 1,660 feet of strata is assigned to the Hyrum Dolomite Member

and 840 feet to the Beirdneau Sandstone Member, than in the Chesterfield Range, where the Hyrum is 380 feet and the Beirdneau, 475 feet (A. L. Benson, written communication, 1963). Moreover, the Beirdneau is considerably sandier and less calcareous on the west than on the east.

Mississippian rocks also are thicker in the Fish Creek Range, where they are incompletely exposed, than in the Chesterfield Range. The Lodgepole Limestone is 650 feet thick on the west and only 260 feet thick on the east; the Little Flat Formation (Dutro and Sando, 1963), 1,460 feet on the west, and only 965 feet on the east. The Monroe Canyon Formation is incompletely exposed on the west and cannot be compared.

CONCLUSIONS

Original distances that separated the sites of deposition of these contrasting sections of individual stratigraphic units may not now be measurable or inferred precisely. Known examples of rapid facies and thickness changes elsewhere make it possible that contrasting Paleozoic stratigraphic sections in the ranges bounding Gem Valley might formerly have been closer than at present. However, we regard this possibility as very unlikely. Indeed, contrasts of some of the units are so striking that we wonder if there has not been some telescoping, possibly along a thrust fault now buried by Cenozoic deposits in Gem Valley, as has been suggested for the north-central part of the valley (Armstrong, 1965). Field evidence for such a fault, however, is lacking.

Stratigraphic data, therefore, make it unlikely that rocks in the Fish Creek and Chesterfield Ranges and those in the Portneuf and Bear River Ranges have been pulled apart during thrusting, or at any other time, to form Gem Valley.

Both the stratigraphic data and the abundance of normal faults recently mapped in the adjoining ranges in the Bancroft and Soda Springs quadrangles support but do not prove graben genesis (Mabey and Armstrong, 1962, p. D74). If Gem Valley is a graben, it could have formed in late Cenozoic time, but here, too, the evidence is meager. Fill in the valley has been estimated from the gravity anomaly to be as much as 9,000 feet thick. Thicknesses of Quaternary lake sediments in the valley [1] have not been determined, but the thickness of the upper Cenozoic Salt Lake Formation, which is also present in the valley, has been estimated to range from 7,000 to 10,000

---

[1] R. C. Bright, 1963, Pleistocene Lakes Thatcher and Bonneville, southeastern Idaho: Minnesota Univ., unpub. Ph.D. thesis.

feet.[2][3] However, the age of the oldest fill in the valley is unknown and probably cannot be determined except by drilling. The presence of extensive basalt in the valley is compatible with tensional origin, but the Pleistocene age of the dated flows [4] indicates that extrusion of the basalt was late and probably associated with block faulting.

REFERENCES

Armstrong, F. C., 1965, Northwestward projection of the Paris thrust fault, southeastern Idaho [abs.]: Geol. Soc. America Spec. Paper 82, p. 317.

Dutro, J. T., and Sando, W. J., 1963, New Mississippian formations and faunal zones in Chesterfield Range, Portneuf quadrangle, southeast Idaho: Am. Assoc. Petroleum Geologists Bull., v. 47, no. 11, p. 1963–1986.

Mabey, D. R., 1963, Regional gravity and magnetic anomalies in southeastern Idaho and western Wyoming [abs.]: Geol. Soc. America Spec. Paper 76, p. 212.

Mabey, D. R., and Armstrong, F. C., 1962, Gravity and magnetic anomalies in Gem Valley, Caribou County, Idaho: Art. 140 *in* U.S. Geol. Survey Prof. Paper 450–D, p. D73–D75.

Mansfield, G. R., 1929, Geography, geology, and mineral resources of the Portneuf quadrangle, Idaho: U.S. Geol. Survey Bull. 803, 110 p.

Oriel, S. S., 1965, Brigham, Langston, and Ute Formations in Portneuf Range, southeastern Idaho [abs.]: Geol. Soc. America Spec. Paper 82, p. 341.

Rubey, W. W., and Hubbert, M. K., 1959, Overthrust belt in geosynclinal area of western Wyoming in light of fluid pressure hypothesis, [pt.] 2 *of* Role of fluid pressure in mechanics of overthrust faulting: Geol. Soc. America Bull., v. 70, no. 2, p. 167-205.

[2] R. C. Bright, 1960, Geology of the Cleveland area, southeastern Idaho : Utah Univ., unpub. M.S. thesis.

[3] Allen Keller, 1962, Structure and stratigraphy behind the Bannock thrust in parts of the Preston and Montpelier quadrangles, Idaho : Columbia Univ., unpub. Ph.D. thesis.

[4] See footnote 1 on p. C3.

STRUCTURE OF A RAY CRATER
AT HENBURY, NORTHERN TERRITORY, AUSTRALIA

By D. J. MILTON and F. C. MICHEL,[1]
Menlo Park, Calif., Houston, Tex.

Abstract.—Crater 3, a circular crater about 200 feet in diameter, was formed in moderately dipping beds of well-cemented sandstone and weak shales overlain by a variable thickness of pediment gravel; it is unique among terrestrial impact craters for displaying rays and ray loops of ejecta similar in pattern to those around craters on the moon. Each ray and loop is made up of a single type of bedrock, the individual fragments of which had been thrown for a distance inversely proportional to the distance of the point of origin from the center of the crater. The larger of these loops is shown to be smaller and narrower than current theory would predict, probably because the models used fail to take into account the finite strength of the bedrock.

The meteorite craters at Henbury, Northern Territory, Australia, were mapped geologically in 1963, as part of a larger program of investigation of meteorite impact structures. Of the dozen or so craters at Henbury, principal interest attaches to the main group of large craters, but the smaller ones also exhibit some notable features. Two of these, craters 3 and 4 of Alderman (1932), are the only known natural terrestrial impact craters at which rays and ray loops of ejecta, in patterns similar to those of rays around craters on the Moon, have been found. This report describes the geology of crater 3, the better exposed of the pair, and discusses its bearing on the problem of the origin of rays of ejecta. Crater 3 is roughly circular, about 200 feet in diameter, and has a relief of 15 feet from floor to rim crest, and 5 feet from the surrounding surface to the crest.

Bedrock at the Henbury crater field is the Pertatataka Formation, of late Precambrian age, composed of alternating beds of sandstone and shale. Despite the age, only the sandstones are well indurated; the shales can be excavated with a shovel. At crater 3 and at the main group, easily erodible shales predominate. These craters, consequently, lie in a "gibber plain," a pediment gravel composed of cobble and smaller subrounded fragments of sandstone and "gray billy" (strongly silicified rock) from the ridges to the south, and rounded pebbles of more distant provenance, in a red silty matrix. The thickness of the gravel depends on the underlying material—it is thin or absent over the more resistant sandstone beds and may be 15 feet or more thick over shale.

The Pertatataka Formation in the vicinity of the crater field has a constant east-west strike and a dip to the south of about 35°. Minor structures in which the beds have other attitudes occur, but are so small and scattered that it may be safely assumed that the bedrock at the site of the crater had the regional attitude before impact.

Nine distinctive bedrock units, either exposed in the crater walls or represented by fragments in the throwout, were mapped (fig. 1). A distinction between broken and somewhat displaced bedrock and throwout would be highly arbitrary and was not made, but in general the transition may be considered to lie at the lip of the crater or, at farthest, the crest of the rim. Attitudes were recorded wherever coherent segments of strata could be found (fig. 1).

---

[1] Rice University, Department of Space Science.
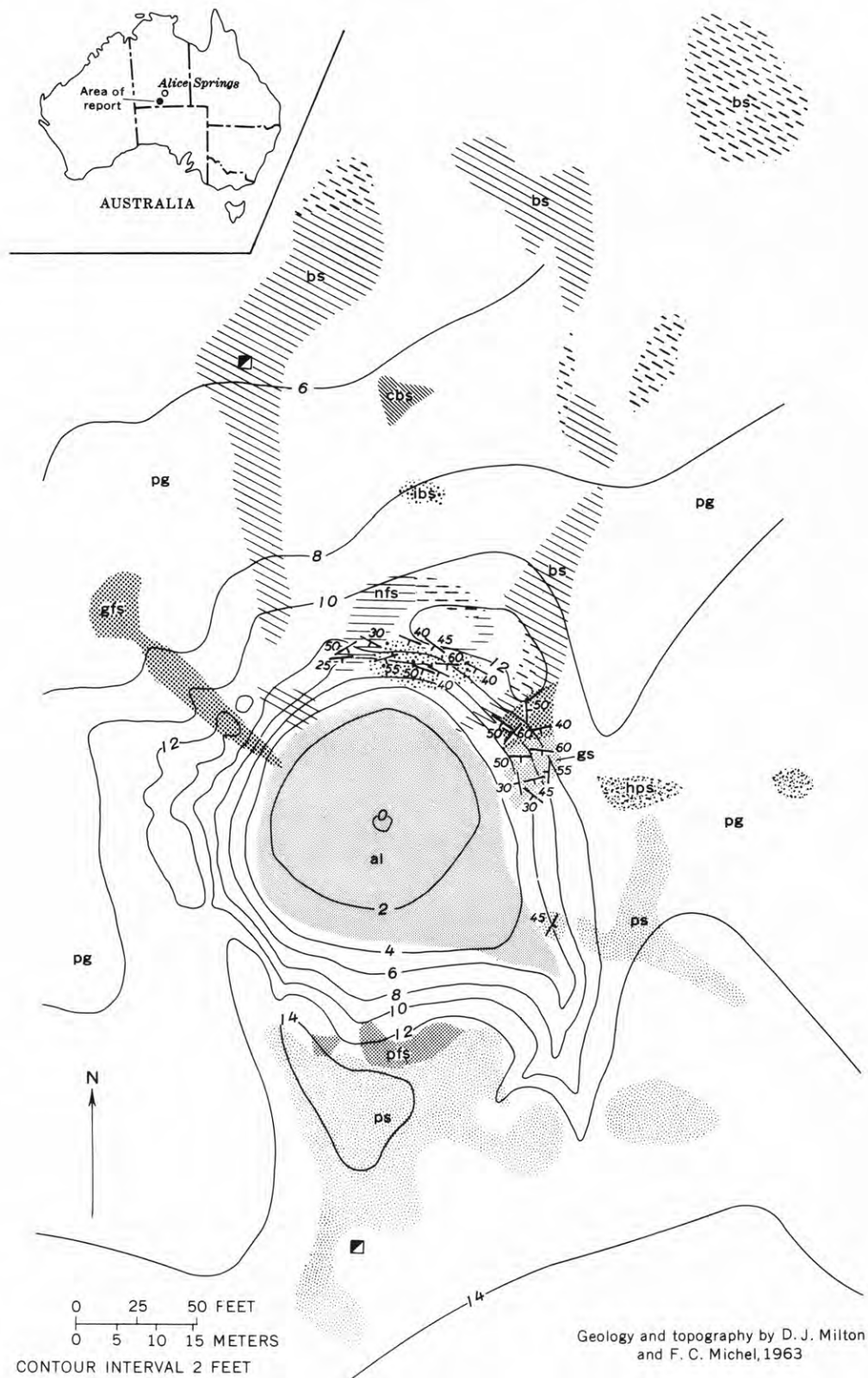
FIGURE 1.—Geologic map and inferred north-south preimpact cross section of crater 3, Henbury, Northern Territory, Australia.
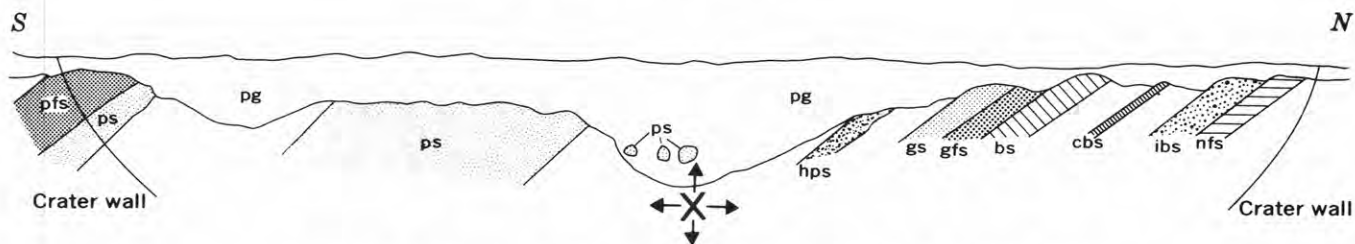
INFERRED PRE-IMPACT CROSS SECTION THROUGH THE CRATER SITE

Unlabeled bedrock units are presumably shale. The center of burst calculated from scaling
relations is marked by X. Scale is approximately × 3 scale of map

EXPLANATION

Pre-crater units in place and in throwout are not differentiated

al

Fine-grained postcrater alluvium

pg

Pediment gravel

Subrounded and rounded rock fragments in a fine-grained
matrix. Undisturbed gravel, throwout composed of gravel, and
gravel redeposited since impact are not distinguished

pfs

Purple flaggy sandstone

Dark sandstone that breaks along micaceous bedding planes

ps

Purple sandstone

Dark poorly bedded sandstone that weathers to irregular rounded
fragments

hps

Hard purple sandstone

Hard sandstone that breaks into blocks as much as 6 inches
thick

gs

Gray sandstone

Thin beds of sandstone interbedded with an unexposed,
presumably shaly, sequence

gfs

Gray flaggy sandstone

Sandstone that breaks into thick platy fragments and shale that
weathers to small chips

bs

Blocky sandstone

Sandstone that breaks into blocks as much as 1 foot on each
side; broken lines indicate sparsely scattered ejecta

cbs

Cubic-breaking sandstone

Sandstone that breaks into blocks as much as 1 or 2 inches on edge

ibs

Irregularly bedded sandstone

Sandstone with nonplanar bedding and poorly developed ripple
marks

nfs

Northern flaggy sandstone

Purplish sandstone that breaks along micaceous bedding planes;
broken lines indicate sparsely scattered ejecta

_40_

Strike and dip of beds

Exploratory pit

FIGURE 1.—Continued

A large part of the walls and rim of the crater is underlain by pediment gravel with a small admixture of bedrock fragments. Undisturbed precrater pediment gravel, with perhaps a few fragments of bedrock ejecta on the surface, can be distinguished only with difficulty from ejecta composed principally of pediment gravel or from such material redeposited in postcrater time. Consequently, the unpatterned areas of figure 1 represent all of these materials.

The schematic north-south cross section of the site before the impact was inferred from the exposures shown on the map (fig. 1). The stratigraphic sequence of 5 of the 6 lower units is known from occurrences in the crater walls. The position in the section of the cubic-breaking sandstone, which was not found in the crater wall, was inferred from the position of fragments in the throwout. The stratigraphic position of the purple sandstone unit is suggested by a somewhat doubtful outcrop on the east wall of the crater; even more dubious outcrops near the southern rim crest suggest that at least some purple sandstone lay immediately below the purple flaggy sandstone unit. Intervals in the section between the labeled units are presumably occupied by shale beds that either had been eroded and replaced to considerable depths by pediment gravel or are represented in the throwout by small nondescript chips that went unnoticed during the mapping.

STRUCTURES IN THE CRATER WALL

In the north wall, the direction of shock propagation was perpendicular to the direction of the strike and was nearly updip, so that the strike of the beds was not markedly affected by the impact. If the assumed preimpact dip is correct, the dips here (and in the northeast wall also) have been somewhat steepened.

More complex deformation is shown in the northeast wall by the gray sandstone and gray flaggy sandstone units (fig. 2). Segments A and B of marker beds retain approximately their original strike. Segment C belongs to the same bed as segment B and presumably was updip nearer the surface before impact. Segment C was shoved outward with a greater displacement on the end originally nearest the center of the crater, resulting in a clockwise rotation. Beds D and E show a similar pattern, with the outer ends retaining their preimpact attitudes and the inner ends rotated clockwise away from the crater center. Segments F and G, which are part of a single bed of gray flaggy sandstone, indicate a more complex pattern.
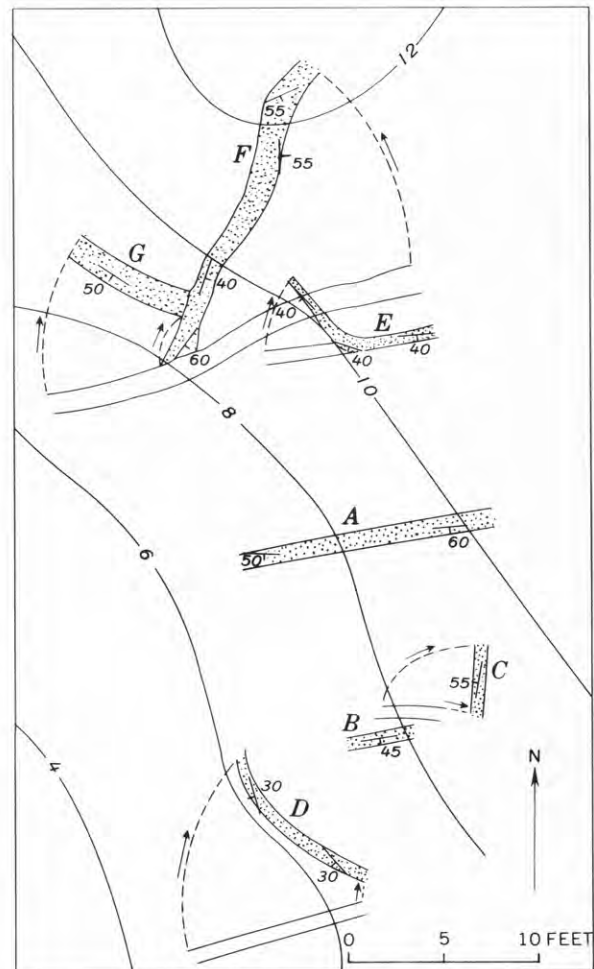
FIGURE 2.—Geologic map of part of the northeast wall of the crater. Marker beds are stippled; their presumed preimpact positions are indicated by unpatterned outline of bed.

Segment F has apparently been rotated counterclockwise, suggesting a zone of unusually great outward displacement lying between the original positions of E and F (which may have been as far apart vertically as horizontally). Segment G, originally downdip, or west of segment F, was displaced farther outward, but with less rotation, than the near end of F and is now wedged tightly against F (fig. 3). In general, deformation involved the rotation of distinct blocks about predominantly vertical axes.

THROWOUT

The most notable feature of crater 3 is the distribution of throwout. Each bedrock unit occurs in discrete delineable areas of throwout, with very little mixing. During his brief reconnaissance, Alderman noted low ridges of sandstone radiating from the

FIGURE 3.—Disturbed bedrock in the northeast wall of crater 3. Gray flaggy sandstone in segment *F* (fig. 2) runs along the right margin past the hammer, and in segment *G* it runs through the foreground. At center are unoriented fragments of blocky sandstone.

crater, which suggested "dikes" of a rock more resistant to erosion. They are, however, not dikes but surficial rays of throwout. A pit dug in the blocky sandstone ray northwest of the crater (fig. 1) showed that broken rock chips and sandstone blocks form a stratum only 5 inches thick overlying undisturbed pediment gravel.

The best developed ray system consists of fragments of the blocky sandstone, lying along a loop the farthest point of which is more than 200 feet from the crater (figs. 4 and 5). On the northeast rim the ray connects with the blocky sandstone in the crater wall. On the northwest rim a gap in the loop about 25 feet across

FIGURE 4.—View craterward along the northwestern ray of blocky sandstone ejecta. Arrow marks exploratory pit indicated on upper part of figure 1. Ray of gray flaggy sandstone ejecta runs from crater to right middle ground (margin of photograph).

is spanned by a patch of silty soil with only scattered pebbles. This patch may possibly be a small filled-in crater superimposed on the rim of crater 3. The ray loop is symmetrical about a radial line from the crater center at right angles to the preimpact strike of the bedrock strata. Scattered fragments of blocky sandstone farther from the crater to the northeast of the main ray may be the remnants of another ray, perhaps an outer loop.

The material in the main loop may reasonably be supposed to be derived from positions near the ground surface along a chord of the crater corresponding to the preimpact outcrop of the blocky sandstone bed. As the distance from the center of gravity of energy release (or, for convenience, center of burst) increases along the chord away from the midpoint, a decrease

FIGURE 5.—Ray loop of blocky sandstone ejecta viewed from northwest rim crest of crater. Ejecta of cubic-breaking sandstone and irregularly bedded sandstone are in right middle ground.

in particle acceleration as well as in angle of ejection would be expected, which would lead to a ray loop with the farthest point on a line from the epicenter at right angles to the strike. Similarly, Shoemaker (1962) has shown that loops of secondary craters around the lunar crater Copernicus were made by fragments that originally lay along chords of the crater. If the dimensions and form of the blocky sandstone ray loop are considered more closely, however, they are found not to match those that would develop in accordance with the simplified theory of cratering applied to Copernicus by Shoemaker.

Shoemaker (1962, p. 331, equation 14) gives a theoretical ballistic range for a throwout fragment from the preimpact surface, which may be rewritten:

$$R = \frac{3Ead}{2\pi\rho g \ (a^2+d^2)^{5/2}}, \qquad (1)$$

where

  R = range of fragment from preimpact to postimpact position,
  E = total energy release,
  a = distance from epicenter to preimpact fragment position,
  d = depth of burst,
  ρ = density of crater material, and
  g = acceleration of gravity.

E and d for crater 3 can be derived by scaling from nuclear craters in alluvium by the relations $E \approx$ (diameter)$^{3.36}$ and $\frac{d}{E^{1/3}} = 0.25 \frac{\text{ft}}{\text{lb}^{1/3}}$ (H. J. Moore, oral communication) where the energy is expressed in equivalent pounds of TNT. Using 200 feet as the crater diameter and scaling from the nuclear craters Teapot Ess or Jangle U (Nordyke, 1961), one finds:

E = 337 tons TNT equivalent $\rbrace$ scaling from Teapot
d = 22 feet $\qquad\qquad$ Ess, or

E = 497 tons TNT equivalent $\rbrace$ scaling from Jangle
d = 25 feet $\qquad\qquad$ U.

The average of the two energies in cgs units is $1.75 \cdot 10^{19}$ ergs. This would be the kinetic energy of an iron meteorite traveling at the modal meteoritic velocity of 15 kilometers/second with a mass of 15 tons, or a sphere 5 feet in diameter.

Applying equation 1 and taking $a = 61$ feet, blocks from the midpoint of the blocky sandstone bed should be thrown out more than 4,400 feet rather than the 245 feet of the actual ray. As the azimuth of ejection moves away from the normal to the chord, the discrepancy between observed and calculated ranges becomes even greater.

The calculated range of ejection would be reduced if the effective depth of burst were less. A hydrodynamic theory of penetration used by Shoemaker (1963) indicates that the Meteor Crater, Ariz., iron meteorite penetrated the ground to 4 or 5 times its thickness. Applied to Henbury crater 3, this yields the same depth of burst as indicated by the scaling relations. The applicability to a small impact crater of either a hydrodynamic theory of penetration or scaling relations from explosion craters is doubtful, but a depth of burst that would yield the actual distance of throwout according to equation 1 would be quite unacceptably shallow.

Equation 1 is thus inapplicable to Henbury crater 3 without modification. Shoemaker (oral communication) has pointed out that the Copernicus model ignores the strength of the material in which the crater formed, a procedure justifiable for large craters but not necessarily so for small ones. Moore and his as-

sociates (1964) have emphasized the dependence of dimensions of hypervelocity craters on the effective strength of the target material. Their work, however, deals with the measurement of craters after formation, and there seems to be no applicable theory for the influence of target strength on the distribution of energy during the process of formation of craters.

Equation 1 is based on an assumption that the energy density is uniform within the shock front. This leads to scaling of crater dimensions as the cube root of the energy and particle velocity as the $-3/2$ power of the distance from the center of burst. Experimental data indicate that the latter exponent is not a constant, but in general takes higher values than that assumed. Chaszeyka and Porzel (1958, p. 81) calculated a decrease of peak overpressure [2] as about the 4.5 power of the distance for explosions in Nevada alluvium. Particle velocity should decrease at half this rate. This calculation is confirmed by Murphey and Vortman (1961, p. 3391) who state that the early surface velocities for the STAGECOACH experiments decreased roughly as the 2.2 power of the depth of burial.

As a gross oversimplification, the exponent 5/2 in equation 1 may be replaced by $1 + \dfrac{x}{2}$, where $-x$ is the scaling power of energy density against distance. To maintain the dimensional balance of the equation, a constant factor must be inserted. Unfortunately, there is no a priori method for knowing this constant factor, so that the ranges of throwout cannot be calculated from a revised formula. However, the shape of the ray loop, whatever its size, depends only on the value of x. The original formula gives a loop much wider in proportion to radial extent than the actual ray. With increasing value of x, the ballistic ranges of fragments from near the ends of the chord decrease more rapidly than the ranges from the center. A match for the actual shape of the ray loop is found at values for x of 8 or 10. These values are higher than any that have been used in crater scaling. They are perhaps significant, not as constants for actual use, but as an indication of the necessity for a more sophisticated theory of cratering, in which the strength of the target material is considered.

Another rather well defined ray loop is made up of fragments of the northern flaggy sandstone. This is much smaller than the blocky sandstone loop, as would be expected from the greater preimpact distance of the bed from the epicenter. Throwout from the irregularly bedded sandstone and from the cubic-break-

---

[2] Shock-induced pressure minus lithostatic pressure.

ing sandstone units is concentrated in patches at distances inversely proportional to the distance between the inferred original positions and the center of the crater. Throwout from the gray flaggy sandstone unit forms a sharply defined linear ray on the west side of the crater (fig. 4), and throwout from the hard purple sandstone unit forms a less definite ray on the east rim.

Throwout from the purple sandstone unit forms a thick widespread blanket rather than a ray system. This is presumably a consequence of its greater thickness and its attitude, more or less normal to the direction of shock propagation. The northward extension of throwout of the purple sandstone on the east rim may have been derived from blocks in the precrater pediment gravel, as suggested in the cross section in figure 1.

POSTCRATER MODIFICATION

Erosion and deposition have modified the crater since it was formed. At crater 2 of Alderman, just west of crater 3, practically no topographic depression remains, but the pebble-free soil and the presence of trees (indicating a bedrock basin that holds water) are evidence of a filled crater. Because crater 3 is larger, it is better preserved, but filling has probably accelerated since the breaching of the southeast rim by a gully (fig. 1). There has been sufficient modification so that it is difficult to reconstruct completely the original form of the crater. The floor of the crater is covered by fine-grained postcrater alluvium sloping inward to a nearly flat pan about 50 feet across. If the original depth matched that calculated by scaling from nuclear craters, the fill in the center of the floor could be as much as 25 to 40 feet thick.

Outside the rim crest, irregularities in what appears to have been an originally hummocky rim have been mostly smoothed out. The purple sandstone ejecta are characterized by large blocks that fragmented either on impact or by later weathering. A pit dug in an area apparently free from throwout only a few feet from several large blocks of purple sandstone (fig. 1) exposed, in descending sequence, a thin capping of desert pavement, $2\frac{1}{2}$ feet of gray soil with small rock chips and occasional large fragments with scarce iron oxide scales, and, at the bottom, typical undisturbed pediment gravel. The upper $2\frac{1}{2}$ feet represents reworked throwout, probably derived from both crater 3 and crater 4, which lies to the south. The immediate postcrater relief of this locality was at least $2\frac{1}{2}$ feet. Less evidence for postcrater modification is found on the northern rim of crater 3, but the 6 inches or so of relief that characterizes the rays is probably the result of differential erosion of the general surface; the finer grained materials are removed more rapidly by sheet wash, leaving the larger sandstone blocks.

REFERENCES

Alderman, A. R., 1932, The meteorite craters at Henbury, central Australia: Mineralog. Mag., v. 23, p. 19–32.

Chaszeyka, M. A., and Porzel, F. B., 1958, Study of blast effects in soil: Chicago, Armour Research Foundation, ARF project D119, final report, 108 p.

Moore, H. J., Gault, D. E., and Heitowit, E. D., 1964, Change in effective target strength with increasing size of hypervelocity impact craters: U.S. Geol. Survey, Astrogeologic studies ann. prog. rept., Aug. 25, 1962 to July 1, 1963, pt. D, p. 52–63.

Murphey, B. F., and Vortman, L. J., 1961, High-explosive craters in desert alluvium, tuff and basalt: Jour. Geophys. Research, v. 66, p. 3389–3404.

Nordyke, M. D., 1961, Nuclear craters and preliminary theory of the mechanics of explosive crater formation: Jour. Geophys. Research, v. 66, p. 3439–3460.

Shoemaker, E. M., 1962, Interpretation of lunar craters, in Kopal, Zdenek, ed., Physics and astronomy of the Moon: New York, Academic Press, p. 283–360.

—— 1963, Impact mechanics at Meteor Crater, Arizona, in Middlehurst, B. M., and Kuiper, G. P., eds., The Moon, meteorites and comets, v. 4 of The solar system: Chicago, Univ. of Chicago Press, p. 301–336.

FOLDING OF THE NAHANT GABBRO, MASSACHUSETTS

By CLIFFORD A. KAYE, Boston, Mass.

Abstract.—On the shore of Nahant, medium-grained gabbro has been broken by closely spaced parallel partings (pseudo-bedding-plane partings) and deformed into a series of anticlines and synclines. From a moderate distance, the rock roughly resembles a folded, thin-bedded sedimentary rock. The spacing of the partings, as many as 8 per inch, varies with the tightness of the folding. The partings were probably produced by shear failures on the concave side of flexed layers of gabbro. Initially, these layers were formed by well-developed sheeting-type jointing. Small reverse-fault displacement on these shear failures produced dilation of the layers which resulted in tension fractures oriented parallel to the direction of the locally resolved compressive stress component. As folding progressed these fractures multiplied and split the pseudobeds into successively smaller units. The process of shear-induced tension also may have produced the sheeting joints and probably was caused by movement along a still-uncovered sizable reverse fault. By compression here is not meant the major compression which caused the fold in the first place but a secondary compressive stress which grew out of internal movement within the fold and as such differs in attitude with position within the fold.

Seven miles northeast of Boston, gabbro and associated peridotite intruded by basic dikes are well exposed along the shores of Nahant, an island that is tied to the mainland by a tombolo. At several places the plutonic rocks are broken by closely spaced parallel joints, or partings, and the rocks are deformed into well-defined folds (fig. 1). From a moderate distance these rocks resemble folded sedimentary rocks to which the folded joints impart a stratified appearance. On close inspection, however, the rocks prove to be medium-grained fresh gabbro, similar to the typical massive plutonic rock seen elsewhere on the island. An explanation for the densely spaced parallel partings and associated folds is not readily evident, for in these shoreline outcrops the rock appears homogeneous in composition and texture, and primary planar structures such as flow banding or mineral lineation are not present. It is, in fact, fairly certain that the structures are the result of elastic deformation of practically homogeneous rock.
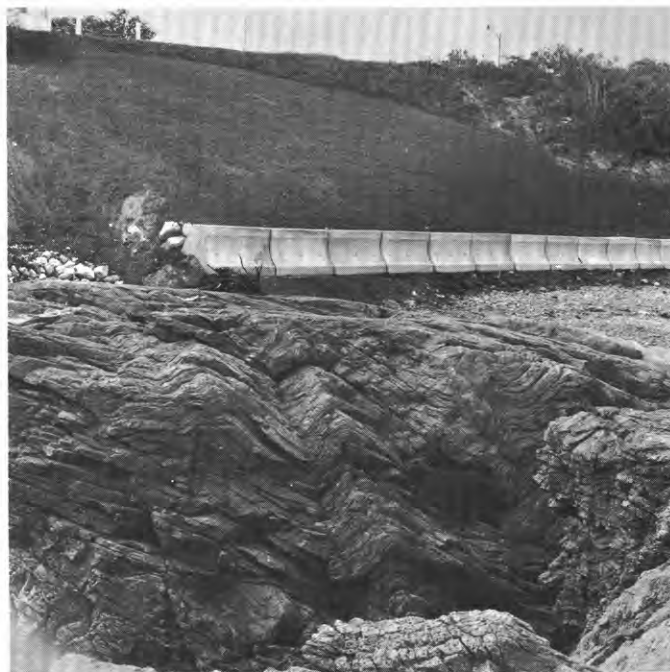
FIGURE 1.—Series of small folds in gabbro, Cedar Point, Nahant, Mass. View southwestward along axes of folds.

DESCRIPTION OF NAHANT GABBRO AND ASSOCIATED ROCKS

The oldest rocks on Nahant are slightly metamorphosed sediments of the Weymouth Formation of Early Cambrian age (Emerson, 1917; LaForge, 1932). These crop out as a small patch at Johns Peril, at the northern tip of the island, and in a very much larger area at the eastern end of the island (fig. 2). The rocks are thin-bedded siliceous argillites with a few thin zones of flesh-colored limestone. Alteration to a massive black hornfels (called "lydite" by Lane, 1889) is rather common at the contact with the gabbro. In eastern Nahant, where the rocks dip about 40° to the northwest, about 400 feet of the formation crops out.

Intruded into the Weymouth Formation is a large body of gabbro and associated peridotite that makes up most of the island. The contact of the gabbro with the Weymouth Formation is exposed at several places. At Great Ledge (fig. 2) the gabbro is concordant with the metasedimentary rocks; but about 200 yards to the west, a small exposure at beach level shows a sharp but very irregular contact. The relation between the gabbroic rocks and the Weymouth Formation in the eastern part of Nahant indicates that the gabbroic body has a highly irregular lateral margin suggestive perhaps of the form of a "Christmas-tree"

EXPLANATION

Beach deposits

Gabbroic complex

Primary flow banding

Mafic dikes

Weymouth Formation
Patterns less dense where rocks are concealed

40
Strike and dip of bedding

Syenite and intrusive breccia

Contact
Dashed where approximately located, dotted where concealed

25
Strike and dip of sheeting

Zone of strong folding

Saunders Ledge

Cedar Point

NAHANT BAY

East Point

Bass Rock

Josephs Beach

BROAD SOUND

Great Ledge

Pea Island

Shag Rocks

Johns Peril

Black Mine

NAHANT

Saunders Ledge

Cedar Point

East Point

Fort Rockman

Bass Rock

70°55'

42°25'

Area of report

MASSACHUSETTS

Geology mapped by C. A. Kaye, 1964

0   500   1000   1500 FEET

FIGURE 2.—Geologic map of eastern Nahant, Mass., showing zone of strong, well-developed folding in gabbro.

laccolith (fig. 2). The gabbroic complex may have been intruded as several sheets or sills separated, at least along the margin, by septa of country rock.

The major rock of the intrusive is medium- to coarse-grained diallage gabbro with minor olivine. Because of the light color of the feldspar, the rock has a mottled appearance more typical of diorite than of gabbro (fig. 6). Tabular to irregular-shaped zones of black peridotite (diallage and olivine in about equal proportions and very minor plagioclase), varying from very coarse grained to medium grained, are interlayered with the gabbro. In places in eastern Nahant, peridotite is in contact with the Weymouth Formation; in others, the normal gabbro is the contact rock. The peridotite apparently is not restricted to the base of the gabbroic body and thus is of only limited value in determining the shape of the intrusion.

Primary flow banding is well developed at several places, though not where the folded pseudobedded rock occurs. On Pea Island (fig. 2), thinly spaced banding dips vertically and strikes northwesterly. Here it probably parallels the contact of the intrusion with the nearby Weymouth Formation. Flow banding at Fort Ruckman consists of alternating thick layers of gabbro and peridotite. At Black Mine the banding is thinner, resembling that on Pea Island.

In addition to gabbro and peridotite, a small mass of fine-grained syenite crops out at Saunders Ledge (fig. 2). Much of this rock has been shattered and injected with basaltic magma, resulting in a striking intrusion breccia.

Recently, Chapman (1962) has described rocks in the coastal region of eastern Maine that are very similar and may be genetically related to the gabbro complex at Nahant. Chapman thinks that the Bays-of-Maine gabbro is Devonian; Emerson (1917) assigned a possible Devonian age to the Nahant gabbro.

Mafic dikes abound on Nahant, cutting both the Weymouth Formation and the gabbro. The largest dikes are steeply dipping and for the most part strike northwest. In figure 2 only a few of the larger ones are shown. Many dikes are compound and by their well-defined zoning show that they were formed by several discrete intrusions. Some of the northwest-striking dikes are folded. A second set of mafic dikes strikes northeasterly (the dikes vary in strike from north to east but the majority strike about northeast). Several dikes of the second set cut across folds without deformation and thus postdate folding.

STRUCTURE OF THE GABBRO

The gabbro is broken in many places by faults. These are easily recognized because the fault surfaces are generally coated with highly polished, slickensided epidote. Most of the faults can be traced only short distances and probably represent only minor displacements.

Jointing of the Nahant gabbro is important because of its role in the formation of the folded structures. Two conspicuous joint sets occur in eastern Nahant. One set strikes northwest and dips steeply. Most of the large compound dikes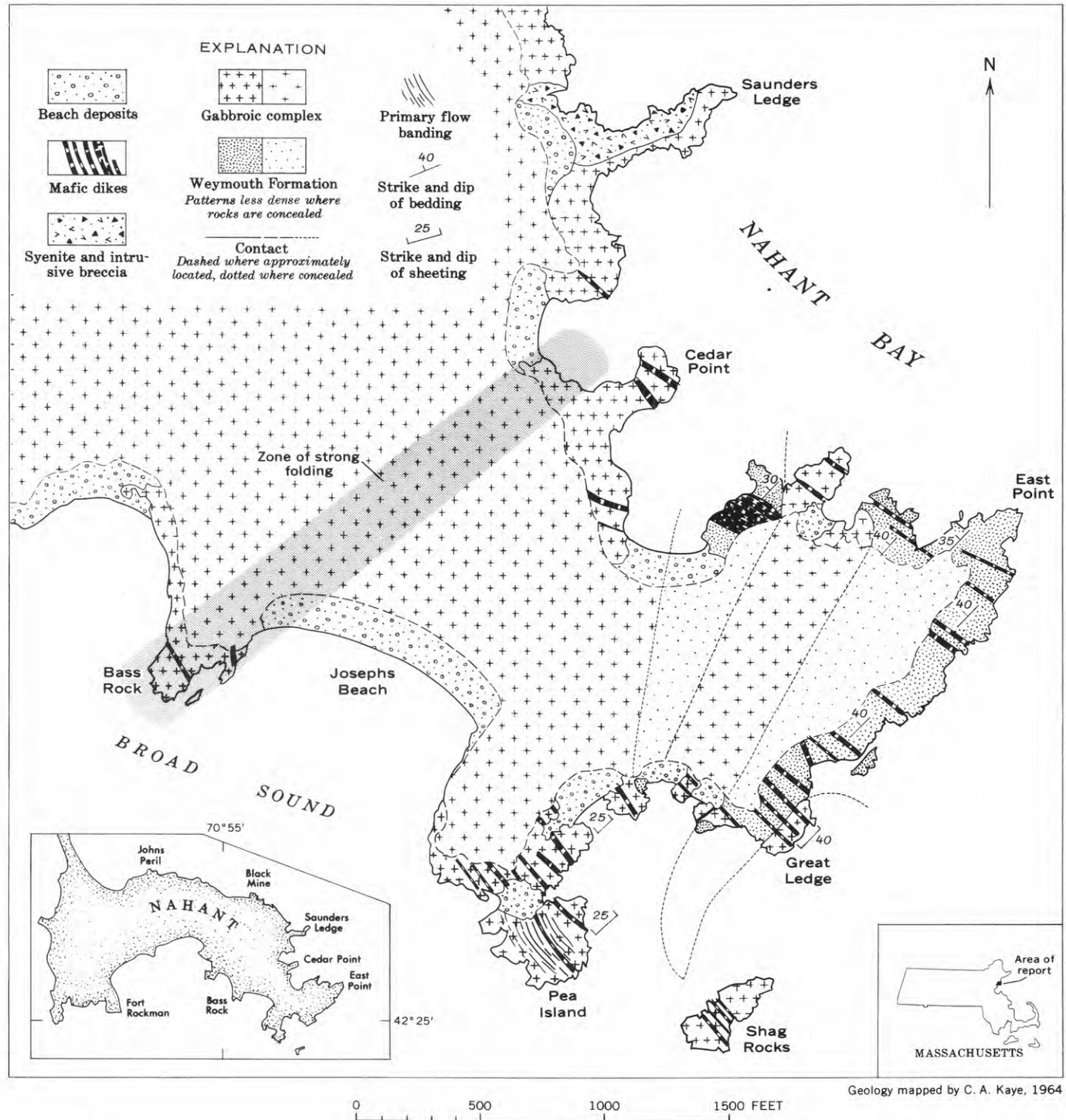 were intruded along these joints. The second set strikes northeasterly and dips about 30°–40° northwest. Joints in the second set are spaced about 1 to 6 feet apart and are rather rigidly parallel. They resemble sheeting although they do not parallel the present surface. A curious fact is that in the eastern part of the island they are parallel, both in strike and degree of dip, to the bedding in the adjacent Weymouth Formation. In fact, they extend from the gabbro across discordant contacts into the Weymouth Formation, where they merge with bedding partings. Because of these joints, the gabbro adjacent to the metasedimentary rocks is eroded into much the same cuesta forms and resembles the Weymouth Formation when seen from afar. One wonders whether there is a causal relationship between the stratification of the Weymouth Formation and sheeting in the adjoining gabbro, or whether this is simply an unusual coincidence. It should be emphasized here, however, that the writer has found no evidence that the gabbro was formed by metasomatic alteration of the metasedimentary rocks.

Although both the sheeting and the very closely spaced joints, or partings, which are the main subject of this paper, give the gabbro the superficial appearance of stratified rock, the two types of jointing should not be confused. As will be explained below, the sheeting is thought to be a necessary prerequisite for the formation of both the folds and the related closely spaced partings in the gabbro. Unlike the sheeting, the partings, or "pseudobedding-plane partings" as they will be called here, vary in spacing from about 3 inches, where the folding is fairly open, to a fraction of an inch, where the folding is tight. The pseudobedding-plane partings have little lateral extent and can be traced for only 25 feet or less in the more open folds. Where folding is tight, they may be less than a foot in length when traced along a rock face. The partings terminate either by merging with other partings at an acute angle or, less commonly, by disappearing into unfractured gabbro (fig. 6).

Folds in thinly pseudobedded gabbro are particularly well developed at two places on the shore of Nahant and can be found in isolated patches in numerous other places. One of the better locations is just west

of Cedar Point (fig. 2), in the rocks flanking the picturesque pocket beach that is reached by the main road through Nahant. The second locality lies on the opposite shore of the island, to the southwest of Cedar Point, at a low rocky promontory called Bass Rock.[1] The two shore localities line up parallel to the axes of the folds, particularly the folds at Cedar Point, and therefore probably occur along the same zone of folding (fig. 2). This zone trends N. 60° E. and is at least 2,200 feet in length, passing out to open water at both ends.

At Cedar Point there are 7 fairly small, tightly folded, parallel anticlines with axes trending N. 60° E. Adjoining these to the south are 3 considerably larger and more open folds (fig. 3). The smaller
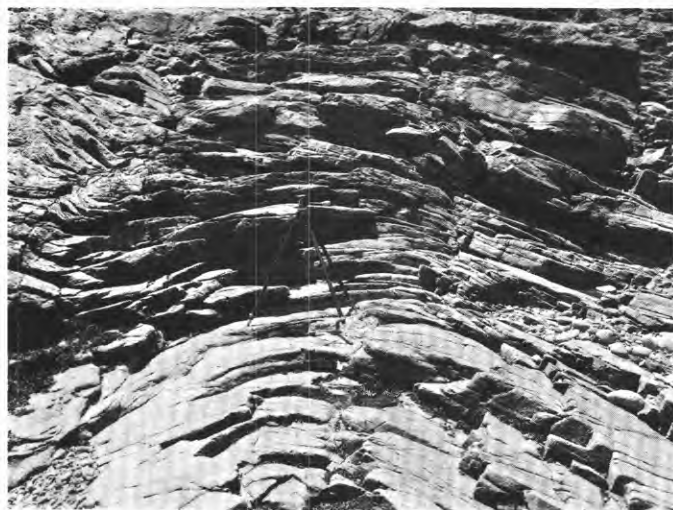
FIGURE 3.—View to southwest along anticlinal axis, Cedar Point, Nahant. This is one of the larger folds in gabbro situated just southwest of the folds shown in figure 1.

anticlines have wave lengths of about 12 feet and amplitudes of about 5 feet, measured from crest to trough. All folds are overturned to the south and have minor drag folds on their flanks (fig. 1).

To the southwest, at Bass Rock, a series of well-developed folds are found. Bass Rock itself is a low rocky platform with an undulating surface. The eroded sides of the platform expose pseudobedding and reveal that the surface is structurally controlled; the low spots coincide with synclines and the highs with anticlines. Two anticlines, trending southwesterly and overturned to the southeast, make up a large part of the platform. A large symmetrical anticline, more than 11 feet high, in partly decomposed coarse-grained mafic gabbro crops out in a wave-eroded cliff behind Bass Rock. On the shore at the southeastern edge of

[1] A recent paper by the author (Kaye, 1964) about this stretch of shore erroneously referred to Cedar Point as Bass Rock.

the folded zone, tight folding cuts across a fine-grained mafic dike.

Study of the pseudobeds and the partings that separate them in vertical rock faces show that the thickness of the pseudobeds varies with the tightness of folding expressed by the radius of curvature. Thus, as the radius of curvature decreases from flank to crest of fold, a single pseudobed splits into several, or even many, pseudobeds. At the crests and troughs of some folds, where the radius of curvature is at a minimum, the pseudobedding-plane partings are only $\frac{1}{8}$ inch apart (fig. 6). A second significant feature is the presence of slickensided chloritic material on the surfaces of freshly exposed pseudobeds; the slickensides are oriented parallel to the dip of the beds.

Lastly, a close examination of the folds shows that they have the geometry of similar folds. In this type of fold, the radius of curvature of the fold does not change progressively from one bed to the next, as is characteristic of concentric folding, but rather remains constant from bed to bed. The geometry of the similar fold requires that either the thickness of a bed (measured normal to the surface of the bed) is greater in crest and trough of the fold than on the flanks, or that adjacent beds are separated by an empty space, or gape, at crest and trough. In this latter case, the bed remains a constant thickness throughout. Figure 4 shows this type of similar folding. The gapes required by the geometry and also the slippage between beds (the fragmentation of line AB) are indicated. In Nahant, small gapes, generally no higher than 3 mm, are found between many pseudobeds at crests and
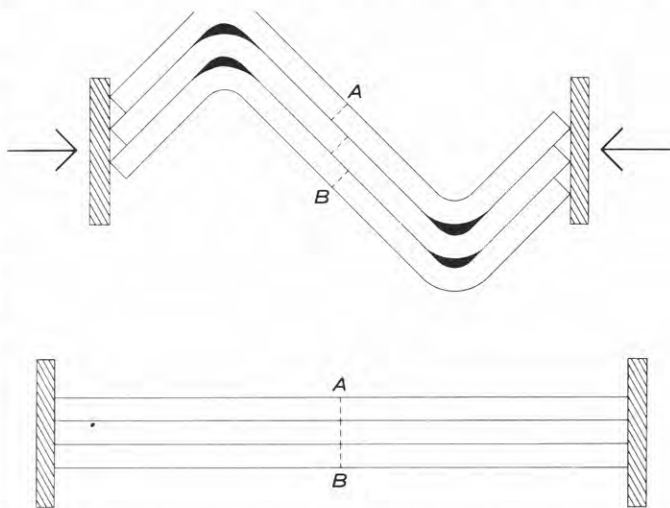
FIGURE 4.—Three-layered prism (below) folded by lateral compression (above). The folding is of the similar type and involves no thickening of the beds in crests and trough. Note the gape (black) at crests and troughs and the slippage between beds as indicated by the fragmentation of line AB.

troughs (fig. 6). The slippage required by this type of folding is expressed at Nahant by the slickensided surfaces of the pseudobeds just described.

ORIGIN OF STRUCTURES

The foregoing observations provide background for a discussion of the origin of the folds and pseudobedding-plane partings. The slickensided bedding planes, the form and distribution of the partings, and the similar geometry of the folds indicate that the folds formed as multilayered flexures and that the partings formed as a consequence, in the manner described below.

The reader is referred to the excellent summary recently published by Donath and Parker (1964) on the mechanics of flexure folding. Here only some of the features necessary to an understanding of the Nahant folds will be discussed. We must first assume the existence of compressive stresses great enough to cause initial flexing of the gabbro. To flex a solid, two or more free surfaces, oriented at an acute angle and preferably parallel to the principal stresses, are required. A thick mass of rock, such as the Nahant gabbro, will flex more readily if many parallel free surfaces are present. Providing that the frictional forces between layers can be overcome by the deformation stress, each layer will flex quasi-independently by slippage between adjacent beds, or layers, in the manner characteristic of similar folding (fig. 4). The force necessary to flex a given thickness of multilayered rock is thereby very much less than if the rock were massive or reacted as a single layer. At Nahant, the well-formed sheeting joints provided parallel free surfaces, and initial multilayered flexing consequently occurred.

A flexure is an elastic deformation. The convex surface is stretched and, in consequence, tensile stresses are developed on that surface while the concave side is shortened and compressive stresses are created there. Both stresses are greatest on the surfaces of the layer and diminish to zero near the midplane of the layer (often called the neutral axis). For a given material the magnitude of the surface stresses varies directly as the thickness of the bed and as the curvature of the fold. If we express curvature by the radius of a circle whose arc matches the curvature, then we can say that the stresses vary inversely as the radius of curvature, at that point.

Figure 5 illustrates for a typical fold the above characteristics of flexures. The radius of curvature at the crest of this flexure is $\frac{1}{4}$ the length of the radius of curvature on the flank of the fold. The relative magnitudes of the stresses at different distances from
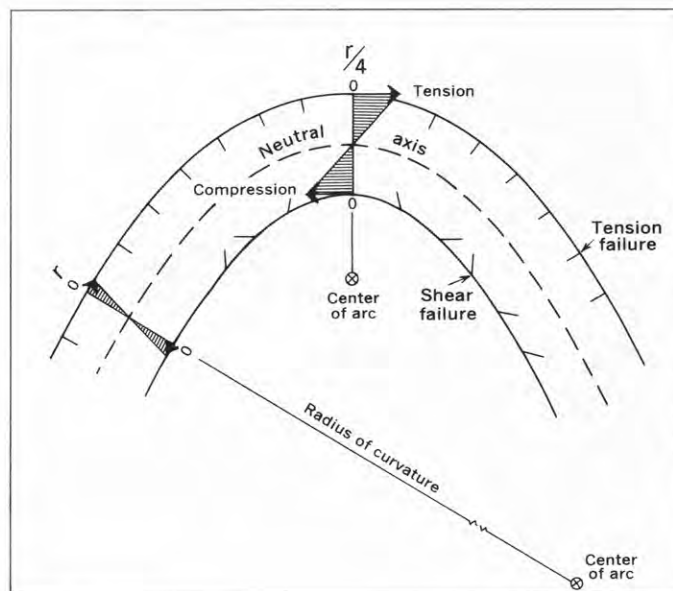
FIGURE 5.—Diagrammatic cross section of a flexed layer. r, radius of curvature.

the neutral axis are shown by the shaded triangles. The triangles indicate that for a given curvature, surface stresses vary directly with the thickness of the layer. As curvature develops during flexing the surface stresses may exceed the strength of the material. The concave side of the bed fails in shear and the convex side in tension. The form taken by these brittle failures is indicated in figure 5. The tension failures are generally normal to the bedding and strike parallel to the strike of the bedding. Shear failures, on the other hand, intersect the bedding at some oblique angle (following Mohr's theory of shear failure), although they, too, strike parallel to the strike of the bedding. If the tensile and shear strength of the rock differ, as they generally do, then failure on one surface will precede that on the other. This failure may, in fact, entirely obviate failure on the other surface, even though initial failure occurred early in the development of the fold. The reason for this is that failure of a surface has the effect of reducing the stresses on that surface; this immediately affects the entire stress field within the bed, shifting the neutral axis toward the opposite surface of the layer. In this way, the effective thickness of the layer is reduced. Progressive failure on one side prevents the stresses on the other side of the bed from reaching the failure point.

Most of the Nahant pseudobedding-plane partings merge with others at an acute angle and in the concave direction of the folds (fig. 6). These partings probably owe their origin to shear failure on the concave surfaces of the flexed pseudobeds, in the manner just

FIGURE 6.—Closeup view of folded gabbro, Cedar Point, Nahant. Note that some pseudobedding-plane partings are isolated and that others merge.

FIGURE 7.—Diagram of flexed layer, showing shear failure on concave side passing into tension failure (long-dashed line). Reverse-fault movement along the surface of failure very much exaggerated. Dilation of layer produced by this movement indicated by stippled zone. Vectors of internal tension are equivalent to this dilation. T, original thickness of bed; t, throw of microfault.

described. They notably differ, however, from the simple shear failure in that for most of their length they are parallel to the layering and therefore, in effect, produce new pseudobeds. From the abundance of these features in the crests and troughs of folds, it is clear that each new layer formed in the above manner also failed, thereby producing other and successively thinner layers. These failed in turn, and so on until folding ceased.

The change in orientation of the partings, from the obliquity of the initial shear failure to parallel fractures, is thought to be the result of tensional stresses produced within the layer by the shear failure itself, transforming the fracture from one of shear at the initial end to one of tension at the propagating end. The manner in which this bed splitting takes place can be understood by reference to figure 7, which represents a flexed pseudobed that has failed in shear on the concave side (the effect is identical in synclines as well as anticlines). The initial failure occurs on the surface and propagates inward. Strain takes the form of reverse faulting on this minute fracture (the displacement on this fault is very much exaggerated in figure 7). The effect of this faulting is to dilate the bed on the acute-angle side of the fault, as can be seen in figure 7, where the original thickness of the bed, T, is increased on the left-hand side by the increment, t, the throw of the microfault. This dilation of the bed

on the acute-angle side of the failure causes internal tensile stresses normal to the surface of the bed, as shown by the arrows. As flexing goes on and shear strain (faulting) continues, internal tension increases and is at a maximum at the tip of the fracture. The orientation of the fracture becomes increasingly controlled by the internal tension and changes from oblique to parallel to the pseudobedding. In effect, the pseudobed is split longitudinally by being wedged apart. This "wedging" action can be likened to shuffling a deck of cards by forcing the ends of the half decks together and at the same time flexing them.

The importance of the gape in similar folding is now evident. The gape represents a release of interbed pressure at fold crest and trough. This is true regardless of whether or not the gape is physically present. In ductile deformation there is a flowage during folding of limb material towards these points of pressure release, resulting in the thickening of beds in crests and troughs and, in effect, the infilling of the space of the gape. On the other hand, in similar folding of brittle rocks, such as we are dealing with in Nahant, the release of pressure at crest and trough is necessary for the microfault displacement on the shear failures. It can be appreciated that if the gabbro pseudobeds had been tightly oppressed at fold crest and trough, shear failure on these surfaces would have been seriously inhibited.

Some pseudobedding partings in the Nahant folds do not merge with other partings, or at least do not do so within the plane of the section in which they are

seen. Instead, these partings are isolated features, dying out into unfractured rock at both ends (fig. 6). Either of two explanations for this structural behavior seems reasonable. The first assumes that these partings may actually commence as shear failures, but that the planes of the cross sections in which we see them do not intersect the shear-failure roots. A second and more probable explanation is that some, if not all, of these partings are, as they appear, isolated tension fractures and that they also are the result of the internal tension of shear origin. There is experimental evidence that isolated tension fractures of this type are formed by shear-induced dilation. For example, Kuenen and de Sitter (1938; also de Sitter, 1956, fig. 9), in compression-box experiments on a thick layer of clay, produced a tight fold passing down into a fault and with multiple isolated tension fractures, parallel to the folded surface of the layer, on the acute-angle side of the fault. These partings resemble the isolated partings at Nahant and probably originated in the same way, namely, by dilation resulting from reverse faulting. Isolated tension fractures parallel to compressive stresses are also a common phenomenon in the triaxial testing of rock cores (Griggs and Handin, 1960, pl. 1). Heard (1960) has noted that this type of brittle failure occurs under low confining pressure or in the absence of interstitial water, or under both conditions. Where conditions are conducive to ductile rather than brittle behavior, as in deep burial and in stress fields of low magnitude but long duration, there is less likelihood that the Nahant type of failure would occur.

Shear-induced tension and the formation of tension fractures that are parallel to the compressive stresses probably form an important geological process. Reverse faults of all sizes must be accompanied by dilation of the rocks on the acute-angle side of the fault. The only exception to this is the rare case where a fault breaks out at the surface. We should therefore expect to find structures similar to those in the Nahant gabbro, although on a larger scale, associated with many reverse faults. Such structures would include reverse faults passing into flat-lying faults of the overthrust type, and flat-lying to gently dipping parallel joints. Where faulting took place under conditions conducive to ductile behavior, these features would probably be absent.

These observations have a bearing on the sheeting of the Nahant gabbro. In light of what has been deduced as to the origin of the smaller parallel fractures (pseudobedding-plane partings), it can be postulated that the sheeting of eastern Nahant was produced by a large northwest-dipping thrust fault. The fault itself may lie at depth and not crop out. Footwall dilation caused by early movement on this fault produced the sheeting. Later movement—and by this is meant later during continuous movement, not a discretely later movement—caused compressive stresses that resulted in flexing and the localized folding. The northeast-trending folded zone (fig. 2) may, in fact, be the surface expression of the thrust and may pass downward into the main fault itself.

The process of shear-induced bed splitting described in this paper is undoubtedly a far from common feature of folded rocks. The factors limiting its occurrence are largely the factors limiting true flexing in geologic folding and can be deduced in general terms. The process represents brittle failure. It would therefore be more common in rocks with high temperature-pressure thresholds between the brittle and the ductile states. Such rocks are generally strongly intermeshed crystalline rocks as opposed to clastic rocks, and ideally, holocrystalline equigranular igneous rocks as opposed to sedimentary and foliated metamorphic rocks. The second limiting factor is rate of strain. Under rapidly applied deformational stresses, most rocks deform as brittle substances. On the other hand, under very slowly applied stresses most rocks deform as ductile materials. Lastly, the shear-induced bed-splitting process requires differential slippage between beds during folding, the principal characteristic of similar folding. This interbed slippage occurs, however, only where frictional resistance to slippage is overcome by the deformational stresses. Since frictional resistance is a function of roughness of bed surfaces and the magnitude of the stresses normal to the bed surfaces, it follows that, everything else being equal, similar folding is more likely to occur at shallow depth where weight of overburden (normal stresses) is at a minimum than under a thick overburden. In summary, shallow burial, rapidly applied deformational stresses, and holocrystalline bedded or sheeted rock provide the ideal conditions for the bed-splitting process that has been deduced from the field evidence at Nahant.

REFERENCES

Chapman, C. A., 1962, Bays-of-Maine igneous complex: Geol. Soc. America Bull., v. 73, p. 883–888.

Donath, F. A., and Parker, R. B., 1964, Folds and folding: Geol. Soc. America Bull., v. 75, p. 45–62.

Emerson, B. K., 1917, Geology of Massachusetts and Rhode Island: U.S. Geol. Survey Bull. 597, 289 p.

Griggs, D. T., and Handin, John, 1960, Observations on fracture and a hypothesis of earthquakes, *in* Griggs, D. T., and Handin, John, eds., Rock deformation: Geol. Soc. America Mem. 79, p. 347–373.

Heard, H. C., 1960, Transition from brittle fracture to ductile flow in Solenhofen limestone as a function of temperature, confining pressure, and interstitial fluid pressure, *in* Griggs, D. T., and Handin, John, eds., Rock deformation: Geol. Soc. America Mem. 79, p. 193–226.

Kaye, C. A., 1964, The upper limit of barnacles as an index of sea-level change on the New England coast during the past 100 years: Jour. Geology, v. 72, p. 580–600.

Kuenen, Ph. H., and de Sitter, L. U., 1938, Experimental investigation into the mechanism of folding: Leidsche Geol. Meded., v. 10, p. 217–239.

LaForge, Laurence, 1932, Geology of the Boston area, Massachusetts: U.S. Geol. Survey Bull. 839, 105 p.

Lane, A. C., 1889, The Geology of Nahant: Boston Soc. Nat. History Proc., v. 24, p. 91–95.

Sitter, L. U. de, 1956, The strain of rock in mountain-building processes: Am. Jour. Sci., v. 254, p. 585–604.

RELATION OF LACCOLITHIC INTRUSION TO FAULTING IN THE NORTHERN PART OF THE BARKER QUADRANGLE, LITTLE BELT MOUNTAINS, MONTANA

By IRVING J. WITKIND, Denver, Colo.

Abstract.—Three anticlines, underlain by laccoliths, are radial to a central stock and are bounded, in part, by normal faults dipping 50° to 60° away from the laccoliths. These faults increase in throw toward the stock. Three separate mechanisms of laccolithic emplacement can be inferred, depending upon: (1) whether the stock or, alternatively, a deeper chamber are considered to have been the source of the magma, and (2) whether the bounding faults that apparently confined the lateral spread of parts of the laccoliths grew out of stresses related to the emplacement of the central stock or, alternatively, of the laccoliths themselves.

The rolling plains of central Montana are broken here and there by discrete, forest-covered mountain groups (index map, fig. 1). One of these is the Little Belt Mountains, chiefly a laccolithic complex, which occupies about 1,250 square miles in parts of Cascade, Judith Basin, Meagher, and Wheatland Counties.

The Little Belt Mountains, first studied by Weed and Pirsson (1900), are currently being restudied as part of a program of laccolithic investigations undertaken by the U.S. Geological Survey. A part of the northern half of the mountains, centering about Barker, Mont., is included in the Barker quadrangle, currently being mapped by the author (fig. 1). Topographic relief totals about 3,000 feet—the valleys are at altitudes of about 5,000 feet, and the mountain ridges at altitudes of about 8,000 feet.

Study of (1) the structural framework of the north flank of the mountains, and (2) the relations of the ore deposits to the igneous intrusions are among the major objectives of this project; this report is a preliminary summary based upon work done during the 1963 and 1964 field seasons.

GEOLOGY

Sedimentary strata exposed in the map area total about 4,600 feet in thickness and include units assignable to 4 systems of the Paleozoic and 2 systems of the Mesozoic (see accompanying table). The major intrusions, mainly felsic rocks, have deformed these strata into quaquaversal domes, and elongate anticlines and synclines. Locally the strata have also been deformed by the emplacement of small mafic plugs.

The volume of the felsic rock (chiefly granite porphyry, syenite porphyry, and quartz-monzonite porphyry) far exceeds the volume of the mafic (chiefly shonkinitic) rocks. The felsic rocks consist mainly of quartz, alkalic and plagioclase feldspar, biotite, and hornblende. The shonkinitic rocks consist chiefly of biotite, augite, olivine, alkalic feldspar, and small amounts of feldspathoids. The age of the igneous rocks has not been determined, but presumably they are either Late Cretaceous or early Tertiary.

The Barker-Hughesville stock, near the center of the Barker quadrangle, is 1 to 1¼ miles in diameter; radiating from the stock are at least 2 tonguelike semiconcordant intrusions (fig. 2). The stock, composed of syenite, has been eroded to a broad valley, whereas the satellitic intrusions form high ridges and peaks. The general configuration of the satellitic intrusions suggests that they are laccoliths; their floors, however, are not exposed. The overall structure seems much like that found in such laccolithic complexes as the Henry Mountains (Hunt, 1953), and the Abajo Mountains (Witkind, 1964) in southeastern Utah. A comparable spatial pattern between parental stock and satellitic laccoliths may also be noted in the Sweetgrass Hills of north-central Montana (C. E. Erdmann, oral communication, 1963).

Extending northeastward from the stock is an elongate anticline whose flanks have been extensively dissected to form wide valleys which reach far back toward the center of the anticline. Near the heads of two of these valleys are rockfalls and outcrops of
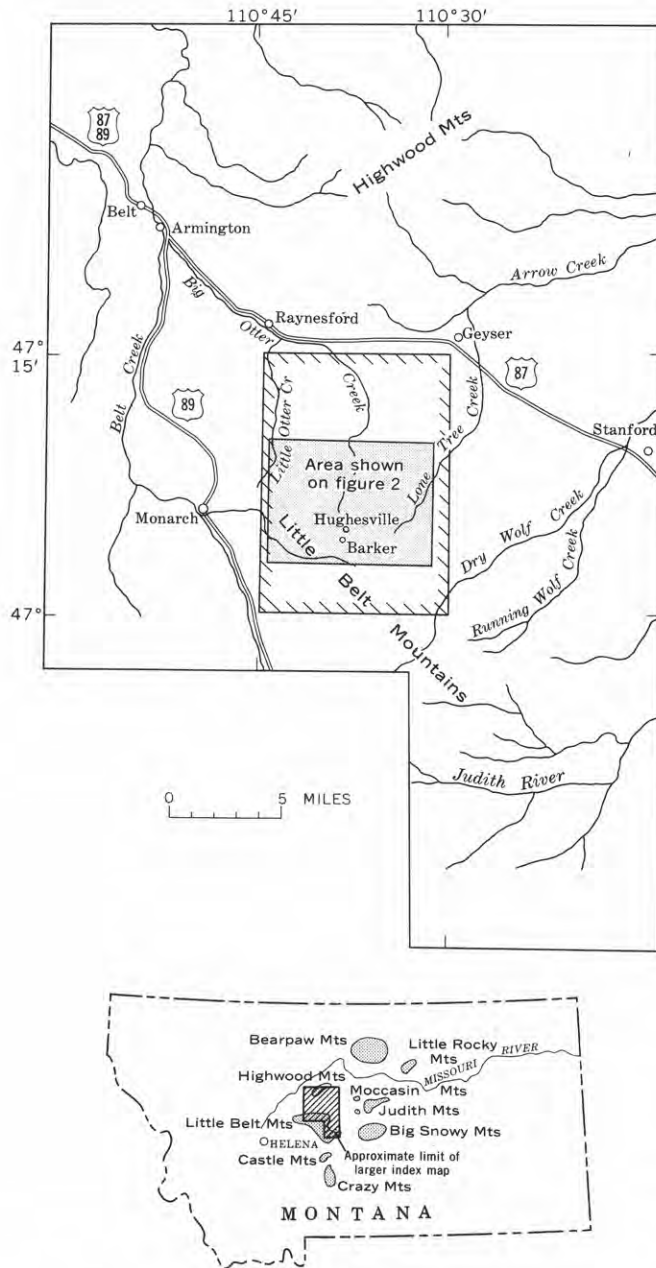
FIGURE 1.—Map of part of central Montana, showing area of report (patterned) within the Barker quadrangle (hachured outline).

quartz-monzonite porphyry which are interpreted as exposed parts of a single partly denuded laccolith, named the Clendennin-Otter laccolith (fig. 2A). The oldest sedimentary unit domed by the laccolith is the Flathead Sandstone.

Extending westward from the stock is a huge mass of granite porphyry here called the Barker laccolith. This intrusion is overlain by Cambrian strata.

To the southeast still another granite-porphyry mass, the Mixes Baldy–Anderson laccolith, extends from the

stock; further work may show this igneous body to be made up of two juxtaposed intrusions. The Middle Cambrian Park Shale is the oldest sedimentary unit domed by this laccolith.

The three mountain masses differ from one another chiefly in the amount of sedimentary cover removed. Both the Barker and Mixes Baldy–Anderson laccoliths are almost wholly denuded, whereas the Clendennin-Otter laccolith is still largely concealed by sedimentary rocks. Each of the structures underlain by a laccolith is bounded on one or more flanks by normal faults which dip 50° to 60° toward the adjacent valleys. Two of these faults lie along radii that extend out from the central stock (fig. 2A). Invariably the main masses of igneous rock are in the upthrown block, and the throw along each fault increases toward the stock. This increase in throw is well shown along the Otter fault. Near its northeast end, about 4 miles from the stock, Madison strata are juxtaposed. About 2 miles to the southwest (near the midpoint of the fault) Jefferson strata of the upthrown block abut Madison beds of the downthrown block. At the west end of the fault, near the proximal end of the Clendennin-Otter laccolith, Cambrian units of the upthrown block are in contact with the downthrown Madison.

The faults seem to have influenced the shape of the developing intrusions. The south flank of the Clendennin-Otter laccolith, for example, is bounded by the Otter fault (fig. 2A). As neither fault gouge nor slickensides were noted along this flank, and as the host rocks are somewhat baked along the contact, the implication is strong that this edge of the laccolith developed against a preexisting fault. Supporting evidence is lent by the fact that the Clendennin fault, along the north flank of the anticline, is followed for part of its length by a northeastward-trending dike which is connected to the Clendennin-Otter laccolith (fig. 2A). It would seem, moreover, that in cross section any one laccolith in this cluster is asymmetric, with one or more very steep flanks, presumably reflecting the presence of the fault plane.

Of the possible interpretations explaining the mode of emplacement of the laccoliths, three seem promising. The first (fig. 2B) assumes that as the stock forced its way upward, the overlying sedimentary strata were initially arched and then broken by a radiating system of normal faults. When the stock came to rest, magma was extruded laterally—and in a radial pattern—along permissive bedding planes (probably below competent stratigraphic units), and incipient laccoliths began to develop with one or more flanks determined by the normal faults. As the laccoliths

EXPLANATION

Chiefly sedimentary rocks

Chiefly igneous rocks

Igneous contact
Dashed where approximately located

Normal fault
Dashed where approximately located
U, upthrown side; D, downthrown side

Approximate outline of
mountain masses
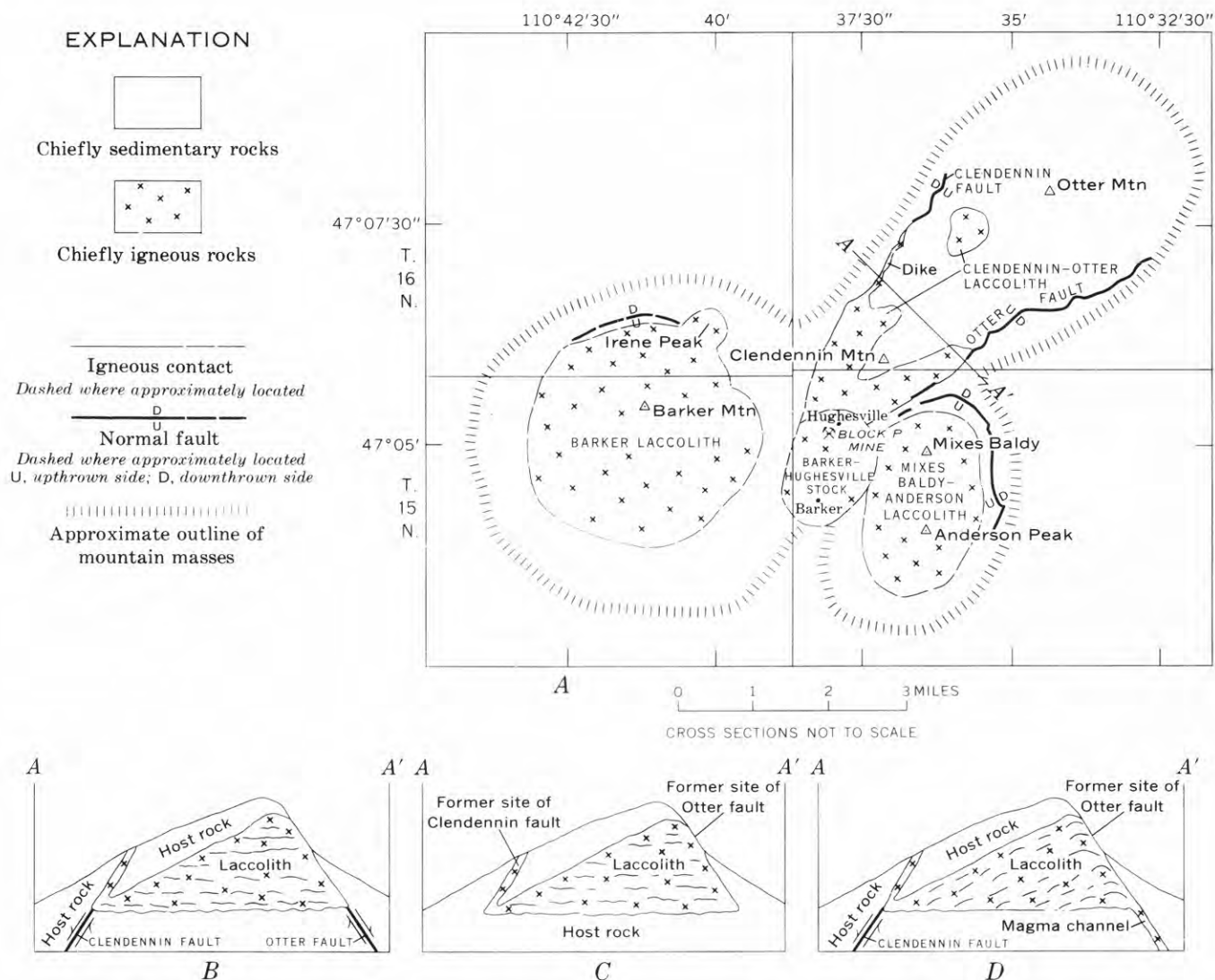
FIGURE 2.—Map and geologic sections showing areal and structural relations of the Barker-Hughesville stock. *A,* Pattern of laccoliths and marginal faults radiating from the stock. *B, C,* and *D,* Diagrammatic sketches of section *A–A'* across the Clendennin-Otter laccolith, illustrating the three alternative explanations for emplacemnt of the laccoliths as described in the text.

expanded they raised and folded back the overlying strata, enlarging each fault. The increase in throw along these faults toward the stock probably reflects the thicker proximal ends of the satellitic laccoliths. In this interpretation the normal faults extend below the laccolithic floors.

The second interpretation (fig. 2*C*) assumes that those faults formed during the upward thrust of the stock guided the emplacement of the satellite laccoliths, but that they were obliterated in the process. The normal faults that now flank the laccoliths were formed as a consequence of the expansion of the laccoliths. Thus, as a laccolith dilated, the overlying strata were raised, arched, and finally broken to form one or

more normal faults. These faults acted as barriers to the lateral spread of the magma, and the laccolith developed with one or more flanks determined by the newly established fault or faults. In this interpretation the faults do not extend below the laccolith floor.

The third interpretation (fig. 2*D*) suggests that the spatial distribution of the laccoliths was entirely dependent upon the fault pattern. Rather than the parent stock serving as the magma source, each fault tapped the magma chamber of the subjacent batholith(?) that gave rise to the stock, and then served as channels for the ascending magma. Wherever the passageways narrowed or closed, or beneath competent stratigraphic units, the magma moved laterally into

the adjacent sedimentary strata to form the laccolith-like bodies. In this interpretation the faults are also postulated to have been formed by the upward thrust of the rising stock.

The increase in throw along the normal faults toward the stock is strong presumptive evidence that the proximal ends of the laccoliths are thickest, suggesting that the laccoliths were fed by the central stock. Thus, either of the first two alternatives, seems more valid than the third hypothesis. The first alternative is preferable (fig. 2B), chiefly because it is doubtful

that an expanding laccolith, thick in its center and thin along its edges, would be able to break the strata at its margins. More likely the faults were already established, and acted as barriers to the lateral spread of the magma. Continued addition of magma resulted in the formation of asymmetric laccoliths having very step flanks terminated by the fault planes. In all three interpretations, it is assumed that the faults and their related fractures in and near the stock then served as channels for ascending hydrothermal fluids which formed ore deposits.

Generalized section of consolidated sedimentary strata exposed along the north flank of the Little Belt Mountains

SYSTEM	SERIES	UNIT		THICK-NESS (feet)	LITHOLOGY
Cretaceous	Lower Cretaceous	Kootenai Formation		500±	Siltstone, shaly, red; conglomeratic sandstone at base.
		UNCONFORMITY			
Jurassic	Upper Jurassic	Morrison Formation		150±	Mudstone, gray; intercalated sandstone beds; coal seam at top.
		Ellis Group	Swift Sandstone	60±	Sandstone, light-brown, thin- to medium-bedded; contains glauconite.
		UNCONFORMITY			
Carboniferous	Pennsyl-vanian	Amsden Formation		50±	Siltstone, shaly, red; light-gray crystalline limestone at base.
	Missis-sippian	Upper Mississippian	Big Snowy Group	Heath Shale	450±	Shale, black, fissile; intercalated thin gray limestone and sandstone beds.
				Otter Formation	260±	Siltstone, light-brown; interleaved light-gray limestone beds.
				Kibbey Sandstone	110±	Siltstone, shaly, red.
			UNCONFORMITY			
		Lower Mississippian	Madison Group	Mission Canyon Limestone	1800±	Limestone, dark-gray, massive; forms cliffs.
				Lodgepole Limestone		Limestone, dark-gray, thin-bedded, fossiliferous; chert in basal beds.
			UNCONFORMITY (?)			
Devonian	Upper Devonian	Three Forks Formation		100±	Siltstone, light-brown and red; black fissile shale near top.
		Jefferson Dolomite		300±	Limestone and dolomite, light-blue to dark-gray.
		Maywood Formation		40±	Siltstone, shaly, red.
		UNCONFORMITY			
Cambrian	Upper Cambrian	Pilgrim Limestone		115±	Limestone, gray, thin-bedded; pebble conglomerate; much glauconite.
	Middle Cambrian	Park Shale		170±	Shale, dark-gray, fissile.
		Meagher Limestone		75±	Limestone, gray, thin-bedded; some glauconite.
		Wolsey Shale		200±	Shale, dark-gray, glauconitic.
		Flathead Sandstone		100±	Sandstone, light-brown, medium- to coarse-grained.
		UNCONFORMITY			
Precambrian crystalline rocks					
		Total sedimentary rocks		4580	

ORE DEPOSITS

The Barker-Hughesville stock was the scene of intense mining activity during the latter part of the last century and the early part of this century. Until 1944, silver (tetrahedrite), lead (galena), and zinc (sphalerite) were mined profitably from the Block P mine, now abandoned and almost wholly filled with water (fig. 2A).

The rich metallic deposits were in or near the stock (Mrs. J. J. McBride, Faith Mining Co.; Mr. Roy Thorson, Barker, Mont., oral communications, 1964), and they apparently were localized along fractures (Spiroff, 1938, p. 559). In the Block P mine, the major vein is concave northward (Spiroff, 1938, p. 559). Future work will attempt to determine whether the normal faults (and their related fractures) extend into the stock, and if so, whether they played an important role in ore localization.

REFERENCES

Hunt, C. B., assisted by Paul Averitt, and R. L. Miller, 1953, Geology and geography of the Henry Mountains region, Utah: U.S. Geol. Survey Prof. Paper 228, 234 p. [1954].

Spiroff, Kiril, 1938, Geologic observations of the Block P mine, Hughesville, Montana: Econ. Geology, v. 33, no. 5, p. 554–567.

Weed, W. H., and Pirsson, L. V., 1900, Geology of the Little Belt Mountains, Montana: U.S. Geol. Survey 20th Ann. Rept., pt. 3, p. 257–595.

Witkind, I. J., 1964, Geology of the Abajo Mountains area, San Juan County, Utah: U.S. Geol. Survey Prof. Paper 453.

COMPOSITION OF JADEITIC PYROXENE
FROM THE CALIFORNIA METAGRAYWACKES

By ROBERT G. COLEMAN, Menlo Park, Calif.

Abstract.—Analyses of purified jadeitic pyroxene from quartz–jadeitic pyroxene–lawsonite–muscovite–glaucophane-bearing metagraywackes from the Franciscan Formation in California indicate the following average molecular composition, in mol percent: Jd 83.8, Di 5.8, Ac 8.6, and Hd 2.6. The optics are: α, 1.670; β, 1.671; γ, 1.678; $2V=60°-68°$; $Z \wedge C\,40°$, with dispersion strong, $r>v$. The monoclinic unit-cell constants are: $a=9.445$ Å, $b=8.620$ Å, $c=5.230$ Å, $\beta=72°31'$, cell volume$=406.1$ Å³. The measured density is 3.32 g/cm³ and the calculated value per unit cell is 3.33 g/cm³.

The presence of significant amounts of pyroxene components other than jadeite in these jadeitic pyroxenes suggests formation at lower pressures and temperatures than those found experimentally for the conversion of albite to pure jadeite+quartz. Petrologic and chemical evidence indicates that the conversion of graywacke to the assemblage quartz-jadeitic pyroxene-lawsonite-muscovite-glaucophane takes place without the introduction of alkalies. The reaction 8 albite+chlorite+$CaCO_3 \rightarrow 5$ jadeitic pyroxene+2 glaucophane+quartz+$2H_2O$+CO_2 may be important in relating greenschist to glaucophane schist facies metamorphism.

The important discovery of Bloxam (1956) that jadeitic pyroxene is an essential metamorphic mineral in many of the recrystallized graywackes of the Franciscan Formation of Jurassic and Cretaceous age stimulated further investigations concerning the distribution of this mineral in these California graywackes (McKee, 1958, 1962a, b; Rose, 1958). Prior to Bloxam's report, de Roever (1955) published an account describing jadeitic pyroxene from the metagraywackes in the Eastern Celebes, and more recently Seki and Shido (1959) have reported similar occurrences in Japan.

These pyroxene-bearing metagraywackes are invariably associated with metamorphic rocks of the glaucophane schist facies that are apparently restricted to post-Paleozoic orogenic belts. The most common mineral assemblages characterizing these metagraywackes are:

1. Quartz-pyroxene-lawsonite-muscovite
2. Quartz-pyroxene-glaucophane
3. Quartz-pyroxene-glaucophane-lawsonite

Metamorphic aragonite has also been found to be a common mineral of these jadeite-bearing metagraywackes (McKee, 1962b; Coleman and Lee, 1962; Brown and others, 1962). The association of quartz and jadeitic pyroxene with varying amounts of lawsonite, glaucophane, and muscovite represents the mineral assemblage characterizing metagraywackes in the glaucophane schist facies (Turner and Verhoogen, 1960). Following recent high-pressure experimental work (Robertson and others, 1957; Birch and LeComte, 1960) on the reaction

$$\text{albite} \rightarrow \text{jadeite} + \text{quartz} \qquad (1)$$
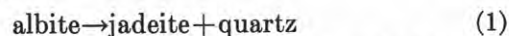
McKee (1960) stated that this equation could be used to demonstrate the extreme pressures necessary to produce jadeite within these metagraywackes. This paper demonstrates that the jadeite of these metagraywackes cannot be considered as pure Jd ($NaAlSi_2O_6$) because it also contains important amounts of other pyroxene components such as Ac ($NaFe^{+3}Si_2O_6$), Di ($CaMgSi_2O_6$), and He ($CaFe^{+2}Si_2O_6$). The presence of such components could therefore lower the pressure-temperature conditions of formation for the pair Jd+Qtz in the system $Na_2O+Al_2O_3+SiO_2$ as established by experimental work. Confirmatory evidence for this proposal is found in Coleman's observation (1961) that jadeitic pyroxenes containing more than 95 percent of the Jd component are restricted to silica-deficient rocks contained within serpentine and that other worldwide occurrences of nearly pure jadeite (>95 percent Jd) are also in such silica-deficient environments (Seki and others, 1960; Morkovkina, 1960; Moskaleva, 1962).

From the above observations regarding the mineral assemblages coexisting with Jd, it is unlikely that the

pyroxene in the quartz-rich graywackes can be a pure end-member jadeite. The experimental work on reaction (1) reveals that the pressure-temperature conditions necessary to produce pure Jd in the presence of quartz are in excess of those predicted during glaucophane schist metamorphism. The purpose of this paper is to show that those jadeitic pyroxenes in the metagraywackes contain noteworthy amounts of other pyroxene components.

MINERALOGY

A sample of jadeite-bearing metagraywackes from Angel Island, San Francisco Bay, Calif., (fig. 1) was used to obtain a pure fraction of the jadeitic pyroxene for chemical analysis and determination of its physical properties. These metagraywackes from Angel Island have been previously described by Bloxam (1956, 1960) and will be discussed within the petrology section. The pyroxene was purified by repeated centrifuging of material less than 325 mesh in methylene iodide. Two fractions were obtained by adjusting the specific gravity of the liquid between 3.30 and 3.34 for the heavy fraction (sample 1, table 1), and between 3.25 and 3.27 for the lighter fraction (sample 2, table 1). The high specific gravity of 3.34 was obtained by supercooling the methylene iodide before centrifuging. Optical examination of the pure concentrates revealed minute dark inclusions which were later found during the chemical analyses to be graphite. X-ray diffraction patterns of these purified concentrates when compared with patterns for known mixtures of jadeite and quartz revealed approximately 0.5 weight percent quartz in sample 1 and 5 weight percent quartz in sample 2. No other impurities were found during the optical and X-ray examination. Sample 2, table 1, was considered too impure for further physical measurements; therefore, all discussions herein will concern only sample 1, table 1.

The chemical analyses were made by a spectrogravimetric method of Stevens and others (1960) which provides a superior analysis, because all major and minor elements present are quantitatively determined. Recalculation of the analysis to 6 oxygens to the unit cell (table 1) shows that the jadeite conforms to the pyroxene formula. However, notable amounts of pyroxene components other than Jd are present. When the composition of this jadeitic pyroxene is compared with the compositions of other pyroxenes from metagraywackes (table 2), it is obvious that these jadeitic pyroxenes contain significant amounts (up to 20 mol percent) of other pyroxene components, the most abundant being Di ($CaMgSi_2O_6$) and Ac ($NaFe^{+3}Si_2O_6$). Therefore, these metamorphic pyroxenes are chemically

TABLE 1.—*Chemical and physical properties of jadeitic pyroxene from metagraywacke, Angel Island, Calif.*

	Sample 1	Sample 2	Sample 1

CHEMICAL PROPERTIES

Chemical composition (weight percent)[1]			Number of ions on the basis of 6 oxygens		
SiO_2	59.2	60.9			
Al_2O_3	21.94	21.38	Si [2]	2.0080	2.0080
Fe_2O_3	1.42	1.36			
FeO	.64	.69	Al	.8847	
MgO	1.04	.85	Fe^{+3}	.0365	
CaO	1.14	1.13	Cr	.0003	
Na_2O	13.7	12.7	V	.0025	
K_2O	.08	.10	Sc	.0002	
H_2O^+	None	.27	Ti	.0128	1.0095
TiO_2	.5	.59	Zr	.0001	
MnO	.03	.02	Fe^{+2}	.0183	
ZrO_2	.009	.014	Mg	.0531	
Cr_2O_3	.010	.014	Mn	.0008	
V_2O_3	.09	.07	Ni	.0001	
NiO	.004	.002	Cu	.0001	
BaO	.003	.010			
BeO	.0005	.002	Na	.9088	
CoO	.0003	.0007	K	.0031	0.9551
CuO	.002	.002	Ca	.0419	
PbO	.002	.002	Sr	.0013	
Sc_2O_3	.008	.008			
Ag	.003	None			
Total	99.88	100.16			
H_2O^-	.05	.06			

PHYSICAL PROPERTIES

Optical properties [3]		Density	
alpha	1.670 ± 0.003	Measured	3.32 ± 0.02 g/cm³.
beta	1.671 ± 0.003		
gamma	1.678 ± 0.003	Calculated	3.33 g/cm³ for
Birefringence	0.008		formula
$2V$	40°		calculated
$Z \vee C$	60°–68°		above.
Dispersion	$r > v$ (strong)		

Unit-cell data [4]	
a	9.445 Å
b	8.620 Å
c	5.230 Å
β	72°31′
Cell volume	406.1 Å³

[1] Chemical analyses by R. E. Stevens, A. A. Chodos, S. T. Neil, A. C. Bettiga, and Elizabeth Godijn.
[2] 0.5 percent SiO_2 subtracted as estimated impurity.
[3] Optical determinations made with sodium light.
[4] Unit-cell data determined by D. E. Appleman from X-ray diffraction powder pattern measurements.

distinct when compared to a pure jadeite, and these chemical differences are reflected by the varying optical properties and unit-cell sizes (table 2). On the other hand, these jadeitic pyroxenes from the metagraywackes contain much more of the Jd component than do the omphacites (table 2), as shown by comparison with omphacite from the Alpine eclogite of the Tiburon Peninsula of California. As noted previously (Cole-

TABLE 2.—*Comparison of jadeitic pyroxenes from metagraywackes*

	Jadeitic pyroxenes from metagraywackes			Jadeite	Omphacite
	1	2	3	4	5
Pyroxene components (molecular percent)					
Jd	86. 0	80. 0	87. 0	96. 5	39. 2
Di	5. 2	6. 5	2. 6	1. 2	40. 2
Ac	5. 9	11. 2	8. 9	2. 3	10. 3
Hd	2. 9	2. 3	1. 5	---------	10. 3
Specific gravity	3. 32	3. 27	3. 29	3. 34	3. 34
Optical properties					
α	1. 670	1. 659	1. 664	1. 654	1. 682
β	1. 671	1. 663	1. 666	1. 657	1. 689
γ	1. 678	1. 670	1. 672	1. 666	1. 705
γ—α	. 008	. 012(?)	. 012(?)	. 012	. 023
$Z \wedge C$	40°	53°	40–50°	34°	48°
$2V$	60–68°	86°	70–75°	70°	69°
Dispersion	$r>v$ strong	$r>v$ strong	$r>v$	None	Weak
Monoclinic unit cell (setting of Wyckoff and Merwin, 1925)					
a	9. 445 Å	---------	---------	9. 402 Å	9. 572 Å
b	8. 620 Å	---------	---------	8. 580 Å	8. 773 Å
c	5. 230 Å	---------	---------	5. 244 Å	5. 253 Å
β	72°31′	---------	---------	72°33′	73°10′
Cell volume	406. 1 Å³	---------	---------	403. 5 Å³	422. 2 Å³

1. Angel Island, Calif.
2. Valley Ford, Calif. (Bloxam, 1956).
3. East-central Celebes (de Roever, 1955).
4. Schist tectonic inclusion in serpentine, Clear Creek, New Idria district, California (Coleman, 1961).
5. Alpine-eclogite, Tiburon Peninsula, Calif. (Coleman and others, report in preparation).

man, 1961), the optical character of these jadeitic pyroxenes is distinct, for they are characterized by a strong dispersion and a lower birefringence than pure jadeite. Additional work is necessary before direct correlations between optical and chemical data can be presented.

X-ray diffraction data have previously been given (Coleman, 1961) for the analyzed pyroxene described in this paper (table 1). As might be expected, the X-ray diffraction powder pattern of the jadeitic pyroxene from the metagraywackes shows a slight shift in the *d*-spacings when compared to the pattern of pure jadeite. This shift reflects a slight increase in cell volume of approximately 3 Å³, resulting from lengthening of the *a* and *b* axes (table 2). By comparison, the Tiburon omphacite illustrates pronounced increase in unit-cell volume (19 Å³) for a pyroxene with less than 50 mol percent Jd. Such volume expansions suggest that formation of those pyroxenes containing components other than Jd may require less pressure than that required to form pure jadeite.

PETROLOGY

The jadeitic pyroxenes from Franciscan metamorphic rocks are generally restricted to metagraywackes;

however, pyroxenes of similar composition have also been described from metabasalts whose composition is spilitic or keratophyric (Coleman and Lee, 1963). These mafic metamorphic rocks belong to the low and intermediate grades of metamorphism (types II and III of Coleman and Lee, 1963), whereas in the higher grade glaucophane schists, omphacite prevails. Only the pyroxene-bearing metagraywackes will be considered here; these metagraywackes are thought to be similar in metamorphic grade to the intermediate (types II and III) metabasalt from the Ward Creek area.

The metagraywackes described in this paper come from three different localities in central California: Angel Island, Valley Ford, and Pacheco Pass (fig. 1). Bloxam (1956, 1959, 1960) has published information concerning the metagraywackes from Angel Island and Valley Ford, and the Pacheco Pass metagraywackes have been discussed by McKee (1962a). The distribution of these metagraywackes within the Franciscan Formation is irregular, and as yet no regional or local patterns have been established, because of insufficient detailed mapping and poor surface exposures. Part of the problem stems from the difficulty of distinguishing metagraywackes from the unmetamor-
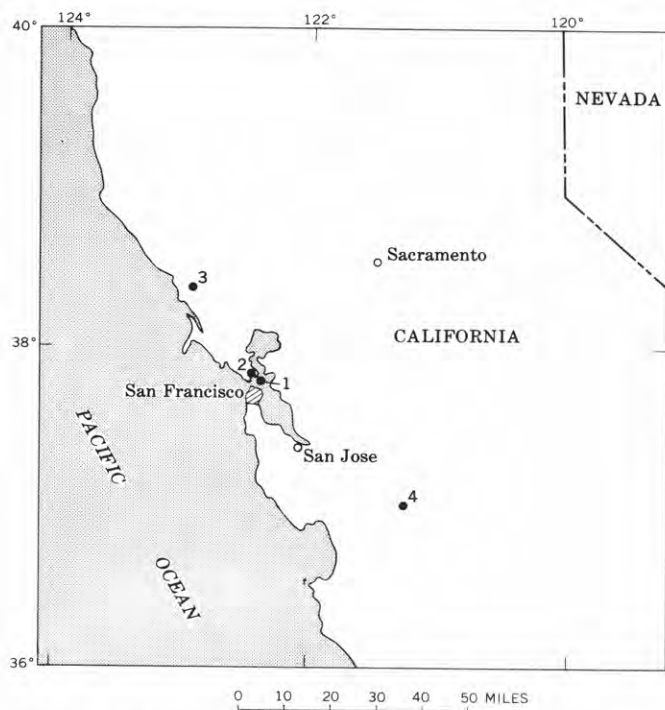
FIGURE 1.—Index map showing location of investigated metagraywackes in California. *1*, Angel Island; *2*, Tiburon Peninsula; *3*, Valley Ford; and *4*, Pacheco Pass.

TABLE 3.—*Modal analyses of metagraywackes, in volumetric percent*

Mineral:	Sample			
	1	2	3	4
Quartz	44. 1	43. 1	30. 7	26. 4
Jadeite	22. 1	25. 3	22. 0	51. 5
Muscovite	25. 0	17. 4	3. 5	5. 4
Lawsonite	1. 3	7. 3	19. 5	7. 2
Glaucophane	---------	. 7	21. 2	7. 1
Carbonate	1. 8	1. 6	---------	---------
Other	5. 6	4. 6	2. 9	2. 4
Specific gravity	2. 77	2. 79	2. 89	2. 97

1. Metagraywacke (80–RGC–58) on western slope of Angel Island above Ft. McDowell at 500-foot contour; from mass of Franciscan graywacke extending from Campbell Point to the crest of Angel Island as shown on the geologic map of the San Francisco North quadrangle, California (Schlocker and others, 1958). This is similar to the metagraywacke from which the analyzed jadeite was obtained, table 1. See table 4 for chemical analyses.

2. Metagraywacke (21–RGC–60) from roadcut along Pacheco Pass (California State Highway 152) approximately 2 miles east of Bell Station on south side of road, Santa Clara County, Calif. See table 4 for analyses.

3 and 4. Metagraywacke (120–RGC–58 and 118–RGC–58) along Ebabias Creek ½ mile from Valley Ford–Freestone Highway, ½ mile south of the Bodega Bay road junction, Sonoma County, Calif. Material similar to that for which chemical analysis is given in table 4, No. 7.

phosed graywackes within the Franciscan Formation. Generally the lack of any metamorphic fabric or megascopic metamorphic minerals precludes positive field identification of these metagraywackes. To help overcome this difficulty, specific gravity of graywacke chips has been checked by using a series of graduated heavy liquids contained in wide-mouth amber jars. The average specific gravity of the Franciscan graywacke is approximately 2.67, whereas that for the pyroxene-bearing metagraywackes is 2.70 or greater.

The study by Bloxam (1960) suggests that 90 percent of the graywackes on Angel Island are metamorphic, but his map does not show the relation of the pyroxene-bearing metagraywackes to the other lithologic units of the island. Later work by Julius Schlocker and Coleman, using the map of Schlocker and others (1958), suggests a very irregular distribution of the metagraywackes which, as yet, cannot be related to structure or associated lithologic units. Bloxam (1960) has also described the pyroxene-bearing metagraywackes from Valley Ford; in this locality the outcrop pattern is limited and the distribution of metagraywacke is very irregular. On the other hand, the Pacheco Pass area described by McKee (1962a) appears to represent a widespread and uniform metamorphism of the graywackes in this area of the Diablo Range. McKee reports that metagraywackes containing jadeitic pyroxene cover a 140-square-mile area and may extend farther north and south along the Diablo Range. In this region McKee has erected a jadeite isograd within the metagraywackes in order to distinguish a zone where metagraywackes containing predominantly quartz-albite-lawsonite-mica change to quartz-jadeite-lawsonite-mica-bearing rocks. Thus in this area widespread continuous metamorphism of graywackes has been established, although the boundaries with the nonmetamorphic rocks are not yet known.

The mineralogical composition of these metagraywackes is usually quite uniform. The modal analyses given for the Angel Island and Pacheco Pass metagraywackes (table 3) are characteristic for most of these rocks. Glaucophane may or may not be present, but in some rocks such as the Valley Ford samples, the glaucophane is sometimes as abundant as the pyroxene. Sedimentary textures of the original graywackes are retained, and rarely does a schistosity or foliation develop.

Quartz is recrystallized and forms mosaic aggregates which contain inclusions of newly formed metamorphic minerals. Quartz veins developed during metamorphism have a similar mosaic texture and contain subhedral to euhedral grains of calcium carbonate and albite. The euhedral albite grains are common in

these veins, but notably jadeitic pyroxene was not found. The groundmass jadeitic pyroxene forms fan-shaped aggregates, produced by clustering of prismatic pyroxene grains. These irregular aggregates are characteristically clouded, because of graphite and quartz inclusions. Albite was not found in these graywackes associated with the jadeitic pyroxene in the groundmass; however, albite is commonly present within the quartz veins. It is obvious that where albite is associated with ferromagnesian minerals, such as chlorite, the two react to form a jadeitic pyroxene. Albite was carefully searched for in the graywackes by separating out density fractions (<2.67) for X-ray diffraction; however only a trace of albite was present in 1 out of 4 samples. Lawsonite is present in all metagraywackes studied and forms small euhedral to subhedral prisms or platelets flattened parallel to (010). Fine-grained muscovite developed along shear planes or as elongated wisps is ubiquitous; the paragonite content of this mica is considered to be less than 5 mol percent. Minor amounts of metamorphic aragonite associated with calcite are often present (McKee, 1962b). The textural evidence suggests that these rocks contain mineral assemblages that are in equilibrium; however the presence of calcite and chlorite associated with aragonite and albite indicates "nonequilibrium" conditions. Calcite invariably replaces aragonite and represents the early stages of weathering or of thermal effects. Where the available albite has reacted to form jadeitic pyroxene or glaucophane, excess chlorite may remain as a stable phase in the albite-deficient zones of the rock. On the other hand, albite forms within quartz veins in the absence of ferromagnesian minerals, demonstrating that end-member jadeite is not stable in the presence of excess silica during metamorphism.

In summary, the metagraywackes are characterized by lack of distinct planar structures and in the field have the same appearance as the unmetamorphosed graywackes. The characteristic mineral assemblage is quartz-jadeite-lawsonite-muscovite with varying amounts of glaucophane, aragonite-calcite, chlorite, and albite. The fact that in most instances these graywackes are in place and lack well-developed metamorphic structures suggests that they are probably equivalent in metamorphic grade to the types II and III metabasalts of Coleman and Lee (1963). Apparently lower grade rocks with a bulk composition equivalent to that of these graywackes have been described by Blake and Ghent (1965). These metasediments contain the assemblage quartz-muscovite-chlorite-albite-

lawsonite-aragonite, which is quite similar to that of the Diablo Range metagraywackes but lacks jadeitic pyroxene and glaucophane. The absence of jadeitic pyroxene could indicate that a lower grade metamorphism may exist for the glaucophane schist facies.

CHEMICAL RELATIONS

The possibility that the presence of jadeite and glaucophane may indicate alkali metasomatism in these rocks has to be considered, as certain authors would restrict the use of the glaucophane schist facies for this reason (Korzhinskii, 1959; Schurmann, 1953; Taliaferro, 1943). Presented in table 4 are 3 new chemical analyses of the jadeite-bearing California metagraywackes along with 4 previous analyses given by Bloxam (1956, 1960). For comparison, average values for unmetamorphosed Franciscan graywackes and for New Zealand graywackes are given, together with newly published averages for all graywackes by Pettijohn (1963). Inspection of these values shows that the composition of the metagraywackes of the Franciscan Formation appears to be nearly identical to that of the average unmetamorphosed graywackes from this formation, as well as to the averages given by Reed (1957) and Pettijohn (1963). One notable characteristic of graywackes is that the Na_2O/K_2O ratio is nearly always greater than 1, as has been shown by Pettijohn (1963). His compilation indicates that graywackes may contain as much as 5.5 weight percent Na_2O, but average between 3 to 4 weight percent. A plot of the N_2O versus K_2O for the Franciscan metagraywackes and unmetamorphosed graywackes and for the average values given in table 4 demonstrates a general overlapping of the Na_2O/K_2O ratios (fig. 2).

The normative albite in the metagraywackes averages 31.3 molecular percent; in the unmetamorphosed Franciscan graywacke the average is 32.5 molecular percent. Reed (1957) has found that the normative albite for 14 New Zealand graywackes averages 32.5 molecular percent. A plot of the normative Ab-Or-An ratios for various graywackes illustrates that there is no significant difference in these ratios among metamorphosed and unmetamorphosed graywackes (fig. 3). Even though a series of analyzed samples representing the change from graywacke to metagraywacke in a single area is not available, the present analytical information strongly indicates that the alkalies were not necessarily mobile components during metamorphism.

Jadeite coexisting with quartz in these metagraywackes is unusual when we consider the reaction
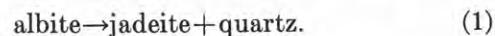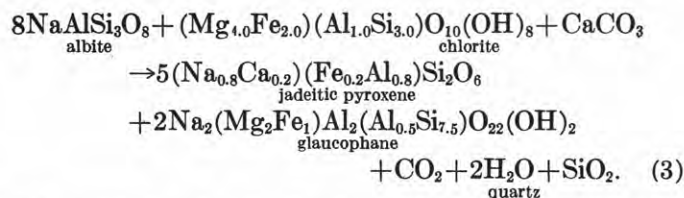
$$albite \rightarrow jadeite + quartz. \qquad (1)$$

TABLE 4.—*Chemical analyses and norms of California jadetized metagraywackes compared with those of average unmetamorphosed graywacke*

	Jadeitized metagraywacke							Unmetamorphosed graywacke		
	1	2	3	4	5	6	7	8	9	10
Chemical composition (weight percent) and specific gravity										
SiO_2	68.2	70.0	67.1	69.77	70.04	70.61	69.14	68.5	69.7	66.7
TiO_2	.62	.51	.55	.41	.14	.53	.37	.5	.6	.6
Al_2O_3	13.00	12.00	13.6	14.82	13.88	11.99	15.08	13.9	14.3	13.5
Fe_2O_3	1.6	1.0	1.3	1.21	.91	1.59	1.51	1.3	1.0	1.6
FeO	2.7	2.8	3.5	1.35	2.26	2.22	.84	3.1	2.5	3.5
MnO	.08	.08	.06	.03	.07	.05	.03	.1	.1	.1
MgO	2.4	3.1	2.4	2.38	2.11	2.82	1.08	2.3	1.2	2.1
CaO	2.0	2.2	2.6	1.99	1.79	2.41	2.79	2.0	1.9	2.5
Na_2O	2.2	2.6	1.4	3.89	4.01	2.86	5.31	3.5	3.5	2.9
K_2O	2.2	2.0	2.0	1.01	.97	1.64	1.28	1.9	2.4	2.0
H_2O^+	3.2	2.7	4.0	2.96	3.15	2.81	1.96	2.7	2.9	2.4
H_2O^-	.5	.16	.33	.20	.25	.20	.08	--------	.4	.6
CO_2	1.0	.38	<.05	.10	.07	.03	--------	.1	.1	1.2
P_2O_5	.1	.10	.19	.08	--------	.07	.12	.1	.2	.2
C	--------	--------	--------	--------	--------	--------	--------	--------	.1	.1
Total	100.00	100.00	100.00	100.20	99.65	99.83	99.59	99.9	99.9	100.4
Specific gravity	2.75	2.79	2.77	2.89	2.91	2.86	2.91	2.67	--------	--------
Catanorm (mol percent)										
Q	33.54	35.94	41.24	33.75	33.50	35.44	24.60	30.55	32.1	--------
Or	13.5	12.5	12.5	6.0	6.0	10.5	8.0	11.5	15.0	--------
Ab	30.0	24.5	13.5	36.5	37.5	28.5	48.5	32.5	32.5	--------
An	3.5	10.5	12.5	9.5	9.0	12.0	13.5	10.0	9.0	--------
C	4.7	2.2	6.0	4.4	3.6	1.3	.1	3.0	3.1	--------
En	7.0	9.0	7.2	7.0	6.0	8.0	3.0	6.6	3.4	--------
Fs	2.3	3.1	4.3	.7	3.2	1.7	--------	3.5	2.4	--------
Ilm	1.0	.8	.8	.6	.1	.8	.6	.6	1.0	--------
Mt	1.8	1.2	1.5	1.4	.9	1.8	1.5	1.4	1.1	--------
Cc	2.6	.2	--------	.2	.2	--------	--------	.2	.2	--------
Ap	.2	.2	.5	.2	.2	.2	.2	.2	.3	--------

1. Metagraywacke (80–RGC–58) on western slope of Angel Island above Ft. McDowell at 500-foot contour; from mass of Franciscan graywacke extending from Campbell Point to the crest of Angel Island as shown on the geologic map of the San Francisco North quadrangle, California (Schlocker and others, 1958). This is similar to the metagraywacke from which the analyzed jadeite was obtained, table 1.
2. and 3. Metagraywacke (21–RGC–60) and metashale (20–RGC–60) from roadcut along Pacheco Pass (California State Highway 152) approximately 2 miles east of Bell Station on south side of road, Santa Clara County, Calif.
4. Metagraywacke (Bloxam 1960, No. 4, table 1, p. 559) from Point Simpton, Angel Island, San Francisco Bay, Calif. Analyst, T. W. Bloxam.
5. Metagraywacke (Bloxam 1960, No. 5, table 1, p. 559) from Point Blunt, Angel Island, San Francisco Bay, Calif. Analyst, T. W. Bloxam.
6. Metagraywacke (Bloxam 1956, No. 1, 302/EC2, table 2, p. 493) eastern El Cerrito, Berkeley Hills, Calif. Analyst, E. H. Oslund.
7. Metagraywacke (Bloxam 1956, No. 2, 302/138e, table 2, p. 493) along Ebabias Creek, ½–mile from the Valley Ford-Freestone highway, ½ mile south of the Bodega Bay road junction, Sonoma County, Calif. Analyst, E. H. Oslund.
8. Average of sixteen analyses of Franciscan graywackes. 1 (Melville, 1891), 1 (Davis, 1918), 1 (Taliaferro, 1943), 1 (Bloxam, 1956), 12 unpublished analyses from U.S. Geological Survey.
9. Average of 14 analyses of lower Mesozoic Alpine graywackes from New Zealand (Reed, 1957, No. 2, p. 22).
10. Mean composition of graywackes based on 61 analyses (Pettijohn, 1963, table 12, p. S15).

Experimental evidence shows that only at extremely high pressures can a pure jadeite exist with quartz (fig. 4). If we assume that the addition of other pyroxene components to jadeite may permit a jadeitic pyroxene to form at lower pressures and temperatures, then it is perhaps reasonable to expect a jadeitic pyroxene to form under conditions characterizing the glaucophane schist facies (fig. 4). The suggested lowering of the curve representing reaction (1) has been plotted in figure 4 and is based on intuitive petrology.

This may, however, be in serious error, as has been pointed out by D. R. Wones, of the U.S. Geological Survey (written communication, 1964). If we assume ideal solution of other pyroxene components in the jadeite, thermodynamic calculations can be designed to estimate the effect of such substitution of components on the stability of reaction (1). These calculations indicate that the intuitive estimate could be much too low as far as the P_{Total} is concerned. On the other hand, we have no evidence that such substitution is

pressures and relatively low temperatures (Simmons and Bell, 1963). The experimental evidence on the stabilities of aragonite and lawsonite given in figure 4 illustrates this point.

At the present stage of experimental evidence, the following equations might be written to characterize

FIGURE 2.—Weight percent Na_2O versus K_2O for metagraywackes and graywackes from the Franciscan Formation, California. Dots, metagraywacke ratios from table 4; circles, unmetamorphosed graywacke ratios (mostly unpublished data); triangles, averages given in table 4.

ideal. Obviously the answer must await further investigation into the effect of these other pyroxene components on the stability of the jadeitic pyroxenes. The presence of aragonite and lawsonite in stable equilibrium with jadeitic pyroxene clearly indicates that these metamorphic rocks are favored by high

FIGURE 3.—Triangular plot of molecular normative feldspar ratios in metagraywackes from the Franciscan Formation (circles) and the average for unmetamorphosed graywackes as taken from table 4 (triangles).

FIGURE 4.—Pressure-temperature diagram showing equilibrium curves determined experimentally by thermodynamic calculations and petrographic evidence. These curves represent reactions that appear to be important in the metamorphism of graywackes in the blue schist facies. The jadeite+quartz→albite reaction is from the experimental work of Birch and LeComte (1960) and the reaction jadeitic pyroxene+quartz→albite+chlorite is inferred from petrographic evidence. The aragonite-calcite curve is from Jamieson (1953) and Clark (1957). The lawsonite→anorthite+H_2O is a calculated curve, and the zoisite+sillimanite+quartz+H_2O field is bounded by experimentally determined lines, both given by Newton and Kennedy (1963). The zeolite field is arbitrarily denoted by a line with a negative slope as suggested by Coombs (1961, fig. 7, p. 212). The suboceanic geothermal gradient is taken from Birch (1955) and could represent conditions during metamorphism of Franciscan graywackes.

possible reactions that could lead to jadeite-bearing metagraywackes:

$$8NaAlSi_3O_8 + 2Ca_{0.5}(Mg_{3.5}Al_{0.5})Si_8O_{20}(OH)_4 nH_2O$$
albite, montmorillonite

$$\rightarrow 5(Na_{0.8}Ca_{0.2})(Mg_{0.2}Al_{0.8})Si_2O_6$$
jadeitic pyroxene

$$+ 2Na_2Mg_3Al_2(Al_{0.5}Si_{7.5})O_{22}(OH)_2$$
glaucophane

$$+ 15SiO_2 + 6H_2O. \quad (2)$$
quartz

769-328 O-65—4

$$8NaAlSi_3O_8 + (Mg_{4.0}Fe_{2.0})(Al_{1.0}Si_{3.0})O_{10}(OH)_8 + CaCO_3$$
<div align="center">albite   chlorite</div>

$$\rightarrow 5(Na_{0.8}Ca_{0.2})(Fe_{0.2}Al_{0.8})Si_2O_6$$
<div align="center">jadeitic pyroxene</div>

$$+2Na_2(Mg_2Fe_1)Al_2(Al_{0.5}Si_{7.5})O_{22}(OH)_2$$
<div align="center">glaucophane</div>

$$+CO_2+2H_2O+SiO_2. \quad (3)$$
<div align="center">quartz</div>

The critical point is the breakdown of both chlorite (montmorillonite) and albite to form jd-pyroxene and glaucophane. Lawsonite can form early and is found coexisting with albite and chlorite in lower grade rocks (Blake and Ghent, 1965; Coombs, 1960; McKee, 1962a).

These reactions can be illustrated by Ernst's diagrams (Ernst, 1963) using the relations between graywacke bulk compositions and the stable mineral assemblages (fig. 5). For greenschist facies regional metamorphism, epidote+chlorite+albite+quartz+muscovite+calcite is the stable assemblage (fig. 5A). Intermediate to the greenschist and glaucophane schist facies is the assemblage lawsonite+albite+chlorite+quartz+muscovite+calcite, where the replacement of epidote by lawsonite may be pressure dependent (fig. 5C). By increasing the pressure ($P_T = P_{H_2O}$) of the system with this bulk composition, reactions (2) and (3) could depict the breakdown of albite+chlorite to jadeite+glaucophane (fig. 5B).

These relations indicate that the greenschist and glaucophane schist facies may be related by the intermediate type containing lawsonite in stable association with albite and chlorite. The close relation between glaucophane schists and alpine-type orogeny suggests that a steeper pressure gradient or a lower thermal gradient characterizes the conditions of formation for the glaucophane schists as compared to those conditions producing greenschists. The intermediate assemblage, lawsonite+albite+chlorite, may be indicative of pressure-temperature conditions intermediate between the glaucophane schist facies and greenschist facies. More detailed fieldwork to determine the distribution of
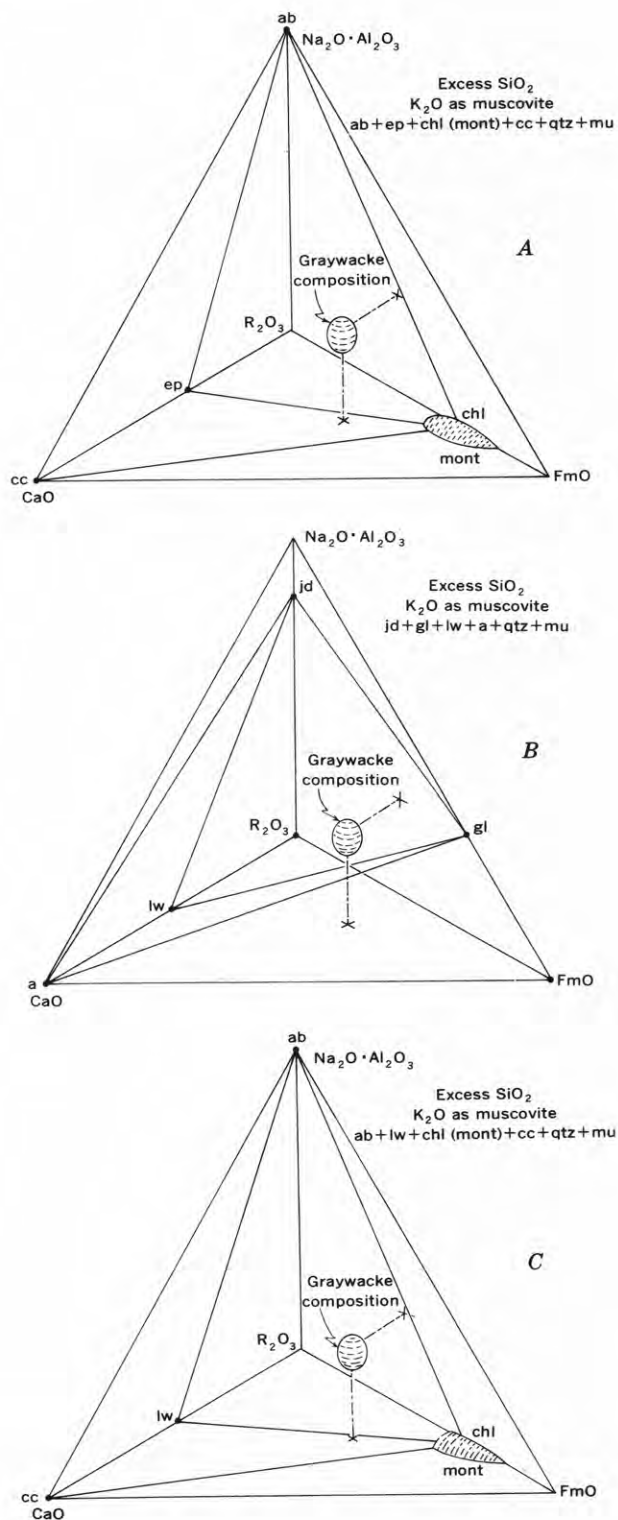

FIGURE 5.—Ernst diagrams (Ernst, 1963) illustrating the possible mineral assemblages that could develop from graywackes during A, greenschist facies; B, blue schist facies; and C, conditions intermediate between greenschist and blue schist facies. All three conditions (A, B, C) require $P_T = P_{H_2O}$, fairly high P_{CO_2}, and excess silica. The graywacke composition represents the average composition as given in table 4. The tetrahedron relates the four components $Na_2O \cdot Al_2O_3 = CaO = FmO = R_2O_3$, and in plotting minerals or rocks, the molecular proportions of $Na_2O \cdot Al_2O_3$, CaO, FmO ($= FeO + MgO$), R_2O_3 ($= Al_2O_3 + Fe_2O_3$) were recast to 100 percent. The abbreviations used are as follows: ab, albite; cc, calcite; ep, epidote; chl, chlorite; mont, montmorillonite; lw, lawsonite; qtz, quartz; mu, muscovite; jd, jadeite; a, aragonite; gl, glaucophane. The chlorite and montmorillonite are shown overlapping in composition; however, no analytical evidence is available to prove or disprove this assumption.

these assemblages in relation to regional structures is necessary before the relations among these metamorphic types can be fully understood.

ACKNOWLEDGMENTS

The author is indebted to several colleagues of the U.S. Geological Survey. Daniel E. Appleman determined the unit-cell data and provided other helpful X-ray information, and Rollin E. Stevens directed the chemical analyses. Julius Schlocker aided in the collection of the materials from Angel Island and helped with the geologic interpretations, and Joan R. Clark and D. R. Wones improved the manuscript by their careful and thoughtful reviews.

REFERENCES

Birch, A. F., 1955, Physics of the crust, *in* Poldervaart, Arie, ed., Crust of the earth—a symposium: Geol. Soc. America Spec. Paper 62, p. 101–117.

Birch, Francis, and LeComte, Paul, 1960, Temperature-pressure plane for albite composition: Am. Jour. Sci., v. 258, p. 209–217.

Blake, M. C., Jr., and Ghent, E. D., 1965. Regional glaucophane-schist-facies metamorphism in the northern Coast Ranges of California [abs.]: Geol. Soc. America Spec. Paper 82, p. 241.

Bloxam, T. W., 1956, Jadeite-bearing metagraywackes in California: Am. Mineralogist, v. 41, nos. 5–6, p. 488–496.

———— 1959, Glaucophane-schists and associated rocks near Valley Ford, California: Am. Jour. Sci., v. 257, no. 2, p. 95–112.

———— 1960, Jadeite rocks and glaucophane schists from Angel Island, San Francisco Bay, California: Am. Jour. Sci., v. 258 no. 8, p. 555–573.

Brown, W. H., Fyfe, W. S., and Turner, F. J., 1962, Aragonite in California glaucophane schists and kinetics of the aragonite-calcite transformation: Jour. Petrology, London, v. 3, no. 3, p. 566–582.

Clark, S. P., Jr., 1957, A note on calcite-aragonite equilibrium: Am. Mineralogist, v. 42, nos. 7–8, p. 564–566.

Coleman, R. G., 1961, Jadeite deposits of the Clear Creek area, New Idria District, San Benito County, California: Jour. Petrology, London, v. 2, no. 2, p. 209–247.

Coleman, R. G., and Lee, D. E., 1962, Metamorphic aragonite in the glaucophane schists of Cazadero, California: Am. Jour. Sci., v. 260, no. 8, p. 577–595.

Coleman, R. G., and Lee, D. E., 1963, Glaucophane-bearing metamorphic rock types of the Cazadero area, California: Jour. Petrology, London, v. 4, no. 2, p. 260–301.

Coombs, D. S., 1960, Lawsonite metagraywackes in New Zealand; Am. Mineralogist, v. 45, nos. 3–4, p. 454–455.

———— 1961, Some recent work on the lower grades of metamorphism: Australian Jour. Sci., v. 24, no. 5, p. 203–215.

Davis, E. G., 1918, The Franciscan sandstone: California Univ. Dept. Geol. Bull., v. 11, no. 1, p. 1–44.

Ernst, W. G., 1963, Significance of phengitic micas from low-grade schists: Am. Mineralogist, v. 48, nos. 11–12, p. 1357–1373.

Jamieson, J. C., 1953, Phase equilibrium in the system calcite-aragonite: Jour. Chem. Physics, v. 21, p. 1385–1390.

Korzhinskii, D. S., 1959, Physico-chemical basis of the analysis of the paragenesis of minerals: New York, Consultants Bur., Inc., v. 142. (Trans. from Russian).

McKee, Bates, 1958, Jadeite alteration of sedimentary and igneous rocks, California [abs.]: Geol. Soc. America Bull., v. 69, no. 12, pt. 2, p. 1612.

McKee, Bates, 1960, Tectonic significance of the phase change—plagioclase → jadeite + quartz [abs.]: Geol. Soc. America Bull., v. 71, no. 12, pt. 2, p. 1926–1927.

———— 1962a, Widespread occurrence of jadeite, lawsonite, and glaucophane in central California: Am. Jour. Sci., v. 260, p. 596–610.

———— 1962b, Aragonite in the Franciscan rocks of the Pacheco Pass area, California: Am. Mineralogist, v. 47, nos. 3–4, p. 379–387.

Melville, W. H., 1891, The chemistry of the Mount Diablo rocks: Geol. Soc. America Bull., v. 2, p. 402–414.

Morkovkina, V. F., 1960, Jadeite rocks in the ultrabasic rocks of the Polar Urals: Akad. Nauk SSSR Ser. Geol. Izv., v. 4, p. 78–82.

Moskaleva, V. N., 1962, K mineralogii pribalkhashskikh zhadeititov (Mineralogy of jadeitites from the Lake Balkhash region), Vses. Mineralog. Obshchestvo Zapiski, Chast. 91. v. 1, p. 38–49.

Newton, R. C., and Kennedy, G. C., 1963, Some equilibrium reactions in the join $CaAl_2Si_2O_8$-H_2O: Jour. Geophys. Research, v. 68, no. 10, p. 2967–2983.

Pettijohn, F. J., 1963, Chemical composition of sandstones—excluding carbonate and volcanic sands: U.S. Geol. Survey Prof. Paper 440–S, 21 p.

Reed, J. J., 1957, Petrology of the lower Mesozoic rocks of the Wellington district: New Zealand, Geol. Survey Bull., n. s., v. 57, 60 p.

Robertson, E. C., Birch, A. F., and McDonald, G. J. F., 1957, Experimental determination of jadeite stability relations to 25,000 bars: Am. Jour. Sci., v. 255, no. 2, p. 115–137.

Roever, W. P. de, 1955, Genesis of jadeite by low-grade metamorphism: Am. Jour. Sci., v. 253, no. 5, p. 283–298.

Rose, R. L., 1958, Pre-Tertiary stratigraphy near Petaluma, California [abs.]: Geol. Soc. America Bull., v. 69, no. 12, pt. 2, p. 1703–1704.

Schlocker, Julius, Bonilla, M. G., and Radbruch, D. H., 1958, Geology of the San Francisco North quadrangle, California: U.S. Geol. Survey Misc. Geol. Inv. Map I–272, scale 1: 24,000.

Schurmann, H. M. E., 1953, Beitrage Zur Glaukophanfrage (2) (Queensland, Kuba, Kalifornien, Val de Bagneo/Schweiz): Neues Jahrb. Mineralogie Abh., v. 85, no. 3, p. 303–392.

Seki, Yotaro, Aiba, Mizuo, and Kato, Chigusa, 1960, Jadeite and associated minerals of metagabbroic rocks in the Sibukawa district, Central Japan: Am. Mineralogist, v. 45, nos. 5–6, p. 668–679.

Seki, Yotaro, and Shido, Fumiko, 1959, Finding of jadeite from the Sanbagawa and Kamuikotan metamorpic belts, Japan: Proc. Japan Acad., v. 35, no. 3, p. 137–138.

Simmons, Gene, and Bell, Peter, 1963, Calcite-aragonite equilibrium: Science, v. 139, p. 1197–1198.

Stevens, R. E., Chodos, A. A., Havens, R. G., Godijn, Elisabeth,

and Neil, S. T., 1960, Combination of gravimetric and spectrographic methods in the analysis of silicates: Art. 228 *in* U.S. Geol. Survey Prof. Paper 400–B, p. B499–B501.

Taliaferro, N. L., 1943, Franciscan-Knoxville problem: Am. Assoc. Petroleum Geologists Bull., v. 27, no. 2, p. 109–219.

Turner, F. J., and Verhoogen, Jean, 1960, Igneous and metamorphic petrology: New York, McGraw-Hill, 2nd ed., 695 p.

Wyckoff, R. W. G., and Merwin, H. E., 1925, The space group of diopside [$CaMg(SiO_3)_2$]: Am. Jour. Sci., 5th ser., v. 9, p. 379–394.

X-RAY DETERMINATIVE CURVE FOR HAWAIIAN OLIVINES OF COMPOSITION Fo$_{76-88}$

By K. J. MURATA, HARRY BASTRON, and W. W. BRANNOCK,

Menlo Park, Calif.

Abstract.—When applied to Hawaiian olivines, Jackson's (1960) X-ray method for determining olivine composition yields a determinative curve that deviates appreciably from the previously established curve for plutonic olivines. The deviation, which is in the direction of a larger unit cell for a given Fo content, is due mainly to the substituent, calcium. Hawaiian olivines contain 0.2 to 0.5 percent CaO, which is an order of magnitude higher than the amounts in the plutonic olivines studied by Hotz and Jackson (1963).

An X-ray diffraction method developed by Jackson (1960) for determining the forsterite content of olivines from the stratiform Stillwater ultramafic complex was found subsequently by Hotz and Jackson (1963) to be applicable to olivines from alpine-type peridotites of Oregon and California. The determinative curve (based on CuKα_1 radiation) for these plutonic olivines is described by the equation

$$2\theta_{062} \text{ (olivine)} - 2\theta_{220} \text{ (LiF)} = 4.4722 - 0.18015 \text{ Fo},$$

in the range of Fo$_{80-95}$.

The method has now been extended to phenocrystic olivines from Hawaiian lavas and to olivines of peridotitic xenoliths from these lavas. The determinative curve for Hawaiian olivines (Fo$_{76-88}$) deviates significantly from the curve established by Hotz and Jackson (1963).

METHOD OF INVESTIGATION

Hawaiian olivines were separated out of crushed lava samples and purified by means of heavy liquids and the isodynamic magnetic separator. The purified samples were analyzed by a combination of chemical, spectrographic, and X-ray fluorescence techniques, and the Fo content was calculated as atomic percent of Mg relative to total octahedral cations. The difference between $2\theta_{062}$ of olivine and $2\theta_{220}$ of LiF was determined on splits of the analyzed samples, according to Jack-

son's method (1960), and the results are given in the accompanying table.

Composition and X-ray measurements of Hawaiian olivines

[Analyses by Harry Bastron, W. W. Brannock, Leoniece Beatty, Lois Jones, and A. C. Bettiga]

Sample No.	Field No.[1]	Fo[2]	FeO (weight percent)	CaO[3] (weight percent)	CaO[4] (weight percent)	MnO (weight percent)	$\Delta 2\theta$[5] (degrees)	Standard deviation[6] (degrees)
1	Ha-1	76.1	20.6	0.25	0.32	0.30	3.126	0.0044
2	MK-19	80.8	16.1	.50	.49	.26	3.050	.0033
3	K-6	82.7	14.8	.43	.45	.22	3.002	.0023
4	K-8	83.4	13.8	.38	.34	.22	2.998	.0043
5	Xen-1MK	84.2	13.8	.21	.22	.24	2.977	.0035
6	Xen-1H	86.2	12.1	.18	.16	.20	2.946	.0042
7	ML-2	86.9	11.3	.28	.28	.18	2.929	.0031
8	Xen-2H	87.7	10.5	.19	.20	.20	2.906	.0032

[1] Ha, MK, K, H, and ML denote samples from Haleakala, Mauna Kea, Kilauea, Hualalai, and Mauna Loa volcanoes, respectively. Xen refers to olivines from peridotitic xenoliths; all others are phenocrystic olivines.
[2] Atomic percent of Mg with respect to total octahedral cations.
[3] Determined by X-ray fluorescence method.
[4] Determined by flame photometry. The results obtained through this method and through the X-ray fluorescence method were averaged for each sample in computing Fo and in plotting figure 2.
[5] Mean of 12 determinations $2\theta_{062}$(olivine)$-2\theta_{220}$(LiF) with Cu radiation.
[6] Standard deviation of the 12 determinations of $\Delta 2\theta$.

DISCUSSION OF RESULTS

A regression analysis of the data on Fo and $\Delta 2\theta$ in the table yields the following equation for a straight-line curve:

$$2\theta_{062} \text{ (olivine)} - 2\theta_{220} \text{ (LiF)} = 4.5644 - 0.018834 \text{ Fo}.$$

The 95-percent confidence interval for the regression equation at Fo$_{84}$ is $\pm 0.011°$ 2θ, corresponding to ± 0.61 Fo. The curve for the equation is given on figure 1. The uncertainty of determination for Hawaiian olivines is about 1.3 times greater than that for the plutonic olivines of Hotz and Jackson (1963). The poorer precision can be ascribed to two factors: (1) the diffraction "lines" of Hawaiian olivines are not as sharp and clean as those of plutonic olivines, probably because of a wider range of composition represented in Hawaiian olivine crystals, and (2) Hawaiian olivines

contain appreciable and variable amounts of calcium, which affect the unit-cell dimensions independent of the Fo:Fa ratio. The content of calcium in plutonic olivines studied by Hotz and Jackson amounts to only a few hundredths of a percent (E. D. Jackson, oral communication).

A comparison is made in figure 1 between the determinative curves for Hawaiian (curve A) and for plutonic (curve B) olivines. In order to be sure that the difference between the two curves is real and not due to some systematic error in our technique, we repeated X-ray measurements on three plutonic olivines of Jackson (1960) and obtained results (shown as crosses in fig. 1) in acceptable agreement with his. In the range Fo_{76-88}, the $\Delta 2\theta$ values for Hawaiian olivines are 0.014° to 0.030° greater than those indicated by the curve for plutonic olivines. That olivines from three Hawaiian peridotitic xenoliths should lie on the same $\Delta 2\theta$ curve as phenocrysts from Hawaiian lavas, and not on the lower curve for plutonic olivines, is of much interest in connection with the problem of the origin of these xenoliths.
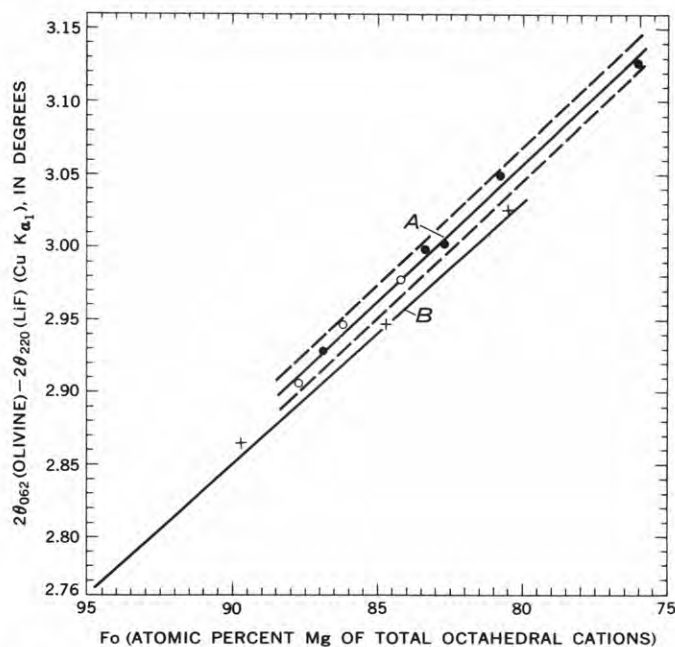
in both figures 1 and 2, mainly to their content of a few to several tenths of a percent of CaO. The radii (Ahrens, 1952) of some of the divalent substituents within the olivine structure are as follows: Mg, 0.66; Ni, 0.69; Fe, 0.74; Mn, 0.80; and Ca, 0.99Å. Because of its large radius relative to all other common substituents, calcium would be expected to affect the unit-cell dimensions of olivine even at low concentrations. Smith and Stenstrom (1965), in fact, have demonstrated how calcium and, to a lesser extent, manganese enlarge the unit cell beyond the dimensions set by the simple Fo : Fa ratio. A restudy of the system diopside-forsterite-silica by Kushiro and Schairer (1963) has further shown that the olivine phase in this classic system is not pure forsterite but contains variable amounts of calcium in solid solution, up to a maximum of about 2.9 weight percent CaO.

In figure 2, the dashed line has been drawn to suggest that the CaO content of Hawaiian olivines may be, in part, a function of the FeO content. But the scatter of points and especially the low CaO content of sample 1 show that factors other than the FeO content are also involved. In contrast to the complicated relation be-

FIGURE 1.—X-ray determinative curve for Hawaiian olivines (A) compared with the curve for plutonic olivines (B) of Hotz and Jackson (1963). Dots, phenocrystic olivines; circles, olivines of peridotitic xenoliths; crosses, remeasurement of three plutonic olivines of Jackson (1960). Dashed lines indicate 95-percent confidence limits for curve A.
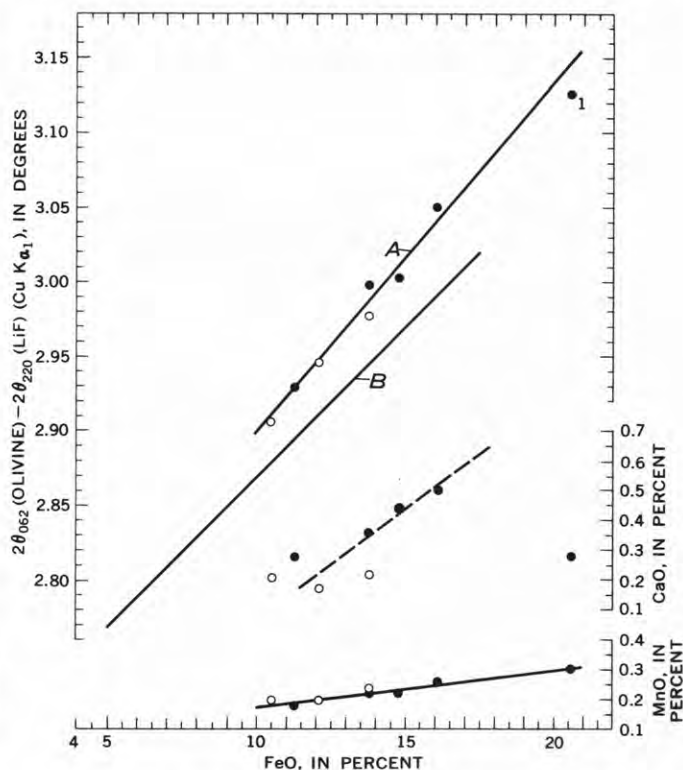
FIGURE 2.—Variation of $\Delta 2\theta$ with weight percent of FeO in Hawaiian olivines (curve A) and in plutonic olivines (curve B), and variation of CaO and MnO with FeO in Hawaiian olivines (all constituents in weight percent). Dots, phenocrystic olivines; circles, olivines of peridotitic xenoliths. Curve B is based on data furnished by P. E. Hotz and E. D. Jackson (written communication).

The $\Delta 2\theta$'s of olivines are plotted in figure 2 against the weight percentage of FeO, and again the separation of the curves for Hawaiian (curve A) and plutonic (curve B) olivines is well shown. We ascribe the higher values of $\Delta 2\theta$ manifested by Hawaiian olivines,

tween CaO and FeO, the increase of MnO with an increase of FeO is very regular.

The present study defines an X-ray determinative curve for Hawaiian olivines of composition Fo_{76-88}, and highlights their content of calcium at a concentration level of several tenths of a percent. Whether volcanic olivines of other provinces also have as much calcium is unknown to us. The possible petrogenetic significance of the calcium content of natural olivines kindles a new interest in this prosaic mineral. In this connection, it must be remembered that conventional chemical methods are inaccurate when used for determining small amounts of calcium in magnesium-rich substances and that the calcium percentages reported in many previous analyses of olivine are questionable. Recourse must be taken to carefully calibrated instrumental methods (spectrographic, X-ray fluorescence, or electron probe) for this particular determination.

REFERENCES

Ahrens, L. H., 1952, The use of ionization potentials. pt. I. Ionic radii of the elements: Geochim. et Cosmochim. Acta, v. 2, p. 155–169.

Hotz, P. E., and Jackson, E. D., 1963, X-ray determinative curve for olivines of composition Fo_{80-95} from stratiform and alpine-type peridotites: Art. 206 in U.S. Geol. Survey Prof. Paper 450–E, p. E101–E102.

Jackson, E. D., 1960, X-ray determinative curve for natural olivine of composition Fo_{80-90}: Art. 197 in U.S. Geol. Survey Prof. Paper 400–B, p. B432–B434.

Kushiro, Ikuo, and Schairer, J. F., 1963, New data on the system diopside-forsterite-silica: Carnegie Inst. Washington Year Book 62, 1962–63, p. 95–103.

Smith, J. V., and Stenstrom, R. C., 1965, Chemical analysis of olivines by the electron microprobe: Min. Mag., v. 34, no. 268 (Tilley volume) p. 436–439.

UPPER TRIASSIC UNDEVITRIFIED VOLCANIC GLASS FROM HOUND ISLAND, KEKU STRAIT, SOUTHEASTERN ALASKA

By DAVID A. BREW and L. J. PATRICK MUFFLER,
Menlo Park, Calif.

Abstract.—Angular clasts of undevitrified basaltic glass occur in bedded calcareous vitric aquagene tuff that is part of a fossiliferous Upper Triassic (Norian) sequence of pillow breccia, pillow lava, massive lava, tuff, and limestone. The glass fragments are of very fine sand to granule size and are tightly cemented by sparry calcite. These fragments have isotropic light-brownish-green cores with a refractive index of 1.588 and narrow isotropic, but perhaps incipiently devitrified light-brown rims with an index of about 1.54. X-ray powder photographs of these fragments show no crystalline material. Other similar fragments in the tuff are patchily devitrified to light-green crystalline material, and still other fragments are thoroughly devitrified and slightly rounded. A K-Ar age of 126 m.y. was obtained on carefully selected fragments of the fresh glass. The discrepancy between this date and the 180–200-m.y. age predicted from the paleontologic evidence is probably due to loss of radiogenic argon.

Glass of demonstrated pre-Tertiary age is uncommon in the geologic record. Simons (1962, p. 882–883) cited a number of descriptions, primarily from Great Britain, but concluded that "Many of these glasses are reported in the older literature, and clear evidence that the glass has not devitrified is commonly not given, but the existence of glass at least as old as Carboniferous seems well established * * *." Pre-Tertiary glasses have been described from only four localities in North America. Ross and others (1929, p. 182) found glassy fragments of pumice enclosed in masses of concretionary calcium carbonate, in upper Cretaceous tuffs in southwestern Arkansas. Barksdale (1951) reported vitrophyric rhyolitic(?) welded tuff of late Late Cretaceous age from western Montana, and Robinson (1963, p. 89–93) reported porphyritic rhyodacite perlite of Late Cretaceous age, also from western Montana. Philpotts and Miller (1963) described glassy pseudotachylites of Precambrian age from southern Quebec.

The locally glassy aspect of the Triassic volcanic rocks in the Keku Strait area of southeastern Alaska was first noted by Buddington (*in* Buddington and Chapin, 1929, p. 139, 141). During geologic mapping of the Keku Strait area in 1963 we collected undevitrified basaltic glass from volcanic rocks of Late Triassic (Norian) age on the northeast side of Hound Island (fig. 1) and noted similar occurrences on the south side of that island and at several localities on Kuiu Island north of Kadak Bay. The geologic setting of the Hound Island volcanic rocks was discussed by Buddington and Chapin (1929, p. 138–144) and by L. J. P. Muffler (report in preparation), and the correlation of these strata with rocks in nearby areas is treated by R. A. Loney and Muffler in a report in preparation.

We wish to thank N. J. Silberling, D. B. Tatlock, and K. J. Murata for helpful reviews of the manuscript.

OCCURRENCE

The glass occurs as fragments in bedded tuff and tuffaceous sandstone that is interbedded with broken-pillow breccia in a section consisting of andesitic-basaltic pillow breccia, aquagene tuff,[1] pillow lava, massive lava, and minor limestone, sandstone, and conglomerate (fig. 2). The pillow breccias and the related aquagene tuffs are similar in sedimentary structure and texture to the Triassic rocks described by Carlisle (1963) from Quadra Island, British Columbia.

---

[1] The term aquagene tuff was defined by Carlisle (1963, p. 61–62), as "* * * a tuff * * * which has been produced by globulation or granulation through quenching, or both, or by a similar process entirely beneath water * * *. 'Aquagene' is preferable to 'subaqueous' since that term has been applied to water-lain subaerial tuffs. Aquagene tuffs are not necessarily palagonite tuffs."
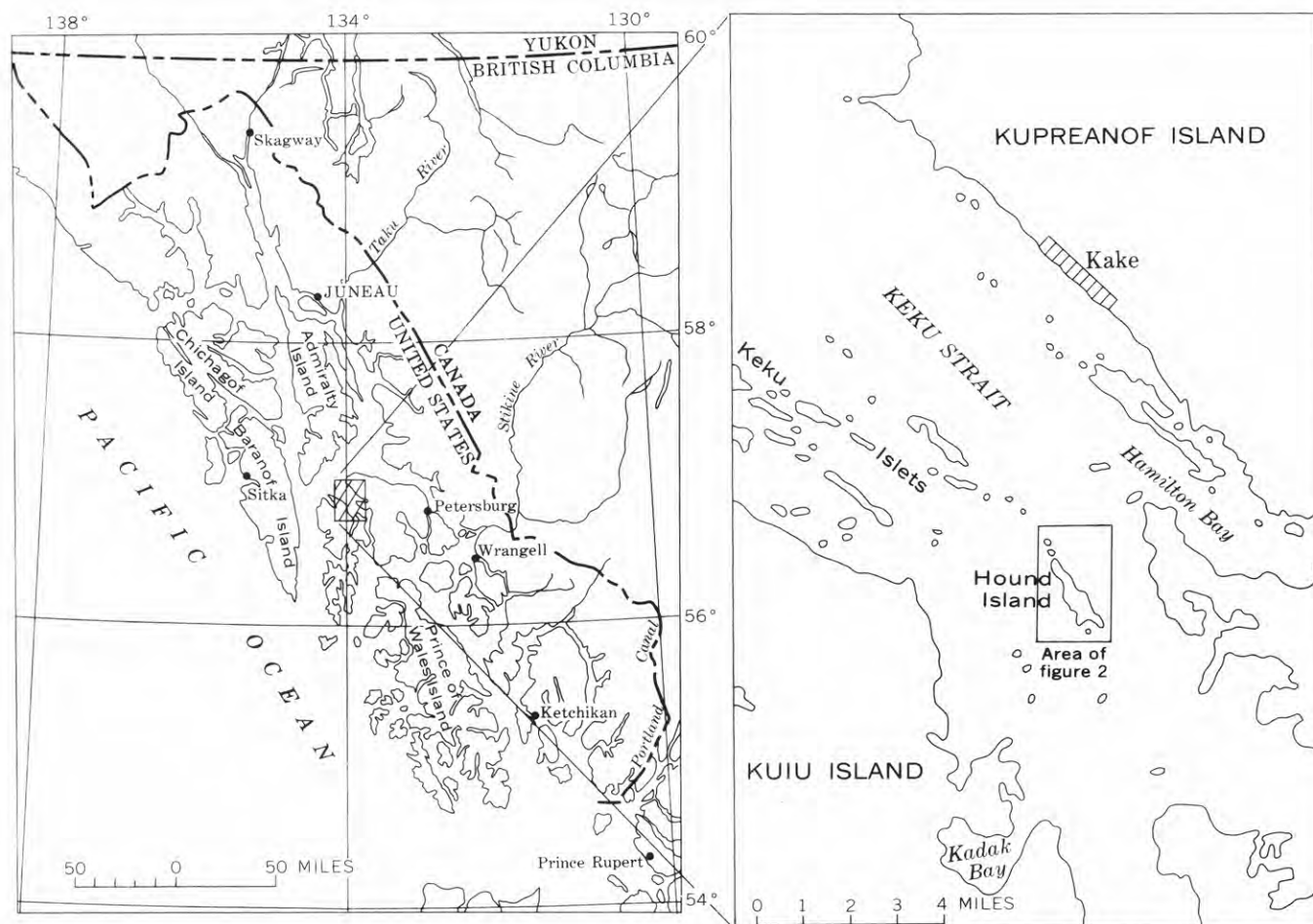
FIGURE 1.—Index map showing the Keku Strait area, southeastern Alaska.

The Hound Island strata are about 1½ miles southwest of the axis of the northwest-trending Keku structural low (Brew, Loney, and Muffler, unpublished manuscript); this structure has also been called the Keku synclinorium. Graywacke and shale of Late Jurassic(?) and Early Cretaceous age and continental sandstone of Tertiary age occur along the axis of the structure. The rocks on Hound Island generally strike north and dip moderately to the east, but significant divergences of attitudes are caused by a series of indistinct gently east-northeast-plunging folds (fig. 2), on the flanks of which are minor low-amplitude, gently plunging warps of various trends. At the northern end of the island a series of dolerite sills have dilated the strata and caused arching that is unrelated to the larger folds mentioned above. Because of the heavy forest cover, the geologic-map features shown in the interior of the island are largely conjectural.

Graphic analysis of the detailed map (fig. 2) indicates that a maximum of about 2,100 feet of strata is exposed on Hound Island. Comparison of the sections

exposed on the northeastern and southwestern sides of Hound Island shows that lateral changes in lithology are common and that the pillow lavas and massive flows are particularly discontinuous. Pillow breccias constitute about 60 percent of the section exposed on Hound Island, aquagene tuff about 15 percent, massive lava about 10 percent, pillow lava 5 percent, limestone and shaly limestone 5 percent, and sandstone and conglomerate 5 percent. Broken-pillow breccia predominates over isolated-pillow breccia by about 4:1. The less prevalent lithic types do not occur in vertically restricted parts of the stratigraphic column and do not show any systematic arrangement in the section. Neither the top or the base of the sequence is exposed; no unconformities are apparent.

Fossils were collected from thin-bedded limestones at five localities on Hound Island (fig. 2). According to N. J. Silberling, of the U.S. Geological Survey (written communication, 1963), one collection (USGS Mesozoic loc. M1899, fig. 2) contains *Halobia* cf. *H. plicosa* Mojsisovics, and the other four collections
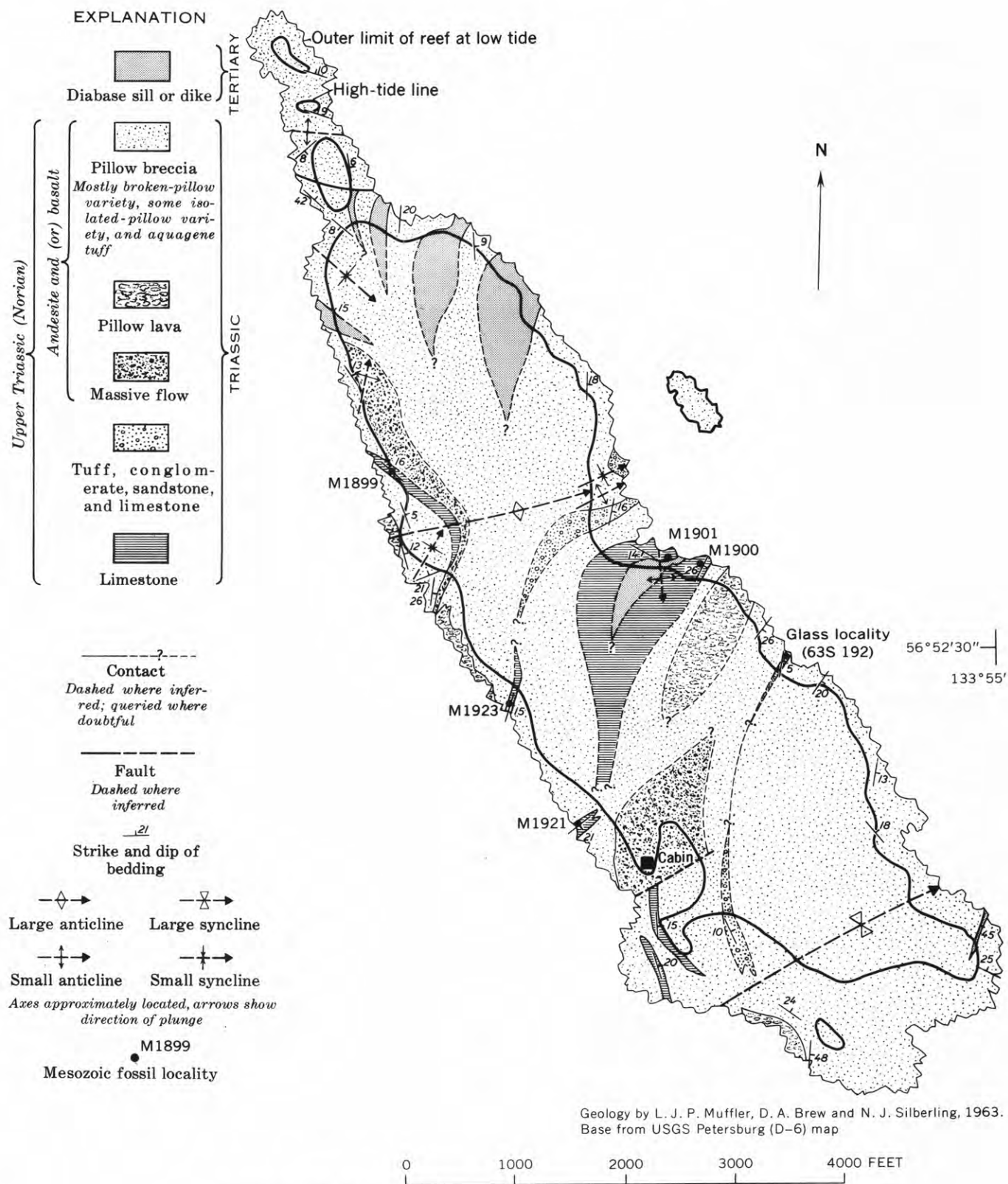
FIGURE 2.—Geologic map of Hound Island, Keku Strait, southeastern Alaska.

(USGS Mesozoic locs. M1900, B1901, M1921, M1923) contain *Halobia* cf. *H. fallax* Mojsisovics. *Monotis scutiformis* cf. *M. s. pinensis* Westermann was also found at locality M1900. These fossils are indicative of an early or middle Norian age. As shown in figure 3 the stratigraphically highest of these localities (M1900 and M1901) are about 370 feet below the horizon from which the glass was collected.

Fossils were not found on Hound Island in strata overlying the glass locality. However, fossils of late Norian age (N. J. Silberling, written communication, 1963) were collected from the same sequence of volcanic rocks at 2 localities within 5 miles of Hound Island, and all of the rocks on Hound Island are unquestionably part of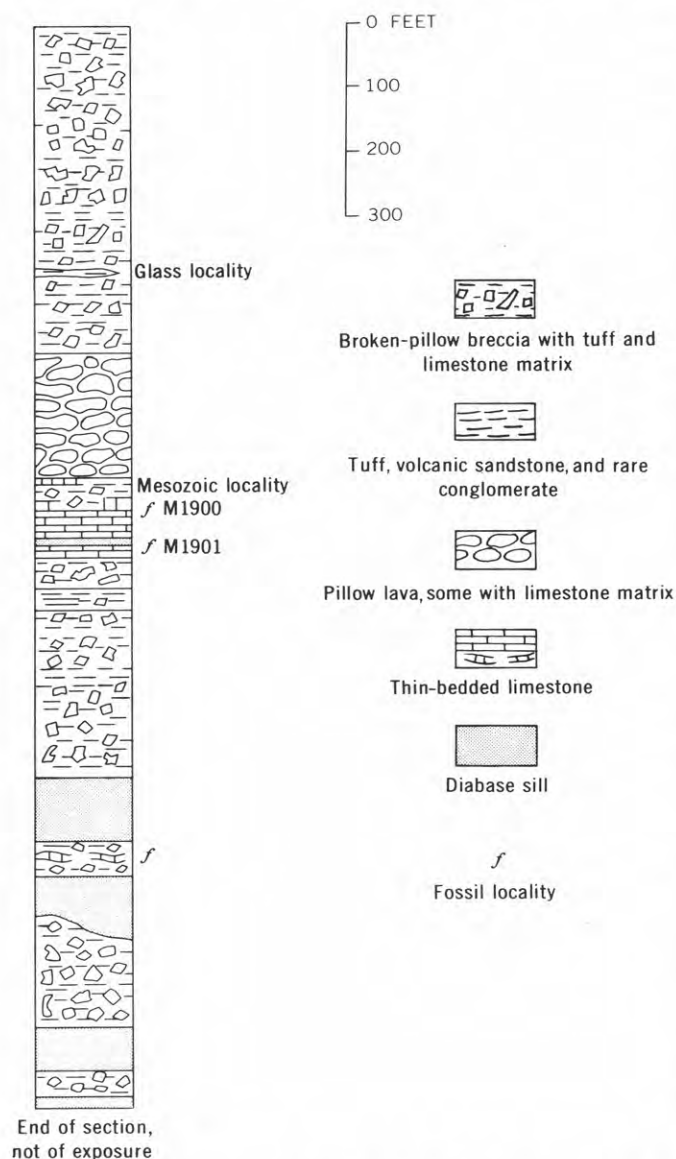 the lithologically distinctive Upper Triassic volcanic unit that is widespread in the Keku Strait area. Post-Triassic rocks in the area are lithologically very different.

PETROGRAPHY AND PETROLOGY

The basaltic glass occurs as angular black clasts of very fine sand to granule size in a unit of brownish-gray-weathering calcareous crossbedded tuff and tuffaceous sandstone that is 10 to 12 feet thick. This unit extends laterally for at least 200 feet across the tidal zone and grades vertically into broken pillow breccia.

The rock is a poorly sorted aggregate of angular fragments of glass that range in size from about 0.10 to 4.00 mm in maximum visible dimension, and average about 0.40 mm (figs. 4 and 5). Some shard-like and spindle-shaped clasts are present. Some specific components are better rounded and somewhat larger,
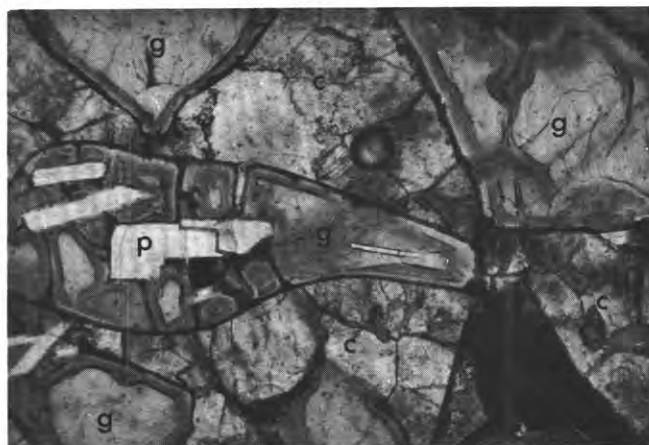
FIGURE 4.—Photomicrograph of calcareous vitric tuff, showing equant and spindle-shaped glass fragments (g), plagioclase laths (p), and calcite matrix (c). × 24. Plane light.
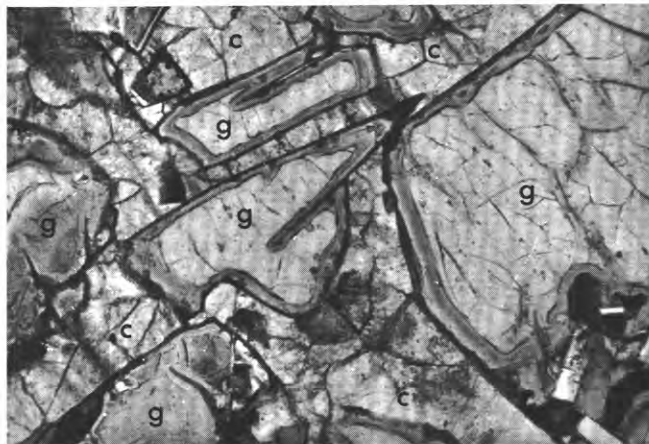
FIGURE 5.—Photomicrograph of calcareous vitric tuff, showing angular glass fragments (g) in calcite matrix (c). × 24. Plane light.

O FEET
— 100
— 200
— 300

Glass locality

Mesozoic locality
ƒ M1900
ƒ M1901

ƒ

End of section,
not of exposure

Broken-pillow breccia with tuff and limestone matrix

Tuff, volcanic sandstone, and rare conglomerate

Pillow lava, some with limestone matrix

Thin-bedded limestone

Diabase sill

ƒ
Fossil locality

FIGURE 3.—Diagrammatic stratigraphic column, northeast side of Hound Island, Keku Strait.

as noted below. The rock is tightly cemented with sparry calcite.

The rock consists of 4 kinds of glass fragments together with other volcanic-rock fragments in a matrix of sparry calcite (average grain size about 0.13 mm) with a dusty appearance. A count of 500 points on a 700-mm^2 thin section by the Chayes method gave the following mode:

	Percent
Fresh light-brownish-green glass (type 1)	31. 0
Fresh light-brownish-green glass with local areas of light-green devitrified glass (type 2)	24. 4
Light-green devitrified glass (type 3)	6. 4
Fresh medium-brown glass (type 4)	1. 4
Various dark volcanic fragments, some glassy, most feldspar rich	7. 4
Calcite matrix	28. 8
Chlorite enclosed in calcite matrix	. 6
Total	100. 0

An X-ray diffractogram of the whole rock shows only peaks indicating the presence of calcite, plagioclase, and chlorite.

Type 1 fragments consist of light-brownish-green perfectly isotropic glass. Refractive index of the glass in sodium light is 1.588 ± 0.002. This index falls in the general range of basaltic glass, and indicates an SiO_2 content of about 50 percent, according to various published curves summarized in Kittleman (1963). The glass has not yet been chemically analyzed. Individual fragments, and the fractures and plagioclase laths within them, are rimmed by a zone, 0.02 to 0.04 mm wide, of light-brown perfectly isotropic material with a refractive index of about 1.54 (figs. 4, 5, and 6). In rock slabs that were etched with hydrofluoric acid and stained for potassium, these narrow rims reacted to the stain whereas the isotropic material of higher index did not. This may be in-

terpreted to indicate incipient devitrification or alteration in the light-brown isotropic zones. An X-ray powder photograph of type 1 glass showed no trace of crystalline material except for the added silicon internal standard.

Type 2 fragments contain varying amounts of light-green anisotropic material as discontinuous patches along the rims (fig. 7), but are otherwise similar to type 1 fragments. This light-green material is devitrified or altered glass.

Both type 1 and type 2 fragments are irregularly fractured and contain a few plagioclase laths of about An_{52}, as determined from extinction-angle and refractive-index data. No crystallites, strain polarization, or perlitic cracks are present in the glass.

Type 3 fragments consist of light-green devitrified glass, similar to, but slightly darker than, the patches of light-green devitrified glass that characterize fragments of type 2. Type 3 fragments are rounded to subrounded, generally larger (average 2.0–3.0 mm) than the type 1 and type 2 fragments, and show a much greater variation in feldspar lath content. They may be slightly older than the other clastic components in the rock.
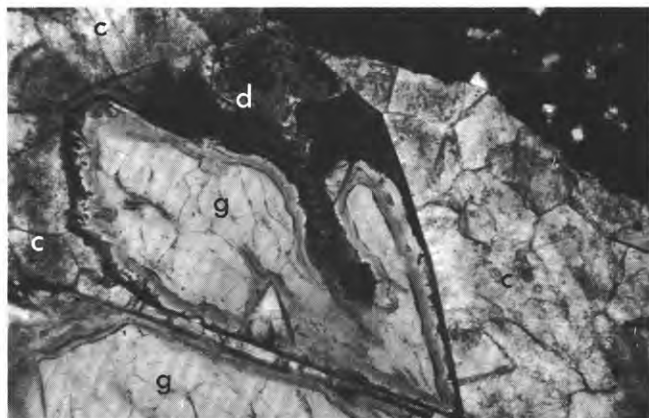
FIGURE 7.—Photomicrograph of a type 2 glass fragment, showing patchy thorough alteration or devitrification (d) of the glass (g), and the adjacent calcite matrix (c). × 24. Plane light.

Type 4 fragments consist of isotropic medium-brown undevitrified glass. These fragments are angular, contain sparse plagioclase laths, and do not have devitrified rims or patches.

The glass-bearing rock may be classified as a bedded calcareous vitric aquagene tuff. Following Carlisle (1963), we consider this tuff to be of submarine origin and the angular fragments to be the result of autocommunication upon quenching. This particular tuff differs from those described by Carlisle (1963) from the Triassic of Quadra Island, British Columbia, in
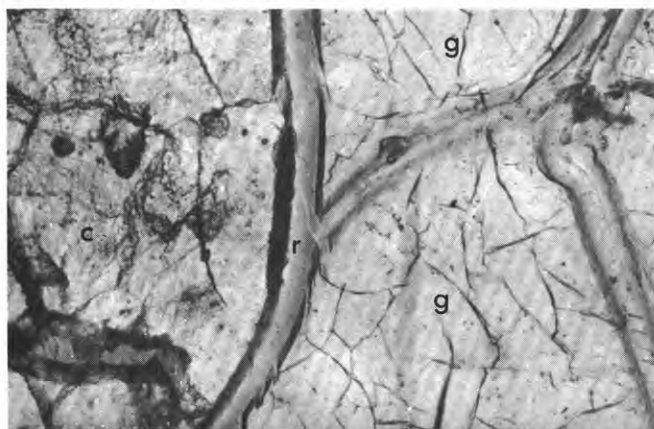

FIGURE 6.—Photomicrograph of edge of type 1 glass fragment (g), showing narrow rim (r) of material with lower refractive index and adjacent calcite matrix (c). × 60. Plane light.

that the matrix is not cogenetic with the fragments but is sparry calcite. We infer from the textures that this calcite was precipitated as cement soon after deposition of the tuff, but cannot exclude the possibility of diagenetic recrystallization of a micritic matrix to form the sparry calcite. Calcite-cemented aquagene tuff is common in the Triassic volcanics of the Keku Strait area, both as bedded tuff and as a matrix in pillow breccia, and grades with increasing amounts of comminuted volcanic detritus into aquagene tuff with a cogenetic matrix. All the glass-bearing rock described in this paper has a sparry calcite matrix, but this type of matrix does not appear to be restricted to the glass-bearing rock.

The vitroclastic texture and the bedded characteristics of this aquagene tuff are striking; texturally the rock may be described as a poorly sorted calcite-cemented sandstone composed of angular clasts with median diameter of 0.10–4.0 mm. Crossbedding and graded bedding were observed in outcrop, and some aquagene tuffs in the Keku Strait area grade laterally and vertically into a dense biomicrite. The presence of fragments of differing angularity and slightly differing lithology also indicates some movement and mixing of the fragments on the sea floor before cementation.

Complete cementation by sparry calcite soon after deposition may have been critical in the preservation of this undevitrified glass. Perhaps the tightly interlocking crystals of calcite prevented circulation of water, and devitrification therefore was inhibited (Marshall, 1961, has suggested that devitrification in the absence of water normally proceeds slowly). Incipient devitrification or alteration (the light-brown isotropic rims) may be due to nucleation around phenocrysts and at fragment boundaries in the presence of intergranular water, whereas the patchy light-green devitrification or alteration of the type 2 fragments may be due to later, restricted circulation of fluids. Devitrification or alteration of the type 3 fragments may have occurred before those clasts were mixed with the fresher type 1 and type 2 fragments.

POTASSIUM-ARGON AGE

The freshness of the type 1 glass fragments and the well-established paleontologic age of the rock prompted an effort to date the glass isotopically. The disaggregated rock was treated with dilute hydrochloric acid to remove the calcite matrix, and the type 1 glass fragments were separated from the remaining rock components by magnetic and hand methods. The results of radiometric dating by J. D. Obradovich (written communication, 1964) are:

K_2O	percent	0.818
Ar^{40}/K^{40}		7.54×10^{-3}
Radiogenic argon	percent	66
Age	m.y.	126

This minimum age falls in the Early Cretaceous, according to the time scale of Kulp (1961). It is believed to be the oldest K-Ar age obtained from a volcanic glass, but is significantly less than the 180–200 m.y. that would be predicted from the paleontologic evidence. The low K-Ar age suggests that radiogenic argon has been lost by diffusion; the slight local devitrification and (or) alteration noted in the sample may have accelerated this diffusion. It is also possible that K_2O was introduced during recent, but unrecognized, alteration.

This undevitrified glass from a vitric tuff of paleontologically determined Norian age is among the oldest volcanic glasses known, and is an exception to the generalization that all undevitrified glass-bearing rocks are no older than Tertiary.

REFERENCES

Barksdale, J. D., 1951, Cretaceous glassy welded tuffs—Lewis and Clark County, Montana: Am. Jour. Sci., v. 249, no. 6, p. 439–443.

Buddington, A. F., and Chapin, Theodore, 1929, Geology and mineral deposits of southeastern Alaska: U.S. Geol. Survey Bull. 800, 398 p.

Carlisle, Donald, 1963, Pillow breccias and their aquagene tuffs, Quadra Island, British Columbia: Jour. Geology, v. 71, no. 1, p. 48–71.

Kittleman, L. R., Jr., 1963, Glass-bead silica determination for a suite of volcanic rocks from the Owyhee Plateau, Oregon: Geol. Soc. America Bull., v. 74, no. 11, p. 1405–1409.

Kulp, J. L., 1961, Geologic time scale: Science, v. 133, no. 3459, p. 1105–1114.

Marshall, R. R., 1961, Devitrification of natural glass: Geol. Soc. America Bull., v. 72, no. 10, p. 1493–1520.

Philpotts, A. R., and Miller, J. A., 1963, A Pre-Cambrian glass from St. Alexis-des-Monts, Quebec: Geol. Mag., v. 100, no. 4, p. 337–344.

Robinson, G. D., 1963, Geology of the Three Forks quadrangle, Montana, with sections on petrography of igneous rocks by H. F. Barnes: U.S. Geol. Survey Prof. Paper 370, 143 p.

Ross, C. S., Miser, H. D., and Stephenson, L. W., 1929, Waterlaid volcanic rocks of early Upper Cretaceous age in southwestern Arkansas, southeastern Oklahoma, and northeastern Texas: U.S. Geol. Survey Prof. Paper 154–F, p. 175–202. [1930]

Simons, F. S., 1962, Devitrification dikes and giant spherulites from Klondyke, Arizona: Am. Mineralogist, v. 47, nos. 7–8, p. 871–885.

SEISMIC-REFRACTION MEASUREMENTS OF CRUSTAL STRUCTURE BETWEEN AMERICAN FALLS RESERVOIR, IDAHO, AND FLAMING GORGE RESERVOIR, UTAH

By RONALD WILLDEN, Denver, Colo.

Abstract.—Interpretation of a reversed seismic-refraction profile recorded between American Falls Reservoir, Idaho, and Flaming Gorge Reservoir, Utah, in May 1963 indicates that the depth to the Mohorovicic discontinuity is about 31 km at American Falls Reservoir and 37 km at Flaming Gorge Reservoir. The existence of an intermediate crustal layer at a depth of about 19 to 21 km beneath the line of profile is well supported by refractions and reflections. The velocity of compressional waves in the mantle just beneath the Mohorovicic discontinuity is about 7.8 km/sec; in the intermediate layer, about 6.9 km/sec; and in the upper crust (beneath the near-surface low-velocity material), about 5.9 km/sec. A prominent phase with an apparent velocity of 8.4 km/sec was recorded at distances of 210 to 325 km from shots at American Falls Reservoir. This phase is believed to be a reflection from a boundary within the mantle.

The U.S. Geological Survey recorded a refraction seismic profile between American Falls Reservoir, on the Snake River, in southeastern Idaho, and Flaming Gorge Reservoir, on the Green River, in northern Utah, during May 1963 (fig. 1). Recordings were made at 35 locations between shotpoints in the 2 reservoirs at the ends of the line. Four shots, of 2,000, 2,000, 4,000, and 6,000 pounds, respectively, were fired at the end shotpoints and 3 shots, of 2,000, 2,000, and 4,000 pounds, respectively, were fired at an intermediate shotpoint in Bear Lake, Utah. Commercial nitro-carbo-nitrate-type blasting agent was used for all shots. The American Falls Reservoir shotpoint was at lat 42°50.14′ N. and long 112°48.66′ W. on the reservoir bottom at a depth of 62 feet for the first 2 shots, and was then relocated at lat 42°51.40′ N. and long 112°47.68′ W. at a depth of 55 feet for the last 2 shots. The Bear Lake shotpoint was at lat 41°56.35′ N. and long 111°17.10′ W. on the lake bottom near the
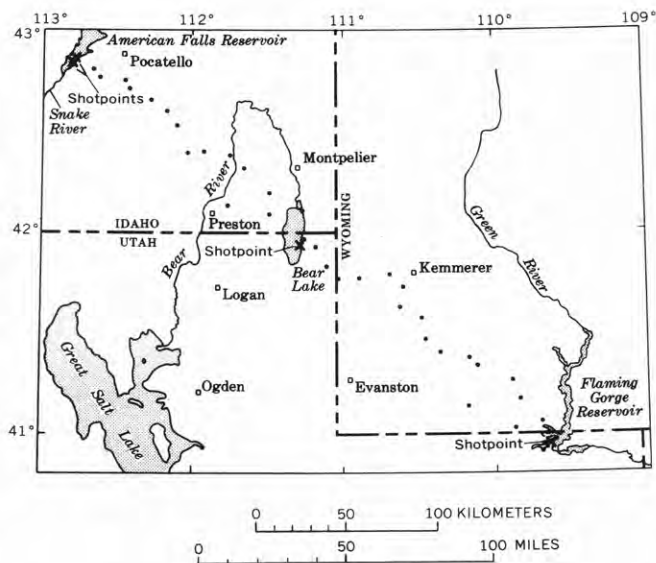
FIGURE 1.—Location of shotpoints (×'s) and recording units (dots) on the seismic-refraction profile from American Falls Reservoir, Idaho, to Flaming Gorge Reservoir, Utah.

steep eastern shore, where water depth ranged from 135 to 165 feet. The Flaming Gorge Reservoir shotpoint was at lat 40°56.77′ N. and long 109°38.43′ W. on the reservoir bottom in water 23 feet deep. The seismic-recording units used in this profile have been described by Warrick and others (1961), and the field procedures have been described by Jackson and others (1963).

GEOLOGY AND PHYSIOGRAPHY

The seismic profile extends from the east edge of the Snake River Plain eastward across the southeastern Idaho–western Wyoming overthrust belt and across the southwestern part of the Green River Basin

to the north flank of the Uinta Mountains. The recording locations between American Falls Reservoir and Bear Lake were at an average elevation of 1,726 meters and those between Bear Lake and Flaming Gorge Reservoir were at an average elevation of 2,036m.

The geology of large parts of the area traversed by this profile was described in early reports by Veatch (1907) and Mansfield (1927). Certain small areas near the profile have been mapped in considerable detail in recent years, and are useful in demonstrating the complexity of the structural features crossed by the profile (Cressman and Gulbrandsen, 1955; Cressman, 1957; Rubey, 1958). Rubey and Hubbert (1959, p. 186-193) have summarized the geology of much of the area crossed by this profile, and the reader is referred to their paper and the earlier reports for a comprehensive discussion of the geology of the area.

Rocks exposed along the profile in the mountain ranges northwest of Bear Lake are mainly middle and lower Paleozoic carbonate and clastic sedimentary rocks and Precambrian quartzite (much of the Brigham Quartzite should probably be considered Pre-

cambrian as recently shown by Oriel, 1964). In the valleys the rocks are primarily Tertiary and Quaternary clastic sedimentary rocks but include basalt flows. Southeast of Bear Lake the rocks for the most part are clastic sedimentary rocks and limestones of Mesozoic and Tertiary age but include some upper Paleozoic clastic and carbonate rocks. Precambrian clastic rocks, mainly quartzites, are exposed in the Uinta Mountains just south of the southeast end of the profile. Older Precambrian metamorphosed carbonate and clastic rocks are exposed in the Bannock Range just north of the profile.

Between American Falls Reservoir and Kemmerer, Wyo., the profile crosses 5 prominent north-trending mountain ranges and intervening valleys. These ranges represent two contrasting structural types. The ranges west of Bear Lake Valley are characterized by gently eastward-dipping strata cut by large high-angle faults (Rubey and Hubbert, 1959, p. 186). The ranges east of Bear Lake Valley are characterized by tight overturned folds, the axial planes of which generally dip westward (Cressman, 1957; Rubey, 1958), and by westward-dipping overthrust sheets with horizontal displacement of at least 10 to 15 miles (Rubey
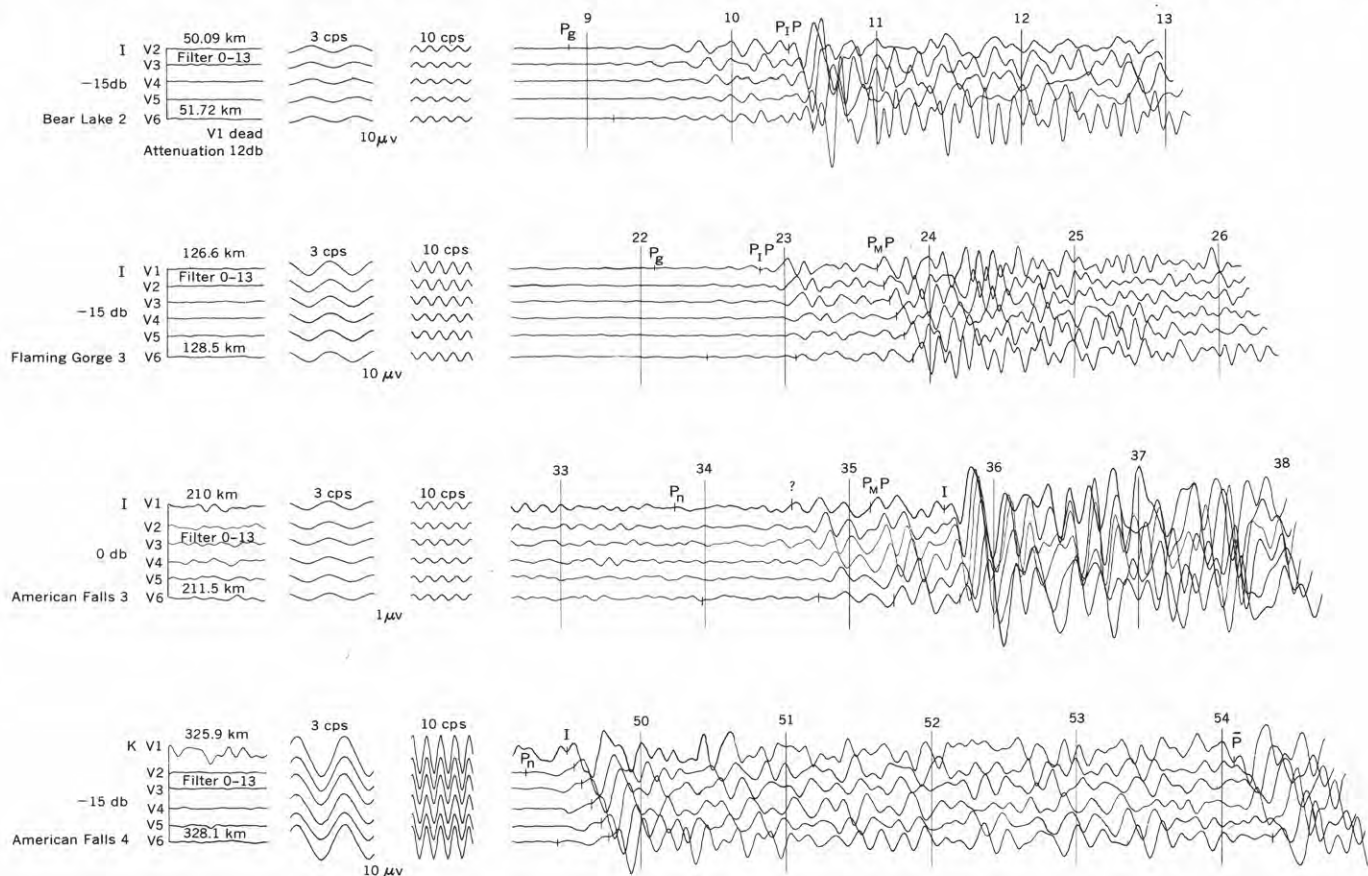

FIGURE 2.—Representative seismograms of the profile from American Falls Reservoir to Flaming Gorge Reservoir. Vertical lines represent seconds after shot time. Instrument calibrations recorded with same instrument adjustments are shown on left.

and Hubbert, 1959, p. 187; Armstrong and Oriel, 1964). Most of the present relief along this part of the profile is due to late Cenozoic displacement on normal faults that bound individual mountain blocks. The pattern of alternating mountains and valleys in southeastern Idaho and adjacent parts of Wyoming and Utah predates the deposition of the Salt Lake Formation (Pliocene) and postdates the deposition of the Wasatch Formation (early Eocene) (Armstrong and Cressman, 1963, p. J20).

From just southeast of Kemmerer, Wyo., to Flaming Gorge Reservoir, the profile crosses the southwest part of the Green River Basin, which represents a third contrasting structural type. The basin is filled with mainly horizontal and very gently dipping practically undeformed strata, which in at least part of the basin attain a thickness of more than 20,000 feet (Jenkins, 1955).

CHARACTERISTICS OF SEISMOGRAMS

All three shotpoints provided relatively efficient conversion of explosive energy to seismic energy, and, except for some locations between American Falls Reservoir and Bear Lake, the quality of the seismograms recorded along the profile is good (fig. 2, p. C45).

American Falls Reservoir shotpoint

The first arrivals (fig. 3) on 8 of 9 seismograms out to a distance of about 88 kilometers represent the direct wave and are designated P_g. The first upward (compressive) motion can be identified on most of these seismograms.
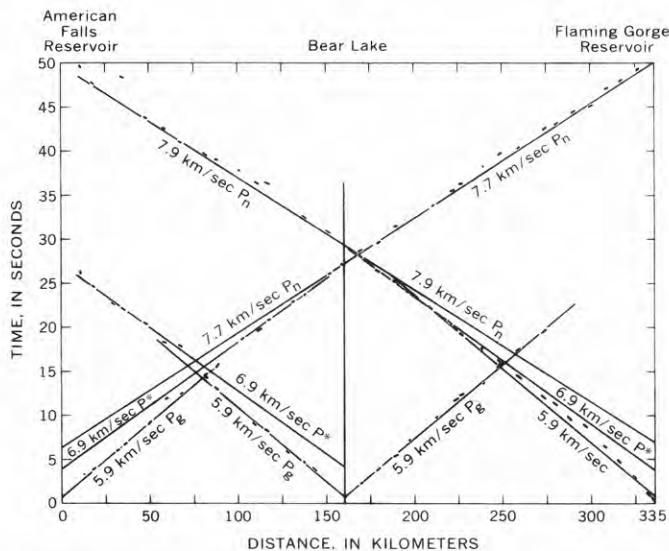
The first arrivals on 5 seismograms in the distance range 102 km to 137 km are identified as a refracted wave from an intermediate layer with a velocity of 6.9 km/sec and are designated P*. A strong secondary arrival recorded on the seismograms in the distance range 35 km to 151 km has been identified as a reflected wave from the upper boundary of this intermediate layer and is designated $P_I P$ (figs. 2 and 4). This arrival is generally the strongest event on the seismograms in the distance range 35 km to 88 km.

Refractions from the Mohorovicic (M) discontinuity, designated P_n, (velocity 7.7 km/sec.) appear as first arrivals on the seismograms from 151 km to the end of the profile at 336 km. Their identification is somewhat questionable on some of the seismograms at distances greater than 280 km. Reflections from the Mohorovicic discontinuity ($P_M P$) can be identified on assorted seismograms from 59 km to 308 km (fig. 4). This event is the strongest arrival on the records in the distance range 101 km to 137 km.

A very strong event appears on the records at a distance of about 210 km (fig. 2) and persists to the end of the profile. It is the strongest event on the records to a distance of 280 km. This phase has the properties of a reflection from a boundary within the mantle and is herein designated I (fig. 4). The apparent velocity of this phase is 8.4 km/sec.

A strong event with an apparent velocity of about 6.0 km/sec appears on 3 of the records near the Flaming Gorge Reservoir end of the profile. This phase is designated $\overline{P}$.

Many other events on the seismograms cannot be correlated from one recording location to the next.

FIGURE 3.—Traveltime curve of first arrivals between American Falls Reservoir and Flaming Gorge Reservoir.
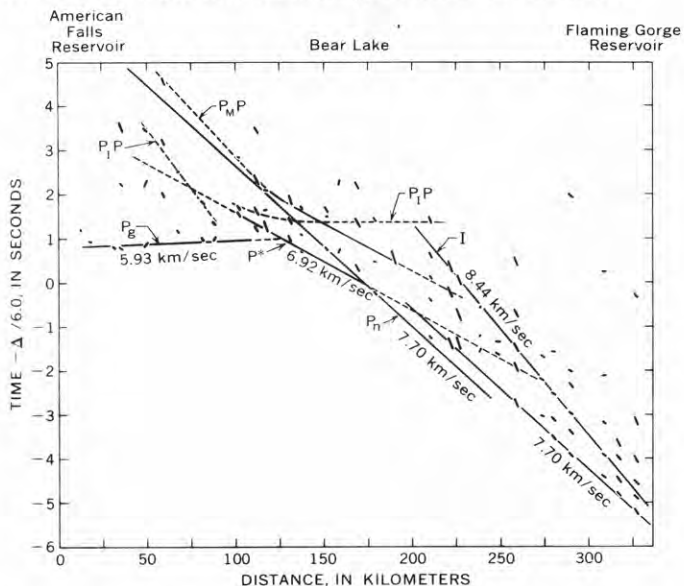

FIGURE 4.—Reduced traveltime curve from American Falls Reservoir to Flaming Gorge Reservoir.

Bear Lake shotpoint

Seismograms recorded from explosions in Bear Lake are similar to those recorded out to distances of about 150 km from shots in both American Falls Reservoir and Flaming Gorge Reservoir.

The first arrivals (fig. 3) on 9 seismograms recorded at distances of 16 km to 101 km toward American Falls Reservoir are designated P_g. A phase identified as P_IP first appears at 43 km and persists to the last recording location at a distance of 149 km from the shotpoint (fig. 5A). This phase is the strongest event on the records. The first arrivals on the seismograms from 112 km to 142 km have an apparent velocity appropriate for a wave refracted from an intermediate layer and are designated P^*.
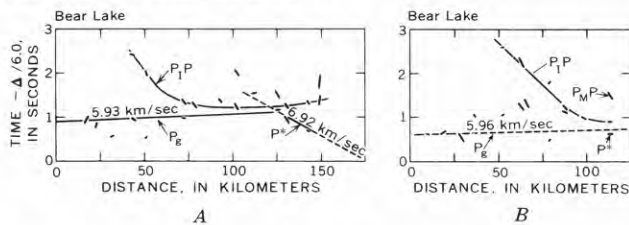
FIGURE 5.—Reduced traveltime curves. A, from Bear Lake toward American Falls Reservoir; B, from Bear Lake toward Flaming Gorge Reservoir.

From Bear Lake toward Flaming Gorge Reservoir the seismograms are much the same except that the profile obtained covers a shorter distance and P^* was identified as a first arrival only on the last record at a distance of 112 km. On this last seismogram the strongest event, which is later than the phase identified as P_IP, has been tentatively identified as a reflection from the Mohorovicic discontinuity and is labeled P_MP (fig. 5B). Such a phase could not be positively identified on the records obtained on the line extending toward American Falls Reservoir.

Flaming Gorge Reservoir shotpoint

The Flaming Gorge Reservoir shotpoint was somewhat more efficient than that at American Falls, and the records obtained from shots at Flaming Gorge Reservoir are generally somewhat better out to a distance of about 200 km. Beyond 200 km the background noise at some recording locations was high enough to obscure first motion on the seismograms, and some records were so noisy that only some of the strong late events could be identified.

Two recording units were laid out end to end and as near the shotpoint as practicable. The closer of these units recorded a direct wave with an apparent velocity of 4.05 km/sec. The two units together indicate a velocity of 4.75 km/sec for the near-surface material.

The first arrivals (fig. 3) on 13 seismograms from 11 to 127 km are the direct wave (P_g). The first upward motion can generally be identified on these records.

The first arrivals on 4 seismograms from 140 km to 166 km are identified as a refracted wave from an intermediate layer (P^*). The reflected wave from the upper surface of this layer (P_IP) appears as a strong secondary event on the records from 39 km to 139 km and in the distance range 39 km to 76 km is the strongest event on the records (fig. 6).
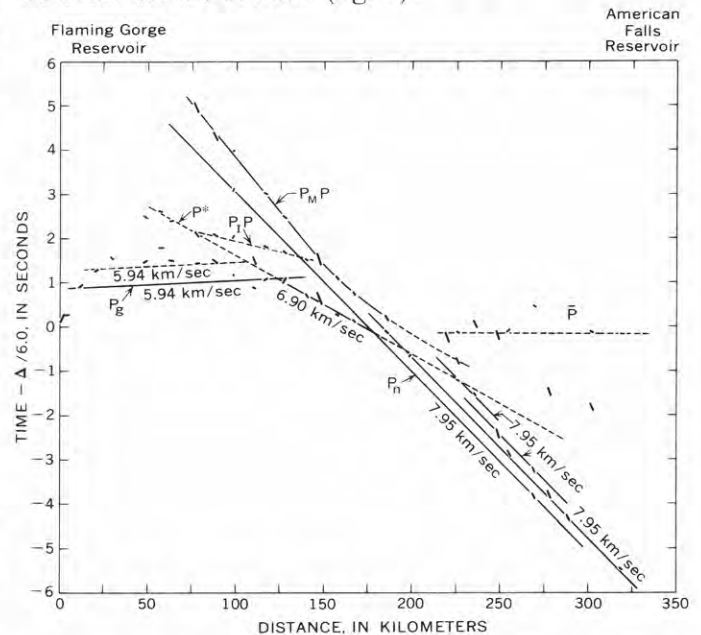
FIGURE 6.—Reduced traveltime curve from Flaming Gorge Reservoir to American Falls Reservoir.

The refracted wave from the Mohorovicic discontinuity (P_n) appears as a first arrival at 184 km and generally persists to the end of the profile, although on most of the records something later than the first motion has been picked. The reflected wave from this discontinuity (P_MP) is first identified at 76 km and persists to 184 km. It is generally the strongest event on the records in this distance range (fig. 6). A large-amplitude low-frequency wave with a velocity of about 6.0 km/sec that has been identified as $\overline{P}$ appears on 6 records in the distance range 225 km to 318 km. This phase is generally the strongest event on the records on which it can be identified. The arrival times of this phase are earlier than traveltimes of the extension of P_g.

No phase comparable to the high-amplitude event identified as I on the semismograms recorded from American Falls Reservoir was recognized on the seismograms recorded from Flaming Gorge Reservoir.

Amplitudes

The amplitudes of prominent phases were measured and tabulated with arrival times.[1] Because the first upward motion could be identified with certainty on only a few of the records, the amplitude was measured as the maximum peak-to-trough displacement in the first few half-cycles of the arrival of each phase. These measurements were converted to ground motion in the manner described by Eaton (1963, p. 5791–5792), and assuming linear scaling to normalize shots to 2,000 lbs. These amplitudes are plotted for each individual profile: American Falls Reservoir to Flaming Gorge Reservoir in figure 7; Flaming Gorge Reservoir

FIGURE 8.—Amplitude (ground displacement) versus distance of prominent phases recorded from shots in Flaming Gorge Reservoir.
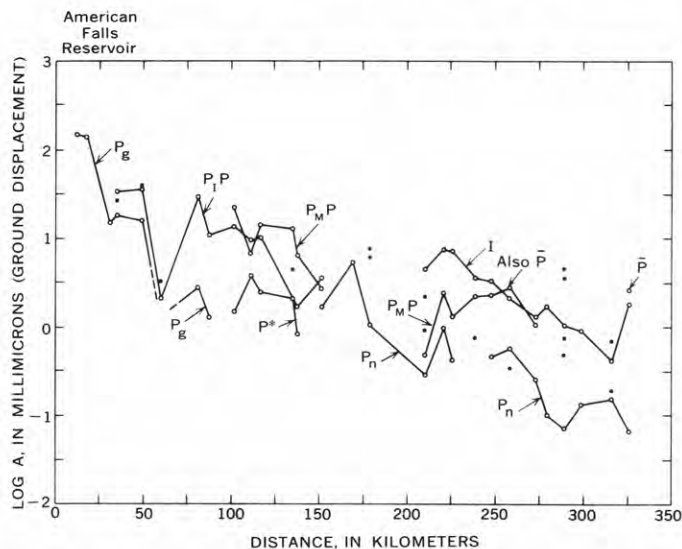

FIGURE 7.—Amplitude (ground displacement) versus distance of prominent phases recorded from shots in American Falls Reservoir.

to American Falls Reservoir in figure 8; and Bear Lake to American Falls Reservoir and Bear Lake toward Flaming Gorge Reservoir in figure 9.

Amplitudes of the refracted waves P_n and P^* and the direct wave P_g generally attenuate rapidly with distance, but there is considerable scatter about any line that would represent a regular decrease in amplitude with distance. P_g is difficult to pick above the noise level at distances near those at which P^* appears as the first arrival. The phase P_n could be picked to the Flaming Gorge end of the profile because of the generally quiet recording locations. In the reverse direction the first motion of P_n generally was not identified owing to the higher noise level.

The reflected events $P_I P$, $P_M P$, and I generally have the largest amplitudes on the seismograms over the

first 50 to 100 km that they appear. The phase $\bar{P}$ is the strongest event on the records on which it can be identified.
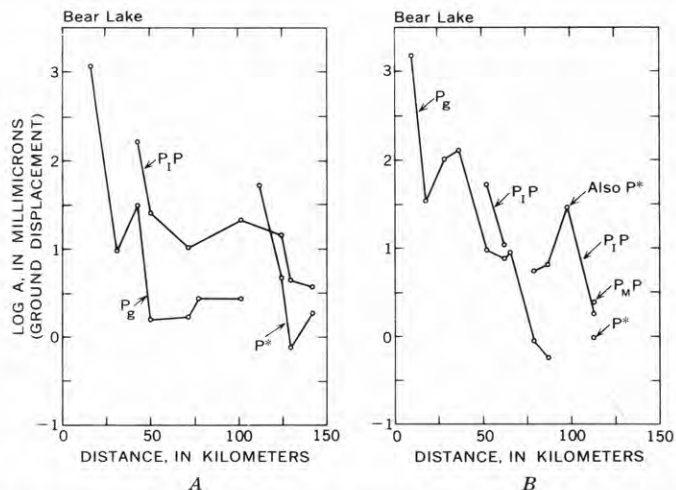
FIGURE 9.—Amplitude (ground displacement) versus distance of prominent phases recorded from shots in Bear Lake. A, Bear Lake toward American Falls Reservoir; B, Bear Lake toward Flaming Gorge Reservoir.

TRAVELTIME AND CRUSTAL STRUCTURE

First arrivals

The equations of the straight lines chosen as the best fit to the observed time of first arrivals are given in table 1. The observed deviation from these lines (fig. 3) is large only for recording locations in the Green River Basin and for the noisy locations near the American Falls Reservoir end of the line that were recorded from shots in Flaming Gorge Reservoir.

[1] Information available in files of the Branch of Crustal Studies, U.S. Geological Survey, Denver, Colo.

TABLE 1.—*Traveltime equations*

Profile	Phase	Traveltimes (seconds)
American Falls Reservoir to Flaming Gorge Reservoir.	P_g	$0.67 + \Delta/5.93$
	P^*	$3.88 + \Delta/6.92$
	P_n	$6.34 + \Delta/7.70$
Bear Lake to American Falls Reservoir__	P_g	$.66 + \Delta/5.93$
	P^*	$4.10 + \Delta/6.92$
Bear Lake to Flaming Gorge Reservoir__	P_g	$.65 + \Delta/5.96$
Flaming Gorge Reservoir to American Falls Reservoir.	P_g	$.70 + \Delta/5.94$
	P^*	$3.76 + \Delta/6.90$
	P_n	$6.97 + \Delta/7.95$

Depth calculations

The depths to the top of the intermediate layer and the Mohorovicic discontinuity have been calculated using first arrivals and velocities from the traveltime curves. The average of the two velocities for the layer immediately beneath the Mohorovicic discontinuity was used to calculate its depth. The computed crustal models are given in table 2. The difference in intercept times and apparent velocities of P_n from American Falls Reservoir and Flaming Gorge Reservoir can be accounted for by a dip of about 1° on the mantle down from American Falls Reservoir toward Flaming Gorge Reservoir.

An approximation of the depth to the reflecting horizon represented by the strong phase I was made by assuming that a traveltime curve for a refracted wave from the same horizon would be tangent to and practically parallel with the segment of the traveltime curve shown on the reduced traveltime graph of figure 4. An intercept time obtained by projecting this line to the zero-distance line and the apparent velocity shown for the phase on figure 4 permit calculation of a total depth to the horizon of about 69 km.

Discussion of results

The existence of an intermediate layer with a velocity of 6.9 km/sec is well established along this profile by two-way refraction coverage and by reflections at both ends of the profile. The depth to the top of the intermediate layer is appreciably greater near Bear Lake than it is near either American Falls Reservoir or Flaming Gorge Reservoir.

The fairly shallow depth to the intermediate layer probably accounts for the refracted wave P^* from the intermediate layer appearing as first arrivals on this line. This phase is rarely observed as a first arrival in the nearby Basin and Range province. The strong phase that is labeled I in this study and that has an apparent velocity of 8.4 km/sec in the distance range 210 km to 325 km has the properties of a reflection from a layer within the mantle. Extending this profile to the southeast with another shotpoint might provide a reversal of this phase, particularly if it emerges as a first arrival, and might permit calculations of its true velocity and the true depth of the reflecting layer. Ryall and Stuart (1963) identified phases with apparent velocities of about 8.4 km/sec recorded at large distances from the Nevada Test Site toward Ordway, Colo. They attributed some of these to a change in velocity of P_n going under the Colorado Plateau but considered one phase with this velocity, which they designed P_c, to be a reflection from a deep-mantle layer. The greater distance at which P_c first appeared on their records suggests that it comes from considerably greater depth than does the phase I on the American Falls-Flaming Gorge Reservoirs profile.

An increase in velocity downward in the upper crustal layer (beneath the low-velocity material) seems to be required to account for the phase $\bar{P}$ arriving appreciably earlier than the projection of the P_g traveltime curve. The apparent velocity of 6.0 km/sec for the phase $\bar{P}$ as contrasted to the velocity of 5.9 km/sec determined for P_g indicates that such a velocity gradient does indeed exist.

Near-surface geology affects the traveltimes recorded along this profile at several places. The most striking effect is the large delay of both P_g and P_n at all re-

TABLE 2.—*Computed crustal model*

Layer	From American Falls Reservoir		From Bear Lake toward American Falls Reservoir		From Bear Lake toward Flaming Gorge Reservoir		From Flaming Gorge Reservoir	
	Velocity (km/sec)	Thickness (km)	Velocity (km/sec)	Thickness (km)	Velocity (km/sec)	Thickness (km)	Velocity (km/sec)	Thickness (km)
1	[1] 3.6	1.5	3.6 (assumed)	1.5	4.0 (assumed)	1.75	[2] 4.05	1.9
2	5.93	18.1	5.93	19.4	---------	---------	5.96	17.6
3	6.92	11.2	---------	---------	---------	---------	6.91	17.3
4	[3] 7.82		---------	---------	---------	---------	7.82	---------
	Total depth to M-discontinuity=30.8 km				Total depth to M-discontinuity=36.8 km			

[1] Average value derived from near-in recordings made from the two American Falls Reservoir shotpoints.
[2] Value derived from a recording unit covering the distance range of 0.39 to 2.75 km from the shotpoint.
[3] Average value of P_n from reduced traveltime curves of figures 4 and 6.

cording locations across the Green River Basin. The early arrival of P_n at the two recording locations closest to Flaming Gorge Reservoir is probably due to thinning of the post-Precambrian strata towards the Uinta Mountains. Other effects that may be attributable in some way to near-surface geology include the delay of P_g at the first two recording locations southeast of American Falls Reservoir. The offset of about ½ second between adjacent recording locations of the traveltime curve for the phase P_1P shown on figure 4 is better explained by a sudden increase in the total thickness of the layer with velocity of 5.9 km/sec. Such an increase could be accomplished by a fault at depth in the area north of Preston, Idaho, that would elevate the crustal block to the west of it somewhat more than 1 km.

CONCLUSIONS

Two-way refraction coverage along this profile indicates a thickening of the crust from about 31 km at American Falls Reservoir to about 37 km at Flaming Gorge Reservoir. The intermediate layer thickens from about 11 km at American Falls Reservoir to about 17 km at Flaming Gorge Reservoir.

The velocity of compressional waves in the crust beneath the near-surface low-velocity material is about 5.9 km/sec along this profile. Compressional waves in the intermediate layer travel with a velocity of 6.9 km/sec, and those in the mantle immediately below the Mohorovicic discontinuity travel with a velocity of 7.8 km/sec. A deeper layer within the mantle with an apparent velocity of 8.4 km/sec is indicated by strong secondary events recorded from shots at American Falls Reservoir.

The crust along this profile is more nearly like that in the Basin and Range province than it is in other provinces covered by U.S. Geological Survey refraction profiles (Pakiser, 1963).

REFERENCES

Armstrong, F. C., and Cressman, E. R., 1963, The Bannock thrust zone, southeastern Idaho: U.S. Geol. Survey Prof. Paper 374–J, p. J1–J22.

Armstrong, F. C., and Oriel, S. S., 1964, Tectonic development of Idaho-Wyoming thrust belt: Am. Assoc. Petroleum Geologists Bull., v. 48, p. 1878.

Cressman, E. R., 1957, Preliminary geologic map of the Snowdrift Mountain quadrangle, Caribou County, Idaho: U.S. Geol. Survey Mineral Inv. Map MF–118.

Cressman, E. R., and Gulbrandsen, R. A., 1955, Geology of the Dry Valley quadrangle, Idaho: U.S. Geol. Survey Bull. 1015–I, p. 257–270.

Eaton, J. P., 1963, Crustal structure from San Francisco, California, to Eureka, Nevada, from seismic-refraction measurements: Jour. Geophys. Research, v. 68, no. 20, p. 5789–5806.

Jackson, W. H., Stewart, S. W., and Pakiser, L. C., 1963, Crustal structure in eastern Colorado from seismic-refraction measurements: Jour. Geophys. Research, v. 68, no. 20, p. 5767–5776.

Jenkins, C. E., 1955, The Pacific Creek deep test, Superior Oil Company No. 1 unit, section 27, T. 27 N., R. 103 W., Sublette County, Wyoming, in Wyoming Geol. Assoc. Guidebook 10th Ann. Field Conf.: p. 153–154.

Mansfield, G. R., 1927, Geography, geology, and mineral resources of part of southeastern Idaho: U.S. Geol. Survey Prof. Paper 152, 453 p.

Oriel, S. S., 1964, Brigham, Langston, and Ute formations in Portneuf Range, southeastern Idaho [abs.]: Geol. Soc. America Special Paper 82, p. 341.

Pakiser, L. C., 1963, Structure of the crust and upper mantle in the western United States: Jour. Geophys. Research, v. 68, no. 20, p. 5747–5756.

Rubey, W. W., 1958, Geologic map of the Bedford quadrangle, Wyoming: U.S. Geol. Survey Geol. Quad. Map GQ–109.

Rubey, W. W., and Hubbert, M. K., 1959, Overthrust belt in geosynclinal area of western Wyoming in light of fluid-pressure hypothesis, pt. 2 of Role of fluid pressure in mechanics of overthrust faulting: Geol. Soc. America Bull., v. 70, p. 167–206.

Ryall, Alan, and Stuart, D. J., 1963, Travel times and amplitudes from nuclear explosions—Nevada Test Site to Ordway, Colorado: Jour. Geophys. Research, v. 68, no. 20, p. 5821–5835.

Veatch, A. C., 1907, Geography and geology of a portion of southwestern Wyoming, with special reference to coal and oil: U.S. Geol. Survey Prof. Paper 56, 178 p.

Warrick, R. E., Hoover, D. B., Jackson, W. H., Pakiser, L. C., and Roller, J. C., 1961, The specification and testing of a seismic-refraction system for crustal studies: Geophysics, v. 26, no. 6, p. 820–824.

SEISMIC FLUCTUATIONS IN AN OPEN ARTESIAN WATER WELL

By JOHN D. BREDEHOEFT, HILTON H. COOPER, JR.,
ISTAVROS S. PAPADOPULOS, and ROBERT R. BENNETT,
Washington, D.C.

Abstract.—The degree to which the water level in an open well responds to a seismic wave is determined by (1) the dimensions of the well, (2) the transmissibility, storage coefficient, and porosity of the aquifer, and (3) the period and amplitude of the wave. The amplitude of the vertical land-surface motion associated with Rayleigh waves may be computed, provided sufficient data regarding the above parameters are available. Conversely, if the amplitude of vertical land-surface motion is known, the water-level fluctuations can be computed. Analysis of the fluctuations caused by the "Good Friday" Alaskan earthquake of March 27, 1964, in a well near Perry, Taylor County, in northern Florida illustrates the theory. This well fluctuated over a range of approximately 15 feet in response to this earthquake.

Water levels in open wells penetrating artesian aquifers, and in some instances water-table aquifers, are known to fluctuate from the effects of earthquakes. To the ground-water hydrologist these earthquake-induced fluctuations may provide a means of obtaining significant information on aquifer characteristics. To the seismologist, they imply the possibility of using wells as seismographs. Rexin and others (1962, p. 18) have suggested, for example, that the response of some wells to long-period waves may be superior to that of conventional long-wave seismographs.

Advances in the theory of aquifer mechanics permit the treatment of a more realistic model of the well-aquifer system subjected to earthquake-induced fluctuations than has been previously considered. The purpose of this paper is to illustrate the theory of seismically induced water-level fluctuations by analyzing the fluctuations in an open artesian well (U.S. Geological Survey observation well Taylor 35) near Perry, Taylor County, in northern Florida, in response to the "Good Friday" Alaskan earthquake of March 27, 1964. The analysis reveals the complexity of the problem, evaluates the variables concerned, and points out where future improvements in the necessary data collection can be made.

THEORY

In order to consider the Perry well in detail it is necessary to abstract briefly the theory of seismically induced water-level fluctuations, which is being presented elsewhere (Cooper and others, 1965).

The water level in the well (Taylor 35) near Perry, Fla., fluctuated over a range (double amplitude) of as much as 15 feet in response to the Good Friday Alaskan earthquake. However, the response of other wells which penetrate the same aquifer was only a fraction of a foot. An obvious explanation of the differing responses is that well-aquifer systems have the essential features of a seismograph and hence magnify the seismic disturbance in differing degrees that depend not only on the characteristics of the well and aquifer, but also on the period of the disturbing wave. Like the seismograph the well-aquifer system consists of a mass (the column of water in the well plus some portion of the water in the aquifer), a restoring force (the difference between the pressure head in the aquifer and the displaced water level in the well), and a damping force (the friction which accompanies the flow of water through the well and aquifer).

The column of water in some wells can oscillate much like the classic spring-suspended mass, as demonstrated by the results of a series of field tests in wells in Florida and Georgia in July 1964. Figure 1 shows the motion of the water level in the well near Perry, Fla., as recorded by a pressure transducer suspended below the water surface during one of these tests. The water in the well was forced to oscillate by periodically raising and lowering a weighted float. The float was then released, and the water continued to
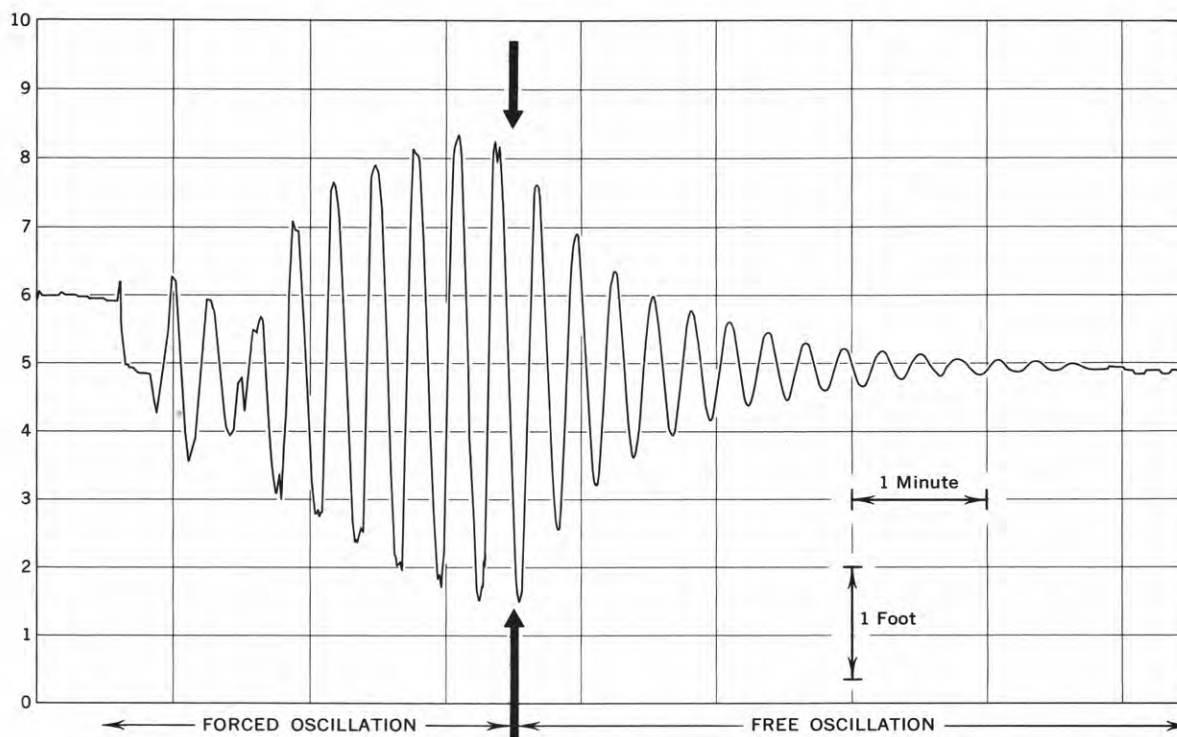
FIGURE 1.—Hydrograph of the well (Taylor 35) near Perry, Fla., during an experiment in which water in the well was forced to oscillate (indicated as forced oscillation on the graph) and then was allowed to oscillate freely (indicated as free oscillation).   The vertical scale is arbitrary.

oscillate in a manner characteristic of free vibration with viscous damping.

Equation of motion

Cooper and others (1965) showed that if friction losses within the well are neglected, the equation of motion of the column of water in the cased portion of the well shown in figure 2 is

$$\rho \pi r_w^2 (H_e+x)\frac{d^2x}{dt^2}+\rho g \pi r_w^2 (H+x)$$
$$=\rho g \pi r_w^2 (H-s_w)+p_o \pi r_w^2 \sin{(\omega t-\eta)}, \quad (1)$$

where

r_w = radius of the well,
$H_e = H+\frac{3}{8}d$ = effective column height,
d = thickness of screened interval,
x = displacement of the water level (positive upward),
ρ = density of water,
g = acceleration of gravity,
s_w = drawdown in the aquifer immediately outside the well screen (positive downward),
$p_o \sin{(\omega t-\eta)}$ = seismically induced fluctuation in the aquifer,
$\omega = 2\pi/\tau$ angular frequency of seismic wave,
τ = period of seismic wave,

η = phase angle, and
t = time.

If x is small relative to H_e, x can be neglected in the inertial term, so that this term is closely approximated by

$$\rho(H_e+x)\frac{d^2x}{dt^2} \approx \rho H_e \frac{d^2x}{dt^2}. \quad (2)$$

Substituting equation 2 in equation 1 and simplifying reduces the equation of motion to

$$\frac{H_e}{g}\frac{d^2x}{dt^2}+x=-s+\frac{p_o}{\rho g}\sin{(\omega t-\eta)}. \quad (3)$$

After no more than one oscillation the drawdown, s_w, is closely described by

$$s_w = \frac{r_w^2}{2T}\left(\frac{dx}{dt}\text{ Ker } \alpha_w - \omega x \text{ Kei } \alpha_w\right), \quad (4)$$

where

T = transmissibility of aquifer,
S = storage coefficient of aquifer, and
$\alpha_w = r_w\sqrt{\omega S/T}.$

The functions Ker α and Kei α, sometimes called Kelvin functions, are the real and imaginary parts of
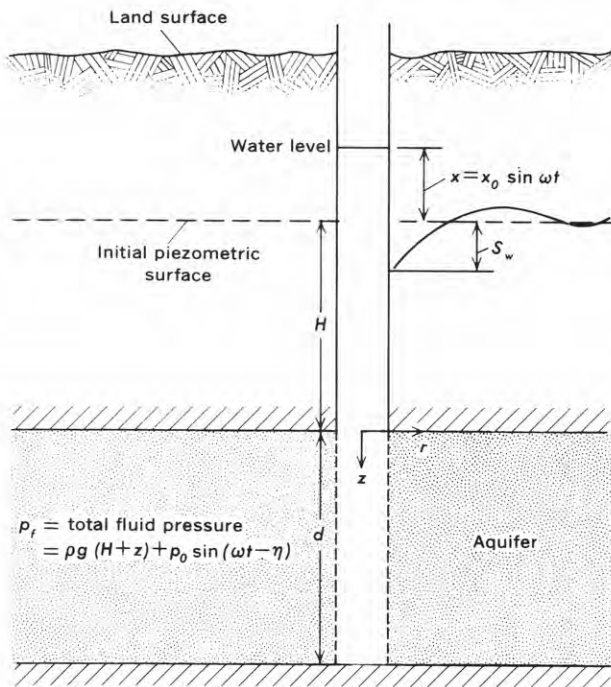
FIGURE 2.—Idealized representation of an open well penetrating an artesian aquifer in which the motion of the water level in the well is caused by fluctuations of pressure head in the aquifer. Symbols are explained in text.

K_0 $(\alpha i^{1/2})$, which is the modified Bessel function of the second kind of order zero.

Amplification

The dynamics of the well-aquifer system are such that the water-level fluctuations in the well can magnify the pressure-head fluctuations in the aquifer. Therefore in order to evaluate the pressure-head fluctuations in the aquifer from the oscillations of the water level in a well it is necessary to establish the "amplification curve" for the particular well in question.

The amplification factor, A, is defined as the ratio of the amplitude, x_0, of the oscillation of the water level in the well to the amplitude, $h_0 = \dfrac{p_0}{\rho g}$, of the pressure-head fluctuation in the aquifer. Accordingly,

$$A = \frac{x_0}{h_0} = \frac{\rho g x_0}{p_0} = \text{amplification factor.} \quad (5)$$

By use of equation 4 equation 3 is solved for the amplitude of the pressure fluctuation, p_0, necessary to produce an oscillation of the water level with an amplitude, x_0.

$$p_0 = x_0 \rho H_e \sqrt{\left[\frac{g}{H_e}\left(1 - \frac{r_w^2 \omega}{2T}\text{Kei }\alpha_w\right) - \omega^2\right]^2 + \left[\frac{r_w^2 g}{2TH_e}\text{Ker }\alpha\right]^2}. \quad (6)$$

Using the relationship $\omega = 2\pi/\tau$ and substituting from equation 6 into equation 5, one finds the amplification factor to be

$$A = \frac{1}{\sqrt{\left(1 - \frac{\pi r_w^2}{T\tau}\text{Kei }\alpha_w - \frac{4\pi^2 H_e}{\tau^2 g}\right)^2 + \left(\frac{\pi r_w^2}{T\tau}\text{Ker }\alpha_w\right)^2}}. \quad (7)$$

An electric analog was designed, constructed and used to analyze the response of a well to a seismic disturbance. The analog results agree remarkably well with the theoretical results.

It is apparent from equation 7 that the amplification is determined by (a) the well geometry (well radius, r_w, and effective height of the column of water in the well, H_e), (b) the aquifer characteristics (transmissibility, T, and storage coefficient, S), and (c) the period τ of the harmonic disturbance. Hence the amplification curve for a particular well can be computed, provided that the well geometry and the aquifer characteristics are known.

For a well such as the one near Perry, Fla., in which the water level will oscillate freely following a disturbance (fig. 1), the frequency of the free oscillation is approximately

$$\omega_w \approx \sqrt{\frac{g}{H_e}}, \quad (8)$$

and the period of the free oscillation is

$$\tau_w = \frac{2\pi}{\omega_w}. \quad (9)$$

The maximum amplification occurs when the harmonic disturbance has a frequency equal to that of the free oscillation of the well.

Relation between fluctuations of pressure head and vertical motion of land surface

Any type of earthquake wave that produces dilatation of the aquifer can cause the water level in a well to fluctuate. Of the types of waves that have been identified with fluctuations in wells, the Rayleigh wave causes the largest motion. A Rayleigh wave produces both dilatation and vertical land-surface motion which can be related to one another theoretically.

In analyses of the properties of aquifers it is commonly assumed that when the aquifer is compressed, the change in volume of the solid material due to deformation of the individual particles is small in comparison to the change in volume of the water (see for example Jacob, 1941, p. 583). This assumption is apparently valid for granular aquifers, but, depending on the pore geometry and Poisson's ratio, it may not be valid for aquifers such as limestone and basalt.

To the extent that the above assumption holds for a given aquifer, nearly all the volume change of a dilatated aquifer goes into a volume change of the water in its pores. Hence the dilatation of the water is nearly equal to that of the aquifer divided by the porosity. The amplitude of the fluctuation of the pressure-head due to the dilatation is, therefore,

$$h_0 = \frac{p_0}{\rho g} = \frac{(\theta_0 E_w/n)}{\rho g}, \tag{10}$$

where

$\theta_0 =$ amplitude of the dilatation,
$E_w =$ bulk modulus of elasticity of water, and
$n =$ porosity of aquifer.

The dilatation can be computed from seismic theory. For a Poisson's ratio of 0.25 the particle motion due to Rayleigh waves in a semi-infinite elastic solid is described (Jeffreys, 1929, p. 91) by

$$u = D(e^{-0.8475kz} - 0.5773e^{-0.3933kz}) \sin k(x-ct),$$

and

$$w = D(0.8475e^{-0.8475kz} - 1.4679e^{-0.3933kz}) \cos k(x-ct), \tag{11}$$

where

u and $w =$ the horizontal and vertical displacements, respectively,
$x =$ distance in the direction of wave travel,
$z =$ depth below surface,
$\lambda =$ length of seismic wave,
$k = 2\pi/\lambda$ wave number,
$c =$ phase velocity, and
$D =$ a constant.

For $z=0$, the last of equations 11 gives the vertical motion of the land surface:

$$w\big|_{z=0} = -0.6204D \cos k(x-ct) = -w_0 \cos k(x-ct), \tag{12}$$

where

$$w_0 = 0.6204D. \tag{13}$$

The dilatation due to the Rayleigh wave is

$$\theta = \frac{\partial u}{\partial x} + \frac{\partial w}{\partial z} = 1.7700\frac{D}{\lambda}e^{-5.3250z/\lambda} \cos k(ct-x). \tag{14}$$

For shallow depths, $z < \lambda/100$, the dilatation is closely approximated by

$$\theta\big|_{z<\lambda/100} = 1.7\frac{D}{\lambda} \cos k(ct-x) = \theta_0 \cos k(ct-x), \tag{15}$$

where

$$\theta_0 = \frac{1.7D}{\lambda}. \tag{16}$$

Substituting from equation 16 into equation 10, we obtain

$$h_0 = \frac{1.7DE_w}{\rho g n \lambda}. \tag{17}$$

The ratio of the change in pressure head to the vertical motion of the well-aquifer system is, from equations 13 and 17,

$$R = \frac{h_0}{w_0} = 2.7\frac{E_w}{\rho g n \lambda}. \tag{18}$$

Magnification of vertical land-surface motion

Using equations 5 and 18 it is possible to define a magnification for a well which, for Rayleigh waves, is comparable to the magnification of a vertical-component seismograph. Thus we define M to be the ratio of the amplitude x_0 of the water-level oscillation to the amplitude w_0 of the land-surface oscillation, and from equations 5 and 18

$$M = \frac{x_0}{w_0} = \left(\frac{x_0}{h_0}\right)\left(\frac{h_0}{w_0}\right) = AR. \tag{19}$$

ANALYSIS OF FLUCTUATIONS IN THE WELL NEAR PERRY, FLA.

Amplification curve

The well near Perry, Fla., is cased with 12-inch pipe to a depth of 189 feet and was completed as a 12-inch open hole in the Floridan aquifer (cavernous limestone) between depths of 189 and 245 feet (fig. 3). The total
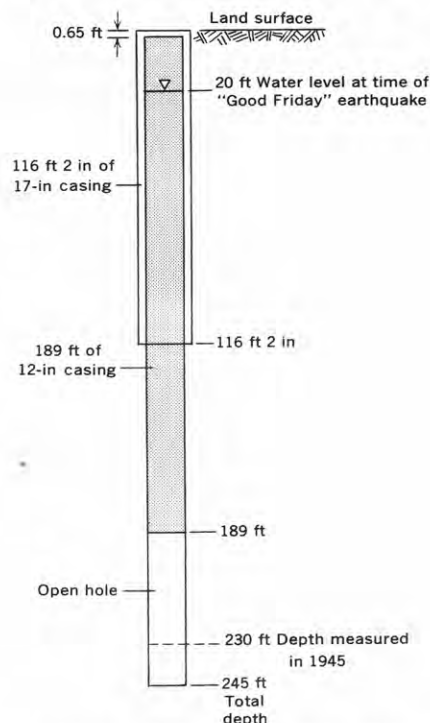

FIGURE 3.—Geometry of the well (Taylor 35) near Perry, Fla., from H. H. Cooper's field notes, 1945.

depth was measured in 1945 to be 230 feet. The depth to water at the time of the earthquake was 20 feet below the land surface. A pumping test of the well indicates that the Floridan aquifer in this area has a transmissibility of approximately 1.4 ft^2/sec (900,000 gal/day ft).

The storage coefficient for a short-period disturbance is truly artesian. Depending upon the porosity, the storage coefficient for that portion of the Floridan aquifer to which the well near Perry responds is within the range of 1×10^{-4} and 1×10^{-6}.

In summary, the pertinent data are

$$H_e = (189-20) + \tfrac{3}{8}(230-189) = 184 \text{ ft},$$
$$r_w = 0.5 \text{ ft},$$
$$T = 1.4 \text{ ft}^2/\text{sec, and}$$
$$1 \times 10^{-6} < S < 1 \times 10^{-4}.$$

Three amplification curves for storage coefficients of 1×10^{-4}, 1×10^{-5}, and 1×10^{-6} were computed from equation 7 for the well (fig. 4), on the basis of these data. Calculations were made using the U.S. Geological Survey Burroughs 220 digital computer. Varying the storage coefficient within the limits indicated does not greatly change the amplification curve (fig. 4), except in a narrow range of frequencies near the point of maximum amplification.

The maximum amplification should occur when the period, τ, of the disturbing force is approximately given by equation 9:

$$\tau = 2\pi\sqrt{\frac{H_e}{g}},$$

which for the Perry well is

$$\tau = 2\pi\sqrt{\frac{184}{32}} = 15.1.$$

This agrees very closely with the observed period of free oscillation of 15 seconds determined by field experiments, shown on figure 1.

Good Friday earthquake

The effect of the Good Friday Alaskan earthquake on the Perry well is shown on the hydrograph (fig. 5). Unfortunately, the recorder advanced the paper at a rate of only 1 inch per day, the usual rate for
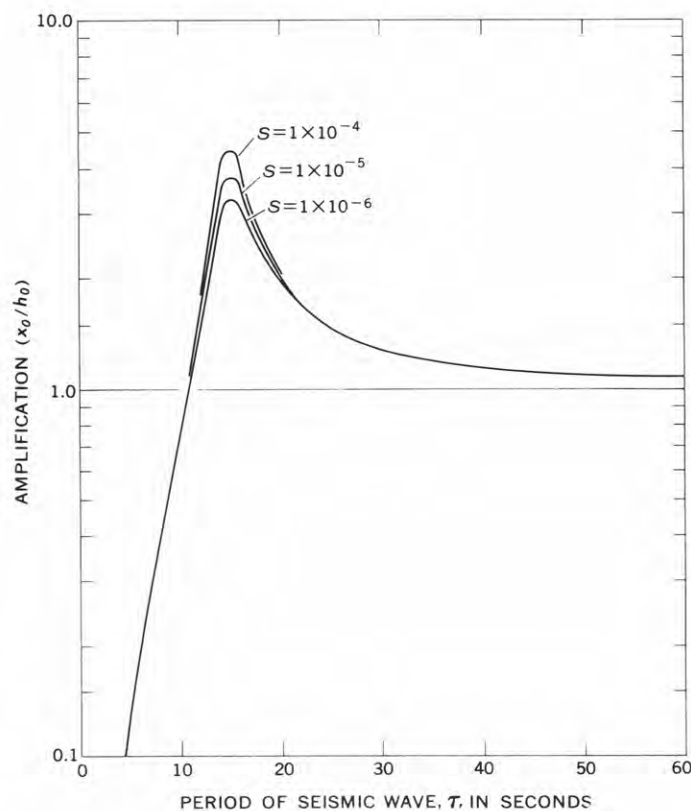

FIGURE 4.—Amplification curves for pressure-head fluctuations in the well (Taylor 35) near Perry, Fla. Symbols are explained in text.
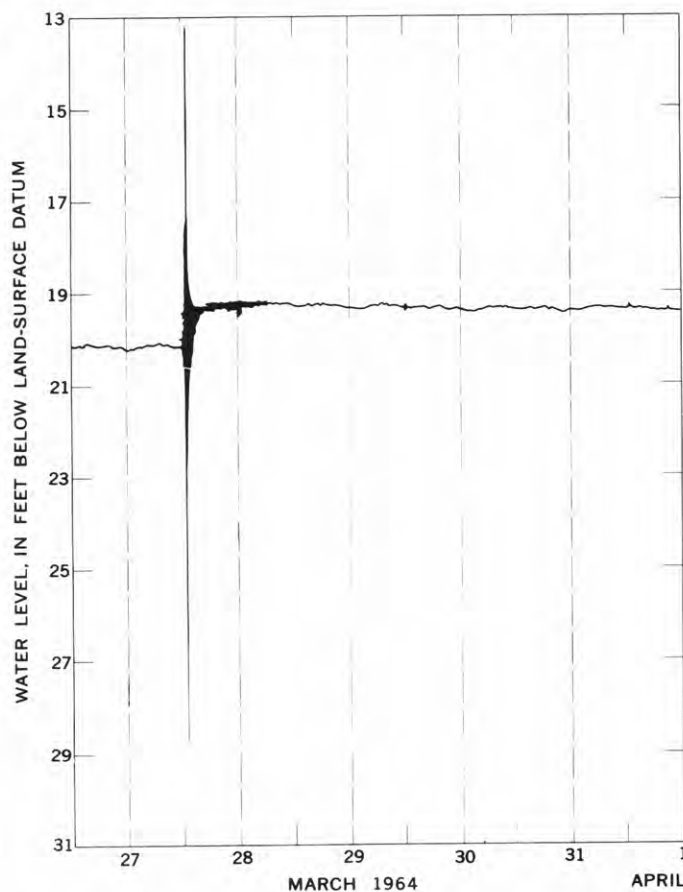

FIGURE 5.—Hydrograph of the well (Taylor 35) near Perry, Fla., showing the fluctuations caused by the Good Friday earthquake.

many observation wells, which makes it impossible to separate individual oscillations in the wave train on the hydrograph. It is, however, possible to interpret the maximum amplitude, x_0, of water-level oscillation. For the Alaskan quake the maximum downward amplitude was about 8 feet and the maximum upward motion was at least 7 feet. The recorder pen may have reversed near the top margin of the chart, in which event the upward fluctuations would have been greater than the 7 feet indicated.

It is obvious from theory that the period of the oscillation must also be known before an interpretation can be made of the earthquake-related pressure changes occurring in the aquifer. The closest seismograph in operation during the earthquake was a standard Wood-Anderson instrument at Cape Kennedy, Fla., approximately 200 miles southeast of Perry. To continue the interpretation we must assume that the ground-surface motion at Cape Kennedy was the same as that at Perry. The U.S. Coast and Geodetic Survey interpreted the maximum vertical ground-surface motion to have occurred with a period of 21 seconds and an amplitude of 3 cm, ± 25 percent (J. Lander, oral communication). However, a variety of Rayleigh waves with a 15-second period and an amplitude of 0.5 cm, ± 25 percent was also observed (J. Lander, oral communication).

Use of the amplification curve for a storage coefficient of 1×10^{-5} (fig. 4) indicates that the amplitude, x_0, of the water-level motion in the well is 1.9 times the amplitude of pressure-head fluctuation, h_0, for a Rayleigh wave having a period of 21 seconds, and 3.7 times the pressure-head fluctuation for a 15-second Rayleigh wave. This means that the amplitude of maximum pressure-head change in the aquifer is approximately, from (5)

$$h_0 = \frac{x_0}{A} = \frac{7.5}{1.9} = 4 \text{ ft,}$$

where $x_0 = 7.5$ feet, the average of the observed maximum upward and downward water-level displacements.

Ground-surface motion and aquifer porosity

Knowing the amplitude, w_0, of both the land-surface motion and the amplitude, x_0, of the water-level oscillation, one can calculate the magnification, M, from equation 19:

$$M = \frac{x_0}{w_0} = \frac{(7.5 \text{ ft})(30.48 \text{ cm/ft})}{3 \text{ cm}} = 76.$$

Since the amplification factor, A, is also known for the 21-second disturbance (fig. 4), R, the ratio of pressure-head change, h_0, to vertical surface motion, w_0, can be calculated from equation 18 or equation 19:

$$R = \frac{h_0}{w_0} = \frac{M}{A} = \frac{76}{1.9} = 40.$$

As equation 18 indicates, R may be calculated from other considerations, provided that the various parameters are known:

$$R = \frac{h_0}{w_0} = 2.7 \frac{E_w}{\rho g n \lambda}.$$

Water at 60°F has a bulk modulus of elasticity, E_w, of about 45 million pounds per square foot and a specific weight, ρg, of about 62.4 pounds per cubic foot. The velocity of Rayleigh waves associated with the Alaskan quake is 3 km/sec (± 25 percent); therefore, the wave length, λ, of the 21-second wave is approximately 63 km, 218,000 feet. The only unknown in (18) is the porosity, which may be computed:

$$n = 2.7 \frac{E_w}{\rho g \lambda R} = \frac{(2.7)(4.5 \times 10^7)}{(62.4)(2.18 \times 10^5)(40)} = 0.22.$$

This porosity represents a weighted average for the total area of influence of the well.

Once the porosity of the aquifer is established, the motion of the water level for the 15-second wave in the Rayleigh wave train may be calculated. The amplitude of the fluctuation associated with the 15-second Rayleigh wave is considerably less than the maximum amplitude of 7.5 feet associated with the 21-second Rayleigh wave, and is, therefore, masked on the hydrograph (fig. 5). From equation 18, R is equal to

$$R = 2.7 \frac{E_w}{\rho g n \lambda} = \frac{(2.7)(4.5 \times 10^7)}{(62.4)(0.22)(1.48 \times 10^5)} = 60,$$

where $\lambda = 45$ km (± 25 percent) $= 148,000$ feet. The amplification factor, A, taken from figure 4 is approximately 3.7 for a 15-second disturbance. The magnification is, therefore,

$$M = AR = 3.7 \times 60 = 222,$$

and the water-level in the well fluctuated with an amplitude of

$$x_0 = M w_0 = 222 \times 0.5 = 111 \text{ cm} = 3.6 \text{ feet.}$$

SUMMARY

This short paper demonstrates the complexity of the water-level response to the seismic disturbance. The land-surface motion can be deduced from the water-level fluctuations, provided that sufficient information is available concerning well geometry, aquifer characteristics, and the nature of harmonic disturbance. Conversely, approximate water-level fluctuations can be deduced from the land-surface motion if the various

necessary parameters are known. The mathematical analysis presented here indicates that unless all these factors are considered, the meaning of seismically induced water-level fluctuations cannot be understood.

The amplification curve for a given open well can be established empirically if the motion of the water level, the fluctuations of pressure in the aquifer, and the period of the oscillation caused by seismic waves are observed. A shut-in well under pressure near the open well but at a sufficient distance to be out of its area of influence would provide a direct means of observing the fluctuation of pressure in the aquifer.

REFERENCES

Cooper, H. H., Bredehoeft, J. D., Papadopulos, I. S., and Bennett, R. R., 1965, Nature of the response of well-aquifer systems to seismic waves: Jour. Geophys. Research. [In press]

Jacob, C. E., 1941, On the flow of water in an elastic artesian aquifer: Am. Geophys. Union Trans., pt. 2, p. 574–586.

Jeffreys, Harold, 1929, The earth: New York, MacMillan Co., 339 p.

Rexin, E. E., Oliver, Jack, and Prentiss, David, 1962, Seismically induced fluctuations of the water level in the Nunn-Bush well in Milwaukee: Seismol. Soc. America Bull., v. 52, p. 17–25.

FRACTIONATION OF URANIUM ISOTOPES AND DAUGHTER PRODUCTS IN URANIUM-BEARING SANDSTONE, GAS HILLS, WYOMING

By JOHN N. ROSHOLT, JR., and CARLOS P. FERREIRA,
Denver, Colo.

Abstract.—At a sandstone-type uranium deposit in the Wentz mine in Natrona County, Wyo., isotopic ratios of U^{234}/U^{238} for 14 samples taken at, or just above, the present level of standing water show that the deposit has a relatively consistent U^{234} deficiency ranging from 7 to 29 percent. Th^{230}/U^{234} and Pa^{231}/U^{235} ratios indicate that the time interval since uranium emplacement near the level of standing water is about 80,000 years and that the time interval generally is greater with increasing distance above the water. The source uranium also appears to be deficient in U^{234}, and the deficiency was maintained in ore by relatively continuous preferential leaching of this isotope.

Significant fractionation of uranium isotopes has been found in roll-type ore bodies in the Shirley Basin, Wyoming (Rosholt and others, 1964a), in the Gas Hills area, Wyoming (Rosholt and others, 1964), and in the Powder River basin, Wyoming, and Slick Rock district, Colorado (Rosholt and others, 1965). In the Powder River basin, U^{234} deficiencies of 40 to 60 percent relative to U^{238} were found in ore in the zone of oxidation above the water table. In the Shirley Basin, U^{234} deficiencies of 7 to 22 percent were found in the ore that occurs below the zone of oxidation. Little variation in U^{234}/U^{238} ratios was found in the relatively unoxidized ore in the Slick Rock district. Ore in the Gas Hills roll feature tended to contain excess U^{234}.

A primary end product of these studies was an interpretation of the mechanism of uranium-isotope fractionation. Total U^{234} is contributed in two ways to the environment in which it is found: (1) those atoms that have been mixed and transported with U^{238}/U^{235} remain with these two isotopes and are not subject to removal by preferential leaching, and (2) atoms generated in place from the radioactive disintegration of U^{238} are subject to differential migration with respect to U^{238}. The term "allogenic U^{234}" was suggested for transported U^{234} in the studies by Rosholt and others (1965); because this uranium is not subject to preferential leaching, subsequent changes in the U^{234}/U^{238} ratios are caused primarily by radioactive decay of U^{234}. The term "authigenic U^{234}" was suggested for those atoms generated in place; this uranium is subject to preferential leaching. Consideration of the dual behavior of U^{234} is of fundamental importance to the interpretation of isotopic distribution of uranium and its daughter products.

This paper compares the radioactive disequilibrium of various samples of uranium ore at, and just above, the present level of standing water in the Wentz mine in Natrona County, Wyo. The Wentz property is a small mine, now closed, in the NW¼ sec. 25, T. 34 N., R. 89 W., at the northeastern end of the Gas Hills district. The location of this deposit with respect to other Gas Hills area ore deposits was shown by Zeller (1957).

The samples referred to in this paper were collected by the senior author and by E. W. Grutt, of the U.S. Atomic Energy Commission, in the summer of 1957 at the point of deepest penetration in the mine. This point was approximately 150 feet horizontally from the portal in the single-drift mine and approximately 60 feet below the topographic surface. The face of the drift was approximately 10 feet wide and 7 feet high, with a few inches of standing water at the face. Sandstone was oxidized in the roof and in the uppermost 1 foot of the face. A sharp demarcation existed between yellow oxidized sandstone in the upper part of the face and dark-gray sandstone in the lower part. The general lithologic variations on the face are shown in figure 1. The upper half of the unoxidized face consisted of several horizontal bands of sandstone whose color alternated every 2 or 3 inches between dark gray and very dark gray. Pyrite-bearing carbon fragments and very dark gray siltstone lenses as much as 1 inch in thickness were irregularly inter-
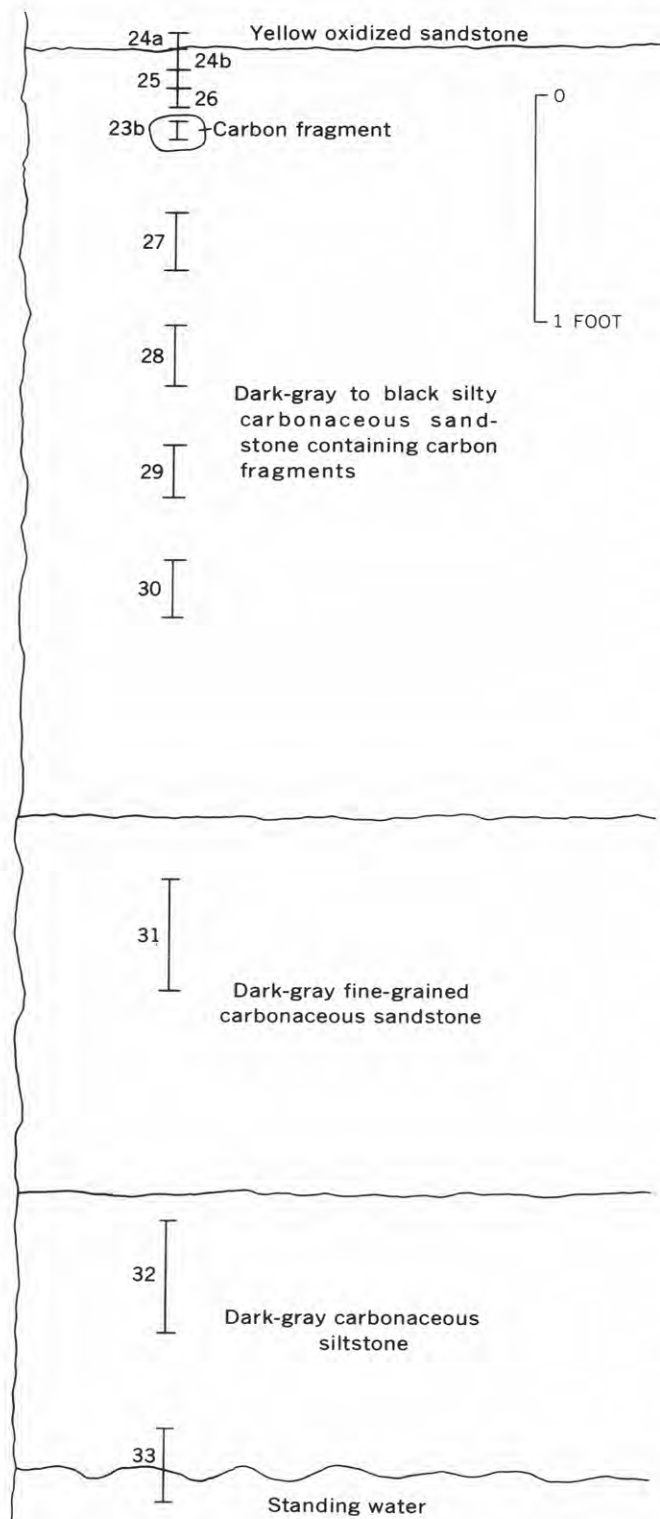
FIGURE 1.—Geologic section showing lithology and stratigraphic position of numbered samples taken from the drift face of the Wentz mine, in the northeastern Gas Hills area, Wyoming.

bedded, in this unit. The lower half of the face consisted of a thick horizontal bed of relatively uniform dark-gray fine-grained sandstone underlain by a thick horizontal bed of equally uniform dark-gray siltstone. The coloration was attributed to a very fine grained mixture of pyrite and disseminated fine-grained specks of carbonaceous material. Some color may have been due to disseminated black uranium minerals that are difficult to identify. There was probably insignificant vanadium mineralization because vanadium did not occur in concentrations greater than 0.01 percent in any of the samples collected.

The face of the drift was sampled at vertical intervals as shown in figure 1. Channel samples weighing about 5 pounds each were collected from 4 of the very dark gray bands on the upper half of the face (Nos. 27, 28, 29, and 30). Three smaller channel samples, weighing about 2 pounds each, were collected across and just below the oxidized sandstone contact (Nos. 24, 25, and 26). The sample across the oxidized sandstone contact was divided later into the oxidized part (24a) and the unoxidized part (24b). A large chip sample (No. 23) containing a carbon fragment from the fifth very dark gray band was also collected from the upper half of the face. Channel samples weighing approximately 10 pounds each were collected from each large unit on the lower half of the face, including an additional sample partly immersed in standing water. Sample 34 is not shown in figure 1; it was obtained from oxidized sandstone in the roof, 10 feet from the portal of the mine.

PROCEDURE

Alpha spectrometry is a convenient method for determining the U^{234}/U^{238} ratio in samples of uranium ore. Electrodeposited uranium is measured following its chemical separation from the sample. The total uranium content of the sample is determined by a separate chemical analysis. The measurement technique and instrumentation are similar to that previously used for alpha spectrometry of thorium isotopes in uranium ores (Dooley and others, 1964, p. 587).

Alpha-particle radioactivity is emitted from U^{238}, U^{235}, and U^{234} in a chemically purified uranium separate. The identifying energies of the uranium isotopes are listed in table 1. Because the radioactivity emitted by U^{235} in a sample is small compared to that emitted

TABLE 1.—*Alpha-particle energies of uranium isotopes*

Isotope	Alpha energy (Mev) and relative atom percent abundance (in parentheses) [1]
U^{238}	4.195 (100)
U^{234}	4.768 (72); 4.717 (28)
U^{235}	4.559 (6.7); 4.520 (2.7); 4.370 (25); 4.354 (35); 4.333 (14); 4.318 (8); 4.117 (5.8)

[1] Alpha spectrum data from Strominger and others (1958, p. 817–818).

by U^{238} and U^{234}, the U^{235} activity was not used in this investigation.

On the basis of previous fluorimetric determinations of uranium, a weighed amount of sample was taken so that, at the most, 100 micrograms of uranium as a final product could be obtained (Francis and Tchang, 1935). The sample was digested with HCl, double attacked with HNO_3, and left on the hot plate until dry. The residue was taken up with approximately 10 milliliters of $6N$ HNO_3, filtered through a very fine filtering membrane, and the solid phase was discarded. The filtered solution was loaded on an anion exchange column (θ 10×120 mm, AG 1—X8, 100–200 mesh, NO_3^{-1} form), after which the column was washed with 2 column volumes of $6N$ HNO_3. The uranium and thorium adsorbed by the resin (Grindler, 1962, p. 215) were eluted with 3 column volumes of H_2O and the eluate was evaporated to dryness. The uranium and thorium nitrates were converted to chlorides by double treatment with HCl. The residue of chlorides was dissolved with approximately 10 ml of $6N$ HCl and loaded on an anion exchange column (θ 5×80 mm, AG 1—X8, Cl^{-1} form) to separate the uranium from the thorium (Grindler, 1962, p. 205). The column was washed with 2 column volumes of $6N$ HCl, and the uranium adsorbed on the resin was eluted with 3 column volumes of H_2O.

To assure complete separation of the uranium from the thorium isotopes, the eluate was repurified by anion exchange in the chloride form. The final eluate was evaporated, and the residue was dissolved with approximately 1 ml of $6N$ HCl after which 8 ml of $2M$ NH_4Cl was added and the pH adjusted to 3–4 with dilute NH_4OH.

The uranium solution was placed in an electroplating cell, and the uranium isotopes were plated on a titanium disk (2.5 centimeters diameter) serving as the cathode, according to the method used by Dooley and others (1964, p. 589). The electroplating process lasted 20 minutes using a current of 1.5–2.0 amperes. Before the anode was taken out of the cell, approximately 5 drops of NH_4OH were added to increase retention of the uranium isotopes as hydrous oxides on the cathode (Ko, 1957). The disk was washed with water, heated for approximately 30 seconds in a gas flame, cooled, and the alpha spectrum of uranium was measured to obtain the U^{234}/U^{238} activity ratio, which is expressed in weight equivalent percent when compared to the reference uranium source which is in radioactive equilibrium.

Radiochemical methods (Rosholt, 1957; Rosholt and Dooley, 1960) were used for the determination of the radioactive daughter products in the decay series below uranium. The results for these daughter products and for U^{234} in table 2 are expressed as equivalents to the

TABLE 2.—*Radioactive-disequilibrium analyses of samples from the Wentz mine, eastern Gas Hills area, Wyoming*

[Isotopes given as percent equivelent of ultimate parent nuclide, except as noted]

USGS Sample No.	Field No. (fig. 1)	eU[1] (percent)	U^{238} [2] (percent)	Pa^{231}	U^{234}	Th^{230}	Ra^{226}	Rn^{222}	Pb^{210}
256377	24a	0.090	0.033	0.11	0.026	0.086	0.16	0.10	0.14
256378	24b	.11	.25	.25	.042	.30	.17	.13	.17
256379	25	.026	.010	.035	.008	.050	.044	.03	.046
256380	26	.087	.11	.15	.079	.11	.063	.05	.062
256375a	[3] 23a	.27	.51	.54	------	.33	.40	.08	.47
256375b	23b	.16	.29	.32	.22	.19	.22	.03	.20
256381	27	.11	.18	.16	.13	.090	.079	.05	.065
256382	28	.078	.081	.15	.059	.094	.097	.06	.081
256383	29	.12	.20	.19	.16	.10	.095	.08	.087
256384	30	.11	.14	.18	.088	.12	.11	.08	.11
256385	31	.35	.66	.50	.55	.31	.20	.11	.18
256386	32	.16	.23	.17	.19	.090	.088	.07	.095
256387	33	.072	.10	.10	.075	.049	.043	.03	.038
256376	[4] 34	.035	.020	.089	.018	.061	.062	.04	.05

Analytical uncertainty of these values is not expected to exceed ± 5 percent except for Rn^{222}, whose uncertainty is not expected to exceed ± 10 percent.
[1] eU (radiometric) assays by J. Angelo.
[2] Based on chemical uranium analyses by H. Lipp, J. Wahlberg, and E. Fennelly.
[3] Selected most carbon-rich part of No. 23.
[4] Not shown in figure 1.

parent nuclides in terms of percent equivalent, which is the amount, in percent of U^{238} under the assumption of radioactive equilibrium, required to support the amount of daughter product actually present in the sample. These units are expressed on the basis of weight percent. The activity ratios, which are numerically identical to equivalent ratios, of U^{234}/U^{238} as determined by alpha spectrometry are shown in table 3. The ratios of Th^{230}/Pa^{231}, determined as Th^{230}/Th^{227} (Rosholt, 1957), and the ratios of Th^{230}/U^{234} and Pa^{231}/U^{234}, calculated from the values in table 2, are listed in table 3 in units of percent equivalent. Based on equivalent units, Pa^{231}/U^{235} is the same as Pa^{231}/U^{238}, assuming no measurable fractionation between U^{235} and U^{238}.

URANIUM EMPLACEMENT AND MIGRATION

One method used for comparison of sample disequilibrium in previous studies (Dooley and others,

TABLE 3.—*Isotopic ratios in samples from the Wentz mine, eastern Gas Hills area, Wyoming*

[Ratios given as radioactive equivalent ratios]

USGS Sample No.	Field No. (fig. 1)	$\dfrac{U^{234}}{U^{238}}$	$\dfrac{Th^{230}}{Pa^{231}}$	$\dfrac{Th^{230}}{U^{234}}$	$\dfrac{Pa^{231}}{U^{235}}$
256377	24a	0.80	0.78	3.3	3.0
256378	24b	.71	1.2	7.1	4.2
256379	25	.84	1.4	6.3	3.5
256380	26	.74	.73	1.4	1.4
256375b	23b	.76	.59	.86	1.1
256381	27	.74	.56	.69	.89
256382	28	.72	.63	1.6	1.9
256383	29	.78	.53	.63	.95
256384	30	.73	.67	1.4	1.3
256385	31	.84	.62	.56	.76
256386	32	.82	.53	.47	.74
256387	33	.75	.49	.65	1.0
256376	34	.93	.69	3.4	4.4

The U^{234}/U^{238} and Th^{230}/Pa^{231} values were measured directly as ratios, and the analytical uncertainties in these values are believed to be ± 1.5 percent and ± 4 percent, respectively. Thus, the analytical uncertainties in the calculated Th^{230}/U^{234} and Pa^{231}/U^{235} ratios are ± 7 percent.

1964, p. 592) is shown in figure 2. Plots of Th^{230}/Pa^{231} versus U^{234}/U^{238} are made and the samples are classified according to type of disequilibrium. The 4 uppermost samples from the mine face (Nos. 24a, 24b, 25, and 26) and the sample of oxidized sandstone from the roof of the mine (No. 34) contain Th^{230} in excess of both U^{234} and U^{238}. Two samples (Nos. 28 and 30) stratigraphically below these 4 upper samples also contain an excess of Th^{230}; all 7 of these samples represent uranium-leached sandstone. The 3 samples nearest the standing water and 2 samples (Nos. 27 and 29) and the carbon fragment (23b) represent Th^{230}-deficient sandstone. There is no systematic difference between the classes of samples and in the amount of U^{234} deficiency, which ranges from 16 to 29 percent for all samples from the mine face. Samples from the Th^{230}-deficient sandstone have a lower Th^{230}/Pa^{231} ratio than the U^{234}/U^{238} ratio, indicating more recent emplacement of uranium than in the uranium-leached sandstone.
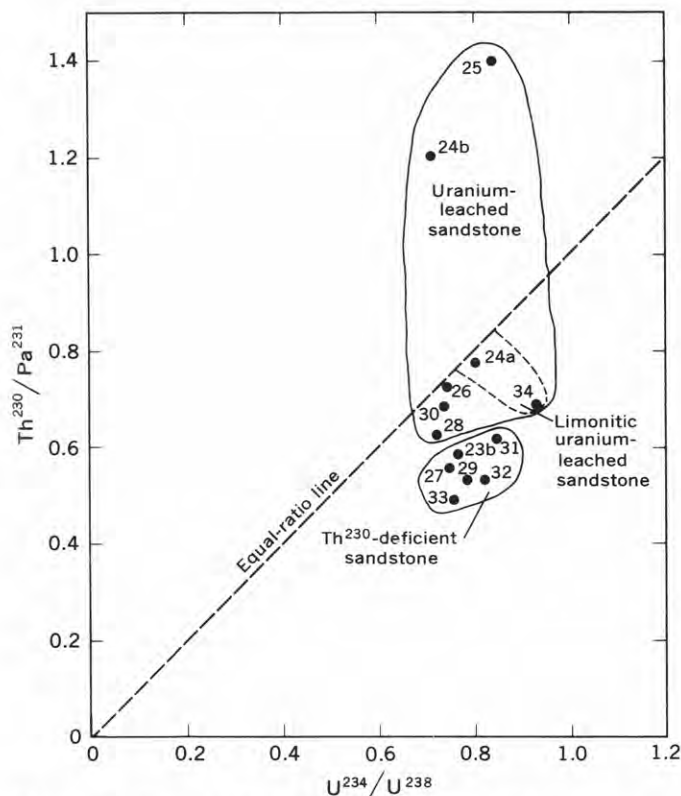
points from the equal-ratio line. A time-interval reference scale is constructed in the lower left-hand part of figure 3 by projecting the distance, normal to the equal-ratio line, of coordinates calculated from the growth of Pa^{231} and Th^{230} from U^{235} and U^{234}. The half-lives used for Pa^{231} and Th^{230} growth are 32,500 years and 75,200 years, respectively.

It appears possible to make a rigorous mathematical derivation for a method of calculating the time interval since emplacement of uranium, on the basis of the variation of the original U^{234}/U^{238} ratio and the amount of preferential leaching of authigenic U^{234}. A description of this technique, which requires determination of the Th^{230}/Pa^{231} and U^{234}/U^{238} ratios present in a sample, and its application to uranium ores from the Gas Hills, Shirley Basin, and Powder River basin, Wyoming, and the Slick Rock district Colorado, is in preparation.

The graphic estimation used in this report appears valid only for those samples that are classified as Th^{230} deficient. Analytical uncertainty in the graphic estimation should not exceed ± 10 percent; however, additional uncertainties of about 20 percent in the estimated time since emplacement could be introduced if uranium was excessively leached from the deposit at a time other than recently. The use of a more rigorous

FIGURE 2.—Plot of Th^{230}/Pa^{231} ratio versus U^{234}/U^{238} ratio in samples showing grouping of uranium-leached sandstone and Th^{230}-deficient sandstone. Location of samples taken at drift face is shown in figure 1.

A graphic representation of the relative chronology of uranium emplacement can be illustrated better by comparison of the log of Th^{230}/U^{234} and the log of Pa^{231}/U^{235} as plotted in figure 3. An approximation of the time interval since emplacement of uranium can be estimated from the minimum distance of sample
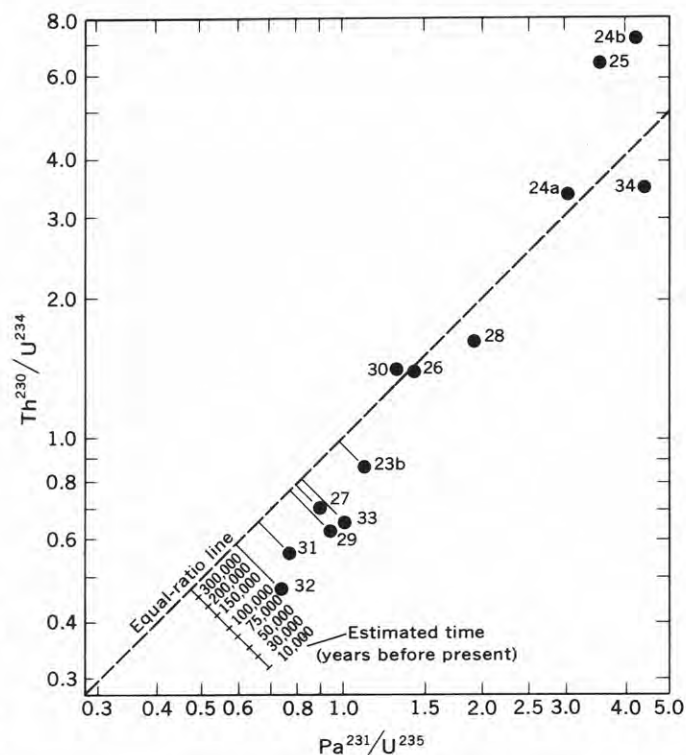

FIGURE 3.—Logarithmic plot of Th^{230}/U^{234} ratio versus Pa^{231}/U^{235} ratio in numbered samples from the Wentz mine. Lengths of lines connecting samples from Th^{230}-deficient sandstone with the equal-ratio line indicate estimated time intervals since emplacement as measured on reference scale.

model for calculating this time interval possibly could reduce the uncertainty in the time interval. Thus the time interval since uranium emplacement in the siltstone near the standing water is about 80,000 years, although it appears that a greater fraction of the uranium has been leached from the sample at the water level. The time interval since emplacement generally becomes greater with increasing distance above the water level.

The analyses of Pa^{231} and Th^{230} and its daughter products from ore of the Wentz mine were included in an earlier report (Rosholt, 1963, p. 202). Addition of U^{234}/U^{238} data determined by the second author of this paper does not significantly alter the interpretations regarding the migration of uranium previously reported for this deposit (Rosholt, 1963, p. 88). Consideration of U^{234}/U^{238} data indicates that the time interval since uranium emplacement was 2 to 3 times greater than that calculated from Th^{230}/Pa^{231} ratios, assuming radioactive equilibrium between U^{234} and U^{238} (Rosholt, 1963, p. 203).

An additional interpretation based on the similarity of U^{234}/U^{238} ratios in all samples indicates that the uranium was deposited with a deficient amount of allogenic U^{234} and that this deficiency was maintained by a relatively continuous preferential leaching of the authigenic U^{234}.

REFERENCES

Dooley, J. R., Tatsumoto, M., and Rosholt, J. N., Jr., 1964, Radioactive disequilibrium studies of roll features, Shirley Basin, Wyoming: Econ. Geology, v. 59, p. 586–595.

Francis, Marcus, and Tcheng-Da-Tchang, 1935, Sur las préparation de couches minces de l'oxyde d'uranium, U_3O_8, par e'lectrolyse: Comptes Rendus de l'Academie de Sciences, Paris, v. 200, p. 1024–1027.

Grindler, J. E., 1962, The radiochemistry of uranium: Natl. Academy of Sciences, Natl. Research Council, NAS–Ns 3050, 350 p.

Ko, Roy, 1957, Electrodeposition of the actinide elements: Nucleonics, v. 15, no. 1, p. 72–77.

Rosholt, J. N., Jr., 1957, Quantitative radiochemical methods for the determination of the sources of natural radioactivity: Anal. Chem., v. 29, p. 1398–1408.

——— 1963, Uranium in sediments: U.S. Geol. Survey open-file rept. 147, 211 p.

Rosholt, J. N., Jr., Butler, A. P., Garner, E. L., and Shields, W. R., 1965, Isotopic fractionation of uranium in sandstone, Powder River basin, Wyoming, and Slick Rock district, Colorado: Econ. Geology, v. 60, p. 199–213.

Rosholt, J. N., Jr., and Dooley, J. R., Jr., 1960, Automatic measurements and computations for radiochemical analyses: Anal. Chem., v. 32, p. 1093–1098.

Rosholt, J. N., Garner, E. L., and Shields, W. R., 1964, Fractionation of uranium isotopes and daughter products in weathered granite and uranium-bearing sandstone, Wind River basin region, Wyoming, in Geological Survey Research 1964: U.S. Geol. Survey Prof. Paper 501–B, p. B84–B87.

Rosholt, J. N., Jr., Harshman, E. N., Shields, W. R., and Garner, E. L., 1964a, Isotopic fractionation of uranium related to roll features in sandstone, Shirley Basin, Wyoming: Econ. Geology, v. 59, p. 570–585.

Strominger, D., Hollander, J. M., and Seaborg, G. T., 1958, Table of isotopes: Reviews of Modern Physics, v. 30, p. 585–904.

Zeller, H. D., 1957, The Gas Hills uranium district and some probable controls for ore deposition, in Wyoming Geol. Assoc. Guidebook 12th Ann. Field Conf., Southwestern Wind River basin, Wyoming: p. 156–160.

PLIOCENE AGE OF THE ASH-FLOW DEPOSITS OF THE SAN PEDRO AREA, CHILE

By ROBERT J. DINGMAN, Lawrence, Kans.

Abstract.—Extensive ash-flow sheets cover a large part of Chile, Bolivia, Argentina, and southern Peru. Biotite separated from four samples of ash flow collected near San Pedro de Atacama, Chile, yielded K-Ar ratios indicative of a Pliocene age. The determined ages range from 4.7 to 7.6 million years and are all well within the time span of the Pliocene according to Holmes' (1960) time scale. The close clustering of the age results, the freshness of the glass and feldspar in the ash flows, and in the same region the lack of demonstrably younger geologic events that could have affected the biotite all lead to the conclusion that the ages obtained are close to the true age of the ash flow in this region.

Extensive ash-flow deposits mantle the slopes of the Andes and the high plain (puna) of Chile, Peru, Bolivia, and Argentina. These deposits cover many thousands of square kilometers and form one of the most extensive geologic units in South America and also one of the most extensive series of ash flows in the world. The area of exposed ash flow in northern Chile is indicated in figure 1. The ash-flow deposits in northern Chile are exposed over an area of about 66,000 square kilometers. The actual extent of the deposits is much greater, as they underlie the sediments in the Pampa del Tamarugal, the Salar de Atacama, and several other basins, and also occur in erosional remnants too small to be shown on figure 1. The maximum thickness of the ash flows is unknown, but Brüggen (1950, p. 123) reports a thickness of 1,000 meters in the Quebrada Tarapacá. Assuming an average thickness of 50 m, the total volume of pyroclastic material in northern Chile is nearly 4,000 cubic kilometers. Addition of the contiguous ash-flow deposits in Argentina, Bolivia, and Peru would increase this figure several fold.

The period of explosive volcanic activity in the region apparently began with a series of relatively minor eruptions of ash building up rapidly to the intense activity that resulted in the deposition of a major ash sheet. In northern Chile the oldest ash flow is the thickest and most extensive of the sequence. For example, Member 2 of the Altos de Pica Formation (Galli and Dingman, 1962) is the oldest major ash flow in the Pica area and is also the thickest and most completely welded. This member extends in the subsurface across the Pampa del Tamarugal to the base of the coastal range. Near Arica the oldest ash flow is also the most extensive and in many localities the thickest and most dense. A few thin lenticular beds of unconsolidated ash are intercalated with the upper few meters of sediments that underlie the first major ash flow. A series of ash-flow deposits and intercalated fanglomerate sediments overlie the major ash sheet throughout much of northern Chile. Volcanic activity continued for several million years and in southern Peru extended on a very minor scale into historic time. The series of ash flows blanketed much of the first major flow except in its western extension. The stratigraphic situation of the ash-flow deposits is analogous to that of the glacial deposits in central North America, where the oldest drift sheet extended farthest to the south and then was partly covered by a series of drift sheets from the other major glaciations, leaving the older, Nebraskan drift exposed to the south of younger drift.
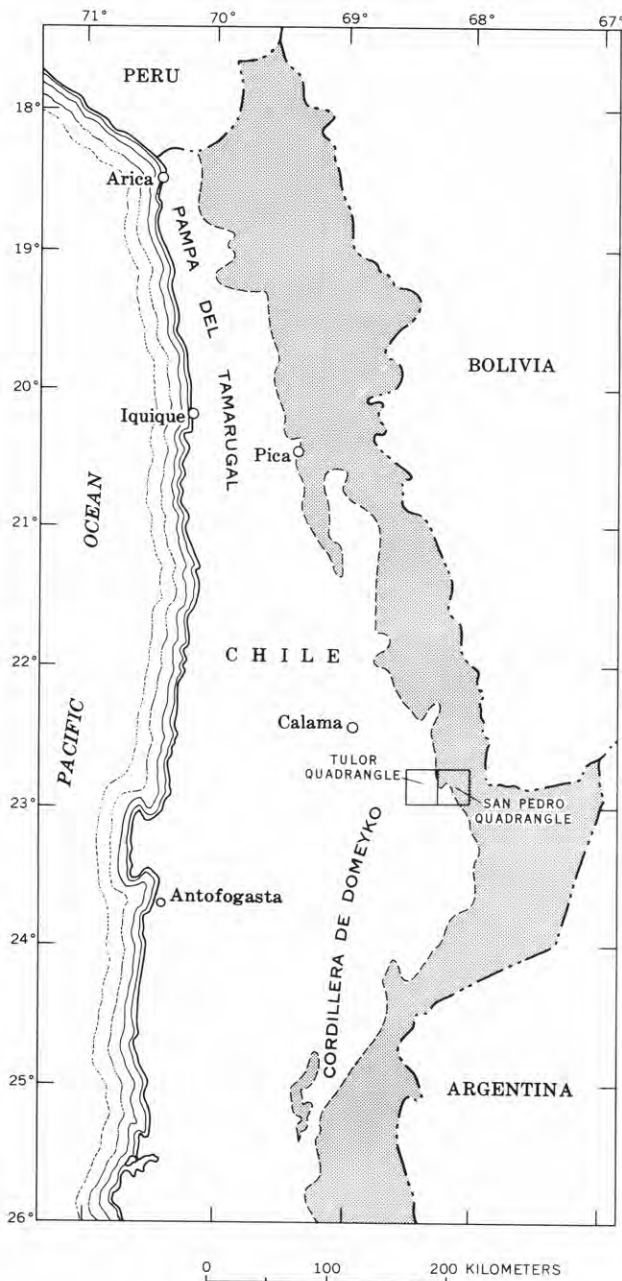
FIGURE 1.—Map of northern Chile, showing approximate extent of outcropping ash-flow deposits (patterned) and the location of the Tulor and San Pedro quadrangles.

The unweathered appearance and relative lack of erosion observed in the field, as well as the unaltered character of the glass and feldspar in thin sections, have caused several authors to postulate a Pleistocene age for these deposits. Other geologists, impressed by the aggregate thickness of the ash flows and the intercalated alluvial deposits, have considered them to be Miocene in age. The interbedded sediments are

continental in origin, and the only fossil evidence for age determination is the identification of a fragment of the jaw bone of a *Nesodon* as being similar to that of a species found in the Miocene of Argentina (Douglas, 1914). The conclusions of various authors regarding the age of the ash-flow series are summarized in table 1.

In 1961 an attempt was made to determine the age of the ash-flow deposits of the Altos de Pica Formation by means of lead-alpha determinations. The small quantities of zircon and the very small fraction of lead developed in these rocks caused ambiguous results, and the calculations could not be used.

Later in 1961, samples for use in the potassium-argon method were collected in the vicinity of San Pedro de Atacama. The geology of this area (fig. 2) was mapped by the author in 1960 and 1961 (Dingman, 1963, 1964). San Pedro de Atacama is located in a structural basin at the western edge of the puna. The puna is covered by late Tertiary ash-flow deposits that dip westward under the sediments of the basin and reappear overlying an elongated zone of salt domes and anticlines which parallel the long axis of the basin. The ash-flow deposits also are exposed in the Cordillera de Domeyko, west of the basin. The basin was filled with fine-grained clastic sediments and evaporites prior to the deposition of the ash flows. The salt domes were formed in Tertiary basin deposits by gravitational gliding (Dingman, 1962). The formation of these structures was mainly completed prior to deposition of the major ash-flow sheets and, therefore, the tuffs lie with angular unconformity over the domal structures. A few thin ash beds are intercalated in the upper 50 m of the folded Tertiary sedimentary rocks. Samples for dating were taken from the oldest major ash-flow sheet from exposures in the Cordillera de Domeyko, the Quebrada de Tambores on the west slope of the basin, and from an exposure in the Cordillera de la Sal. Sample 2 (table 2) was taken from an ash bed intercalated in the Tertiary strata. This bed dips vertically at the same locality.

The ash-flow deposits in the San Pedro area increase in density and hardness to the west toward the volcanic vents of fissures from which they originated. In the sampled locality the deposits are pale-yellowish-brown moderately hard tuff. The matrix consists of unaltered to slightly altered glass shards that are curved and welded. Axiolitic structure occurs but is not common. The phenocrysts are of biotite, oligoclase, and less commonly quartz, amphibole, and opaque

TABLE 1.—*Tertiary and Quaternary formations containing ash-flow deposits in northern Chile and adjoining areas*

[From Dingman and Lohman, 1963, p. C70]

Period	Epoch	Bolivia (Douglas, 1914)	Bolivia (Ahlfeld, 1946)	Peru (Jenks, 1948)	Chile (Brüggen, 1950)	Argentina (Groeber, 1957)	Chile (Galli and Dingman, 1962)	Chile (Doyel and Henriquez, written communication, 1962)	Chile (Dingman, 1963)
Quaternary	Pleistocene				Riolítica Formacion[1] (Chile)		Altos de Pica Formation	Lluta Formation[1]	Unnamed formation of ash-flow deposits[1]
Tertiary	Pliocene		Estratos del Rio Mauri[1]			Araucaniano Formacion	Altos de Pica Formation	Lluta Formation[1]	Unnamed formation of ash-flow deposits[1]
Tertiary	Miocene	Mauri Volcanic Series[1]			Liparítica Formacion[1] Riolítica Formacion[1]		Altos de Pica Formation	—??—	San Pedro Formation Tambores Formation
Tertiary	Oligocene			Corcoro System	? Chacani Volcanics ?		Altos de Pica Formation	Putani Formation Arica Formation	San Pedro Formation Tambores Formation
Tertiary	Eocene			Corcoro System			Altos de Pica Formation	Putani Formation Arica Formation	San Pedro Formation Tambores Formation
Tertiary	Paleocene				San Pedro Formacion		Altos de Pica Formation	Putani Formation Arica Formation	San Pedro Formation Tambores Formation

[1] Stratigraphically and lithologically equivalent to the Altos de Pica Formation.

minerals. The biotite phenocrysts are euhedral, range in length from 0.2 to 1.6 mm, and have inclusions of magnetite, apatite, and scarce zircon. The aspect of the rock, both in hand specimen and in thin section, is fresh or slightly altered.

The biotite was separated from the four San Pedro samples in the laboratories of the Instituto de Investigaciones Geológicas by Fernando Munizaga and was sent to the U.S. Geological Survey in Washington, D.C., for age determinations by the potassium-argon method. The results are given in table 2. According to the geologic time scale proposed by Holmes (1960) the calculated ages are all well within the time span assigned to the Pliocene Epoch. Because (1) all 4 age results cluster closely (6.3 ± 1.3 million years), (2) the rocks are apparently fresh, and (3) younger geologic events that could have influenced the po-

TABLE 2.—*K-Ar ages of biotite from the ash-flow deposits*

[Analysts: R. W. Kistler and P. Elmore, U.S. Geological Survey]

Field No.	K_2O (percent)	K^{40} (ppm)	Ar^{40} (ppm)	Radiogenic Ar^{40} (percent)	Ar^{40}/K^{40}	Age (million years)
1	7.79	7.89	0.00351	31	0.000445	7.6
2	7.86	7.96	.00248	19	.000311	5.3
3	6.42	6.50	.00289	34	.000444	7.6
4	7.77	7.87	.00217	16	.000276	4.7

Decay constants:
K^{40}: 0.585×10^{-10} yr^{-1} (electron capture)
4.72×10^{-10} yr^{-1} (beta decay)
Abundance ratio:
$K^{40}=1.22\times10^{-4}$ g/g K

tassium-argon ratios are not known in the region, the ages obtained are believed to be close to the true age of the ash-flow sheet in this region.
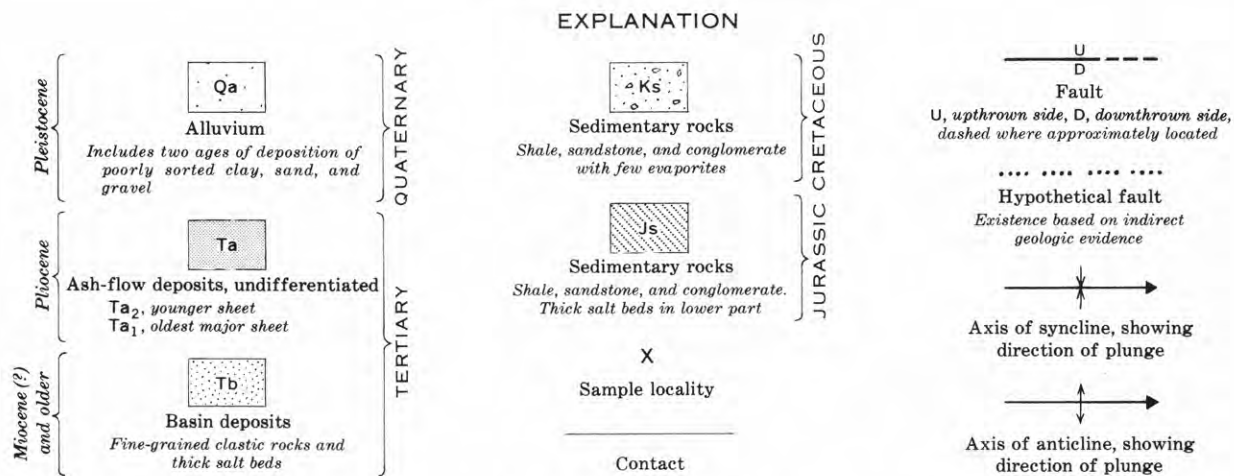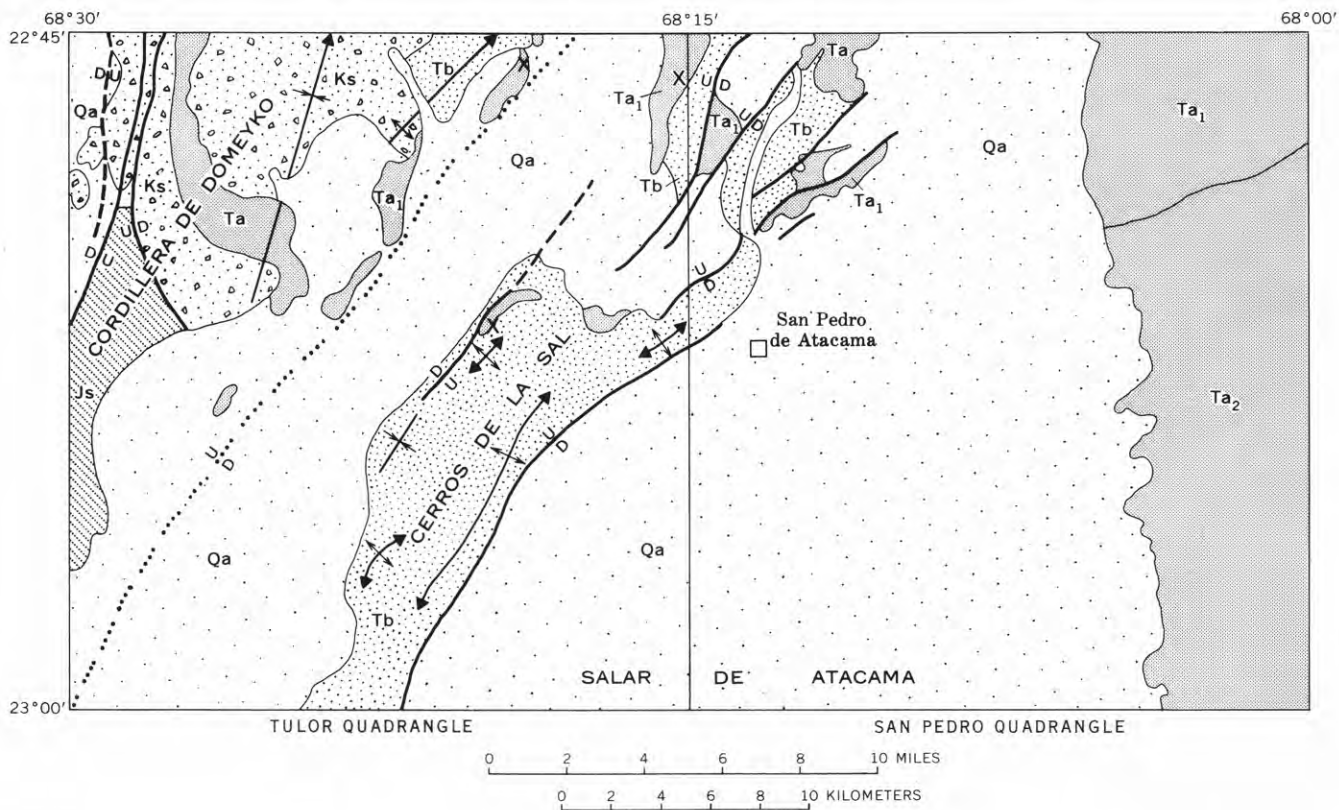
FIGURE 2.—Generalized geologic map of the San Pedro and Tulor quadrangles, Antofagasta province, Chile.

REFERENCES

Ahlfeld, Friedrich, 1946, Geología de Bolivia: La Plata, Argentina, Mus. La Plata Rev. (nueva serie), Sección Geol., v. 3, p. 3–370.

Brüggen, Juan, 1950, Fundamentos de la geología de Chile: Santiago, Chile, Inst. Geográfico Militar, 374 p.

Dingman, R. J., 1962, Tertiary salt domes near San Pedro de Atacama, Chile: Art. 147 *in* U.S. Geol. Survey Prof. Paper 450–D, p. D92–D94.

―――― 1963, Quadrangulo Tulor, Antofogasta Province, Chile: Santiago, Chile, Inst. Inv. Geol., Carta Geol. de Chile, v. 4, no. 11, 35 p., 1 pl., 7 figs.

―――― 1964, Quadrangulo San Pedro: Santiago, Chile, Inst. Inv. Geol., Carta Geol. de Chile. [In press]

Dingman, R. J., and Lohman, K. E., 1963, Late Pleistocene diatoms from the Arica area, Chile: Art. 78 *in* U.S. Geol. Survey Prof. Paper 475–C, p. C69–C72.

Douglas, J. A., 1914, Geological sections through the Andes of Peru and Bolivia, I. From the coast of Arica in the north of Chile to La Paz and the Bolivian "Yungas": Geol. Soc. London Quart. Jour., v. 70, p. 1–53.

Galli, C. O., and Dingman, R. J., 1962, Quadrangulos Alca, Pica, Matilla y Chacarilla: Santiago, Chile, Inst. Inv. Geol., Carta Geol. de Chile, v. 3, nos. 2, 3, 4, and 5, 125 p., 11 pl., 12 figs.

Groeber, Pablo, 1957, Chile, pt. 7 *of* Amerique Latine, *in* Hoffstetter and others, Lexique Stratigraphique International: Paris, France, Comm. Stratigraphy, Internat. Geol. Cong., v. 5, p. 195.

Holmes, Arthur, 1960, A revised geological time scale: Edinburgh Geol. Soc. Trans., v. 17, pt. 3, p. 204.

Jenks, W. F., 1948, Geologia de la Hoja de Arquipa: Lima, Peru, Dirección de Minas y Petroleo Bull. 9.

JURASSIC AGE OF A MAFIC IGNEOUS COMPLEX, CHRISTIAN QUADRANGLE, ALASKA

By H. N. REISER, M. A. LANPHERE, and W. P. BROSGE,
Menlo Park, Calif.

Abstract.—Potassium-argon age determinations, one on plagioclase from diorite, the other on hornblende from leucogabbro, indicate that a large mafic igneous complex in the Christian quadrangle, northeastern Alaska, was emplaced in Jurassic time. Recently identified pollen and spores indicate that some of the intruded sedimentary rocks are Triassic in age.

Potassium-argon ages here described indicate a Jurassic age for a large complex of mafic igneous rocks located in the Christian quadrangle, about 25 miles southeast of the Brooks Range, in northeastern Alaska. Intruded sedimentary rocks dated as Triassic on the basis of pollen and spores provide a maximum limiting age for the emplacement of the complex. One of the two potassium-argon determinations was made on hornblende, a mineral found by past experience to give a reliable minimum age. In view of these factors the measured potassium-argon ages are believed to be close to the true age of the complex.

Rocks of this complex have previously been described as Carboniferous or Mesozoic in age by Mertie (1929), and as late Paleozoic in age by Brosgé and Reiser (1962). The complex consists mostly of hypabyssal intrusive rocks, but includes some extrusive and some plutonic rocks. Smaller bodies of similar rocks in and north of the Brooks Range have previously been assigned a tentative Jurassic age on the basis of field relations (Smith and Mertie, 1930; Patton and Tailleur, 1964). However, the only certainly identified Jurassic volcanic rocks in this region have been volcaniclastic beds in the Arctic foothills of the range that contain Middle Jurassic fossils (Patton and Tailleur, 1964; Jones and Grantz, 1964).

GEOLOGIC SETTING

The igneous complex occurs in a structural basin. Upper Paleozoic and lower(?) Mesozoic sedimentary rocks dip toward and beneath the complex, and large inclusions of sedimentary rocks also occur within the complex (fig. 1). Most of the rocks surrounding the complex are Devonian carbonate rocks and Devonian and Devonian(?) clastic rocks, but the rocks in actual contact with the complex are mostly chert, shale, and graywacke of late Paleozoic to Triassic age.

The lower part of the cherty sequence is a unit of bedded radiolarian chert and varicolored shale and argillite. The apparent stratigraphic position of this chert unit with respect to Devonian(?) and Mississippian units in and immediately north and northeast of the area covered by figure 1 indicates that the chert unit may be of Late Devonian, Early Mississippian, and post-Mississippian age. On the basis of the Triassic flora described below, some of the chert may be of Triassic age. Chert of this unit bounds the igneous complex for most of its length and also occurs within the complex.

Twelve large sheared blocks of Triassic and possibly older sedimentary rocks occur as inclusions in the igneous complex. These blocks consist of (1) shale; (2) graywacke, calcareous graywacke, and sandy limestone with interbedded chert, argillite, and rare volcaniclastic beds; and (3) interbedded shale and quartz sandstone. One small block of graywacke (locality 63ARr58, fig. 1, lat 67°38½' N., long 144°47' W.) whose contacts with the igneous rocks are covered, contains unidentifiable plant trash and a few plant microfossils. Richard A. Scott, of the U.S. Geological Survey (written communication, 1964), has identified 11
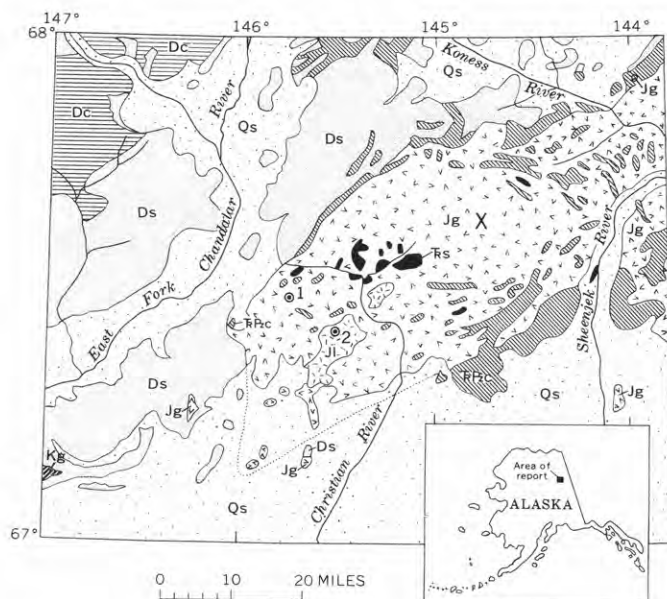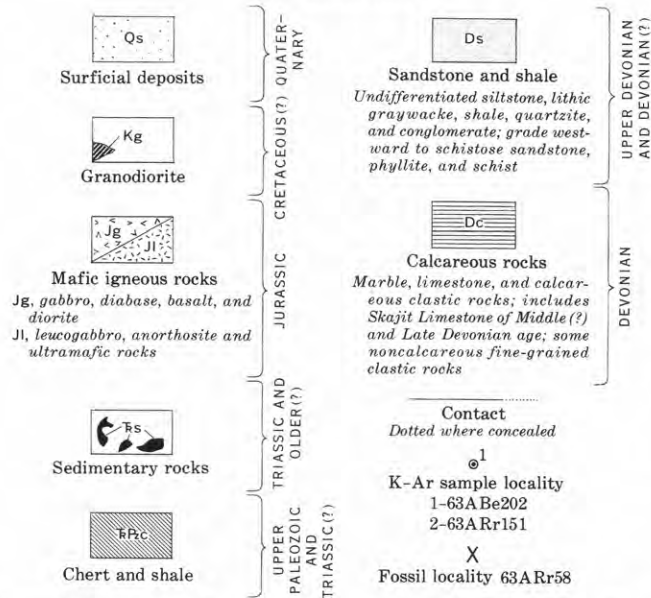
FIGURE 1.—Generalized geologic map of the Christian River area, Alaska, showing K-Ar sample localities and fossil locality.

genera of pollen and spores and has assigned this collection a Triassic age. According to Scott,

The poor preservation and limited number of specimens preclude identification of species. . . . The sample was originally dated as Permian or Triassic on the basis of the occurrence of *Taeniaesporites*. Of the newly recognized genera, *Vitreisporites*, *Gnetaceaepollenites*, and *Concavisporites* are not known from rocks older than Triassic. . . . *Striatites* has not been recorded from rocks as young as Late Triassic. Neither . . . *Striatites* nor *Taeniaesporites* is present in a large Rhaetic . . . assemblage from western U.S. . . . In summary, a Triassic age can now be assigned to sample 63ARr58 . . . .

Some of the graywackes correlated with this fossiliferous Triassic graywacke are interbedded with chert and argillite. Consequently, some of the chert in the

underlying chert-shale unit may well be of Triassic age.

IGNEOUS COMPLEX

The igneous complex is roughly oblong. It trends northeastward and is approximately 80 miles long and 30 miles wide. The sedimentary rocks adjacent to the northwestern and southeastern contacts, as well as most of the included layers of sedimentary rock, strike parallel to the margins of the complex and dip generally inward toward its center. Partial mapping of the northeast end of the body (not shown on fig. 1) indicates that the rocks along that margin also dip inward. The northwestern boundary of the complex is sharp and may be in part a fault, but at the eastern boundaries (not shown) the mafic rocks seem to extend on into the sedimentary rocks for about 20 miles in a series of irregularly distributed sills and dikes.

There is little evidence of intrusive effects at the margin of the complex and at its contacts with the inclusions. Most contacts between the complex and the sedimentary units are covered. Except for development of biotite in sandstone at one locality, thermal metamorphic effects are limited to the calcareous rocks. Calcareous graywacke is epidotized at one locality, and the many thin limestone beds that occur east of the map area are completely recrystallized, locally epidotized and generally almost completely silicified. At a few localities interpenetrating contacts, crosscutting and partly sheared contacts, and bands of fine-grained rubble interpreted to be chill zones were observed.

The igneous complex can be divided into two distinctly different groups of mafic rocks. The predominant group is dark and consists largely of gabbro, diabase, basalt, and diorite. The other group, which is restricted to the southwestern portion of the complex, is light colored, and consists primarily of banded hornblende leucogabbro. Exposed contacts between these two groups were not seen, so their relation could not be established.

The gabbro, diabase, and basalt that compose the group of dark rocks all have practically the same mineralogical composition. The plagioclase is commonly labradorite. Clinopyroxene is the dominant ferromagnesian mineral, but hornblende, both deuteric and secondary, also occurs. Iron oxides and apatite are common accessory minerals.

A closely related but somewhat less calcic and more siliceous phase representing a late stage of crystallization is indicated by local occurrences of diorite, quartz diorite, and quartz gabbro. Mertie (1929) determined that zoned feldspars in the quartz gabbro have labradorite cores and oligoclase rims. Oligoclase also oc-

curs in these rocks in myrmekitic intergrowths with quartz.

Generally the dark rocks are hydrothermally altered. The ferromagnesian minerals are chloritized and the plagioclase is clouded with alteration products. The plagioclase in some rocks is saussuritized and in others is partially altered to chlorite and illite.

The light-colored group of rocks consists of inter-banded hornblende leucogabbro, anorthosite, horn-blende gabbro, pyroxenite, and peridotite. Most of these rocks occur as frost-riven rubble. The leuco-gabbro is the most abundant of the light-colored rocks and consists of bands of almost pure labradorite separated by thinner bands of dark-green ferromagne-sian minerals. The bands range from thin streaks to bands several inches thick. Layering on a larger scale is suggested by alternating bands of rubble of leuco-gabbro, hornblende gabbro, and pyroxenite. Locally the leucogabbro intrudes hornblende peridotite and olivine gabbro.

Hornblende is the dominant ferromagnesian mineral in the leucogabbro, but clinopyroxene and some olivine are also found. In thin section the plagioclase and ferromagnesian minerals of the leucogabbro and anorthosite are fresh and unaltered. The rocks are allotriomorphic granular and some show mortar struc-ture. Protoclastic texture is evident in several thin sections where twisted and fractured plagioclase grains display curved twinning lamellae and undulating ex-tinction.

Some of the hornblende is later than the clino-pyroxene and olivine, but the hornblende of the dated specimen seems to be older than some of the feldspar. In the band of coarse-grained leucogabbro from which specimen 63ARr151 comes, stringers of only partly granulated labradorite penetrate cracks in the large hornblende crystals.

AGE

Potassium-argon ages were measured on partly al-tered plagioclase from a sample of diorite (63ABe202) from the dark group of rocks and on fresh hornblende from a sample of leucogabbro (63ARr151) from the light group.

The plagioclase of sample 63ABe202 is clouded with chlorite and illite as observed in thin section. However, an X-ray diffraction pattern of the separate used for potassium-argon analysis indicates that it is practically pure plagioclase.

The plus-or-minus value assigned each age (see ac-companying table) is the estimated standard devia-tion of analytical precision. We assume that the po-tassium-argon ages are minimum ages because there is no

Potassium-argon ages of minerals from a large intrusive complex, Christian quadrangle, Alaska

[Potassium analyses by H. C. Whitehead and L. B. Schlocker; argon analyses by M. A. Lanphere]

Field No.	Mineral	Location	K_2O (weight percent)	Ar^{40}_{rad} (moles/g)	$\dfrac{Ar^{40}_{rad}}{Ar^{40}_{total}}$	Apparent age (millions of years)
63ABe202__	Plagio-clase.	Lat 67°30′ N., long 145°45′ W.	1.12 1.13 ___ 1.125(avg)	2.677×10^{-10}	0.69	155±6
63ARr151__	Horn-blende.	Lat 67°28′ N., long 145°31′ W.	.246 .250 .254 .254 ___ .251(avg)	0.6503×10^{-10}	.51	168±8

K^{40} decay constants:
$\lambda_\epsilon = 0.585\times10^{-10}$ per year
$\lambda\beta = 4.72\times10^{-10}$ per year
Abundance ratio: $K^{40}/K = 1.19\times10^{-4}$ atom percent.

evidence that hornblende or plagioclase inherit signifi-cant amounts of radiogenic argon during crystalliza-tion.

The two ages agree within analytical uncertainty, and both results indicate a Jurassic age for the com-plex according to Kulp's (1961) compilation of the geologic time scale. The results suggest an Early or Middle Jurassic age, but more analyses should be made before such a specific age is assigned to the complex.

An investigation of mineral-age stability under con-tact-metamorphic conditions (Hart, 1964) and the re-sults of several geochronologic studies have shown that hornblende has very high retentivity for argon during thermal events that have affected a rock since its ini-tial crystallization. It has been shown that horn-blende generally gives a reliable crystallization age for an igneous or metamorphic rock. Thus, we consider the 168 million-year hornblende age to be not only a minimum age but the best available estimate for the time of emplacement of the complex. The hornblende age also is considered more reliable than the plagioclase age because the argon-retention properties of horn-blende are much better known than those of plagio-clase.

A Carboniferous or Mesozoic age was originally as-signed to the dark rocks of the igneous complex ex-posed along the Sheenjek River (Mertie, 1929) be-cause of the close association and intrusive relation of these rocks with the chert-shale unit. Mertie regarded this chert-shale unit as probably Late Devonian or Early Mississippian in age, but possibly Triassic in age. Brosgé and Reiser (1962), on the other hand, considered the chert and shale near the East Fork of the Chandalar to be late Paleozoic, probably Devonian, in age, and believed the igneous rocks to be volcanic

correlatives of the associated chert. New field data show that the igneous complex is largely intrusive, an interpretation strongly supported by the age results here described.

REFERENCES

Brosgé, W. P., and Reiser, H. N., 1962, Preliminary geologic map of the Christian quadrangle, Alaska: U.S. Geol. Survey open-file report, 2 sheets.

Hart, S. R., 1964, The petrology and isotopic-mineral age relations of a contact zone in the Front Range, Colorado: Jour. Geology, v. 72, p. 493–525.

Jones, D. L., and Grantz, Arthur, 1964, Stratigraphic and structural significance of Cretaceous fossils from the Tiglukpuk Formation, northern Alaska: Am. Assoc. Petroleum Geologists Bull., v. 48, no. 9, p. 1462–1474.

Kulp, J. L., 1961, Geologic time scale: Science, v. 133, no. 3459, p. 1105–1114.

Mertie, J. B., Jr., 1929, The Chandalar-Sheenjek district, Alaska: U.S. Geol. Survey Bull. 810–B, p. 87–139.

Patton, W. W., Jr., and Tailleur, I. L., 1964, Geology of the Killik-Itkillik region, Alaska: U.S. Geol. Survey Prof. Paper 303–G, p. 409–500.

Smith, P. S., and Mertie, J. B., Jr., 1930, Geology and mineral resources of northwestern Alaska: U.S. Geol. Survey Bull. 815, 351 p.

FIRST OCCURRENCE OF GRAPTOLITES
IN THE KLAMATH MOUNTAINS, CALIFORNIA

By MICHAEL CHURKIN, JR., Menlo Park, Calif.

Abstract.—Silurian graptolites have been found recently in the Klamath Mountains in shale and siltstone of the Gazelle Formation below its fossiliferous Payton Ranch Limestone Member (Middle or Upper Silurian). They confirm that part of the Gazelle Formation is at least as old as Middle Silurian. The graptolites provide a potentially useful tool in establishing the stratigraphic succession in this structurally complex region.

Corals and brachiopods of Ordovician(?), Silurian, and Devonian age and trilobites of Silurian age have been reported from isolated exposures of limestone near the northeastern edge of the Klamath Mountains, Calif. (Wells and others, 1959; Churkin, 1961), but up to now only unidentifiable fossil fragments have been found in the much thicker siltstone, graywacke shale, chert, conglomerate, and volcanic portions of the stratigraphic section. Many of the contacts of fossiliferous limestones with interstratified detrital rocks are sheared and faulted, and an important thrust fault (Wells and others, 1959; Churkin and Langenheim, 1960) further complicates reconstruction of the stratigraphic succession. Thus graptolites discovered by the writer in fine-grained detrital rocks that form most of the section offer promise of being a useful tool in establishing the stratigraphic succession and structures in the Klamath Mountains.

Along Lime Gulch, just west of Gazelle, in northern California, more than 600 feet of interbedded graywacke, shale, siltstone, bedded chert, and conglomerate is overlain by nearly 200 feet of massive limestone that contains Silurian fossils (Churkin and Langenheim, 1960). This entire sequence of beds, which belongs to the Gazelle Formation, is overlain in thrust-fault contact by phyllite and semischist. The limestone at the top of the Gazelle Formation in the Lime Gulch area has been named and mapped separately as the Payton Ranch Limestone Member, of Middle or

Late Silurian age, by Churkin and Langenheim (1960, p. 259, 262). Its type locality, about 1 mile northeast of Payton Ranch, was designated as the east side of the high peak (elevation 4,320 feet) in NE¼SW¼ sec. 6, T. 42 N., R. 6 W., Yreka quadrangle, Siskiyou County, Calif. The type section is 188 feet thick.

The graptolites reported in this article were collected from dark-gray siltstone and silty shale of the Gazelle Formation, in a small saddle (elevation 4,080 feet) at the northwestern tip of a south-sloping knob of the Payton Ranch Limestone Member in Lime Gulch, NE¼NW¼SW¼ sec. 12, T. 42 N., R. 7 W., Yreka 15-minute quadrangle, Siskiyou County, Calif. (fig. 1). The graptolites are preserved as faint impressions on light-gray (weathered) bedding surfaces.

The graptolitic siltstone and shale appear to be about 50 feet stratigraphically below the base of the Payton Ranch Limestone Member, but the lower contact of the limestone is faulted and the original stratigraphic separation between the graptolite-bearing rocks and the Payton Ranch may have been greater.

The graptolite collection consists of 40 individual specimens, most of which are so poorly preserved that only generic identification is possible. Species and species groups of monograptids, identified by the writer, are listed below with their stratigraphic ranges.

Monograptus sp. indet. (spirally coiled rhabdosome); spirally coiled monograptids indicate an upper Llandovery (late Early Silurian) age.

Monograptus sp. indet. (rhabdosome nearly straight, hooked thecae); monograptids with hooked thecae range from upper Llandovery through Wenlock (Middle Silurian).

Monograptus sp. indet. (rhabdosome straight, thecae of *M. vomerinus* type); species with thecae of *M. vomerinus* type range from upper Llandovery through Wenlock.
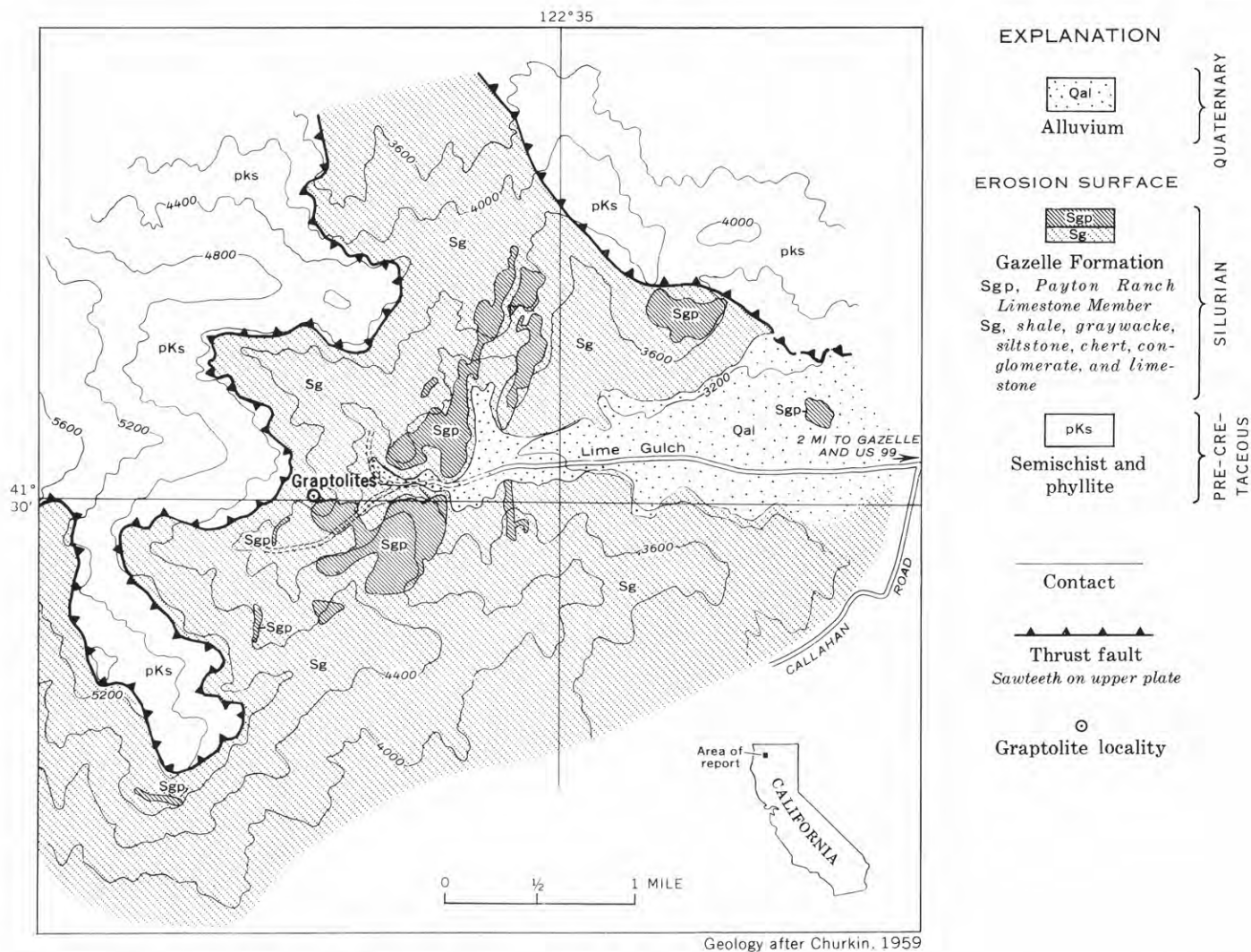
FIGURE 1.—Generalized geologic map of the Lime Gulch area, Siskiyou County, Calif., showing the graptolite locality described in text.

Monograptus sp. indet. (thin rhabdosome, straight to slightly curved; thecae simple and straight); Silurian. *Retiolites geinitzianus* (Barrande)?; ranges from upper Llandovery through lowest Wenlock.

The Gazelle Formation was assigned a Late Silurian age by Wells and others (1959), on the basis of corals and brachiopods from its Payton Ranch Limestone Member. The formation was assigned a Middle or Late Silurian age on the basis of trilobites from thin-bedded shale and limestone farther south (Churkin, 1961). The presence of the graptolites described here indicates that the shale and siltstone in the Gazelle Formation may be uppermost Llandovery (latest

Early Silurian) or Wenlock (Middle Silurian) in age, thus confirming that part of the Gazelle is a least as old as Middle Silurian.

REFERENCES

Churkin, Michael, Jr., 1961, Silurian trilobites from the Klamath Mountains, California: Jour. Paleontology, v. 35, p. 168–175.

Churkin, Michael, Jr., and Langenheim, R. L., Jr., 1960, Silurian strata of the Klamath Mountains, California: Am. Jour. Sci., v. 258, p. 258–273.

Wells, F. G., Walker, G. W., and Merriam, C. W., 1959, Upper Ordovician(?) and Upper Silurian formations of the northern Klamath Mountains, California: Geol. Soc. America Bull., v. 70, p. 645–650.

A PROPOSED REVISION OF THE SUBALKALINE INTRUSIVE SERIES OF NORTHEASTERN MASSACHUSETTS

By R. O. CASTLE, Los Angeles, Calif.

Abstract.—The subalkaline intrusive series of northeastern Massachusetts as given by C. H. Clapp in 1921 is revised to include the following units: (1) the Sharpners Pond Tonalite, (2) the Newburyport Quartz Diorite as mapped south and west of Boxford, (3) a "younger subalkaline intrusive series" defined by Toulmin in 1964, and (4) the Andover Granite. Inclusion of the Andover Granite with the "alkalic" intrusive series is rejected owing chiefly to its continuity with the demonstrably pre-"alkalic" Sharpners Pond Tónalite.

SUMMARY OF INTRUSIVE SERIES IN NORTHEASTERN MASSACHUSETTS

The plutonic rocks contained within that section of northeastern Massachusetts shown in figure 1 fall into a minimum of 3 and perhaps as many as 5 or 6 naturally defined groups known as intrusive series.
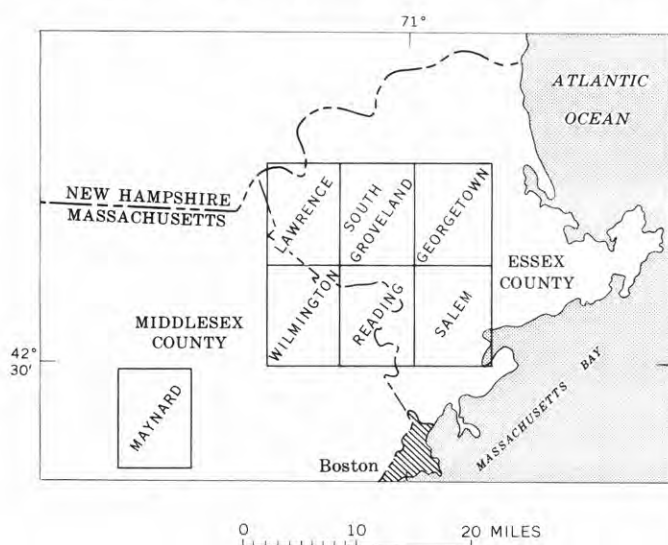

FIGURE 1.—Index map of northeastern Massachusetts, showing location of quadrangles referred to in this report.

An intrusive series may be defined, in turn, as a set of plutonic igneous rocks closely associated in time and space, with no implication as to magma source or sources. Currently recognized intrusive series in northeastern Massachusetts include at least the following: (1) an unnamed series consisting chiefly of the Dracut Diorite and Ayer Granite, (2) an "alkalic" intrusive series, and (3), a subalkaline intrusive series.

The Dracut Diorite and Ayer Granite (Emerson, 1917, p. 223) lie generally north and west of a major fault trending east-northeast through the southern part of the city of Lawrence. The relation between this sequence and the other intrusive rocks of northeastern Massachusetts is not entirely clear; however, as it seems to be sharply separated areally from the other plutonic rocks of this area, which occur largely or entirely to the south of the major fault alluded to above, the Dracut and Ayer sequence need not be considered further here. The remaining intrusive rocks of northeastern Massachusetts, particularly those in Essex County, generally have been referred to one or the other of two major series to which Clapp (1921) gave the names "alkaline" and "subalkaline."

The rocks of the alkaline series have been studied by a number of geologists and recently have been investigated in detail by Toulmin (1960, 1964). Toulmin (1964, p. A24) has renamed Clapp's alkaline group the " 'alkalic' intrusive series;" he has retained the general term "because many of the rocks in the series contain peralkaline minerals," but the term has been enclosed by quotation marks, for "chemical analyses of the rocks do not support a peralkaline character for the series as a whole." According to Toulmin (1964), the rocks of the "alkalic" series are characterized by relatively low calcium content, relatively high alkali-

alumina and iron-magnesium ratios, and a general absence of alteration and deformation.

The subalkaline intrusive series heretofore has been investigated only cursorily. Clapp (1921, p. 21-25) concluded from his studies of the igneous rocks of Essex County that the Salem Gabbro-Diorite, the Newburyport Quartz Diorite, and the Dedham Granodiorite comprised his subalkaline group. He (1921, p. 29) suggested, moreover, that the Andover Granite be included, along with the Quincy Granite and Beverly Syenite, in the alkaline group. Emerson (1917, p. 218, 220-221), on the other hand, felt that the Andover was unrelated to Clapp's alkaline group and belonged to a still later epoch of igneous activity. Mapping in the Salem quadrangle led Toulmin (1964) to divide Clapp's subalkaline group into "older" and "younger" subalkaline intrusive series, both of which are clearly separable from the still younger "alkalic" intrusive series. According to Toulmin (1964, p A10), the Salem Gabbro-Diorite and the Newburyport(?) Quartz Diorite constitute the "older subalkaline intrusive series" of probable early Paleozoic or Precambrian age. Undifferentiated diorite and gabbro, a medium-grained granodiorite-adamellite body cropping out along a zone trending northeast through Middleton and Topsfield, and the Topsfield Granodiorite have been grouped together by Toulmin (1964, p. A18-A24) as the "younger subalkaline intrusive series" of probable middle Paleozoic age.

REDEFINITION OF THE SUBALKALINE INTRUSIVE SERIES

Recent bedrock studies in the Lawrence, Wilmington, South Groveland, and Reading quadrangles by the writer, and the Salem quadrangle by Toulmin (1964), have made possible a more explicit definition of the subalkaline intrusive series than was previously possible. The field relations and lithologic characteristics of the igneous rocks examined in these five quadrangles indicate that the subalkaline series should be redefined to include at least the following: (1) the intrusive igneous rocks west of long 71°00′ W. and northwest of Middleton and Topsfield centers formerly mapped with the Salem Gabbro-Diorite (Emerson, 1917, pl. X; Clapp, 1921, pl. 1), (2) the Newburyport Quartz Diorite as mapped south and west of Boxford, (3) the "younger subalkaline intrusive series" of Toulmin, and (4) the Andover Granite. The major units of the subalkaline intrusive series as defined here (fig. 2) are units 1 and 4 of the above listing. Revision of the series is based chiefly on the probable continuity between these two major units; inclusion of other rocks with the subalkaline series is based in turn on their probable correlation with either unit 1 or 4. In addition to the rocks tabulated above, at least two other separately mapped intrusive formations in Middlesex County, and perhaps the Salem Gabbro-Diorite as well, ultimately may be found to belong to the subalkaline intrusive series. Although geographic as opposed to compositional names are to be preferred in the naming of intrusive series, the original name for this series is retained here in substance and form; little benefit would accrue by changing or modifying the name, for it has been firmly established by Clapp and perpetuated by Toulmin.

Sharpners Pond Tonalite

The name Sharpners Pond Tonalite is adopted here for the generally melanocratic plutonic rocks west of long 71°00′ W. and northwest of Middleton and Topsfield centers formerly mapped with the Salem Gabbro-Diorite. The type locality is taken as Sharpners Pond (fig. 2), approximately 4¼ miles west of Topsfield; although only one facies is well developed in the immediate vicinity of the pond, the name has been extended to the entire spectrum of rocks comprising this formation. The name Salem Gabbro-Diorite is no longer considered appropriate for these rocks for the following reasons: (1) an average mode for all the rocks mapped with the Sharpners Pond Tonalite probably would fall well within the range of tonalite and well outside that of gabbro-diorite, and (2) according to Toulmin (1964, p. A18) the rocks of the Sharpners Pond cropping out in the northwest corner of the Salem quadrangle (the undifferentiated diorite and gabbro of his designation) "are clearly distinguishable from the gabbro and diorite of the Salem area" and may have been emplaced during a much later period of igneous activity than the type-Salem. The chief differences between the type-Salem and the Sharpners Pond Tonalite noted by Toulmin are: (1) the less deformed and altered nature of the Sharpners Pond, (2) the apparently total absence of pyroxene (augite) from the Sharpners Pond as contrasted with its common occurrence in the Salem and, (3) the abundance of crosscutting trap dikes among the outcrops of the Salem as opposed to their general absence in exposures of the Sharpners Pond.

The Sharpners Pond Tonalite has been divided into the following facies: (1) hornblende diorite, (2) biotite-hornblende tonalite, and (3) biotite tonalite. Selected representative modes from each of the Sharpners Pond facies are presented in the accompanying table. All three facies are transitional with each other on both map and outcrop scale; where age relations may be established within or among the
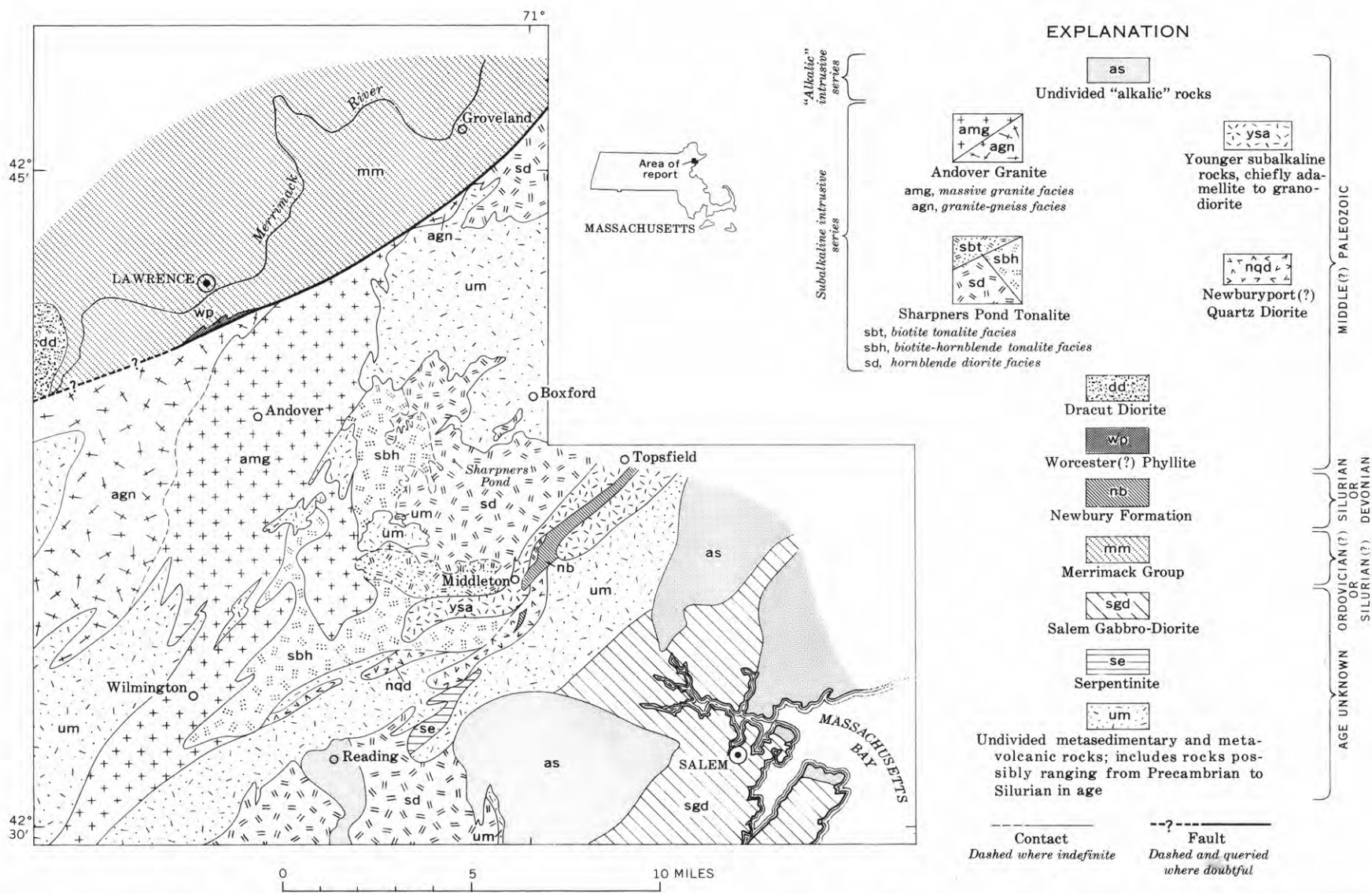
FIGURE 2.—Generalized geologic map showing distribution of major rock units in part of northeastern Massachusetts. Map is based on work by Toulmin (1964, pl. 1) and Castle, and covers parts of Lawrence, South Groveland, Wilmington, Reading, and Salem quadrangles, shown on figure 1.

separately mapped facies, the more felsic rocks are consistently younger. The distribution of the Sharpners Pond Tonalite over that part of northeastern Massachusetts that has been mapped in detail is given on figure 2. The Sharpners Pond, as shown on figure 2, occupies at least 40 to 50 square miles of northeastern Massachusetts; it may occupy as much as 90 square miles if rocks to the northeast mapped with the Salem Gabbro-Diorite and Newburyport Quartz Diorite ultimately are found to belong to the Sharpners Pond. Those parts of the Sharpners Pond Tonalite studied in detail consist chiefly of massive to somewhat foliated, generally medium grained and equigranular intrusive rocks. They range in color from dark greenish gray or black to light gray. Their modal compositions fall generally in the tonalite-diorite range. Leucocratic gabbros occur locally but extremely rarely; granodiorites are far more common but are confined exclusively to those areas mapped with the biotite tonalite facies.

Andover Granite

The Andover Granite, the other major unit of the redefined subalkaline intrusive series, was named by Clapp [1] for exposures of granite, aplite, and pegmatite in and around Andover, Mass. The Andover, like the Sharpners Pond, can be broken into a number of mappable facies; for purposes of this discussion it is divide into a granite gneiss and a massive granite facies. The individual facies of the Andover are generally transitional and roughly contemporaneous; the crystallization period of the more pegmatitic granite, however, probably ranged somewhat beyond that of the other facies. The distribution of the Andover Granite over a part of northeastern Massachusetts is given in figure 2; it occupies roughly 90 to 95 square miles within and beyond the map area of figure 2 (Emerson, 1917, pl. X).

The rocks of the Andover range in color from light gray to chalky white. They are characterized by widely ranging fabrics within a relatively narrow compositional range. The granite gneiss facies is slightly to intensely foliated, whereas the rocks of the massive granite facies are generally devoid of planar structures. The texture ranges from typically granitic,

[1] C. H. Clapp, 1910, The igneous rocks of Essex County, Massachusetts: Massachusetts Inst. Technology, abstract of thesis, 12 p.

Selected representative modal analyses of rocks from the Sharpners Pond Tonalite and the Andover Granite

[From 491 to 1002 points counted per thin section; all values in volume percent; the number of analyses is weighted in favor of the biotite tonalite facies and massive granite facies in order to better illustrate their transitional nature; Tr., trace]

	Sharpners Pond Tonalite												Andover Granite														
	Hornblende diorite facies			Biotite-hornblende tonalite facies			Biotite tonalite facies						Massive granite facies											Granite-gneiss facies		
	A	B	C	D	E	F	G	H	I	J	K	L	M	N	O	P	Q	R	S	T	U	V	W	X	Y	Z
Quartz			4.3	14.7	18.6	13.1	25.7	28.7	28.4	30.4	27.2	29.0	28.6	28.6	31.0	34.3	35.5	31.6	29.6	35.0	30.9	31.2	30.7	26.8	31.7	31.6
Plagioclase	52.3	51.8	48.6	48.9	47.2	46.2	56.1	49.7	49.5	39.4	39.9	28.2	46.0	42.3	36.9	31.0	28.3	27.5	27.0	24.0	37.1	33.6	33.0	32.8	28.2	28.4
(An content; [1] mol percent)	(47)	(37)	(32)	(32)	(35)	(36)	(25)	(33)	(31)	(28)			(22)	(24)	(20)	(12)	(15)	(10)		(5)	(12)	(13)	(15)	(15)	(8)	(7)
Microcline								1.2	3.4	18.0	23.0	33.0	13.0	18.3	21.2	27.3	28.0	34.8	38.8	28.6	24.7	32.6	31.6	30.0	34.8	28.8
Hornblende	36.8	33.6	18.9	17.6	22.3	13.9	3.9	1.1																		
Biotite		7.3	12.9	16.6	9.9	22.7	12.0	16.6	7.4	8.4	6.8	4.6	9.1	5.2	9.6	2.8	4.3	.4	3.3		2.0	.4	2.1	5.8	2.3	
Chlorite	1.7	1.5	2.4		.9				5.0	1.0	.8	.2	.4	.2	.5	1.0	3.5	1.4			.6	.1	.4	.4	.5	.1
White mica			1.4					.3	3.6	1.8	1.4	2.2	.9	3.5	.3	1.7		4.3	1.0	11.8	4.4	1.6	2.1	4.2	1.7	11.2
Epidote	3.0	.5	2.3	.4	.3	.9	.1	1.3	1.8	1.0	.7	2.4	1.0	1.8	.4	1.4	Tr.		.1	.4	.4	.1		.2	.4	
Sphene				1.2	.4	2.3	.4	.5	.6		.2		.5													
Apatite	.8	1.0	3.2	.5	.1	.7	1.4	.3	.2	Tr.	.1	Tr.	.1	.1	.1		.2					.1				
Zircon or thorite		.1			.1			Tr.				Tr.				.1		Tr.							Tr.	
Garnet														Tr.		.1		.2		Tr.	.3			Tr.	.4	.1
Carbonate			.6	Tr.	.1																					
Opaque	5.4	2.8	6.8	.1	.1	.2	.4	.3	.2				.4			.5				.1	.2		.1			

A. Diorite 2,600 ft S. 80° E. of eastern tip of Creighton Pond, Middleton.
B. Diorite along western edge of Rabbit Pond, Andover (occurs within biotite-hornblende tonalite facies).
C. Biotitic diorite 1,000 ft N. 60° E. of intersection of Reading-Wakefield-Woburn town lines, Reading.
D. Biotite-hornblende tonalite 2,900 ft S. 33° E. of Gray St.–Boston St. intersection, North Andover.
E. Biotite-hornblende tonalite 2,100 ft S. 73° E. of Winter St.–Foster St. intersection, North Andover.
F. Biotite-hornblende tonalite 2,700 ft N. 70° W. of Mill St.–Jenkins Rd. intersection, Andover.
G. Biotite tonalite 1,200 ft N. 55° E. of Salem St.–Woburn St. intersection, Wilmington.
H. Biotite tonalite 2,400 ft west of Maple St.–Main St. intersection, North Reading.
I. Biotite tonalite along north shore of Middleton Pond, 2,250 ft S. 56° W. of summit of Wills Hill, Middleton.
J. Biotite granodiorite 2,800 ft south of Marblehead St.–Forrest St. intersection, North Reading.
K. Biotite granodiorite along east side of Haverhill St., 350 ft south of Haverhill St.–North St. intersection, North Reading.

L. Biotite adamellite 1,900 ft N. 60° W. of southeastern tip of Swan Pond, North Reading.
M. Granodiorite 200 ft north of Berry Pond, North Andover.
N. Granodiorite 2,200 ft N. 14° W. of Harold Parker Rd.–Middleton Rd. intersection, North Andover.
O. Granodiorite 2,350 ft N. 50° E. of Andover Country Club clubhouse, Andover.
P. Adamellite 5,800 ft N. 89° E. of North St.–Haverhill St. interstion, North Reading.
Q. Adamellite 750 ft S. 68° W. of Church St.–Wildwood St. intersection, Wilmington.
R. Granite 1,100 ft S. 9° E. of Woburn St.–Salem St. intersection, Wilmington.
S. Granite 1,400 ft S. 15° W. of Shawsheen Ave.–Aldrich Rd. intersection, Wilmington.
T. Granite 950 ft S. 59° E. of Woburn St.–Park St. intersection, Wilmington.
U. Granodiorite 3,100 ft N. 43° E. of Elm St.–Summer St. intersection, Andover.
V. Adamellite 2,900 ft S. 10° E. of Haverhill St.–Main St. intersection, Andover.
W. Adamellite 3,650 ft S. 53° E. of Shawsheen St.–Lowe St. intersection, Tewksbury.
X. Adamellite-gneiss 1,800 ft N. 26° W. of Foster Rd.–Gray St. intersection, Billerica.
Y. Granite-gneiss at Kendall St.–North St. intersection, Tewksbury.
Z. Muscovite adamellite-gneiss 1,500 ft N. 66 E. of Mt. Vernon St.–Beacon St. intersection, Lawrence.

[1] All plagioclase compositions are based on flat-stage determinations and are considered accurate to no more than ±4 mol percent.

medium grained, allotriomorphic, through typically pegmatitic, extremely coarse grained, and locally hypidiomorphic. The Andover Granite is essentially adamellitic, and relatively few rocks included with the Andover lie to either side of this composition. Selected representative modes are presented in the table.

Relationship between the Sharpners Pond Tonalite and the Andover Granite

Several lines of evidence point to a consanguineous or at least broadly transitional relation between the Sharpners Pond Tonalite and the Andover Granite: (1) As the Andover Granite is traced eastward at the relatively broad scale of the geologic map, particularly in the area southeast of Andover center, it is seen to be smoothly transitional with the biotite tonalite facies of the Sharpners Pond. A comparable transitional relation involving the Andover exists with neither the other facies of the Sharpners Pond nor the surrounding country rock. (2) Rocks clearly identifiable with the massive granite facies of the Andover grade imperceptibly into biotite tonalite of the Sharpners Pond over the area of a single outcrop. (3) The modal analyses presented in the table show a generally smooth variation from the mafic Sharpners Pond to the felsic Andover Granite. The sequence of emplacement among these transitional rocks, in which the more felsic rocks of the table are consistently younger, suggests that the series followed a liquid line of descent toward the granite minimum, just as would be expected in a normal comagmatic series. Toulmin (written communication, 1961) has pointed out that this mafic to felsic trend of emplacement is not necessarily simply a function of differentiation toward the granite minimum; it may reflect in part a refusion of older felsic rock which might then have remained fluid even after the more mafic rock had solidified. Had this mechanism been operative on a large scale, however, apparent reversals of the mafic to felsic trend might reasonably be expected from place to place. (4) The modal analyses in the table show that there is not only chemical continuity but phase continuity as well between the Andover and Sharpners Pond; thus it is inferred that both groups of rocks have had similar histories and have been emplaced and crystallized under similar conditions. A comparable suggestion of environmental continuity is provided by the fact that the two-feldspar rocks from both the Sharpners Pond and Andover are characterized by the same extremely intricate, allotriomorphic grain-boundary configurations.

It is virtually certain, then, that the Andover Granite and Sharpners Pond Tonalite belong to a continuous plutonic series. This continuity might normally imply a simple comagmatic relation whereby the two descended from a single parent magma; there is some evidence, however, indicating a more complex history. The generally bimodal nature of the subalkaline series (reflected in the overwhelmingly tonalitic character of the Sharpners Pond and the essentially adamellitic nature of the Andover, together with the volumetrically insignificant development of granodiorite in both formations) suggests that the Sharpners Pond Tonalite and Andover Granite may have been precipitated from partly mixed yet separately derived magmas. This possibility tends to be supported, moreover, by the fact that the occurrence of granodiorite is confined to an outcrop area in and around the biotite tonalite facies of the Sharpners Pond. Accordingly, if the former existence of separate magmas may be assumed, it seems unlikely that both were generated within the same region of the earth's crust or subcrust. It is at least conceivable, therefore, that the Andover magma may have arisen through palingenesis of a metasedimentary-metavolcanic sequence well within the crust, whereas the Sharpners Pond magma may have been derived through the fractional melting of mantle material.

There is little point in continuing to include the Andover Granite with the "alkalic" series, as proposed by Clapp, if only for the reason that it is clearly transitional with the demonstrably pre-"alkalic" Sharpners Pond Tonalite. There are other reasons as well, however, for excluding the Andover from the "alkalic" intrusive series. As shown by the ubiquitous development of mortar structure, broken and bent feldspar twins, and other evidence, the foliated fabric of the rocks within the granite gneiss facies and parts of the massive granite facies derives from their synkinematic emplacement and crystallization or postemplacement deformation; since the rocks of the "alkalic" series are mainly undeformed, it is probable that they were intruded later in the orogenic cycle. Furthermore, although otherwise chemically comparable, the alkali-alumina ratio is much lower in the Andover than in the "alkalic" granites, supporting the subalkaline identification of the Andover and its separation from all other rocks presently included with the "alkalic" intrusive series. The relatively aluminous character of the Andover is suggested by the prominence of muscovite; it is particularly conspicuous in the norm. Corundum fails to appear in the norm of the "alkalic" granites, whereas it occurs in all the norms of the Andover Granite calculated so far (one specimen, for example, contained 4.59 percent norma-

tive corundum). Chemically similar granites from the separate series, moreover, differ sharply in their essential and varietal phase composition. The rocks of the Andover are chiefly two-feldspar granites; the "alkalic" granites, on the other hand, are characteristically "single" feldspar, perthitic rocks. In addition, micas comprise the chief varietal phases of the Andover Granite, whereas the alkalic granites are dominantly hornblendic. These phase differences suggest completely dissimilar plutonic environments.

Newburyport(?) Quartz Diorite

Rocks shown as Newburyport (?) Quartz Diorite on figure 2 have been included provisionally with the subalkaline intrusive series simply because where they crop out south of Middleton center they are similar to, and transitional with, rocks clearly identifiable with the biotite-hornblende tonalite facies of the Sharpners Pond. Differences between the two units are chiefly of secondary origin and are manifested by a somewhat higher degree of alteration and deformation within those rocks that have been mapped with the Newburyport(?).

"Younger subalkaline intrusive series"

The adamellites and granodiorites included with the "younger subalkaline intrusive series" by Toulmin also are correlated tentatively with the redefined subalkaline intrusive series. Although this correlation derives in part from the fact that both the "younger" subalkaline rocks and the Newburyport(?) Quartz Diorite bear the same apparent relation to the Newbury Formation (see below), it is based primarily on the correspondence in phase composition and texture between the adamellites of the "younger" series and the rocks of the Andover. The adamellites are two-feldspar rocks in which mica (altered biotite) occurs as the chief varietal mineral; they are characterized, moreover, by the same extremely intricate grain-boundary configuration that marks the Andover. These same characteristics suggest as well that the "younger" subalkaline rocks are unrelated to the "alkalic" intrusive series for many of the same reasons that the Andover must be unrelated to the "alkalic" series. By the same token the Squam Granite cropping out immediately east of Middleton center (Clapp, 1921, pl. 1) also must be unrelated to the "alkalic" series, for Toulmin (1964, pl. 1) has shown that the rocks in this area included with the Squam by Clapp actually belong with his "younger" subalkaline series.

It is at least conceivable, however, that the "younger" subalkaline rocks of figure 2 actually do form a unique intrusive series. The pink to red color, the generally felsic composition, and the occurence of rounded (resorbed?) quartz phenocrysts in the granodiorites suggest that the "younger" subalkaline group may be correlative with the similarly constituted and spatially associated volcanic rocks of the Newbury Formation (Toulmin, 1964, p. A71–A72). Since none of the other rocks of the redefined subalkaline intrusive series (with the possible exception of the Newburyport(?) Quartz Diorite) are thought to bear a corresponding relation to known volcanic rocks in northeastern Massachusetts, the suspicion remains that the "younger" subalkaline rocks may belong to a separate intrusive series.

TENTATIVE CORRELATIONS

Those rocks in Essex County formerly mapped with the Dedham Granodiorite (Clapp, 1921, pl. 1) are at least in part correlative with either the Andover Granite or the "younger" subalkaline rocks; they accordingly belong in part or perhaps entirely with the redefined subalkaline intrusive series. Hansen (1956, p. 46) has defined a small pluton cropping out in the northeast section of the Maynard quadrangle as the Assabet Quartz Diorite. Generally similar lithologies and the fact that both bear the same relations to the Andover Granite and surrounding metamorphic rocks indicate that the Assabet and Sharpners Pond probably are correlative, and that the Assabet, too, belongs with the subalkaline intrusive series. Rocks cropping out in the Maynard quadrangle and originally included with the Andover by Emerson (1917, pl. X) but subsequently mapped as the Acton Granite (Hansen, 1956, p. 48–50; M. E. Willard, oral communication, 1951), almost certainly should be included with the redefined subalkaline intrusive series. The fabric, phase composition, and field relations of the Acton are identical with parts of the massive granite facies of the Andover, and the two (as Emerson suspected) are clearly equivalent.

Although a correlation between the Salem Gabbro-Diorite and Sharpners Pond Tonalite tentatively has been rejected, their separation cannot be demonstrated with certainty (Toulmin, 1964, p. A70), and the possible inclusion of the Salem with the redefined subalkaline intrusive series should not yet be dismissed. In the first place, continuity between the Sharpners Pond and Salem is suggested specifically by the fact that the Sharpners Pond becomes generally more mafic as it is traced toward the relatively femic type Salem. Secondly, the fact that the Sharpners Pond is thought to be less altered and deformed than the Salem may be attributable to differences in either its mode of emplacement (that is, the degree of crystallin-

ity obtaining in the magma of the Sharpners Pond as contrasted with that of the Salem) or its geographic position relative to major tectonic lineaments; the fresher aspect of the Sharpners Pond is not necessarily attributable to intrusion during a distinctly later orogeny.

AGE OF THE SUBALKALINE INTRUSIVE SERIES

The age of the subalkaline intrusive series remains in doubt, but the available evidence now indicates that the series probably evolved during middle Paleozoic time. Its minimum age may be fixed in a general way through the relation of the series with the "alkalic" intrusive series. Field evidence suggests that at least one member of the "alkalic" series of eastern Massachusetts is very doubtfully younger than earliest Pennsylvanian (Emerson, 1917, p. 188; Knox, 1944, p. 137–138), and there is nowhere evidence of intrusion of the Carboniferous rocks of the Boston basin by rocks assigned to the "alkalic" series. A K-Ar hornblende age of 345±15 million years obtained by Hurley and others (1960, p. 289) from the "alkalic" Cape Ann Granite of Essex County suggests a minimum age of earliest Carboniferous (Holmes, 1960, p. 204) for this unit, and a recent Rb-Sr whole-rock age determination by Bottino (1963, p. 79) indicates that the Cape Ann may be as old as 415±10 million years (roughly Middle Silurian according to Holmes, 1960, p. 204). In any event, since the "alkalic" rocks are known to be intrusive into the subalkaline series over a wide area, and the reverse relation is nowhere known to occur, the subalkaline series is improbably younger than early Carboniferous and perhaps no younger than Middle Silurian. Perhaps the best evidence pertaining to the maximum age of the subalkaline series stems from its relation to the Upper Silurian Newbury Formation. Studies by Toulmin (1964, p. 17) and N. P. Cuppels (1964, written communication) in the Salem and Georgetown quadrangles respectively have shown that the Newbury Formation is transected and probably, although not certainly, intruded by the Topsfield Granodiorite (or its correlatives). Where it occurs in the Reading quadrangle the Newbury Formation is transected by the Newburyport(?) Quartz Diorite (see fig. 2), which, together with the occurrence of a stepped contact between the Newburyport(?) and rhyolitic rocks of the Newbury exposed over a distance of 3 to 4 feet, suggests that the Newbury is intruded by the Newburyport(?)

as well as by the Topsfield. A further suggestion of a maximum Silurian age for the subalkaline intrusive series derives from the occurrence within the Merrimack Group (of probable Middle Silurian age as designated by Billings, 1956, p. 103–104) of several massive pegmatite lenses correlated by the writer with the Andover Granite. Radiometric dates are not yet available for any of the rocks of the redefined subalkaline series; dates on the intrusives of the Fitchburg pluton (Rodgers, 1952, p. 419; Webber and others, 1956, p. 580; Lyons and others, 1957, p. 535), with which the subalkaline series may be correlative, simply support its probable minimum Carboniferous age.

REFERENCES

Billings, M. P., 1956, The geology of New Hampshire, pt. II. Bedrock geology: New Hampshire State Plan. and Devel. Comm., 203 p.
Bottino, M. L., 1963, Whole-rock Rb-Sr studies of volcanics and some related granites, in Hurley, P. M., and others, Variations in isotopic abundances of strontium, calcium, and argon and related topics: U.S. Atomic Energy Comm., 11th Ann. Prog. Rept. for 1963, Massachusetts Inst. Technology, NYO-10, 517, Contract AT(30-1)-1381, p. 65–84.
Clapp, C. H., 1921, Geology of the igneous rocks of Essex County, Massachusetts: U.S. Geol. Survey Bull. 704, 132 p.
Emerson, B. K., 1917, Geology of Massachusetts and Rhode Island: U.S. Geol. Survey Bull. 597, 289 p.
Hansen, W. R., 1956, Geology and mineral resources of the Hudson and Maynard quadrangles, Massachusetts: U.S. Geol. Survey Bull. 1038, 104 p.
Holmes, Arthur, 1960, A revised geological time-scale: Edinburgh Geol. Soc. Trans., v. 17, p. 183–216.
Hurley, P. M., and others, 1960, Variations in isotopic abundances of strontium, calcium, and argon and related topics: U.S. Atomic Energy Comm., 8th Ann. Prog. Rept. for 1960, Massachusetts Inst. Technology, NYO-3941, Contract AT(30-1)-1381, 289 p.
Knox, A. S., 1944, A carboniferous flora from the Wamsutta formation of southeastern Massachusetts: Am. Jour. Sci., v. 242, p. 130–138.
Lyons, J. B., Jaffe, H. W., Gottfried, David, and Waring, C. L., 1957, Lead-alpha ages of some New Hampshire granites: Am. Jour. Sci., v. 255, p. 527–546.
Rodgers, John, 1952, Absolute ages of radioactive minerals from the Appalachian region: Am. Jour. Sci., v. 255, p. 411–427.
Toulmin, Priestly, 3d, 1960, Composition of feldspars and crystallization history of the granite-syenite complex near Salem, Essex County, Massachusetts, U.S.A.: Internat. Geol. Cong., 21st, Copenhagen, 1960, Rept. pt. 13, p. 275–286.
——— 1964, Bedrock geology of the Salem quadrangle and vicinity, Massachusetts: U.S. Geol. Survey Bull. 1163-A, p. A1–A79.
Webber, G. R., Hurley, P. M., and Fairbairn, H. W., 1956, Relative ages of eastern Massachusetts granites by total lead ratios in zircon: Am. Jour. Sci., v. 254, p. 574–583.

GNEISSIC ROCKS IN THE SOUTH GROVELAND QUADRANGLE, ESSEX COUNTY, MASSACHUSETTS

By R. O. CASTLE, Los Angeles, Calif.

Work done in cooperation with the Massachusetts Department of Public Works

Abstract.—Detailed mapping in the South Groveland quadrangle has made possible the division of the gneissic rocks in this area into two formations to which the names Fish Brook Gneiss and Boxford Formation have been assigned. The Fish Brook Gneiss is a relatively uniform fine- to medium-grained, quartz-plagioclase gneiss; it is either an isolated intrusive rock predating the subalkaline intrusive series of this area or an ancient "dome" gneiss similar to those of western New England. The Boxford Formation consists of a lower member composed chiefly of mica schists and quartz-feldspathic gneisses and an upper member composed of generally thinly layered, very fine grained, compositionally heterogeneous but predominantly amphibolitic rocks; it is thought to be correlative with the Rye Formation of southeastern New Hampshire and perhaps correlative with the Marlboro Formation of eastern Massachusetts.

The igneous rocks of Essex County, Mass., have been investigated in relative detail by several geologists (Clapp, 1921; Toulmin, 1964); the associated metasedimentary and metavolcanic rocks, on the other hand, have received little attention. Emerson (1917, pl. X), for example, lumped the metamorphic rocks in the South Groveland quadrangle of Essex County into the following categories; (1) Merrimack Quartzite (included within the Merrimack Group of Billings, 1956, p. 44), (2) Marlboro Formation, and (3) gneisses and schists of undetermined age. Clapp (1921, pl. 1) generalized still further by including the "gneisses and schists of undetermined age" with the Andover Granite. Recent mapping in the South Groveland quadrangle, however, has permitted a more explicit definition of the metamorphic rocks of this area than was previously possible; the chief purpose of this paper, accordingly, is to briefly describe two newly defined formations that together comprise the metamorphic rocks in the South Groveland quadrangle exclusive of the Merrimack Group.

Stratigraphic relations between the Merrimack Group and the remaining metamorphic rocks of the South Groveland quadrangle are not directly determinable; the two groups are separated by a major fault passing through the northern half of the quadrangle (fig. 1) and can be related only through probable correlatives in southeastern New Hampshire. Regardless of their relation to the Merrimack Group, however, the occurrence and general character of the gneissic rocks south of the major fault correspond in part to those of the older metamorphic rocks in southeastern New Hampshire and elsewhere in eastern Massachusetts; the gneissic rocks of this area consequently may provide a link between these two areas of older metamorphic rocks.

FISH BROOK GNEISS

The name Fish Brook Gneiss is introduced here for an irregularly shaped gneiss body cropping out in the southeast quarter of the South Groveland quadrangle (fig. 1); the name and type locality have been selected for the good exposures of this unit in the vicinity of Fish Brook, in Boxford. Part of the Fish Brook Gneiss formerly was mapped with the Andover Granite and the remainder was included with either the Marlboro Formation or the Salem Gabbro-Diorite (Emerson, 1917, pl. X).

The typical Fish Brook Gneiss is a pearly white to very light gray, distinctly foliated but generally unlayered biotite-quartz-plagioclase rock. The foliation in the gneiss is manifested chiefly by oriented biotite flakes; owing to a southerly diminution in biotite, however, the foliated nature of the Fish Brook is less marked toward the south. The textures in the Fish Brook Gneiss characteristically range from fine to
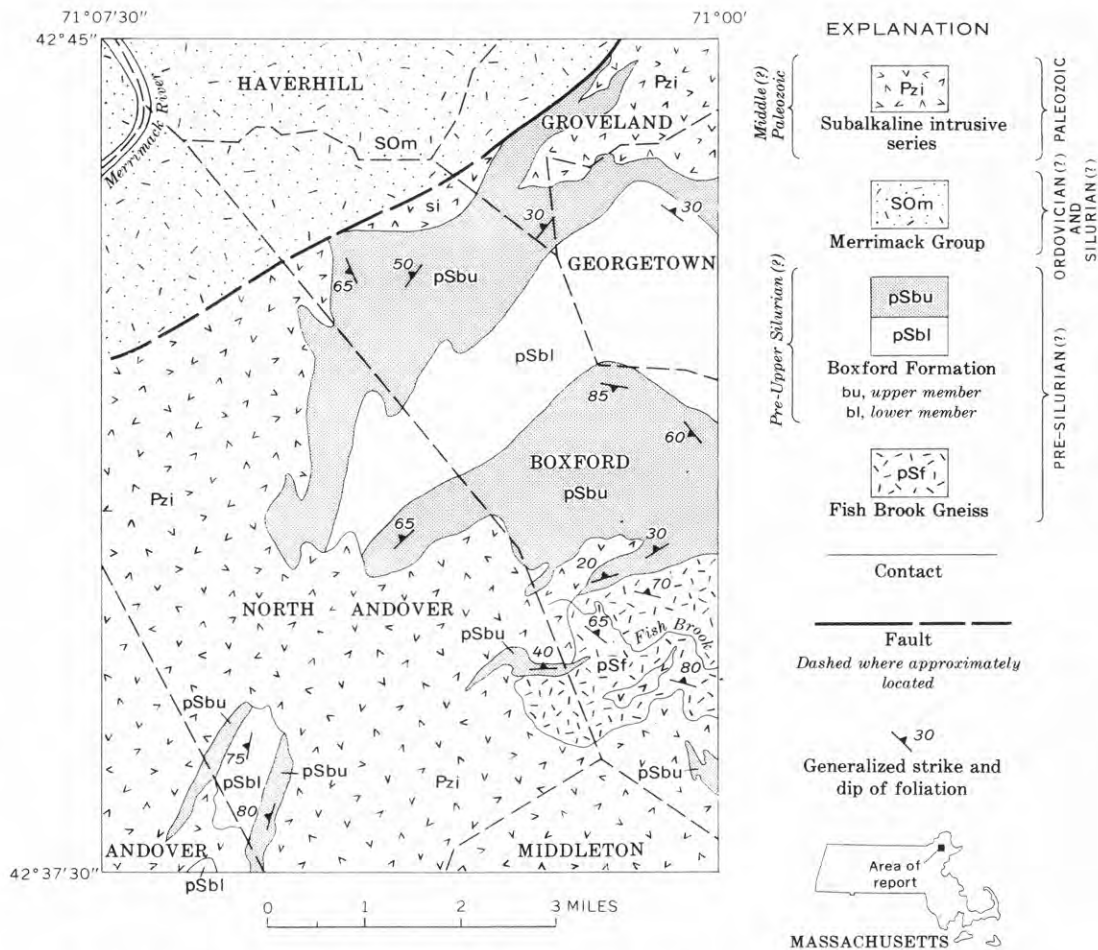
FIGURE 1.—Generalized geologic map of the South Groveland quadrangle, Massachusetts.

medium grained and granoblastic to hypidioblastic. Plagioclase constitutes as much as 55 percent of the gneiss and its composition over the entire unit is thought to average around An_{25}. Quartz is the other major constituent of the gneiss and locally accounts for as much as 40 percent of the rock. Representative modes are presented in table 1.

Inclusions of amphibolite, thinly layered biotite gneiss, and other rock types known to occur in the adjacent Boxford Formation have been found within the Fish Brook Gneiss, particularly along its northern contact. Most of these inclusions are irregularly shaped, and some are little more than schlieren; others, however, occur as small rectangular blocks as much as a foot or more in length. The foliation of the gneissic host commonly is roughly continuous with that in the inclusions, but it locally wraps or "flows" around the edges of these inclusions.

The configuration of the contact of the Fish Brook Gneiss with the diorite and tonalite of the locally occurring subalkaline intrusive series, together with the truncation of the Fish Brook foliation and the Fish

Brook–Boxford contact by this same series (fig. 1), strongly suggests that the Fish Brook Gneiss has been intruded by the subalkaline rocks. In addition, mafic rocks thought to belong to the subalkaline series were seen (although rarely) crosscutting the gneiss in individual outcrops.[1] Any possibility that the Fish Brook Gneiss may postdate the subalkaline intrusive series accordingly seems very unlikely. Felsic intrusives, whether related to the subalkaline intrusive series or not, are relatively uncommon within the outcrop area of the Fish Brook Gneiss. A diffuse, nebulously defined zone of massive very coarse grained biotite granite and pegmatite does occur, however, along the northern edge of the gneiss; although clearly younger, these granitic rocks are in gradational contact with the gneiss and merge imperceptibly into it.

The Fish Brook Gneiss is either a plutonic igneous rock that has been intruded against the adjacent Box-

---

[1] Fine-grained, porphyritic diorite crosscuts the Fish Brook Gneiss in exposures near the Boxford-North Andover town line, immediately south of the contact of the Fish Brook Gneiss with the outlier of the Boxford Formation, and small dikes of medium-grained diorite have intruded the gneiss in exposures south of Fish Brook near the eastern edge of the quadrangle.

TABLE 1.—*Modal analyses of rocks from the Fish Brook Gneiss*

[All values in volume percent; Tr., trace]

	A	B	C
Quartz	32. 9	39. 6	39. 7
Plagioclase	54. 0	53. 0	54. 1
Microcline		5. 8	Tr.
Hornblende	1. 6		. 7
Biotite	9. 8		4. 1
Chlorite	. 2	1. 0	. 1
White mica	. 7		
Epidote	. 2	. 2	. 4
Apatite	. 3		. 1
Opaque material	. 3	. 4	. 8

A. Biotite gneiss 300 ft S. 60° E. of Towne Rd.–Main St. intersection, Boxford. Points counted: 1000.
B. Quartz-plagioclase gneiss 3,300 ft N. 54° W. of intersection of Boxford–Middleton–North Andover town lines, North Andover. Points counted: 500.
C. Biotite gneiss 1,700 ft N. 29° E. of Lawrence Rd.–Main St. intersection, Boxford. Points counted: 1000.

ford Formation, or a highly metamorphosed "dome" or "core" gneiss of either igneous or sedimentary ancestry. Supporting a simple intrusive origin is the fact that the composition of the gneiss locally accords with that of a clearly intrusive biotite tonalite known to crop out 4 or 5 miles southwest of the type locality of the Fish Brook. A correlation between these two is considered improbable, however, since the tonalite almost certainly forms a relatively young member within the same subalkaline intrusive series currently thought to crosscut the Fish Brook Gneiss exposed in the South Groveland quadrangle. The foliation of the Fish Brook Gneiss, moreover, is discordant with respect to (1) the Boxford–Fish Brook contact and (2) the long axis of the Fish Brook Gneiss body itself. These structural features (fig. 1), together with the absence of any crosscutting relations with the Boxford Formation, are generally inconsistent with any derivation requiring that the Fish Brook be intrusive into the adjacent rocks.

It is conceivable, of course, that the foliation in the Fish Brook Gneiss is of postintrusive metamorphic origin; this possibility is suspect, however, owing to the apparent discordance in foliation between the Fish Brook and the adjacent Boxford Formation. It seems equally, if not more likely, therefore, that the Fish Brook is a core or dome gneiss. According to this interpretation the gneiss is a unit of considerable antiquity that may have been subjected to a pre-Boxford deformation and metamorphism and subsequently was overlain or onlapped by the Boxford Formation. This interpretation would account for the partly discordant relations between the two formations and at the same time explain the crude conformity between the Fish Brook–Boxford contact and the internal structure of the Boxford Formation. The dome-gneiss hypothesis is deficient chiefly in its failure to explain

the occurrence of the Boxford-type inclusions contained within the Fish Brook. However, the development of diffuse patches of granite within the gneiss is suggestive of local palingenesis, and it is at least conceivable that these xenolithlike inclusions have been ingested by a gneissic host that was at one time highly plastic if not actually molten.

It is remotely possible that the Fish Brook Gneiss and Boxford Formation are in fault contact, and that the temporal relation between the two (and thereby the origin of the Fish Brook) consequently may be indeterminate. This possibility is considered improbable for two reasons: (1) there is no evidence of movement along any of the contacts between the two formations; and (2) the postulated faulting would have to have been of a geometric complexity sufficient to explain the presence within the Fish Brook of large, angularly discordant outliers of the Boxford Formation such as the one shown athwart the Boxford–North Andover town line south of Fish Brook (fig. 1).

Should the Fish Brook Gneiss prove to be a post-Boxford intrusive, it would be unique in the sense that felsic intrusives predating the subalkaline intrusive series are otherwise unknown in northeastern Massachusetts. Should the Fish Brook be shown to be a dome gneiss, on the other hand, it might prove equally unique; it would then become the only unit in northeastern Massachusetts or southeastern New Hampshire known to predate the Boxford Formation or its equivalents.

BOXFORD FORMATION

The name Boxford Formation is introduced here for a group of conspicuously foliated rocks cropping out abundantly in the east-central section of the South Groveland quadrangle. The name and type locality have been chosen for the good exposures of this unit in the northwest half of the town of Boxford (fig. 1). The main outcrop belt of the Boxford Formation is about 4 miles wide; the formational thickness cannot be accurately determined but it probably exceeds 5,000 feet. Most of the rocks included with this newly defined formation originally were mapped with the Salem Gabbro-Diorite; a relatively small fraction were mapped with the Marlboro Formation and undifferentiated gneisses and schists (Emerson, 1917, pl. X).

The Boxford Formation is divided here into lower and upper members; the stratigraphic relation between the two is not certainly demonstrable locally, but in a spatial sense at least the upper member of this designation clearly overlies the lower member and it is assumed that this geometric relation is a reflection of

their relative ages. The lower member of the Boxford consists chiefly of conspicuously foliated, although generally obscurely layered, fine- to medium-grained mica schists and quartzo-feldspathic gneisses, together with apparently subordinate amounts of amphibolite. The schists are characteristically crumbly, commonly stained by iron oxides, and poorly exposed; the gneisses and amphibolites are better exposed and seemingly less altered. Estimated modes of representative rocks from the lower member of the Boxford Formation are presented in table 2. These modes are based upon visual estimates of the abundance of minerals observed in this formation and represent approximations at best.

The upper member of the Boxford crops out far more conspicuously than the lower member and is well

TABLE 2.—*Estimated modes of rocks from the Boxford Formation*

[All values in volume percent; Tr., trace]

	Lower member		Upper member								
	A	B	C	D	E	F	G	H	I	J	K
Quartz	43	20	--	--	47	15	--	--	5	25	10
Plagioclase	47	5	20	30	20	19	60	--	60	--	4
Microcline	--	--	--	--	20	--	--	--	--	--	--
Hornblende	--	--	25	65	5	--	16	--	--	--	--
Tremolite	--	--	--	--	--	--	--	--	14	--	--
Actinolite	--	--	--	--	--	--	--	90	--	--	--
Diopside	--	--	15	--	--	--	--	--	--	--	--
Biotite	8	20	25	--	6	--	--	--	--	15	--
Chlorite	--	--	3	--	--	15	2	5	3	2	6
White mica	--	35	--	--	--	45	7	--	--	37	63
Epidote	--	--	--	1	--	--	3	2	4	--	--
Sillimanite	--	8	--	--	--	--	--	--	--	3	5
Andalusite	--	10	--	--	--	--	--	--	--	15	7
Garnet	--	--	--	--	--	2	--	--	--	--	--
Apatite	--	--	--	--	--	--	3	--	--	--	--
Sphene	--	--	4	Tr.	1	--	5	--	6	--	--
Carbonate	--	--	8	--	--	--	2	--	--	--	--
Opaque material	2	2	--	4	1	4	2	3	8	3	5

A (R–199). Quartz-feldspar gneiss along Andover bypass, 2,000 ft north-northeast of Rocky Hill Rd.–Andover bypass intersection, Andover (south of map area, fig. 1).

B (G–210). Quartz-mica schist near crest of knoll 1,900 ft northwest of Pine Plain Rd.–Willow Rd. intersection, Boxford.

C (G–19). Thinly layered calc-silicate gneiss 2,300 ft northnorthwest of Washington St.–Willow Rd. intersection, Boxford.

D (G–20). Amphibolite 2,800 ft north-northeast of Washington St.–Main St. intersection, Boxford.

E (G–170). Thinly layered quartz-feldspar gneiss 3,200 ft south-southeast of Washington St.–Uptack St. intersection, Groveland.

F (G–171). Mica schist 2,500 ft southeast of Washington St.–Salem St. intersection, Groveland.

G (G–682). Thinly layered gneiss at northern tip of Towne Pond, Boxford.

H (G–63). Actinolite schist from inlier of Boxford Formation near Brooks School, North Andover.

I (G–42). Fine-grained gneiss 2,000 ft east-southeast of summit of Byers Hill, Boxford.

J (G–42). Mica schist 2,000 ft east-southeast of summit of Byers Hill, Boxford (interlayered with I).

K (G–823). Sericite schist 2,200 ft north-northeast of Salem St.–Summer St. intersection, North Andover.

exposed throughout much of Boxford and Georgetown. It is composed entirely of conspicuously foliated, generally thinly layered, very fine grained, hypidioblastic rocks. The foliation in the upper member is manifested as a simple schistosity or a very thin layering in which the individual layers probably average less than 1 mm in thickness; where both layering and schistosity are present together, the schistosity apparently parallels the layering, which is in turn probably, but not certainly, mimetic to the original bedding. (Unambiguously defined primary structures have not been recognized by the writer in any of the outcrops of the Boxford Formation.) The rocks of the upper member range widely in composition from amphibolite to sericite schist; amphibolites and hornblende-plagioclase gneisses are the most abundant rock types represented. Estimated modes of representative rocks from the upper member of the Boxford Formation are presented in table 2. These modes are based upon visual estimates of the abundance of minerals observed in this section and represent approximations at best.

The compositional heterogeneity of the Boxford Formation suggests a complex depositional history. The earliest deposits apparently were argillaceous to arenaceous sediments; increasing abundance of amphibolite toward the top of the formation is thought to reflect increasing vulcanism.

The Boxford Formation, along with the Fish Brook Gneiss, has been isolated from the other metasedimentary and metavolcanic rocks of northeastern Massachusetts through faulting and intrusion; suggested correlations between the Boxford and other units are consequently highly speculative. The Boxford strikes southwest toward a belt of metamorphic rocks that have been mapped by the writer with the Marlboro Formation, and the broad compositional similarity between these two units suggests that they are very likely correlative. This suggested correlation, however, may prove impossible to demonstrate, for the Boxford and Marlboro are separated over a distance of 4 or 5 miles by a broad expanse of intrusive rocks. A major structural discontinuity, moreover, may separate the two units as well, and the associated intensive and extensive deformation of the Marlboro Formation cropping out directly south of the South Groveland quadrangle precludes any detailed comparison of the two formations.

A unit with which the Boxford is almost certainly correlative is the Rye Formation of southeastern New Hampshire. The Rye Formation, according to Billings (1956, p. 38–39), consists of a lower metasedi-

mentary member composed chiefly of feldspathic mica schist and an upper metavolcanic member composed of amphibolite and fine-grained biotite gneiss; this description of the Rye accords roughly with that of the Boxford. The writer has examined parts of the Rye Formation, moreover, and has noted that the lithology of the upper member in particular is strikingly similar to that of the upper member of the Boxford. Whether or not the probable equivalence of the Boxford and Rye Formations can be demonstrated through detailed areal studies is problematical. They are separated by a sizable plutonic complex over a distance of about 14 miles, and it is not now known whether appreciable volumes of earlier metamorphic rocks are included within this complex. The chief stratigraphic significance of the Boxford Formation, then, may derive from the fact that its occurrence tends to support a correlation between the older metamorphic rocks of southeastern New Hampshire (Rye Formation) and the Marlboro Formation of eastern Massachusetts. This equivalence was suggested almost half a century ago by Katz (1917, p. 167–168) but remains unconfirmed.

If the postulated equivalence of the Boxford and Rye Formations is accepted, the Boxford is almost certainly pre-Devonian and probably pre-Silurian. The Rye Formation is overlain around the Rye anticline of southeastern New Hampshire by the totally dissimilar Merrimack Group (R. F. Novotny, oral communication, 1957); inasmuch as the Merrimack Group is very doubtfully younger than Early Devonian and probably is Middle Silurian in age (Billings, 1956, p. 99–105), the Rye Formation is probably no younger than Silurian.

An alternate approach to the age of the Boxford is suggested by its probable equivalence with the Marlboro Formation. Emerson (1917, p. 24) assigned the Marlboro to the Algonkian(?); several workers (Rodgers and others, 1959, p. 56; Dixon, 1964, p. C2), however, have indicated that the Marlboro Formation is very probably correlative with the Putnam Group of eastern Connecticut, tentatively assigned by Dixon and others (1962) to the "Ordovician(?)" and considered "certainly pre-Pennsylvanian and probably early Paleozoic in age" by Dixon (1964, p. C2). Moorbath and others (1962, p. 7), moreover, have been able to date the Northbridge Granite Gneiss of eastern Massachusetts by the Rb-Sr whole-rock method as 535±15 million years (probably an original, premetamorphic age); inasmuch as Emerson (1917, p. 24, 155) considered the Northbridge to be overlain "normally" by the Westboro Quartzite and the ubiqui-

tously associated Marlboro Formation, a maximum age of Late Cambrian (on the time scale of Holmes, 1960) is implied for the Marlboro, thereby supporting its presumed "Ordovician(?)" or "early Paleozoic" age.

Emerson's structural interpretation, however, is open to doubt, for H. R. Dixon (written communication, 1964) recently has suggested that the Marlboro and Northbridge may be in fault contact; their relative ages, as a consequence, may not be directly determinable. Moorbath and others (1962), moreover, have shown that a $Sr^{87}/Sr^{86} : Rb^{87}/Sr^{86}$ whole-rock value for the Milford Granite falls precisely on the whole-rock isochron defined by the Northbridge Granite Gneiss; since the Milford is almost certainly intrusive into the Marlboro Formation (Emerson, 1917, p. 165), the possibility exists that both the Northbridge and the Milford postdate the Marlboro, and that the Marlboro and Boxford are, in turn, older than Late Cambrian. This suspicion of a pre-Ordovician or even Precambrian age for the Marlboro is forcefully supported by a recently defined Rb-Sr whole-rock isochron of 558±20 million years for the main mass of the Dedham Granodiorite (Ramo and Fairbairn, 1963, p. 53), several large masses of which intrude the "Algonkian(?)" (Marlboro and Westboro) rocks west of Boston (Emerson, 1917, p. 175–176).

REFERENCES

Billings, M. P., 1956, The geology of New Hampshire; pt. II. Bedrock geology: New Hampshire State Plan. and Devel. Comm., 203 p.

Clapp, C. H., 1921, Geology of the igneous rocks of Essex County, Massachusetts: U.S. Geol. Survey Bull. 704, 132 p.

Dixon, H. R., 1964, The Putnam Group of eastern Connecticut: U.S. Geol. Survey Bull. 1194–C, p. C1–C12.

Dixon, H. R., Lundgren, Lawrence, Snyder, G. L., and Eaton, Gordon, 1962, Colchester nappe of eastern Connecticut, in Abstracts for 1962: Geol. Soc. America Spec. Paper 73, p. 139.

Emerson, B. K., 1917, Geology of Massachusetts and Rhode Island: U.S. Geol. Survey Bull. 597, 289 p.

Holmes, Arthur, 1960, A revised geological time-scale: Edinburgh Geol. Soc. Trans., v. 17, p. 183–216.

Katz, F. J., 1917, Stratigraphy in southwestern Maine and southeastern New Hampshire: U.S. Geol. Survey Prof. Paper 108–I, p. 165–177.

Moorbath, S. and others, 1962, Rb-Sr investigation of the Northbridge Granite-Gneiss, Massachusetts, in Hurley, P. M., and others, Variations in isotopic abundances of strontium, calcium, and argon and related topics: U.S. Atomic Energy Comm., 10th Ann. Prog. Rept. for 1962, Massachusetts Inst. Technology, NYO–3943, Contract AT(30–1)–1381, p. 7–8.

Ramo, Alan, and Fairbairn, H. W., 1963, Preliminary age study of the Dedham granitic rocks, in Hurley, P. M., and others, Variations in isotopic abundances of strontium, calcium, and

argon and related topics: U.S. Atomic Energy Comm., 11th Ann. Prog. Rept. for 1963, Massachusetts Inst. Technology, NYO–10, 517 Contract AT(30–1)–1381, p. 53–54.

Rodgers, John, Gates, R. M., and Rosenfeld, J. L., 1959, Explanatory text for preliminary geological map of Connec-

ticut, 1956: Connecticut Geol. and Nat. History Survey Bull. 84, 64 p.

Toulmin, Priestly 3d, 1964, Bedrock geology of the Salem quadrangle and vicinity, Massachusetts: U.S. Geol. Survey Bull. 1163–A, p. A1–A79.

STRATIGRAPHY OF THE UPPER PART OF THE YAKIMA BASALT IN WHITMAN AND EASTERN FRANKLIN COUNTIES, WASHINGTON

By JAMES W. BINGHAM and KENNETH L. WALTERS, Tacoma, Wash.

Abstract.—Stratigraphic sections measured about 70 miles and 130 miles east of Sentinal Gap, Wash., on the Columbia Plateau, show a rock sequence similar to the one described by J. H. Mackin in 1961 near Sentinel Gap. The newly measured sequence, in the upper part of the Yakima Basalt, consists of (in descending order) the nonporphyritic Priest Rapids Member, the porphyritic Roza Member, and the sparsely porphyritic Frenchman Springs Member. The key stratigraphic marker is a flow in the Roza Member. The existence of the sequence at widely spaced localities in central and eastern Washington suggests that it is continuous and mappable over large areas of the plateau.

The basalt of the Columbia Plateau, outlined on figure 1, recently was designated the Columbia River Group by Waters (1961), who divided this group into two formations, the Yakima Basalt and the Picture Gorge Basalt, on the basis of exposures in northeastern Oregon. There the Yakima Basalt unconformably overlies the Picture Gorge Basalt (Waters, 1961, p. 588, 591). The Yakima Basalt extends from the Cascade Range eastward to the Rocky Mountains and from the Columbia and Spokane Rivers southward into northern Oregon. The areal extent of the Picture Gorge Basalt is not known.

Mackin (1961) described a stratigraphic sequence in the upper part of the Yakima Basalt in the Columbia River valley between Priest Rapids Dam and Vantage (fig. 1) and in the Yakima River valley near Roza Station. He named the units of this sequence, in descending order, the Priest Rapids, Roza, and Frenchman Springs Basalt Members. The units differ in lithology: the Priest Rapids is nonporphyritic

and consists of 1 to 4 flows, the Roza is porphyritic and consists of 1 or 2 flows, and the Frenchman Springs is sparsely porphyritic to nonporphyritic and consists of 3 to 6 flows. These units are hereby adopted as the Priest Rapids, Roza, and Frenchman Springs Members of the upper part of the Yakima Basalt.

The sequence described by Mackin (1961) at Sentinel Gap near Vantage has been mapped by M. J. Grolier and J. W. Bingham (report in preparation) in the Columbia Basin Irrigation Project area as far east as Sulphur Lake (fig. 1), about 60 miles east of the area described by Mackin.

Sections which show this stratigraphic sequence have been measured by the authors at two additional localities to verify the presence of the sequence eastward from the Columbia Basin Irrigation Project of the U.S. Bureau of Reclamation. These localities are (1) Devils Canyon near Kahlotus, and (2) Yakawawa Canyon southwest of Pullman, 70 miles and 130 miles, respectively, east of Sentinel Gap. Table 1 describes the sequence at these two localities and in Sentinel Gap and gives the number of flows and their total thickness at each place.

Figure 2 shows the regional correlation and relative thickness of the members at 5 control points over a distance of about 175 miles along section *A–A'* shown on figure 1. The thickening and basining of certain members of the sequence in the central part of the plateau, as shown on figure 2, are attributed to subsidence which continued during the time of extrusion of the flows that make up this sequence.
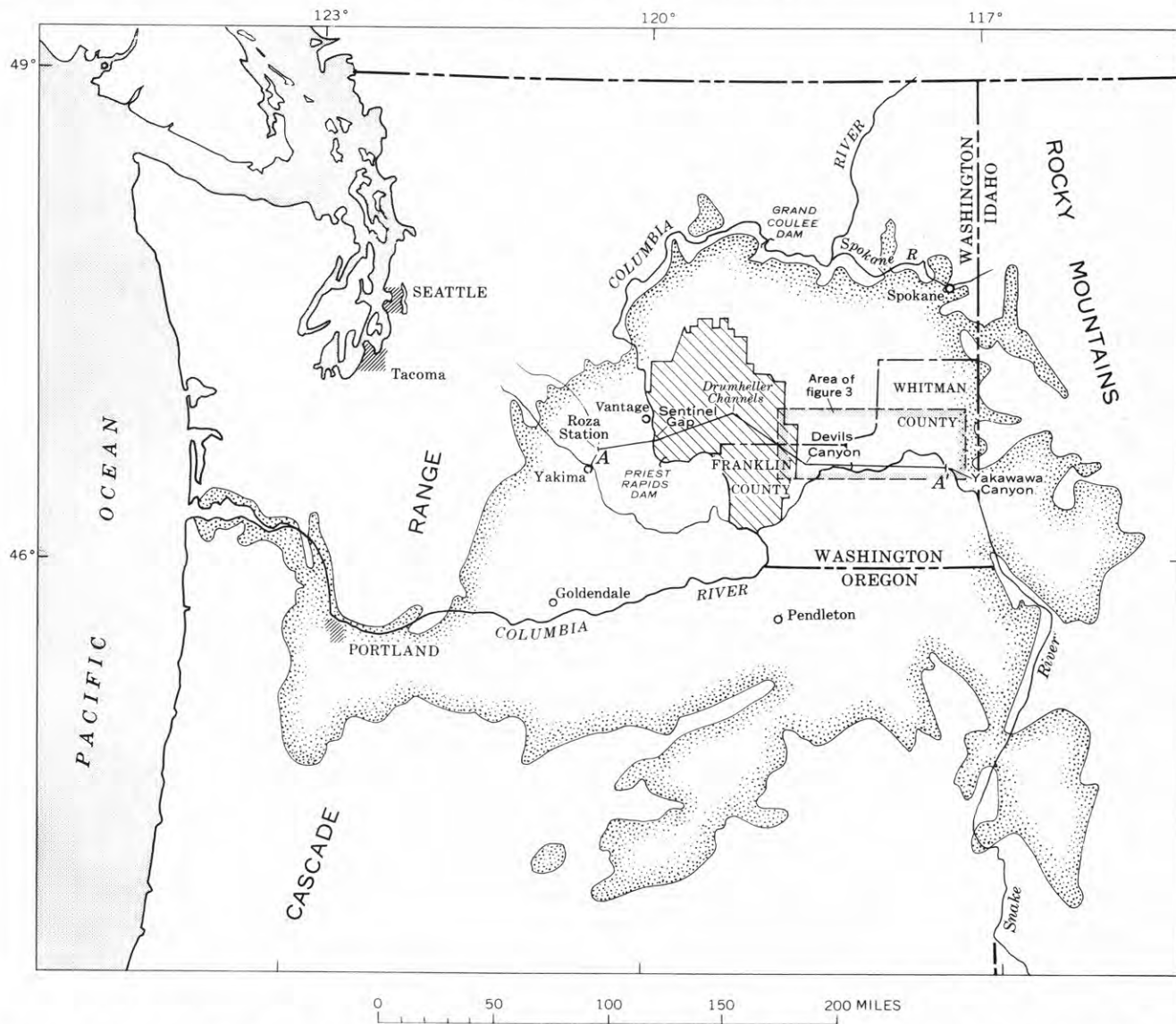
FIGURE 1.—Areal extent of the Columbia River Group (stippled border) (after Waters, 1961) in the northern part of the Columbia Plateau. The Columbia Basin Irrigation Project area is shown by diagonal pattern. Section *A–A'* is shown on figure 2.

In addition to identification of the sequence in the stratigraphic sections measured at Devils and Yaka-wawa Canyons, parts of the sequence were recognized at 18 places from near Connell eastward into eastern Whitman County, where K. L. Walters is preparing a ground-water report. The locations of these places are shown on figure 3 and described in table 2. In those places where less than the full sequence occurs, the stratigraphic relations are consistent; either the topographic relief is not sufficient to expose the entire section or the upper part of the section has been removed by erosion.

The number of flows in each member differs from place to place. However, the single flow of the Roza Member, described by Mackin in the Columbia River valley near Sentinel Gap and in Yakima River canyon,

TABLE 1.—*Comparison of three members in the upper part of the Yakima Basalt at three localities in southeastern Washington*

| Member	Description	Sentinel Gap (Mackin, 1961)		Devils Canyon		Yakawawa Canyon	
		Number of flows	Total thickness (feet)	Number of flows	Total thickness (feet)	Number of flows	Total thickness (feet)
Priest Rapids___	Medium- to coarse-grained basalt; grayish black where fresh, red-brown to green where weathered; nonporphyritic and diktytaxitic. Very large columns with spherical fractures normal to the column axis are common. Includes Quincy Diatomite Bed of Mackin (1961, p. 25) or its equivalent in places.	4	220±25	1	50±10	2(?)	100±20
Roza_____	Medium- to coarse-grained basalt; dark blue gray or dark reddish gray where fresh, red-brown where weathered; porphyritic with uniformly distributed transparent lath-shaped phenocrysts averaging 1 cm in length. Large columns with platy partings and entablatures with swirling platy partings are common.	1	110±10	2	160±15	1	80±10
Frenchman Springs.	Fine- to medium-grained basalt; dark gray to black; sparsely porphyritic with unevenly distributed, roughly equidimensional, partly resorbed, shattered, yellowish-white phenocrysts averaging 1 cm in diameter. Includes Squaw Creek Diatomite Bed of Mackin (1961, p. 21) or its equivalent in places.	3	365±20	6	265±15	3	230±10
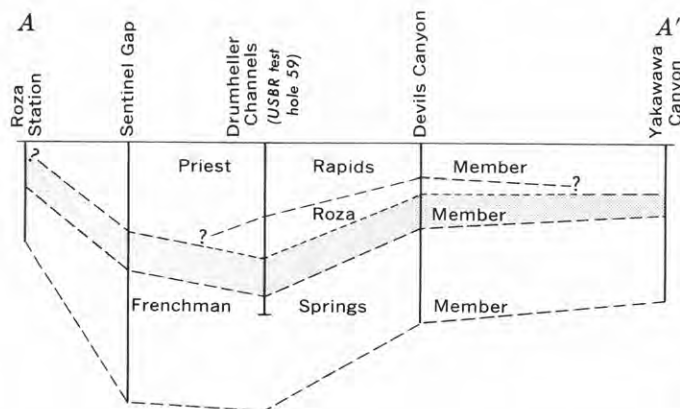
FIGURE 2.—Diagrammatic sketch of section A–A' (fig. 1), showing the basalt sequence discussed in text. The top of the Priest Rapids Member in the measured sections is alined horizontally to emphasize midbasin thickening of the members. The key flow in the Roza Member is shown by pattern. Data for Drumheller Channels from U.S. Bureau of Reclamation test hole 59.

is present at nearly all the localities visited and appears to be continuous over thousands of square miles. This flow is a key stratigraphic marker throughout most of the Columbia Basin Irrigation Project area (Grolier and Bingham, report in preparation) even

where the Roza consists of more than one flow, and has been observed by the authors as far north as 10 miles south of Grand Coulee Dam, as far south as Pendleton, Oreg., and as far west as the vicinity of Goldendale. Wherever exposed within the 175-mile reach from the Yakima area to eastern Whitman County the key flow is relatively uniform in thickness and retains its characteristic lithology. The apparent continuity of this flow over such a great area is difficult to explain. Optimum conditions of (1) volume, viscosity, and temperature of magma, (2) locations of vents, and (3) topographic relief must have prevailed to permit such extensive spreading of lava.

The similarity of the succession of flows in the measured sections, and the fact that the members are mappable over most of the intervening distances, lead us to conclude that the sequence in Yakawawa Canyon, although different in its number of flows, is the same as that described by Mackin at Sentinel Gap. On the basis of this conclusion the area covered by the Priest Rapids, Roza, and Frenchman Springs Members of the Yakima Basalt can be assumed to extend into Whitman County.
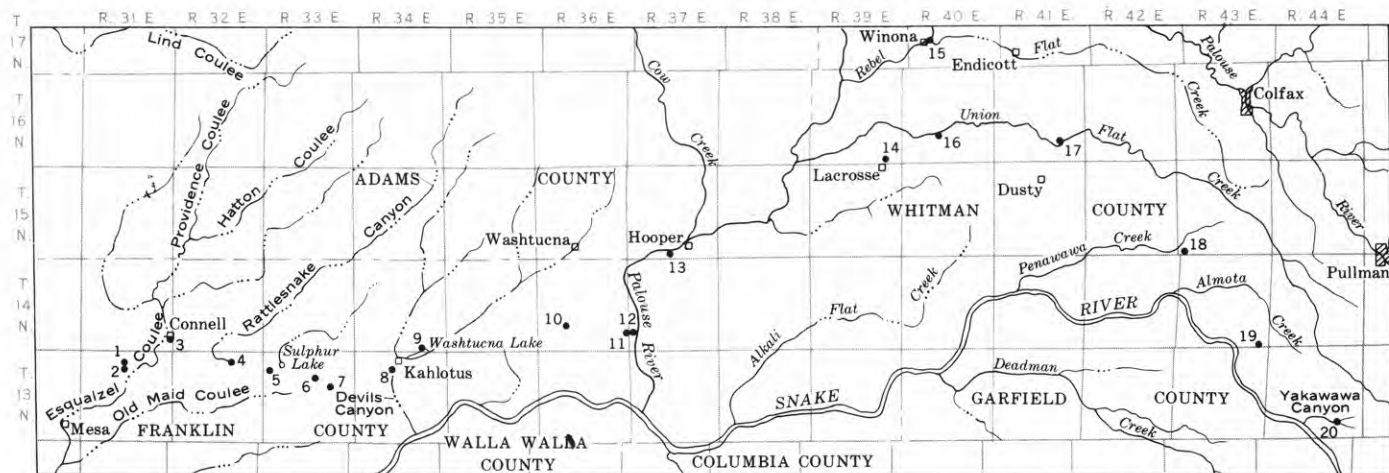
FIGURE 3.—Area of southeastern Washington in which segments of the stratigraphic sequence in the upper part of the Yakima Basalt were examined.   Numbers refer to descriptions in table 2.   Location of area is shown on figure 1.

TABLE 2.—*Parts of basalt sequence exposed at 20 places in southeastern Washington*

No. on fig. 3	Location [1]	Member or members identified	No. of fig. 3	Location [1]	Member or members identified
1	13/31–4SE¼	Saddle Mountains Basalt Member of Mackin (1961) over one flow of the Priest Rapids Member, over Roza Member.	12	14/37–30SW¼	Frenchman Springs Member over lower basalt flows.
2	13/31–9NE¼	Roza Member over Frenchman Springs Member in gully.	13	15/37–33SE¼	Roza Member over Frenchman Springs Member.
3	14/31–36NE¼	Roza Member in roadcut.	14	16/39–35SE¼	Priest Rapids Member over equivalent of Quincy Diatomite Bed of Mackin (1961) (table 1), over Roza Member.
4	13/32–3SE¼	Priest Rapids Member over Roza Member.			
5	13/33–7NW¼	Do.	15	17/40–29NW¼	Roza Member only.
6	13/33–10SW¼	Do.	16	16/40–28NW¼	Priest Rapids Member over Rosa Member.
7	13/33–14NW¼	Do.	17	16/41–26SW¼	Do.
8	13/34–9NW¼	Devils Canyon section (table 1).	18	15/43–31SW¼	Do.
9	14/34–35SW¼	Roza Member, along road.	19	14/43–36SW¼	Do.
10	14/36–29NE¼	Priest Rapids Member over Rosa Member.	20	13/44–26SW¼ 13/44–35NW¼	}Yakawawa Canyon section (table 1).
11	14/36–25SE¼	Roza Member over Frenchman Springs Member.			

[1] The first two numbers of each location code refer to the township and range, respectively; the number and letters following the hyphen refer to the section and quarter section. All are in the northeast quadrant, Willamette meridian and base line.

REFERENCES

Mackin, J. H., 1961, A stratigraphic section in the Yakima Basalt and the Ellensburg Formation in south-central Washington: Washington Div. Mines and Geology Rept. Inv. 19, 45 p.

Waters, A. C., 1961, Stratigraphic and lithologic variations in the Columbia River Basalt: Am. Jour. Sci., v. 259, p. 583–611.

PREVIOUSLY UNDESCRIBED MIDDLE(?) ORDOVICIAN, DEVONIAN(?), AND CRETACEOUS(?) ROCKS, WHITE MOUNTAIN AREA, NEAR McGRATH, ALASKA

By C. L. SAINSBURY, Denver, Colo.

Abstract.—Marine carbonate and clastic rocks approximately 6,000–6,500 feet thick are dated by fossils as Middle(?) Ordovician and Devonian(?) in age. The marine strata are in fault contact along the Farewell fault with 8,100 feet of quartz conglomerate of Cretaceous(?) age. The rocks are unmetamorphosed.

Geologic mapping of mercury deposits discovered in 1958 (Sainsbury and MacKevett, 1960) has given information on the stratigraphy of a thick section of marine lower Paleozoic and continental Cretaceous(?) rocks hitherto undescribed in this part of Alaska (index map, fig. 1). The lower Paleozoic rocks have been dated by two collections of Middle(?) Ordovician and Devonian(?) fossils. The dated Middle(?) Ordovician beds are underlain by several thousand feet of marine carbonate and clastic rocks. The Farewell fault, a major fault of the Alaska lineament (Sainsbury and Twenhofel, 1954), brings the lower Paleozoic rocks in fault contact with a thick conglomerate believed to be of Cretaceous(?) age. This conglomerate may be correlative with the Lower Cretaceous Cantwell Formation, which is widespread some 100 miles east in the Alaska Range (Capps, 1940). The general geology of the White Mountain area is shown on figure 1.

The Middle(?) Ordovician rocks comprise an estimated 4,500–5,000 feet of unmetamorphosed miogeosynclinal marine sediments. The lower part contains shale, calcareous quartzo-feldspathic sandstone, siliceous siltstone and chert, and argillaceous limestone. These grade upward into medium-bedded gray limestone and argillaceous limestone which is in part chert bearing (fig. 2). The lowermost beds of the Middle(?) Ordovician are intricately folded and faulted near the Farewell fault, the true thickness of these folded rocks has not been determined accurately. The overlying beds are less deformed; the given thickness of these units is based in part on planetable mapping and in part on photogrammetric measurements along sections traversed on foot. The part of the section compiled from planetable maps is identified on figure 2 and is at the east end of the line of section *A–A* on figure 1. The remainder of the section is compiled from photogrammetric measurements tied to field-observation points on the southeast slopes of White Mountain just south of the line of section. The thicknesses measured from the planetable map are considerably more accurate than those measured from photogrammetric points. The geologic structure shown on the geologic section is considerably simplified, particularly in that part west of White Mountain, where many small-scale, tight folds complicate the main anticline.

The Middle(?) Ordovician rocks are dated by fossils in a collection (USGS 3140-CO) made by Sainsbury. The one brachiopod in this collection was identified by G. A. Cooper, of the U.S. National Museum, as *Christiania?* sp. (written communication, 1960). Jean M. Berdan, of the U.S. Geological Survey, reported (written communication, 1960) the following ostracodes from the same hand specimen:

> *Oepikella* sp.
> *Brevibolbina?* sp.
> *Pyxion?* sp.
> *Leperditella* sp.
> *Krausella* sp.
> Ostracodes, undetermined.

All the forms listed above, with the possible exception of *Pyxion*, range from the Middle to the Late Ordovician. However, the general aspect of the fauna and the absence of Late Ordovician species suggest that this collection is more probably Middle than Late Ordovician in age.

These Middle(?) Ordovician rocks are in part similar to Ordovician rocks described by Brooks (1911, p. 67–71) from the South Fork of the Kus-
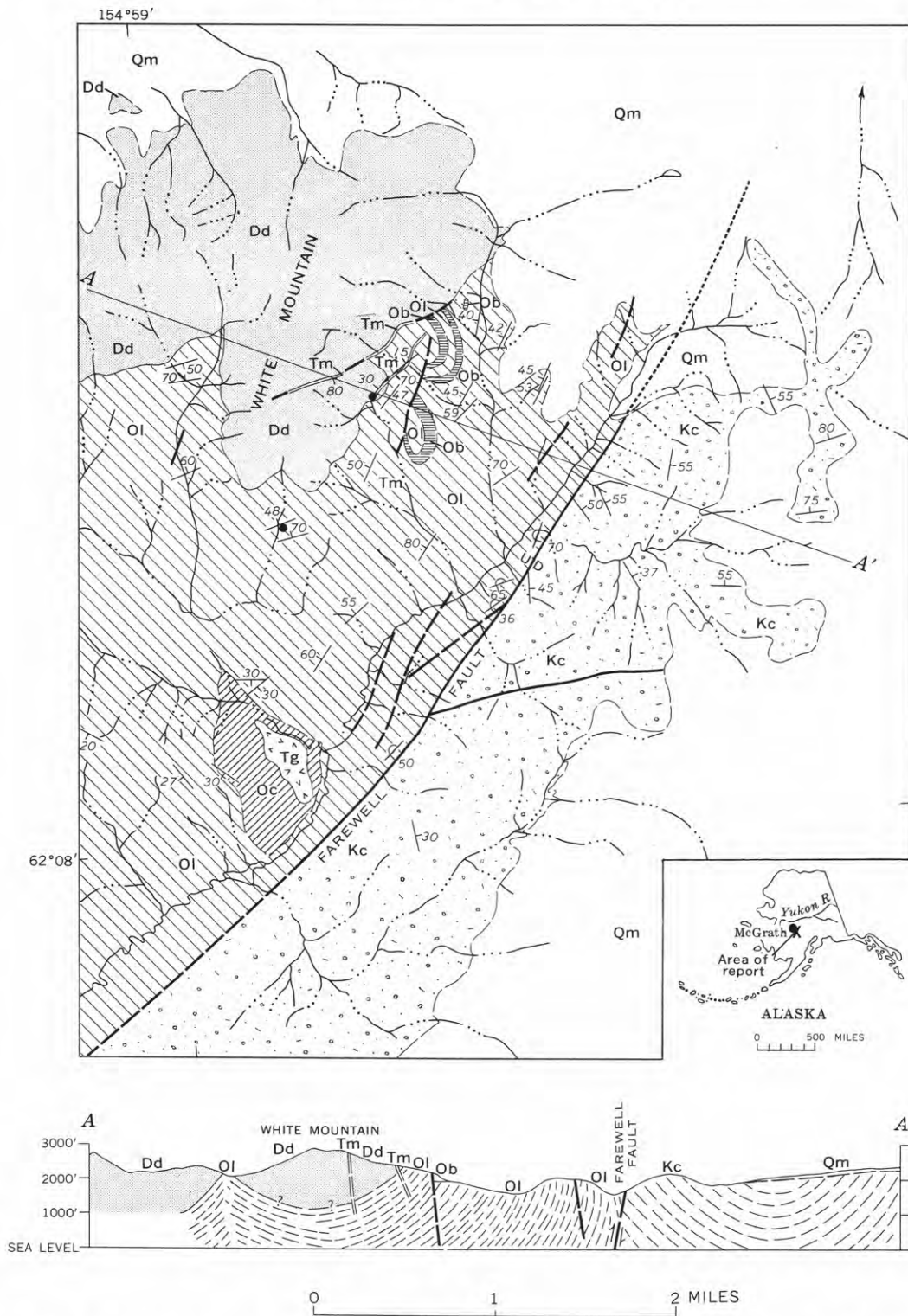
FIGURE 1.—Reconnaissance geologic map and structure section of the White Mountain area, south-central Alaska.
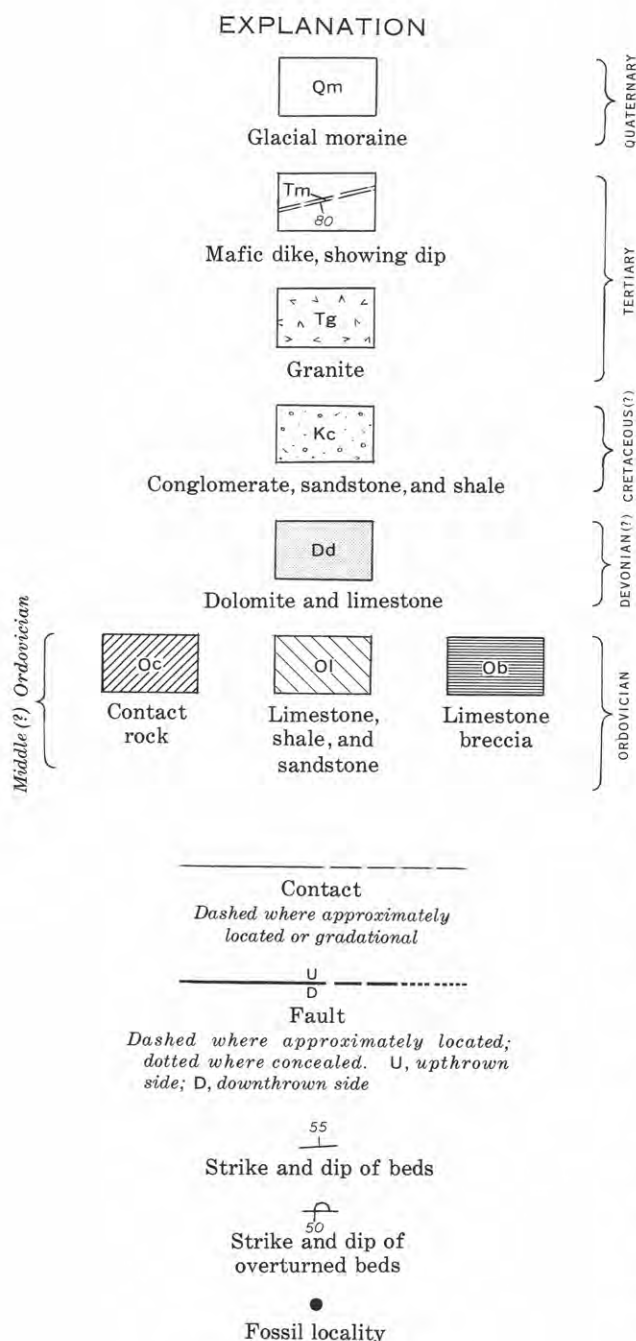
EXPLANATION

Qm

Glacial moraine

Tm
80

Mafic dike, showing dip

Tg

Granite

Kc

Conglomerate, sandstone, and shale

Dd

Dolomite and limestone

Oc

Contact
rock

Ol

Limestone,
shale, and
sandstone

Ob

Limestone
breccia

QUATERNARY

TERTIARY

CRETACEOUS(?)

DEVONIAN(?)

ORDOVICIAN

Middle (?) Ordovician

Contact
*Dashed where approximately
located or gradational*

U
D

Fault
*Dashed where approximately located;
dotted where concealed.* U, *upthrown
side;* D, *downthrown side*

55

Strike and dip of beds

50

Strike and dip of
overturned beds

●

Fossil locality

FIGURE 1.—Explanation.

kokwim River and the Tatina River some 50 miles east in the Alaska Range, the nearest known exposures of rocks of Ordovician age.

As the fossils which date the Middle(?) Ordovician rocks were collected approximately 3,800 feet above the base of the section, the lowermost beds shown in the section (fig. 2) may be considerably older than Middle Ordovician.

About 1,500 feet of limestone and dolomite overlies the Middle(?) Ordovician rocks, possibly with fault contact or with unconformity, and are considered here to be Devonian(?) in age. The base of the Devonian(?) rocks is brecciated where examined in two places, suggesting a fault contact; however, there is no angular discordance with the underlying rocks.

A sample of algal limestone (USGS coll. 5592-SD) from the lower part of the massive limestone and dolomite sequence contains an archaeocyathid associated with corals. Concerning the corals, W. A. Oliver, Jr., of the U.S. Geological Survey, reports (written communication, 1960):

This collection includes four rugose corals referable to a single species of a type which is certainly post-Ordovician and probably Silurian or Devonian in age. The species appears to be close to the genus *Leptoinophyllum* which is of Devonian age, but the material is inadequate for positive identification and a Silurian age cannot be ruled out.

Helen Duncan, of the U.S. Geological Survey, studied the algal and archaeocyathid material and reports (written communication, 1964):

The most conspicuous fossil is an unusual organism that has been named *Aphrosalpinx* and considered to be an archaeocyathid by Russian specialists who work on that group. Hitherto *Aphrosalpinx* has been recorded only from the northern and central Ural Mountains where it is said to occur in rocks of Ludlow age. The Alaskan specimen seems to be essentially identical with the Russian species *A. textilis* Miagkova, a circumstances that suggests contemporaneity of the Alaskan and Russian occurrences. However, the Russian literature dealing with *Aphrosalpinx* does not give adequate information on the associated fauna. Furthermore, in my opinion, there is uncertainty regarding the stratigraphic significance of some other faunal assemblages from the northern Urals that have been called Late Silurian. Under the circumstances, I think it would be hazardous to conclude that the Alaskan *Aphrosalpinx* provides indisputable evidence of Silurian age.

As Mr. Oliver has pointed out, the associated corals certainly look more like something I should expect to find in the Devonian. Inasmuch as the two lines of faunal evidence now available seem to conflict, the precise age of the unit in question cannot be determined until fossils with tested diagnostic value are obtained. In the meantime, I favor considering the horizon as Devonian(?).

The rocks here called Devonian(?) are lithologically similar to dolomitic rocks described by Cady and others (1955, p. 24–27) and assigned by them to the
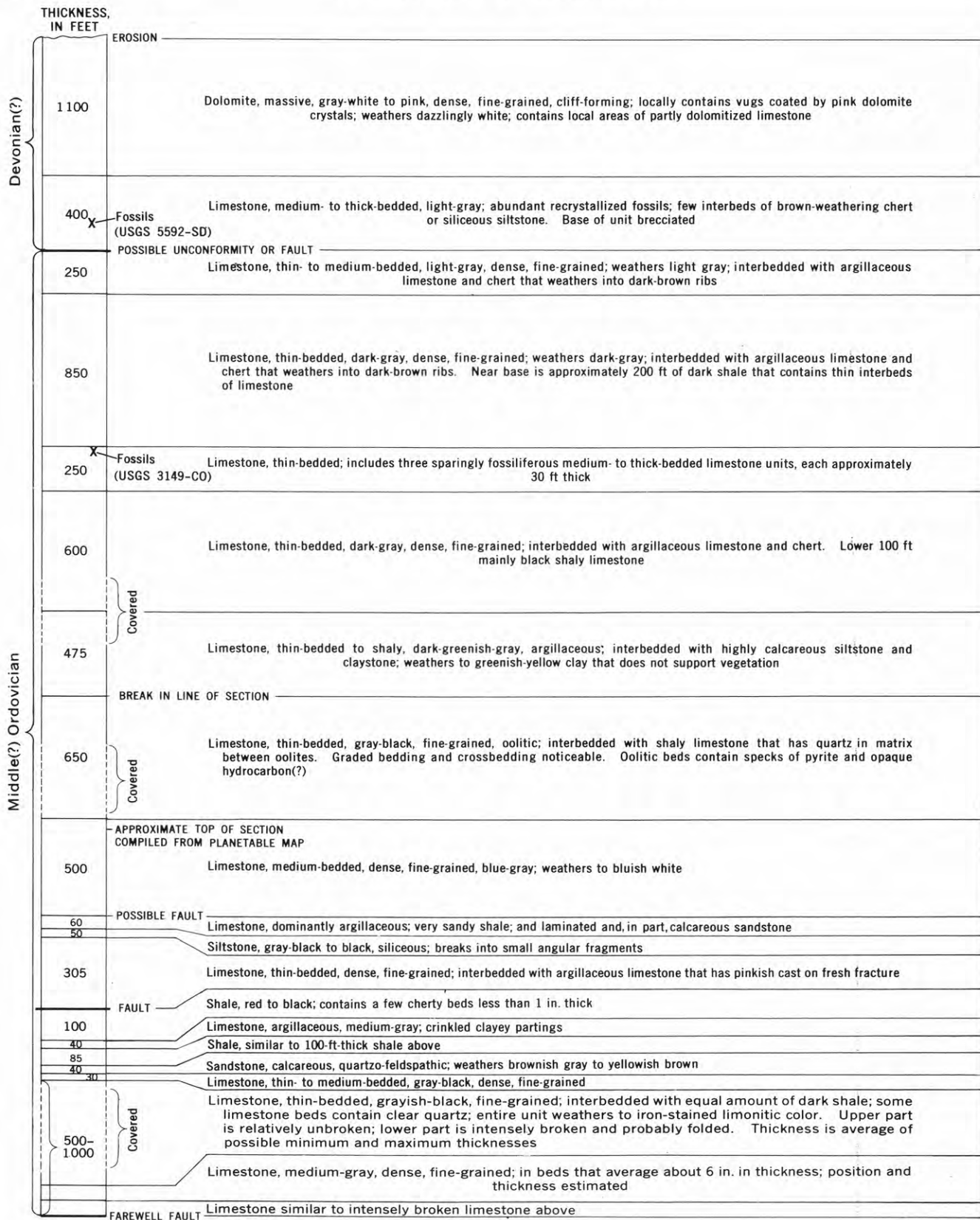
THICKNESS, IN FEET

EROSION

Devonian(?)

1100 — Dolomite, massive, gray-white to pink, dense, fine-grained, cliff-forming; locally contains vugs coated by pink dolomite crystals; weathers dazzlingly white; contains local areas of partly dolomitized limestone

400 X — Fossils (USGS 5592–SD) — Limestone, medium- to thick-bedded, light-gray; abundant recrystallized fossils; few interbeds of brown-weathering chert or siliceous siltstone. Base of unit brecciated

POSSIBLE UNCONFORMITY OR FAULT

Middle(?) Ordovician

250 — Limestone, thin- to medium-bedded, light-gray, dense, fine-grained; weathers light gray; interbedded with argillaceous limestone and chert that weathers into dark-brown ribs

850 — Limestone, thin-bedded, dark-gray, dense, fine-grained; weathers dark-gray; interbedded with argillaceous limestone and chert that weathers into dark-brown ribs. Near base is approximately 200 ft of dark shale that contains thin interbeds of limestone

X Fossils (USGS 3149–CO)
250 — Limestone, thin-bedded; includes three sparingly fossiliferous medium- to thick-bedded limestone units, each approximately 30 ft thick

600 — Limestone, thin-bedded, dark-gray, dense, fine-grained; interbedded with argillaceous limestone and chert. Lower 100 ft mainly black shaly limestone

Covered
475 — Limestone, thin-bedded to shaly, dark-greenish-gray, argillaceous; interbedded with highly calcareous siltstone and claystone; weathers to greenish-yellow clay that does not support vegetation

BREAK IN LINE OF SECTION

650 — Covered — Limestone, thin-bedded, gray-black, fine-grained, oolitic; interbedded with shaly limestone that has quartz in matrix between oolites. Graded bedding and crossbedding noticeable. Oolitic beds contain specks of pyrite and opaque hydrocarbon(?)

APPROXIMATE TOP OF SECTION COMPILED FROM PLANETABLE MAP

500 — Limestone, medium-bedded, dense, fine-grained, blue-gray; weathers to bluish white

POSSIBLE FAULT

60 / 50 — Limestone, dominantly argillaceous; very sandy shale; and laminated and, in part, calcareous sandstone

Siltstone, gray-black to black, siliceous; breaks into small angular fragments

305 — Limestone, thin-bedded, dense, fine-grained; interbedded with argillaceous limestone that has pinkish cast on fresh fracture

FAULT — Shale, red to black; contains a few cherty beds less than 1 in. thick

100 — Limestone, argillaceous, medium-gray; crinkled clayey partings

40 — Shale, similar to 100-ft-thick shale above

85 / 40 — Sandstone, calcareous, quartzo-feldspathic; weathers brownish gray to yellowish brown

30 — Limestone, thin- to medium-bedded, gray-black, dense, fine-grained

500–1,000 — Covered — Limestone, thin-bedded, grayish-black, fine-grained; interbedded with equal amount of dark shale; some limestone beds contain clear quartz; entire unit weathers to iron-stained limonitic color. Upper part is relatively unbroken; lower part is intensely broken and probably folded. Thickness is average of possible minimum and maximum thicknesses

Limestone, medium-gray, dense, fine-grained; in beds that average about 6 in. in thickness; position and thickness estimated

FAREWELL FAULT — Limestone similar to intensely broken limestone above

FIGURE 2.—Stratigraphic column of lower Paleozoic rocks, White Mountain, Alaska.

Holitna Group of Devonian, Silurian, and Ordovician (?) age. The nearest exposures of the Holitna Group are about 70 miles southwest of White Mountain.

The Cretaceous (?) rocks which lie southeast of the Farewell fault comprise an estimated 8,100 feet of quartz conglomerate with interbedded black to brown shale; these rocks grade upward into microconglomerate and coarse sandstone with interbedded quartz conglomerate and shale. Scour channels and crossbedding are common, and coal fragments were found at several places. The quartz in the conglomerate is principally vein quartz. The conglomerate is here correlated provisionally with the Cantwell Formation of Early Cretaceous age (Capps, 1940, p. 77), which

is widespread and thick in the Alaska Range about 100 miles to the east.

REFERENCES

Brooks, A. H., 1911, The Mt. McKinley region, Alaska: U.S. Geol. Survey Prof. Paper 70, 234 p.

Cady, W. M., Wallace, R. E., Hoare, J. M., and Webber, E. J., 1955, The central Kuskokwim region, Alaska: U.S. Geol. Survey Prof. Paper 268, 132 p.

Capps, S. R., 1940, Geology of the Alaska Railroad region: U.S. Geol. Survey Bull. 907, 201 p.

Sainsbury, C. L., and MacKevett, E. M., Jr., 1960, Structural control in five quicksilver deposits in southwestern Alaska: U.S. Geol. Survey Prof. Paper 400–B, p. B35–B38.

Sainsbury, C. L., and Twenhofel, W. S., 1954, Fault patterns in southeastern Alaska [abs.]: Geol. Soc. America Bull., v. 65, no. 12, pt. 2, p. 1300.

PRESENCE OF THE OSTRACODE *DREPANELLINA CLARKI* IN THE TYPE CLINTON (MIDDLE SILURIAN) IN NEW YORK STATE

By JEAN M. BERDAN and DONALD H. ZENGER,[1]

Washington, D.C., Claremont, Calif.

Abstract.—The ostracode *Drepanellina clarki*, previously unreported from New York State, has been found in a thin zone in the uppermost Clinton beds—the upper part of the Herkimer Sandstone of Chadwick (1918)—immediately below the base of the overlying Lockport Formation in the Rome and Utica quadrangles in east-central New York. The horizon of *Drepanellina clarki* appears to be stratigraphically above Gillette's *Paraechmina spinosa* Zone in the Herkimer. The presence of *Drepanellina* in the type Clinton extends the geographic range of the genus and permits a more direct correlation of the Clinton with the *Drepanellina clarki* Zone of Ulrich and Bassler elsewhere in the Appalachian region.

In the course of a stratigraphic study of the Herkimer Sandstone of Chadwick (1918), the uppermost Clinton unit in east-central New York, Zenger discovered an ostracode assemblage characterized by *Drepanellina clarki* Ulrich and Bassler just beneath the base of the overlying shaly Ilion Member of the Lockport Formation. His provisional identifications of this species and of the genera *Paraechmina* and *Dizygopleura* were confirmed by Berdan, who has also provided additional specific assignments. *Drepanellina clarki* is one of the species used for zoning the Clinton in the central Appalachians. Because it had not hitherto been reported from New York, its discovery permits a closer correlation between New York and Maryland and raises some questions about the equivalence of the Rochester Shale, the Herkimer Sandstone, and beds correlated with them in Maryland.

Acknowledgments.—The fieldwork on the Herkimer by Zenger was supported by Grant No. 928–63 from the Geological Society of America. The writers are grateful to Professor A. O. Woodford for the critical reading of the manuscript.

HERKIMER SANDSTONE

The Herkimer Sandstone, named by Chadwick (1918, p. 551), has been restudied by Zenger, who will publish details of the stratigraphy and petrography at a later date. It crops out in a narrow belt that extends from the Oneida quadrangle eastward across the Rome, Utica, and Winfield quadrangles and into the Richfield Springs quadrangle, where it pinches out (fig. 1). Most workers, including Gillette (1947, p. 112) and Fisher (1959), regarded the Herkimer as the eastern, nearshore equivalent of the more fossiliferous Rochester Shale of central and western New York. The Rochester, in turn, was correlated with the *Drepanellina clarki* Zone of the McKenzie Forma-
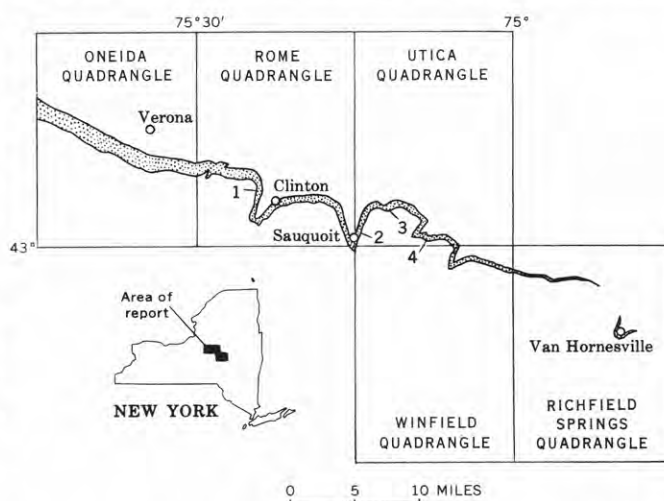
FIGURE 1.—Outcrop belt (stippled) of the Herkimer Sandstone of Chadwick (1918) in east-central New York, and localities of *Drepanellina clarki* horizon. *1*, College Hill. *2*, Sauquoit. *3*, Starch Factory Creek. *4*, Moyer Creek. Distribution of the Herkimer based in part on information from the geologic map of New York by the New York State Geological Survey (1962).

tion of Maryland. These correlations were based on the evidence of various groups of fossils, especially the ostracodes.

OSTRACODE ZONES

The exceptional value of ostracodes for Clinton correlations in the Appalachian region was first recognized by Ulrich and Bassler (1923). They established 9 ostracode zones, 3 in each of the lower, middle, and upper parts of the Clinton (Ulrich and Bassler, 1923, p. 349). The three zones in the upper part of the Clinton are, in ascending order, the *Bonnemaia rudis* Zone, the *Mastigobolbina typus* Zone, and the *Drepanellina clarki* Zone. The last, the youngest of the Clinton zones, was unequivocally correlated with the Rochester Shale by Ulrich and Bassler (1923, p. 386), largely because of the presence of *Paraechmina spinosa* (Hall), *P. abnormis* (Ulrich), and *Dizygopleura symmetrica* (Hall) in both; however, they recognized that the other known ostracodes in the Rochester do not occur in the *Drepanellina clarki* Zone of Maryland and Pennsylvania, and that *D. clarki* does not occur in New York.

Gillette (1947), in his detailed study of the Clinton Group in New York, was able to find only 5 of the 9 zones proposed by Ulrich and Bassler. In the upper part of the Clinton he recognized the *Mastigobolbina typus* Zone and an overlying zone which he designated the *Paraechmina spinosa* Zone. The latter he considered equivalent to the *Drepanellina clarki* Zone of Maryland, although he preferred to name it for the most common ostracode in the Rochester Shale because *D. clarki* had not been found in New York. The accompanying table shows Gillette's two upper Clinton zones, the rock units containing these zones in the type Clinton of east-central New York, and the corresponding zones of Ulrich and Bassler in Maryland.

Ostracode zones in the upper part of the Clinton Group in east-central New York, and equivalent zones of Ulrich and Bassler (1923)

[Adapted from Gillette (1947, p. 22-23)]

	New York		Maryland
	Uppermost two ostracode zones of Gillette	Rock units representing these zones	Equivalent ostracode zones of Ulrich and Bassler
Upper part of Clinton Group	*Paraechmina spinosa*	Herkimer Sandstone	*Drepanellina clarki*
		Kirkland iron ore	
	Mastigobolbina typus	Willowvale Shale	*Mastigobolbina typus*
		Westmoreland iron ore	

Gillette (1947, p. 24), like Ulrich and Bassler, based his correlation on the presence of *Paraechmina spinosa* in both the Rochester in New York and the *D. clarki* Zone of Maryland. Other *D. clarki* Zone ostracodes mentioned by Gillette (1947, p. 106) as occurring in the Rochester are *Paraechmina postica* Ulrich and Bassler, *Dizygopleura proutyi* Ulrich and Bassler, and "*Beyrichia*" *veronica* Ulrich and Bassler. Although ostracodes in the Herkimer are sparse and poorly preserved, Gillette (1947, p. 70) listed *Paraechmina spinosa*, *P. postica*, *Dizygopleura proutyi*, and "*Beyrichia*" *veronica* from the lower 14 feet of this formation along Dawes Quarry Creek in Clinton, and hence he correlated this unit with the Rochester Shale to the west.

Problems of identification affect present-day assessment of the significance of the *Paraechmina spinosa* Zone. Gillette's identification of *Dizygopleura* "*proutyi*" in the Rochester and Herkimer may require revision; according to Swartz (1933, p. 233, 234) *D.* "*proutyi*" is based on the female dimorphs of *Kloedenella cornuta* (Ulrich and Bassler) and of *K. cornuta praenuntia* Swartz. It now appears likely that the form from the Rochester, identified by Gillette as *D. proutyi*, is the female of the common Rochester species *D. symmetrica*. The ostracodes which are most abundant in the Rochester Shale have been listed by Copeland (1962, p. 10). These include *Paraechmina spinosa*, *P. abnormis*, *P. postica*, *Dizygopleura symmetrica*, and "*Ctenobolbina*" *punctata* Ulrich. Although *P. postica* is also recorded from the Rochester by Gillette, Berdan has never seen it in Rochester collections from western New York. Moreover, no specimens of beyrichiid ostracodes which could be referred to "*Beyrichia*" *veronica* have as yet been found in the Rochester, and it seems possible that the form from western New York identified by Gillette as "*Beyrichia veronica*" may have been "*Ctenobolbina*" *punctata*, another common Rochester species. Oddly enough, Gillette does not mention *Paraechmina abnormis*, *Dizygopleura symmetrica*, or "*Ctenobolbina*" *punctata* as occurring in western New York, although all three were originally described from the Rochester shale and are very abundant. Should Gillette's identifications of Rochester ostracodes prove to be incorrect, his correlation of the *Paraechmina spinosa* Zone of New York with the *Drepanellina clarki* Zone of Maryland would be greatly weakened.

OSTRACODES IN THE HERKIMER SANDSTONE

All ostracodes found by Zenger in the Herkimer thus far are from the western and central parts of the outcrop belt (Oneida, Rome, and Utica quad-

FIGURE 2.—Specimens of *Drepanellina clarki* Ulrich and Bassler from locality 4 on Moyer Creek, Utica 15-minute quadrangle, New York. *a*, Latex impression of slab showing appearance of *D. clarki* and associated ostracodes in rock, × 4. *b, c,* Tecnomorphic internal molds of two right valves; × 30; *c* shows part of the shell. *d*, Internal mold of heteromorphic right valve, × 30. *e*, Internal mold of heteromorphic left valve, × 30.

rangles). In this area the Herkimer is 60 to 70 feet thick and consists of a sequence of interbedded light-gray sandstone, gray dolomitic sandstone, gray crinoidal dolomite, reddish hematitic sandstone, and dark-gray shale. Poorly preserved fossils are common in some beds; brachiopods and pelecypods are the most abundant. The western part of the Herkimer is underlain by a thin distinctive hematitic unit, the Kirkland iron ore of Gillette (1947), and the contract appears to be gradational. The upper contact of the

Herkimer with the Ilion Member of the Lockport Formation has been considered as unconformable by Gillette (1947, p. 113), but Zenger (1962, p. 2252; 1965) regards this contact as transitional.

The ostracodes in the Herkimer are generally poorly preserved. Most of those in the upper part of the formation are internal molds, and only a few of them show any shell material. In addition to *Drepanellina clarki* Ulrich and Bassler (fig. 2), other ostracodes suggestive of the *D. clarki* Zone of Maryland have been

found at Moyer Creek (see locality 4 in list of localities), although some, such as *Velibeyrichia* sp., are not suitably preserved for specific identification. Zenger has also found another ostracode horizon about 15 feet above the base of the Herkimer along Stony Creek, 2 miles south-southwest of Verona, in the Oneida quadrangle. There the ostracodes are preserved as external molds on a bedding surface. *Paraechmina spinosa* (Hall) and *P. abnormis* (Ulrich) can be identified with reasonable certainty and there are a few specimens which may represent *P. postica* Ulrich and Bassler. This is probably the same horizon found by Gillette on Dawes Quarry Creek, although fewer species are present in the Stony Creek exposures than at Dawes Quarry Creek. On the basis of the data gathered thus far, it appears that *Drepanellina clarki* may occur above the *Paraechmina spinosa* assemblage in the Herkimer.

The presence of the *Drepanellina clarki* Zone in New York extends its geographic distribution northward from its previously reported most northerly occurrence in Pennsylvania, and permits a direct correlation between the uppermost type Clinton and the equivalent beds of the central Appalachian area. The full significance this correlation may ultimately have will not be clear, however, until further studies have been made on the extent, both lateral and vertical, of *Drepanellina* in New York. Thus far this ostracode is known only from a very thin zone at the top of the Herkimer. One critical question is whether it is stratigraphically significant that, as seems to be true in eastern New York, the *Drepanellina* horizon lies above the *Paraechmina spinosa* assemblage. Swartz (1935, figs. 3, 4) indicated that *P. spinosa*, *P. abnormis*, and *P. postica* occur together in the *Drepanellina clarki* Zone of Maryland and Pennsylvania, but he showed *P. postica* extending higher in the section than the other species of *Paraechmina*. The ostracode association in the upper part of the Herkimer at the Moyer Creek locality, where ostracodes are more abundant and better preserved than at the other localities studied, lacks any of the characteristic Rochester species; however, it includes *Drepanellina clarki*, *D. modesta*, *Paraechmina postica*, and *Dizygopleura* sp. cf. *D. swartzi*, an assemblage typical of the *Drepanellina clarki* Zone in Maryland. It is possible that this difference from the Rochester is due to facies control, but it is also possible, as previously suggested by Swartz (1935, p. 1182), that most of the Rochester of western New York is slightly older than the *D. clarki* Zone of the central Appalachian area.

In the western part of the State, in the vicinity of Lockport and Niagara Falls, *Paraechmina spinosa* and associated forms occur up to about 3 or 4 feet from the top of the Rochester. The uppermost part of the Rochester appears to be essentially barren of fossils, and is overlain by thin-bedded dolomite of the DeCew Member of the Lockport Dolomite, which is also nearly unfossiliferous. If facies control is critical, *Drepanellina* may never have occurred in western New York. A hasty search in these beds by Berdan in the summer of 1964 failed to locate any specimens, but the possibility of its existence in the uppermost part of the Rochester or in the DeCew should be kept in mind by Clinton stratigraphers. Other evidence (Zenger, 1962; 1965) suggests that the upper part of the Herkimer in east-central New York is younger than the upper part of the Rochester in the western part of the State. Thus the possibility that *Drepanellina* occurs even above the DeCew, in the lower part of the Lockport of western New York, should not be overlooked.

DESCRIPTION OF LOCALITIES

Drepanellina clarki has been found at the four numbered localities shown on figure 1 and described below.

1. College Hill

Section along the east-flowing tributary of Oriskany Creek just north of College Hill, roughly parallel to and 0.7 miles north of Route 412, west of Clinton, in the south-central part of the Rome 15-minute quadrangle. *Drepanellina clarki* occurs with the gastropod *Hormotoma* in the uppermost few feet of the Herkimer, which consists of medium-dark-gray to dark-gray crinoidal dolomite. This thin zone is at an altitude of about 700 feet, and is immediately below shale and stromatolitic dolomite of the Ilion Member of the Lockport Formation.

2. Sauquoit

Section along the west-flowing tributary of Sauquoit Creek midway between and approximately parallel to Roberts Road and Laughlin Road, about 1 mile north-northeast of Sauquoit, in the southeast ninth of the Rome 15-minute quadrangle and the southwest part of the Utica 15-minute quadrangle. The uppermost 4 feet of the Herkimer (below the dark-gray shale and stromatolitic dolomite of the overlying Lockport) consists of medium-bedded coarse-grained crinoidal dolomite and intercalated dark-gray fissile to chippy shale. *Drepanellina clarki* is found in both the shale and the dolomite, where it is associated with *Hormotoma*, *Tentaculites*, *Trimerus*, *Leptaena*, and

others. The sequence is at an altitude of about 910 feet.

3. Starch Factory Creek

Section along the west-flowing tributary of Starch Factory Creek from 0.8 to 1.0 mile northwest of Stewart Corners, in the southwest part of the Utica 15-minute quadrangle. Immediately below the linguloid-bearing shales of the Ilion Member of the Lockport are a couple of feet of dark-gray shales and intercalated gray medium-grained thin- to medium-bedded sandy crinoidal dolomite which has poorly preserved specimens of *Drepanellina clarki* with *Hormotoma* and *Tentaculites* on shaly parting surfaces. These uppermost fossiliferous beds are at an altitude of about 1,180 feet.

4. Moyer Creek

Section along the south branch of Moyer Creek about 1.3 miles east-northeast of Parker Corners, in the south-central part of the Utica 15-minute quadrangle. At this locality the uppermost 2 feet of Herkimer consists of gray shales and gray thin- to medium-bedded slightly sandy crinoidal dolomite. Relatively well preserved specimens of *Drepanellina clarki* (fig. 2) occur in the dolomite layers and are associated with other ostracodes which include *Drepanellina modesta*, *Paraechmina postica*, *Aechmina* sp., *Dizygopleura* sp. cf. *D. swartzi*, and *Velibeyrichia* sp. Specimens of

Hormotoma and *Tentaculites* are abundant. The elevation of this thin zone is about 1,060 feet.

REFERENCES

Chadwick, G. H., 1918, Stratigraphy of the New York Clinton: Geol. Soc. America Bull., v. 29, p. 327–368.

Copeland, M. J., 1962, Canadian fossil Ostracoda, Conchostraca, Eurypterida and Phyllocarida: Geol. Survey of Canada Bull. 91, 57 p.

Fisher, D. W., 1959, Correlation of the Silurian rocks in New York State: New York State Mus. and Sci. Service, Geol. Survey Map and Chart Ser. No. 1. [1960]

Gillette, Tracy, 1947, The Clinton of western and central New York: New York State Mus. Bull. 341, 191 p.

New York State Geological Survey, 1962, Geologic map of New York: New York State Mus. and Sci. Service, Geol. Survey Map and Chart Ser. No. 5.

Swartz, F. M., 1933, Dimorphism and orientation in ostracodes of the family Kloedenellidae from the Silurian of Pennsylvania: Jour. Paleontology, v. 7, p. 231–260.

——— 1935, Relations of the Silurian Rochester and McKenzie Formations near Cumberland, Maryland, and Lakemont, Pennsylvania: Geol. Soc. America Bull., v. 46, p. 1165–1194.

Ulrich, E. O., and Bassler, R. S., 1923, Paleozoic Ostracoda; Their morphology, classification and occurrence, *in* Maryland Geological Survey, Silurian: p. 271–391.

Zenger, D. H., 1962, Proposed stratigraphic nomenclature for Lockport Formation (Middle Silurian) in New York State: Am. Assoc. Petroleum Geologists Bull., v. 46, p. 2249–2253.

——— 1965, Stratigraphy of the Lockport Formation (Middle Silurian) in New York State: New York State Mus. and Sci. Service Bull. [In press]

MIOCENE MACROFOSSILS
OF THE SOUTHEASTERN SAN JOAQUIN VALLEY, CALIFORNIA

By WARREN O. ADDICOTT, Menlo Park, Calif.

Abstract.—Marine mollusks referable to the principal divisions of the California Miocene chronology occur in the southeastern San Joaquin Valley. Early and middle Miocene assemblages occur in the Kern River area northeast of Bakersfield. The Barker's Ranch fauna of this area is the standard for the middle Miocene "Temblor stage." New data from current biostratigraphic studies in the Kern River area indicate that this important faunal unit ranges from near the base of the Olcese Sand to the top of the Round Mountain Silt. Middle and late Miocene macrofossils occur in the Tejon Hills near Arvin.

Molluscan fossils representative of the three principal time-stratigraphic divisions of the California Miocene chronology, the Vaqueros, Temblor, and Briones-Cierbo-Neroly "stages" [1] of Weaver and others (1944), occur in two principal areas along the southeastern margin of the San Joaquin Valley, near the Kern River and in the northern Tejon Hills (fig. 1). Marine mollusks referable to the "Vaqueros" and "Temblor stages", the traditional early and middle Miocene divisions of the Pacific coast chronology, are abundant in the foothills between the Kern River and Poso Creek, about 15 miles northeast of Bakersfield. Beds of unusually well preserved fossils in the upper part of the Olcese Sand of Diepenbrock (1933) have yielded the classic Barker's Ranch fauna. This fauna is the standard of reference (Anderson, 1905, p. 190–191) for the "Temblor stage" of the macrofossil chronology. Mollusks and echinoids of middle and late Miocene age are present in the northern Tejon Hills near Comanche Point. There are other scattered records of Miocene fossils from the margin of the valley, and also a few subsurface records from well cores.

Biostratigraphic studies in progress on the early and middle Miocene molluscan faunas of the Kern River area and middle and late Miocene assemblages from the northern Tejon Hills are briefly summarized in order to record new data of potential use in local and regional faunal correlation. Stratigraphic ranges of a few of the abundant and characteristic Miocene mollusks of the southeastern San Joaquin Valley are defined herein and most of these species are figured. Principal interest is in the Barker's Ranch fauna, the largest Miocene molluscan fauna of the Pacific coast. This fauna, previously known from a few localities in a limited stratigraphic interval embracing the contact between the Olcese Sand and the Round Mountain Silt of Diepenbrock (1933), has been informally used as the standard for middle Miocene correlation on the Pacific coast. New biostratigraphic data from the Kern River area indicate that this unit extends from near the base of the Olcese Sand to the top of the Round Mountain Silt.

References to specimen numbers and localities in the accompanying paper are abbreviated as follows:

UCLA—University of California, Los Angeles.
UCMP—University of California Museum of Paleontology, Berkeley.
UCR—University of California, Riverside.
USGS Cenozoic loc. M—U.S. Geological Survey, Menlo Park, Calif.
USNM—U.S. National Museum, Washington, D.C.

HISTORY OF PALEONTOLOGIC INVESTIGATION

W. P. Blake, geologist-mineralogist assigned to a U.S. War Department Pacific Railroad Survey party, discovered the marine strata of the Kern River area while encamped on Ocoya [Poso] Creek in August 1853. Blake collected poorly preserved casts and molds of several mollusks from sandstone on the south bank of Poso Creek, and several shark teeth from near the top of the marine section. Field sketches of the fossiliferous material from sandstone beds now included in the

---

[1] Quotation marks are used hereafter to signify that these chronostratigraphic units have not been formally defined.
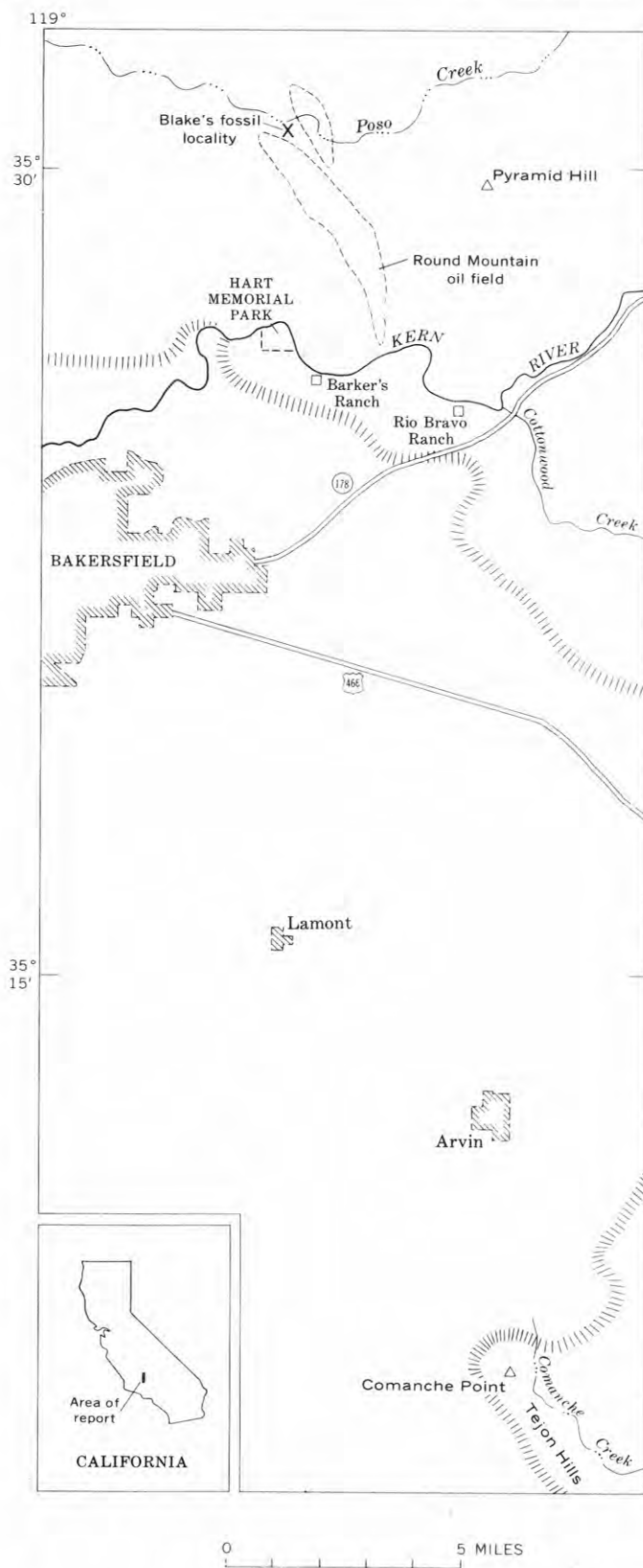
FIGURE 1.—Index map of southeastern San Joaquin Valley, Calif. Hachures represent western edge of foothills.

Olcese Sand were sent to T. A. Conrad in Philadelphia for identification. From these drawings Conrad (1855) described 12 new species and concluded that the fossils were Miocene.

The exceptionally well preserved fossils of the Kern River drainage area apparently were not discovered until about 40 years later when Watts (1894) listed a fauna of 33 mollusks, identified by J. G. Cooper, from localities along the Kern River. F. M. Anderson (1905) first associated the name Temblor with marine strata and macrofossils of the Kern River area. In this and subsequent publications (Anderson, 1911; Anderson and Martin, 1914) a fauna of 89 species, including 48 newly described gastropods and pelecypods, were reported from the vicinity of John Barker's Ranch on the Kern River. The assemblage later became known as the Barker's Ranch fauna. In 1905 Anderson (p. 190–191) concluded that the molluscan assemblage from the vicinity of Barker's Ranch was "the most typical fauna of the Lower Miocene of the California interior." It thereby serves as a standard for his synonymous "Temblor Group" of that area, a unit predicated largely on biostratigraphic criteria. Subsequent usage has been to recognize the Barker's Ranch fauna as the standard of reference for the "Temblor stage." Anderson (1911) recognized 3 faunal zones in a 2,000-foot marine section along the Kern River. The lowest unit, best exposed at Pyramid Hill, was named the A zone; it was later correlated with the Vaqueros Formation [2] by Loel and Corey (1932) on the basis of larger collections. The B zone included the Barker's Ranch fauna. The C zone included the shark-tooth bed and a few mollusks near the top of the marine section. Mollusks of the B and C zones are referable to the "Temblor stage." Additional species from the Barker's Ranch fauna were described by Keen (1943).

The molluscan paleontology of the northern Tejon Hills area has been less thoroughly studied. Clark (in Merriam, 1916) first reported Miocene fossils from that area, including 9 species of early or middle Miocene age east of Comanche Creek and 27 species of late Miocene age at Comanche Point; Clark's list of late Miocene species has appeared in several subsequent papers. Additional late Miocene taxa were reported by Addicott and Vedder (1963).

MOLLUSCAN BIOSTRATIGRAPHY

Kern River-Poso Creek area

The principal stratigraphic occurrence of Miocene macrofossils of this area is depicted in figure 2.

[2] Loel and Corey's Vaqueros Formation (1932), a chronostratigraphic unit, is the basis of the Vaqueros "stage" of later usage.

FIGURE 2.—Stratigraphic ranges of selected mollusks in Miocene formations of the Kern River area.

Names originally proposed for subsurface units are frequently used as subdivisions of Anderson's (1911) original Temblor Group in surface mapping; these include the Walker Formation and Vedder Sand of Wilhelm and Saunders (1927), Jewett Sand of Godde (1928), Olcese Sand and Round Mountain Silt of Diepenbrock (1933), and Freeman Silt of Kleinpell (1938).

A few nonmarine mollusks and plant fossils have been reported from strata close to the surface type section of the Walker Formation near Bena (Dibblee and Chesterman, 1953).

Although marine fossils are not reported from exposures of the Vedder Sand, the "Vaqueros stage" guide fossil *Turritella inezana* Conrad and other species have been recovered from well cores not far from the outcrop.

The lowest occurrence of fossiliferous strata is at Pyramid Hill (secs. 14 and 15, T. 28 S., R. 29 E.), where the basal marine conglomerate, here included in the Jewett Sand, lies unconformably on the Walker Formation. This unit is recognized as the "Grit Zone" of the Pyramid Hill Sand (Ferguson, 1944) in the subsurface. It includes such index species of the "Vaqueros stage" as *Lyropecten magnolia* (Conrad), *Ostrea vaquerosensis* Loel and Corey, and *Crassatella granti* (Wiedey). In addition to these and other stratigraphically restricted species, there is a previously unreported element of northern mollusks characteristic of late Oligocene to middle Miocene formations of Oregon and Washington including *Epitonium clallamense* Durham, *Miopleiona weaveri* Tegland, *Priscofusus* aff. *P. geniculus* (Conrad), *Priscofusus medialis* (Conrad), *Bruclarkia yaquinana* (Anderson and Martin), and *Mytilus middendorffi* Grewingk.

Macrofossils are less abundant in the overlying fine- to very fine-grained part of the Jewett Sand. Several species in the basal conglomerate, including the variable pectinid *Vertipecten nevadanus* (Conrad) [*Pecten bowersi* Arnold, *P. perrini* Arnold, and *P. kernensis* Hertlein are synonyms] extend upward into this part of the formation. Two species apparently restricted to the Vaqueros Formation of Loel and Corey (1932), *Chlamys hertleini* (Loel and Corey) and *Ostrea eldridgei yneziana* Loel and Corey, are locally concentrated in oyster biostromes in the upper part of the Jewett Sand.

The overlying Freeman Silt, sometimes included with the Jewett Sand as Freeman-Jewett, contains scattered small pelecypods, including *Acila conradi* (Meek), that represent a muddy, moderate-depth environment unlike that represented by the characteristic inner sublittoral-zone fossils of the "Temblor" and

"Vaqueros stages." The fauna of the next higher formation, the Olcese Sand, is here included as the lowest part of the "Temblor stage." It establishes an upper limit for the Vaqueros-Temblor boundary in the Kern River area. The lower limit of the "Temblor stage" occurs above the highest *Ostrea-Chlamys* biostromes of the Jewett Sand. Macrofossils of the intervening Freeman Silt represent a facies too poorly known to be assigned to either "stage."

The Olcese Sand is divisible into three lithostratigraphic units: (1) a lower fine- to very fine-grained sandstone with scattered fossiliferous calcarenites containing a fauna of about 40 to 50 species, (2) a coarse-grained current-bedded sand and gravel unit that is largely nonmarine, and (3) an upper unit of about 100 to 200 feet of fine- to medium-grained sand with several fossil beds toward the top. There is a gradational change from medium- to fine-grained sand in the upper part of the Olcese Sand to sandy siltstone or mudstone in the overlying Round Mountain Silt. The fauna of the upper part of the Olcese Sand is best represented in the area southwest of the Round Mountain oil field; mollusks of the lower part of the Round Mountain Silt are abundant along the Kern River east of the Rio Bravo Ranch. There is no pronounced faunal break between the two formations.

The Baker's Ranch molluscan fauna is typically developed in the upper part of the Olcese Sand on the north side of the Kern River between Hart Memorial Park and the south end of the Round Mountain oil field. It is named for Barker's Ranch headquarters, once located near the center of sec. 5, T. 29 S., R. 29 E.,

---

EXPLANATION OF FIGURE 3

a. *Ostrea titan* Conrad. × ¾. USNM 649163. Santa Margarita Formation, Comanche Point, USGS Cenozoic loc. M1702.
b. *Lyropecten crassicardo* (Conrad). Right valve. × ⅔. USNM 649164. Santa Margarita Formation, Comanche Point, USGS Cenozoic loc. M1619.
c. *Florimetis biangulata* (Carpenter). × 1. USNM 649165. Same locality as b.
d. *Lucinisca nuttalli* (Conrad). × 1. USNM 649166. Same locality as b.
e. *Chlamys hertleini* Loel and Corey. × 1. UCLA 39412. "Top of Pyramid Hill Sand" [Jewett Sand of this paper], UCLA loc. MB2000.
f. *Ostrea eldridgei yneziana* Loel and Corey. × 1. UCMP 36551. Approximately 170 ft above base of Jewett Sand, UCMP loc. B1654.
g. *Ostrea vaquerosensis* Loel and Corey. × ¾. UCMP 36552. Basal Jewett Sand, UCMP loc. B1659.
h. *Thais packi* Clark. × 2. USNM 649167. Basal Jewett Sand, USGS Cenozoic loc. M1591.
i. *Lyropecten magnolia* (Conrad). × ½. UCR 1185–b. Basal Jewett Sand, UCR loc. 1185.
j. *Epitonium (Cirsotrema) clallamense* Durham. × 1½. UCMP 36553. Basal Jewett Sand, UCMP loc. B1665.
k. *Vertipecten nevadanus* (Conrad). Right valve. × 1. UCMP 36554. About 40 ft above base of Jewett Sand, UCMP loc. B1673.
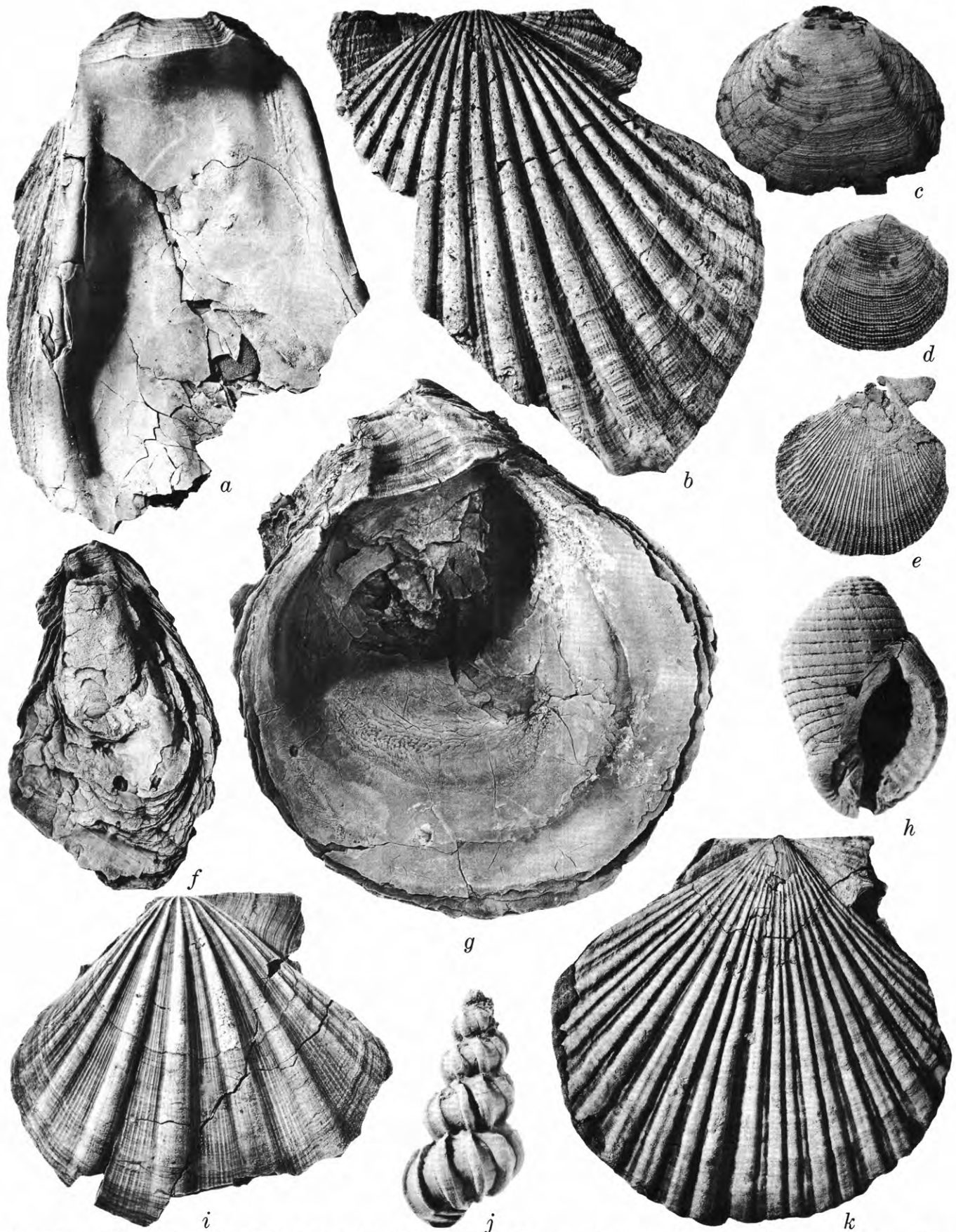
FIGURE 3.—Mollusks of the Jewett Sand of Godde (1928) and Santa Margarita Formation in the Kern River and northern Tejon Hills areas of California.

on the south side of the Kern River. Studies in progress by the author on the mollusks of this unit indicate a fauna of about 200 species, including many undescribed ornate gastropods of tropical affinities. Some of the mollusks restricted to the upper part of the Olcese Sand and the Round Mountain Silt are *Nassaris arnoldi* (Anderson), *Trophon kernensis* Anderson, *Crepidula rostralis* (Conrad), *"Thesbia" ocoyana* (Anderson and Martin), *Megasurcula howei* Hanna and Hertlein, and *Tellina nevadensis* (Anderson and Martin). Other characteristic species that also occur lower in the section include *Bruclarkia barkeriana* (Cooper), *Trophosycon kernianum* (Cooper), *Conus owenianus* Anderson, *Molopophorus anglonanus* (Anderson), and *Chione temblorensis* (Anderson).

The Round Mountain Silt is about 400 feet thick in the vicinity of the Kern River. The lower 150 feet consists of light-gray to chocolate-brown carbonaceous sandy mudstone with scattered mollusks, including locally abundant articulated valves of *Anadara osmonti* (Dall). A bed containing abundant *Turritella ocoyana* Conrad and *Amiantis mathewsoni* (Gabb) occurs near the top of the overlying diatomaceous mudstone and shale along the west side of Cottonwood Creek south of State Highway 178. A diatom flora of 80 species has been described from the Round Mountain Silt by Hanna (1932). The upper 100 feet of the Round Mountain Silt along the Kern River includes a fine- to very fine-grained sand containing abundant shark teeth and marine mammal bones near the base and fossiliferous sandstone beds near the top. Both were included in Anderson's C zone (1911). There are about 40 species of mollusks including abundant *Dosinia merriami* Clark in the upper sandstone beds. Nearly all of these mollusks also occur in the upper part of the Olcese Sand. The studies of marine vertebrates of the C zone were summarized by Church (1958).

Nonmarine gravel and sand referable to the Cottonwood Creek Formation of Hackel and Krammes (1958), possibly correlative with the Santa Margarita Formation of local subsurface usage, overlie the Round Mountain Silt along the Kern River. At the Fruitvale oil field, immediately west of Bakersfield, late Miocene fossils have been reported from cores of the Santa Margarita Formation by Gale (*in* Preston, 1931). The assemblage includes 55 species.

A few of the characteristic mollusks from Miocene formations of the Kern River area are illustrated in figures 3 and 4, appearing on pages 105 and 107.

Northern Tejon Hills

Miocene megafossils are abundant in the vicinity of Comanche Point. East of Comanche Creek, a small macrofossil assemblage of middle Miocene age occurs in fine-grained sandstone, originally mapped as "Vaqueros Sandstone" by Hoots (1930) but now recognized as Olcese Sand (T. W. Dibblee, oral communication, Feb. 1965). Fossils occur in a 20- to 100-foot stratigraphic interval above granitic basement rocks. Recent collections from 5 localities in this area have increased the assemblage to 33 taxa (see accompanying table). Fossils occur in concretionary strata characterized by abundant barnacles, *Aequipecten andersoni* (Arnold), and *Mytilus* spp. The small echinoid *Vaquerosella andersoni* (Twitchell) is sufficiently abundant in two areas to form so-called button beds (loc. M1709, M1716). The fauna is correlated with the "Temblor stage" fauna of the Kern River area.

At Comanche Point, fossil mollusks occur in a 20-foot interval of marine sandstone and conglomerate near the top of a 400-foot section of Santa Margarita Formation measured by Savage (1955). Abundant *Lyropecten crassicardo* (Conrad) and *Ostrea titan* Conrad occur in conglomerate at the base of this unit that overlies green to varicolored mudstone and sandstone containing terrestrial vertebrates referred to the Clarendonian Stage of Savage (1955). Above the conglomerate is 10 to 15 feet of light-yellowish-brown sand with scattered fossiliferous concretions which have yielded about 60 species of mollusks (Addicott

---

EXPLANATION OF FIGURE 4

a, b. *Bruclarkia barkeriana* (Cooper). × 1. UCMP 36555. Upper part of Olcese Sand, UCMP loc. B1600.

c. *Bruclarkia barkeriana* forma *santacruzana* (Arnold). × 1. UCMP 36556. About 80 ft stratigraphically below top of Olcese Sand, UCMP loc. B1603.

d. *Neverita (Glossaulax) andersoni* (Clark). × 1. UCMP 36557. About 25 ft below top of Olcese Sand, UCMP loc. B1593.

e. *Tellina nevadensis* Anderson and Martin. × 1. USNM 649168. Near top of Olcese Sand, USGS Cenozoic loc. M1599.

f. *Nassarius arnoldi* (Anderson). × 5. USNM 649169. Lower part of Round Mountain Silt, USGS Cenozoic loc. M1604.

g. *"Thesbia" ocoyana* (Anderson and Martin). × 2. USNM 649170. Near top of Olcese Sand, USGS Cenozoic loc. M1602.

h. *Cancellaria dalliana* Anderson. × 1½. UCMP 36558. Upper part of Olcese Sand, UCMP loc. B1598.

i. *Oliva californica* Anderson. × 1½. UCMP 36559. Same locality as *a.*

j. *Megasurcula howei* Hanna and Hertlein. × 1½. UCMP 36560. Near top of Olcese Sand, UCMP loc. B1597.

k, n. *Trophon kernensis* Anderson. × 1. UCMP 36561. Same locality as *a.*

l. *Molopophorus anglonanus* (Anderson). × 1½. UCMP 36562. Same locality as *h.*

m. *Aequipecten andersoni* (Arnold). × 1½. USNM 649178. Upper part of Olcese Sand, USGS Cenozoic loc. M1597.

o. *Turritella ocoyana* Conrad. × 1. UCMP 36563. Round Mountain Silt, UCMP loc. B1588.

p. *Chione (Chionopsis) temblorensis* (Anderson). × 1. UCMP 36564. UCMP loc. B1599.

q. *Ostrea ashleyi* Hertlein. × ⅗. UCMP 36565. About 70 ft below top of Olcese Sand, UCMP loc. B1643.
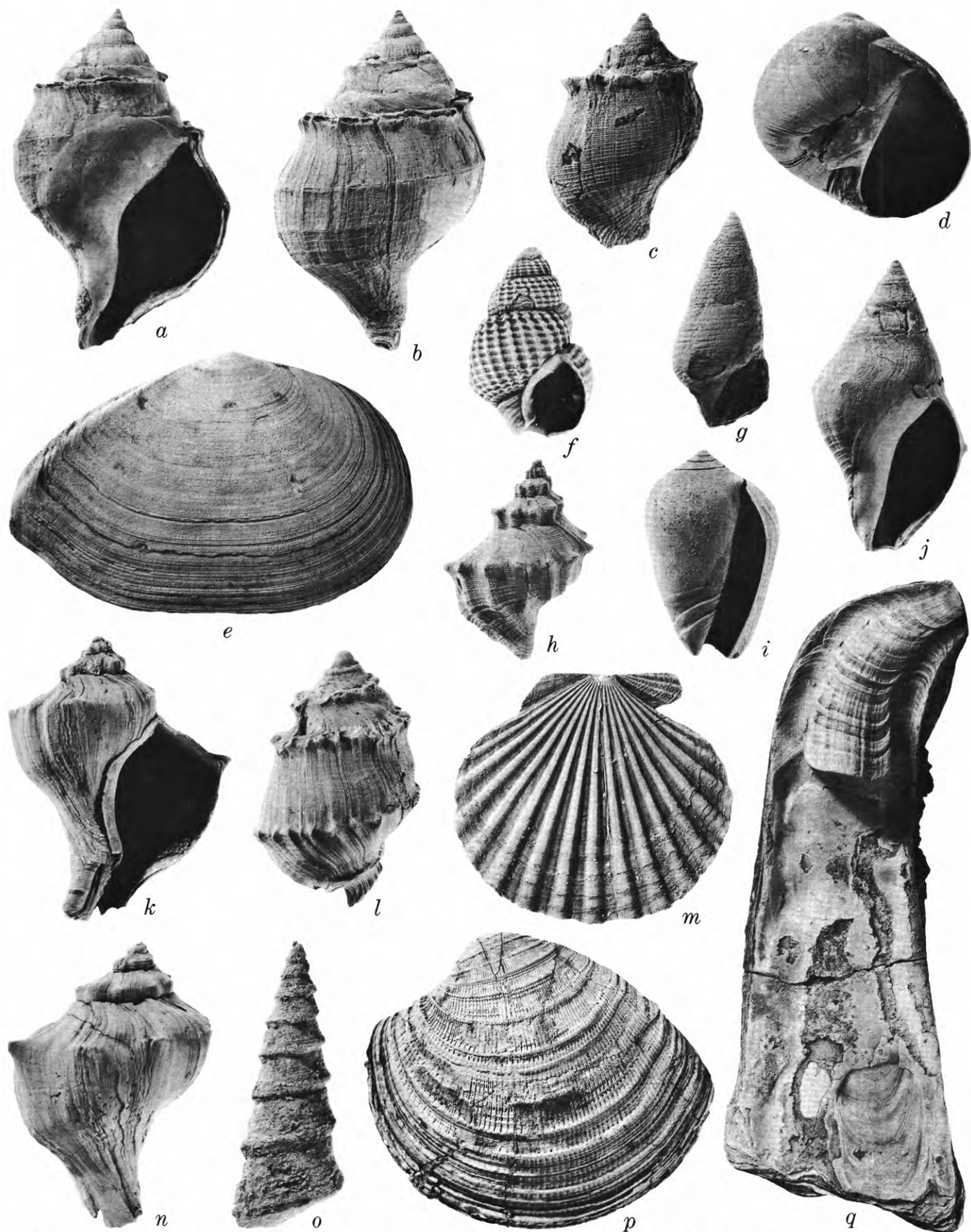
FIGURE 4.—Mollusks of the Olcese Sand and Round Mountain Silt of Diepenbrock (1933) in the Kern River area, California.

and Vedder, 1963), many represented by external molds. This assemblage clearly indicates a post-Temblor, late Miocene age and a correlation with the fauna of the Santa Margarita Formation of the California Coast Ranges. Characteristic mollusks from localities

at Comanche Point are *Nassarius pabloensis* (Clark), *"Fusinus" fabulator* Nomland, *Lucinisca nuttalli* (Conrad), *Dosinia merriami occidentalis* Clark, and *Clementia pertenuis* (Gabb). Some of these species are illustrated on figure 3.

Middle Miocene macrofossils from the northern Tejon Hills area

[×, present; sp., species undetermined; ?, doubtful identification; FI, field identification]

	USGS Cenozoic localities				
	M1713	M1712	M1714	M1709	M1716
Echinoids:					
Diadema sp. (spines)				×	×
Vaquerosella andersoni (Twitchell)				×	×
Vaquerosella cf. *V. merriami* (Anderson)					×
Gastropods:					
Calliostoma sp		×			
Turritella ocoyana Conrad			×		
Serpulorbis sp			×		
Calyptraea sp		×			
Neverita andersoni (Clark)		sp.?	FI		
Ficus (Trophosycon) kernianum Cooper		?	×		
?*Trophon* sp		×		×	
Thais cf. *T.* n. sp. Lutz	×				FI
Mitrella sp		×			
Oliva californica Anderson		×			
Conus owenianus Anderson			×		
Terebra cooperi Anderson		×	?		
Turricula? cf. *T. ochsneri* (Anderson and Martin)		×			
Pelecypods:					
Anadara sp		×			
Glycymeris sp		×			
Modiolus sp		×			
Mytilus cf. *M. expansus* Arnold			×	sp.	FI
Mytilus middendorffi Grewingk			FI		
Ostrea ashleyi Hertlein?		×			
Aequipecten andersoni (Arnold)	FI	×		×	×
Hinnites giganteus (Gray)				×	
Lucina excavata Carpenter		×			
Lucinoma acutilineata (Conrad)			×		
Miltha sanctaecrucis (Arnold)		?	×		
Trachycardium vaquerosensis (Arnold)			×		
Chione aff. *C. temblorensis* Anderson		×			
Dosinia cf. *D. merriami* Clark		×			
Spisula albaria Conrad		×			
Panope abrupta (Conrad)		×			
Barnacle:					
Balanus sp	FI				×

M1713. 3,300 ft south, 450 ft west of NE cor. sec. 19, T. 32 S., R. 30 E., Arvin quadrangle.

M1712. 150 ft north, 2,400 ft west of SE cor. sec. 29, T. 32 S., R 30 E., Tejon Hills quadrangle.

M1714. 2,100 ft south, 1,300 ft west of NE cor. sec. 30, T. 32 S., R. 30 E., Tejon Hills quadrangle.

M1709. SW¼NW¼NW¼ sec. 29, T. 32 S., R. 30 E., Tejon Hills quadrangle.

M1716. 1,250 ft south, 1,050 ft east of NW cor. sec. 29, T. 32 S., R. 30 E., Tejon Hills quadrangle.

REFERENCES

Addicott, W. O., and Vedder, J. G., 1963, Paleotemperature inferences from late Miocene mollusks in the San Luis Obispo-Bakersfield area, California: Art. 77 *in* U.S. Geol. Survey Prof. Paper 475–C, p. C63–C68.

Anderson, F. M., 1905, A stratigraphic study in the Mount Diablo Range of California: California Acad. Sci. Proc., 3d ser., Geology, v. 2, p. 155–248, pls. 13–33.

———— 1911, The Neocene deposits of Kern River, California, and the Temblor Basin: California Acad. Sci. Proc., 4th ser., v. 3, p. 73–148.

Anderson, F. M., and Martin, Bruce, 1904, Neocene record in the Temblor basin, California, and Neocene deposits of the San Juan district, San Luis Obispo County: California Acad. Sci. Proc., 4th ser., v. 4, p. 15–112, pls. 1–10.

Church, C. C., 1958, Macropaleontology, *in* San Joaquin Geol. Soc. Guidebook 1958 Spring Field Trip, Round Mountain Area: p. 12–13, 18–19.

Conrad, T. A., 1855, Report of Mr. T. A. Conrad on the fossil shells collected in California * * *: U.S. 33d Congress, 1st sess., House Ex. Doc. no. 129, p. 5–20.

Dibblee, T. W., and Chesterman, C. W., 1953, Geology of the Breckenridge Mountain quadrangle, California: California Div. Mines Bull. 168, 56 p.

Diepenbrock, Alex, 1933, Mount Poso oil field: California Oil Fields, v. 19, no. 2, p. 4–35.

Ferguson, G. C., 1944, East side San Joaquin Valley, Bakersfield, California, *in* Weaver, C. E., and others, Correlation of the marine Cenozoic formations of western North America: Geol. Soc. America Bull., v. 55, p. 581–583, chart facing p. 596.

Godde, H. A., 1928, Miocene formations in the east side fields of Kern County: California Oil Fields, v. 14, no. 1, p. 5–15.

Hackel, Otto, and Krammes, K. F., 1958, Stratigraphy, *in* San Joaquin Geol. Soc. Guidebook 1958 Spring Field Trip, Round Mountain Area: p. 10–11, 14–15.

Hanna, G. D., 1932, The diatoms of Sharktooth Hill, Kern County, California: California Acad. Sci. Proc., 4th ser., v. 20, p. 161–263.

Hoots, H. W., 1930, Geology and oil resources along the southern border of San Joaquin Valley, California: U.S. Geol. Survey Bull. 812–D, p. 243–332.

Keen, A. M., 1943, New mollusks from the Round Mountain Silt (Temblor) Miocene of California: San Diego Soc. Nat. History Trans., v.10, no. 2, p. 25–60, pls. 3, 4.

Kleinpell, R. M., 1938, Miocene stratigraphy of California: Tulsa, Okla., Am. Assoc. Petroleum Geologists, 450 p.

Loel, Wayne, and Corey, W. H., 1932, The Vaqueros Formation, lower Miocene of California; I, Paleontology: California Univ., Dept. Geol. Sci. Bull., v. 22, no. 3, p. 31–410, pls. 4–65.

Merriam, J. C., 1916, Mammalian remains from the Chanac Formation of the Tejon Hills, California: California Univ., Dept. Geology Bull., v. 10, no. 9, p. 111–127.

Preston, H. M., 1931, Report on Fruitvale oil field: California Oil Fields, v. 16, no. 4, p. 5–24.

Savage, D. E., 1955, Nonmarine lower Pliocene sediments in California—A geochronologic-stratigraphic classification: California Univ., Dept. Geol. Sci. Bull., v. 31, no. 1, p. 1–26.

Watts, W. L., 1894, The gas and petroleum yielding formations of the central valley of California: California Mining Bur. Bull. 3, 100 p.

Weaver, C. E., and others, 1944, Correlation of the marine Cenozoic formations of western North America [Chart 11]: Geol. Soc. America Bull., v. 55, no. 5, p. 569–598.

Wilhelm, V. H., and Saunders, L. W., 1927, Report on the Mount Poso Oil Field: California Oil Fields, v. 12, no. 7, p. 5–12.

NEW EVIDENCE ON LAKE BONNEVILLE STRATIGRAPHY AND HISTORY FROM SOUTHERN PROMONTORY POINT, UTAH

By R. B. MORRISON, Denver, Colo.

Abstract.—Pluvial-lake history revealed by study of new exposures on Promontory Point, Utah, is summarized as follows: Two lacustral episodes which preceded Lake Bonneville are correlated with the Kansan and Illinoian Glaciations, respectively. Episodes of lake desiccation and soil formation which separated and followed these lacustral episodes are correlated with the Yarmouth and Sangamon Interglaciations, respectively. At least four lake cycles occurred in early Lake Bonneville (Alpine) time, which is correlated with the Bull Lake Glaciation. In late Lake Bonneville time, correlated with the Pinedale Glaciation, there were 4 lake cycles: 2 high (earlier) ones recorded by the Bonneville Formation and 2 lower ones by the Draper Formation. Several of the main interlacustral episodes of marked lake recession or desiccation are marked in the deposits by soil profiles; the newly named Promontory Soil, separating the Alpine and Bonneville Formations, is particularly well developed.

The sequences of pluvial-lake deposits of the Great Basin surpass all other types of continental deposits— alluvial, colluvial, eolian, and even glacial—in the completeness and sensitivity of their records of Quaternary climatic changes. The most complete records are those of late Pleistocene Lake Bonneville and of its neighbor to the west, Lake Lahontan. The history of the lakes can best be deciphered by detailed stratigraphic studies in areas of exceptional exposure. Many more large-scale fluctuations of the lakes are now recognized than were known a few years ago. Fine subdivision of the stratigraphic record and correlation of the thin stratigraphic units through their entire altitude range are necessary to recognize more fluctuations and to determine the maximums and minimums of the various oscillations in lake level. However, in most areas, exposures are not adequate for detailed subdivision of the record and for correlation of thin units. This problem of making reliable correlations has confounded, to some degree, every attempt to unravel the history of Lake Bonneville by intensive stratigraphic study. Every stratigraphic worker has wished for exposures more continuous than those provided by the accidents of natural erosion or by small artificial openings such as roadcuts and ordinary gravel pits.

These hopes were largely fulfilled during 1955–57 when two huge gravel pits were excavated for the Southern Pacific Co. on Promontory Point, Box Elder County, Utah (fig. 1), to provide fill for completion of the railroad causeway across Great Salt Lake. Exposures in these pits were studied intensively during the summers of 1962 and 1963. The larger gravel pit is in Little Valley, on the western slope of the Promontory Range, 5 miles from the southern end of Promontory Point. It is 1.8 miles long, and along much of its length it is about 0.3 miles wide and extends more than 50 feet below the original land surface. The other pit, in a valley 2 miles to the south, is considerably smaller, but its lowest exposures are at an altitude about 200 feet lower than those in the Little Valley pit (or within 60 feet of the altitude of Great Salt Lake in June 1951—4,200 feet—that is shown on recent topographic quadrangle maps). These pits provide exposures of deposits of Lake Bonneville and other Quaternary sediments and soils over a total vertical range of 900 feet (to within 120 feet of the elevation of the highest shoreline); moreover, they are unrivaled for their continuity and their completeness of stratigraphic detail. Both valleys provided excellent lodgement for the lake sediments and sheltered the deposits from much of the wave erosion.

The history of lake fluctuations shown on figure 2 is based on the alternation, in the stratigraphic succession of two types of deposits and features. Lake maximums are recorded by shore deposits at high levels and by deep-water sediments which overlie older shore deposits. Low levels of the lake are represented by unconformities due to subaerial erosion, by weathering profiles, by terrestrial sediments that overlie lake deposits, and by shore deposits that are intercalated with
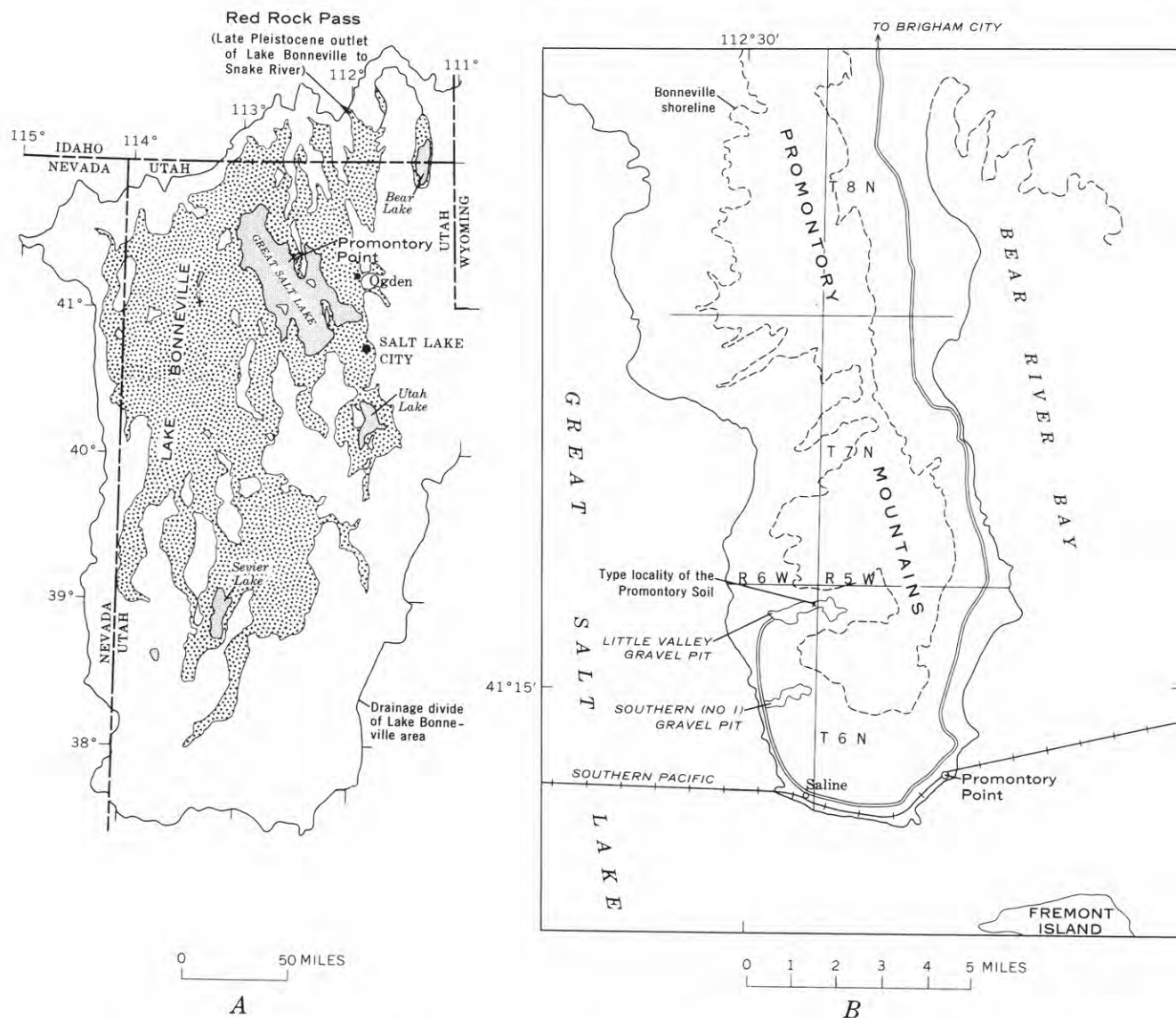
FIGURE 1.—Lake Bonneville, Great Salt Lake, and Promontory Point. *A*, Map showing extent of Lake Bonneville. Great Salt Lake and Promontory Point are at upper center. *B*, Map of Promontory Point, showing locations of Little Valley gravel pit (type locality for Promontory Soil) and southern (No. 1) gravel pit.

those formed in deeper water. The altitudes of various lake levels are inferred from the altitudes of the deposits.

PRE-LAKE BONNEVILLE UNITS

Deposits of pre-Lake Bonneville age comprise 2 lacustrine units, 2 interlacustrine units, 2 soils with very strong weathering profiles, and a distinctive bed of volcanic ash (fig. 2). These deposits invariably underlie the sediments of Lake Bonneville and coeval and younger sediments.

The older pre-Lake Bonneville lacustrine unit rests directly on bedrock in lower parts of the pits; it is exposed at altitudes of between 4,670 and 4,315 feet. The highest exposure appears to be below the highest

shoreline of the lacustral interval that this unit records. The unit is almost entirely cobble and pebble gravel that generally has well-rounded clasts, is nonfossiliferous, and is as much as 30 feet thick. The older pre-Lake Bonneville interlacustrine unit, locally present above the older lake unit, consists of variable amounts of alluvial-fan gravel (generally quite angular), colluvium (mostly slopewash, also angular), and, in its upper part, loess that commonly contains some interbedded silty to gravelly colluvium. It is exposed at altitudes as low as 4,318 feet. At the base of this unit a bed of pure white volcanic ash, nearly 2 feet in maximum thickness, crops out locally on the south side of the Little Valley pit. H. A. Powers (U.S. Geological Survey, written communications, 1962) considers that

Figure (left side)

INFERRED LAKE OSCILLATIONS

(Lake level in feet above sea level)

TIME | 4500 | 5000

Recent
- Alluvium, colluvium
- Early Recent soil
- Alluvium, colluvium
- Midvale Soil
- Loess, minor alluvium
- Draper Formation: middle member — lower member
- Graniteville Soil — Bonneville shoreline 5250 ft
- Bonneville Fm — Upper member — Interlacustrine diastem; alluvium, colluvium
- White marl member — 5220+
- Alluvium and colluvium of Bonneville age
- Promontory Soil

Pleistocene
- 4800± ft — Weak soil
- Interlacustrine diastem; local alluvium, colluvium
- 5280? ft
- Alpine Formation — Interlacustrine diastem; local alluvium, colluvium
- 5150+ ft
- Moderately strong soil
- Interlacustrine diastem; local alluvium, colluvium
- 5050+ ft
- Alluvium and colluvium of Alpine age

Time scale much compressed from the Wisconsin[2] above

- Dimple Dell Soil
- Younger pre-Lake Bonneville interlacustrine unit and disconformity
- Younger pre-Lake Bonneville lacustrine unit
- Pre-Dimple Dell soil
- Older pre-Lake Bonneville interlacustrine unit and disconformity
- Pearlette Ash Member equivalent
- Older pre-Lake Bonneville lacustrine unit
- Bedrock

APPROXIMATE AGE, IN THOUSANDS OF YEARS, BEFORE PRESENT

TENTATIVE CORRELATIONS

ROCKY MOUNTAIN GEOLOGIC-CLIMATIC STANDARD[1]	MIDCONTINENT REGION TIME-STRATIGRAPHIC DIVISIONS[2]
Pinedale-Neoglacial interglaciation	
Pinedale Glaciation (Late stade / Middle stade / Early stade)	Valderan substage
	Twocreekan substage
	Woodfordian substage
Bull Lake-Pinedale interglaciation	Farmdalian substage
Bull Lake Glaciation	Altonian substage
Sacagawea Ridge-Bull Lake interglaciation	Sangamonian stage
Sacagawea Ridge Glaciation	Illinoian stage
Cedar Ridge-Sacagawea Ridge interglaciation	Yarmouthian stage
Cedar Ridge Glaciation	Kansan stage

(Wisconsinan stage / Lake Bonneville Group indicated on chart)

[1] After Richmond (1964a, 1964b).

[2] Wisconsinan units from Frye and Willman (1960,1963); pre-Wisconsinan units from Leverett (1899) and Frye and Leonard (1952).

FIGURE 2.—Stratigraphy and tentative stratigraphic correlation of Quaternary deposits, and summary of lake oscillations at southern Promontory Point, Utah.

petrographically the ash is probably correlative with the Pearlette Ash Member (of the Sappa Formation) of Kansas.

A very strong weathering profile, the pre-Dimple Dell soil, is developed on the older pre-Lake Bonneville interlacustrine deposits (or, where they are missing, on the older pre-Lake Bonneville lacustrine unit), but not on younger deposits. It is seen only in buried occurrences, beneath the younger pre-Lake Bonneville lacustrine or interlacustrine units at locations sheltered from strong wave or stream erosion. It is exposed at altitudes as low as 4,320 feet. This soil is a maximal Brown soil. Its B horizon is a deep, somewhat reddish, brown (hue 7.5 YR), is moderately to strongly clayey, has weak to strong prismatic-blocky structure, and is as much as 3 feet thick where least eroded. The underlying Cca (calcareous) horizon is typically 4 to 5 feet thick and generally is well cemented by $CaCO_3$.

The younger pre-Lake Bonneville lacustrine unit, about 25 feet in maximum thickness, lies on the pre-Dimple Dell soil or, where the soil is missing, on unweathered older lacustrine or interlacustrine deposits. It consists of gravel, sand, silt, and clay, with some marl and in places small amounts of tufa. Locally it contains shells of snails, pelecypods, or both. This unit is exposed at altitudes between 4,325 and 4,980 feet; there is no evidence that its highest exposure records the highest shoreline of the lake in which it was deposited. Two samples (L–775L and L–775M)[1] of snail shells, collected at different times from the same site and bed in the younger pre-Lake Bonneville lacustrine unit at an altitude of 4,874 feet, gave rather widely divergent radiometric ages. Their radiocarbon ages are 28,500±1,500 years and 25,400±2,500 years, respectively. Two Th^{230}–U^{234} determinations of the age of the first sample are 89,000±8,000 years and 97,000±6,000 years, and two like determinations of the age of the second sample are 128,000±25,000 years and 212,000±30,000 to 40,000 years.[1] The unit that yielded these samples is overlain in the same exposure by fan gravel of the younger pre-Lake Bonneville subaerial unit that bears the Dimple Dell Soil; therefore the snails are certainly of pre-Lake Bonneville age. Consequently, according to the correlations presented in this paper, the C^{14} ages are much too young. The Th^{230}–U^{234} ages are too young for the first sample but probably are in the right order of magnitude for the second sample.

The younger pre-Lake Bonneville interlacustrine unit locally overlies the younger lacustrine unit. It consists of fan gravel (as much as 30 feet thick), col-

[1] Aaron Kaufman, 1964, Th^{230}–U^{234} dating of carbonates from Lakes Lahontan and Bonneville: Columbia Univ., Ph. D. thesis, 249 p.

luvium, and a little loess, and thus it resembles the older lacustrine unit except for the absence of volcanic ash. Its lowest exposure is at an altitude of 4,325 feet.

At southern Promontory Point the Dimple Dell Soil, named in a study of eastern Jordan Valley, Utah (Morrison, 1965a), is developed on deposits of the younger pre-Lake Bonneville interlacustrine unit, or on older deposits where those are absent, but not on the Alpine Formation. This soil is nearly as strongly developed as the pre-Dimple Dell soil, and it is of comparable thickness, but its B horizon typically is slightly less red and slightly less clayey, its structure is less well developed, and its Cca horizon is somewhat thinner and less well cemented. These contrasts are well shown in exposures which show both soils, separated by one or more of the intervening sedimentary units. Below the highest shorelines the younger soil is found only where it was buried by younger deposits, in places especially sheltered from subsequent erosion. Above the highest shoreline it is preserved locally as a relict soil on old alluvial fans. Its lowest exposure is at an altitude of 4,328 feet.

Inasmuch as the deposits of Lake Bonneville are correlated with the Bull Lake and Pinedale Glaciations (Morrison, 1961a, b; Richmond, 1961, 1964a) (see fig. 2), which are correlative with the Wisconsinan stage of Frye and William (1960, 1963; see also Richmond, 1962, table 11; Morrison;[2] and Morrison, 1965b), the Dimple Dell Soil is in turn correlated with the Sangamon Soil of the Great Plains–Midwest region, and therefore with the later part of the Sangamon Interglaciation and with the Sangamonian stage of Frye and Leonard (1952). The pre-Dimple Dell soil is correlated with the Yarmouth Soil of the Great Plains–Midwest region, with the later part of the Yarmouth Interglaciation, and with the Yarmouthian stage of Frye and Leonard (1952). Other correlations of the pre-Lake Bonneville succession with the Rocky Mountain and midwestern glacial successions are given on figure 2. According to this reasoning the bed of volcanic ash in the older pre-Lake Bonneville interlacustrine unit is late Kansan, and therefore is equivalent to the Pearlette Ash Member of the Sappa Formation in Kansas, supporting the correlation that has been made by H. A. Powers (see p. C111) on petrographic grounds.

DEPOSITS OF LAKE BONNEVILLE AGE

The main stratigraphic units of Lake Bonneville age are subdivided, defined, and correlated mainly on the basis of intercalated weathering profiles (soils), which

generally are the best stratigraphic markers in the succession. The lacustrine sediments of this age, which comprise the Lake Bonneville Group (Hunt, 1953), are here divided into the Alpine (oldest), Bonneville, and Draper Formations. Interlacustrine sediments (alluvium, colluvium, and loess of several ages, in units which are not formally named) and weathering profiles are intercalated with various parts of the Lake Bonneville Group.

Alpine Formation

The Alpine Formation, named by Hunt (1953), comprises the earlier deposits of Lake Bonneville. It is intermediate in age between the Dimple Dell Soil and the Promontory Soil (described in the next section of this report) and is correlated with the "yellow clay" of Gilbert (1890); it is equivalent to the Alpine Member of the Little Cottonwood Formation in eastern Jordan Valley, Utah (Morrison, 1965a). The Apline overlies the Dimple Dell soil and the younger pre-Lake Bonneville subaerial deposits with minor or no unconformity, and underlies the Promontory Soil and immediately older subaerial sediments with local unconformity. It is the thickest formation in the Lake Bonneville Group, reaching a maximum thickness of about 100 feet on southern Promontory Point. This formation is mainly gravel; it ranges from boulder gravel to pebble gravel, with local interbeds of sand and a few beds of silt and marl, and at a given locality contains the coarsest shore gravel in the Lake Bonneville Group. It forms the bulk of three conspicuous bay bars across Little Valley.

Several diastems, formed as a result of lake recession, occur within the Alpine Formation. They are marked by unconformities which record subaerial exposure and local erosion, and by discontinuous wedges of alluvium or colluvium which in some places bear weak to moderately strong weathering profiles. These intra-Alpine interlacustrine diastems and subaerial units within the Alpine Formation separate the formation into at least four wedges representing separate lake cycles. Unfortunately, individual diastems are only locally discernible. They are especially difficult to trace through the gravelly shore facies zone in determining the highest altitude reached by each tongue of the Alpine. Preliminary determinations are as follows: The oldest known wedge of the Alpine can be identified at least as high as 5,050 feet; the diastem immediately above it is locally identifiable at least as low as 4,700 feet and in places is associated with 1 to 4 feet of colluvium or alluvium bearing a moderately strong weathering profile. The second Alpine wedge can be traced as high as 5,150 feet and

[2] R. B. Morrison, 1964, Soil stratigraphy—principles, application to differentiation and correlation of Quaternary deposits and landforms, and applications to soil science: Nevada Univ., Ph. D. thesis, 178 p.

probably extends somewhat higher; the overlying diastem has been identified as low as 4,850 feet. The third wedge of the Alpine is exposed in the Little Valley gravel pit as high as 5,150 feet and may extend to the all-time highest shoreline of Lake Bonneville (at an average altitude of about 5,280 feet). That shoreline is marked by a prominent bouldery shore terrace which extends to about 30 feet above the Bonneville shoreline, bears the Promontory Soil, and is of Alpine age, but whether it marks the second or the third Alpine maximum is not certain. The diastem overlying the third wedge can be identified as low as 4,700 feet. It locally bears a foot or two of alluvium or colluvium and a weak soil. The youngest of the Alpine wedges, several feet in maximum thickness, extends to an altitude of approximately 4,800 feet.

Radiocarbon analysis of snail shells from a local marl bed in the upper part of the third wedge of the Alpine, at 4,791 feet altitude, gave an age of 40,000 $\pm$2,000 years (Rubin and Alexander, 1960, sample W-875); C^{14} analysis of another sample (L-775G) from this location gave an age of $\approx$ 37,000 years, and Th^{230}-U^{234} analysis indicated an age of 37,000 $\pm$1,500 and 40,000 $\pm$1,500 years (two determinations).[3] These ages support the correlations made herein.

Unconformity and subaerial units of post-Alpine–pre-Bonneville age

A widespread unconformity between the Alpine and Bonneville Formations records subaerial exposure and local erosion; locally a few inches to several feet of alluvium, or both, occurs along this unconformity. A strongly developed weathering profile, the Promontory Soil, is preserved on these deposits or along the unconformity in many places. The unconformity, subaerial deposits, and soil, identified at altitudes as low as 4,267 feet, attest to a major interval of probably complete lake desiccation.

Promontory Soil.—The Alpine Formation and the post-Alpine pre-Bonneville subaerial sediments locally bear a strongly developed weathering profile that is here named the Promontory Soil. This soil typically separates the Alpine and Bonneville Formations in the sheltered places where it has been preserved from wave erosion that occurred during deposition of the Bonneville Formation. Its type locality, and the one that best displays both its stratigraphic relations and a well-preserved profile, is a bench face in the north-central part of the Little Valley gravel pit, in the SE¼NE¼ sec. 1, T. 6 N., R. 6 W., at about 4,825±10 feet altitude (fig. 1). In all exposures at southern Promontory Point the Promontory Soil is a Brown soil

or (locally) a Calcisol. Its B horizon is 1 to (rarely) 2 feet thick where least eroded, deep brown (hue 7.5 YR to 10 YR), generally only slightly clayey, and generally structureless (massive) or (locally) weakly prismatic-blocky. The underlying Cca horizon, which commonly is the only part of the profile preserved in locations where the soil has been partly eroded by waves, has moderately strong to strong calcium carbonate concentration or even cementation, and usually it is about 2½ feet thick. In several places the profile of the Promontory Soil is compound, two soil profiles being present but separated by a few inches to 2 feet of alluvium or colluvium. Evidently the intervening sediment was deposited during a minor interval of deposition within the main soil-forming interval.

Bonneville Formation

As it is used in this discussion the Bonneville Formation includes all the lake sediments that are younger than the Alpine Formation (fig. 2) and older than the Draper Formation (which is discussed in a later section of this report). This usage differs slightly from the definition by Hunt (1953) and the modification of it by Bissell (1963, p. 111–112). They include in the Bonneville the lacustrine sediments believed to have been formed during the post-Alpine lake cycle in which water rose to the Bonneville shoreline[4] and, presumably, overflowed at Red Rock Pass; but they distinguish beds deposited during recession of the lake, at and below the Provo shoreline, as the Provo Formation. (Bissell also included in the Provo the sediments which were laid down in a separate subsequent lake cycle that did not quite reach the Provo shoreline and which here are designated as the lower member of the Draper Formation.) The present investigation showed, however, that on southern Promontory Point the Provo shoreline is scarcely marked by deposits of the Provo Formation, so that it is not feasible there to distinguish the Provo Formation. As used here the Bonneville Formation extends below the Provo shoreline and includes the main part of the Provo Formation (in the usage of Hunt and of Bissell) but excludes the upper part, which is here assigned to the Draper Formation. In this usage the Bonneville Formation is identical with the combined

---

[3] See footnote 1 on p. C112.

[4] The Bonneville shoreline was defined by Gilbert (1890) as the highest shoreline of Lake Bonneville. He also believed that this shoreline was of the same age in all parts of the Lake Bonneville basin, and that it marked the maximum of the lake cycle that overflowed at Red Rock Pass, Idaho. It now is established that the highest shoreline of this lake cycle is not everywhere the highest shoreline, because of differential warping resulting from isostatic rebound. (At southern Promontory Point one of the shorelines of Alpine age is higher; see above on this page.) Therefore, in this paper the term "Bonneville shoreline" refers to the highest shoreline of the last lake cycle that rose to the high-shore zone, and presumably caused Lake Bonneville to overflow at Red Rock Pass.

Bonneville and Provo Members of the Little Cotton-wood Formation in eastern Jordan Valley, Utah (Morrison, 1965a), and to the Bonneville Formation as used in the Salt Lake City area (Van Horn, 1965). This formation is younger than the Promontory Soil and is older than the Graniteville Soil (which is discussed below); consequently these soils are excellent markers for differentiating the Bonneville Formation and other lake units.

The Bonneville Formation comprises two wedges of lacustrine sediment separated by an interlacustrine diastem. The lacustrine wedges record at least two deep-lake cycles, both of which rose above the highest exposures in the gravel pits; one, presumably the second, rose to the Bonneville shoreline.[5] The lower wedge is here called the white marl member, after its distinctive offshore facies that was first described and named the White Marl by Gilbert (1890). The upper wedge of the Bonneville Formation is here called the upper member.

The shore facies of the white marl member is lacustrine gravel and sand that generally resembles the shore facies of the Alpine Formation except that typically it is finer grained and has little or no coarse gravel, even on mountain shores that were most exposed to waves. The offshore facies of this member, which commonly begins within a few feet of the shore, is the most prominent and widespread marker unit in the Lake Bonneville succession. At southern Promontory Point this facies is informally named the white marl bed and typically is silt and silty fine sand; it is generally highly calcareous, thick bedded to massive, and faintly laminated. Small gastropod shells are abundant in many places. This facies is from about 1 to 20 feet thick, and is pale green to nearly white except in the upper several inches to 3 feet where it generally is pale pinkish gray to pale pink and forms the "pink marker bed" of Goode and Eardley (1960). At southern Promontory Point the white marl bed typically is somewhat less white and contains more silt and clay and fewer nearly pure marl beds than it does in areas farther west and southwest. The white marl bed at southern Promontory Point is widely exposed at elevations between 4,320 and 5,220 feet in the gravel pits and in a few wash-bank exposures; it extends to within 30 feet of the Bonneville shoreline. The gravelly shore facies extends higher, but its upper limit cannot be precisely located in the poor exposures available at this altitude.

The diastem that separates the white marl member from the upper member became evident only after tracing of beds above and below it. In most places it is a nearly smooth surface that slightly crosscuts the bedding of the underlying white marl member locally. In places it is marked by a discontinuous line of pebbles and cobbles and rarely by lenses of colluvial or alluvial gravel. It has been traced to an altitude as low as 4,470 feet in Little Valley and as low as 4,323 feet in the valley to the south. At no place does this diastem bear a true weathering profile. The pink zone at the top of the white marl member directly and persistently underlies this diastem and locally cuts across underlying strata. The pink color likely is due to incipient weathering during the lake recession recorded by the diastem.

The upper member of the Bonneville Formation is similar to the white marl member, especially in its gravelly to sandy shore facies; the two members cannot be differentiated where their shore gravels directly overlie one another. The offshore facies of the upper member is mainly thick- to thin-bedded silty fine sand and medium sand; the percentage of sand increases upward. Gastropod shells commonly are present and locally are abundant. This facies superficially resembles that of the white marl member, except that it is relatively noncalcareous and generally is sandier and somewhat darker. It commonly is overlain by several feet of regressive shore gravel and gravelly sand of the upper member.

The upper member extends to the Bonneville shoreline, which lies at an average altitude of about 5,250 feet at Little Valley. Presumably the overflow of Lake Bonneville at Red Rock Pass was initiated during the lake maximum that is marked by this shoreline. There is no indication in the upper member at Little Valley of a conspicuous recessional stillstand at the Provo shoreline level.

Radiocarbon age determinations for samples from the Bonneville Formation at Little Valley fit a reasonable chronologic sequence and support the correlations made herein. Radiocarbon analysis of wood from a local bog deposit of carbonaceous silt at the base of the white marl member at an altitude of about 4,775 feet indicated an age of 20,600±500 years (Rubin and Alexander, 1960, sample W-876). Wood (sample L-775N of Kaufman) from the base of the white marl member at about 4,650 feet was determined to be 20,800±300 years old.[6] The age of snail shells in two samples (L-775I and L-775J) from a lens of lake-reworked alluvium at the diastem between the white marl member and upper member, at about 4,890 feet, was determined to be 15,300±400 and 15,400±300 years, respectively.[6] Snail shells from the upper, regressive part of the upper member at about 4,725

_____

[5] See footnote 4 on preceding page.

[6] See footnote 1 on p. C112.

feet altitude were found to be 12,780±350 years old (Ives and others, 1964, sample W-943); another sample of snail shells (sample L-775K of Kaufman) from the same stratigraphic position but from 4,826 feet altitude was found to be 11,700±300 years old[6]. From this evidence, together with radiocarbon dates from material from the Bonneville Formation elsewhere, it appears that the lake maximum to which the Bonneville shoreline was related occurred between 15,000 and 12,000 years ago.

Disconformity between the Bonneville and Draper Formations and associated subaerial units

A disconformity records subaerial exposure and minor erosion between the Bonneville and Draper Formations. The disconformity is best marked by the Graniteville Soil (described in the following section), although fan gravel and colluvium, from several inches to several feet thick, are associated with it locally. The disconformity has been identified at an altitude as low as 4,250 feet, and the Graniteville Soil as low as 4,330 feet, attesting to complete or nearly complete desiccation of the lake.

Graniteville Soil.—The Graniteville Soil is a strongly developed weathering profile intermediate in age between the Bonneville Formation (and alluvium and colluvium of post-Bonneville–pre-Draper age) and the Draper Formation. It was first defined on this basis in eastern Jordan Valley (Morrison, 1965a), where at its type locality it occurs as a relict soil on the Bonneville Member (of the Little Cottonwood Formation) on the Bonneville shoreline terrace. On southern Promontory Point the Graniteville invariably is a Brown soil only slightly less strongly developed than the Promontory Soil; it resembles the latter so closely that commonly the two soils are difficult to distinguish unless their stratigraphic relations are exposed in sequence. The B horizon of the Graniteville is 1 to 1½ feet thick, brown (hue 7.5 YR to 10 YR, slightly lighter than typical for the Promontory Soil), slightly clayey, and generally structureless (though locally moderately prismatic-blocky). The Cca horizon generally is about 2 feet thick, and commonly it has a somewhat lesser concentration of $CaCO_3$ than the Promontory Soil. Unlike the Promontory, the Graniteville invariably seems to be a single soil. The Graniteville is much more widely preserved than the Promontory Soil, with little or no erosion of its profile below even the highest shoreline of Draper age. Above this shoreline it occurs both as a relict soil and as a soil buried by younger alluvium and colluvium.

---

[6] See footnote 1 on p. C112.

Draper Formation

The Draper Formation is defined in eastern Jordan Valley, Utah (Morrison, 1965a), as the lake sediments intermediate in age between the Graniteville and Midvale Soils. (The Midvale Soil is discussed in the next section of this report.) In Jordan Valley the Draper comprises three wedges of lacustrine sediments separated by interlacustrine diastems; the lacustrine wedges, called the lower, middle, and upper members, respectively, of the Draper Formation record the last three known cycles of Lake Bonneville, all of which were comparatively low and brief. At southern Promontory Point only the lower and middle members have been identified. These consist of discontinuous lenses of pebble gravel a few inches to 4 feet thick, commonly separated by comparable thicknesses of fan gravel. The lower member extends to about 4,770 feet, and the middle member to about 4,470 feet. The interlacustrine diastem between these two members can be recognized as low as 4,280 feet.

POST-LAKE BONNEVILLE DEPOSITS AND SOILS

Post-Lake Bonneville deposits, overlying the Draper Formation and local subaerial deposits coeval with it, are mainly fan gravel and colluvium (slopewash), and locally, some loess. Two weathering profiles are in places intercalated with these deposits; these are the Midvale Soil (older) and an early Recent soil. The post-Lake Bonneville deposits older than the Midvale Soil are correlated with the early part of the altithermal interval. They are composed mainly of loess and silty alluvium and colluvium derived from reworking of loess, with few lenses of gravelly alluvium. Their lithology suggests that the interval during which they were deposited was arid and windy.

Midvale Soil.—The Midvale Soil, defined in eastern Jordan Valley, Utah (Morrison, 1965a), is a moderately mature pedocal, considerably less well developed than the Graniteville and Promontory Soils. It has a B horizon that generally is less than a foot thick, structureless, and light brown, and grades into a Cca horizon that is about 1½ feet thick and has a relatively moderate concentration of calcium carbonate (depending upon parent material). This soil has undergone little subsequent erosion, and is widespread. It is presumed to have formed during the later part of the altithermal interval of Antevs (1948, 1952), from about 4,500 to 3,800 years ago. It is a correlative of the Toyeh Soil of the Lake Lahontan area, that has been suggested as a logical marker for the Pleistocene-Recent boundary in the Great Basin (Morrison, 1961c; 1965a, b).

The Midvale Soil is overlain locally by younger gravelly to silty alluvium and slopewash that has a maximum thickness of 25 feet. Intercalated with these Recent deposits in places is another, weakly developed weathering profile, which is correlated with the early Recent soil in eastern Jordan Valley (Morrison, 1965a). This soil is so weakly developed that it has only the barest suggestion of a B horizon (a "color" B horizon of soil scientists), which is generally less than 5 inches thick; also there commonly is no discernible $CaCO_3$ concentration below the B horizon.

Lacustrine deposits of Recent (post-Midvale) age have not been identified on southern Promontory Point.

CORRELATION OF POST-SANGAMON DEPOSITS AND SOILS WITH THE ROCKY MOUNTAIN AND MIDWEST-ERN SUCCESSIONS

In recent studies of the Little Cottonwood–Bells Canyon and eastern Jordan Valley areas, south of Salt Lake City, Utah (Richmond, 1961, 1964a; Morrison, 1961a, 1965a), the Graniteville Soil was not recognized in the glacial sequence nor the Promontory Soil in the lacustrine sequence. Hence the Graniteville Soil was incorrectly correlated with the post-Bull Lake soil, and consequently the Bonneville Member of the Little Cottonwood Formation (and lake rise to the Bonneville shoreline) was miscorrelated with the late stade of the Bull Lake Glaciation. From the less ambiguous succession revealed at southern Promontory Point, it now is evident that on the basis of similar relative weathering-profile development the Promontory Soil should be correlated with the post-Bull Lake soil, and the Midvale Soil with the post-Pinedale soil. On the basis of this argument and of the available radiocarbon dates the Bonneville Formation is correlated with (1) the early and middle stades of the Pinedale Glaciation (see fig. 2)—the white marl member with the early till, and the upper member with the middle till of this glaciation; and (2) with the Woodfordian substage of Frye and Willman (1960, 1963). The Draper Formation is correlated with the upper till of the Pinedale Glaciation and with the Valderan substage of Frye and Willman (1960, 1963). The Alpine Formation now is correlated with the Bull Lake Glaciation in its entirety, and with the Altonian substage of Frye and Willman (1960, 1963). The Promontory Soil is further correlated with the Farmdalian substage of Frye and Willman (1960, 1963), and the Graniteville Soil is correlated with the Brady Soil of the Great Plains region and with the Twocreekan substage of Frye and Willman (1960, 1963).

INTERPRETATION OF LAKE HISTORY

The lake history recorded in the stratigraphic succession at southern Promontory Point can be summarized as follows:

Two long-lasting deep-lake intervals older than Lake Bonneville are evident. During the earlier of these, of Kansan age and correlated with the Cedar Ridge Glaciation in the Rocky Mountains, the lake rose to an altitude of at least 4,670 feet; during the second interval, of Illinoian age and correlated with the Sacagawea Ridge Glaciation in the Rocky Mountains, the lake rose to at least 4,980 feet. The highest exposures of the deposits that record these lake intervals are below the highest shoreline of Lake Bonneville, but the floor of the Great Salt Lake basin was several hundred feet lower when these lakes existed (prior to subsequent deposition), so the pre-Lake Bonneville lakes were comparable to Lake Bonneville in depth. During a major recessional interval between the times of the two middle Pleistocene lakes the water level fell at least as low as 4,318 feet and the Great Salt Lake basin probably was as completely desiccated as it is now. Another major interlacustral period occurred after the time of the younger pre-Lake Bonneville lake, and the water level again fell to at least 4,325 feet altitude, and probably complete desiccation occurred, prior to the advent of Lake Bonneville.

Early Lake Bonneville history is recorded mainly by the Alpine Formation. The several interlacustrine diastems within this unit separate at least 4 wedges of lacustrine sediments, recording at least 4 separate lake cycles, all correlative with the Bull Lake Glaciation in the Rocky Mountains. The maximums of these 4 lake cycles in this area appear to have been at altitudes of (oldest to youngest) at least 5,050 feet, more than 5,100 feet, at least 5,150 feet and probably 5,280 feet, and about 4,800 feet, respectively. During the intervening recessions the lake levels went at least as low as 4,700, 4,850, and 4,700 feet, respectively.

Middle Lake Bonneville time, correlative with the Bull Lake–Pinedale interglaciation in the Rocky Mountains, was another fairly long interval of probably complete lake desiccation. The later part of this interval is thought to have been considerably warmer than now, on the basis of the strong chemical weathering manifested by the Promontory Soil.

Late Lake Bonneville time is recorded by the Bonneville and Draper Formations and the intervening Graniteville Soil, all correlative with the Pinedale

Glaciation in the Rocky Mountains. The Bonneville Formation represents deposition during two lake cycles; during the first, when the white marl member was deposited, the lake rose to within a few feet of the Bonneville shoreline; during the second lake cycle, represented by the upper member, the lake rose to the Bonneville shoreline and presumably overflowed at Red Rock Pass. Between these cycles there was a short-lived but deep recession, to at least as low as 4,323 feet. Following the rise to the Bonneville shoreline was another deep recession, and the lake level fell at least as low as 4,250 feet. Formation of the Graniteville Soil during this interval demonstrates that the climate became considerably warmer than that of the present.

The final phase of Lake Bonneville is evinced by the Draper Formation, which on southern Promontory Point records two lake cycles that rose as high as about 4,770 and 4,470 feet, respectively. During the intervening recessional interval the lake level dropped at least as low as 4,280 feet.

Early post-Lake Bonneville time is correlated with the altithermal age of Antevs. During this interval, from about 7,000 or 6,500 years to about 3,800 years ago, lake levels remained at least as low as now and probably Great Salt Lake was completely dry at times. The early part of this warm interval was arid and characterized by strong wind activity. The later part, at the end of the Pleistocene Epoch, was somewhat less arid, as is shown by the formation of the Midvale Soil. Data on lake history during the Recent Epoch are not available from this area.

This revised interpretation of Lake Bonneville history supplements all previous ones in recognizing several additional lake cycles in both early and late Lake Bonneville times. If the various Alpine lake cycles are grouped together as the early deep-lake period of Lake Bonneville, and if the lake cycles recorded by the Bonneville and Draper Formations are grouped as the late deep-lake period, my interpretation is in accord with the conclusions of Gilbert (1890), Antevs (1952, 1955), Ives (1951), Hunt (1953), Bissell (1963), and Eardley and others (1957) on the relative ages of, and maximum heights reached during, the two main deep-lake intervals. The post-Alpine–pre-Bonneville desiccation was of interglacial magnitude, but not so long lasting as inferred by Gilbert and by Eardley and others. The revised correlation of the last occupation of the Bonneville shoreline with the Pinedale Glaciation agrees with the conclusions of Blackwelder (1931), Antevs, as revised (1952, 1955), and Ives (1951); its correlation with the middle stade

of this glaciation is supported by this portion of the radiocarbon chronology.

REFERENCES

Antevs, Ernst, 1948, Climatic changes and pre-white man, in The Great Basin, with emphasis on glacial and postglacial times: Utah Univ. Bull., v. 38, no. 20, p. 168–191.
——— 1952, Cenozoic climates of the Great Basin: Geologische Rundschau, v. 40, no. 1, p. 94–108.
——— 1955, Geologic-climatic dating in the West: Am. Antiquity, v. 20, no. 4, p. 1.
Bissell, H. J., 1963, Lake Bonneville—geology of southern Utah Valley, Utah: U.S. Geol. Survey Prof. Paper 257–B, p. 101–130.
Blackwelder, Eliot, 1931, Pleistocene glaciation in the Sierra Nevada and Basin Ranges: Geol. Soc. America Bull., v. 42, no. 4, p. 865–922.
Eardley, A. J., Gvosdetsky, Vasyl, and Marsell, R. E., 1957, Hydrology of Lake Bonneville and sediments and soils of its basin: Geol. Soc. America Bull., v. 68, no. 9, p. 1141–1202.
Frye, J. C., and Leonard, A. B., 1952, Pleistocene geology of Kansas: Kansas Geol. Survey Bull. 99, 230 p.
Frye, J. C., and Willman, H. B., 1960, Classification of the Wisconsinan Stage in the Lake Michigan glacial lobe: Illinois Geol. Survey Circ. 285, 16 p.
——— 1963, Development of Wisconsinan classification in Illinois related to radiocarbon chronology: Geol. Soc. America Bull., v. 74, p. 501–506.
Gilbert, G. K., 1890, Lake Bonneville: U.S. Geol. Survey Mon. 1, 438 p.
Goode, H. D., and Eardley, A. J., 1960, Lake Bonneville—a preliminary report on the Quaternary deposits of Little Valley, Promontory Range, Utah [abs.]: Geol. Soc. America Bull., v. 71, p. 2035.
Hunt, C. B., 1953, General geology, in Hunt, C. B., Varnes, H. D., and Thomas, H. E., Lake Bonneville—geology of northern Utah Valley, Utah: U.S. Geol. Survey Prof. Paper 257–A, p. 11–45.
Ives, P. C., Levin, Betsy, Robinson, R. D., and Rubin, Meyer, 1964, U.S. Geological Survey radiocarbon dates VII: Radiocarbon, v. 6, p. 37–76.
Ives, R. L., 1951, Pleistocene valley sediments of the Dugway area, Utah: Geol. Soc. America Bull., v. 62, no. 7, p. 781–797.
Leverett, Frank, 1899, The Illinois glacial lobe: U.S. Geol. Survey Mon. 38, 817 p.
Morrison, R. B., 1961a, New evidence on the history of Lake Bonneville from an area south of Salt Lake City, Utah: Art. 333 in U.S. Geol. Survey Prof. Paper 424–D, p. D125–D127.
——— 1961b, Correlation of the deposits of Lakes Lahonton and Bonneville and the glacial sequences of the Sierra Nevada and Wasatch Mountains, California, Nevada, and Utah: Art. 332 in U.S. Geol. Survey Prof. Paper 424–D, p. D122–D124.
——— 1961c, A suggested Pleistocene-Recent (Holocene) boundary for the Great Basin region, Nevada-Utah: Art. 330 in U.S. Geol. Survey Prof. Paper 424–D, p. D115–D116.
——— 1965a, Lake Bonneville—Quaternary stratigraphy of eastern Jordan Valley south of Salt Lake City, Utah: U.S. Geol. Survey Prof. Paper 477. [In press]

Morrison, R. B., 1965b, Quaternary geology of the Great Basin, *in* Wright, H. E. and Frey, D. G., eds., The Quaternary of the United States: Princeton, N.J., Princeton Univ. Press, Review volume, 1965 Cong., Internat. Assoc. for Quaternary Research (INQUA). [In press]

Richmond, G. M., 1961, New evidence of the age of Lake Bonneville from the moraines in Little Cottonwood Canyon, Utah: Art. 334 *in* U.S. Geol. Survey Prof. Paper 424–D, p. D127–D128.

—— 1962, Quaternary stratigraphy of the La Sal Mountains, Utah: U.S. Geol. Survey Prof. Paper 324, 135 p.

—— 1964a, Glaciation of Little Cottonwood and Bells Canyons, Utah: U.S. Geol. Survey Prof. Paper 454–D, 100 p.

—— 1964b, Three pre-Bull Lake tills in the Wind River Mountains, Wyoming—a reinterpretation, *in* Geological Survey Research 1964: U.S. Geol. Survey Prof. Paper 501–D, p. D104–D109.

Rubin, Meyer, and Alexander, Corrine, 1960, U.S. Geological Survey radiocarbon dates V: Am. Jour. Sci. Radiocarbon Supp., v. 2, p. 129–185.

Van Horn, Richard, 1965, Engineering implications and geology, Hall of Justice excavation, Salt Lake City, Utah; sect. 2. Late Wisconsin and Recent stratigraphy: Utah Geol. and Mineralog. Survey Report. [In press]

GLACIATION IN THE NABESNA RIVER AREA, UPPER TANANA RIVER VALLEY, ALASKA

By ARTHUR T. FERNALD, Washington, D.C.

Abstract.—Morainal deposits define two major glaciations—the Black Hills Glaciation of Illinoian age and the Jatahmund Lake Glaciation of Wisconsin age. Nonglacial terrace deposits, consisting of an upper unit of Wisconsin age (W-1174; 25,800 years B.P.) and a lower unit thought to be of Sangamon age (W-976; older than 42,000 years), are correlated with the glacial sequence.

The Nabesna River area, on the north side of the Alaska Range in east-central Alaska (fig. 1), provides type localities for two major glaciations in the upper Tanana River valley. No other glacial advances have been recognized within the piedmont or lowland areas; the adjacent Yukon-Tanana uplands on the north side of the Tanana River were unglaciated. In both the episodes recognized, glaciers from the Wrangell Mountains flowed northward through the Alaska Range via the Nabesna River valley, and spread out on the bordering piedmont (fig. 2). There, the Nabesna glacier was joined by local glaciers that originated in the Alaska Range and flowed down the Cheslina River valley, west of the Nabesna valley, and down the Stuver Creek valley on the east. At several places ice of the older, more extensive glaciation projected through the Black Hills into the lowland of the Tanana River, but ice of the younger glaciation was restricted to the piedmont.

During the older glaciation, here named the Black Hills Glaciation, the Nabesna glacier advanced northeastward across the piedmont to the Black Hills and there deposited drift up to a maximum altitude of about 3,000 feet above sea level. The ice reached its most northerly advance along the present course of the Nabesna River. The largest morainal remnant is on the west side of Stuver Creek, where it in part straddles the Black Hills and in part flanks them. Its subdued morainal topography consists of a series of rounded terraces on the flanks of the Black Hills;

and of knobs and ridges with smooth crests and gentle slopes separated by broad shallow depressions on the summit. Gray till, consisting of cobble- to boulder-sized fragments in a matrix of sandy silt, is exposed at the type section (locality 1 on fig. 2) for deposits of the Black Hills Glaciation. A high percentage of the rocks are basaltic or andesitic types that are characteristic of the volcanic Wrangell Mountains.

A complex series of prominent end moraines on the piedmont was deposited during the later Jatahmund Lake Glaciation, here named after the largest lake
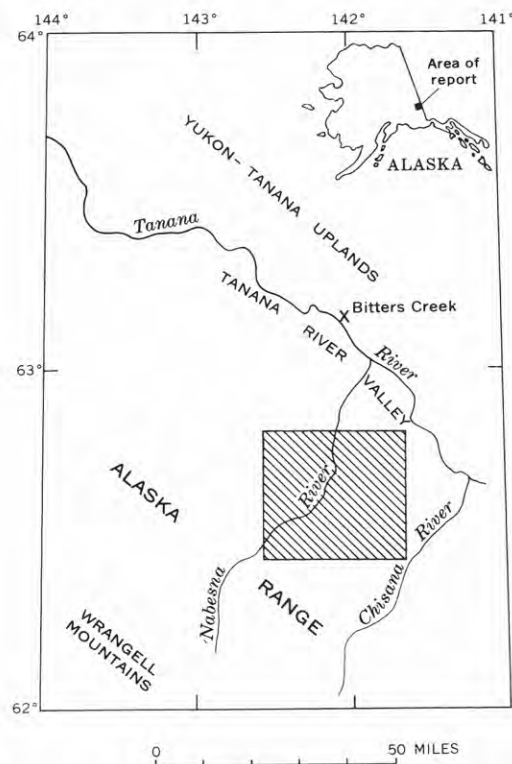
FIGURE 1.—Index map of part of east-central Alaska, showing area of this report (patterned).
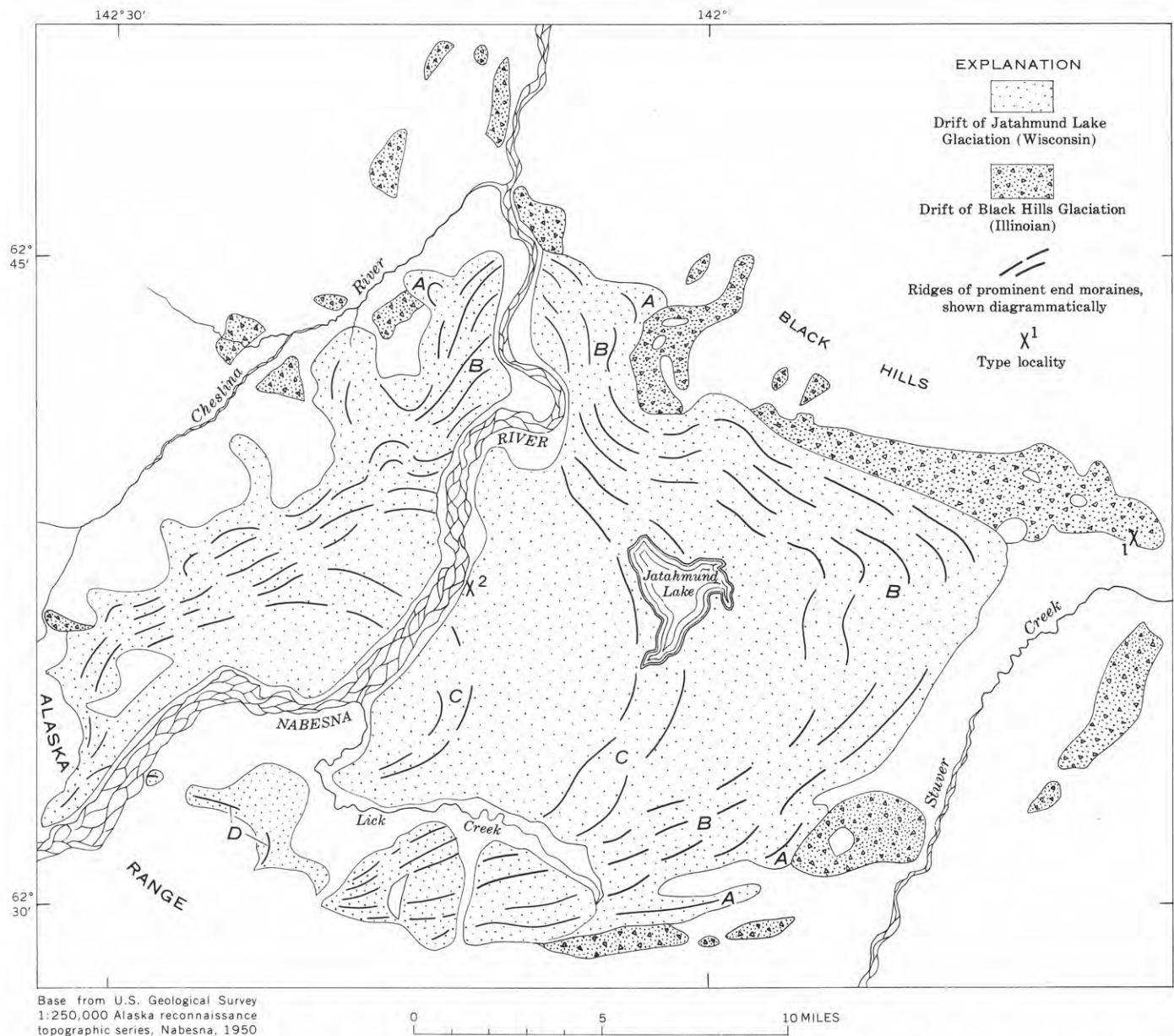
FIGURE 2.—Distribution of drift of the Nabesna glacier on the north side of the Alaska Range.   A, Stuver moraine; B, Takomahto Lake moraines; C, Lick Creek moraines; D, Pickerel Lakes moraines.

confined by the moraines. For convenience of reference, two marginal lakes, a crosscutting stream, and a nearby hill provide local names for the moraines, as outlined on figure 2. A belt of exceedingly rough, hummocky massive moraines (the Takomahto Lake moraines, B on fig. 2), from 1 to 4 miles wide, dominates the series. It outlines the outer limit of the deposits for most of its distance, but at several places a small older moraine (Stuver moraine, A) extends as much as a mile beyond it. Successively less extensive moraines are present on the piedmont (Lick Creek moraines, C), and the youngest of the series is near the foot of the Alaska Range (Pickerel Lakes moraines, D). All the moraines

are characterized by sharp angular ridges, knobs, and hollows that are strikingly different from those of the Black Hills moraines. A high bluff of gray drift along the Nabesna River (locality 2) is the type section for deposits of the Jatahmund Lake Glaciation. The drift is till that contains pebble- to boulder-sized fragments in a matrix of sand and silt and that is interbedded with poorly stratified gravel consisting of well-rounded pebbles, cobbles, and boulders in a sandy matrix. A high percentage of the rocks are volcanic and are similar in lithology to those in the older drift.

Assignments of Illinoian and of Wisconsin ages, respectively, to the two glaciations are based on topo-

graphic modification of the moraines, on their relation to radiocarbon-dated nonglacial deposits, and on their sequential analogy with those of other regions in Alaska. The intense modification of the moraines of the Black Hills Glaciation, in contrast with excellent preservation of the moraines of the Jatahmund Lake Glaciation, clearly indicates that a significant interval of time separated the formation of the two.

The complex series of Jatahmund Lake moraines represents a major glacial episode but apparently a single glaciation, because no significant time break is recognizable within the series. The moraines also represent the last glaciation in the area, for no end moraines are present upvalley except small ones near the present Nabesna Glacier front. The moraines are therefore considered to be of Wisconsin age. This age assignment is in agreement with recent studies that suggest that Wisconsin time encompasses the pulsations of a single major glaciation, post-Sangamon in age (Flint, 1962).

Organic material in silt that overlies the Pickerel Lakes moraine is radiocarbon dated at 2,000±300 years Before Present (W–1169; Ives and others, 1964, p. 65). The inclusion of this moraine with Jatahmund Lake units implies that the terminus of the Nabesna Glacier, located 35 miles upvalley, has been confined to within this distance in post-Wisconsin time. A similar restriction, characteristic of that of other Alaskan glaciers with a northern exposure, is illustrated by Russell Glacier, which is located between the Nabesna Glacier and the Canadian border. Capps (1916, p. 74) showed that Russell Glacier retreated more than 7,800 years ago from a site 8 miles from its present terminus, where a 39-foot peat section is exposed. He based this age on an accumulation rate of 1 foot of peat in 200 years; a layer of volcanic ash 7 feet down within the section was estimated to be 1,400 years old. The age of the ash, and by implication the peat accumulation rate, has been closely confirmed by radiocarbon analyses; the ash fell between 1,750 and 1,520 B.P. (Fernald, 1962).

Radiocarbon-dated terrace deposits beyond the glaciated area, on the north side of the Tanana River, at Bitters Creek (fig. 1), have been correlated with the glacial sequence. The character of the deposits and the stratigraphic positions of the radiocarbon samples are shown in the composite section in figure 3. The lower 15-foot organic-rich unit, which lies beneath an unconformity and which is dated as older than 42,000 years, is considered to be a deposit of the last interglacial event, of Sangamon age, and is thus correlated with the Black Hills—Jatahmund Lake interval. The
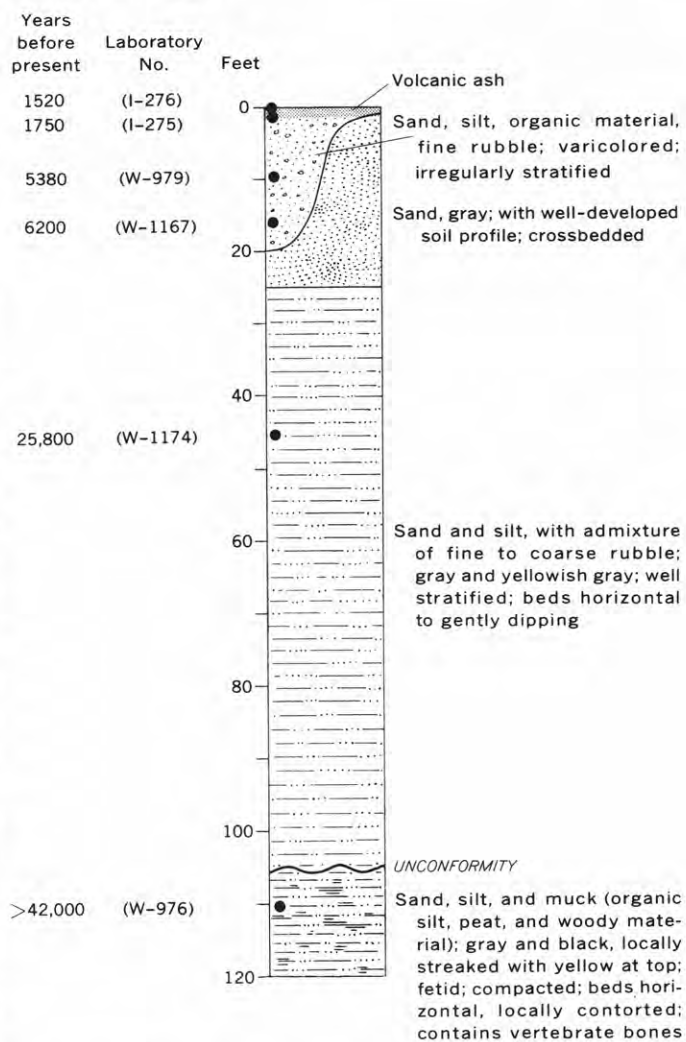
FIGURE 3.—Composite section of terrace deposits between the Tanana River at Bitters Creek (Riverside bluff), and adjacent Yukon-Tanana uplands (lat 63°10′ N., long 142°07′ W.). Large black dots in column show position of radiocarbon-dated samples. Volcanic ash near top of column is bracketed between the 1,750- and 1,520-year old samples. *I*, dated by Isotopes, Inc., Westwood, N.J.; *W*, dated by U.S. Geological Survey Radiocarbon Laboratory.

overlying unit of organic-poor deposits, 80 feet thick, reflects aggradation during the last major glaciation and is correlated with the Jatahmund Lake Glaciation. The date of nearly 26,000 years before present for a thin organic zone (45 feet below the surface) is within the limits of a Wisconsin interstadial event that is well recognized in the central North American sequence (Flint, 1962). Sand of eolian origin that mantles the terrace is considered to be of Wisconsin age also; it is locally overlain by alluvial-colluvial fill that has a minimum age of 6,200 years. Three radiocarbon dates from within dune sand elsewhere in the lowland have related intensive eolian activity with the last major glaciation (Fernald, 1965).

REFERENCES

Capps, S. R., 1916, The Chisana-White River district, Alaska: U.S. Geol. Survey Bull. 630, 130 p.

Fernald, A. T., 1962, Radiocarbon dates relating to a widespread volcanic ash deposit, eastern Alaska: Art. 11 *in* U.S. Geol. Survey Prof. Paper 450–B, p. B29–B30.

——— 1965, Late Quaternary chronology, upper Tanana River valley, eastern Alaska [abs.]: Geol. Soc. America Spec. Paper. 82, p. 60–61.

Flint, R. F., 1962, Status of the Pleistocene Wisconsin stage in central North America: Science, v. 139, p. 402–404.

Ives, P. C., Levin, Betsy, Robinson, R. D., and Rubin, Meyer, 1964, U.S. Geological Survey Radiocarbon Dates VII: Radiocarbon, v. 6, p. 37–76.

RECENT HISTORY OF THE UPPER TANANA RIVER LOWLAND, ALASKA

By ARTHUR T. FERNALD, Washington, D.C.

Abstract.—Twenty radiocarbon analyses provide dates for the following events that postdate late Quaternary glaciation and eolian activity: (1) Stabilization of dunes initiated in late Wisconsin and postglacial times probably was completed more than 5,000 years ago. (2) Alluvial-colluvial filling along lowland borders began 10,500 to 6,000 years ago and continues today. (3) Deposition of fluvial-lacustrine sediments in the lowland has become widespread within the last 3,000 years.

Surficial deposits that cover the northwest-trending lowland of the upper Tanana River in east-central Alaska (fig. 1) include dune sand, alluvial-colluvial sediments, fluvial-lacustrine sediments, and volcanic ash. The chronology of the deposits, as dated by 20 radiocarbon analyses that give a range in age of 850 to 12,400 years, is summarized in this paper; the climatic implications of the deposits are not considered here. Data on the samples, grouped by type of deposit, are given on figure 2. Dates and descriptions of individual samples analysed in the Washington laboratory of the U.S. Geological Survey have been published (Ives and others, 1964, p. 60–69). Location of the samples is shown on a sketch map of all surficial deposits of the valley (fig. 1) that are mappable at this scale. Older deposits in terraces along the Tanana River have been correlated with a glacial sequence established in the piedmont area along the Nabesna River, where the Black Hills Glaciation of Illinoian age and the Jatahmund Lake Glaciation of Wisconsin age have been defined (see article beginning on p. C120 of this chapter, and Fernald, 1965b).

Eolian sand occurs in completely stabilized dune fields that are scattered over the lowland. Dunes in 3 areas (Tenmile Creek, Northway, and Beaver Creek; see fig. 1) were initially stabilized at 12,400 years Before Present (W-1212), 11,250 B. P. (I-302), and 8,200 B.P. (W-1206), respectively. These dates were obtained from thin organic beds within the uppermost parts of the dunes, at depths between 5 and 7 feet;

evidently most of the sand was deposited previously, but some deposition continued afterward. All dune fields have been inactive for a time sufficiently long to permit development of soils; the fields were stabilized prior to deposition of a volcanic ash between 1,520 and 1,750 B.P. (Fernald, 1962). Dunes in 2 areas (Beaver Creek and Bitters Creek) were completely stabilized by 10,230 B.P. (W-980) and 6,200 B.P. (W-1167), respectively, as dated from overlying organic-rich, alluvial-colluvial sediments. In all the fields the crests of the dunes have well-developed soil profiles and the hollows commonly have peaty soils. On the basis of this weathering and of the dates available, an age of more than 5,000 years is suggested for complete stabilization of the dune fields.

Mixed alluvial and colluvial deposits, transported by running water and by mass movement, have accumulated along the borders of the lowland and in the lower parts of tributary valleys within the uplands. These deposits are exposed in terrace escarpments where major streams and lakes of the lowland abut the uplands. They contain variable amounts of irregularly stratified sand, silt, rubble, and organic material; much of the sand and silt is reworked eolian sediment. In places, as at Bitters Creek, the fill overlies dune sand and a thick series of organic-poor deposits that have been related to aggradation during Wisconsin time (Fernald, 1965a). A measured section of the fill, nearly 20 feet thick, is given below. As is indicated by the radiocarbon dates, sediment accumulation began sometime before 6,200 B.P. It amounted to more than 5 feet between that date and 5,380 B.P. and occurred at a rate of approximately 7 feet per 1,000 years. Thereafter, the rate of accumulation averaged about 2 feet per 1,000 years, but the accumulation has been minimal during the last 1,500–2,000 years.

Radiocarbon-dated organic material from 3 other localities (Beaver Creek, Tahamund Lake, Porcupine Creek), collected at the lowest exposed depths (between
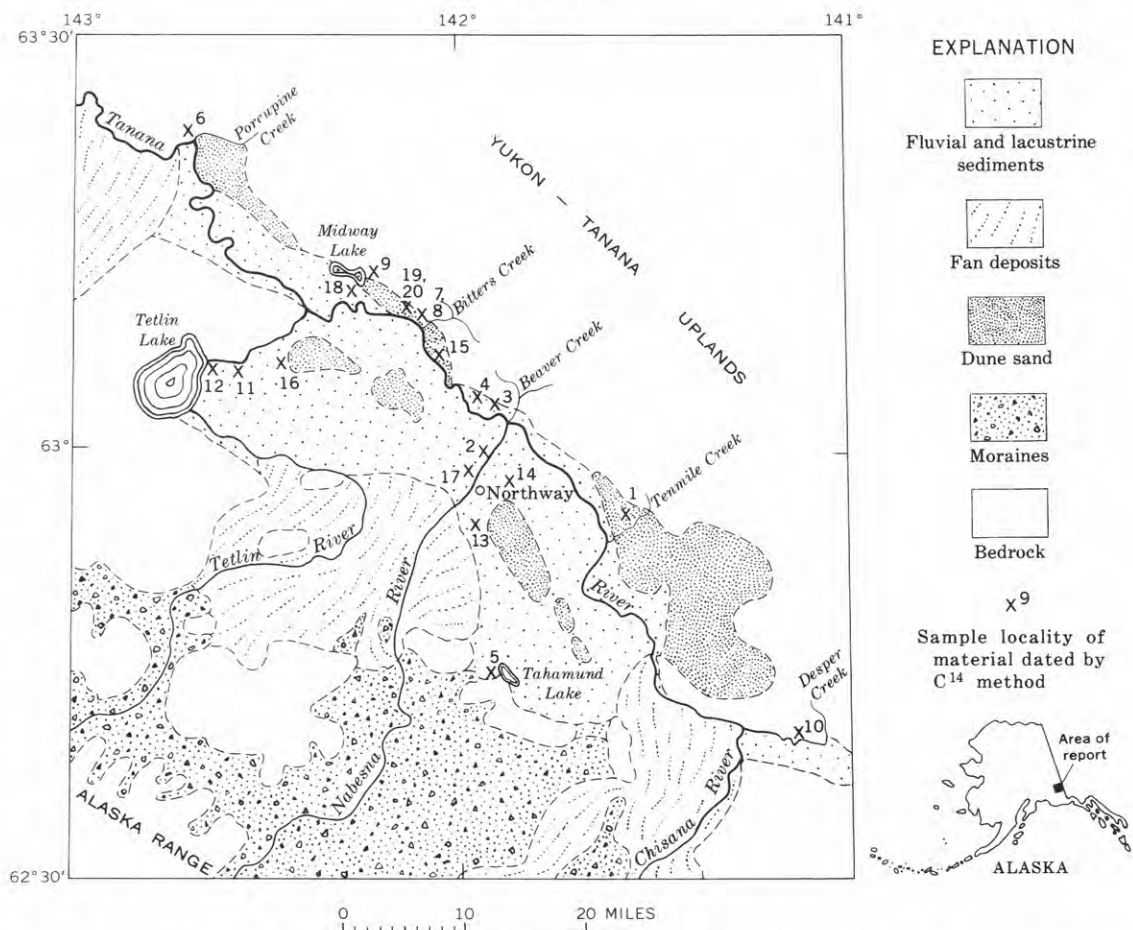
FIGURE 1.—Index map of part of east-central Alaska, showing the upper Tanana River valley, and sample localities.

6.5 and 15 feet below the surface), has an age of 10,230, 8,175, and 6,930 years, respectively. In an exposure at Midway Lake, the age of organic material at a depth of 6 feet is 5,300 years. Similar material, 3 feet down

Measured section of alluvial-colluvial deposits between the Tanana River at Bitters Creek (Riverside bluff) and the adjacent Yukon-Tanana uplands; lat 63°10′ N., long 142°07′ W.

[Ages and laboratory numbers given for dated materials: I, Isotopes, Inc., Westwood, N.J.; W, U.S. Geological Survey Radiocarbon Laboratory]

	Thickness (feet)
Silt and peat_____	0. 7
Volcanic ash (between 1,520 and 1,750 B.P., I-276 and I-275, from an age determination at a nearby locality)_____	. 5
Silt, sand, fine granite rubble, organic material; varicolored; irregularly stratified_____	8. 2
Tree stumps, in place (5,380 B.P., W-979)_____	. 7
Sand, silt, fine granite rubble, peat, organic debris; varicolored; irregularly stratified_____	5. 6
Peat, black (6,200 B.P., W-1167)_____	. 1
Sand and silt, grayish-yellow; with minor organic material; irregularly bedded_____	3. 5
Eolian sand, gray, crossbedded; grains frosted and of uniform size; contact with overlying sand and silt indistinct_____	Covered

in an exposure along Desper Creek, has an age of 3,120 years. The deposits, although diverse in character because of local controls, do show a generally similar chronology: earliest organic-bearing accumulations began during the period between 10,500 and 6,000 B.P.; greatest accumulations apparently occurred chiefly around 6,000–5,500 B.P.; minimal accumulations have occurred during the last 1,500–2,000 years (that is, since deposition of the volcanic ash). The average rate of accumulation has been about 1½ feet per 1,000 years.

A complex of fluvial and lacustrine sediments underlies most of the lowland, where the sediments occur in broad meander belts developed by the Tanana and tributary rivers, and in broad lake-dotted low terraces. The flood plains are now being enlarged by lateral migration of the rivers against dune fields in the lowland and, on the north side of the lowland, against terraces. The stream and lake deposits consist principally of sand, silt, and organic material. On the south side of the lowland they overlie organic-poor sand and gravel. At two such sites radiocarbon ages of 6,170 and 3,000

	Locality No.	Laboratory No.	Depth, in feet	Radiocarbon date, in years before present
Volcanic ash	20	I-276	1.3	1520±100
	19	I-275	2	1750±110
Fluvial-lacustrine sediments	18	I-278	3.5	850±90
	17	I-303	2.5	1270±80
	16	W-1171	2.5	1550±300
	15	W-978	7	2000±250
	14	I-279	3	2400±100
	13	W-1210	4.3	2560±250
	12	I-274	10	3000±120
	11	W-1173	9.5	6170±300
Alluvial-colluvial sediments	10	W-1209	3	3120±250
	9	I-277	6	5300±250
	8	W-979	9.7	5380±260
	7	W-1167	16	6200±300
	6	W-1170	15	6930±300
	5	I-305	6.5	8175±175
	4	W-980	14	10,230±300
Dune sand	3	W-1206	6.5	8200±300
	2	I-302	7	11,250±250
	1	W-1212	5.5	12,400±450

FIGURE 2.—Summary of data on radiocarbon samples from the upper Tanana River valley, Alaska. Location of samples shown on figure 1. Finite dates shown by dots; sample numbers enclosed by parentheses. Source of radiocarbon dates: *I*, Isotopes, Inc., Westwood, N.J.; *W*, U.S. Geological Survey Radiocarbon Laboratory.

years have been obtained for the underlying deposits in terrace exposures along the Tetlin River. Six ages from within the deposits, obtained from organic material in cut banks along rivers and lakes at lowest exposed depths (between 7 and 2.5 feet), range in age from 2,560 to 850 years. Thus, development of the lowland has become widespread within the last 3,000 years. The ash layer deposited between 1,750 and 1,520 B.P. is present on low terraces within the lowland, but it is not present on slip-off slopes of meandering rivers. It has been reworked into the deposits that were laid down at the time of the ash fall and are now intermediate in altitude between the low terraces and the slip-off slopes.

The recent events in the upper Tanana River lowland that postdate late Quaternary glaciation and eolian activity are summarized as follows:

(1) Stabilization of dunes was initiated in late Wisconsin and postglacial times (12,400 B.P., 11,250 B.P., 8,200 B.P.). All dunes were probably stabilized more than 5,000 years ago (10,230 B.P., 6,200 B.P.).

(2) Deposition of organic-bearing alluvium-colluvium along the borders of the lowland and within tributary valleys began between about 10,500 and 6,000 years ago (19,230 B.P., 8,175 B.P., 6,930 B.P., 6,200 B.P.) and has continued to the present. In one 20-foot section, more than 5 feet of sediment accumulated between 6,200 B.P. and 5,380 B.P.

(3) Deposition of fine-grained organic-bearing fluvial and lacustrine sediments has become widespread in the lowlands within the last 3,000 years. The deposits on the south side of the lowland overlie sand and

gravel (6,170 B.P., 3,000 B.P.); elsewhere the flood plains have expanded against dune fields and terraces.

REFERENCES

Fernald, A. T., 1962, Radiocarbon dates relating to a widespread volcanic ash deposit, eastern Alaska: Art. 11 *in* U.S. Geol. Survey Prof. Paper 450–B, p. B29–B30.
——— 1965a, Glaciation in the Nabesna River area, upper Tanana River valley, Alaska, *in* U.S. Geological Survey Research 1965: U.S. Geol. Survey Prof. Paper 525–C, p. C120–C123.
——— 1965b, Late Quaternary chronology, upper Tanana River valley, eastern Alaska [abs.]: Geol. Soc. America Spec. Paper 82, p. 60–61.
Ives, P. C., Levin, Betsy, Robinson, R. D., and Rubin, Meyer, 1964, U.S. Geological Survey Radiocarbon Dates VII: Radiocarbon, v. 6, p. 37–76.

MAXIMUM EXTENT OF LATE PLEISTOCENE CORDILLERAN GLACIATION IN NORTHEASTERN WASHINGTON AND NORTHERN IDAHO

By PAUL L. WEIS and GERALD M. RICHMOND,
Washington, D.C., Denver, Colo.

Abstract.—Late Pleistocene glaciers in northeastern Washington and northern Idaho were considerably less extensive than has been previously supposed. Ice which was part of a single large sheet farther north formed a number of lobes that were for the most part valley glaciers near their southern margins. Ice-contact deposits, landforms, and ice-modified bedrock were used as criteria for determining the outermost position of the ice margins. Deposits south of those margins that were once considered to be till are now thought to have formed as a result of the catastrophic floods from glacial Lake Missoula.

The location of the late Pleistocene ice margin, which was the maximum extent of Cordilleran glaciation in the vicinity of Spokane, Wash., has been investigated repeatedly. Most previous workers concluded that at its maximum extent the ice crossed Spokane Valley and covered a considerable area of the adjoining Columbia Plateau to the south or southwest. Recent investigations lead us to the conclusion that the ice was much less extensive, and that at its outermost position the ice margin actually lay considerably farther north.

Although many workers have considered various aspects of the Pleistocene history of the Spokane area, only Bretz (1923a, 1928), Bretz and others (1956), and Flint (1936, 1937) have studied the area intensively. They published maps showing what they believed was the extent of the ice in northeastern Washington. No one attempted to map the ice margin eastward into Idaho (fig. 1). In this paper we reexamine the criteria and evidence used by these workers, and offer alternative criteria, new data, and new conclusions.

PREVIOUS INVESTIGATIONS

Early workers placed the general position of the ice margin on the surface of the Columbia Plateau south of Spokane, largely because of a deposit at Cheney which was long thought to be till (Leverett, 1917;

Large, 1922; Freeman, 1926; Bryan, 1927) and which contains striated stones (Flint, 1937). The interpretation of that deposit as till influenced subsequent workers in the area. We believe that the deposit at Cheney, and other deposits on this part of the plateau, are of flood origin; that the margin of the ice lay east and north of Spokane; and that the ice extended south of Spokane Valley and abutted the plateau only in a small area along the Spokane River northwest of the city (fig. 1).

Bretz (1923a, b) based his location of the ice margin on topography, outwash deposits, loess deposits, erratic boulders, and deposits that he believed to be till. In much of the area between Spokane and the mouth of the Spokane River, about 50 miles to the west, the short north-flowing tributaries of the river drain parts of the Columbia Plateau that lack the thick cover of loess characteristic of parts of the plateau farther south. Bretz (1923b, p. 622) attributed the absence of loess cover to ice scour, but because only the loess appeared to have been removed he concluded that the ice there had been relatively thin. He ascribed the presence of erratics in deposits of gravel on the plateau in the southern part of Spokane to glacial ice, and concluded that the degree of weathering of some was evidence that they had not been transported far, and thus that the ice did not advance far south of that point (Bretz, 1923a, p. 581).

Flint (1935, 1936, 1937) studied the drift border across the entire area that lies between the Cascade Mountains on the west and the Idaho border on the east. He used a variety of criteria to determine the location of the ice margin, but in the area near Spokane he believed that only three could be applied: deposits of till, erratic stones, and ice-modified topography. The ice margin he suggested was based on his interpretation of various deposits and topographic features in

the area, but the use of erratics, as he pointed out (Flint, 1937, p. 210), required that the location of the ice margin was already approximately known:

... non-basaltic rocks from the highlands (to the north) have thus far been found only in the general district in which till appears in the sections. Hence, the stones may be used in mapping the drift border in places where till has not been found.

Similar boulders are found in and adjacent to the scabland tracts, but as boulders in such positions may well have been waterborne beyond the glaciers, they have not been used in determining the drift border.

Flint (1937, p. 210, 216-218) described the well-known deposit at Cheney, Wash., and listed 15 other localities south of the Spokane River and in the valley of the Little Spokane River where he inferred till to
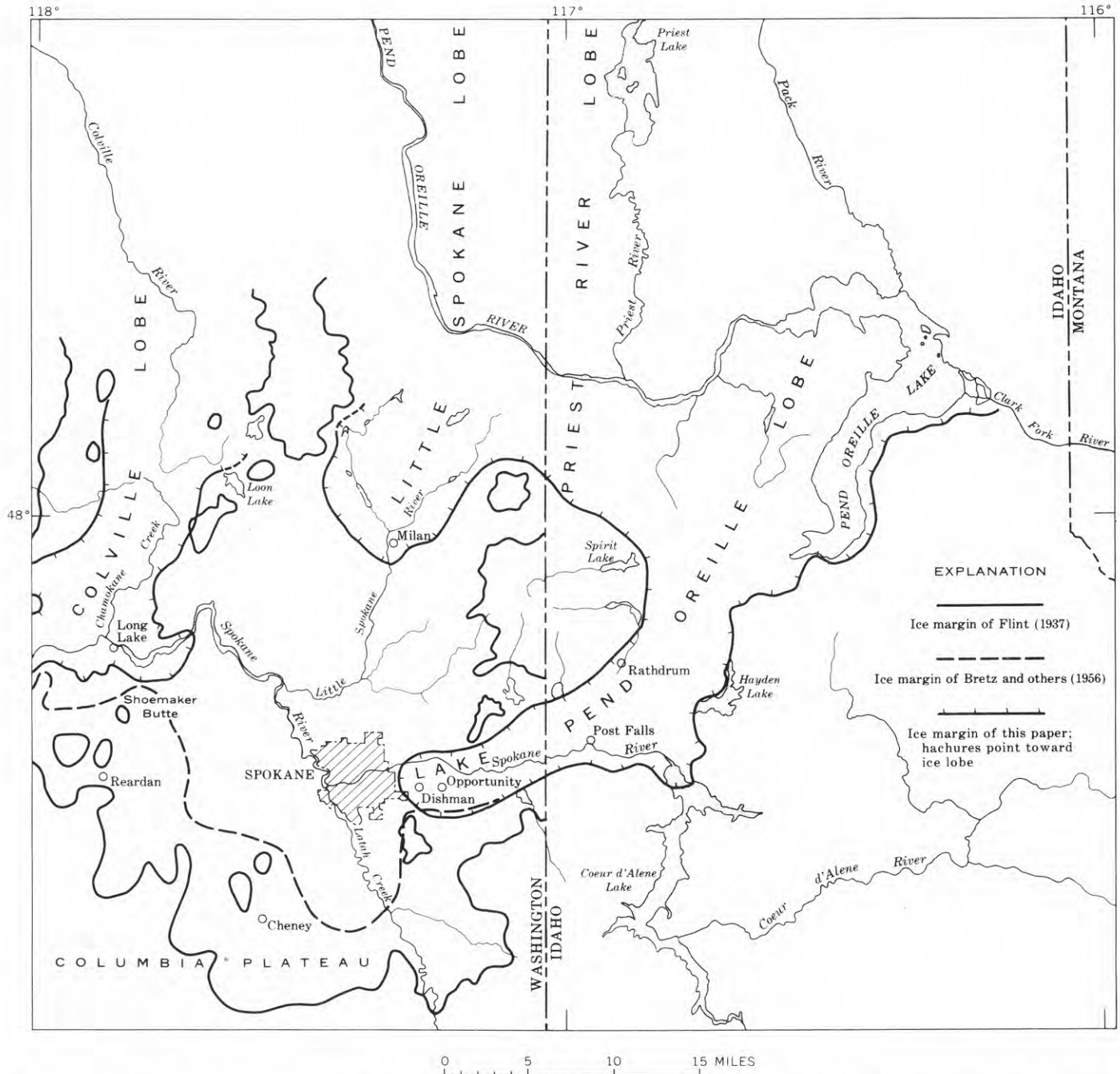
FIGURE 1.—Late Pleistocene ice margins in the vicinity of Spokane, Wash., as mapped by Bretz and others (1956), Flint (1937), and Weis and Richmond (this paper).

be present. The authors have reexamined all these localities and concluded that till occurs at only two. At Flint's locality 1, north of the confluence of the Spokane and Columbia Rivers, a layer of compact silty clay till with erratic stones occurs in roadcuts beneath several feet of massive stone-free compact loess. At one of several roadcuts indicated at Flint's locality 14, a lenticular mass of soft, gray calcareous massive till which consists of silt, clay, and erratic stones is 18 inches thick and extends 30 feet along the cut; it is interbedded with clean fine-grained flat-bedded lake sand of very uniform texture. This till may be a deposit from an iceberg grounded near the shore of a lake.

The deposits at Flint's other localities appear to us to fall into three categories: (a) flood gravel that is coarse and open-textured, with angular to subrounded and, in part, percussion-shattered stones; it contains some erratics but is characterized by an abundance of locally derived basalt (Flint's localites 2, 13, 14, 15); (b) weakly to well bedded brown loess that was reworked by floodwater; it contains granules and small angular fragments of arkosic detritus, or thin lenticular beds of such detritus (Flint's localities 3, 4, 5, 6, 7, 8, 9); and (c) colluvial mantle resting on kaolinized granitic rock and overlain by pre-flood brown loess that contains one or more buried soils; the colluvium contains rounded to angular pebbles of quartz, feldspar, and quartzite, and locally bears a bright-red clayey soil (Flint's localities 10, 11, 12).

The deposit at Cheney, Wash., is now covered by a building. However, at another locality three-fourths of a mile distant, at the south edge of Cheney (NW½ SE¼ sec. 12, T. 23 N., R. 41 E.), there is an extension of the same barlike feature along the west margin of the Cheney-Palouse flood spillway; it contains open-textured flood gravel that has coarse angular to subangular stones in an earthy matrix. It is not till. The deposit abuts hills of loess to the west but is not covered by loess.

Flint (1936, p. 1854; 1937, p. 221) concluded that numerous deposits in tributary reentrants along the margin of the valley east of Spokane are remnants of a once-continuous outwash fill. We believe that they are more complex. In most exposures they consist of two units separated by a sharp erosional disconformity. The lower unit consists of sand or sandy gravel characterized by poor sorting, channel-and-fill crossbedding, slump structures, and sharp changes in texture. We infer that unit to consist of ice-contact deposits formed by ice-margin streams. The upper unit also consists of sand or sandy gravel, but is characterized by moderate to good sorting, long foreset beds that dip downvalley across the mouths of tributary valleys, and subangular, percussion-shattered cobbles. We infer these deposits to be of flood origin.

Flint (1937, p. 211) noted certain differences in topography on loess-covered hills north and south of his inferred drift border near Reardan, Wash. (fig. 1). He ascribed the topography north of his drift border to glaciation. Becraft and Weis (1963, p. 42–44, fig. 6) disagreed, concluding that the lack of clear examples of glacial erosion, and the absence of erratic gravels except where they could be accounted for by the scabland floods, make glaciation appear unlikely. Furthermore, no compaction or deformation of loess attributable to overriding by ice can be found. The topography itself, although somewhat subdued as compared with loess hills farther south, bears a normal, mature drainage pattern that suggests neither present nor former derangement such as is characteristic of morainal topography. Further, loess deposits are generally thinner near the north edge of the Columbia Plateau than farther south, and are thinnest on the high hills that Flint shows as nunataks, where in fact the loess deposits should be thickest if the high hills actually represent unglaciated remnants.

NEW EVIDENCE AND INTERPRETATIONS

Criteria we used to infer the limits of glaciation include the distribution of the following: till, ice-contact deposits, ice-scoured bedrock surfaces, ice polish, and morainal topography. Supplemental evidence in the form of deeply weathered residuum was also used. Where residually weathered material, devoid of erratics, is found in patches on spurs and ridge crests where it would be highly susceptible to glacial erosion, these localities are inferred to lie outside, or above, the position of the ice margin.

The Cordilleran ice sheet advanced south into the Spokane region in four major valley lobes. From east to west they are the Lake Pend Oreille lobe (Rathdrum lobe of Anderson, 1927), the Priest River lobe, the Little Spokane lobe, and the Colville lobe (fig. 1). Flint (1937) concluded that at its maximum extent the ice in all these lobes coalesced, filling the Spokane Valley and spilling southward over a considerable area of the adjoining Columbia Plateau. We have concluded that the ice was much less extensive. We believe that no ice reached the surface of the Columbia Plateau east of long 117°45′ W., that the ice from the Lake Pend Oreille lobe occupied only that part of Spokane Valley east of Spokane, that the Little Spokane lobe ended about 15 miles north of Spokane, and that the

Colville lobe extended no more than about 2½ miles south of the Spokane River and reached the surface of only a small part of the Columbia Plateau.

Ice of the Lake Pend Oreille lobe moved south into the valley of the Spokane River, then westward along the valley to Spokane. Till, locally covered by a veneer of flood deposits, underlies several square miles northwest of Hayden Lake, Idaho, at elevations of 2,400 to 2,700 feet. About 2½ miles east of Post Falls, Idaho, a large remnant of a kame reaches an elevation of about 2,350 feet; thus the ice there must have reached at least that elevation.

The Lake Pend Oreille lobe was confined to the valley of the Spokane River between Post Falls and Spokane. Only the lower 100 feet or so of spur ridges along the valley are smooth enough to suggest a significant amount of erosion by ice, and west of Spokane no such smoothed surfaces are present. Many surfaces below about 2,500 feet along the valley have large areas of bare outcrop, but the distribution and surface irregularity of the outcrops suggest scour by floodwater rather than by ice. The only ice-polished surfaces are less than 100 feet above the valley floor; remnants of that ice polish are known at points southeast and northwest of Opportunity, Wash., and near the north and south sides of the valley immediately east of Spokane.

Ice-contact deposits, disconformably overlain by flood sand and gravel, block or partly block all the valleys that are tributary to the Spokane Valley between Rathdrum, Idaho, and Dishman, Wash. (fig. 1). East of the boundary between Washington and Idaho most of the deposits are kame terraces. The deposits are characterized by horizontal bedding, by channel crossbedding, by poor to good sorting, and by materials composed of coarse to fine sand and granule gravel, with local layers of pebbles and cobbles, and scattered boulders. West of the State boundary the deposits are mainly kame deltas; they consist of well-sorted sand and granule gravel in long deltaic foreset beds which contain a few local and probably ice-rafted stones. The most westerly deposits, near Dishman, Wash., suggest the approximate western limit of the ice. The deltaic character of the deposits indicates that the glacier terminated in a lake which has been called glacial Lake Spokane (Large, 1922; Anderson, 1927).

The maximum elevation of these ice-contact deposits decreases westward from about 2,400 feet just north of Rathdrum, Idaho, to about 2,350 feet southeast of Spokane. The original surfaces have been channeled and somewhat lowered by subsequent flood erosion in many places. Whether channeled or not, the kame tops are evidence that the ice margin at one time stood at least that high.

Although the maximum elevation reached by the ice cannot be measured directly, an upper limit can be found. Deeply weathered residuum is present in many places on the hills bordering Spokane Valley. Its exact age is unknown, and is probably not the same in all exposures, but this residuum is clearly older than recognizable glacial deposits. Some of the deposits are on ridge crests, spurs, and similar surfaces that would have been denuded had glacial ice moved over them. The maximum elevation of the ice margin must therefore be below them. Two examples of this deeply weathered residuum are on a ridge crest near the boundary between Washington and Idaho, at an elevation of about 2,650 feet, and on a ridge south of Opportunity, Wash., at 2,400 feet. These occurrences are among those that provide reference points for the line below which the ice margin must lie.

Although the precise upper limits of the Lake Pend Oreille lobe are not known, it appears that at the maximum extent of the ice its upper surface in Spokane Valley stood somewhere between the top of the highest kame and the bottom of the lowest easily eroded residuum. Similarly, although the lower surface of the ice lobe cannot be recognized precisely, we believe that it probably stood somewhere between the lowest exposed ice polish on bedrock and the lowest level at which glacial gravel occurs in Spokane Valley. Using all available data, we conclude that at the Washington-Idaho boundary the ice was between 650 and 1,000 feet thick, and that at its terminus near Spokane, it had a maximum thickness of 250 to 700 feet.

We have not studied the outer limit of the Priest River lobe in detail. At the maximum of glaciation it probably merged with the Lake Pend Oreille lobe to the east and with the Little Spokane lobe to the west.

The Little Spokane lobe is believed to have reached its maximum stand in the vicinity of Milan, Wash. (fig. 1). The exact location of the outer limit is not known, in part because no end moraine is preserved. However, the distribution of the deposits from glacial Lake Spokane, and of the hills that are covered by deeply weathered granite residuum devoid of erratics, limits the possible extent of the ice south of Milan to approximately that shown on figure 1.

At its maximum extent, the Colville lobe abutted the basalt rim of the Columbia Plateau about 2½ miles south of Long Lake, Wash., on the Spokane

River, where deposits of lake sand form a large kame delta (Flint, 1936, p. 1854) at an elevation of about 2,350 feet. The kame is capped by flood gravel. To the south the distribution of deep residual weathered rock, locally overlain by loess and bearing no erratic material, shows that the ice did not reach the north side of Shoemaker Butte. North of the Spokane River the western margin of the lobe retained a body of water called glacial Lake Wellpinit (Flint, 1936, p. 1856; Becraft and Weis, 1963, p. 51). Along the eastern margin the ice probably approached Loon Lake, which is dammed by glacial outwash, but must not have extended southeast beyond the lake because pinnacles and sharp crests present on deeply weathered granite there could not have been preserved under moving ice.

SUMMARY AND CONCLUSIONS

The problem of the maximum extent of the Cordilleran ice sheet near Spokane has been obscured by the controversy of 30 years ago regarding the flood origin of the channeled scabland, a concept now widely accepted. We now know that the scabland floods occurred when the water that ponded in glacial Lake Missoula, in western Montana, breached its ice dam at the mouth of the Clark Fork River (Bretz and others, 1956; Pardee, 1942). The great volume of water thus released could take only one course, southwestward to Spokane and across parts of the Columbia Plateau. Earlier workers, unaware of the full scope and effects of the floods, were understandably misled by some of its deposits and found ice-margin features difficult to recognize where flood effects were most severe. In fact, we now realize that where flood effects are particularly severe the precise location of the ice margin will probably never be known.

Present evidence leads us to the conclusion that the Lake Pend Oreille lobe ended near the east side of Spokane and never extended westward to join the Little Spokane lobe as postulated by both Bretz and Flint. We also conclude that although ice locally abutted the Columbia Plateau on the south side of Spokane Valley near Shoemaker Butte it did not encroach over an extensive area of the plateau as previously supposed.

The relations between ice margins, flood deposits, and glacial lake deposits are complex, both in position and in time. We believe that except where flood effects were most severe, a much more detailed picture of those relations can be worked out. We hope that this note will serve to refocus attention on that possibility.

REFERENCES

Anderson, A. L., 1927, Some Miocene and Pleistocene drainage changes in northern Idaho: Idaho Bur. Mines and Geology, Pamph. 18, 29 p.

Becraft, G. E., and Weis, P. L., 1963, Geology and mineral deposits of the Turtle Lake quadrangle, Washington: U.S. Geol. Survey Bull. 1131, 73 p.

Bretz, J H., 1923a, Glacial drainage on the Columbia Plateau: Geol. Soc. America Bull., v. 34, p. 573–608.

—— 1923b, Channeled scablands of the Columbia Plateau: Jour. Geology, v. 31, p. 617–649.

—— 1928, Channeled scabland of eastern Washington: Geog. Review, v. 18, p. 446–477.

Bretz, J H., Smith, H. T. U., and Neff, G. E., 1956, Channeled scablands of Washington; new data and interpretations: Geol. Soc. America Bull., v. 67, p. 957–1049.

Bryan, Kirk, 1927, The "Palouse soil" problem: U.S. Geol. Survey Bull. 790, p. 21–45.

Flint, R. F., 1935, Glacial features of the southern Okanogan region: Geol. Soc. America Bull., v. 46, no. 2, p. 169–194.

—— 1936, Stratified drift and deglaciation of Eastern Washington: Geol. Soc. America Bull., v. 47, p. 1849–1884.

—— 1937, Pleistocene drift border in eastern Washington: Geol. Soc. America Bull., v. 48, p. 203–231.

Freeman, O. W., 1926, Mammoth found in loess in Washington: Sci., new ser., v. 64, p. 477.

Large, Thomas, 1922, Glacial border of Spokane: Pan-Am. Geologist, v. 38, p. 359–366.

Leverett, Frank, 1917, Glacial formations in the Western United States [abs.]: Geol. Soc. America Bull., v. 28, p. 143–144.

Pardee, J. T., 1942, Unusual currents in glacial Lake Missoula, Montana: Geol. Soc. America Bull., v. 53, p. 1569–1600.

BIRCH CREEK PINGO, ALASKA

By DANIEL B. KRINSLEY, Washington, D.C.

Abstract.—The Birch Creek pingo is a large open-system pingo near Circle, Alaska. The top of the pingo has collapsed, forming a crater which is partly filled by a shallow pond. The stratigraphy exposed in the bluffs of the crater suggests that there was permafrost in the area during the period 6,950±400 years B.P. to 5,720±65 years B.P., which coincides with the postglacial thermal maximum. The local base level has been reduced at least 5 feet in the last 5,720±65 years, and the pingo has been updomed during this time.

Pingos (Eskimo name for hills rising above a tundra plain) are mounds or hills which have been updomed by hydrostatic pressure in areas underlain by permafrost. The hydrostatic pressure may result from hydraulic head related to an adjacent slope (Porsild, 1938, p. 47); pingos formed in this way are designated open-system pingos. Hydrostatic pressure resulting from volume expansion of water on freezing, as permafrost advances into a closed, unfrozen pocket, may form closed-system pingos (Müller, 1959, p. 97; Mackay, 1963, p. 84–85). Open-system pingos range in size from mounds a few feet in height and basal width to hills 90 feet high and 1,550 feet wide at their base (Müller, 1959, p. 29). Closed-system pingos are generally larger and may reach a height of 300 feet and basal diameter of ½ mile (Smith, 1913, p. 28).

DESCRIPTION OF BIRCH CREEK PINGO

The Birch Creek pingo is a forested elliptical hill rising 49 feet above a stream terrace near Circle, in east-central Alaska. It lies at lat 65° 42′ N. and long 144° 24′ W., about 1¾ miles southwest of the Steese Highway bridge crossing Birch Creek. Its maximum north-south and east-west dimensions are 1,450 and 1,200 feet, respectively, as measured across the 650-foot contour, which marks its base (fig. 1).

The proximity of Birch Creek pingo to the valley side, to ice mounds, and to another pingo on the valley side, as well as the development of all these features in an area of discontinuous permafrost (Fer-

rians, 1965), suggests that the Birch Creek pingo is of the open-system type. Open-system pingos are common in the Yukon-Tanana upland (which includes Birch Creek valley) (Holmes and others[1]), but closed-system pingos have not been identified there to date.

The top of the Birch Creek pingo forms a crater with 20-foot bluffs and steep forested slopes that surround a shallow pond. Two saddles on the northern crater rim may mark the positions of former outlets; the northwest saddle, 3 feet above the surface of the pond, is muddy adjacent to the pond. The present outlet at the southwest corner of the pond is connected to a small stream south of the pingo. Discharge at the outlet was approximately ½ gallon per minute in mid-August 1963. The water temperature was 61°F. near the shore of the pond and 64°F. at the outlet.

The north-south profile of the pingo is generally symmetrical, with outer slopes of 22° and inner (crater) slopes of 35°. The east-west profile is asymmetrical, with a steep outer slope of 28° and an inner slope of 33° on the west, and with an outer slope of 25° and an inner slope of 42° on the east. The pingo is encircled by a shallow depression containing two small lakes on the west and black-spruce muskeg on the north and east. A small stream to the south, which drains the southern lake, flows west into an oxbow of Birch Creek. The pingo and the surrounding drainage system are 500 feet from the base of the west slope of Birch Creek valley, on a terrace that is 5 feet above the present flood plain, and 1 mile from Birch Creek. A compound system of ice mounds and a smaller pingo with a central pond lie against the valley slope 1,000 feet northwest of the Birch Creek pingo.

---

[1] G. W. Holmes, D. M. Hopkins, and H. L. Foster, Distribution and age of pingos of interior Alaska: Internat. Conf. Permafrost, Purdue Univ., 1963, Proc.
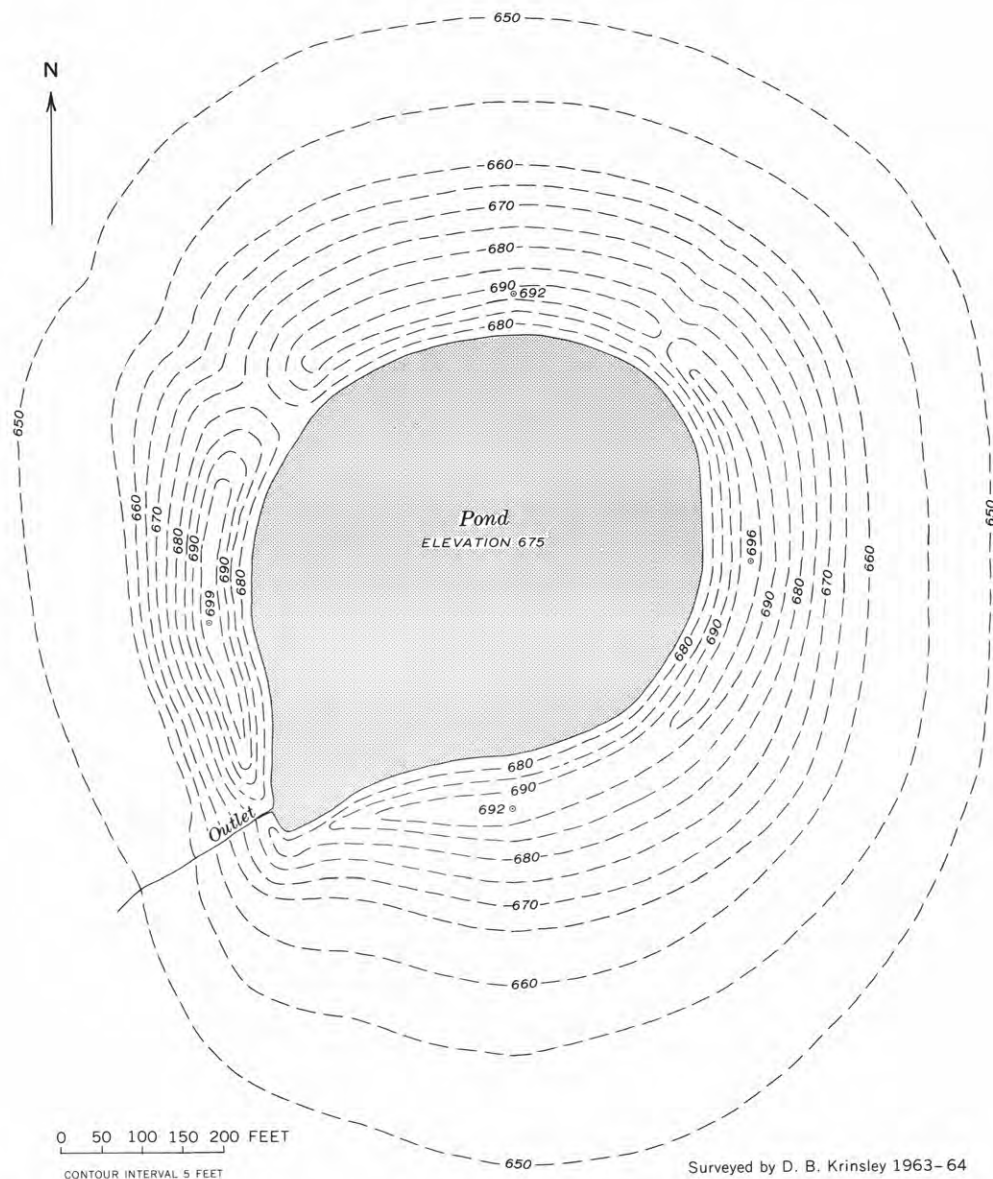
FIGURE 1.—Topographic map of the Birch Creek pingo, Alaska. The average altitude of the surrounding terrace, on which the pingo is situated, is about 650 feet.

Around the base of the pingo the frost table (measured in late August in 1963 and in 1964, and considered to be the permafrost table) is 20 to 29 inches beneath the surface. Near the top of the outer slopes the frost table is about 50 inches beneath the surface; inside the crater, in contrast, it is more than 6 feet beneath the surface. The frost table has receded laterally, outward, as the crater pond has induced peripheral thawing. Permafrost lies 18 to 30 inches below the surface in Birch Creek valley but is absent locally in the better drained terrace gravels and in sandy deposits adjacent to Birch Creek. The thickness of the permafrost in Birch Creek valley is not known.

The crater rim, no longer underlain by frozen soil, has collapsed locally in crescent-shaped segments that are delineated by narrow cracks concentric to the faces of the inner bluff. The large size of the pingo and its relatively smooth outer slopes suggest that little degradation has occurred since it was updomed, and that the original ice core is probably still present.

A 20-foot vertical section was prepared on the east side of the crater by scraping the face of the bluff and by partially excavating the foot. All the stratified materials observed in the section dip 17° east. The basal part of the section is not convoluted and contains 11 feet of stratified brown sandy pebble gravel and well-oxidized pebble gravel. These coarse

materials are overlain by a 2-inch zone of wood fragments in sand which, in turn, is covered by 3 feet of slightly convoluted stratified medium-grained buff to gray sand. The contact between the convoluted sand and the underlying gravel is sharp. Two and a half inches of nearly pure fibrous peat, which is not convoluted, overlies the convoluted sand. The peat is overlain by 6 feet of stratified sandy silt that has not been deformed. Some of the sandy silt, between less permeable buff to gray zones, has been oxidized brownish red. Near-surface sandy silt, just beneath the 2-inch-thick cover of organic material, is not oxidized.

AGE RELATIONS

The organic materials in the vertical section were dated by the radiocarbon method by Long (1965), of the Smithsonian Institution. The age of the wood fragments at the top of the lower, gravel zone is 6,950±400 years (sample SI-123), and that of the fibrous peat (above the convoluted sand) 5,720±65 years (sample SI-122). The 3-foot bed of slightly convoluted medium sand was thus deposited less than 6,950±400 years ago in a flood-plain or lacustrine environment. The convolutions, which postdate the sand, suggest the development of frost structures by congeliturbation (Bryan, 1946, p. 633). It seems unlikely that frost structures would have developed in sand covered by a water body (Lachenbruch, 1957, p. 1515); therefore, the local water table must have been at least 3 feet below the land surface when the frost structures developed. The absence of frost structures in the underlying stratified gravel is best explained by assuming that the gravel was saturated and frozen (Nichols[2]). The later deposition of the peat, 5,720± 65 years ago, indicates a bog environment, which in turn suggests that the local water table had risen at least 3 feet.

Nichols[2] described a similar bluff exposure along the east side of Tolsona Creek, Alaska. There, an ice mass extended upward into a layer of contorted gravel in which a peat layer was folded. The contorted gravel was unconformably overlain by undisturbed bedded sand which contained two peat layers. The folded peat was dated as 6,910±250 years B.P. (before present, that is, before A.D. 1950) (sample W-717, Rubin Alexander, 1960, p. 166), and the lower peat layer in the bedded sand was dated as 5,850±320 years B.P. (Meyer Rubin, written communication on sample W-1304, 1963).

These dates and their nearly exact counterparts from Birch Creek bracket a period which occurred

during the postglacial thermal maximum (9,000 to 3,000 years B.P. according to Ahlmann, 1953, p. 38, and 7,500 to 4,000 years B.P. according to Flint, 1957, p. 377). During the climatic amelioration of the postglacial thermal maximum, which has been recorded in southern Alaska (Karlstrom, 1961, p. 302) and in the southwest Yukon Territory (Krinsley, 1965, p. 293), permafrost developed at Tolsona Creek and probably was present beneath the convoluted sand at Birch Creek. These data suggest that even during the postglacial thermal maximum, conditions in local areas were not sufficiently responsive to the general rise in the mean annual temperature to prevent the formation or maintenance of permafrost.

The upper 6 feet of stratified fine to medium, sandy silt at Birch Creek, which suggests a quiescent-water environment, probably was deposited in an oxbow of Birch Creek. If the stratified sandy silt had not been updomed in the pingo, the upper part of this material would now be 5 feet above the present level of Birch Creek. Therefore, the local base level has been reduced at least 5 feet in the last 5,720±65 years, and the pingo has been updomed during this time.

The 3 feet of convoluted sand, between the wood fragments and the peat, accumulated at an average rate of approximately 1 foot per 410 years. If we assume a uniform rate of accumulation, the upper 6 feet of stratified sandy silt would have been deposited in 2,460 years. On the basis of this assumption, the pingo could have been updomed less than 3,260 (5,720—2,460) years ago.

A mature forest of white spruce and aspen approximately 100 years old covers the outer and the inner (crater) slopes of the pingo. There is no evidence of rotten or charred stumps to suggest a previous forest growth. The trunk of a 145-year-old white spruce on the north shore of the pond was leaning steeply toward the pond along its lower 2 feet, but was growing vertically above the tilted lower part. On the basis of observed growth rates of white spruce this tree is believed to have been growing on stable ground at the margin of the pond during the last 100+ years. Other old trees at the shoreline show similar deformation. Several trees which were growing at the shoreline have recently fallen into the pond, and low vegetation adjacent to them has been inundated, which suggests a very recent change in environment.

These observations suggest that the pingo may be only a few hundred years old, and that there has been a relatively long period of stability (100+ years) since the updoming. The diameter of the pond is now

[2] D. R. Nichols, Permafrost in the Recent Epoch: Internat. Conf. Permafrost, Purdue Univ., 1963, Proc.

being enlarged by recession of the bluffs and by a rise in water level caused by infilling of peripheral debris, partial flooding by water previously frozen in the crater rim, and by precipitation.

The unusually high temperature of the pond water (61°F. to 64°F.) suggests that the pond is well insulated from the ice core by a thick layer of silt. In the vicinity, other lakes and ponds not associated with ice have similar water temperatures during August.

Carbon 14 evidence suggests that the pingo was up-domed less than 5,720±65 years ago. This maximum age is similar to the maximum ages of the closed-system pingo in the Thelon Valley, N.W.T., Canada, which was dated as 5,500±250 yeas B.P. (Craig, 1959, p. 509); and to the open-system Sitiyak pingo in the Mackenzie delta area, N.W.T., Canada, which was dated as 6,800±200 years B.P. (Müller, 1962, p. 284). These maximum ages indicate that the pingos are post-Wisconsin (Karlstrom, 1961, p. 306) frost features of which some may have developed during the cooler period following the postglacial thermal maximum (altithermal) (Karlstrom, 1961, p. 306-307). Other pingos are younger frost features of which many have formed recently.

REFERENCES

Ahlmann, H. W., 1953, Glacier variations and climatic fluctuations: Am. Geog. Soc., ser. 3, 51 p.

Bryan, Kirk, 1946, Cryopedology, the study of frozen ground and intensive frost-action with suggestions on nomenclature: Am. Jour. Sci., v. 244, no. 9, p. 622–642.

Craig, B. G., 1959, Pingo in the Thelon Valley, Northwest Territories: Geol. Soc. America Bull., v. 70, p. 509–510.

Ferrians, O. J., Jr., 1965, Permafrost map of Alaska: U.S. Geol. Survey Misc. Geol. Inv. Map I–445. [In press].

Flint, R. F., 1957, Glacial and Pleistocene geology: New York, John Wiley and Sons, Inc., 553 p.

Karlstrom, T. N. V., 1961, The glacial history of Alaska; its bearing on paleoclimatic theory, in Symposium on solar variations, climatic change, and related geophysical problems: New York Acad. Sci. Ann., v. 95, art. 1, p. 290–340.

Krinsley, D. B., 1965, Pleistocene geology of the southwest Yukon Territory, Canada: Jour. Glaciology, v. 5, no. 40, p. 385–397.

Lachenbruch, A. H., 1957, Thermal effects of the ocean on permafrost: Geol. Soc. America Bull., v. 68, p. 1515–1530.

Long, Austin, 1965, Smithsonian Institution radiocarbon measurements II: Am. Jour. Sci., Radiocarbon Supp., v. 7, 1965. [In press]

Mackay, J. R., 1963, The Mackenzie delta area, N.W.T.: Canada Dept. Mines and Tech. Surveys Mem. 8, 202 p.

Müller, Fritz, 1959, Beobachtungen über Pingos: Medd. om Grønland, v. 153, 127 p.

Müller, Fritz, 1962, Analysis of some stratigraphic observations and radiocarbon dates from two pingos in the Mackenzie delta area, N.W.T.: Arctic, v. 15, p. 278–288.

Porsild, A. E., 1938, Earth mounds in unglaciated arctic northwestern America: Geog. Rev., v. 28, p. 46–58.

Rubin, Meyer, and Alexander, Corrine, 1960, U.S. Geological Survey radiocarbon dates V: Am. Jour. Sci., Radiocarbon Supp., v. 2, p. 129–185.

Smith, P. S., 1913, The Noatak-Kobuk region, Alaska: U.S. Geol. Survey Bull. 536, 160 p.

⚒

QUATERNARY STRATIGRAPHY OF THE DURANGO AREA, SAN JUAN MOUNTAINS, COLORADO

By GERALD M. RICHMOND, Denver, Colo.

Abstract.—Study of the type localities of Quaternary strati-graphic units defined by Atwood and Mather in 1932 in the Durango area shows that their Wisconsin moraines are of Pine-dale age. Although some of their Durango moraines are of Bull Lake age, their type Durango moraine represents the youngest of three pre-Bull Lake glaciations, the Sacagawea Ridge Glacia-tion. The Florida Gravel is outwash of Sacagawea Ridge age and may represent two glacial advances. The Oxford Gravel is colluvium of middle to late Pleistocene age. The Bridgetimber Gravel and some deposits of the Bayfield Gravel represent out-wash of two pre-Sacagawea Ridge glaciations, the Cedar Ridge and Washakie Point (older) glaciations. Other deposits of Bayfield Gravel are residually weathered from pre-Quaternary conglomerate.

The town of Durango, Colo., lies at the mouth of the canyon of the Animas River, at the south edge of the San Juan Mountains in southwestern Colorado (fig. 1). Quaternary deposits are widespread in the vicinity of the

FIGURE 1.—Index map of Colorado, showing location of the Durango area.

town and to the south and east in the drainage basins of the Animas, Florida, and Los Pinos Rivers. The area includes many of the type localities of stratigraphic units mapped by Atwood and Mather (1932) throughout the San Juan Mountains. These stratigraphic units, as defined by Atwood and Mather, are given in table 1.

TABLE 1.—*Quaternary stratigraphic units in the San Juan Moun-tains, as defined by Atwood and Mather (1932)*

Pleistocene:
    Wisconsin Till and outwash gravel
    Oxford Gravel (interglacial)
    Durango Till and outwash gravel
    Florida Gravel (interglacial)
    Cerro Till
Pliocene(?):
    Bridgetimber Gravel and Bayfield Gravel

The writer has restudied the deposits in the Durango area, and their stratigraphic relations, during a series of visits over the past several years. The purpose of this paper is to present certain additional information about the deposits and a revised interpretation of the origin and age of some of them.

The Animas River flows in a deep glaciated valley for nearly 60 miles from its headwaters north of Silver-ton, in the heart of the San Juan Mountains, to the town of Durango, where the late Pleistocene glaciers terminated. Just downstream from the town the river passes through a series of hogback ridges that mark the south edge of the mountains, and flows southward into New Mexico in an open valley bordered by outwash terraces.

During each late Pleistocene glaciation an icecap, some 1,200 square miles in area as mapped by Atwood and Mather (1932), formed over the central part of the San Juan Mountains. It was the source of the glaciers in the valley of the Animas River, and also of glaciers in the valleys of the Florida and Los Pinos Rivers to the east. The cap ice flowed across the eastern rim of the valley of the Animas River at many
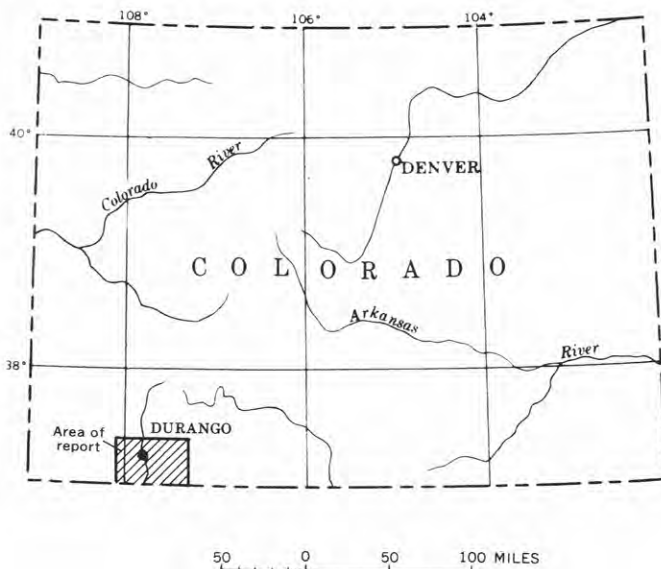
TABLE 2.—*Correlation of Quaternary deposits in the Durango, Colo., area with glaciations |in the Wind River Mountains, Wyo., area*

Midcontinent	Wind River Mountains, Wyo.		Durango area, San Juan Mountains, Colo.
			Immature zonal soil.
Late Wisconsin	Pinedale Glaciation	Late stage	Wisconsin moraines and outwash gravel.
		Middle stage	
		Early stage	
	Interglaciation		Mature zonal soil.
Early Wisconsin	Bull Lake Glaciation	Late stage	Some Durango moraines and some Durango outwash gravel.
		Early stage	
	Interglaciation		Very strongly developed soil.
Illinoian	Sacagawea Ridge Glaciation		Type end moraine of Durango Till; some Durango outwash gravel and Florida Gravel.
	Interglaciation		Very strongly developed soil.
Kansan	Cedar Ridge Glaciation		Gravel on Mesa Mountains, gravel on lower surface of Bridgetimber Mountain, and some deposits of Bayfield Gravel.
	Interglaciation		Very strongly developed soil.
Nebraskan	Washakie Point Glaciation		Bridgetimber Gravel on upper surface of Bridgetimber Mountain and some deposits of Bayfield Gravel.

points and was undoubtedly responsible for that glacier's being the longest in the Southern Rocky Mountains.

In the following discussion, the Quaternary deposits of the area are correlated with glaciations defined in the Wind River Mountains of Wyoming (Blackwelder, 1915; Moss, 1951; Holmes and Moss, 1955; Richmond, 1948, 1962, 1964), which have become a standard for correlation in the Rocky Mountains. From oldest to youngest, these glaciations are: Washakie Point, Cedar Ridge, Sacagawea Ridge, Bull Lake, and Pinedale. A summary correlation of the Quaternary deposits of the Durango area, as interpreted by the writer, with the glaciations in the Wind River Mountains is given in table 2. Two stades of Recent Neoglaciation, the Temple Lake and Gannett Peak, are also recognized in both areas, but will not be discussed here. The deposits are described from youngest to oldest because they are most readily identified in that order.

YOUNGER GLACIAL DEPOSITS

Pinedale Glaciation

Two hummocky arcuate end moraines, 50 to 60 feet high, extend across the valley of the Animas River at Durango at an altitude of 6,650 feet (figs. 2, 3). Both are bouldery and relatively fresh in appearance. The till is loose and sandy.

The moraines are separated by a swale underlain by

outwash gravel which extends from the upstream moraine through narrow channels in the downstream moraine. The latter moraine overlies proglacial gravel across which the ice had advanced. An outwash terrace segment, less than 25 feet above the Animas River, extends downstream from each moraine through the town of Durango. Weathering of the two moraines is identical. The soil consists of a humic A horizon, 2 to 4 inches thick, over a weakly oxidized pale-yellowish-brown B horizon, 10 to 14 inches thick. The profile displays almost no clay illuviation. These moraines were described by Atwood and Mather (1932), who considered them to be of Wisconsin age. Their characteristics are similar to moraines of the early and middle stages of the Pinedale Glaciation in the Wind River Mountains, Wyo.

A gravel outwash plain extends upstream from the moraines for a distance of 12 miles, rising gradually to an ice-contact front and local end-moraine segments at an altitude of 6,800 feet. This front probably marks a readvance of the ice during the late stage of Pinedale Glaciation.

Bull Lake Glaciation

Remnants of two older morainal arcs occur just downstream from the Pinedale moraines at Durango at an altitude of 6,750 feet (figs. 2, 3). The inner moraine is 60 to 120 feet high, and the outer moraine

pe and pm—Early and middle stades, Pinedale Glaciation (Wisconsin stage of Atwood and Mather, 1932)
be and bl—Early and late stades, Bull Lake Glaciation (not recognized by Atwood and Mather, 1932)
s—Sacagawea Ridge Glaciation (type end moraines of Durango stage of Atwood and Mather, 1932)

FIGURE 2.—End moraines at Durango, San Juan Mountains, Colo.

for example, along Dallas Creek west of Ridgeway (Richmond, 1954), they mapped moraines having these characteristics as deposits of Durango Till.

Two outwash terraces extend downstream from the Bull Lake moraines at Durango. At the moraines they are 100 and 170 feet above the river, but 7 miles downstream they are only 80 and 150 feet above it. They transect the end moraine of the type Durango Till and lie at a lower level than its outwash plain. The lower of the two terraces is the more widespread; the upper occurs as isolated segments along the valley wall and in places is covered by younger alluvial fan deposits. The soil on these terraces is similar to that on the Bull Lake moraines, but south of the mountain front it has a Cca horizon 18 to 24 inches thick. Equivalent terraces lie downstream from Bull Lake moraines along the Florida and Los Pinos Rivers.

Sacagawea Ridge Glaciation

The end moraine of the type Durango Till (Atwood and Mather, 1932) is a broad, gently sloping ridge that rests on a rock bench 300 to 350 feet above the Animas River east of Durango, at an altitude of 6,950 to 7,000 feet (figs. 2, 3). The till is compact, bouldery, unsorted, and composed of rock types from the Animas River drainage basin. The soil developed on it consists of a red (2.5 YR), plastic, clayey B horizon more than 6 feet thick, underlain by a thicker Cca horizon impregnated and partially cemented with calcium carbonate. The very mature form of the moraine, its position in the canyon at a considerable height above the river, and the very strong degree of development of the soil on it are typical characteristics of deposits of the youngest of three pre-Bull Lake glaciations in the Wind River Mountains, called the Sacagawea Ridge Glaciation.

An outwash plain of bouldery gravel, 300 feet above the river, extends downstream from the moraine. It was mapped as Durango outwash by Atwood and Mather. Four segments of a higher gravel-capped terrace, 500 feet above the river (fig. 4), occur just south of the first hogback ridge downstream from Durango. These were mapped as Florida Gravel by Atwood and Mather and inferred to be of interglacial origin. The material on the most northerly segment forms a knob 40 to 50 feet above the flat surface of the other segments and consists of coarse unsorted bouldery debris that is either till or outwash deposited near ice. The writer infers therefore that these higher terrace deposits represent an early advance of the Sacagawea Ridge Glaciation.

The Florida Gravel at its type locality on Florida Mesa, west of the Florida River (fig. 4), caps two dissected bedrock benches. The gravel is 20 to 30

is 30 to 50 feet high. These moraines outline two stands of the ice beyond those of the Pinedale Glaciation. They are separated from the Pinedale deposits by a terrace scarp. The moraines are more mature in appearance, less bouldery, and more dissected than the Pinedale moraines, and the till in them is also more compact than that of the Pinedale moraines. The soil has been eroded from them in most exposures, but where preserved it consists of a thin A horizon overlying an oxidized dark-yellowish-brown B horizon, 18 to 30 inches thick.

The characteristics of these moraines are similar to those of the Bull Lake Glaciation of the Wind River Mountains, Wyo., the early and late stades of which they are inferred to represent. Atwood and Mather did not recognize these moraines at Durango. However, along the Florida and Los Pinos Rivers to the east as well as in other parts of the San Juan Mountains, as,

pe and pm—Early and middle stades, Pinedale Glaciation (Wisconsin stage of Atwood and Mather, 1932)
be and bl —Early and late stades, Bull Lake Glaciation
s—Sacagawea Ridge Glaciation (type end moraine of the Durango stage of Atwood and Mather, 1932)

FIGURE 3.—Sequence of moraines at Durango, Colo.   Photograph by Whitman Cross.

feet thick and bears a very strongly developed red clayey soil 3 to 5 feet thick like that on the type Durango Till but with an underlying massive Cca horizon 2 to 3 feet thick. The soil is overlain by deposits of loess 3 to 15 feet thick which give the bench a gently undulating surface. The presence of a mature zonal soil in the upper part of the loess suggests that most of it is of Bull Lake age. However, the immature zonal soil at the surface of the loess indicates that the uppermost part was deposited or locally reworked in Pinedale time. The gravel on the lower and more extensive part of Florida Mesa can be traced upstream along the Florida River to moraines of Sacagawea Ridge age. To the west the deposit merges with outwash from the end moraine of the type Durango Till. The higher part of the mesa is more dissected, and is at the same level as the four high terrace segments south of Durango. The gravel deposits on both benches were included in the Florida Gravel by Atwood and Mather (1932). They are here inferred to represent outwash of two advances of the ice during Sacagawea Ridge Glaciation.

OLDER GLACIAL AND INTERGLACIAL DEPOSITS

Atwood and Mather (1932) described an ancient till of precanyon origin on many upland divides in the San Juan Mountains. They named this the Cerro Till from a type locality on Cerro Summit at the north edge of the mountains. R. G. Dickinson (this chapter, p. C147), after restudy of this area, considers the type deposit to be nonglacial and of landslide and mass-wasting origin. The term Cerro Till has therefore been abandoned. As is pointed out by Dickinson, however, this does not preclude the possibility that other deposits mapped as Cerro Till by Atwood and Mather may be till.

In the Durango area, though no distinct precanyon till has been found, there are widespread thick deposits of precanyon gravel whose characteristics suggest a fluvioglacial origin. These include deposits mapped as Bridgetimber Gravel and Bayfield Gravel by Atwood and Mather (1932), who judged them to be of Pliocene(?) age.

Bridgetimber Gravel

At its type locality the Bridgetimber Gravel caps Bridgetimber Mountain (fig. 4), whose highest part is
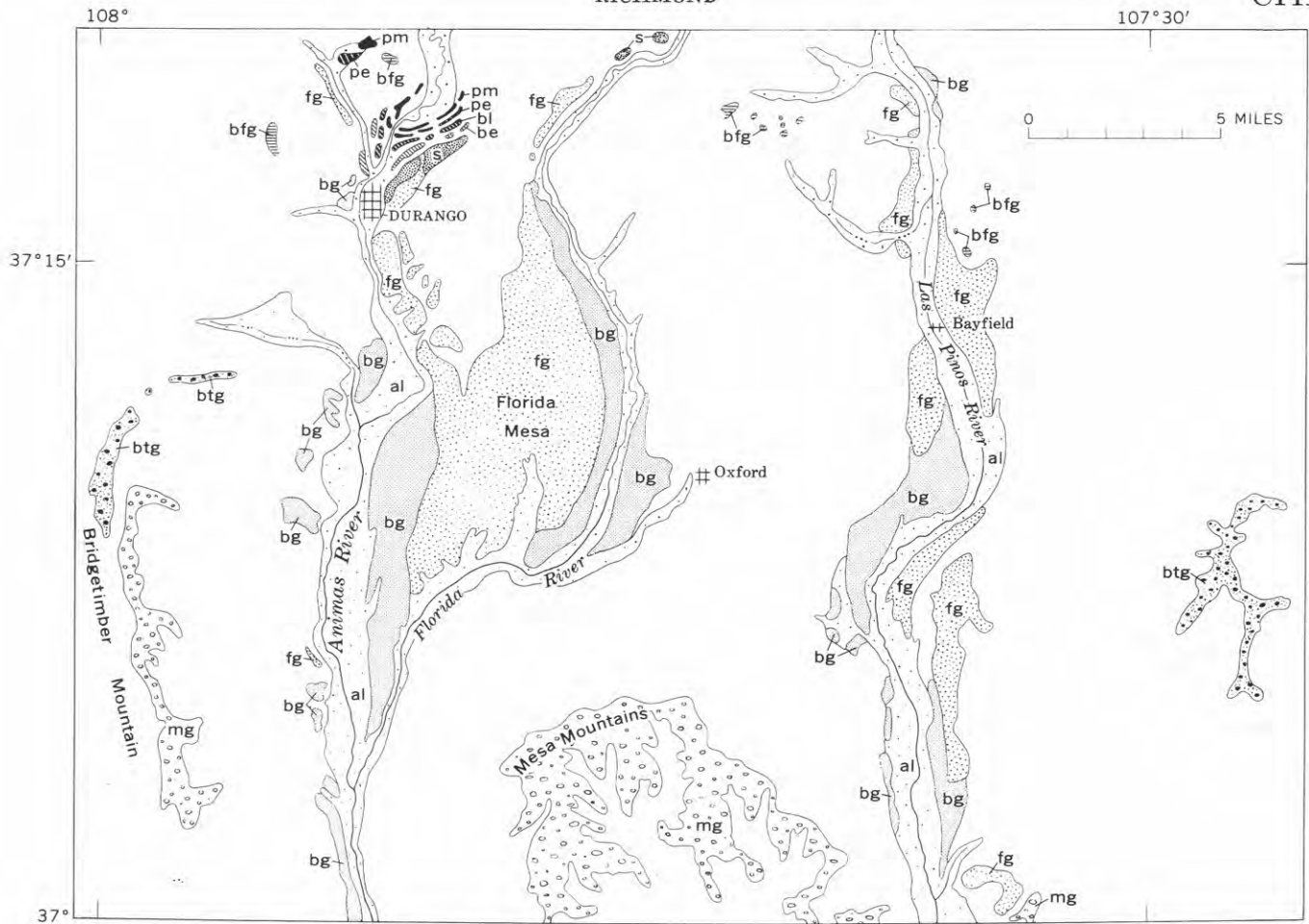
pe and pm—End moraines of early and middle stades of Pinedale Glaciation (Wisconsin stage of Atwood and Mather)
al—Outwash and alluvium of Pinedale and Neoglacial age (Wisconsin and Recent alluvium of Atwood and Mather)
be and bl—End moraines of early and late studies of Bull Lake Glaciation
bg—Outwash of Bull Lake Glaciation (includes some Durango outwash deposits of Atwood and Mather)
s—End moraines of Sacagawea Ridge Glaciation (Durango stage of Atwood and Mather)
g—Florida Gravel—outwash of Sacagawea Ridge Glaciation (considered to be pre-Durango interglacial gravel by Atwood and Mather; includes some Durango outwash deposits of Atwood and Mather)
mg—Gravel on Mesa Mountains—outwash of Cedar Ridge(?) Glaciation (included in Bridgetimber Gravel by Atwood and Mather)
btg—Bridgetimber Gravel—outwash of Washakie Point(?) Glaciation (considered Pliocene(?) in age by Atwood and Mather)
bfg—Bayfield Gravel—in part glacial or fluvioglacial deposits of pre-Sacagawea Ridge age; in part residual pebble gravel weathered from conglomerate in Animas Formation (considered Pliocene(?) in age by Atwood and Mather)

FIGURE 4.—Quaternary deposits of the Durango area, San Juan Mountains, Colo. (modified after Atwood and Mather, 1932).

approximately 2,000 feet above the Animas River. Mapped as a single unit by Atwood and Mather, the deposit rests on 2 distinct erosion surfaces, one 400 feet above the other. The gravel on the lower surface of Bridgetimber Mountain is 20 to 40 feet thick and was derived predominantly from the drainage of the Animas River. The deposits lie at an altitude of about 7,800 feet at the northeast edge of Bridgetimber Mountain and extend continuously southward for about 8 miles, at a gradient of 40 feet per mile, to an altitude of 7,500 feet. Similar deposits cap the Mesa Mountains (fig. 4), on a projection of this gradient 10 miles to the southeast. This gravel is here distinguished separately, though informally, as gravel on the Mesa Mountains. Its lack of sorting and the abundance of boulders and soled and faceted shapes suggest a fluvioglacial origin.

It is correlated tentatively with the Cedar Ridge Glaciation of the Wind River Mountains.

The gravel on the upper surface, to which the term Bridgetimber Gravel will be restricted for purposes of this paper, is 75 to 100 feet thick at the northeast edge of Bridgetimber Mountain but thins rapidly to between 10 and 15 feet in thickness 2 miles to the south along the west edge of the mountain. It consists of pebbles, cobbles, and boulders with an abundant sandy matrix at the north end of the mountain, but with very little fine-grained matrix to the south. Most of the cobbles and boulders are 6 to 18 inches in diameter, but some boulders are as much as 5 feet across. The stones are commonly rounded, but at the north end of the mountain many have a soled and faceted shape. However-no striated stones were found. The material is pre, dominantly of quartzite, but some is diorite, monzonite,

and sandstone derived from the La Plata Mountains to the northwest.

The deposit is thoroughly weathered to a depth of about 10 feet. Crystalline rocks in the weathered zone are mostly rotted and crumbly, and the matrix is clayey. Rock fragments below the weathered zone are fresh and the matrix is sandy. The color of the weathered zone is reddish brown; that of the fresh deposit is grayish brown. Though the evidence is certainly not incontrovertible, the writer considers the marked change in thickness, in abundance of matrix, and in abundance of soled and faceted stones from north to south along the deposit to suggest its origin as outwash along the edge of an upland glacier. These deposits are tentatively correlated with the Washakie Point Glaciation of the Wind River Mountains.

Bayfield Gravel

The Bayfield Gravel of Atwood and Mather (1932, p. 84) includes a variety of deposits. That at the type locality, on "* * * the highest part of Animas City Mountain, 3½ miles north of Durango" (fig. 4), includes abundant cobbles of quartzite and quartz ranging from 4 to 10 inches in diameter. The deposit lies at an altitude of 8,170 feet on a northward projection of the surface of the Mesa Mountains and of the lower surface of Bridgetimber Mountain, and is correlated with the gravel on those surfaces and hence with the Cedar Ridge Glaciation. A similar deposit lies at altitudes between 8,100 and 8,200 feet, 3 miles southwest of Durango.

Deposits of Bayfield Gravel found by Atwood and Mather (1932, p. 85) "* * * in the hogback region between the Animas and Los Pinos Rivers" (fig. 4), at altitudes of about 8,100 feet, are composed of pebbles of quartzite, jasper, quartz, and andesite derived by weathering of local exposures of conglomerate beds in the Animas Formation of Cretaceous and Paleocene age. Deposits of Bayfield Gravel on flat-topped hills east of the Los Pinos River and 3 to 5 miles north of Bayfield (fig. 4) are those from which the term Bayfield Gravel is derived (Atwood and Mather, 1932, p. 85). The writer found only a few widely scattered rounded stones on these hills. Some are pebbles like those in nearby conglomerate in the Animas Formation. Others are cobbles of quartzite, schist, or gneiss, and may have been let down from a sheet of gravel that formerly extended across the area at the level of a projection of the surface of the gravel on the Mesa Mountains. The summits of the hills are at altitudes of 7,550 to 7,800 feet, approximately on this projection.

Still another deposit called Bayfield Gravel by Atwood and Mather caps the southern sector of the flat-topped divide east of the Los Pinos River (shown as Bridgetimber Gravel on fig. 4). This deposit is 20 to 40 feet thick and is composed of cobbles and boulders of quartzite and other rocks derived from the San Juan Mountains to the north. It is deeply weathered like that on Bridgetimber Mountain but is locally cemented at depth by calcium carbonate. The deposit rests on a surface at an altitude of about 8,500 feet, comparable to the upper surface on Bridgetimber Mountain; it appears to be correlative with the Bridgetimber Gravel, and hence with the Washakie Point Glaciation.

OXFORD GRAVEL

Atwood and Mather (1932) defined the Oxford Gravel from deposits in an area between the Los Pinos and Florida Rivers in which the town of Oxford is located (fig. 4). They described the deposits as consisting of a veneer of gravel and widespread silt, intergradational with gravel in a terrace that is intermediate between terraces of Durango (Sacagawea Ridge) and Wisconsin (Pinedale) ages. They considered the Oxford Gravel to be deposits of interglacial origin. The intermediate terrace gravel is mostly of Bull Lake age and of glacial rather than interglacial origin. The Oxford Gravel, upslope from the terraces, is a widespread veneer of cobbles that mantles a much-dissected, irregular terrain having a relief of several hundred feet, and formed by mass wasting from a thick pre-canyon fluvioglacial gravel formerly existing in the vicinity of Oxford, and now preserved on the Mesa Mountains to the south (fig. 4). The gravel veneer extends to elevations as high as a projection of the surface of the Mesa Mountains. As the material is mainly quartzite, it has persisted through several cycles of erosion and was probably let down intermittently from the beginning of dissection of the gravel on the Mesa Mountains to the present by slopewash, creep, and solifluction. The Oxford Gravel is thus a colluvial unit, probably formed under both glacial and interglacial climates, and ranging in age from middle to late Pleistocene. As such it is not stratigraphically significant to subdivision of the Quaternary of the area. It is not shown on table 2. The silt, mapped with the gravel by Atwood and Mather, is mainly of eolian origin and largely of Bull Lake age.

REFERENCES

Atwood, W. W., and Mather, K. F., 1932, Physiography and Quaternary geology of the San Juan Mountains, Colorado: U.S. Geol. Survey Prof. Paper 166, 176 p.

Blackwelder, Eliot, 1915, Post-Cretaceous history of the mountains of central western Wyoming: Jour. Geology, v. 23, p. 97–117, 193–217, 307–340.

Dickinson, R. G., 1965, Landslide origin of the type Cerro Till, southwestern Colorado, in Geological Survey Research 1965: U.S. Geol. Prof. Paper 525–C, p. C147–C151.

Holmes, G. W., and Moss, J. H., 1955, Pleistocene geology of the southwestern Wind River Mountains, Wyoming: Geol. Soc. America Bull., v. 66, p. 629–654.

Moss, J. H., 1951, Early man in the Eden Valley [Wyo.]: Pennsylvania Univ. Mus. Mon. 6, p. 9–92.

Richmond, G. M., 1948, Modification of Blackwelder's sequence of Pleistocene glaciation in the Wind River Mountains, Wyoming [abs.]: Geol. Soc. America Bull., v. 59, p. 1400–1401.

———— 1954, Modification of the glacial chronology of the San Juan Mountains, Colorado: Science, v. 119, p. 177.

———— 1962, Three pre-Bull Lake tills in the Wind River Mountains, Wyoming: Art. 59 *in* U.S. Geol. Survey Prof. Paper 450–D, p. D132–D136.

———— 1964, Three pre-Bull Lake tills in the Wind River Mountains, Wyoming—a reinterpretation, *in* Geological Survey Research 1964: U.S. Geol. Survey Prof. Paper 501–D, p. D104–D109.

DISTRIBUTION OF PLEISTOCENE GLACIERS
IN THE WHITE MOUNTAINS OF CALIFORNIA AND NEVADA

By VALMORE C. LaMARCHE, JR., Menlo Park, Calif.

Abstract.—Cirques, U-shaped valleys, moraines, and till provide evidence of Pleistocene glaciation of the semiarid White Mountains. Only eastward-draining canyons were glaciated. Cirques developed on the lee side of broad summit uplands in areas where drifting snow could accumulate.

Recent ground and air reconnaissance of the White Mountains of eastern California and adjacent Nevada provides evidence of Pleistocene valley glaciation on the east side of the range. Evidence of glaciation was noted briefly by Blackwelder (1934) and by Anderson (1937); the physiographic effects of the glaciers were discussed by Beaty,[1] and Hall [2] has mapped some of the glacial deposits. However, no general description of the glacial geology has been published, even though the White Mountains rank among the highest and most extensively glaciated ranges in the Great Basin.

The White Mountains consist of a linear north-trending fault block of granitic and metamorphic rocks, locally veneered by thin basalt flows, that has been elevated and tilted eastward since late Tertiary time (Knopf, 1918). A rolling upland surface along the crest of the range is 8,000 feet above the flanking desert basins. The crest maintains an average altitude greater than 12,000 feet for a distance of 25 miles, reaching 14,246 feet at White Mountain Peak. Because it is in the precipitation shadow of the Sierra Nevada, 30 miles to the west, the range has a relatively dry climate. The mean annual precipitation at 12,500 feet is only 15.5 inches (Pace [3]).

Despite their general aridity the White Mountains underwent at least one Pleistocene glaciation. Glacially sculptured topography and associated surficial deposits show that several eastward-draining canyons were occupied by small glaciers (fig. 1). Cirques are located east of the crest, from Boundary Peak on the north to Sheep Mountain on the south. Their floors range in altitude from 11,200 feet to 12,500 feet, and many contain tarns and small moraines. Perennial snowbanks and small stratified ice masses cling to the walls of the highest cirques, but there are no glaciers. U-shaped valleys extend eastward from cirques along the crest of the range. Deposits of till as thick as 400 feet make up broad, arcuate steps on the valley floors. On the north fork of Chiatovich Creek there are 3 distinct terminal or recessional moraines which have been deeply incised by axial stream channels; the end moraine farthest downstream is about 4 miles from the cirques. Along the north fork of Cottonwood Creek paired lateral moraines lie 300 feet above the stream; the till, resting on metamorphosed dolomite, contains boulders of granite and metamorphic rocks exposed near the crest of the range.

There is some evidence of an extensive early ice advance that is not represented by easily recognizable moraines. The canyons of Middle Creek, Chiatovich Creek, and Indian Creek, near the northern end of the White Mountains, retain their U-shaped cross profiles to the eastern front of the range. If the valley forms are due to an early glaciation, they indicate that the ice moved 6 to 8 miles down the canyons from the cirques, or nearly twice as far as the later maximum advance. Any early ice advance must have been much less extensive to the south, however. The lower canyons of the north and south forks of McAfee Creek were evidently not glaciated, for they narrow abruptly, at an altitude of about 8,500 feet, 2 to 3 miles from the cirques. If there were early glaciers, their limited downcanyon penetration probably was due to the lower altitude and lesser snows of the southern crest of the range.

[1] C. B. Beaty, 1960, Gradational processes in the White Mountains of California and Nevada: California Univ., Berkeley, Calif., Ph. D. thesis.

[2] M. L. Hall, 1964, Intrusive truncation of the Precambrian-Cambrian succession in the White Mountains, California: California Univ., Berkeley, Calif., M. A. Thesis.

[3] Nello Pace, 1963, Climatological data summary for the decade 1 January, 1953 through 31 December, 1962 from the Crooked Creek Laboratory and the Barcroft Laboratory: California Univ. White Mountain Research Sta., Berkeley, Calif. [Duplicated report].
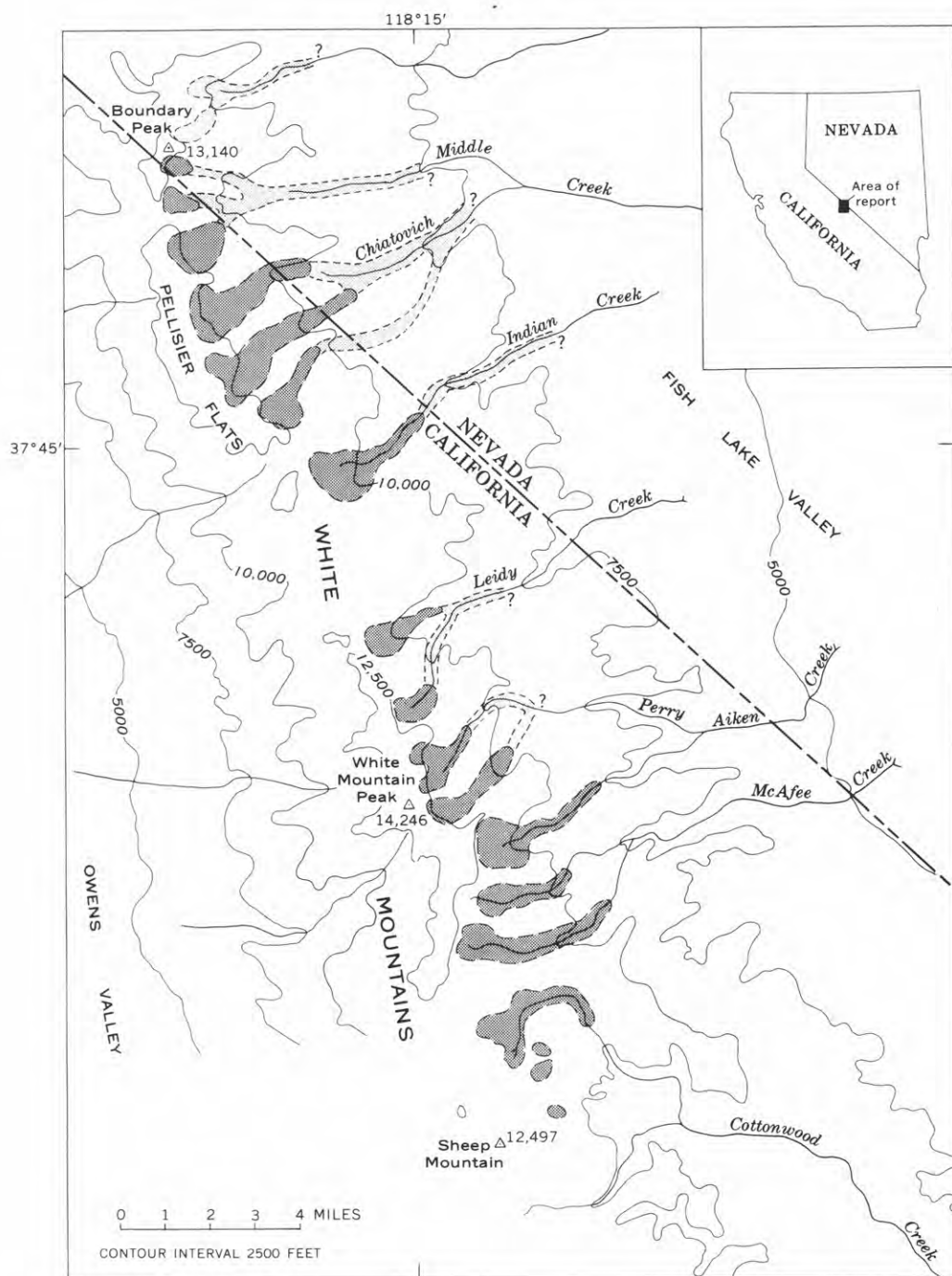
FIGURE 1.—Glaciated areas (darker pattern) in the White Mountains. Lighter pattern indicates areas of possible glaciation.

FIGURE 2.—View south from Pellisier Flats toward White Mountain Peak. Note snowbank at head of cirque in foreground and subdued topography along crest of range north of peak.

Although only the higher areas in the White Mountains supported valley glaciers, the size and distribution of the glaciers were related to other topographic factors. For example, (1) there is no evidence of cirque development on the west side of the range. (2) To the north,

the largest glaciers were fed from cirques along the eastern edge of Pellisier Flats (fig. 2), a broad plateau on the range, but the equally high narrow crest of nearby Boundary Peak had only small cirque glaciers. (3) Near the southern limit of glacial activity the broad summit upland slopes to the east. Along its western margin are 2 unglaciated ridges that rise to an altitude of about 12,500 feet. On the abrupt eastern edge of the upland, 2 miles distant and 1,000 to 1,500 feet lower, were 3 small glaciers.

Pleistocene glaciers in the semiarid White Mountains thus seem to have been related to cirques that developed in the lee of rolling crestal areas over a large range of altitudes. The unprotected summit flats were the sources of snow that drifted to sheltered slopes along the eastern side of the crest.

REFERENCES

Anderson, G. H., 1937, Granitization, albitization and related phenomena in the northern Inyo Range of California-Nevada: Geol. Soc. America Bull., v. 48, p. 1–74.

Blackwelder, Elliot, 1934, Supplementary notes on Pleistocene glaciation in the Great Basin: Wash. Acad. Sci. Jour., v. 24, p. 217–222.

Knopf, Adolph, 1918, A geological reconnaissance of the Inyo Range and the eastern slope of the southern Sierra Nevada, with a section on the stratigraphy of the Inyo Range, by Edwin Kirk: U.S. Geol. Survey Prof. Paper 110, 130 p.

LANDSLIDE ORIGIN OF THE TYPE CERRO TILL, SOUTHWESTERN COLORADO

By ROBERT G. DICKINSON, Denver, Colo.

Abstract.—Geologic study of the hummocky and bouldery surficial debris comprising the type Cerro Till indicates that the material was deposited by mass-wasting processes, primarily landsliding, instead of by a piedmont glacier. The name Cerro Till is abandoned because till does not occur in the type area.

Bouldery material in hummocky surficial deposits at Cerro Summit (fig. 1), traversed by U.S. Highway 50 about 15 miles east of Montrose, Colo., was named the Cerro Till by Atwood (1915). Geologic study by the writer indicates that the materials in these and similar deposits to the south along the west flank of Cimarron Ridge, also mapped as Cerro Till by Atwood and Mather (1932), are mass-wasting debris formed primarily by landsliding. The name Cerro Till is here abandoned because till does not occur in the type area. This does not imply that all the material previously mapped as Cerro Till in the area of the San Juan Mountains is not till. Each deposit should be reevaluated on the basis of its local geologic setting, and appropriate new names should be established.

GEOGRAPHIC AND GEOLOGIC SETTING

Cerro Summit, altitude about 7,950 feet, is on the divide between the Uncompahgre River and Cimarron Creek, a tributary of the Gunnison River. Bedrock of the area is mostly Upper Cretaceous Mancos Shale. Locally, in the area south of Cerro Summit and west of Cimarron Ridge, the Mancos Shale is overlain by poorly consolidated sandstone and shale of the Upper Cretaceous Pictured Cliffs Sandstone and of the Fruitland and Kirtland Shale Formation (the Mesaverde Formation of Atwood and Mather, 1932, p. 102). Cimarron Ridge consists of Late Cretaceous and Tertiary volcanic conglomerates and tuff breccias locally capped by welded tuffs of the Tertiary Potosi Volcanic Group. Most of these units are extremely susceptible to landsliding because they are poorly
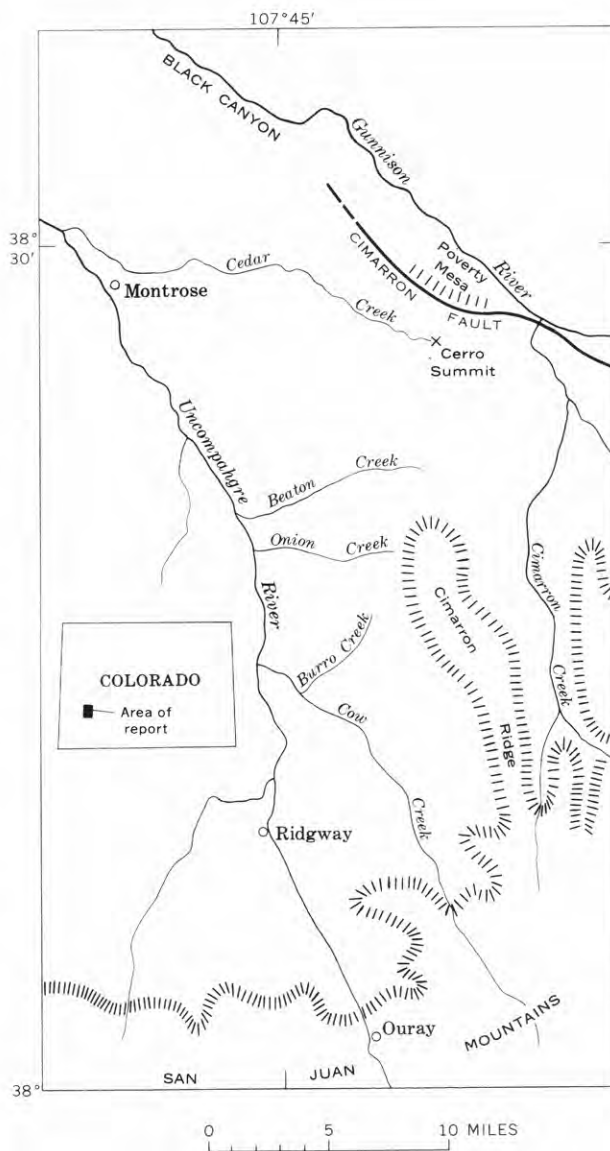
FIGURE 1.—Index map of the Cerro Summit area, southwestern Colorado.

consolidated and contain abundant argillaceous material.

About 1½ miles north of Cerro Summit, Precambrian metamorphic rocks are exposed in high south-facing cliffs along a fault-line scarp that marks the position of the Laramide Cimarron fault. This escarpment forms the southern boundary of Poverty Mesa (Vernal Mesa on the map of Atwood and Mather, 1932, pl. 1). The mesa surface is an exhumed late Paleozoic and early Mesozoic peneplain cut on Precambrian rocks. Small patches of Jurassic rocks and Tertiary conglomerate, tuff breccia, and welded tuff are present on Poverty Mesa.

The debris covering the hill slopes at Cerro Summit was first described as till by Hills (1884, p. 42). Atwood (1915, p. 14), established the type area of the Cerro Till at Cerro Summit. Later, Atwood and Mather (1932, p. 102) described the debris at Cerro Summit as a "heterogeneous mixture of various materials ranging in size from the finest rock flour to boulders 25 feet in length—a typical glacial till." The Cerro Till, as mapped by Atwood and Mather (1932, pl. 1), covers a large semicontinuous area from Poverty Mesa southward for about 20 miles along the west flank of Cimarron Ridge. Several small areas which were also mapped as Cerro Till occur along the north and west flanks of the San Juan Mountains and east of Pagosa Springs on the southwest flank of the San Juan Mountains.

Since the study by Atwood and Mather (1932), little work has been done on the glacial deposits of the San Juan Mountains. Several workers (Smith, 1936, p. 841; Richmond, 1954, p. 614; Bush and others, 1959, p. 343) have correlated glacial deposits in the San Juan area with the Cerro Till, but no one has attempted to reevaluate the various exposures in light of the revised glacial sequence now recognized in the Rocky Mountain region (Richmond, 1964).

Howe (1909, p. 16) emphasized in his report on the landslides of the San Juan Mountains that older landslides can easily be mistaken for glacial moraine unless the internal character of the deposit can be examined. W. R. Hansen (oral communication, 1961), working in the Black Canyon area just north of Cerro Summit, suspected from a cursory examination that the bouldery debris in the Cerro Summit area is not of glacial origin.

The writer's study has been limited to the area north and west of Cimarron Ridge, including the type area at Cerro Summit. None of the other areas previously mapped as Cerro Till have been investigated.

SURFICIAL DEPOSITS IN THE CERRO SUMMIT AREA

Surficial deposits, chiefly landslide debris, form an almost continuous cover over the bedrock in the area from the Cimarron fault southward to the vicinity of Cow Creek, about 20 miles south of Cerro Summit. Locally, the surficial deposits include alluvium, colluvium, and alluvial-fan gravels, but these materials are not pertinent to this discussion and will not be described here. The landslide origin of most surficial material in the Cerro Summit region is evident from the topography, as shown on aerial photographs (figs. 2 and 3). At Cerro Summit, however, some landslides are not apparent from the topography shown on aerial photographs because the forms have been changed by later weathering and erosion. For example, much of the surface at Cerro Summit is strewn with boulders that weather from the landslide debris, giving the surface an appearance of old glacial moraine.

Deposits whose structural and lithologic features are typical of those in the Cerro Summit area are well exposed in the highway cut at Cerro Summit. This cut, about 55 feet deep, extends through the middle of an elongate hill that joins the irregular sloping surface to the south with the hilly area to the north (fig. 2). The well-exposed material in the western part of the highway cut seems, on casual observation, to be entirely undisturbed Mancos Shale. Careful examination shows, however, that the shale does not have regular bedding and that stringers of crushed shale cut across the bedding in the outcrop.

In the eastern part of the highway cut the deposit consists of bouldery debris in the upper 5 to 10 feet, intermixed bouldery debris and crushed shale in a middle zone, and badly crushed Mancos Shale in the lower part. The bouldery debris in the upper part of the cut has a matrix of sandy clay derived in part from fresh Mancos Shale and in part from weathered bedrock. The boulders, of locally derived types, are mostly rounded porphyritic volcanic and granitic rocks, 6 inches to 2 feet in diameter. Some larger angular boulders, as much as 4 feet in diameter, consist of welded tuff derived from the Potosi Volcanic Group. The wide distribution of large boulders of Potosi welded tuff, which are present throughout the surficial deposits in the Cerro Summit area and locally scattered over a widespread area of the Mancos Shale northeast of Montrose, probably indicates that the original extent of Potosi welded tuff was greater than is shown by present outcrops (W. R. Hansen, written communication, 1964). Most of the other rock types in the bouldery debris occur in the Tertiary conglomerates on Poverty Mesa and in Cimarron Ridge. Poorly defined crude scratches or striations that could be mistaken for glacial striations occur on a few of the smaller rounded boulders. Similar scratches, however, can be found on boulders in undoubted landslide deposits elsewhere in the area. Flint (1947, p. 66)
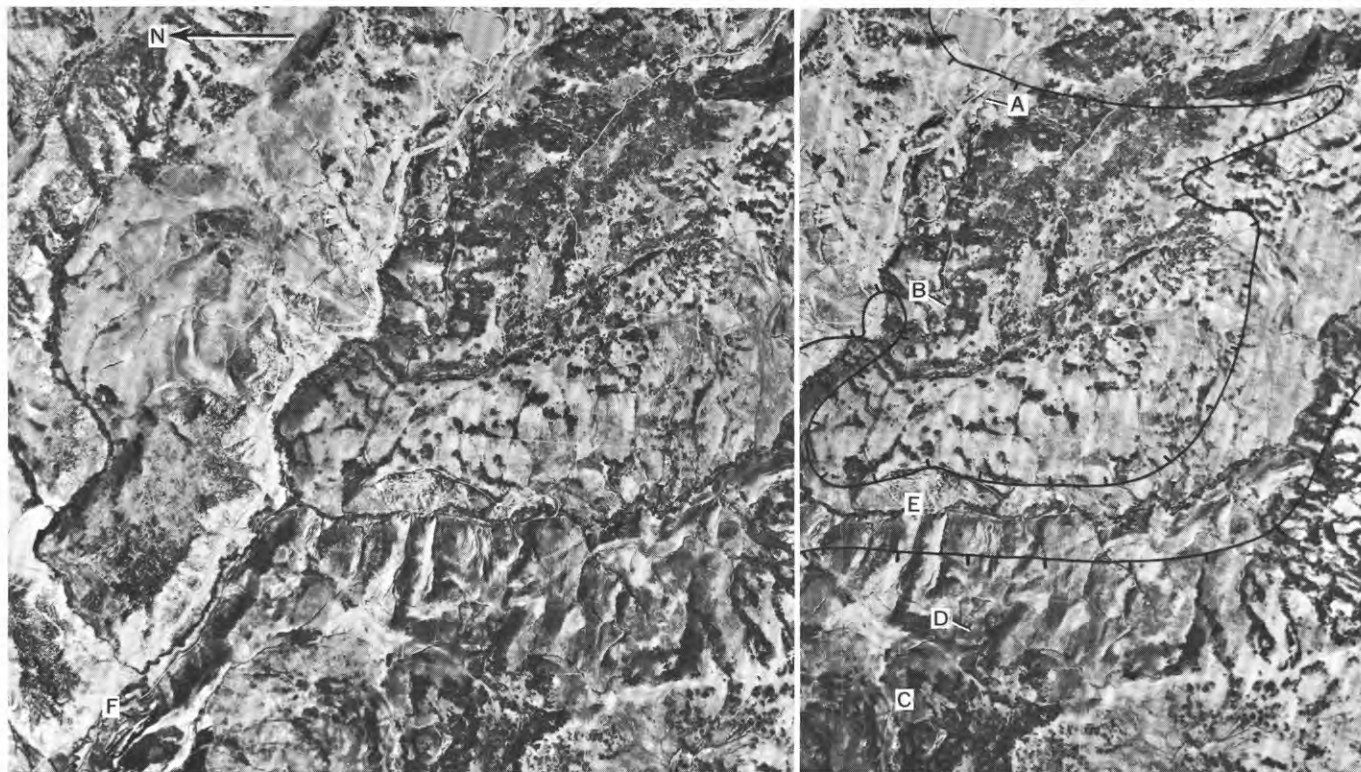
Figure 2.—Stereogram of the Cerro Summit area.   The approximate contact of the Cerro Till as mapped by Atwood and Mather (1932) is marked by the hachured line.   The supposed till is on the hachure side.   *A*, Cerro Summit; *B*, landslide scarps along the abandoned Denver and Rio Grande Western Railroad; *C*, landslide scarps on hillside; *D*, superposed younger landslide debris; *E*, younger landslide scarps; and *F* (lower left corner), recent landslides which buried the Denver and Rio Grande Western Railroad in 1942.   (Photographs, U.S. Army Map Service, 137 AV 2059-2060, approximate scale 1 : 60,000.)

concludes that striations on stones can be produced by any heavy mass flowing according to fluid dynamics, and that reasonable evidence of glacial origin must be determined before a striation is interpreted as glacial. The hypothesis that the boulders were transported to Cerro Summit by a glacier (Atwood and Mather, 1932, p. 82) is thus no longer required to explain the character of the surficial materials.

The crushed shale in the lower part of the cut consists of small fragments of shale, mostly less than half an inch in diameter, enclosed in a shale-derived clayey matrix.   A banded flow structure which resembles that formed by creep occurs in the intermixed zone.   Both creep and earthflow produce flow structure in shale, and it is usually difficult to determine the origin of the structure by examination of only the upper part of the deposit.   This flow structure, however, would not have been formed by glacial action.

Locally, on the elongate hill at Cerro Summit and on the hills north of Cedar Creek, the bouldery surficial debris includes angular boulders of pink and white coarse-grained pegmatite which were derived from the cliffs north of the Cimarron fault.   The presence of these Precambrian rocks at Cerro Summit indicates that some of the debris was derived from the north,

rather than entirely from the south as was concluded by Atwood and Mather (1932, p. 82).

The mode of emplacement of the bouldery debris at the top of the highway cut at Cerro Summit is not readily determined from exposures or from topographic expression as shown on aerial photographs (fig. 2). The hill at Cerro Summit is rounded and otherwise expressionless.   The debris covering the hill supports vegetation—consisting mostly of sagebrush, oak bush, and serviceberry—that has a distinctively mottled pattern similar to that on landslide deposits elsewhere in the area.   As exposed in the highway cut, the hill seems to consist mainly of broken and crushed shale with some bouldery material on the surface of the hill. Downcutting is evident in the area and the hill has probably been eroded from landslide debris.   The bouldery debris could be part of the original landslide debris or could have been emplaced by landslide and creep prior to erosion of the hill to its present shape.

The following brief discussion of some nearby landslide deposits is given because Atwood and Mather (1932) interpreted these deposits as till.   Many landslide scarps west of Cerro Summit are evident on aerial photographs.   These scarps and the associated hummocky landslide debris below the scarps occur both on

the upland hillsides (fig. 2, localities *C, D*) and along the valley sides (fig. 2, locs. *B, E, F*). That landsliding has occurred at various times is shown by crosscutting scarps, superposed landslides (fig. 2, loc. *C*), and landslide scarps that are sharper and fresher (fig. 2, loc. *E*) in appearance than others in the area. The landsliding along the valleys occurred after the valleys were cut. Geologic study by the writer in the Bostwick Park area, 5 miles northwest of Cerro Summit, indicates that most of the downcutting along Cedar Creek occurred during post-Bull Lake time.

Most of the surficial deposits west of Cimarron Ridge are compound features that formed by repeated mudflow, earthflow, and slumping movements. Many of these features are evident on figure 3, a stereogram of the Beaton Creek area. A large, hummocky, tongue-shaped lobe of an earthflow deposit occurs in the northwest corner of the stereogram. Slump scarps occur along the ridge south of the earthflow tongue and elsewhere in the area. Mudflows which originated in the headward reach of Onion Creek, in the southwest part of figure 3, overrode older landslide debris for more than 3 miles.

North of Burro Creek, 200 to 300 feet of older, eroded, and dissected landslide debris caps the inter-stream divide. The landslide character of this debris is not evident on aerial photographs. In the SW¼ SW¼ sec. 1, T. 46 N., R. 8 W., New Mexico principal meridian, about 2½ miles above the mouth of Burro Creek, a roadcut about 60 feet below the top of the deposit exposes large masses of sandstone and shale and boulders of conglomerate and breccia, 10 feet or more in diameter, enclosed in a matrix of bouldery mudstone and crushed shale and sandstone. The larger bodies of soft sandstone and shale have been squeezed and drawn into lenticular masses. Slickensides, indicating movement along slip planes within the deposit, are evidence of the landslide origin of the material. This debris is part of an earthflow and mudflow that descended from the east for a distance of several miles.

CONCLUSIONS

Geologic study of the surficial deposits in the Cerro Summit area and to the south along the west flank of Cimarron Ridge indicates that the deposits formed by mass-wasting processes, primarily by landsliding. These surficial deposits cover most of the bedrock but do not form a continuous, blanketlike deposit. The topographic expression of much of the debris is that
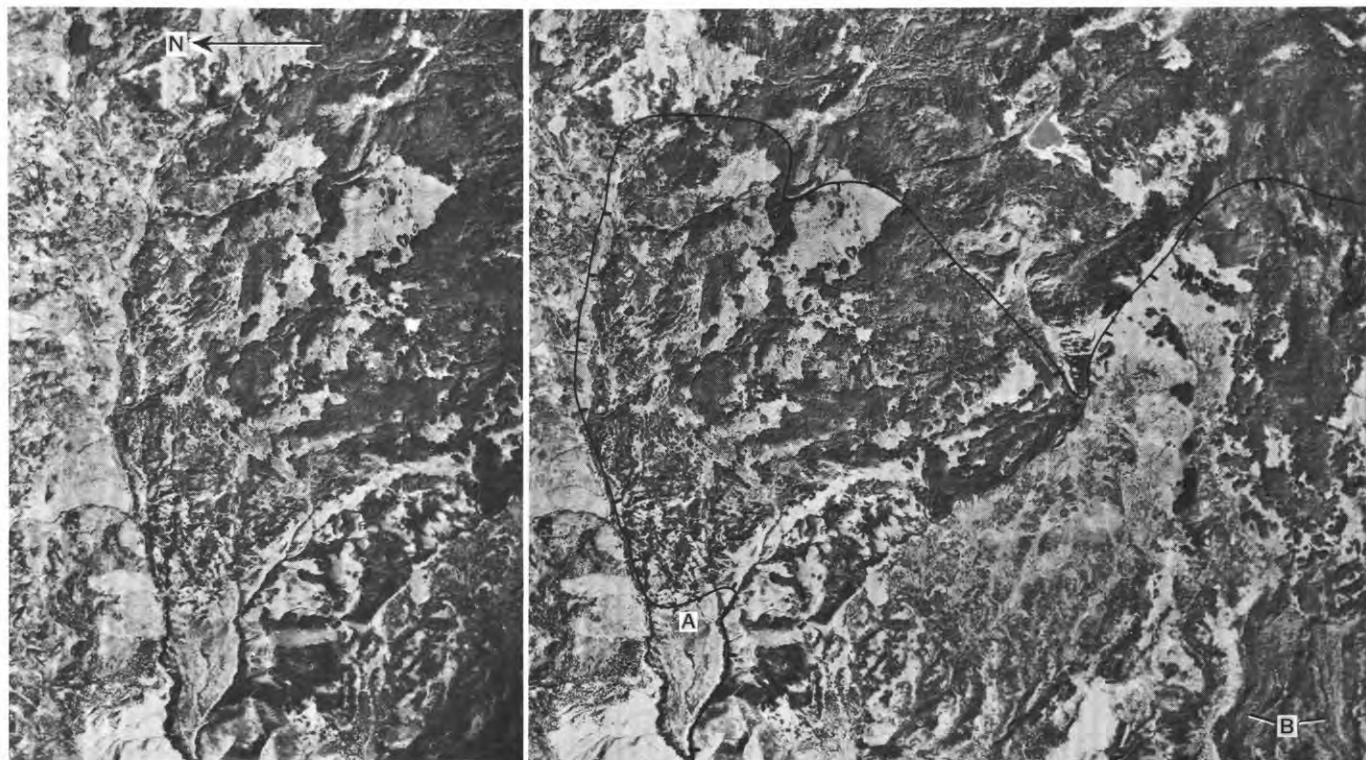
FIGURE 3.—Stereogram showing extensive landslide in the Beaton Creek area. The approximate contact of the Cerro Till as mapped by Atwood and Mather (1932) is marked by the hachured line. The supposed till is on the hachure side. *A* (lower left), contact crosses the toe of a massive earthflow; and *B* (lower right corner), mudflows mapped as till. (Photographs, U.S. Army Map Service, 137 AV 2058-2059, approximate scale 1:60,000.)

characteristic of landslides. Detailed examination of the internal character of some deposits shows the presence of slickensides and crushing, disorientation, or mixing of rock that indicate a landslide origin of the debris. Poorly defined scratches or striations occur on some boulders, but similar scratches can be found on boulders in landslide deposits in the area. In the debris at Cerro Summit the presence of Precambrian pegmatite that is from outcrops about 1½ miles to the north indicates that the debris is locally derived and was not transported into the area from the south. The landsliding occurred at various times and the resulting deposits are, therefore, of different ages.

The surficial deposits in the Cerro Summit area are not till as indicated by Atwood (1915) and Atwood and Mather (1932). Because till does not occur at Cerro Summit, the type area of the Cerro Till (Atwood, 1915), the stratigraphic name is abandoned. New terminology should be established for the older tills in the San Juan Mountains region.

REFERENCES

Atwood, W. W., 1915, Eocene glacial deposits in southwestern Colorado: U.S. Geol. Survey Prof. Paper 95–B, p. 13–26.

Atwood, W. W., and Mather, K. F., 1932, Physiography and Quaternary geology of the San Juan Mountains, Colorado: U.S. Geol. Survey Prof. Paper 166, 176 p.

Bush, A. L., Bromfield, C. S., and Pierson, C. T., 1959, Areal geology of the Placerville quadrangle, San Miguel County, Colorado: U.S. Geol. Survey Bull. 1072–E, p. 299–384.

Flint, R. F., 1947, Glacial geology and the Pleistocene epoch: New York, John Wiley and Sons, Inc., 589 p.

Hills, R. C., 1884, Extinct glaciers of the San Juan Mountains, Colorado: Colorado Sci. Soc. Proc., v. 1, p. 39–46.

Howe, Ernest, 1909, Landslides in the San Juan Mountains, Colorado: U.S. Geol. Survey Prof. Paper 67, 58 p.

Richmond, G. M., 1954, Modification of the glacial chronology of the San Juan Mountains, Colorado: Science, v. 119, no. 3096, p. 614–615.

———— 1964, Three pre-Bull Lake tills in the Wind River Mountains, Wyoming—a reinterpretation, in Geological Survey Research 1964: U.S. Geol. Survey Prof. Paper 501–D, p. D104–D109 [1965].

Smith, H. T. U., 1936, Periglacial landslide topography of Canjilon Divide, Rio Arriba County, New Mexico: Jour. Geology, v. 44, no. 7, p. 836–860.

GEOMORPHIC SIGNIFICANCE OF A CRETACEOUS DEPOSIT IN THE GREAT VALLEY OF SOUTHERN PENNSYLVANIA

By KENNETH L. PIERCE, Flemingsburg, Ky.

Abstract.—A lignitic terrestrial deposit of Late Cretaceous age appears to rest on more than 170 feet of residuum from carbonate rocks. After accumulation, probably in a sink, this deposit may have been lowered hundreds of feet by solution of the underlying carbonate rocks. This lowering of the deposit is consistent with regional rates of erosion and with evidence of lowering of other Appalachian surficial deposits.

Fossil pollen and spores from an unusual surficial deposit in the Great Valley of southern Pennsylvania have been found by Tschudy (1965) to be of Late Cretaceous (probably late Turonian to early Campanian) age. This deposit is the first of Cretaceous age reported from the Valley and Ridge province of the central Appalachians, and it represents one of the few paleontologically dated features of the controversial Mesozoic and Cenozoic history of the region. The term "Pond Bank deposit" is here applied to the pollen-bearing Cretaceous sediment and the materials associated with it. At present only the age, location, and topographic position of this deposit are clearly established. The deposit is part of a thick mantle of surficial materials largely composed of clayey residuum from the weathering of carbonate rocks. The absence of deep exposures prohibits definition of surficial formations. This report presents some possible geomorphic interpretations of the deposit; I hope that it will stimulate further investigation into the character and significance of this and similar Appalachian deposits.

In 1864–65 an iron-mining company sank a 70-foot drainage shaft between two iron-ore pits near Pond Bank, Pa. This shaft, now filled with trash and surficial debris, is reported to have struck about 18 feet of lignite containing discernible fragments of plants. Lesley (1865) discussed the occurrence and published a letter from the mine superintendent, G. B. Weistling, de-scribing it. Using geomorphic arguments, Lesley (1865, p. 480) concluded that the lignite " * * * must be of latest Tertiary age." Stose (1909, p. 12–13, 16–17) later studied the surficial geology of the area; he concluded that the Harrisburg topographic surface and the Pond Bank deposit are of early Tertiary age.

The shaft in which the lignite was found is located on the southeast side of the Great Valley, at the foot of South Mountain (fig. 1). The deposit lies on rather flat terrain near the mouth of English Valley, a small gently-sloping valley bordered by ridges of Lower Cambrian clastic rocks. When I visited the area in 1961 the discovery shaft was filled in, so that only the mine dump was available for sampling. No lignite similar to that described by Weistling was found; perhaps this material has weathered or was burned for fuel. The pollen-bearing material obtained from the mine dump is a black carbonaceous clay containing about 80 percent silt and clay, 10 percent organic material, and 10 percent quartz sand. Numerous charcoal-like seeds, nuts, and fragments of wood are present in the carbonaceous clay, although none of those collected were preserved well enough to be identified.

GEOLOGIC SETTING OF THE LIGNITIC DEPOSIT

Lignite is reported (Lesley, 1865, p. 481) to have been found between 41 and 64 feet below the surface. At a depth of 64 feet a drift was driven for 48 feet, mainly in lignite but in a light-colored clay near the end. The geomorphic position of the lignite is only a little below the local drainage and at about the same altitude as the larger streams where they leave South Mountain.

As is described on figure 2, the lignite is overlain by locally derived clay, sand, and lumps of iron oxide.
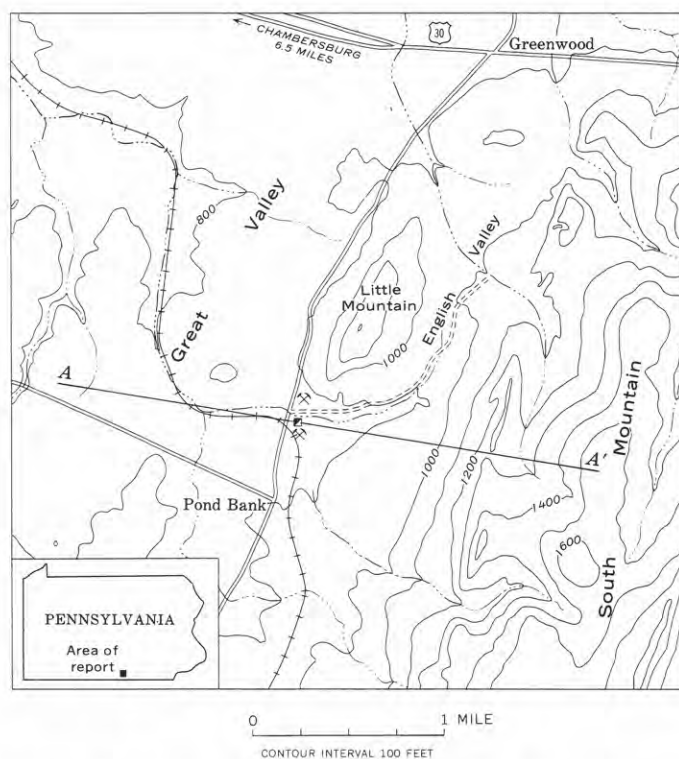
FIGURE 1.—Map showing location of the Pond Bank deposit. Shaft in which lignite was found is shown by half-shaded square in center of figure; Pond Bank pits shown by mine symbols. Map is from east-central part of Chambersburg 15-minute quadrangle. Shaft is located 1,250 feet north of lat 39°52'30" N. and 11,150 feet west of long 77°30' W. Section A–A' is shown on figure 3.

FIGURE 2.—Columnar section from the shaft in which lignite was found at Pond Bank. Section modified from Weistling (*in* Lesley, 1865, p. 480–482).

percentages of insoluble constituents in these units, are given on figure 4.

OTHER LIGNITIC DEPOSITS IN THE APPALACHIAN REGION

Lignitic materials have been reported from several localities in the Appalachians from Nova Scotia to Georgia. The nearest lignitic deposit is at Ironton, Lehigh County, Pa. (Lewis, 1881, p. 283), on the north side of the limestone belt in the Great Valley and 110 miles northeast of Pond Bank. Lignite at Brandon, Vt., is considered by Barghoorn and Spackman (1950,

Materials similar to those described on figure 2 were found in the mine dump.

The lignite is probably underlain by clays residual from Lower Cambrian carbonate rocks. Although the thickness of surficial materials beneath the Pond Bank deposit is not reported, mine descriptions indicate that the materials are at least 170 feet thick and maybe as much as 335 feet.[1] In mines upvalley from the discovery shaft the total thickness of surficial materials is reported to be 110 feet (d'Invilliers, 1887, p. 1432).

The unconsolidated materials beneath the lignitic deposit unconformably overlie nearly horizontal Tomstown Dolomite (figs. 3 and 4). The bedrock units in the vicinity of the lignitic deposit, and estimates of the

FIGURE 3.—Cross section showing present structural location of the Pond Bank deposit (after Stose, 1909). Surficial material indicated by fine stipple; the known lignite is around shaft in surficial materials. Location of cross section is shown on figure 1. €a, Antietam Sandstone; €t, Tomstown Dolomite; €w, Waynesboro Formation; €e, Elbrook Formation. Reconstructed position of Tomstown-Waynesboro and Waynesboro-Elbrook contacts shown by dashed lines.

[1] d'Invilliers (1887, p. 1431) reports that "two sets of levels are driven at Little Pond Bank and the ore stoped from them, the lifts being about 200 feet vertically apart." Carbonate bedrock was found in one of the drifts (Frazer, 1877, p. 250), apparently along the lower level. Air shafts from one of the levels were driven up into the old open cut, which was about 35 feet deep (d'Invilliers, 1887, p. 1431; Lesley, 1892, p. 249). It is not possible to determine which level was immediately below these open cuts. If it was the upper level, the lower level was 300 to 400 feet below the surface (200 feet between levels plus 100 to 200 feet between the first level and the surface). If it was the lower level, then the upper level was probably at the horizon of the ore mined in the open cuts (about 35 feet) and the lower level was 200 feet below at a depth of 235 feet. Thus the lignite appears to overlie at least 171 feet (235 minus 64) and possibly as much as 336 feet (400 minus 64) of surficial materials.

Lithology	Estimated insoluble material (percent)	Estimated thickness of residuum formed by insoluble material (feet)	Description and thickness
	10 to 15	300 to 450	Elbrook Formation (3000 feet). Light-gray shaly limestone and calcareous shale with a few thick limestone beds.
	50 to 70	140 to 200	Waynesboro (Rome) Formation (1000 feet). Slabby sandstone, hard sandy purple shale; limestone in middle of formation.
	5 to 15	20 to 80	
	20 to 30	40 to 60	
	8 to 15[1]	70 to 140 (for upper 900 ft)	Tomstown (Shady) Dolomite (1000 feet). Massive and thin- bedded dolostone with thin shaly interbeds.
	90	- -	Basal Cambrian clastic rocks (6000 feet). Antietam, Harpers, and Weverton Formations.

[1] In northern Virginia the Tomstown Dolomite contains an average of 10 percent or more of insoluble material (King, 1943, p. 20).

FIGURE 4.—Columnar section of Cambrian rocks in the vicinity of the Pond Bank deposit (after Stose, 1909). Percentages of insoluble constituents estimated on the basis of analyses of similar carbonate rocks. Present position of Pond Bank lignitic deposit, relative to stratigraphic column of bedrock, is indicated by black dot, and other surficial materials by crosshatching.

p. 346) to be of early Tertiary age. Lignite near Shubenacadie, Nova Scotia, 800 miles northeast of Pond Bank, is of Early Cretaceous age (Stevenson, 1959, p. 34; Stevenson and McGregor, 1963). South of Pond Bank, surficial lignite is reported in northeastern Tennessee (Bridge, 1950, p. 193; King and Ferguson, 1960, p. 91); and in the Valley and Ridge province 600 miles south of Pond Bank, leaf prints from lignitic material associated with the Georgia and Alabama bauxite deposits were considered by R. W. Brown to be of Cretaceous or early Tertiary age (oral communication *in* Bridge, 1950, p. 194; see also Cloud and Brown, 1944). Lignite is also present in the Cretaceous coastal-plain deposits, including those about 100 miles east of Pond Bank in Maryland, New Jersey, and southeastern Pennsylvania.

All Appalachian lignitic accumulations and associated deposits either overlie carbonate bedrock (or, in Nova Scotia, sulfate bedrock) or they lie at the stratigraphic position of the base of soluble rock already removed by solution. They also occur on the valley floors at the inferred position of the classical Harrisburg topographic surface, and are commonly associated with surficial deposits of iron oxide, manganese, and bauxite. Many

of these occurrences of lignite have been regarded as indicative of the age of the topographic "surface" with which they are associated. Bridge (1950, p. 197), for instance, considers the Harrisburg surface or valley-floor peneplain and associated surficial deposits to be of the same age as the unconformity between the Paleocene Midway Group and the Eocene Wilcox Group of the Atlantic and Gulf Coastal Plains. As is discussed below, the assumption that the lignitic deposits date the topographic "surface" on which they rest may not be justified, for it appears possible or even likely that deposits such as that at Pond Bank have been lowered hundreds of feet as a consequence of solution of the underlying bedrock.

GEOMORPHIC SIGNIFICANCE OF THE POND BANK DEPOSIT

Near Pond Bank, during Late Cretaceous time, plant remains accumulated and were preserved in a wet depression. The presence of numerous specimens of the fern genus *Azolla* in the lignite is believed to indicate deposition in a lake, pond, or fresh-water swamp, because all modern species of this genus are confined to such environments (R. H. Tschudy, written communication, 1964). The depression containing the body of water is thought to have been a sink, for carbonate rocks underlie the area. This watery area was surrounded by forest, as is indicated by wood, conifer and angiosperm pollen, and fern spores in the lignitic sediment. No marine fossils were noted in the Pond Bank pollen and spore assemblage, and in particular no marine hystrichospheres or dinoflagellates such as are commonly found in marine, nearshore polleniferous deposits (R. H. Tschudy, written communication, 1964). Thus the Pond Bank deposit accumulated in a nonmarine environment.

This terrestrial deposit demonstrates subaerial exposure of the Great Valley during part of Late Cretaceous time, and therefore indicates a subaerial environment for the higher and more landward part of the Valley and Ridge province to the west. It does not support the hypothesis of marine deposits in a Cretaceous coastal-plain cover over the Valley and Ridge province (Johnson, 1931) during the interval of Pond Bank deposition. If marine deposits accumulated during Late Cretaceous time, and even during Early Cretaceous time, it seems likely that such deposits should be present at least locally in the Valley and Ridge province because terrestrial deposits of similar antiquity are preserved at numerous localities. Except where the Gulf Coastal Plain overlaps the southern Appalachians, no marine Cretaceous rocks have been found in the Valley and Ridge province. Nonmarine deposits in the western part of a coastal-plain cover (Johnson,

1931, p. 49–50) might have been preserved during lowering of the land surface. Thus, if the Pond Bank deposit has been lowered by more than 1,500 feet, it conceivably represents the nonmarine portion of the coastal-plain cover postulated by Johnson.

The original elevation of the Pond Bank deposit relative to the present topography is uncertain, and it is possible that the deposit was lowered considerably during solution of the underlying carbonate rocks. Such topographic lowering of other Appalachian surficial deposits is indicated by evidence from the following four localities: (1) White and Denson (1952, p. 8) suggest an average lowering in excess of 150 feet for the northwestern Georgia bauxite deposits. Their conclusion is based on the present vertical distribution of the deposits and Bridge's (1950, p. 195) hypothesis that streams flowing from crystalline rocks carried the bauxite to the sites of deposition. (2) In northeastern Tennessee, King and Ferguson (1960, p. 91 and fig. 24) describe nearly vertical streaks of lignite along the margin of a surficial bauxite deposit. Considerable deformation, probably by slumping resulting from solution of the underlying carbonate rocks, is indicated by the tilted and smeared lignite beds, and by the "disrupted lignitized wood" and "macerated carbonaceous material" in the beds. (3) Across the Great Valley from Pond Bank, accumulations of weathered gravel are marked by sinks and ridges with a local relief of more than 30 feet, indicating at least an equal amount of differential solution of the underlying carbonate rocks after deposition of the gravel.[2] (4) Accumulations of residuum 100 to 250 feet thick have been noted mantling carbonate rocks in Virginia and Tennessee (King, 1950, p. 55 and fig. 16; King and Ferguson, 1960, p. 50–51; Rodgers, 1948, fig. 3). On a gentle slope, formation of a thickness of 100 feet of such residuum derived from carbonate rocks having 10 percent insoluble material requires that the uppermost and oldest part of the residuum be lowered by 900 feet.

An estimate of the possible amount of lowering of the Pond Bank deposit can be made on the basis of the following assumptions: (1) that there is at least 170 feet of residuum beneath the lignite (see footnote 1) and that nearly all of this residuum formed after deposition of the Pond Bank deposit, (2) that the minimum amount of insoluble material in the bedrock is as shown on figure 4, and (3) that the Pond Bank deposit and residuum now lie about 100 feet above the base of nearly horizontal Tomstown Dolomite (fig. 3). If the Pond Bank deposit originally accumulated on top of the middle unit of the Waynesboro Formation (fig. 4), about 1,600 feet vertically above the present

contact between the residuum and bedrock, a residuum estimated to be a minimum of 140 feet thick could have been formed by solution of the intervening rocks (figs. 3 and 4), and in the process the deposit would have been lowered by more than 1,400 feet. If this amount of lowering has taken place, then the Late Cretaceous position of the deposit was several hundred feet above the highest mountains now present in the area. The thickness of the post-Pond Bank residuum may be considerably greater than 140 feet (see footnote 1), and thus lowering may have been considerably greater than 1,400 feet.

Estimates of the average amount of material eroded from the Appalachians since the Pond Bank deposit accumulated, about 85 million years ago (numerical age estimated from Kulp, 1961, fig. 1), can be obtained from the volume of coastal-plain and ocean-floor sediments, or, with much less reliability, from the modern rate of erosion of the Appalachians. According to Menard (1961, p. 155) an average of about 25,000 feet of rock has been eroded from the Appalachians since early Cretaceous time (125 million years ago); on the basis of a constant rate of erosion, this indicates an average of more than 15,000 feet of erosion since Pond Bank time. On the basis of dissolved load in a stream draining the Nittany arch, Ewing (1885) calculated the modern rate of solution of carbonate rock to be 1 foot in 9,000 years; an extrapolation of this rate indicates about 9,000 feet of erosion since Pond Bank time. A compilation by Gilluly (1964, p. 486) indicates that the modern rate of total erosion in the northern Appalachians is 0.86 inch per 1,000 years; an extrapolation of this rate indicates about 6,000 feet of erosion since Pond Bank time. In another study by Judson and Ritter (1964, p. 3399) the computed rate of regional denudation in the North Atlantic region of the United States is 1.9 inches per 1,000 years. This rate, by extrapolation, suggests that more than 13,000 feet of erosion may have occurred since Pond Bank time. In summary, all these estimates indicate an average erosion of the Appalachians of at least several thousand feet since Pond Bank time.

On the other hand, if no lowering of the Pond Bank deposit has occurred, little solution of the underlying carbonate rocks can have taken place and the deposit must initially have been laid down on the surficial material it now overlies. If this be true, the deposit accumulated on the valley-floor "partial peneplain" and the major features of the present topography are relics of Late Cretaceous time. Under conditions similar to those in a nearby Appalachian basin studied by Hack (1960), the surface and ground waters that flow by Pond Bank from the forested quartzitic terrain of South Mountain and Little Mountain are probably

---

[2] K. L. Pierce, 1964, Bedrock and surficial geology of the McConnellsburg quadrangle: Yale Univ., Ph. D. thesis, p. 135.

rather acid. It is quite unlikely that, throughout the last 85 million years, these acidic ground and surface waters have not dissolved enough carbonate rock to cause some lowering of the Pond Bank deposit. As was discussed earlier in this paper, deformed sheets of weathered gravel along the western side of the Great Valley indicate solutional lowering by at least several tens of feet. At least an equal amount of lowering should have affected the Pond Bank deposit, for it lies at the foot of the mountains in a topographic position similar to that of the weathered gravel accumulations and probably is fully as old.

REFERENCES

Barghoorn, E. S., and Spackman, William, 1950, Geological and botanical study of the Brandon lignite and its significance in coal petrology: Econ. Geology, v. 45, p. 344–357.

Bridge, Josiah, 1950, Bauxite deposits of the southeastern United States, in F. G. Snyder (ed.), Symposium on the mineral resources of the southeastern United States: Knoxville, Univ. Tennessee Press, p. 170–201.

Cloud, P. E., Jr., and Brown, R. W., 1944, Early Cenozoic sediments in the Appalachian region (Alabama and Georgia) [abs.]: Geol. Soc. America Bull., v. 55, p. 1466.

d'Invilliers, E. V., 1887, Report on the iron ore mines and limestone quarries of the Cumberland-Lebanon Valley: Pennsylvania Geol. Survey 2d, Ann. Rept. 1886, pt. IV, p. 1409–1567.

Ewing, A. L., 1885, An attempt to determine the amount and rate of chemical erosion taking place in the limestone (Calciferous to Trenton) valley of Center County, Pa., and hence applicable to similar regions throughout the Appalachian region: Am. Jour. Sci., 3d ser. v. 29, p. 29–31.

Frazer, Persifor, Jr., 1877, Report of progress in the counties of York, Adams, Cumberland, and Franklin: Pennsylvania Geol. Survey 2d, C–2, p. 201–400.

Gilluly, James, 1964, Atlantic sediments, erosion rates, and evolution of the continental shelf; some speculations: Geol. Soc. America Bull., v. 75, 483–492.

Hack, J. T., 1960, Relation of solution features to chemical character of water in the Shenandoah Valley, Virginia:

Art. 179 in U.S. Geol. Survey Prof. Paper 400–B, p. B387–B390.

Johnson, D. W., 1931, Stream sculpture on the Atlantic slope, a study in the evolution of Appalachian rivers: New York, Columbia Univ. Press, 142 p.

Judson, Sheldon, and Ritter, D. F., 1964, Rates of regional denudation in the United States: Jour. Geophys. Research, v. 69, no. 16, p. 3395–3401.

King, P. B., 1943, Manganese deposits of the Elkton area, Virginia: U.S. Geol. Survey Bull. 940–B, p. 15–55.

——— 1950, Geology of the Elkton area, Virginia; U.S. Geol. Survey Prof. Paper 230, 82 p.

King, P. B., and Ferguson, H. W., 1960, Geology of northeasternmost Tennessee: U.S. Geol. Survey Prof. Paper 311, 136 p.

Kulp, J. L., 1961, Geologic time scale: Science, v. 133, p. 1105–1114.

Lesley, J. P., 1865, On the recent discovery of lignite in Pennsylvania: Am. Philos. Soc., Proc. 9, p. 463–482.

——— 1892, A summary description of the geology of Pennsylvania: Pennsylvania Geol. Survey 2d, Final Rept. v. 1, p. 1–719.

Lewis, H. C., 1881, The iron ores and lignite of the Montgomery County Valley: Acad. Nat. Sci. Philadelphia, Proc. 32, p. 282–291.

Menard, H. W., 1961, Some rates of regional erosion: Jour. Geology, v. 69, p. 154–161.

Rodgers, John, 1948, Geology and mineral deposits of Bumpass Cove, Unicoi and Washington Counties, Tenn.: Tennessee Div. Geology Bull. 54, 82 p.

Stevenson, I. M., 1959, Shubenacadie and Kennetcook map-areas, Colchester, Hants, and Halifax Counties, Nova Scotia: Geol. Survey Canada Mem. 302, 88 p.

Stevenson, I. M., and McGregor, D. C., 1963, Cretaceous sediments in central Nova Scotia, Canada: Geol. Soc. America Bull., v. 74, p. 355–356.

Stose, G. W., 1909, Mercersburg-Chambersburg, Pa.: U.S. Geol. Survey Geol. Atlas, Folio 170, 19 p.

Tschudy, R. H., 1965, An Upper Cretaceous deposit in the Appalachian Mountains, in Geological Survey Research 1965: U.S. Geol. Survey Prof. Paper 525–B, p. B64–B68.

White, W. S., and Denson, N. M., 1952, The bauxite deposits of Floyd, Bartow, and Polk Counties, northwest Georgia: U.S. Geol. Survey Circ. 193, 27 p.

SOME POTENTIAL MINERAL RESOURCES OF THE ATLANTIC CONTINENTAL MARGIN [1]

By K. O. EMERY, Woods Hole, Mass.

Abstract.—Preliminary findings from a current geological investigation indicate that the continental shelf and the upper part of the continental slope off the Atlantic coast of the United States may be the site of large deposits of construction sand, phosphorite, manganese oxide, and petroleum. The sand covers most of the continental shelf, the phosphorite occurs near the top of the continental slope and its southward extension inshore of the Blake Plateau, and manganese nodules are common on the Blake Plateau. Petroleum source beds and structures appear to be most favorable along (1) a seaward extension of the Cape Fear Arch, (2) the outer part of the continental shelf from south of Boston northeastward probably to the Grand Banks of Newfoundland, and (3) a probable fault zone southeast of New York City.

A broad regional study of the geology of the continental shelf and slope off the Atlantic coast of the United States was begun in late 1962 as a joint program of the U.S. Geological Survey and the Woods Hole Oceanographic Institution (Emery and Schlee, 1963). The study includes investigations of topography, sediments, lithology, and geological structure. By the end of 1964 a topographic compilation was completed, with a series of four general charts and many more-detailed small ones (Uchupi, 1965; R. M. Pratt, report in preparation). General sampling of the sea floor also was nearly finished, with about 1,800 large surface samples from an 18-kilometer grid that extends from shore to depths as great as 4,000 meters. In addition, about 8,000 km of continuous seismic profiles were run at 50- to 100-km spacing. Preliminary examination of the results permits the outlining of the shallower portions of the region that are most likely to contain mineral deposits of economic value (fig. 1). Additional detailed dredging and study of geological and geophysical data should narrow the areas of maximum interest and possibly reveal additional areas not shown by figure 1.

SAND AND GRAVEL

The most widespread resource to be exploited from the surface of the continental shelf is probably sand and gravel for construction use as concrete aggregate, road material, and material for beach widening. As shown by D'Amico (1964), the value of sand and gravel quarried on land in the United States during 1963 was $849 million, or about 20 percent of the total value of all nonmetallic minerals other than fuels. For sea-floor operations, this relation is apt to be more heavily weighted in favor of sand and gravel because of the wide distribution, great thickness, lack of overburden, and cheap barge transportation of these materials. The samples that have been obtained to date show relict sand to be present throughout most of the length of the continental shelf, extending from an average depth below sea level of about 20 m to a depth of 80 to 140 m near the shelf edge (fig. 1). Thickness of the sand is as much as 60 m. The sand consists mainly of quartz and feldspar, and it is coarser grained than the modern sediment occurring both landward and seaward of it. Sediment on the shelf just north of Miami is highly calcareous and thus is unsuitable for many construction purposes. Surface sediment in the Gulf of Maine (off Boston and Portland, fig. 1) consists chiefly of silty clay and poorly sorted mixtures of clay, silt, sand, and gravel.

The relict nature of the sand on most of the continental shelf is indicated by a grain size coarser than that of sand nearer shore, and by the typical presence of iron stain and solution pits. The relict sand also contains occasional shells of the common edible oyster that normally lives at depths of only a few meters within coastal estuaries and lagoons. Radiocarbon ages obtained for several specimens range from 8,000 to 11,000 years (Merrill and others, 1965). In summary, the relict sand appears to consist of ancient shore deposits
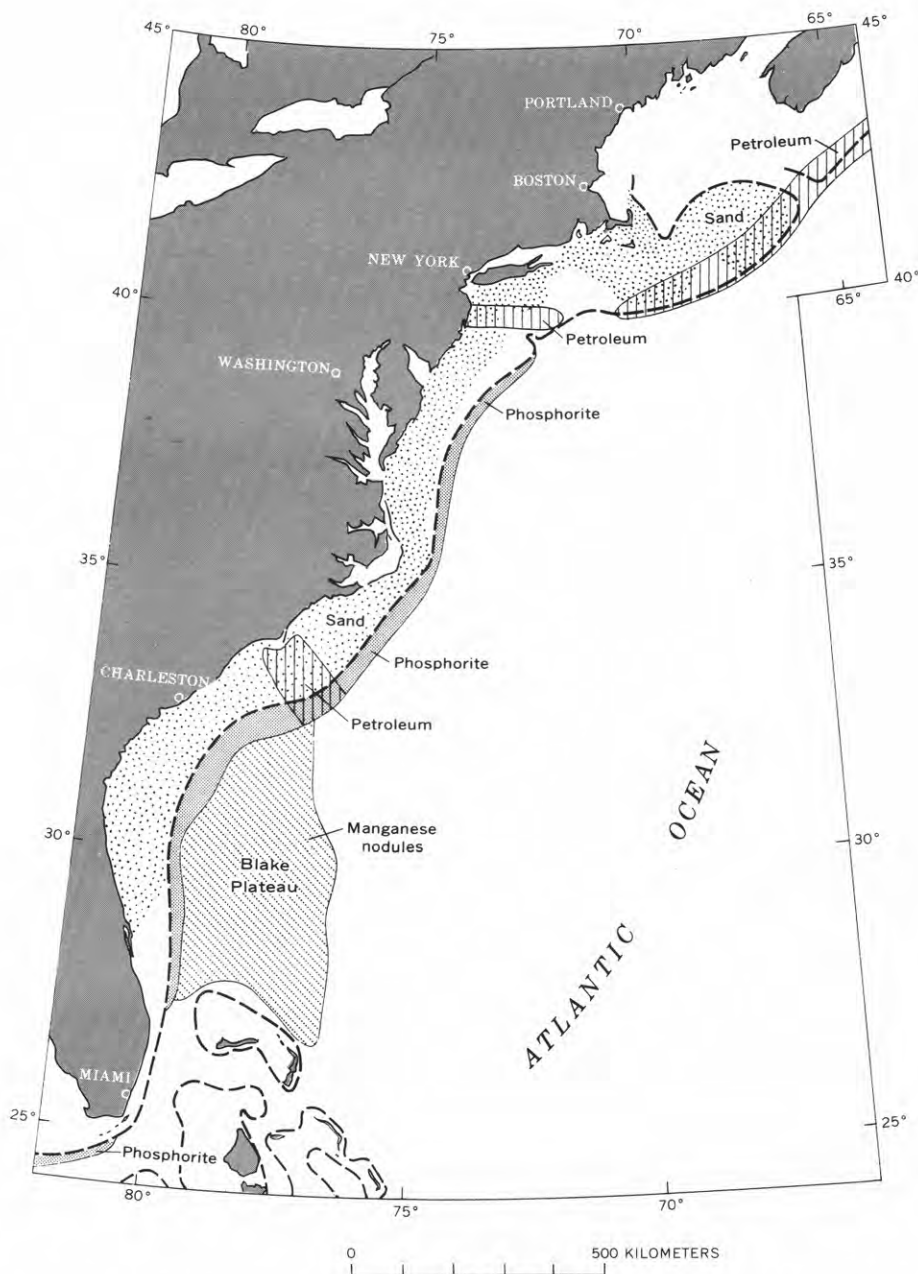
FIGURE 1.—Distribution of the most favorable areas for some potential mineral resources off the Atlantic coast of the United States. The dashed line denotes the position of the edge of the continental shelf, about 80 m deep in the south and about 140 m in the north. The area indicated for manganese nodules corresponds to the surface of the Blake Plateau.

that were formed as the ocean transgressed the continental shelf at the end of the latest glacial epoch. Supporting evidence for that environment of deposition is given by the presence of submerged terraces and beach ridges on the shelf. The independence of the offshore relict sand from the inshore modern sand means that the relict sand probably can be mined without disturbing the shoreline equilibrium.

Gravel is subordinate to sand on the continental shelf, but it may be abundant in two general areas. One of these is a large gravel fan off New York City, where gravel must have been deposited by the Hudson River as a sheet perhaps in a manner similar to that of the widespread gravels on the Atlantic Coastal Plain (Schlee, 1957; 1964). The other area is atop the northern margin of Georges Bank (the shelf projection

southeast of Boston, fig. 1), where residual gravels from glacial till, glacial outwash, and Tertiary strata have been concentrated by the winnowing action of tidal currents.

PHOSPHORITE

Phosphorite nodules occur in many surface samples from beyond the edge of the continental shelf. They appear to be most abundant between depths of about 200 and 500 m on the East Florida Escarpment, a 1° slope that leads downward from the continental shelf to the Blake Plateau (fig. 1). They are present but probably less abundant on the top few hundred meters of the continental slope between the Blake Plateau and the vicinity of New York City, and they are still less common on the continental slope east of New York City. The nodules are brown dense masses as large as 8 cm in diameter, and they have the X-ray and optical characteristics of apatite.

The phosphorite is associated with glauconite. Both materials are authigenic deposits and are typical of shallow sea-floor environments that have a very low rate of accumulation of detrital or biogenic sediments. The area of their maximum concentration is just such an environment. However, there is a strong probability that the phosphorite is residual from weathering and erosion of outcrops of phosphatic strata. On the adjacent land several Miocene and Pliocene formations contain phosphorite that is exploited chiefly for fertilizer. The seaward regional dip should permit these formations to crop out on the slope, if the slope is a fault partly mantled with sediments, as Sheridan and others (1965) indicate is true of the East Florida Escarpment. Topographic irregularities on the slopes also suggest that narrow structural terraces were developed by outcrops of resistant strata (Heezen and others, 1959). The question of quantity and quality of the phosphorite can be determined only by detailed sampling and laboratory analyses. During 1963 the total value of phosphorite mined on land in the United States was only about $140 million (D'Amico, 1964); thus mining of it from the sea floor may be uneconomical.

MANGANESE NODULES

Many samples and bottom photographs (Pratt, 1963) have shown an abundance of nodules and crusts of manganese oxide on the Blake Plateau (fig. 1) between depths of 750 and 1,050 m. The nodules occur in a thin blanket of globigerina and pteropod ooze lying on Pliocene and Miocene limestones. They range in size from sand grains to flat masses nearly a meter in length, but the majority are subspherical nodules 10 to 20 cm in diameter. The encrustations are solid-looking

coatings on the bottom, covering continuous areas of at least 10 sq m, the space depicted by underwater photographs that show them; they are rarely if ever removed by sampling devices.

Analyses reported by Mero (1960, 1962) suggest that the nodules from the Blake Plateau are of low quality for metallurgical purposes as compared with those that have been dredged from the deep-sea floor of the Pacific Ocean. However, it is possible that higher quality nodules occur at the seaward side of the Blake Plateau, which is more distant from diluting detrital sediments. The nearness of the Blake Plateau to ports and its relatively shallow depth may permit this area of the sea floor to be one of the first to be economically exploited for manganese. The total value of manganese of comparable quality mined in the United States during 1961 was only about $1.5 million (D'Amico, 1964), but the manganese nodules from the sea floor contain trace elements (mainly cobalt, nickel, and copper) perhaps more valuable than their manganese matrix.

PETROLEUM

A sizable fraction of the oil and gas production of the world already comes from the shallow sea floor off the coasts of the United States and Europe, and in the Persian Gulf. The Atlantic Coastal Plain sediments are not very petroliferous, but farther seaward these sediments become thicker, more marine, and possibly better source beds of petroleum. Suitable petroleum-bearing structures may be associated with large tectonic structures that exist in three main areas shown by figure 1. The southern area is along a seaward extension of the Cape Fear arch, which is well known on the adjacent land. A second area just southeast of New York City follows a major strike-slip fault. The northern area underlies the continental shelf between two tectonic troughs mapped by Drake and others (1959). The basement rock of the ridge between the troughs is overlain by 1.5 to 2.5 km of Cretaceous to Pliocene strata. Farther southwest the ridge underlies deep water of the continental slope, but farther northeast it becomes shallower in the vicinity of Sable Island (beyond the limits of fig. 1) and it probably extends to the northwestern part of the Grand Banks of Newfoundland. Detailed geophysical exploration may reveal the presence of isolated high portions of the ridge worthy of testing by drilling.

At the base of the continental slope is a broad gently sloping feature, the continental rise. Continuous seismic profiling indicates that it consists of numerous interbedded strata of alternating high and low acoustic impedence. These layers probably consist of sandy

turbidites separated by clayey hemipelagic beds—a flyschlike deposit. Future testing by drilling may show that the clays are petroleum source beds and that the sands are reservoir beds (Emery, 1963).

CONCLUSIONS

Areas having particular potential for construction sand, phosphorite, manganese nodules, and petroleum have been outlined in a general way (fig. 1) from preliminary results of a continuing study of the Atlantic continental margin. Further planned investigation should pinpoint the best parts of these areas for such resources. Whether any of them will eventually be exploited depends upon future developments in marine engineering and a favorable cost-price relation.

REFERENCES

D'Amico, K. J., 1964, Statistical summary: U.S. Bur. Mines, Minerals Yearbook, 1963, v. 1, p. 129–175.

Drake, C. L., Ewing, Maurice, and Sutton, G. M., 1959, Continental margins and geosynclines; The east coast of North America north of Cape Hatteras *in* Physics and chemistry of the earth, v. 3: London, Pergamon Press, p. 110–198.

Emery, K. O., 1963, Oceanographic factors in accumulation of petroleum: 6th World Petroleum Conference, Frankfurt/Main, Germany, sec. 1, paper 42, p. 483–491.

Emery, K. O., and Schlee, J. S., 1963, The Atlantic continental shelf and slope, a program for study: U.S. Geol. Survey Circ. 481, p. 1–11.

Heezen, B. C., Tharp, Marie, and Ewing, Maurice, 1959, The floors of the oceans, I. The North Atlantic: Geol. Soc. America Spec. Paper 65, p. 1–122.

Merrill, A. S., Emery, K. O., and Rubin, Meyer, 1965, Ancient oyster shells on Atlantic continental shelf: Science, v. 147, p. 398–400.

Mero, J. L., 1960, Mineral resources on the ocean floor: Mining Congress Jour., v. 46, p. 48–53.

—— 1962, Ocean-floor manganese nodules: Econ. Geology, v. 57, p. 747–767.

Pratt, R. M., 1963, Bottom currents on the Blake Plateau: Deep-Sea Research, v. 10, p. 245–249.

Schlee, John, 1957, Upland gravels of southern Maryland: Bull. Geol. Soc. America, v. 68, p. 1371–1410.

—— 1964, New Jersey offshore gravel deposit: Pit and Quarry Mag., v. 57, no. 6, p. 80, 81, 95.

Sheridan, R. E., Drake, C. L., Nafe, J. E., and Hennion, J., 1965, Seismic-refraction measurements of the continental margin east of Florida: Geol. Soc. America Spec. Paper 82, p. 183.

Uchupi, Elazar, 1965, Maps showing relation of land and submarine topography, Nova Scotia to Florida: U.S. Geol. Survey, Misc. Geol. Inv. Map I–451. [In press]

COMPOSITION OF BASALTS DREDGED FROM SEAMOUNTS OFF THE WEST COAST OF CENTRAL AMERICA

By CELESTE G. ENGEL and THOMAS E. CHASE,[1]
La Jolla, Calif.

Abstract.—Two alkali basalts and a third, intermediate in composition between tholeiitic and alkali basalts, have been dredged from the surficial parts of three submarine volcanoes on the Cocos Ridge, eastern Pacific Ocean. The two alkali basalts contain (in weight percent, calculated water free): SiO_2, 44.6; $Na_2O + K_2O$, 4.8 to 5.8; and appreciable amounts of the trace elements Ba, Sr, and Zr. The intermediate type contains: SiO_2, 48.8; $Na_2O + K_2O$, 3.7; and smaller amounts of most trace elements except Cu. Alkali basalts, similar to those from the Cocos Ridge, form the apical parts of most large volcanoes throughout the oceans.

Expedition Criss-Cross of the Scripps Institution of Oceanography, University of California, successfully dredged samples of volcanic rock from the near-surface parts of three seamounts west and southwest of Cocos Island, and north of the Galapagos Islands, in the Pacific Ocean. This note discusses the chemistry and petrography of these submarine igneous rocks.

The forms of the submarine volcanoes from which the samples were dredged are shown in figure 1. These features lie along the northwest flank of Cocos Ridge, which extends from about lat 2° N. and long 94° W. to the southwest coast of Costa Rica and Panama (fig. 1). The Cocos Ridge, in turn, is a spur of the huge East Pacific Rise (Menard, 1960).

All the rocks recovered in the dredge hauls are basalts. Locations of the samples and depths of dredge sites are given at the bottom of the accompanying table. Dredge hauls ranged in depth from 150 to 250 fathoms.

Sample 312 was recovered from the upper part of a submarine volcano about 180 miles north of the Galapagos Islands and 290 statute miles southwest of Cocos Island (fig. 1). It is a light-gray dense basalt. In thin section the rock has a diabasic to fluidal structure and contains (in volume percent): plagioclase, 58; augite,

[1] U.S. Bureau of Commercial Fisheries.

Chemical composition of basalts dredged from seamounts off the west coast of Central America

	Sample 312		Sample 314		Sample 316	
	Original	Water free	Original	Water free	Original	Water free
Oxides, in weight percent [1]						
SiO_2	48.34	48.83	44.90	45.57	42.95	44.61
TiO_2	1.97	1.99	2.85	2.89	2.81	2.92
Al_2O_3	16.36	16.53	22.80	23.13	19.10	19.84
Fe_2O_3	2.59	2.62	1.91	1.94	4.03	4.18
FeO	7.38	7.46	4.69	4.76	5.60	5.81
MnO	.17	.17	.12	.12	.16	.16
MgO	6.23	6.29	5.09	5.16	6.65	6.90
CaO	11.97	12.09	9.16	9.30	9.37	9.73
Na_2O	2.91	2.94	4.00	4.06	3.50	3.63
K_2O	.79	.80	1.76	1.79	1.15	1.19
H_2O+	.27	--------	.54	--------	1.84	------
H_2O-	.55	--------	.66	--------	1.46	------
P_2O_5	.28	.28	1.26	1.28	.99	1.03
Total	99.81	--------	99.74	--------	99.61	------
Elements, in parts per million [2]						
Ba	220	--------	740	--------	810	------
Co	33	--------	22	--------	27	------
Cr	46	--------	120	--------	180	------
Cu	62	--------	34	--------	48	------
Ga	22	--------	19	--------	20	------
La	<80	--------	120	--------	<80	------
Nb	31	--------	82	--------	70	------
Ni	45	--------	63	--------	60	------
Sc	38	--------	30	--------	33	------
Sr	320	--------	740	--------	440	------
V	290	--------	250	--------	320	------
Y	40	--------	52	--------	52	------
Yb	4	--------	4	--------	5	------
Zr	150	--------	340	--------	260	------

Ag <3, B <30, Be <2, Mo <5.

Sample 312. Paramount Bank; lat 3°20′ N., long 90°45′ W. Depth 165 fathoms.

Sample 314. Unnamed seamount; lat 4°58′ N., long 87°28′ W. Depth 250 fathoms.

Sample 316. West Cocos Seamount; lat 5°28′ N., long 88°33′ W. Depth 150 fathoms.

[1] Major element analyses by C. G. Engel.
[2] Quantitative spectrographic analyses (±15 percent) by R. G. Havens.
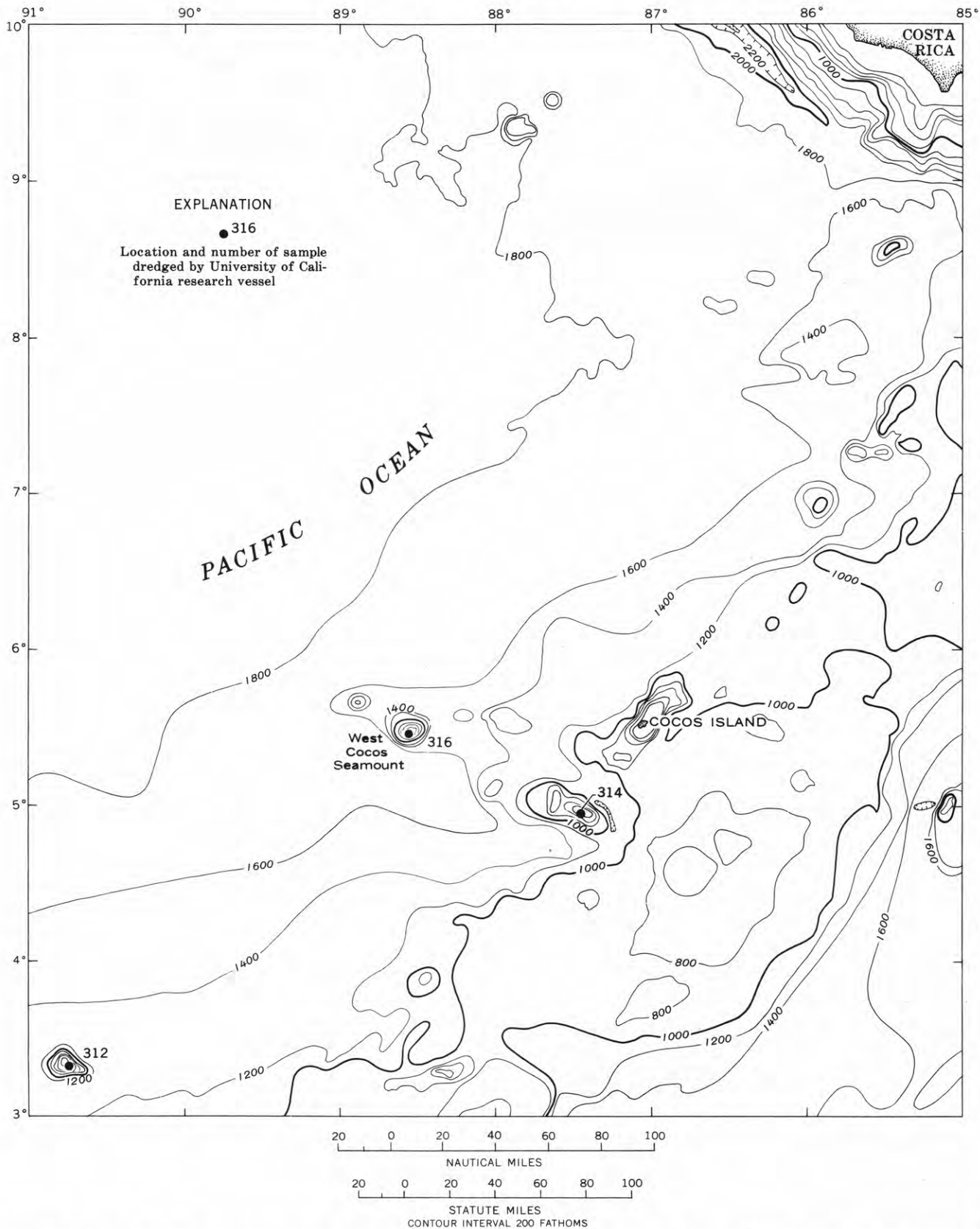
FIGURE 1.—Submarine topographic chart of part of Cocos Ridge, off the west coast of Central America, showing locations of samples dredged during Expedition Criss-Cross. Topography from Topographic Charts 13 and 14, U.S. Bureau of Commercial Fisheries.

38; opaque minerals, 3; and alteration products, principally palagonite, 1. The chemical composition of basalt 312 (see table) is intermediate between the composition of low-potassium oceanic tholeiites and typical alkali basalts of submarine volcanoes and islands. The average K_2O content of low-potassium tholeiites is 0.17 weight percent, whereas typical alkali basalts capping submarine volcanoes and islands contain about 1.5 weight percent of K_2O (Engel and Engel, 1963; 1964a; 1964b). Tholeiitic basalts similar in composition to basalt 312 also occur on the Galapagos Islands (Banfield and others, 1956). Tholeiites are, however, commonly subordinate to alkali basalts on the islands and higher submarine volcanoes of the East Pacific Rise.

Sample 314 is a gray vesicular porphyritic alkali basalt from the crest of an unnamed seamount (see table and fig. 1). It contains vesicles and tubules as much as 7 mm long. In thin section the rock consists of the following constituents (in volume percent): a fine-grained groundmass, principally a mat of plagioclase and opaque minerals, 45; labradorite phenocrysts, 18; olivine, clear and unaltered, 5; vesicles, 27; opaque minerals, 4; and calcite, lining walls of vesicles, about 1.

Sample 316 is a gray vesicular porphyritic alkali basalt from the upper part of the West Cocos Seamount. It contains almond-shaped vesicles that are as much as 20 mm long. The phenocrysts are labradorite and pale pink augite. The rock contains (in volume percent): plagioclase, 60; augite, 20; opaque minerals, 8, and vesicles, 6. It is the most altered of the basalts studied and contains approximately 6 volume percent palagonite and other alteration products. Both of the alkali basalts 314 and 316 contain numerous tiny crystals of apatite.

The concentrations of trace elements in the basalts (see table) reflect their major element compositions. Distinct differences exist between the amounts of trace elements in basalt 312 and the amounts in the alkali basalts 314 and 316. The alkali basalts contain more Ba, Sr, Zr, Nb, Cr and Ni, than does basalt 312. The increases in amounts of Ba, Sr, and Zr, with an increase in sodium and potassium in the alkali basalts, are predictable on the basis of chemical coherence and have been observed in the Hawaiian lava series by Wager and Mitchell (1953). The enrichment of Cr and Ni in the alkali basalts, 314 and 316, could hardly be predicted and appears to be anomalous. There is less Cu in the alkali basalts than in basalt 312.

The composition and occurrence of the basalts 312, 314, and 316 are consistent with what is known regarding volcanic rocks throughout other parts of the East Pacific Rise (Chubb and Richardson, 1933; Bandy, 1937; Banfield and others, 1956; Engel and Engel, 1963, 1964b). Cappings of the higher volcanoes are composed largely of alkali basalts and other members of the alkali-rich series. The deeply submerged flanks of the East Pacific Rise appear to consist largely of low-potassium, tholeiitic basalts. Engel and Engel (1964a, 1964b) have suggested that this low-potassium basalt represents the primary magma erupted from the mantle. The alkali basalts and derivative alkali-rich members appear to be derived from the low-potassium basalts by magmatic differentiation.

REFERENCES

Bandy, N. C., 1937, Geology and petrology of Easter Island; Geol. Soc. Am. Bull., v. 48, p. 1589–1610.

Banfield, A. F., Behre, C. H., Jr., and St. Clair, David, 1956, Geology of Isabela (Albemarle) Island, Archipielago de Colon (Galapagos): Geol. Soc. Am. Bull., v. 67, p. 215–234.

Chubb, L. J., and Richardson, Constance, 1933, Geology of Galapagos, Cocos, and Easter Islands: Bernice P. Bishop Museum Bull. 110, 67 p.

Engel, A. E. J., and Engel, C. G., 1964a, Composition of basalts from the Mid-Atlantic Ridge: Science, v. 144, no. 3624, p. 1330–1333.

——— 1964b, Igneous rocks of the East Pacific Rise: Science, v. 146, no. 3643, p. 477–485.

Engel, C. G., and Engel, A. E. J., 1963, Basalts dredged from the northeastern Pacific Ocean: Science, v. 140, no. 3573, p. 1321–1324.

Menard, H. W., 1960, The East Pacific Rise: Science, v. 132, no. 3441, p. 1737–1746.

Wager, L. R., and Mitchell, R. L., 1953, Trace elements in a suite of Hawaiian lavas: Geochim. et Cosmochim. Acta, v. 3, p. 217–223.

ON THE STATISTICS OF THE ORIENTATION OF BEDDING PLANES, GRAIN AXES, AND SIMILAR SEDIMENTOLOGICAL DATA

By A. E. SCHEIDEGGER, Urbana, III.

Abstract.—It is shown that the mean of a series of axes in space (normals to bedding planes, long axes of sand grains, and so forth) is not given by the vector mean of the individual axes (as commonly assumed in the literature), but should be calculated as the eigenvector of a certain symmetric matrix. This, then, represents the direct analog of taking the arithmetic mean value of linear data. It also is the correct extension of Krumbein's well-known method based on doubling the angle of circularly distributed data to three dimensions. An example is given.

A problem that occurs on many occasions in the study of transport and deposition of sediments is that of making a statistical evaluation of a multitude of observed axes. This problem occurs, for example, in analyzing the orientation of crossbedding planes or the orientation of sand grains deposited on a bar. It is necessary to find a "best" axis for each series of axes (the normals to the bedding planes and the long axes of the sand grains), since one always wishes to summarize the multitude of observed data in some useful fashion. The problem of finding a best (sometimes loosely called "mean") axis for a series of axes is therefore an extremely important one.

The method of finding a best axis for a series of axes which is presently usually considered as most applicable (see, for example, Steinmetz, 1962; Potter and Pettijohn, 1963) is one which seems to be due originally to Reiche (1938); it is that of computing the vector mean of the individual axes.

It is easy to see, however, that the procedure of computing the vector mean of a series of axes is not a satisfactory one for finding the best of these axes. A vector is a directed quantity, an axis is not. Hence, in order to assign a vector to each axis, it is necessary to make a convention with regard to the side of the axes in which the corresponding vector is supposed to point. One might be inclined to say, for instance, that the direction of every axis shall be taken thus that it points down-ward, or in the direction of some hypothetical mean flow direction. However, such a procedure immediately assigns a peculiar significance to an arbitrarily chosen direction (for example, the vertical). The resulting best axis of a series of axes is therefore dependent on the particular choice of this arbitrarily chosen direction. Clearly, one ought to define a best axis in such a fashion that it depends only on the series of individual axes, and not, in addition, on some arbitrary choice such as a vertical direction.

A common way to get around the above difficulty is to draw a contour map on a unit sphere for the density (number per unit solid angle) of axes that fall in a certain direction. The axis with the greatest density is, then, the best for the series of individual axes. Unfortunately, this procedure can be used only if the number of individual axes in the series under consideration is very great, which is not always true. Thus, in many cases some analytical type of averaging of the original series of axes will be required.

In this paper, it is shown that the mean of a series of axes in space should be calculated as the eigenvector of a certain symmetric matrix.

STATISTICAL ARGUMENT

In order to propose a method for the determination of the best axis of a series of axes, it will be necessary to make a few fundamental postulates. Setting up such postulates is, of course, to a certain extent arbitrary; the postulates represent a priori assumptions (they are axiomatic) that cannot further be justified, except by the principle of correspondence with the theory of

errors of Gauss. As is well known, if one has a series of N points on a line (the position coordinate being given by the distance x_i of each point from some origin—point O on the line) the mean $\bar{x}$ is given by

$$\bar{x}=\sum_{i=1}^{i=N} x_i/N$$

The justification for taking $\bar{x}$ as representing the mean of the points follows from the a priori assumption that the *deviation* $|\bar{x}-x_i|$ of each point from the mean position $\bar{x}$ is subject to a Gaussian probability distribution

$$P_i=\text{const } e^{-k(x_i-\bar{x})^2},$$

where k is the parameter of the distribution. The assumption of the particular form of P_i as a Gaussian distribution is completely axiomatic; it cannot be further justified except by saying that it is reasonable from a physical standpoint. If the deviations are due to many random effects, the central-limit theorem of probability theory asserts that, in time, P_i will approach a Gaussian distribution. The best position $\bar{x}$ may then be found by postulating it in such a way that the total probability P_{tot} of the distribution

$$P_{tot}=\prod_{i=1}^{i=N} P_i$$

becomes a maximum. Clearly

$$P_{tot}=\text{const } e^{-k\Sigma(x_i-\bar{x})^2}$$

becomes a maximum if the exponent of the exponential is a minimum; that is, if the sum $\Sigma(x_i-\bar{x})^2$ is a minimum. This condition leads to the well-known method of least squares.

The above theory is useful in many instances for the description and representation of linear data. Their mean $\bar{x}$ and standard deviation

$$\sigma^2=\frac{1}{N}\Sigma(x_i-\bar{x})^2$$

gives a good idea of the distribution of the points on a line.

The task is to find a suitable generalization of the above procedures so that they can be applied to a series of axes in three-dimensional space.

Let us denote the N axes by $\vec{n}_i$, with components n_{ix}, n_{iy}, n_{iz}, in the x, y, z direction (these directions are assumed to represent an orthogonal system), respectively. It is assumed that $\vec{n}_i$ represents unit vectors in either direction of the corresponding axes. The "mean" of these axes will be a unit vector denoted by $\pm\vec{X}_1$

(components x_1, y_1, z_1). The deviation of $\vec{n}_i$ from $\vec{X}_1$ will be represented by the angle $-\pi/2\leq\phi\leq\pi/2$ between $\vec{X}_1$ and $\vec{n}_i$. If the probability distribution of ϕ is to be a generalization of a Gaussian distribution, we postulate that, for small ϕ, this distribution *shall* be Gaussian. In addition, we have to postulate that the probability distribution in ϕ is periodic modulo π (because we are dealing with axes), and thus that the hemisphere is our fundamental domain. Finally, we postulate that the probability distribution depends on a parameter k and that for $k=0$ one has a completely random distribution on the hemisphere.

These three postulates are satisfied by the following distribution:

$$P_i=\text{const } e^{k \cos^2\phi}.$$

Indeed, one has for small ϕ,

$$P_i=\text{const } e^{k(1-\phi^2+\cdots)}=\text{const } e^{-k\phi^2},$$

which is Gaussian. Furthermore,

$$P_i(\phi)=P_i(\phi+\pi)$$

and

$$P_i(k=0)=\text{const},$$

as required.

We now proceed as in the linear case, and seek the position of x such that the total probably

$$P_{tot}=\prod P_i$$

becomes a maximum. The cosine is nothing but the scalar product $(\vec{n}_i\vec{X}_1)$; thus

$$P_{tot}=\text{const } e^{k\Sigma(\vec{n}_i\vec{X}_1)^2}.$$

Clearly, P_{tot} is a maximum if $\Sigma(\vec{n}_i\vec{X}_1)^2$ is a maximum. The task, thus, is to maximize F (with $\vec{X}$ a unit vector with components x, y, z):

$$F=\Sigma(n_i\vec{X})^2$$

under the condition that $|\vec{X}|=1$. In components, this yields

$$F=a_{11}x^2+a_{22}y^2+a_{33}z^2+2a_{12}xy+2a_{13}xa+2a_{23}yz$$

with

$$a_{11}=\Sigma n_{ix}^2$$
$$a_{22}=\Sigma n_{iy}^2$$
$$a_{33}=\Sigma n_{iz}^2$$
$$a_{12}=a_{21}=\Sigma n_{ix}n_{iy}$$
$$a_{13}=a_{31}=\Sigma n_{ix}n_{iz}$$
$$a_{23}=a_{32}=\Sigma n_{iy}n_{iz}$$

Thus, the problem is to maximize F (a quadratic form) under the condition that $x^2+y^2+z^2=1$.

This is a classical problem; the solution for $\vec{X}$ is that it must be the eigenvector $\vec{X}_1$ of the matrix a_{ik} corresponding to the largest eigenvalue λ_1. This eigenvalue also is the value of F for $\vec{X}=\vec{X}_1$. Thus

$$\lambda_1 = \Sigma(\vec{n}_i \vec{X}_1)^2 = \Sigma \cos^2\phi_i$$

or

$$\sigma_1{}^2 = \frac{\lambda_1}{N} = \frac{1}{N}\Sigma \cos^2\phi_i$$

is the mean square of the cosines of the deviation angles.

The distribution of the axes may therefore be characterized by the 3 normalized eigenvectors of the matrix a_{ik} and the 3 eigenvalues, divided by N. It appears that this type of characterization is the logical generalization of the usual characterization of linear values by their mean and standard deviation, to a distribution of axes in space.

Mathematically, the above can also be expressed by stating that a distribution of axes in space may be characterized by the symmetric tensor A_{ik} where

$$A_{ik} = \frac{1}{N} a_{ik},$$

with a_{ik} as defined above.

One may call the tensor A_{ik} the "orientation tensor" for the axes under consideration. If the orientation tensor, referring to some type of axes, be calculated for some standard area around each point on a map, one obtains a tensor field indicative of the statistical orientation of these axes. By drawing the horizontal projections of the trajectories tangent to the principal directions of the orientation tensor at every point, one obtains an interesting visualization of the statistical distribution of the axes in question in the area investigated.

The eigenvalue technique for the characterization of special elements appears to have been proposed for the first time by Fara and Scheidegger (1963) for axes scattering around a plane; the statistical justification of the procedure for axes, in somewhat different form, was given by the writer in connection with the analysis of fault-plane solutions of earthquakes (Scheidegger, 1964). However, it is clear that this procedure is perfectly general and therefore directly applicable to sedimentation studies.

In two dimensions, the above eigenvalue technique amounts to the same thing as the method doubling the angles and then adding the vectors, which was proposed by Krumbein (1939). It is thus seen that the eigenvalue technique is the correct extension of Krumbein's method from 2 to 3 dimensions.

APPLICATION

We apply the technique proposed in this paper to the characterization of a series of crossbedding planes which were studied by Rusnak (1957). In the accompanying table, we list Rusnak's data on observed crossbedding dip direction and inclination. The azimuth is always taken clockwise from north, the inclination is the angle with the horizontal plane.

In order for our method for determining the statistical distribution of axes to be applicable, Rusnak's data were first to be translated into data that refer to spatial axes. In order to do this, one has to construct the normals to the dipping planes; the result of this calculation is shown in the table. The poles to the crossbedding planes are given by their azimuth and plunge (smallest angle between axis and horizontal plane).

Observed dip of crossbedding and calculated axes normal to bedding planes

Location	Dip of crossbedding (from Rusnak, 1957)		Axes normal to bedding planes		
	Direction (degrees)	Inclination (degrees)	Axis number	Azimuth	Plunge (degrees)
SE¼NW¼ sec. 31, T. 2 N., R. 1 E., Schuyler County, Ill.	1	12	1	S. 1 W.	78
	45	10	2	S. 45 W.	80
	69	22	3	S. 69 W.	68
	70	15	4	S. 70. W.	75
	78	8	5	S. 78 W.	82
	96	28	6	N. 84 W.	62
	110	6	7	N. 70 W.	84
	280	12	8	S. 80 E.	78
	285	13	9	S. 75 E.	77
	335	19	10	S. 25 E.	71
	352	26	11	S. 8 E.	64
	355	5	12	S. 5 E.	85
	357	25	13	S. 3 E.	65
NE¼SW¼ sec. 17, T. 8 N., R. 3 E., Fulton County, Ill.	5	25	14	S. 5 W.	65
	325	22	15	S. 35 E.	68
	340	15	16	S. 20 E.	75
	340	28	17	S. 20 E.	62
SW¼NE¼ sec. 19, T. 8 N., R. 3 E., Fulton County, Ill.	15	22	18	S. 15 W.	68
	130	17	19	N. 50 W.	73
	331	4	20	S. 29 E.	86
SW¼NE¼ sec. 20, T. 8 N., R. 3 E., Fulton County, Ill.	40	22	21	S. 40 W.	68

The next task is to calculate the matrix a_{ik} from the parameters of the $N=21$ axes, using the formulas given above. The matrix is

$$\begin{pmatrix} 1.332 & -0.118 & -3.487 \\ -.118 & .755 & -.804 \\ -3.487 & -.804 & 18.913 \end{pmatrix}$$

The eigenvalues of this matrix are

$$\lambda_1 = 19.611$$
$$\lambda_2 = 0.963$$
$$\lambda_3 = 0.426$$

The eigenvector corresponding to the largest eigenvalue has the azimuth α_1 and plunge β_1:

$$\alpha_1 = \text{S. } 12.27° \text{ W.}$$
$$\beta_1 = 78.97°$$

This axis represents the "mean" of the individual axes. Similarly, the eigenvector corresponding to the smallest eigenvalue has the azimuth α_3 and plunge β_3:

$$\alpha_3 = \text{N. } 42.58° \text{ E.}$$
$$\beta_3 = 9.56°.$$

The third eigenvector is simply the normal to the two others. The generalized standard deviations $\sigma_i^2 = \lambda_i/N$ are

$$\sigma_1^2 = 0.934$$
$$\sigma_2^2 = 0.046$$
$$\sigma_3^2 = 0.020$$

The characterizing tensor $A_{ik} = a_{ik}/N$ is

$$\begin{pmatrix} 0.063 & -0.006 & -0.166 \\ -.006 & .036 & -.038 \\ -.166 & -.038 & .901 \end{pmatrix}$$

It is interesting to plot the above data and best axis. The normals of the plane on a polar graph are shown in figure 1 by dots. The eigenvector corresponding to λ_1 is shown by a circle-and-cross symbol. It is seen that it falls into a region where one would expect it to lie. The scattering of the axes could also be expressed, instead of by σ_1^2, by an angle ϕ such that

$$\phi = \arccos \sigma_1.$$

This angle is 14.90° in the above case.

Translated back into planes, one might summarize the above data by saying that the mean plane has a dip direction of N. 12.27 E. and an inclination of 90° $-\beta_1 = 11.03°$. The standard scattering angle is 14.90°. The dip direction of the least-fitting plane (that corresponding to the smallest eigenvalue) to the series of bedding planes is S. 42.58° W. and its inclination is 80.44°. The corresponding scattering angle is $\phi_3 = \arccos \sigma_3 = 81.81°$.

The two (that is, the "best" and "least") fitting planes with their scattering angles characterize the distribution of bedding planes observed by Rusnak.
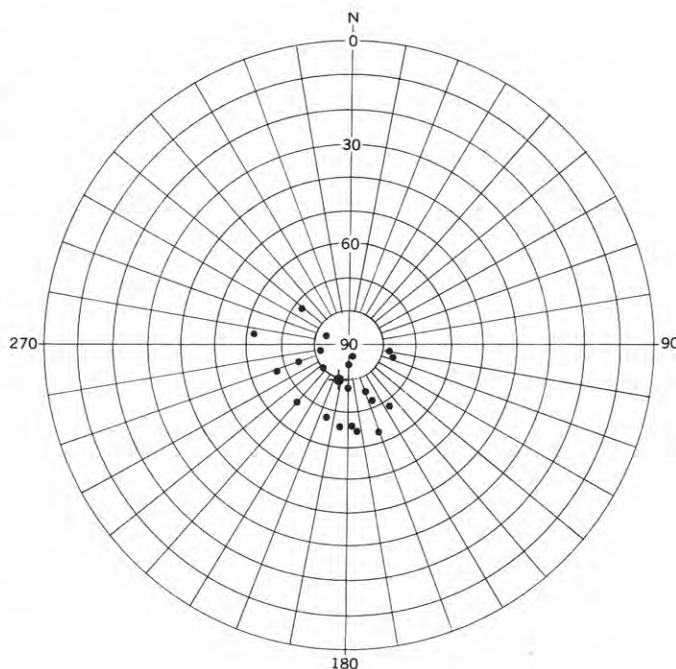
FIGURE 1.—Axes normal to bedding planes plotted in stereographic projection of lower hemisphere (after Rusnak, 1957) are shown by dots. "Best" axis (as calculated in this paper) is shown by circle-and-cross symbol.

REFERENCES

Fara, H. D., and Scheidegger, A. E., 1963, An eigenvalue method for the statistical evaluation of fault plane solutions of earthquakes: Seismol. Soc. Am. Bull., v. 53, p. 811–816.

Krumbein, W. C., 1939, Preferred orientation of pebbles in sedimentary deposits: Jour. Geol., v. 47, p. 673–706.

Potter, P. E., and Pettijohn, F. J., 1963, Paleocurrents and basin analysis: Berlin, Springer Verlag. 296 p.

Reiche, Parry, 1938, An analysis of cross-lamination: the Coconino sandstone: Jour. Geol., v. 46, p. 905–932.

Rusnak, G. A., 1957, A fabric and petrologic study of the Pleasantview sandstone: Jour. Sed. Petrology, v. 27, p. 41–55.

Scheidegger, A. E., 1964, The tectonic stress and tectonic motion direction in Europe and western Asia as calculated from earthquake fault plane solutions: Seismol. Soc. Am. Bull., v. 54, p. 1519–1528.

Steinmetz, Richard, 1962, Analysis of vectorical data: Jour. Sed. Petrology, v. 32, p. 801–822.

A SPECTROPHOTOMETRIC METHOD FOR THE DETERMINATION OF TRACES OF GOLD IN GEOLOGIC MATERIALS

By H. W. LAKIN and H. M. NAKAGAWA, Denver, Colo.

Abstract.—Gold in a sample is dissolved with sodium bromate and hydrobromic acid and extracted from dilute hydrobromic acid with ethyl ether. The ether is evaporated, and the aqueous solution of the residue is extracted with 4,4'-bis(dimethylamino) thiobenzophenone (TMK) in isoamyl alcohol. The absorbance of the red gold-TMK complex is proportional to the amount of gold present. As little as 20 ppb gold can be determined. Thallium interferes with the determination when present in large amounts. About 25 analyses can be made per man-day.

A sensitive method for the determination of trace amounts of gold in geologic materials (soil, gossan, and silicified limestone) would be useful in geochemical exploration for ore deposits of lead, bismuth, silver, copper, and zinc as well as for gold. Martinet and Cuper (1961) and Pakhomova and Vysotskaya (1963) have developed methods to meet this need. These methods yield satisfactory results, but repeated evaporation, filtration, precipitation, and subsequent solution make the methods tedious and lengthy.

Several spectrophotometric methods for the determination of microgram quantities of gold have been published and reviewed critically by Sandell (1959), Beamish (1961), and Chow and Beamish (1963).

Recently, Daiev and Jordanov (1964) have determined 0.5 to 60 parts per million Au in copper-bearing, lead-bearing, and mixed concentrates with N,N'-tetramethyl-o-tolidine as the color-forming reagent. Stanton and McDonald (1964) have determined as little as 0.09 ppm Au in 20-g samples of soils, with Brilliant green as the color-forming agent. Cheng and Lott (1961) studied 4,4'-bis (dimethylamino) thiobenzophenone (thio-Michler's ketone=TMK) and its related compounds as sensitive reagents for gold and concluded that TMK offers the highest sensitivity among the common colorimetric reagents for gold.

The separation of minute amounts of gold from the overwhelming quantities of other elements present in a sample large enough to yield a representative value is the difficulty inherent in all spectrophotometric methods for traces of gold in geologic materials. The ease of reduction of gold and its tendency to become adsorbed on glass and sample-residue particles compound this difficulty. The method presented below offers a simple means of separation of gold and its subsequent measurement.

The gold and gold minerals in the sample are dissolved with concentrated hydrobromic acid and sodium bromate; the excess bromine resulting from the reduction of the bromate ion is expelled by evaporation; then the acid solution and the unattacked sample residue are transferred to a separatory funnel, and the sample solution is diluted to give a final acid concentration of about $3N$. Two extractions of this solution and residue with ethyl ether yield a recovery of more than 99 percent of the gold in the ether phase. Subsequent wash of the ether with $1.5N$ HBr removes the iron, silver, mercury, and most of the palladium extracted from the sample. The ether is evaporated; the residue taken up in water, the solution buffered, and shaken with a TMK solution in isoamyl alcohol to give a red gold–TMK complex in the yellow TMK solution; the intensity of the color of the red complex is proportional to the amount of gold in the sample. A 5-gram sample is easily handled, and 0.1 microgram (gamma=microgram) of Au can be measured which gives a sensitivity of 0.02 ppm.

Any gold minerals completely enclosed in insoluble particles such as quartz would not be brought into solution and the resulting values in the analysis would below. The sample must, therefore, be ground to a powder to insure a reasonable attack of the gold. As fine grinding may result in loss of gold by plating onto the grinding equipment a reasonable compromise must be reached with each type of sample studied.

Hydrobromic acid, sodium bromate, and bromine are used to dissolve gold and gold minerals. Solution is just as complete as with aqua regia, and tedious evaporations are avoided.

Although Goldschmidt (1954) gives 0.001 ppm for the abundance of gold in the lithosphere, DeGrazia and Haskin (1964) suggest a crustal abundance of 0.0025 ppm. Their characteristic values of gold content, obtained by a neutron-activation method of analysis, range from 0.0024 ± 0.0018 ppm for acid igneous and metamorphic rocks, through 0.0047 ± 0.0016 for shales and 0.006 ± 0.0035 ppm for sandstone, to 0.012 ± 0.007 for pelagic clays. From this work it appears that a sensitivity of 0.02 ppm is 2 to 8 times the normal abundance of gold in various rock types. This sensitivity should give adequate data for mineral exploration; it should reveal enrichment of gold by hydrothermal or weathering processes. It has been used in a study of ancient placer deposits in a conglomerate (J. C. Antweiler, written communication, 1965).

PROCEDURE

Sample solution

Roast 5 g of pulverized sample at red heat for 10 to 20 minutes in a porcelain dish. Transfer to a 150-milliliter beaker, mix thoroughly with about 2 g of sodium bromate and wet with water. Rapidly pour 40 ml of concentrated HBr[1] into the beaker containing the roasted sample and sodium bromate. Warm on steam bath for 1 hour, then transfer to a hotplate and evaporate to a final volume of 20–25 ml.

Extraction

Transfer the entire contents of the beaker (solution and undissolved residue) to a 125-ml separatory funnel, using 30–40 ml of water to effect the transfer and to dilute the acid to approximately $3N$ HBr. Add 50 ml of ethyl ether, shake vigorously for 3 minutes and transfer the ether to another separatory funnel. Add 25 ml of ether to the aqueous sample solution and shake for 3 minutes. Combine the ether extracts and wash twice by shaking with 40- and 25-ml portions of $1.5N$ HBr. If the second wash acid is colored, a third wash is necessary.

Estimation

Put about 1 ml of water in a 150-ml beaker and add the ether phase from the extraction; evaporate on a steam bath until no odor of ether remains. Do not evaporate to dryness. Dilute to 10 ml with water. To an aliquot in a 50-ml beaker add enough water to make the volume approximately 10 ml, add 2.5 ml of NTA solution and adjust the pH to 3.0 ± 0.2 with NH_4OH or H_3PO_4. Transfer the contents of the beaker to a 125-ml separatory funnel and add 3 ml of dilute thio-Michler's ketone. Shake 3 minutes and allow phases to separate. Discard aqueous layer and wash organic phase with water. Drain off the water and add a few drops of ethyl alcohol to collect the last traces of water. Discard the water and transfer the organic phase to a cuvette and read the absorbance in a spectrophotometer at 545 millimicrons. Compare absorbance with standard curve to determine the amount of gold, in gammas, and convert to parts per million.

Preparation of standard curve

To five 25-ml portions of $3N$ HBr, each containing 1 g of iron as ferric bromide, in separatory funnels add 0, 0.1, 0.5, 1.0, and 1.5 micrograms of gold and shake for 3 minutes with 25 ml of ethyl ether. Transfer the ether to another separatory funnel, add another 25-ml portion of ether to each aqueous phase and shake for 3 minutes. Combine the ether extracts and wash twice with 25-ml portions of $1.5N$ HBr. Transfer the ether phases to 150-ml beakers containing 1 ml water, evaporate the ether on a steam bath and proceed as in estimation. Repeat several times and plot the average absorbance of six or more replicates versus the gold content to obtain a reliable curve for routine work.

Reagents

Standard gold solution (0.1 percent): Dissolve exactly 1.0000 g of Au in $HBr–Br_2$ and heat gently to expel excess Br_2. Cool and dilute to 1,000 ml with concentrated HBr.

Dilute gold solution (0.0001 percent): Dilute 0.1 ml of 0.1-percent Au solution to 100 ml with $1.5N$ HBr. Prepare fresh daily.

Hydrobromic acid, concentrated, reagent grade, distilled.

Hydrobromic acid, $1.5N$: Dilute 172 ml of concentrated HBr to 1 liter with water.

Sodium bromate, powder, reagent grade.

Ethyl ether, reagent grade.

Nitrilo triacetic acid (NTA) solution (10 percent): To 10 g of NTA in 50 ml of water add NaOH pellets until solution is complete. Dilute to 100 ml with water. The pH of this solution should be about 3.3.

Thio-Michler's ketone: Dissolve 14.25 mg of 4,4'-bis(dimethylamino) thiobenzophenone in 400 ml of isoamyl alcohol. Heat gently to hasten solution. Cool and dilute to 500 ml with isoamyl alcohol. Protect from light.

Dilute thio-Michler's ketone: Dilute 25 ml of stock solution to 75 ml with isoamyl alcohol. Keep cold and protect from light.

Isoamyl alcohol, reagent grade.

Extraction of gold with isopropyl and ethyl ethers

The extraction coefficient of gold from hydrobromic acid solutions with isopropyl ether and ethyl ether was investigated by McBride and Yoe (1948) for gold concentrations ranging from 10 to 1,000 gammas of Au per milliliter. They recommended isopropyl ether and $2.0–2.5N$ HBr for separation of gold from much iron. In order to determine the effectiveness of these solvents in extracting gold from solutions containing 0.0025 to 0.05γ of Au per milliliter, the following experiments were made with gold-198 as a tracer. With equal volumes of the aqueous and organic phases the percentage of gold extracted into the isopropyl ether increased from 15 percent with $0.5N$ HBr through 45 percent with $2.5N$ acid to 86 percent with 5.5 and $6.0N$ HBr. However, the presence of other ions increased the effectiveness of the extraction. With a stock solution containing 6.3 g of Na, 18.3 g of Mg, 48 g of Al, 6 g of K, 9 g of Ca, 3.5 g of Ti, 0.4 g of Mn, and 18 g of Fe per liter, the

---

[1] The rapid addition of hydrobromic acid is necessary to provide sufficient volume to dissolve most of the bromine produced during the initial violent reaction.

extraction of gold with isopropyl ether from $5N$ HBr was 91 to 93 percent and from $6.5N$ acid was more than 97 percent. At this high acidity most of the iron is extracted with the gold, interfering with the subsequent measurement of gold.

Extraction of gold with ethyl ether is efficient at much lower acidities. With equal volumes of the aqueous and ether phases, 81 percent of the gold was extracted from $1N$ HBr and 88 percent from $1.5N$ acid after a 1 minute shaking in each case. With the stock solution, described above, 87 percent was extracted from $1N$ HBr and 95 percent from $1.5N$ acid. Very little ferric bromide is extracted under these conditions. With two 3-minute extractions using equal volumes, more than 99 percent of the gold was extracted into the ether phase from $1.5N$ HBr.

Adsorption of gold

Gold is strongly adsorbed by the sample residue· Five samples of low-grade ore from the Cripple Creek mining district, Cripple Creek, Colo., were roasted, spiked with Au^{198} as $AuBr_3$ and digested with hydrobromic acid and bromine. The samples were transferred to centrifuge tubes, centrifuged, and the supernatant liquid decanted. The residues were mixed thoroughly with 10 ml of water, centrifuged, the wash water decanted, and the residues washed again with 10 ml of water. The residues contained from 41.5 to 64.4 percent of the radioactive gold, and an average of 55 percent. When the hot concentrated hydrobromic acid was decanted from another sample residue 86 percent of the radioactive gold remained with the residue.

The answer to this problem is to make the ether extraction with the sample solution and residue in the separatory funnel. As the ether removes gold from the aqueous phase the adsorbed gold goes into solution. With gold-198 as a tracer it was found that only 0.4 percent of the Au remained in the sample residue after two ether extractions.

The aqueous solution of gold obtained after the ether solution should not be allowed to stand overnight, as gold is apparently adsorbed by the glass vessel and low values are obtained.

Interferences

Several elements form colored compounds with thio-Michler's ketone. According to Cheng and Lott those elements are ruthenium (III), rhodium (III), iridium (III), mercury, silver, palladium, copper (I), and gold; however in their proposed bromide-TMK procedure for auric gold only mercury, silver, and palladium represent interferences because the others do not form colored compounds in an organic medium. Neither mercury nor silver interfere in quantities up to 0.4 percent.

Samples containing larger quantities of mercury could be tolerated since during the roasting process the mercury would be volatilized. Palladium forms a pink compound and becomes an interference in quantities greater than 300 γ.

Thallium (III) reacts at pH 3 with TMK to give a blue complex. The complex of thallium with NTA, however, is adequate to prevent interference with the gold determination, except in samples with unusually high thallium content. Only 4 samples out of more than 1,200 analyzed in our laboratories contained sufficient thallium to cause interference. In these cases smaller sample aliquots were taken and no blue color was evident. With 2.5 ml of 10-percent solution of NTA 30 γ of Tl increases the absorbance at 545 $m\mu$ to give a value twice that obtained with 0.1 γ of Au.

Antimony is extracted by ethyl ether from $3N$ HBr solution and some remains in the ether phase. On dilution of the residue from the ether evaporation, hydrolysis of the antimony bromide yields a white precipitate which causes difficulty in taking an aliquot of the solution. This has been experienced only with high-grade antimony ores.

In addition to the above interferences, cadmium and uranium were found to interfere—1 milligram of either element gave a color equivalent to 0.1 γ of Au.

Among the anions, Cheng and Lott reported that acetate, tartrate, chloride, sulfate, and dichromate had no effect on the determination of gold with TMK. The only interfering anion seems to be bromide, and when present in excess it diminishes the sensitivity of the method. Care must therefore be taken to avoid transfer of droplets of the hydrobromic acid solution with the ether into the beaker for evaporation.

Bromine produced during digestion of the sample can be a very serious interference if it is not entirely removed. A trace of bromine left in the sample solution is adequate to oxidize the TMK, causing a green color. Boiling the hydrobromic acid-bromine solution of the sample eliminates the bromine.

PRECISION AND ACCURACY

Table 1 shows the repeatability obtained with standard gold solutions run through the analytical procedure. These data may be used to draw a standard curve or the average absorbance of 0.018 per 0.1 μg of Au may be used to calculate the gold content. The large relative standard deviation of the absorbance for 0.1 gamma of Au (26 percent) is expectable for the lower limit of a spectrophotometric procedure.

Another test of repeatability is shown in table 2. Three samples of gold ore were run repeatedly by the TMK method. Five-gram samples were extracted with ethyl ether, and appropriate aliquots of the

aqueous solution were taken to react with TMK. Gold is usually present in geologic materials as discrete particles of the metal or of gold minerals. This situation makes it difficult to take sample splits that contain the same amount of gold. The variation between replicate determinations on these gold ores is greater than the variation obtained with standard gold solutions (table 1). It is reasonable to assume that these larger differences reflect differences in the gold content of the respective 5-g subsamples used for analysis.

The gold content obtained by the TMK method in a number of gold ores is compared with that obtained by

TABLE 1.—*Repeatability of spectrophotometric method, using standard gold solutions in ferric bromide*

[Data represent nine replications at each gold concentration]

Gold taken (γ, micrograms)	Absorbance of gold TMK at 545 mμ [1]				Relative standard deviation (percent)	Absorbance per 0.1 γ Au
	Minimum	Maximum	Average	Standard deviation		
0.1	0.010	0.031	0.0195	0.0052	26.0	0.0195
0.5	.079	.095	.087	.0046	5.4	.0175
1.0	.157	.185	.1725	.0083	4.8	.0172
1.5	.243	.300	.272	.0168	6.1	.0181
Average						0.0181

[1] Absorbance of the gold solutions was measured against their respective blank solutions as the null section.

TABLE 2.—*Repeatability of TMK method on gold-ore samples from Clear Creek County, Colo.*

Lab. No.	Description of sample	Number of determinations	Gold content (ppm)				Relative standard deviation (percent)
			Maximum	Minimum	Average	Standard deviation	
234557	Vein sample, Treasure Vault mine	9	1.00	0.60	0.81	0.13	16.1
224707	Chip sample, Ella No. 1, Lawson area	4	.98	.73	.81	.10	12.3
223181	Gold Anchor mine, Alice Creek district	5	24.0	18.4	21.7	2.01	9.3

fire assay in table 3: The TMK method is designated to determine gold in the range 0.02 to 3.0 ppm, but analyzed samples are not available with gold contents below 0.5 ppm. However, the data in table 3 indicate that the method is adequate to screen samples for gold content and to determine if further sampling and fire assays are desirable. The method provides a simple reasonably accurate procedure for determining gold in the range 0.02 to 3 ppm at a rate of about 25 analyses per man-day, thus bridging the gap between fire assay and neutron-activation procedures.

TABLE 3.—*Comparison of data by TMK method with fire assay on gold ore from Clear Creek County, Colo.*

Sample No.	Description and location	Gold content (ppm)	
		Average of duplicate analysis, by TMK method	Fire assay [1]
216092	Vein sample from unknown mine	[2] 0.83	0.68
222893	Galena sphalerite breccia ore, Silver Creek area	1.57	1.37
229657	Mill heads, Goldridge mill, Central City district [3]	1.16	1.37
222897	Quartz pyrite, copper, sphalerite ore, Silver Creek area	3.75	4.80
223184	Grab sample from dump Gold Anchor mine	6.42	6.84
223180	Channel sample Gold Anchor mine	14.3	10.3
224702	Quartz-pyrite-sphalerite, Lawson area	[2] 24.4	26.5

[1] Parts per million calculated from ounces/ton of fire assay by D. W. Skinner, U.S. Geological Survey, Denver, Colo.
[2] Average of triplicate analysis.
[3] Gilpin County, Colo.

REFERENCES

Beamish, F. E., 1961, A critical review of colorimetric and spectrographic methods for gold: Anal. Chem., v. 33, p. 1059–1066.

Cheng, K. L., and Lott, P. F., 1961, 4,4′-Bis (dimethylamino) thiobenzophenone (thio-Michler's ketone) and its related compounds as sensitive reagents for gold—Microchemical techniques, *in* Microchemical journal symposium series, v. 2: New York, Interscience Publishers, 1181 p.

Chow, A., and Beamish, F. E., 1963, Studies of titrimetric spectrophotometric methods for the determination of gold: Talanta, v. 10, no. 8, p. 883–90.

Daiev, Ch., and Jordanov, N., 1964, Photometric method for the determination of small amounts of gold with N,N-tetramethyl-o-tolidine (Tetron): Talanta, v. 11, no. 3, p. 501–6.

DeGrazia, A. R., and Haskin, Larry, 1964, On the gold contents of rocks: Geochim. et Cosmochim. Acta, v. 28, p. 559–564.

Goldschmidt, V. M., 1954, Geochemistry (edited by Alex Muir): London, Oxford Univ. Press, 730 p.

Martinet, R., and Cuper, J., 1961, Rapid determination of gold in soils, ores, waters, and laterites: Franc., Rep., Bur. Rech. Geol. Miniere, Bull. no. 2, 47–66.

McBride, W. A. E., and Yoe, J. H., 1948, Colorimetric determination of gold as bromoaurate: Anal. Chem., v. 20, p. 1094–99.

Pakhomova, K. S., and Vysotskaya, T. A., 1963, Determination of gold during complex geochemical studies: Sibirsk. Otd. Akad. Nauk SSSR, Ser. Geol. 1963, v. 16, p. 75–80.

Sandell, E. B., 1959, Colorimetric metal analysis, 3d ed.: New York, Interscience Publishers, 1032 p.

Stanton, R. E., and McDonald, Alison J., 1964, The determination of gold in soil with Brilliant green: Analyst, v. 89, no. 13, p. 767–770.

A FIELD METHOD FOR THE DETERMINATION OF SILVER IN SOILS AND ROCKS

By H. M. NAKAGAWA and H. W. LAKIN, Denver, Colo.

Abstract.—A rapid sensitive and specific field method useful in geochemical exploration has been developed for the determination of silver in geologic materials. In this method the sample is digested with nitric acid, and the silver is extracted with triisooctyl thiophosphate (TOTP) in benzene and stripped from the organic phase with dilute hydrochloric acid. Silver is then measured indirectly by its catalytic action on the persulfate oxidation of manganous ion to permanganate. The lower limit of sensitivity of the method is 0.01 ppm. Soils, rocks, oxides and sulfide ores have been analyzed, and the results agree favorably with analyses by fire assay. The data are also compared with results obtained by semiquantitative spectrographic analyses on concentrates of 23 different minerals. About 80 determinations can be made per man-day.

Several available colorimetric methods for the analysis of silver are adequate for many purposes and types of material (Sandell, 1959; Snell and others, 1959; Kodama, 1963), but the need for a reliable, rapid, and sensitive method satisfactory for exploration purposes has led to the development of the procedure described in this paper.

The most generally suitable reagents at the present time for the colorimetric determination of small amounts of silver are p-dimethyl-aminobenzilidenerhodanine and dithizone (Sandell, 1959). Neither reagent, however, is selective nor sensitive enough for the desired conditions, and in order to isolate silver tedious precipitation or ion-exchange procedures are involved.

In the proposed method the sample is digested with nitric acid and silver is extracted with triisooctyl thiophosphate (TOTP) in benzene (Handley and Dean, 1960) and stripped from the organic phase with dilute hydrochloric acid. Silver is then determined indirectly by its catalytic action on the persulfate oxidation of manganous ion to permanganate (Underwood and others, 1952; Lai and Weiss, 1962). The simplicity of the method allows for about 80 determinations per man-day.

Although TOTP is not a specific extractant for silver it is highly selective, and according to Handley and Dean only mercury, tantalum, and, to a lesser degree, vanadium are extracted by TOTP from a nitric acid solution containing 35 elements. These three elements are not considered as being interferences, because they do not catalyze the above reaction. Palladium catalyzes the oxidation, but is only partly stripped from the TOTP by $0.3N$ HCl. Because as much as 30 gammas (gamma $= \gamma =$ microgram) of Pd only doubles the effect of 0.1 γ of Ag, the procedure is nearly specific for silver.

DESCRIPTION AND DISCUSSION OF METHOD

Sample solution

Solution of silver in geologic materials is usually effected by digesting the finely ground sample with boiling nitric acid followed by a sodium carbonate fusion of the insoluble residue (Hillebrand and others, 1953; Almond and others, 1949). Potassium pyrosulfate fusion has also been used as a preliminary attack of the sample (Sandell, 1959). Samples of assayed materials were (1) digested with concentrated HNO_3, (2) fused with $K_2S_2O_7$ and digested with $8N$ HNO_3 and (3) fused with $K_2S_2O_7$ and digested with $8N$ H_2SO_4. Treatments (1) and (2) were followed by extraction from $8N$ HNO_3 with 30-percent TOTP in benzene. Treatment (3) was followed by extraction from $8N$ H_2SO_4 with 30-percent TOTP in benzene. Very little difference was observed between the three treatments and extractions. With Ag^{110} as a tracer, 95 percent of the silver was extracted from the $8N$ H_2SO_4 as compared to 99 percent from $8N$ HNO_3. The nitric acid digestion and extraction are favored for their simplicity and repeatability.

Extraction of silver from TOTP solutions

The removal of silver from the organic phase into an aqueous medium is a necessity for performing sub-

sequent analytical steps. Handley and Dean (1960) state that 93 percent of the Ag in TOTP solution can be extracted with an equal volume of dilute NH_4OH. Consequently, attempts to strip the silver from the TOTP were made with dilute NH_4OH. Recovery of silver was inconsistent and incomplete, ranging from 40 percent to 75 percent after 2 extractions. Sodium hydroxide was also tried, but it also yielded inconsistent and poor recoveries. The most effective stripping from the organic phase was accomplished by using dilute HCl. One wash with an equal volume of $0.3N$ HCl removed 97–99 percent of the silver. The optimum concentration of HCl is $0.3N$, because the stripping ability of acid of this concentration is the highest that can be obtained without having any adverse effects on the catalytic reaction used for estimation. It has been stated that 7 milligrams of Cl^{-1} gives an error of 1 standard deviation in the determination of 0.10γ of Ag (Underwood and others, 1952).

Silver ions tend to be adsorbed on the glass, and this adsorption becomes the source of serious error in very dilute solutions. For this reason the analyses must be carried out with dispatch. Silver left in the $0.3N$ HCl may be partially lost from solution after standing overnight. This adsorption makes it necessary to carefully clean test tubes between analyses with dilute sodium cyanide solution followed by several rinses with metal-free water.

Interferences

Interferences are known for each phase of this procedure, but the method in its entirety is believed to be virtually specific for silver. Besides silver, palladium is the only element extracted to an appreciable extent by TOTP, and able to catalyze the oxidation reaction of manganous ion to permanganate. Mercury, tantalum, and, to a lesser degree, vanadium (Handley and Dean, 1960) are also extracted, but none of these elements catalyze the oxidation reaction. Large amounts of manganese prevent the formation of purple permanganate by producing brown manganous dioxide, but manganese is not extracted by TOTP. No interference was observed when the following salts and metals were dissolved with concentrated HNO_3 and subjected to the proposed method of analysis for silver: 50 mg each of TeO_2, $Au°$, $KReO_4$, $(NH_4)_2IrCl_6$, $(NH_4)_3RhCl_6·1\frac{1}{2}H_2O$, $(NH_4)_2[Ru(H_2O)Cl_5]$, $(NH_4)_2$ $OsCl_6$, $(NH_4)_2PtCl_6$ and $Ta°$; 200 mg each of Bi_2O_3, $CoCl_2$, $CrCl_3$, $TlNO_3$, $K_2TiO(C_2H_4)_2·2H_2O$, Nb_2O_5, MoO_3, $CdCl_2$, $SnCl_2$, Na_2WO_4, $K(SbO)C_4H_4O_6·\frac{1}{2}H_2O$, V_2O_5, and $HgCl_2$; 500 mg each of $PbCl_2$, $NiCl_2$, $ZnCl_2$ and As_2O_3; and 2 g each of $FeCl_2·4H_2O$, $CuSO_4$ and $Cu(NO_3)_2·3H_2O$. The tests indicated that these ele-

ments or compounds are tolerated in the quantities likely to be met in most samples. At first, copper was thought to be an interference because 2 grams each of $CuSO_4$ and $Cu(NO_3)_2·3H_2O$ gave respective Ag values of 0.1γ and 0.2γ, although no test for copper could be obtained in the $0.3N$ HCl extract. We concluded that silver contamination in the salts used was responsible for the positive results because the interference was removed by the first extraction with TOTP. The second extraction of the same nitric acid solution yielded excellent blanks without a trace of enhancement of the oxidation of manganese, indicating no interference from copper.

The chief interferences are Pd^{+2}, Cl^{-1} and organic matter due to TOTP. Palladium becomes objectionable in quantities greater than 32 micrograms because it increases a $0.1-\gamma$ standard twofold, but such a concentration in a sample would be extremely rare and is therefore not too serious. Excess Cl^{-1} leads to resulting low values, but the quantity used in this method is tolerated without any loss of sensitivity. The most serious interference arises from incomplete separation of the organic and aqueous acid phases. Small amounts of TOTP remaining in the hydrochloric acid extract form a yellow wax when heated with persulfate. The simultaneous formation of wax and purple permanganate leads to low results. This condition is remedied by a preliminary heating of the acid solution with potassium persulfate prior to taking an aliquot for the catalytic procedure.

Sensitivity, precision, and accuracy

The sensitivity of this method is due to the catalytic procedure. It has long been known that reactions of this type are extremely sensitive and involve primarily a rate measurement. Therefore, the time and temperature of such reactions and the concentration of the reactants must be carefully controlled. For the proposed silver method the critical aspects of the catalytic phase are temperature of reaction and concentration of oxidant. A salt bath is used to keep the temperature between 98°–100°C, and an excess of potassium persulfate is maintained to insure the dependency of rate of oxidation of manganous ion to permanganate upon the amount of silver present.

The reproducibility in the range 0.01–5 parts per million is shown by replicate analyses of 8 samples presented in table 1. The large relative standard deviations of 63 percent, 46.8 percent, and 47.9 percent obtained for 3 samples in table 1 are probably caused by lack of homogeneity of the sample. A relative standard deviation of 20 to 50 percent appears to be a reasonable measure of the precision of the method.

TABLE 1.—*Replicate determinations of silver*

[Determinations in parts per million]

Sample No.	Analyses of separate subsamples							Mean	Relative standard deviation (percent)
	1	2	3	4	5	6	7		
64–2730	5	5	4	3	3	3	3	3.7	25.7
64–2740	5	2.5	2.5	3		3	4	3.3	29.5
114938	2	3	2	2.4	3.2	2	3	2.5	27.1
114939	1	1.5	1.5	1.2	1.2	1.2	1.6	1.3	16.6
64–2722	.75	.75	.3	.4	.12	.12	.6	.43	63.0
64–2733	.3	.12	.28	.4	.14			.25	46.8
64–2743	.05	.05	.04	.04	.02	.01	.02	.03	47.9
114933	.05	.02	.02	.04	.02	.01	.02	.03	21.5

The reliability of the method is based on analysis of samples having assayed values. Unfortunately, samples of known silver content in the range for which this method is intended are unavailable. Therefore, the accuracy of the method is determined on samples containing as much as 50 ppm of Ag as indicated in table 2. There is satisfactory agreement between

TABLE 2.—*Comparison of silver values obtained from different weights of the same sample by the proposed field method and by fire assay*

[Values given in parts per million]

Sample No.	Proposed field method					Fire assay [1]
	Sample weight (grams)				Average silver value	
	0.1	0.2	0.5	1.0		
223188	60	50	60	30	50	50
91400	2	3.8	6	4	3.95	4.8
612953	5	3.5	4	7.5	5	7

[1] Parts per million calculated from ounces per ton; assay by D. W. Skinner, U.S. Geological Survey, Denver, Colo.

various weights of the same sample. However, the precision of the method increases with the quantity of silver present, up to 5 ppm as observed in table 1. A rough measure of reliability is given (table 3) by comparison with semiquantitative spectrographic results obtained over a wide range of silver content for concentrates of 23 minerals.

REAGENTS AND APPARATUS

Potassium persulfate, reagent-grade.

Nitric acid, concentrated, reagent-grade.

Nitric acid, 8N: Dilute 1 part of concentrated HNO_3 with 1 part of demineralized water.

Triisooctyl thiophosphate in benzene: Dilute 300 milliliters of TOTP with 700 ml of benzene.

Hydrochloric acid, 0.3N: Dilute 25 ml of concentrated HCl to 1 liter with demineralized water.

Phosphoric acid, reagent-grade: Dilute 1 to 1 with demineralized water.

Manganous sulfate: Dissolve 0.5 g of $MnSO_4 \cdot H_2O$ in 500 ml of demineralized water.

TABLE 3.—*Comparison of silver content in diverse minerals as determined by the proposed field method and by semiquantitative spectrographic methods*

[Semiquantitative spectrographic analyses by Pauline J. Dunton, U.S. Geological Survey, Denver, Colo.]

Major component of sample	Method	
	Proposed field (ppm)	Semiquantitative spectrographic (ppm)
Arsenopyrite	30	30
Allanite	2	1.5
Cervantite	.5	7
Chalcopyrite	150	300
Cerussite	100	300
Descloizite	.7	1.5
Galena	600	700
Gold quartz and pyrite	7.5	7
Glauconite	10	7
Hemimorphite	3.5	7
Hydrozincite	30	15
Molybdenite	10	15
Niccolite	50	70
Psilomelane	.5	1.5
Pyrrhotite	3.5	7
Pyrite	4	3
Pentlandite	4	3
Smaltite	>1600	700
Scheelite	400	700
Thorite	>8	1.5
Tetrahedrite	4000	7000
Anglesite	500	1500
Antimony	200	300

NOTE.—Figures are reported to the nearest number in the series 7, 3, 1.5, 0.7, 0.3, 0.15, etc., in percent, and converted to parts per million.
60 percent of the reported results may be expected to agree with the results of quantitative methods.

Silver standard solution, 0.01 percent in 0 1N HNO_3: Dissolve 0.158 g of $AgNO_3$, in 1,000 ml of 0.1N HNO_3 solution.

Culture tubes, 16- by 150-mm: Calibrate at 5 and 10 ml.

Culture tubes, 18- by 150-mm: Calibrate at 5 ml.

Electric hot plate with magnetic stirrer.

Aluminum block, drilled to accommodate 16-mm culture tubes. Hot plate, magnetic stirrer, and block with capacity of 13 tubes are available commercially.

Magnets: teflon-coated bars, 0.5 in. long.

Water bath, aluminum, 7-in × 13-in, 5-in deep: The temperature of the water bath must be between 98° and 100° C. Add sodium chloride as necessary to raise boiling point at higher altitudes.

Test-tube rack, to accommodate 18-mm culture tubes: A woven-wire rack with handles to fit in water bath with capacity of 48 tubes.

Test-tube rack, to accommodate 16-mm culture tubes, capacity 48 tubes.

2 automatic pipets, 5 ml.

Pipets, measuring, 10 ml, calibrated in 0.1 ml.

Pipets, measuring, 1 ml, calibrated in 0.01 ml.

Pipets, micro, 0.005 ml.

Scoops, 0.2 g, 0.5 g, and 2 of 1-g capacity.

PROCEDURE

Sample solution

1. Place 1 g (or one 1-g scoopful) of the finely powdered sample in a 16- by 150-mm culture tube.
2. Add one Teflon-covered magnet and 5 ml concentrated HNO_3.
3. Place the tube, containing sample and HNO_3, in the aluminum heating block over a magnetic stirrer and allow the acid to boil for 30 minutes. Adjust the heat so that the upper portion of the culture tube serves as a condenser, thus conserving the HNO_3.
4. Add 5 ml of demineralized water and again heat to boil.
5. Allow to cool.

Extraction

1. Add 5 ml of the TOTP solution to the contents of the culture tube, stopper the tube with a cork, and shake the tube for 1 minute.
2. Allow the phases to separate and transfer the organic phase with an automatic pipet to a second 16- by 150-mm culture tube.
3. Add 10 ml 0.3N HCl to the second tube, stopper with a clean cork, and shake the tube for 1 minute.
4. Remove and discard the organic phase with an automatic pipet.

Oxidation of TOTP in 0.3N HCl extract

1. Transfer 5 ml of the 0.3N HCl extract to an 18- by 150-mm culture tube. If a smaller aliquot is taken make the volume up to 5 ml with 0.3N HCl.
2. Add 1-g scoopful of $K_2S_2O_8$, place in a boiling water bath at 98°–100°C and heat for 10 minutes.
3. Remove and cool the solution.

Estimation

1. To the cool solution add 1 ml of H_3PO_4, 1 ml of $MnSO_4$ solution, 5 ml of demineralized water, and 5–6 1-g scoopfuls of $K_2S_2O_8$.
2. Mix thoroughly with glass stirring rod and again place in boiling water bath.
3. After heating for 10 minutes at 98°–100°C, remove the sample solution from the boiling water bath and chill rapidly in an ice bath.

4. When cold, crush with a stirring rod the crystals of $K_2S_2O_8$ and K_2SO_4 that crystallized on cooling. Leave in ice bath until the upper inch or so of the permanganate solution is clear.
5. Compare the sample solution with standards prepared at the same time.

Preparation of standards

Pipet 10 γ of Ag into a tube containing 5 ml of 1+1 HNO_3. Add 5 ml of TOTP and shake for 1 minute. Allow the phases to separate and transfer the organic layer to a second tube containing 10 ml of 0.3N HCl. Shake for 1 minute and discard organic layer. Transfer appropriate aliquots of the HCl solution, corresponding to 0, 0.005, 0.01, 0.05, 0.1, 0.2, 0.4, and 0.8 γ of Ag, into tubes containing 5 ml of 0.3N HCl. Add 1 g of $K_2S_2O_8$ to each tube and heat in boiling water bath at 98°–100°C for 10 minutes. Cool and add 1 ml of H_3PO_4, 1 ml of $MnSO_4$, 5 ml of demineralized water and approximately 5–6 g of $K_2S_2O_8$. Place in boiling water bath and proceed as with sample. The acid permanganate solution fades slowly, so standards must be made with each group of samples. The samples and standards may be kept in an ice bath for about an hour without any noticeable fading.

REFERENCES

Almond, Hy, Stevens, R. E., and Lakin, H. W., 1949, A confined-spot method for the determination of traces of silver in soils and rocks, pt. 7 of Contributions to geochemistry, 1949: U.S. Geol. Survey Bull. 992, p. 71–81.

Handley, T. H., and Dean, J. A., 1960, Triakyl thiophosphates—selective extractants for silver and mercury: Anal. Chemistry, v. 32, p. 1878.

Hillebrand, W. F., Lundell, G. E. F., Bright, H. A., and Hoffman, J. I., 1953, Applied inorganic analysis, 2d ed.: New York, John Wiley and Sons, 1034 p.

Kodama, Kazunobu, 1963, Methods of quantitative inorganic analysis: New York, Interscience Publishers, 507 p.

Lai, M. G., and Weiss, H. V., 1962, Cocrystallization of ultramicro quantities of elements with thionalid—Determination of silver in seawater: Anal. Chemistry, v. 34, no. 8, p. 1012–1015.

Sandell, E. B., 1959, Colorimetric metal analysis, 3d ed: New York, Interscience Publishers, p. 802–820.

Snell, F. D., Snell, C. T., and Snell, C. A., 1959, Colorimetric methods of analysis including photometric methods, v. IIA: Princeton, N.J., D. Van Nostrand Company, 793 p.

Underwood, A. L., Burrill, A. M., and Rogers, L. B., 1952, Catalytic determination of submicrogram quantities of silver: Anal. Chemistry, v. 24, p. 1597.

DIURNAL VARIATIONS OF THE CHEMICAL QUALITY OF WATER IN TWO PRAIRIE POTHOLES IN NORTH DAKOTA

By HUGH T. MITTEN, Sacramento, Calif.

Abstract.—Maximum (or minimum) values for the concentrations of dissolved oxygen and CO_3^{-2}, and the ratio of the ion activity product to the equilibrium constant for calcite (IAP/K_{eq}) in the water of two prairie potholes occurred at about the times of highest (or lowest) temperature. The concentration of HCO_3^{-1} did not vary consistently with time or temperature, and concentration of dissolved oxygen decreased as the concentration of CO_2 in the water increased. Water in both potholes was supersaturated with calcite. The presence of a colloidal or undissociated form of calcium carbonate, or the effects of organic matter, may be responsible for the apparent lack of calcite in the top part of the bed of one pothole.

Thousands of depressions known as prairie potholes dot the surface of the Coteau du Missouri in North Dakota (Shjeflo and others, 1962). Atmospheric precipitation, evapotranspiration, ground-water movement, and solution of deposited salts cause large fluctuations in water quality in most of these potholes. Moreover, the chemical quality of water may differ considerably from one pothole to another. This paper describes diurnal variations in concentrations of HCO_3^{-1}, CO_3^{-2}, and dissolved oxygen, and the equilibrium conditions with respect to calcite, in the water of prairie potholes.

The Coteau du Missouri forms the eastern edge of the Missouri Plateau glaciated section of the Great Plains physiographic province (fig. 1). The Coteau characteristically has poorly drained knob-and-kettle topography and local relief of 20 to 100 feet. It is underlain by glacial drift of variable thickness; most of the drift is till, but stratified ice-contact and outwash deposits occur locally. Probably most of the potholes were formed as irregularities in the moraine due to uneven distribution of the drift. Many of the potholes, however, may be kettles; a distinction between origins generally is difficult.

Data were collected at two potholes in Dickey County, N. Dak., pothole A in the SE¼NW¼, SW¼NE¼ sec. 16, T. 129 N., R. 66 W., and pothole B in the SW¼SE¼ sec. 19, T. 129 N., R. 66 W. These potholes,
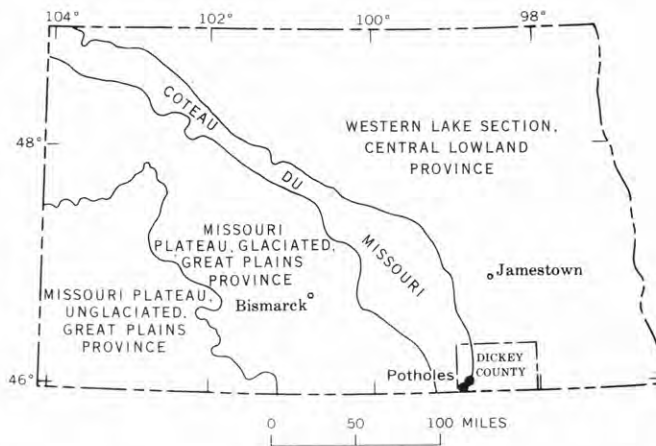
FIGURE 1.—Index map of North Dakota, showing physiographic units and location of the prairie potholes investigated (after Lemke, 1960).

which are numbered 5 and 6A in a broad study of prairie potholes by the U.S. Geological Survey, will be referred to as potholes A and B, respectively, in this paper. Both potholes have an elliptical outline and gently sloping bottoms, and each had a water-surface area of about 15 acres and a depth of 2 to 3 feet at time of sampling. Each pothole is in the bottom of a depression surrounded by low rounded grass-covered hills. At pothole B, emergent vegetation—mostly cattails—extends outward about 50 feet from the shore. No emergent vegetation was present in pothole A or in the central part of pothole B, but suspended green algae were abundant in both potholes.

Water samples were collected in late August and early September 1963, about every 2 hours over a period of about 30 hours at pothole A, and for about 46 hours at pothole B. The samples were collected from a rubber raft at a reference point near the center of each pothole. All samples were collected about 1 foot below the water surface. Samples intended for the determination of calcium, magnesium, and iron

were acidified and filtered; those for the determination of other major constituents were not treated in the field. Sufficient field measurements of pH, alkalinity, air and water temperatures, and the altitudes of the sampling sites, were made to permit calculation of the ionic strength of the solution and of the total concentration of the carbonate species (Barnes, 1964; Hem, 1961). The dissolved-oxygen content of the water water also was determined in the field.

Analytical results were tabulated with a computer program prepared by Fred Sower of the Computation Branch of the U.S. Geological Survey. This program provides a thermodynamic description of the natural waters and used the analytical values from the standard laboratory analyses for all but the carbonate species, which were determined by field titration. This program can be used to compare the analyzed amount of the calcium ion with the amount required to equilibrate the water with calcite if carbonates are in solution. Calcite and aragonite, as described by Back (1961), are the stable phases of $CaCO_3$ at the temperatures and pressures of the earth's surface. The equilibrium for calcite was considered in this study.

Pothole A contained a magnesium sulfate type of water, and pothole B contained a magnesium sulfate bicarbonate type (table 1). The water in both potholes, however, also contained significant concentrations of calcium. The concentrations of all constituents varied no more than a few parts per million throughout the sampling period. Sampling and laboratory errors can account for most of these variations. However, temperature, amount of dissolved oxygen, ratio of ion activity product to equilibrium constant for calcite, and concentration of CO_3^{-2} changed consistently with the time of day (figs. 2 and 3).

TABLE 1.—*Typical quality of water in potholes A and B during sampling period*

[Results in equivalents per million]

	Pothole A	Pothole B
Date	Aug. 31, 1963	Sept. 4, 1963
Time	2130	2200
Calcium (Ca)	7. 48	3. 99
Magnesium (Mg)	26. 16	7. 07
Sodium (Na)	6. 35	1. 35
Potassium (K)	1. 15	. 69
Bicarbonate (HCO₃)	4. 72	6. 12
Carbonate (CO₃)	. 21	. 39
Sulfate (SO₄)	35. 81	6. 54
Chloride (Cl)	. 51	. 25

The concentration of dissolved oxygen is dependent on photosynthesis, which in turn is related to water temperature and the distribution of sunlight hours. Photosynthetic activity and, therefore, the concentration of dissolved oxygen reached a peak in the afternoon and a low point in the early morning. During the day, plants use carbon dioxide and give off oxygen;
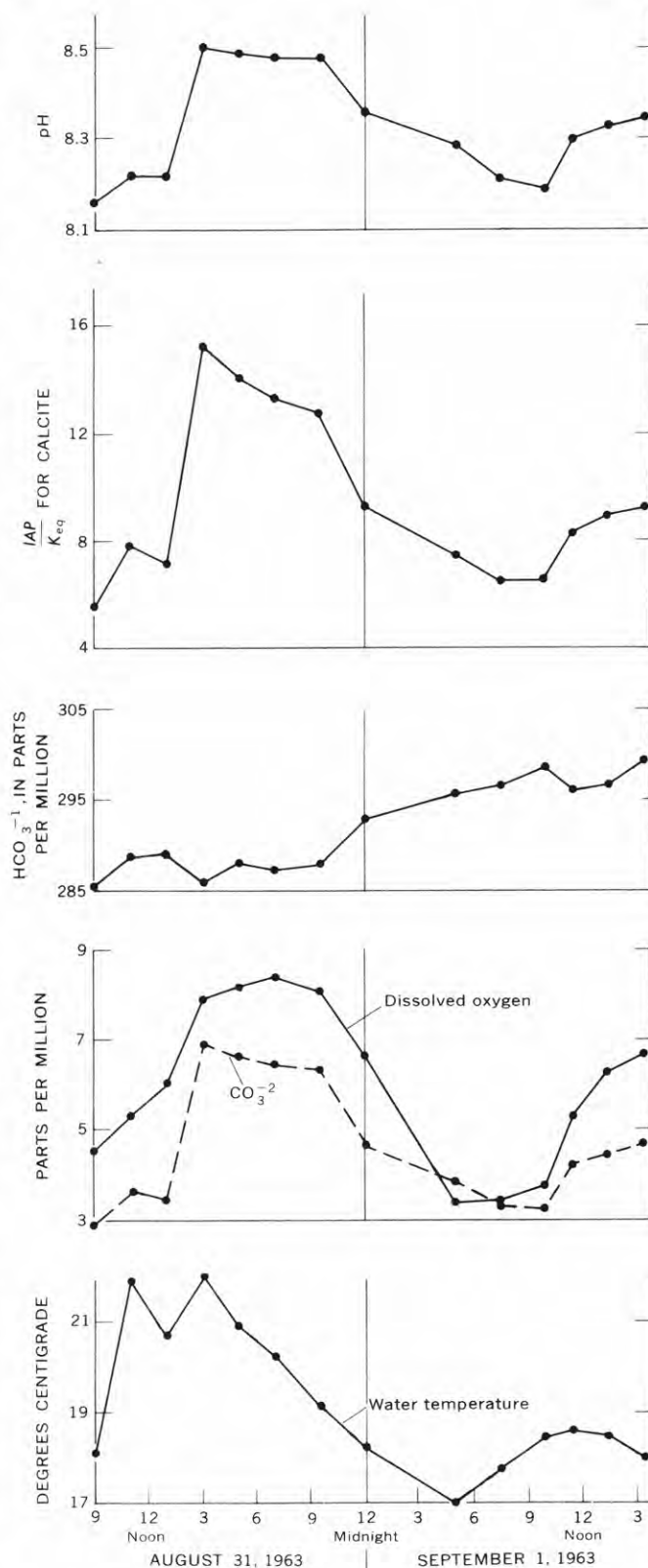
FIGURE 2.—Graphs of data from pothole A, showing time versus concentration of CO_3^{2-}, HCO_3^{-1}, and dissolved oxygen; and time versus water temperature, pH, and IAP/K_{eq}.
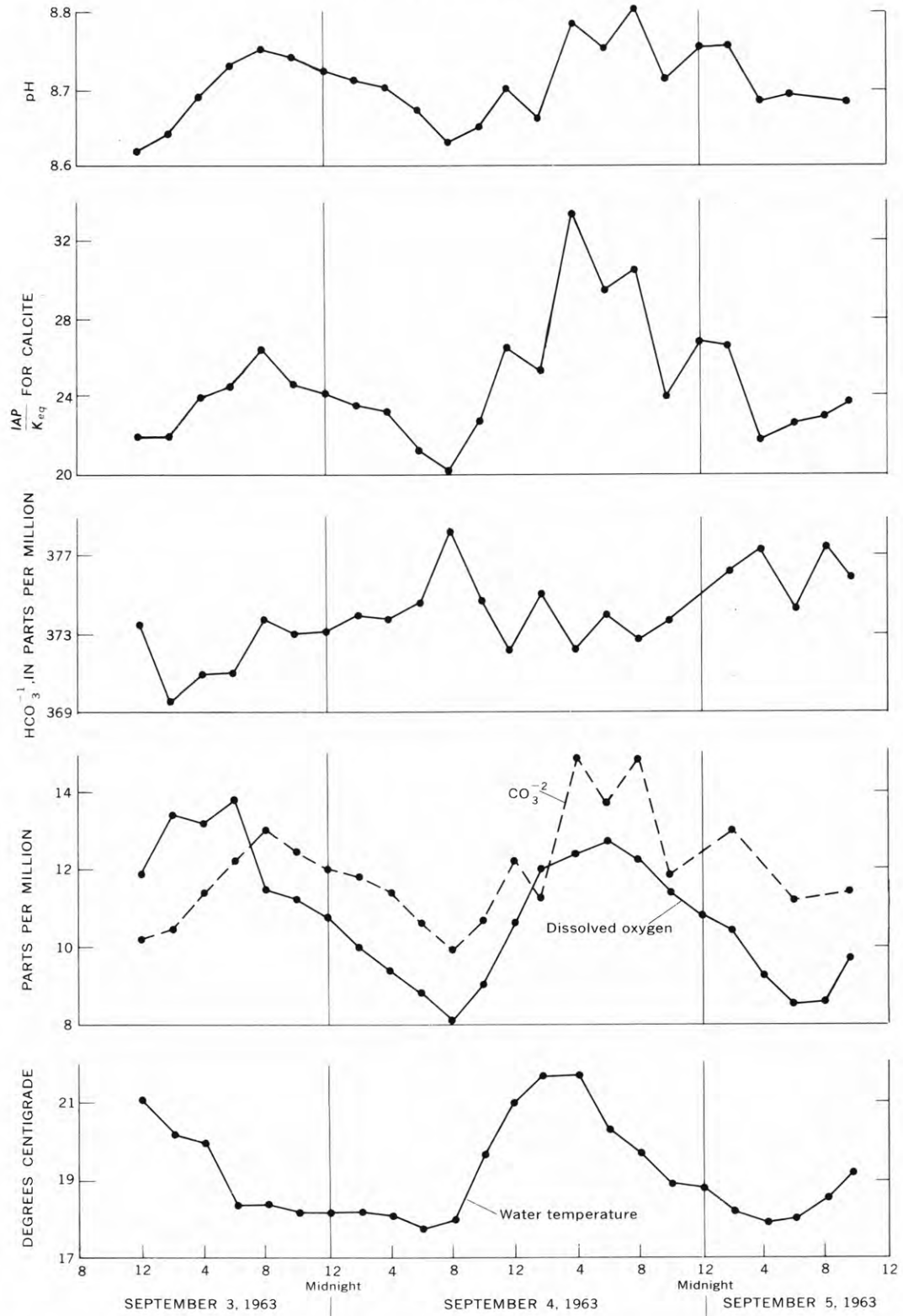
FIGURE 3.—Graphs of data from pothole B, showing time versus concentration of CO_3^{-2}, HCO_3^{-1}, and dissolved oxygen; and time versus water temperature, pH, and IAP/K_{eq}.

during the night, they use oxygen and give off carbon dioxide. The relations between the concentrations of carbon dioxide as determined from computer analysis and dissolved oxygen as determined in the field are shown on figure 4. The anomalous points above the curve for pothole B are from data collected during the first part of the study and probably were caused by high concentrations of carbon dioxide or dissolved oxygen in rain that fell in pothole B just before the sampling began.

In most natural surface waters, pH is dependent on the carbonate equilibria, which in turn are related to temperature. Although the concentration of HCO_3^{-1} did not change consistently with temperature, generally the highest (or lowest) values for pH and for the concentration of CO_3^{-2} occurred at or shortly after the times when the water temperatures were highest (or lowest) in the potholes (figs. 2 and 3).

Table 2 shows values for pH, CO_3^{-2}, and HCO_3^{-1} determined in the field at the time that the samples were collected, and the corresponding values for the same samples determined in the laboratory about 2 months later. The pH and concentration of CO_3^{-2} decreased in the samples from both potholes; the concentration of HCO_3^{-1} decreased slightly in the samples from pothole A, and remained about the same in samples from pothole B. Such changes may have been caused by loss of CO_2 from the solutions through the polyethylene sample bottles, or by loss of CO_2 when the bottles were opened in the laboratory, after photosynthetic action during the interval between collection and analysis. As has been pointed out by other workers (Back, 1961, p. 10; Roberson and others,

1963) analyses for alkalinity and pH intended for the study of mineral equilibria should be made in the field.

TABLE 2.—*Change in field and laboratory values for HCO_3^{-1}, CO_3^{-2}, and pH*

Sample collected		pH		Bicarbonate (HCO₃) (ppm)		Carbonate (CO₃) (ppm)	
Date in 1963	Time	Field	Laboratory	Field	Laboratory	Field	Laboratory
Pothole A							
Aug. 31____	0900	8. 16	7. 78	286	280	2. 8	0
Do_____	1500	8. 50	7. 79	286	280	6. 9	0
Do_____	2130	8. 48	7. 63	288	281	6. 3	0
Pothole B							
Sept. 3_____	1600	8. 69	8. 00	371	374	11	0
Do_____	2200	8. 74	7. 92	373	373	12	0
Sept. 4_____	0400	8. 70	7. 89	374	374	11	0

As was discussed by Garrels (1960) and by Back (1961), if calcite and all ionic species dissolved in the water are in equilibrium, calcium carbonate saturation in water depends on the following reactions:

$$CaCO_3 \text{ (calcite)} \rightleftharpoons Ca^{+2} + CO_3^{-2} \qquad (1)$$

$$CO_3^{-2} + H^{+1} \rightleftharpoons HCO_3^{-1} \qquad (2)$$

$$HCO_3^{-1} + H^{+1} \rightleftharpoons CO_2 + H_2O \qquad (3)$$

$$H^{+1} + OH^{-1} \rightleftharpoons H_2O \qquad (4)$$
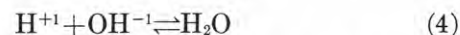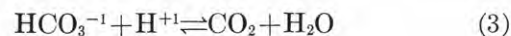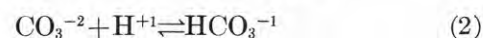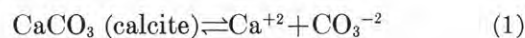
For (1) the ion activity product, IAP, by definition is

$$IAP = [Ca^{+2}] [CO_3^{-2}]$$
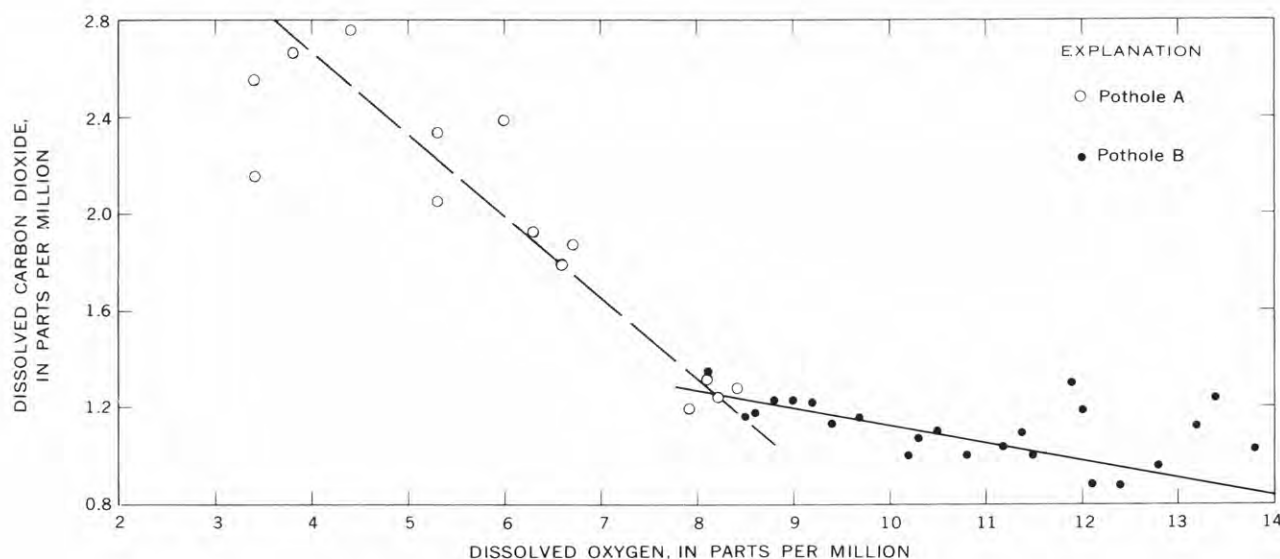
FIGURE 4.—Graphs of dissolved oxygen versus CO_2.

The activity of the calcium ion $[Ca^{+2}]$ is calculated from

$$[Ca^{+2}]=m_{Ca^{+2}}\gamma_{Ca^{+2}},$$

where $m_{Ca^{+2}}$ is the molality and $\gamma_{Ca^{+2}}$ is the ion activity coefficient determined from the Debye-Hückel equation. The activity of the carbonate ion $[CO_3^{-2}]$ is calculated from the equations

$$K_2=\frac{[H^{+1}]\,[CO_2^{-2}]}{[HCO_3^{-1}]}$$

and

$$[H^{+1}]=10^{-pH}$$

and

$$[HCO_3^{-1}]=m_{HCO_3^{-1}}\gamma_{HCO_3^{-1}},$$

where K_2 is the second dissociation of carbonic acid. The pH is measured in the field; $[HCO_3^{-1}]$ is determined from the concentration of bicarbonate, $m_{HCO_3^{-1}}$, from field data; and $\gamma_{HCO_3^{-1}}$ is calculated from the Debye-Hückel equation.

The ratio of IAP for (1) to the equilibrium constant for calcite (K_{eq}) for (1) indicates the degree of saturation of calcite in water. At any temperature, if $IAP/K_{eq}=1$ the solution is saturated with respect to calcite; if $IAP/K_{eq}>1$ the solution is supersaturated; and if $IAP/K_{eq}<1$ the solution is unsaturated.

The ratio IAP/K_{eq} for calcite varied diurnally in potholes A and B; high (or low) values occurred about the same time that the water temperatures were highest (or lowest). In both potholes all values of IAP/K_{eq}

for calcite exceed 1; therefore, the waters in both potholes are supersaturated with respect to calcite, and calcite might have been expected to have been precipitated from solution. However, B. F. Jones (written communication, 1964) found that a mud sample from the top of the bed of pothole B contained no calcite, dolomite, or magnesite. The sample contained more than 50 percent quartz and organic material, and subordinate but roughly equal amounts of montmorillonite, plagioclase, and mica. The reason for lack of precipitated carbonate is not clear; calcium carbonate may be in a colloidal or undissociated form, or the effects of organic matter may be responsible.

REFERENCES

Back, William, 1961, Calcium carbonate saturation in ground water, from routine analyses: U.S. Geol. Survey Water-Supply Paper 1535–D, 14 p.

Barnes, Ivan, 1964, Field measurement of alkalinity and pH: U.S. Geol. Survey Water-Supply Paper 1535–H, 17 p.

Garrels, R. M., 1960, Mineral equilibria at low temperature and pressure: New York, Harper and Brothers, 254 p.

Hem, J. D., 1961, Calculation and use of ion activity: U.S. Geol. Survey Water-Supply Paper 1535–C, 17 p.

Lemke, R. W., 1960, Geology of the Souris River area, North Dakota: U.S. Geol. Survey Prof. Paper 325, 138 p.

Roberson, C. E., Feth, J. H., Seaber, P, R., and Anderson, Peter, 1963, Differences between field and laboratory determinations of pH, alkalinity, and specific conductance of natural water: Art. 115 in U.S. Geol. Survey Prof. Paper 475–C, p. C212–C215.

Shjeflo, J. B., and others, 1962, Current studies of the hydrology of prairie potholes: U.S. Geol. Survey Circ. 472, 11 p.

PHYSICAL AND CHEMICAL HYDROLOGY OF GREAT SALT LAKE, UTAH

By D. C. HAHL, M. T. WILSON, and R. H. LANGFORD,
Salt Lake City, Utah

Abstract.—Since 1851 the stage of Great Salt Lake has ranged from a high of 4,211.6 feet above mean sea level (in 1873) to a low of 4,191.35 feet (in 1963). In 1873 and 1963 the dissolved-solids concentrations of the brine were about 15 and 28 percent, respectively, but the composition of the dissolved solids remained virtually constant. About 2 million tons of dissolved solids (chiefly sodium and chloride) and 1 million acre-feet of water annually were contributed to the lake by surface sources during the 1960 and 1961 water years. In 1873 the lake contained about 6 billion tons of solids in about 30 million acre-feet of water, and in 1963 about 4 billion tons in about 9 million acre-feet. Two parts of the lake separated by a causeway built in 1957 are affected differently by inflow and evaporation. The resulting differences in density and head cause two-directional flow, near the surface and at depth, respectively, through culverts in the causeway and probably through the fill itself.

Levels of closed lakes change continuously in response to climatic changes and tend to maintain equilibrium between inflow to the lakes and evaporation from their surfaces. The chemical characteristics of lake water change with changes in stage and volume. A general downward trend in the level of Great Salt Lake since the early 1870's has long been of concern and has caused speculation regarding possible desiccation of the lake. Changes in the lake's chemical composition, which affect the commercial extraction of minerals from the brine and the recreational uses of the lake, have been of more recent concern. In recent years the U.S. Geological Survey has studied the chemical hydrology of Great Salt Lake and its surficial inflow in cooperation with the University of Utah and the Utah Geological and Mineralogical Survey. Recent studies, which have shown the hydrology of Great Salt Lake to be very complex, are being continued to gather information systematically on the physical and chemical characteristics of the lake. This article reviews changes in stage and salinity of the lake since records began in 1851, describes the results of a mineral-inflow study made

during the water years 1960–61, discusses the chemical character of the lake brine, and presents some results of the current study of mineral transport within the lake.

Great Salt Lake, in northern Utah and the northeastern part of the Great Basin, is the largest surface-water body in the Western Hemisphere which does not drain to the ocean. It is the remnant of Lake Bonneville, a Pleistocene lake which, while not directly associated with continental glaciation, was formed as a result of the same climate which caused extensive glaciation. Lake Bonneville had an area of about 20,000 square miles at its highest level during late Pleistocene time; it reached a depth of 1,000 feet before overflowing the rim of the basin at Red Rock Pass, about 20 miles northwest of Preston, Idaho, and discharging to the ocean through the Portneuf, Snake, and Columbia Rivers. With the return of warm and dry climate, evaporation from the lake surface exceeded inflow and the lake receded.

CHANGES IN WATER LEVEL

When the pioneers reached Great Salt Lake in 1847 its water-surface elevation was about 4,200 feet above mean sea level (fig. 1) and its maximum depth was about 35 feet. During a series of wet years from 1862 to 1868 the stage of the lake rose almost 12 feet; precipitation for that 7-year period provided a greater water supply to the Great Basin than for any similar period during the past several hundred years. Evidence from shorelines and vegetation (Gilbert, 1890, p. 242–243) shows that for some centuries the level of the lake had been lower than that recorded in 1865. The maximum recorded elevation of the lake was 4,211.6 feet in 1873, but during a series of dry years from 1873 to 1904 the stage receded almost 16 feet. Since 1904 the lake level has fluctuated between about
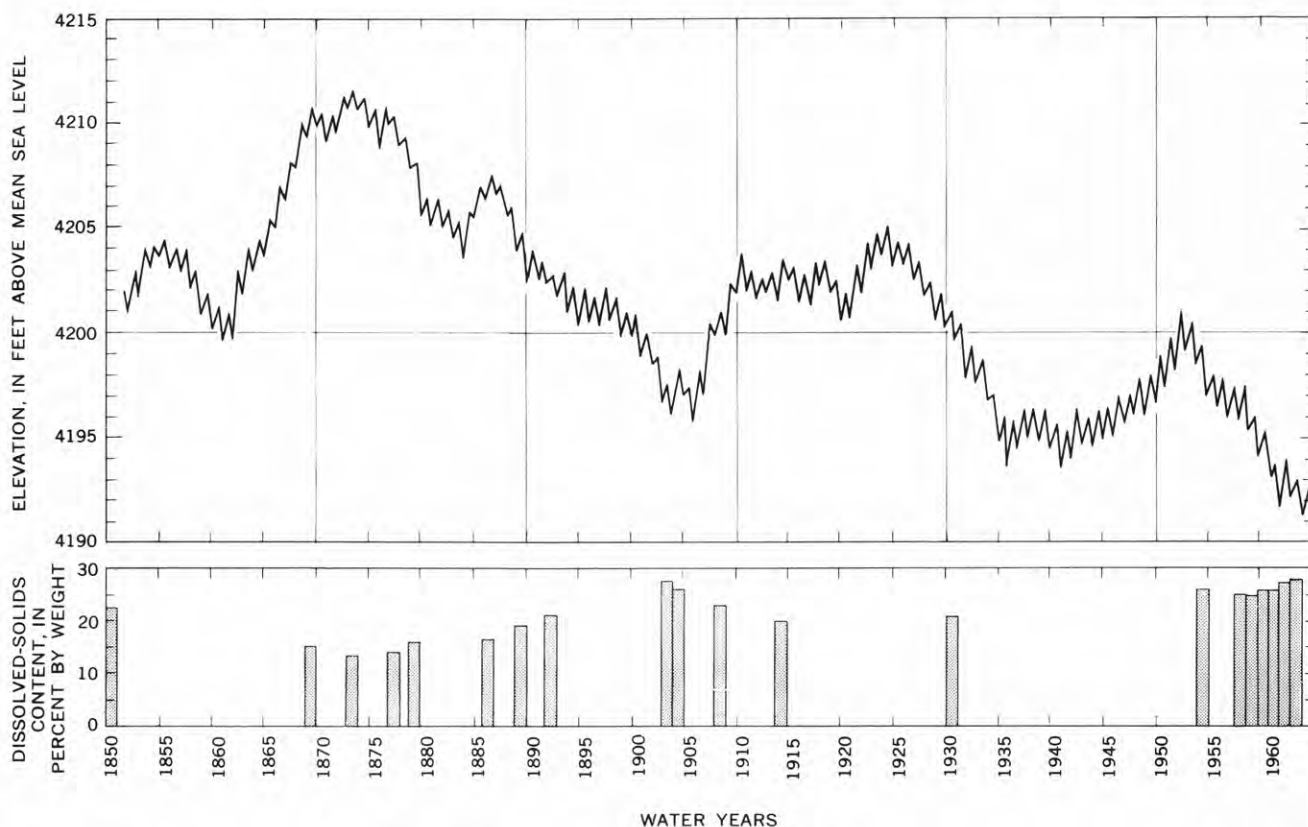
FIGURE 1.—Hydrograph of Great Salt Lake (above), showing yearly maximum and minimum lake-surface elevations, 1851–1963; and bar graph showing the dissolved-solids content of the brine (below).

4,191 and 4,205 feet; the greatest decrease in stage (11 feet) was during the drought period of the late 1920's and early 1930's. The lowest stage recorded was 4,191.35 feet, on November 1, 1963.

Large changes in streamflow are soon reflected by changes in lake stage. During 1907 the lake stage increased 3 feet, and during 1909, 2 feet. During the drought years of 1931, 1934, and 1961 the stage of the lake dropped about 2 feet each year. Although the stage is affected by increased consumptive use of water in the basin, the general downward trend since 1873 does not necessarily mean that the lake will dry up in the near future. The lake tends to maintain a balance between the amount of water evaporated from its surface and the amount of water contributed to it by surface streams, by ground-water inflow, and by precipitation on its surface. During a period of dry years the stage falls, the surface area decreases rapidly, and the mineralization increases. All these changes favor decrease in the total volume of evaporation, and less inflow is required to maintain the lower lake stage. Conversely, during a period of wet years the stage rises, the surface area increases appreciably, and mineralization decreases; thus, a larger volume of

evaporation compensates for the greater inflow. Over a period of years the lake's surface elevation therefore tends to stabilize. At the high stage in 1873 the area of the lake's surface was about 2,400 square miles; at the low stage in 1963 it was about 940 square miles.

DISSOLVED-MINERAL INFLOW

Preliminary findings of Diaz (1963) show that the Bear River and the drains which discharge municipal and industrial waste water contributed more than half of the 2 million tons of dissolved solids that entered Great Salt Lake in 1960 from surface sources; the Jordan River and the springs which discharge near the lakeshore contributed about one-third. These findings were substantiated in a later report (Hahl and Langford, 1964) in which similar data were presented for the 1961 water year. Although the dissolved-solids inflow was less during 1961 (1.7 million tons), the relative amounts contributed by the several sources remained the same as in 1960. Ground-water inflow during 1960 and 1961 was estimated to be half a million acre-feet annually, and the dissolved-solids load contributed by ground water was estimated to be half a million tons annually.

About 82 percent of the surface inflow of water to the lake during the water years 1960–61 came from the Bear, Jordan, and Weber Rivers; however, only about 55 percent of the dissolved-mineral load was contributed by these three rivers. The remainder of the mineral load was contributed chiefly by springs, drains, and sewage canals (Hahl and Langford, 1964).

The most abundant dissolved mineral constituents entering the lake during the 2-year period were sodium and chloride. Figure 2 shows the chemical characteristics of surface inflow to the lake from its major tributaries. The constituents of the dissolved solids in the surface inflow during the 1960 and 1961 water years are shown in table 1.

TABLE 1.—*Constituents of the dissolved solids, in percent by weight*

Silica, SiO_2	1. 3
Calcium, Ca^{+2}	7. 1
Magnesium, Mg^{+2}	3. 7
Sodium, Na^{+1}	22. 7
Potassium, K^{+1}	1. 5
Bicarbonate as carbonate, CO_3^{-2}	12. 8
Sulfate, SO_4^{-2}	14. 3
Chloride, Cl^{-1}	36. 3
Nitrate, NO_3^{-1}	. 3
Total	100. 0

Downstream changes in water quality, depicted diagrammatically on figure 2, result from changes in environment. For example, most runoff in the three major streams entering Great Salt Lake originates as snowmelt or rainfall in the Uinta Mountains and Wasatch Range, in the eastern part of the drainage basin. This runoff is of the bicarbonate type and is generally of excellent chemical quality. In the lower reaches of these rivers, evapotranspiration, return flows from irrigated lands, discharge of industrial and municipal wastes, and ground-water inflow cause the water quality to change; sodium, chloride, and sulfate become major dissolved constituents.

CHEMICAL CHARACTER OF THE BRINE

The concentration of dissolved solids (in percent by weight) in the lake brine has ranged from about 15 percent during the high lake stages of the 1870's to about 28 percent during the low lake stages of the early 1900's and 1960's (fig. 1). The relation between lake stage or lake volume and dissolved-solids concentration is nearly linear between stages of about 4,195 and 4,205 feet. A preliminary review of historical data indicates that the dissolved-solids concentration of the brine appears to approach a maximum of 28 to 29 percent when lake volume is less than about 10 million acre-feet, and a minimum of 13 to 14 percent when volume is 25 to 30 million acre-feet.

Although the dissolved-solids concentration of the brine changes with time, the percentage composition of the dissolved solids has remained constant over the past hundred years. Sodium and chloride are the predominant constituents; sulfate, magnesium, and potassium are present in lesser amounts; and calcium, bicarbonate, and other substances are minor constituents. Extremes observed during 1959–61, average concentrations of individual constituents dissolved in the brine of the southern arm of the lake, and discharge-weighted average concentrations of surface inflow are given in table 2.

TABLE 2.—*Concentrations of dissolved constituents in Great Salt Lake brine and surface inflow, 1959–61*

[Concentrations in parts per million unless otherwise indicated]

Constituent or property	Great Salt Lake			Surface inflow (discharge-weighted average) [3]
	Maximum [1]	Minimum [1]	Average [2]	
Silica (SiO_2)	7. 0	4. 2	5. 3	18
Aluminum (Al)	2. 6	2. 5		
Iron (Fe)	. 11	. 02	. 04	
Calcium (Ca)	463	265	319	94
Magnesium (Mg)	9, 440	6, 920	8, 050	49
Sodium (Na)	92, 200	77, 800	85, 700	300
Potassium (K)	5, 570	3, 810	4, 550	20
Lithium (Li)	56	29		
Bicarbonate (HCO_3)	398	266	327	344
Sulfate (SO_4)	22, 600	12, 100	17, 400	188
Chloride (Cl)	158, 000	133, 000	147, 000	475
Fluoride (F)	7. 4	5. 9		
Iodide (I)	. 60	. 26	. 41	
Nitrate (NO_3)	154	61	82	4. 1
Boron (B)	36	21		
Dissolved solids, calculated	285, 000	240, 000	263, 000	1, 320
Density, g/ml at 20°C	1. 221	1. 186	1. 208	1. 000

[1] Observed extremes (from analyses of samples collected in southern arm of lake during June 1959–November 1961).
[2] Average of analyses of samples collected in southern arm of lake in April, July, and October 1960, and January–February 1961.
[3] For water years 1960 and 1961.
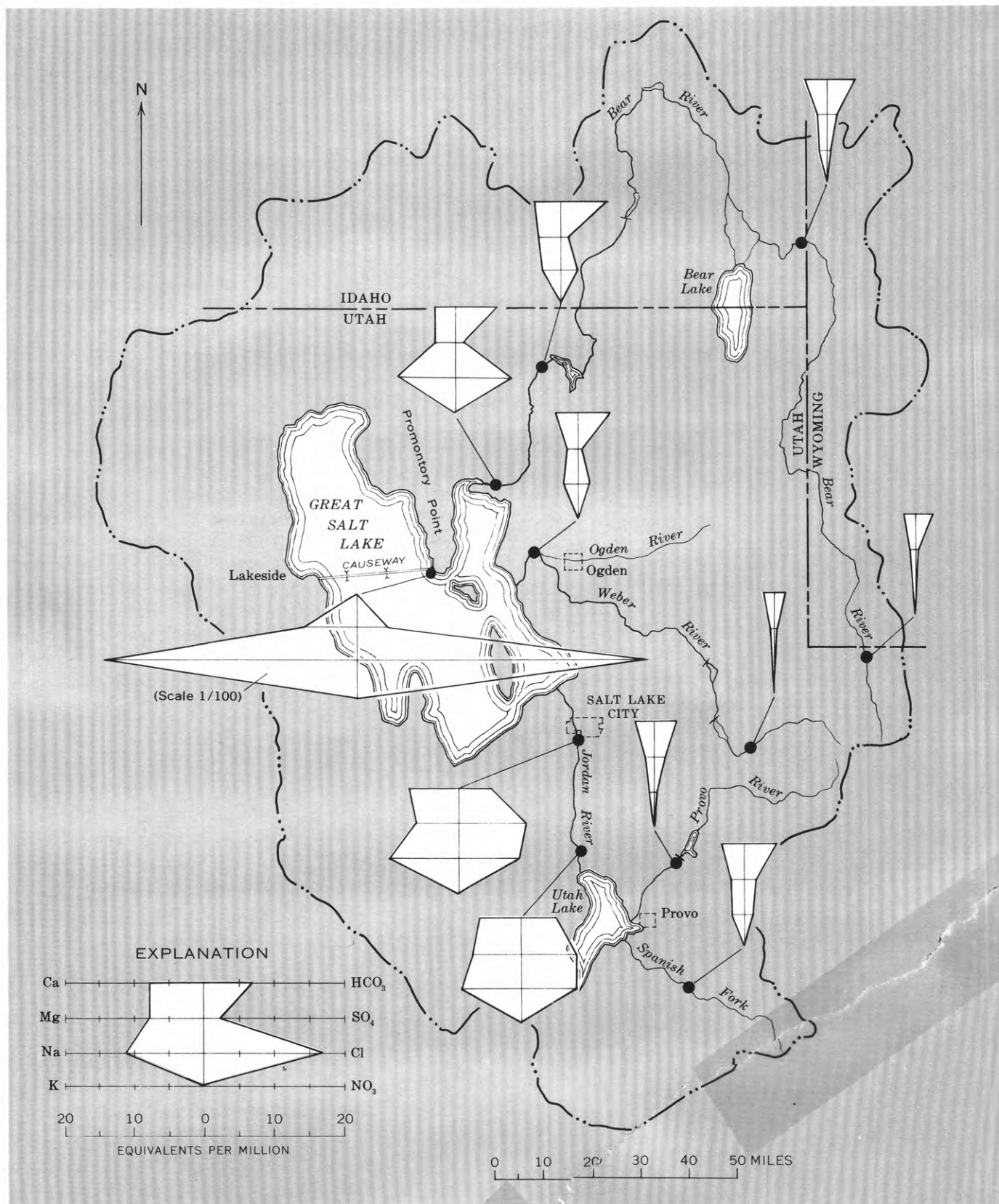
FIGURE 2.—Chemical quality of water at selected sampling sites in the Great Salt Lake basin (enclosed by dashed and dotted line). Sampling sites are shown by large dots, and the dissolved-solids content of the water is indicated by chemical diagrams. The horizontal scale of the chemical diagram for Great Salt Lake is only 1/100 of that of the other diagrams.

The amount of mineral matter dissolved in the brine also fluctuates with lake volume. In 1873, when the lake was at its highest recorded stage, the lake volume was about 30 million acre-feet and the brine contained about 6 billion tons of dissolved solids. In contrast, at the low stage of November 1963, the volume was about 8.7 million acre-feet and the brine contained about 4 billion tons of dissolved solids.

Because the dissolved-solids concentration of the brine is about 200 times that of the surface inflow (table 2), it is virtually unaffected by the minerals being delivered to the lake each year. The effect of inflow is to change the volume of the lake and, thus, to act as a diluent. With increasing volume the dissolved-solids concentration of the brine decreases, but the total amount of mineral matter dissolved in the brine increases. This increase in total dissolved solids seems to result mainly from re-solution of salts that had been precipitated on the lakebed and shore or otherwise left behind as the volume was decreasing. Therefore, the chemical characteristics of the brine are controlled mainly by the minerals dissolved in the brine and by the salts on the lakebed which are available for solution. Physiographic features of the lakebed, and aquatic life in the brine, may also affect the dissolved-solids concentration and chemical character of the brine.

EFFECT OF A CAUSEWAY ON CONCENTRATION

In the late 1950's a causeway was constructed across the lake between Promontory Point and Lakeside. As a result, one-third of Great Salt Lake is now separated from the main body of brine by a permeable fill of quarry-run rock. Two culverts, each 15 feet wide, allow free flow of brine through the fill to a depth of about 10 feet (the lake here is about 25 feet deep). The southern arm of the lake is fed mainly by relatively fresh water from the major tributaries (Bear, Weber, and Jordan Rivers), but the northern arm has been fed (since 1957) mainly by brine which flows northward through the fill and culverts. Therefore, the dissolved-solids concentration in the northern arm probably will fluctuate less, and the brine will become more concentrated there, than in the southern arm. The amount of seasonal change in concentration in the southern part of the lake is determined largely by the amount of inflow from the major tributaries. During years of low runoff, the lake volume decreases and the brine approaches saturation; during years of high runoff the volume increases and the brine becomes less concentrated.

Because about 95 percent of the total surface inflow (about 2 million acre-feet per year as a long-term average) enters the southern arm of the lake, the water level there is higher during the season of greatest inflow than in the northern arm, and brine movement should be from the southern to the northern arm. Inflow is greatest during the spring and is relatively small during the summer months when evaporation is the greatest. When evaporation equals inflow, usually during the months of July and November, the levels of the lake on each side of the causeway approach equilibrium. Flow through the fill during these periods should be small except when other influences such as wind increase the level on one side and decrease it on the other. On several occasions after periods of calm weather, however, flow from the northern to the southern arm of the lake was observed. Velocity profiles in the culverts, measured twice within 3 weeks during the fall of 1963, showed that the upper 4 feet of water in the culverts flowed northward while the lower 5 feet flowed southward. On November 14, 1963, the difference in head between the mean lake surface on the southern and northern sides of the fill was about three-fourths of an inch. The brine flowing northward had a density about 2 percent less than that of the brine flowing southward. On the basis of these observations we conclude that density differences coupled with small head differences probably can cause opposing flows to occur simultaneously through the fill as well as through the causeway openings.

Older observations, of which there are relatively few, suggest that there are no great differences in concentration from point to point in the lake or from one part of a vertical section to another. Recent data indicate, however, that inflowing tributary waters and precipitation falling on the lake tend to form a layer at the lake surface which persists for some time before the fresher water mixes with the brine beneath. Such a layer, observed in the lake about 12 miles from the mouth of Bear River, south of the causeway, and west of Promontory Point, seemed to persist for several weeks in spite of a moderate windstorm during that period.

These discoveries of simultaneous two-directional flow between the two arms of the lake, and of the presence of a layer of dilute water on the surface of the brine, which show the chemical and physical environment in Great Salt Lake to be more complex than was formerly realized, should be helpful in studies of evaporation from the brine and of mineral transport in the lake.

REFERENCES

Diaz, A. M., 1963, Dissolved-salt contribution to Great Salt Lake, Utah: U.S. Geol. Survey Prof. Paper 450-E, p. E163-E165.

Gilbert, G. K., 1890, Lake Bonneville: U.S. Geol. Survey Mon. 1, 438 p.

Hahl, D. C., and Langford, R. H., 1964, Dissolved-mineral inflow to Great Salt Lake and chemical characteristics of the Salt Lake brine, pt. II. Technical report: Utah Geol. and Mineralog. Survey Water-Resources Bull. 3., 40 p.

Hahl, D. C., and Mitchell, C. G., 1963, Dissolved-mineral inflow to Great Salt Lake and chemical characteristics of the Salt Lake brine, pt. I. Selected hydrologic data: Utah Geol. and Mineralog. Survey Water-Resources Bull. 3, 40 p., 1 fig.

A COMPARISON OF THE CHEMICAL COMPOSITION OF RAINWATER AND GROUND WATER IN WESTERN NORTH CAROLINA

By R. L. LANEY, Tucson, Ariz.

Abstract.—In western North Carolina, the change in the character of the dissolved constituents from rainwater to ground water is apparently rapid. Rainwater contains less than 12 ppm of dissolved solids and has a calcium sulfate-calcium bicarbonate composition. Silica makes up less than 0.2 ppm of the dissolved solids. Ground water has a mixed-cation bicarbonate composition and generally contains less than 0.4 ppm of sulfate. More than half the ground water sampled contains less than 50 ppm of dissolved solids, of which 40 to 50 percent is silica. The outstanding differences in chemical composition of these two waters result from the solution of magnesium, sodium, and silica in the ground, and the removal of sulfate. Sulfate might be removed from rainwater by anion exchange with clay minerals or by bacterial reduction.

Although shallow ground water in western North Carolina is derived largely or entirely from precipitation, there are striking differences in the composition of dissolved solids in rainwater and in ground water. In order to determine whether transitional chemical characteristics exist between these two types of water, the chemical composition of rainwater was compared with that of ground water that contains small amounts of dissolved solids.

This report presents data obtained during cooperative ground-water investigations in the Blue Ridge physiographic province of western North Carolina. The area of investigation covers about 7,200 square miles and is drained by the Hiwassee, Little Tennessee, French Broad, Yadkin, and Catawba Rivers. The mean annual precipitation ranges from less than 45 inches in the eastern part of the area to more than 75 inches at higher altitudes. The location of the area and the distribution of rainfall-sampling sites are shown on figure 1.
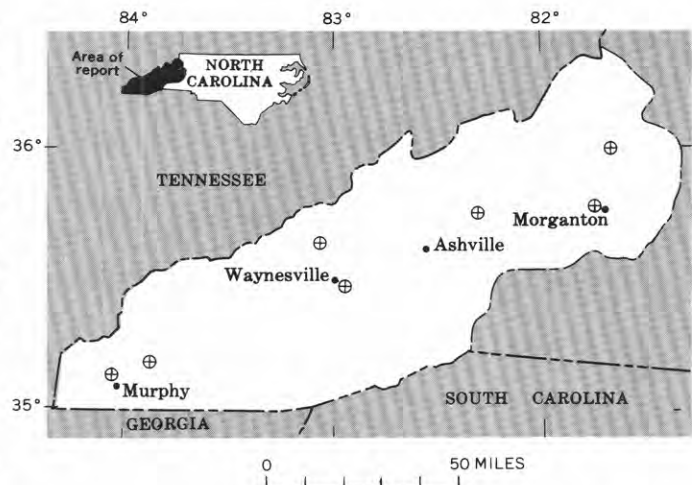
FIGURE 1.—Map of western North Carolina, showing location of sites (circled crosses) where samples of rainwater were collected.

During the sampling period, July 1962 to May 1963, a total of 33 samples of rainwater was collected at 8 U.S. Weather Bureau cooperative-observer sites. Each sampling station was equipped with a 2- by 2- by 2-foot enclosure whose top stood 5 feet above the ground. The top surface was covered with a 25- by 25-inch piece of corrugated Fiberglas that drained the rainwater into a Fiberglas-lined trough; the water then flowed through polyethylene tubing into a polyethylene bottle inside the enclosure. The collecting surface was covered with canvas between rains, so that samples of water could be collected from single rains without collecting the dust that fell between rains. Contamination introduced into the samples from the

canvas is believed to be less than that which would have come from the dust.

Three hundred and twenty-one ground-water samples were obtained from wells and springs. Where possible, samples from wells were taken at the wellhead after a brief period of pumping; where this was not possible, the samples were collected from household faucets. All samples of spring water were obtained from the reservoir overflow of improved springs.

Standard methods described by Rainwater and Thatcher (1960) were used in making all the water analyses.

The concentration of dissolved solids in the rainwater ranges from 2.2 to 11 ppm. The water has a calcium sulfate-calcium bicarbonate composition, and sulfate is the principal anion in more than half the samples. Silica concentrations range from 0.0 to 0.3 parts per million. Gambell (1963) and Gambell and Fisher (1964) show that calcium and sulfate are the principal cation and anion, respectively, in rainwater in southern Virginia and eastern North Carolina. Generally, the average concentrations of constituents in western North Carolina agree with those on maps which show isopleths of concentrations of rainwater in the United States (Junge and Werby, 1958).

In the ground water, the relative abundance of the three principal cations—calcium, magnesium, and sodium—depends on the chemical composition of the host rocks. In this area these rocks include granites, gneisses, schists, metasedimentary and metavolcanic rocks, and some ultramafic rocks. Their wide range in composition is reflected by a wide range in the composition of the solids dissolved in the ground water. Bicarbonate is the most abundant anion, and sulfate is the least abundant anion. Silica makes up 40 to 50 percent of the dissolved solids. More than half the ground-water samples contained less than 50 ppm of dissolved solids. The ground water that has a low concentration of dissolved solids is most useful for comparison with the rainwater because the purpose of this report is to look for a transitional relation in the chemical compositions of rainwater and ground water. For convenience, only ground water that contains less than 30 ppm of dissolved solids was used in the comparison. The ground-water samples used are divided into two groups—those containing 9 to 20 ppm of dissolved solids and those containing 21 to 30 ppm—to determine whether a gradual transition in chemical character exists from rainwater to ground water as the dissolved solids of the ground water increase. By this procedure three suites of analyses of approximately the same size were obtained.

The average sulfate concentration is 2.0 ppm in the rainwater but only 0.4 ppm in the ground water (see accompanying table). On the other hand, the average content of silica is 0.1 ppm in rainwater but 7.0 ppm in ground water. Ratios of principal chemical constituents in the two waters are shown in figure 2, and the groupings of points for both cations and anions show a striking difference in chemical composition of the rainwater and the ground water. On the other hand, there is little or no difference in the groupings for the two suites of ground-water analyses. Thus there
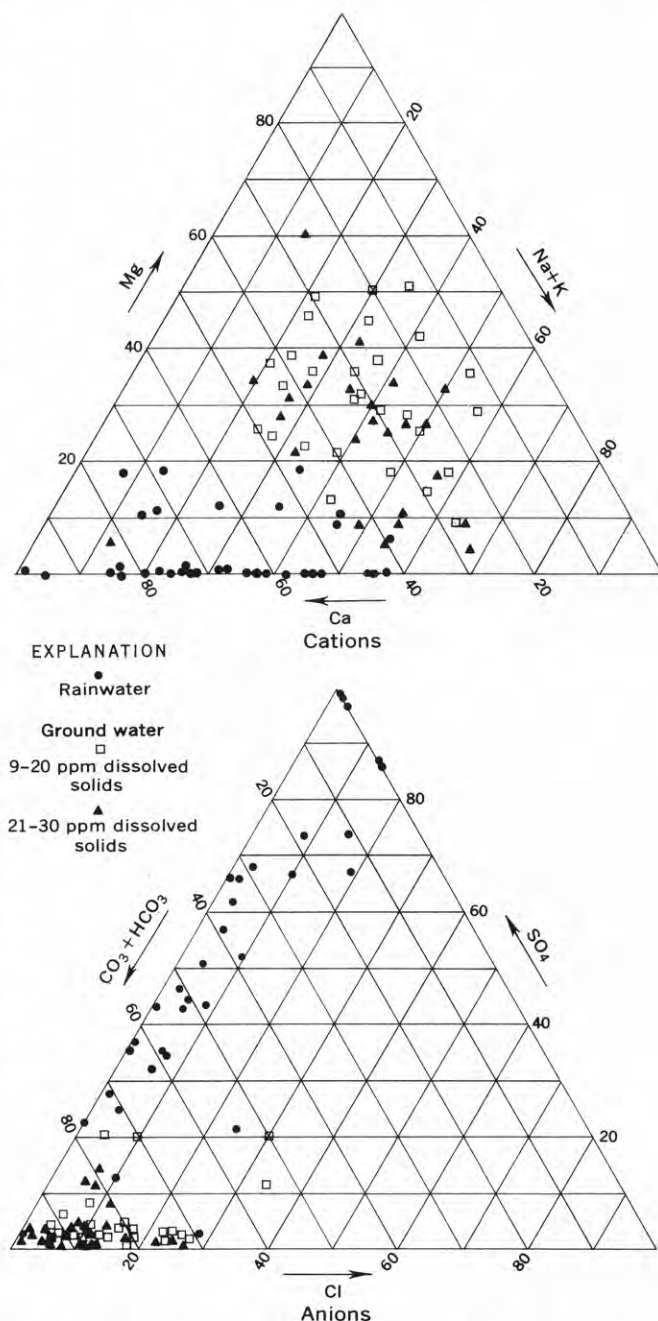
FIGURE 2.—Water-analysis diagrams showing percentage reacting values of the principal ions in rainwater and in ground water in western North Carolina.

appears to be no gradual transition in composition from rainwater to ground water in this area. Although no quantitative information is available, the residence time for some of the ground water probably is short. If this assumption is correct, the change in chemical composition as rain infiltrates and becomes ground water may be rapid. Feth and others (1964) found that the chemical composition of snowmelt in the Sierra Nevada changes almost instantly on contact with soil and saprolite.

Average concentrations of dissolved solids in rainwater and ground water from western North Carolina

[In parts per million]

	Rainwater (33 analyses)	Ground water	
		9 to 20 ppm of dissolved solids (28 analyses)	21 to 30 ppm of dissolved solids (27 analyses)
Calcium (Ca)	0.9	1.0	1.8
Magnesium (Mg)	.0	.6	.8
Sodium (Na)	.4	1.0	1.8
Potassium (K)	.2	.6	.8
Bicarbonate (HCO₃)	2.0	8.0	14
Sulfate (SO₄)	2.0	.4	.4
Chloride (Cl)	.2	.9	1.0
Silica (SiO₂)	.1	7.0	11
Dissolved solids:			
Range	2.2–11	9–20	21–29
Average	5.1	15	25
Less SiO₂	5.0	8.0	16
Specific conductance (micromhos at 25°C):			
Range	4–28	10–32	18–47
Average	13	17	27

The decrease in the concentration of sulfate as rainwater becomes ground water may be due to anion exchange with clay minerals or to sulfate reduction. Feth and others (1964) report that in the Sierra Nevada both sulfate and chloride are removed from solution by anion exchange with clay minerals. Bear (1955, table 4.4) shows that 100 grams of kaolinitic clay at pH 6.9 will exchange 0.7 milliequivalents of sulfate, and that at pH 6.25 it will exchange 4.6 meq of sulfate. The anionic change in the transition from rainwater to ground water involves a concomitant decrease of the amount of sulfate and an increase in the amount of bicarbonate. Inasmuch as bicarbonate is not a common ion in clay minerals (Grim, 1953, p. 126), sulfate reduction may be a more likely mechanism to explain the change from a sulfate to a bicarbonate composition. This reaction can be written (Hem, 1959, p. 223):

$$SO_4^{-2} + CH_4 \xrightarrow{\text{(bacteria)}} HS^{-1} + H_2O + HCO_3^{-1}.$$
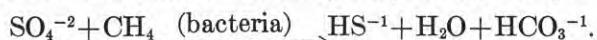
Sulfur is released as H_2S gas, and bicarbonate is subsequently increased. Other hydrocarbons besides methane could act as oxidizable substances. Conditions favorable for this reaction commonly prevail in the mat of decaying leaf litter on the surface of the soil. McKenzie and others (1960), in a study of the translocation of iron in the formation of podzols in Michigan, report that the A horizon had a lower redox potential than the underlying B horizon. Podzols occur in western North Carolina; if a relatively low redox potential occurs in the surface horizon of the soil, it may account for the reduction of sulfate.

There is an increase of about 70 times in silica content when rainwater becomes ground water (see table). High percentages of silica in ground water result from the weathering of silicate minerals. A surplus of silica commonly remains after alteration of the original silicate minerals to clay minerals, and part of this silica is readily available for solution by rainwater that comes in contact with rock and soil. The solution of silica is one of the principal chemical changes that occurs when the rainwater becomes ground water. The data in the accompanying table show that the total amount of ionic constituents increased less than two times.

The outstanding features of the change from rainwater to ground water in western North Carolina, in terms of the chemistry of the water, are thus: (1) an apparent lack of gradational members between typical analyses of rainwater and of ground water; (2) a change from a calcium sulfate and calcium bicarbonate composition to a mixed-cation bicarbonate composition; and (3) a marked solution of silica.

REFERENCES

Bear, F. E., 1955, Chemistry of the soil: New York, Reinhold Pub. Corp., 373 p.

Feth, J. H., Roberson, C. E., and Polzer, W. L., 1964, Sources of mineral constituents in water from granitic rocks, Sierra Nevada, California and Nevada: U.S. Geol. Survey Water-Supply Paper 1535–I, 70 p.

Gambell, A. W., 1963, Sulfate and nitrate content of precipitation over parts of North Carolina and Virginia: Art. 114 *in* U.S. Geol. Survey Prof. Paper 475–C, p. C209–C211.

Gambell, A. W., and Fisher, D. W., 1964, Occurrence of sulfate and nitrate in rainfall: Jour. Geophys. Research, v. 69, no. 20, p. 4203–4210.

Grim, R. E., 1953, Clay mineralogy: New York, McGraw-Hill Book Co., 384 p.

Hem, J. D., 1959, Study and interpretation of the chemical characteristics of natural water: U.S. Geol. Survey Water-Supply Paper 1473, 269 p.

Junge, C. E., and Werby, R. T., 1958, The concentration of chloride, sodium, potassium, calcium, and sulfate in rainwater over the United States: Jour. Meterology, v. 15, p. 417–425.

McKenzie, L. J., Whiteside, E. P., and Erickson, A. E., 1960, Oxidation-reduction studies on the mechanism of B horizon formation in Podzols: Soil Sci. Soc. America Proc., v. 24, p. 300–305.

Rainwater, F. H., and Thatcher, L. L., 1960, Methods for collection and analysis of water samples: U.S. Geol. Survey Water-Supply Paper 1454, 301 p.

LIGHT-DEPENDENT QUALITY CHANGES IN STORED WATER SAMPLES

By KEITH V. SLACK and DONALD W. FISHER,

Menlo Park, Calif., Washington, D.C.

Abstract.—Composition of replicate samples of natural water stored in polyethylene bottles of three degrees of transparency was nearly identical after storage. After exposure for 3 months to alternating 12-hour light and dark periods, pH ranged from 9.27 to 10.17, HCO_3 was not detected in most samples, CO_3 concentration ranged from 7 to 13 ppm, and free CO_2 and NO_3 were below detection. After an additional 2 months of dark storage, pH had decreased 2 units relative to that of the samples during illumination, concentration of free CO_2 and HCO_3 had increased greatly, and CO_3 was below detection. Observed changes are attributed to photosynthesis by algae which developed in the samples during illumination, and to re-solution of substances following death and decay of the algae in the dark.

Most water-quality studies are based on laboratory analyses, many of which do not accurately represent the natural composition of the water. Altered sample composition may result from physical and chemical changes and from several types of biological processes, the most important of which are production and consumption of organic matter. Both photosynthetic and chemosynthetic production are recognized, depending upon the energy source; in both cases substances are removed from solution by algae and certain bacteria to form new organic materials. Other types of bacteria and fungi decompose organic matter to simpler substances, many of which go into solution as inorganic ions. Phosphorus, nitrogen, silicon, sulfur, carbon, oxygen, and hydrogen are the common elements involved, although many other major and minor constituents of water also are concentrated or released by living organisms.

METHOD OF INVESTIGATION

Studies were made to evaluate the effects of photosynthesis on water samples during storage. Three different types of 2-liter polyethylene bottles were selected for testing: clear transparent, white translucent, and amber translucent. Presumably, photosynthesis within the bottles should be a function of both light intensity (and hence of sample-bottle opacity) and spectrum (and hence of sample-bottle color).

Replicate water samples were obtained in March 1963 from Rock Creek in Washington, D.C., and from the Cacapon River between the towns of Largent and Great Cacapon, W. Va. Clean bottles were rinsed three times with the source water, filled, capped, and sealed with tape. Upon reaching the laboratory, all bottles were maintained at 25°C and exposed to alternating 12-hour periods of darkness and light. The intensity of the light was approximately 1/10 that of full sunlight. After 3 months, complete analyses were made of each sample. The bottles were then resealed and stored in complete darkness for 2 months, after which a second set of analyses was made. Care was used to prevent contamination of the samples during the brief time that the bottles were open for the first set of analyses. The effects of contamination or of the increased air spaces in the sample bottles after the first analyses are believed to be insignificant factors in changed sample composition between the two conditions of storage.

RESULTS

As is shown in the accompanying table, no significant difference was found among samples in the three types of bottles after dark-light storage. Blue-green and other algal growths were present, and the compositions of all samples showed evidences of photosynthesis. The pH ranged from 9.27 to 10.17, and because of the high pH the amount of bicarbonate could not be determined directly. In most samples the carbonate concentration ranged from 7 to 13 parts per million. Concentrations of free CO_2 and NO_3 were below the level of detection.

During the period of dark storage, pH decreased 2 units to the range 7.15 to 8.02, and free CO_2 and bicarbonate concentrations increased greatly; carbonate

Composition of water samples from Cacapon River, W. Va., and Rock Creek, Washington, D.C., after storage in three types of polyethylene bottles

[Replicate analyses were made after exposure of the samples to alternating 12-hour light-dark cycles for 3 months, and again after storage in total darkness for 2 months]

	Type of polyethylene bottle											
	Clear transparent				White translucent				Amber translucent			
	Illuminated		Dark		Illuminated		Dark		Illuminated		Dark	
Cacapon River, W. Va.												
Conductivity (micromhos)	65	67	64	65	71	72	65	67	66	67	65	64
pH	9.58	9.53	7.20	7.30	9.85	9.77	7.15	7.20	9.47	9.53	7.25	7.30
Chemical constituents (ppm):												
CO_2			2.1	1.8			2.4	2.2			1.9	1.7
HCO_3	6	6	21	23			21	22	6	5	21	21
CO_3	7	7			9	10			7	8		
OH					1	0						
SO_4	7.6	6.8	8.8	9.2	8.0	7.0	8.6	9.6	8.9	8.0	8.6	9.2
NO_3	.0	.0	.01	.02	.0	.0	.03	.03	.0	.0	.05	.12
PO_4	.05	.06	.02	.01	.24	.05	.00	.00	.07	.06	.00	.00
Cl	1.1	1.0	1.3	1.3	1.1	1.0	1.3	1.3	1.1	1.0	1.3	1.2
F	.0	.0			.0	.0			.0	.0		
B									<.05			
Ca	7.8	7.8	7.0	6.5	7.0	7.6	7.0	7.5	7.2	8.4	7.0	7.4
Mg[1]	1.4	1.4	2.1	3.0	1.6	1.4	2.2	2.4	1.5	1.1	2.0	2.2
Na	1.3	1.2	1.4	1.2	1.3	1.3	1.3	1.3	1.3	1.3	1.2	1.2
K	1.2	1.2	1.3	1.3	1.2	1.2	1.3	1.3	1.3	1.2	1.3	1.3
SiO_2	5.8	4.7	5.9	4.7	6.3	6.3	7.0	6.6	5.4	5.3	6.1	5.7
Rock Creek, Washington, D.C.												
Conductivity (micromhos)	172	160	177	185	172	177	174	179	173	180	182	183
pH	10.15	9.27	7.80	7.39	10.17	10.16	7.82	8.02	10.14	10.15	7.82	7.85
Chemical constituents (ppm):												
CO_2			1.3	3.6			.05	.08			0.5	1.2
HCO_3		26	51	55			48	51			52	54
CO_3	11	8			9	12			13	13		
OH	3				4	2			2	2		
SO_4	16	12	17.6	17.2	15	12	17.6	17.6	14	14	17.6	17.6
NO_3	.0	.0	.01	.00	.0	.0	.01	.01	.0	.0	.03	.03
PO_4	.07	.06	.00	.00	.05	.06	.01	.03	.05	.09	.00	.00
Cl	17	16	16	16	18	15	16	16	17	16	16	16
F	.0	.0			.0	.0			.0	.0		
B						<.05						
Ca	17	16	17	17	17	17	17	17	18	18	17	18
Mg[1]	.5	2.7	4.2	5.4	.1	.2	3.5	5.1	.1	.4	4.7	5.5
Na	9.4	9.6	9.5	9.6	9.6	9.4	9.6	9.6	9.6	9.6	9.5	9.7
K	2.3	2.3	2.4	2.4	2.3	2.3	2.4	2.4	2.3	2.2	2.4	2.4
SiO_2	6.6	8.9	12.2	13.7	5.9	6.2	10.8	12.0	6.9	7.1	12.1	13.0

[1] Calculated as the difference between total hardness and calcium.

ion was not detected. Silica increased in the Rock Creek water, perhaps due to dissolution of diatom frustules. Nitrate and SO_4 increased in all samples. Surprisingly, PO_4 concentration was higher in the illuminated samples than in the continuously dark samples; this effect is tentatively attributed to uptake of PO_4 by increased bacterial populations in the dark. The large change in Mg concentration between the two storage conditions was unexpected and cannot be explained from available data.

The major compositional changes are readily explained on the basis of CO_2 uptake for photosynthesis and of utilization of nutrients to support algal growth during the illuminated period. Photosynthesis may be represented by

$$6\ H_2O + 6\ CO_2 = C_6H_{12}O_6 + 6\ O_2.$$
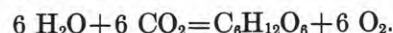
As carbon dioxide is depleted the equilibrium between bicarbonate ion and its dissociation products shifts to the right, resulting in a higher pH. Thus,

$$HCO_3^{-1} = CO_2 + OH^{-1}.$$
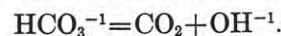
Along with depletion of the bicarbonate, additional hydroxyl ions result from the reaction of the carbonate ion:

$$CO_3^{-2} + H_2O = CO_2 + 2\ OH^{-1}.$$
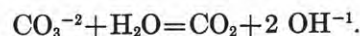
The death and decay of plants during dark storage releases CO_2, with a consequent drop in pH. Other elements and groups (such as NO_3 and SiO_2) are similarly liberated as a result of decomposition of the photosynthetic products.

CONCLUSIONS

Relatively dilute waters were used in these tests. Changes of magnitude similar to those observed may not occur in more highly buffered waters; however, the changes in composition of Rock Creek samples were as large as those of the more poorly buffered Cacapon River samples. Probably the greater degree of organic enrichment in Rock Creek favored biological activity within the stored samples.

The initial composition of the water samples was not determined because the objective of the experiment was to test for differences among samples stored in the three types of bottles. Analyses of samples collected from the same streams at other times indicate that the pH and the concentration of carbonate species in the experimental samples, at the time of collection, resembled those under the condition of dark storage.

When precise results are required, analyses of unstable constituents should be completed in the field if practicable. If analyses must be made in the laboratory the samples should be protected as described by Rainwater and Thatcher (1960, p. 27–30). When analyses cannot be completed promptly, dark storage will help prevent changes in sample composition resulting from the growth of photosynthetic organisms. Because no such benefit was demonstrated for any of the bottle types tested, dark storage should be ensured by wrapping sample bottles in opaque material such as aluminum foil, or by storing them in light-tight containers.

REFERENCE

Rainwater, F. H., and Thatcher, L. L., 1960, Methods for collection and analysis of water samples: U.S. Geol. Survey Water-Supply Paper 1454, 301 p.

PATTERNS OF DISSOLVED OXYGEN IN A THERMALLY LOADED REACH OF THE SUSQUEHANNA RIVER, PENNSYLVANIA

By KEITH V. SLACK and FRANK E. CLARKE,

Menlo Park, Calif., Washington, D.C.

Abstract.—Dissolved-oxygen conditions in the West Branch of the Susquehanna River were investigated at stations above and below a steam-electric powerplant. The river receives strip-mine drainage and moderate quantities of municipal wastes upstream from the reach affected by thermal loading. Relatively high concentrations of dissolved oxygen in the river at these stations are attributed chiefly to the shallow depth of the river and to a slow rate of organic decomposition in the acid water. When studied in October, a diurnal fluctuation in concentration of dissolved oxygen was found only above the plant. Light- and dark-bottle tests with river water showed zero net production of oxygen above the powerplant and a net loss of oxygen below it. A significant quantity of oxygen is believed to be added to the river above the powerplant by streambed plants but not by phytoplankton. Below the outfall, reduced algal abundance probably results from the effects of chemical and fine-sediment wastes from the plant.

FIGURE 1.—Diurnal changes in water temperature, West Branch of the Susquehanna River, Pa., October 16–17, 1962. Station A was above the Shawville steam-electric powerplant and station B was below it.

SETTING

Dissolved-oxygen conditions in a thermally loaded river were investigated by two methods at stations above and below the source of heat. Observations were made on October 16–17, 1962, near the Shawville powerplant on the West Branch of the Susquehanna River, Pa. Messinger (1963) described a study of heat dissipation conducted on this stream during the same period.

The reach of the stream studied receives treated wastes from Clearfield and other small upstream communities, but the chemical quality of the river water is dominated by strip-mine drainage. During our work pH was about 4 and sulfate concentration was about 200 parts per million. Discharge was 350 cubic feet per second and ground-water inflow was negligible.

The generally high concentration of dissolved oxygen observed during this investigation probably is the result of (1) shallow water depth, which favors atmospheric reaeration, (2) slow rate of oxygen utilization by decomposable organic matter in the acid water, and (3) oxygen production by riverbed plants.

Station B was at an altitude of 1,040 feet, in the heated section below the dam at the Shawville plant. Station A, at 1,050 feet, was above the cooling pond for the plant, 1.8 miles above the dam. Discharge of condenser-cooling water increased water temperature an average of 13°C at station B over that at station A (fig. 1).

METHODS

The concentration of oxygen in the river water was measured at 2- to 3-hour intervals to determine diurnal

changes. The azide modification of the Winkler method was used.

The standard light-and-dark-bottle ("L and DB") technique of Gaarder and Gran (1927) was used to estimate the contribution of photosynthetic oxygen to the river by phytoplankton. Strickland (1960) critically reviewed the method and concluded that the maximum analytical precision is 0.017 ml oxygen per liter (0.024 ppm). In this procedure a large, thoroughly mixed water sample is divided into three parts. Oxygen concentration in one subsample is determined immediately to establish the initial condition. Clear glass-stoppered 300-ml BOD (Biochemical Oxygen Demand) bottles, designated "light" bottles, are filled with a second subsample. Another set of BOD bottles, covered with opaque material and designated "dark" bottles, are filled with the third subsample. Pairs of light and dark bottles are submerged in the water for a predetermined period, after which dissolved oxygen is measured in each bottle. Normally, the dissolved-oxygen content increases in the light bottles and decreases in the dark bottles. The increase of oxygen in the light bottles is interpreted as the excess of oxygen production over oxygen utilization in respiration ("net photosynthesis") by the enclosed organisms. Oxygen decrease in the dark bottles is attributed to respiration by microscopic plants and animals. Thus "gross" production of oxygen during the test period is the difference between the light- and dark-bottle values at the end of the experiment, assuming that respiration is the same in both bottles.

During the 24-hour test, replicate light and dark bottles were suspended side-by-side just beneath the water surface at each station in such a way that the bottles were kept in constant motion by the current. A deflector was arranged at station A to prevent shading of bottles by accumulations of drifting leaves.

RESULTS

The river was supersaturated with oxygen at all times at station B and during most of the daylight hours at station A (fig. 2). However, the dissolved-oxygen concentration was less below the powerplant as a result of decreased solubility of the gas at the higher water temperature. Above the plant dissolved oxygen varied diurnally; maximum values occurred during the day, and minimum concentration and minimum saturation were observed at 0230 hours EDT. The diurnal change in dissolved oxygen at station A strongly suggests a light-dependent control such as photosynthesis, although details in the pattern of change appeared to result from a combination of factors. The gradual decrease in dissolved-oxygen concentration between about 1700 hours and 2330 hours is thought to represent
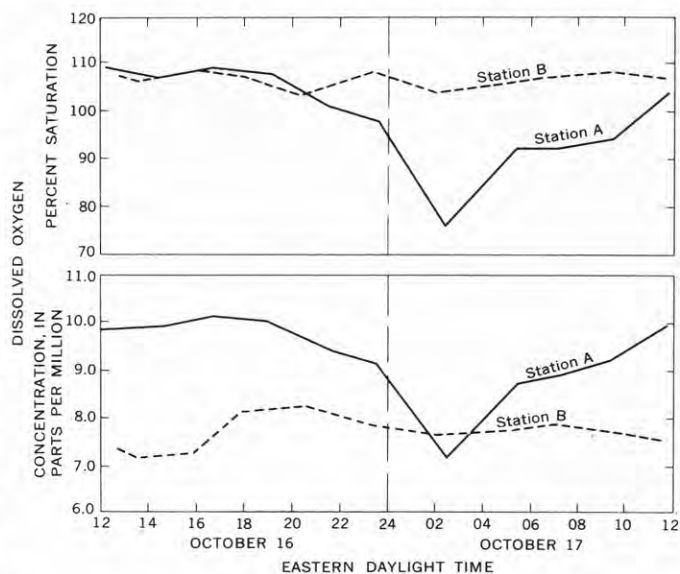
FIGURE 2.—Diurnal change in dissolved oxygen, West Branch of the Susquehanna River, Pa., October 16–17, 1962. Station A was above the Shawville steam-electric powerplant and station B was below it.

oxygen uptake for respiration following cessation of photosynthesis. The predawn increase in dissolved oxygen may represent either recovery to normally higher levels following passage of a slug of low-oxygenated water, or an interruption of the usual nocturnal sag in dissolved-oxygen concentration by a mass of more highly oxygenated water. Light showers of rain observed at the study area during the observation at 2330 hours may have been the source of additional oxygen in the river water if they also occurred upstream. At station B the dissolved-oxygen pattern was complicated by powerplant operations. For example, the observation at 1800 hours showed that river temperature had decreased and suspended sediment had increased abruptly; these changes are believed to have been a result of backwashing of intake-filter screens. These changes in quality were accompanied by increased dissolved-oxygen concentration but by decreased percent saturation. Flushing of filter screens is thought to affect dissolved oxygen concentration at station B chiefly by contributing to unfavorable conditions for the growth of benthic plants.

Results of the light- and dark-bottle tests are shown in the accompanying table. At station A, above the powerplant, there was no change in dissolved-oxygen concentration in any bottle during the exposure period; this indicates zero net production of oxygen. At station B, oxygen concentration decreased in all bottles, showing a negligible population of phytoplankton and negligible biochemical uptake. However, more oxygen was present in the dark bottles than in the light bottles,

Changes in dissolved oxygen in light and dark bottles after 24-hour exposure, West Branch of the Susquehanna River, Pa., October 16–17, 1962

Station	Initial dissolved oxygen (ppm)	Average final dissolved oxygen (ppm)		Average dissolved-oxygen change (ppm)	
		Light bottle	Dark bottle	Light bottle	Dark bottle
A	9.8	9.8	9.8	0.0	0.0
B	7.4	6.6	7.0	−.8	−.4

a theoretically impossible result in view of the assumption of equal respiration in all bottles.

Although the light- and dark-bottle method is not sufficiently sensitive for use in waters of very low productivity, the differences observed in this study are well within the accuracy obtainable. Higher dark-bottle than light-bottle readings have been reported for a number of lakes. Hutchinson (1957, p. 617), discussing similar observations in a Connecticut lake, suggested that increased depletion of oxygen in the light bottles may result from a stimulation effect of light on zooplankton. Gessner and Pannier (1958) demonstrated that respiration rates of some photosynthetic organisms are dependent on oxygen concentration. Thus, the absence from the dark bottles of the high oxygen tensions which occur in the light bottles may cause the respiration rates in the dark bottles to be too low. Dugdale and Wallace (1960) reported numerous observations of dark-bottle readings which were higher than light-bottle readings in two Alaskan lakes. In addition to possible biological causes, these authors suggested that loss of oxygen from the initial sample prior to fixing, or photochemical oxidation of humic material in light bottles, might explain higher dark-bottle values. Eberly (1963) considered that anomalous dark-bottles values in Indiana lakes might result from release of free oxygen in the dark by a species of blue-green algae, *Oscillatoria agardhi*.

It is unlikely that any one mechanism will explain all the reported cases of anomalous dark-bottle values. In our tests, photochemical oxidation of some substance from the powerplant is a possibility. Slightly higher light-bottle temperature, resulting in more rapid oxygen utilization, is believed to be a contributing factor. Higher light-bottle temperatures are explained by a greenhouse effect resulting from near-surface exposure of the bottles. During the study all bottles were assumed to be at the temperature of the surrounding water, but in later tests under similar conditions, light-bottle temperatures exceeded those of dark bottles and of flowing water by at least 0.5°C.

The photosynthesis tests suggest that phytoplankton did not contribute significantly to the oxygen resources during this study. However, other plants were present, rooted or otherwise attached to the streambed, and they probably contributed significant quantities of oxygen to the river above the powerplant. Gas bubbles, thought to be oxygen produced by photosynthesis, were abundant on benthic algal films during the day. Difficulties in sealing an enclosure to the rocky streambed prevented measurement of this contribution. Photosynthetic-oxygen production was not significant at station B, as is indicated by the lack of diurnal change in oxygen content (fig. 2). Moreover, only 1 genus of attached algae (exclusive of diatoms) was found at station B, in contrast to the 8 genera found at station A. Undoubtedly, water temperatures at station B often exceed the highest observed during our brief study, but the direct effect of temperature on attached algae is probably small. A more important control on algal abundance is thought to be chemical and fine-sediment wastes resulting from operation of the powerplant.

REFERENCES

Dugdale, R. C. and Wallace, J. T., 1960, Light and dark bottle experiments in Alaska: Limnology and Oceanography, v. 5, no. 2, p. 230–231.

Eberly, W. R., 1963, Oxygen production in some northern Indiana lakes: Proc. 17th Indust. Waste Conf., Purdue Univ., Eng. Bull. v. 47, no. 2, p. 733–747.

Gaarder, Torbjorn, and Gran, H. H., 1927, Investigations of the production of plankton in the Oslo Fjord: Rapp. et Proc.-Verb., Cons. Internat. Explor. mer., v. 42, p. 1–48.

Gessner, Fritz, and Pannier, Federico, 1958, Influence of oxygen tension on respiration of phytoplankton: Limnology and Oceanography, v. 3, no. 4, p. 478–480.

Hutchinson, G. E., 1957, Geography, physics, and chemistry; v. 1 *of* A treatise on limnology: New York, John Wiley and Sons, 1015 p.

Messinger, Harry, 1963, Dissipation of heat from a thermally loaded stream: Art. 104 *in* U.S. Geol. Survey Prof. Paper 475–C, p. C175–C177.

Strickland, J. D. H., 1960, Measuring the production of marine phytoplankton: Fisheries Research Board of Canada Bull. 122, 172 p.

EFFECT OF LAND USE ON THE LOW FLOW OF STREAMS IN RAPPAHANNOCK COUNTY, VIRGINIA

By H. C. RIGGS, Washington, D.C.

Abstract.—Analysis of discharge measurements for nine small streams in the Piedmont physiographic province, made during summer and fall in the years 1961–64, indicates that discharge per square mile is directly related to the percentage of the drainage basin which is cleared of trees and brush. Clearing of land along the stream channel seems to produce a greater effect on discharge than clearing over the basin generally. This effect of clearing is most pronounced at extremely low levels of discharge and becomes negligible at high discharges.

Discharge measurements made on 20 small streams in the Hazel River basin, in Rappahannock County, Va., indicate that during summer and fall some of these streams consistently produce higher base flows per unit area than others. The measurements for the nine streams originating in the Piedmont were studied to find the reason for these differences. Figure 1 shows the 9 streams and the measuring sites, both of which are referred to by number because only 3 of the streams are named.

Seven sets of discharge measurements and one set of discharge estimates are available. Each set consists of a discharge for each of the 9 streams, made within a 1- or 2-day period, at least several days after any appreciable rain. The measurements were made during the period May through November, in the years 1961 to 1964.

The most obvious differences in discharge are between streams 4 and 5. Although these streams flow in the same direction, have somewhat similar drainage patterns, and drain areas of similar size (3.69 and 3.76 square miles, respectively), all measured discharges of stream 4 were appreciably smaller than those for stream 5 made at comparable times. Geologic factors which may lead to differences in stream discharge include characteristics of rocks, soils, and topography.

Almost all the area occupied by the streams sampled (fig. 1), including the tract which contains streams 4 and 5, is underlain by granite, gneiss, and other crystalline
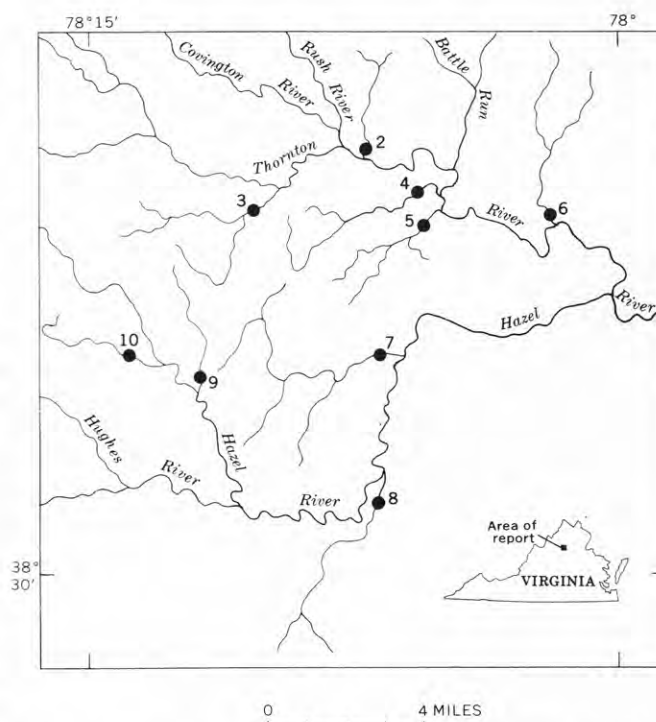
FIGURE 1.—Map of part of the Hazel River basin, Virginia, showing streams used in this analysis. Dots indicate measuring sites.

rocks (Virginia Division of Mineral Resources, 1963). The drainage pattern shown on figure 1 suggests structural control of stream courses, but streams 4 and 5 are near one another, trend generally parallel to one another along the regional strike of the rocks, and thus appear from the geologic map to be in similar environments. Significant differences in rock types and structure may be present, but they are not recognizable on a geologic map at this scale (1:500,000).

The soils in the area have been mapped in detail by the U.S. Department of Agriculture (1961). Included in the description of each soil type is a hydrologic rating

which indicates the ability of the soil to take in water during periods of sustained rainfall. Four rating classes were used—high, medium, low, and very low. Most of the soils in the basins of streams 4 and 5, as well as those in the basins of the other seven streams, are in the medium class. Only a few small areas of soils in different rating classes are scattered throughout the basins. Thus, the difference in discharge between streams 4 and 5 appears not to be a result of differences between the soils.

Topographic form and relief are not greatly different among the nine basins, nor is there sufficient relief to cause an appreciable difference in precipitation. Specific topographic characteristics such as depth of incision of the channels, elevation of the measuring sites, and stream slopes were considered, but no relation between these factors and stream discharge could be found.

The chief dissimilarity found between the basins of streams 4 and 5 is in the amount of cleared land in each. In its natural state the land was covered with a fairly dense growth of brush and trees, largely deciduous. As shown on the 1961 topographic map of the Sperryville quadrangle, scale 1:62,500, 32 percent of the basin of stream 4 above the measuring site and 49 percent of the basin of stream 5 above the measuring site were cleared. Most of the cleared land is now (1964) in pasture or hay, with a small amount in other crops. The basin of stream 4, with 17 percent less cleared land, produced a lower discharge than the basin of stream 5. Thus, these data suggested that the size of the low flow yielded by a basin is related to the area of cleared land in the basin.

Verification of this hypothesis was sought by relating each of the eight sets of discharge measurements of the streams to drainage area and to percentage of basin cleared, by means of graphic multiple regression. Each set of measurements for streams 3, 4, 5, 7, 8, and 9 produced a graphic relation from which an equation of the following form was derived:

$$\log Q = a + b \log A + b_1 \log C, \qquad (1)$$

where Q is discharge in cubic feet per second; A is drainage area in square miles; C is the percentage of basin cleared; and a, b, and b_1 are coefficients. The coefficients of the eight equations are listed in table 1. Six of eight values of coefficients b_1 (of the percentage of land cleared) are greater than zero, and these coefficients are inversely related to the general magnitude of discharge in the area as represented by the discharge of stream 7 (fig. 2). The best index of the general level of discharge would be the discharge of a fairly large stream unaffected by clearing of forest. Of the streams in this group, stream 7 most closely meets these criteria. Use of the regression coefficient b_1 in
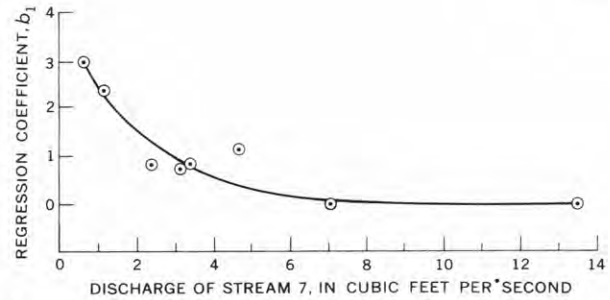
FIGURE 2.—Effect, on discharge, of percentage of cleared land, as related to magnitude of discharge (data from table 1).

the relation of figure 2 is justified because drainage area and percentage of cleared land are unrelated and thus the regression coefficients b and b_1 are statistically independent. Data from streams 2, 6, and 10 are not consistent with equation 1.

This analysis suggests that low flows during the summer and fall are better sustained in basins having a large proportion of cleared land than in basins which are largely timbered; that the influence of cleared land is greatest when the general level of discharge is lowest; and that the influence becomes negligible at a high discharge level. However, this conclusion can be stated only tentatively because data from 3 of the 9 streams were not used in the analysis. If the percentage of basin cleared is to be used as an index of the effect of the land use on low flows, additional factors need to be included in the analysis.

Plants reduce the water available for streamflow by intercepting precipitation on their leaves, from which it evaporates, and by removing moisture from the soil by transpiration. The magnitude of these effects tends to be greater for trees than for smaller plants. Thus clearing of forest would be expected to reduce streamflow, but the magnitude of the change in streamflow due to clearing is related to other characteristics of the drainage basins in a complex manner, and no simple relation exists. For example, Kilpatrick (1964) showed that, at times, parts of a basin may not contribute to

TABLE 1.—*Regression coefficients in equation 1, and corresponding discharges of stream 7*

Date of measurement	Regression coefficients			Discharge of stream 7 (cubic feet per second)
	a	b	b_1	
Oct. 30–31, 1961	−2.47	1.11	1.1	4.62
June 26, 1962	−.10	1.13	0	13.4
Sept. 24–25, 1962	−1.90	1.13	.7	3.15
May 15–16, 1963	−.40	1.08	0	7.00
Aug. 6–7, 1963	−6.05	1.28	3.0	.67
Oct. 21, 1963 [1]	−4.31	1.26	2.4	[1] 1.1
June 25, 1964	−1.83	1.00	.8	3.30
November 14, 1964	−2.07	1.00	.8	2.41

[1] Discharge estimated in field.

the base flow of a stream; and Dunford and Fletcher (1947) reported that important gains in water yield during the growing season resulted from cutting only the riparian vegetation (that is, vegetation growing on the banks of the river) in a small basin in Coweeta Experimental Forest, N.C. Thus the location of the cleared land in a basin may be a significant factor in its effect on streamflow.

Adequate moisture is commonly available near the stream channel for maximum transpiration, but on hillsides and ridges the soil moisture is often limited so that the amount of soil moisture rather than the type of plant cover determines the amount of transpiration. If it is assumed that the change in transpiration is the major effect of clearing of forest, then it seems likely that clearing along the stream channel would produce a greater change in streamflow than clearing of an area away from the stream channel. On the basis of this assumption an index of the amount of cleared land was defined as the percentage of length of the lower half of the stream which is cleared of trees and brush for at least 300 feet on each side of the channel. Such index values, measured on the topographic map for the nine streams, are not precise but are thought to be of the right order of magnitude.

These index values of percentage of channel cleared in the lower half of the basin (designated D) were used to develop graphic regressions subsequently expressed in the form

$$\log Q = a_1 + b_2 \log A + b_3 \log D, \qquad (2)$$

where the other symbols are as previously defined. All nine streams fit equation 2. Results are given in table 2. The curve which expresses the relation of b_3 to the discharge of stream 7 (shown on fig. 3) is similar to the curve shown on figure 2. Thus, analysis by equation 2 yields a conclusion similar to that already drawn. The second analysis, which confirms the first, is considered the more reliable because it uses data from all nine streams in the area studied.

These analyses strongly suggest (1) that the differences among low flows of the nine streams are related to differences in the proportions of cleared land in the basins, (2) that clearing of the land helps sustain summer and fall base flows of streams in the Hazel River
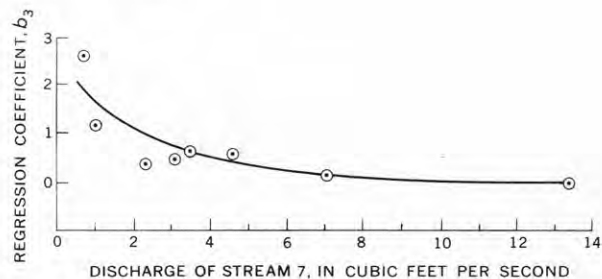
FIGURE 3.—Effect, on discharge, of percentage of basin surface cleared within 300 feet of the channel in the lower half of the basin, as related to the magnitude of discharge (data from table 2).

basin, and (3) that the land-clearing effects are proportionately greatest at the lower discharge ranges. For the purpose of increasing summer and fall base flows, the areas whose clearing is most effective appear to be those adjacent to the stream channels.

TABLE 2.—*Regression coefficients in equation 2, and corresponding discharges of stream 7*

Date of measurement	Regression coefficients			Discharge of stream 7 (cubic feet per second)
	a_1	b_2	b_3	
Oct. 30–31, 1961	−1.82	1.27	0.62	4.62
June 26, 1962	−.30	1.42	0	13.4
Sept. 24–25, 1962	−2.12	1.49	.64	3.15
May 15–16, 1963	−.72	1.11	.15	7.00
Aug. 6–7, 1963	−6.66	1.80	2.65	.67
Oct. 21, 1963	−3.54	1.52	1.20	[1] 1.1
June 25, 1964	−1.72	.98	.68	3.30
Nov. 14, 1964	−1.30	.98	.37	2.41

[1] Discharge estimated in field.

REFERENCES

Dunford, E. G., and Fletcher, P. W., 1947, Effect of removal of stream-bank vegetation upon water yield: Am. Geophys. Union Trans., v. 28, p. 105–110.

Kilpatrick, F. A., 1964, Source of base flows of streams: Internat. Union of Geodesy and Geophysics, General Assembly at Berkeley, Internat. Assoc. of Sci. Hydrology Publ. 63, p. 329–339.

U.S. Department of Agriculture, 1961, Soil survey, Rappahannock County, Virginia: Soil Conserv. Service Soil Survey Series 1958, no. 11, 85 p.

Virginia Division of Mineral Resources, 1963, Geologic map of Virginia: Charlottesville, Va., Virginia Department of Conservation and Economic Development.

SEASONAL ERASURE OF THERMAL STRATIFICATION IN PRETTY LAKE, INDIANA

By JOHN F. FICKE, Fort Wayne, Ind.

Abstract.—Data on temperature and concentration of dissolved oxygen in a small Indiana lake were used in describing the erasure of stratification of the lake water during the warm autumn of 1963. A measurable thermocline was observed to drop within a few feet of the bottom before it was erased in late November. Upon turnover of lake water the uniform lake temperature was about 0.6°C higher than the temperature of the hypolimnion while the lake was stratified.

Lakes of moderate depth located in temperate zones usually become stratified during the summer. The zone of less dense warm water near the surface of a stratified lake, called the epilimnion, is subject to wind action which produces relatively uniform temperatures and a uniform distribution of microbiological and chemical constituents. The colder, more dense region near the lake bottom, commonly called the hypolimnion, is subject to limited mixing and circulation. In lakes of at least moderate depth, sunlight usually cannot penetrate to the hypolimnion in sufficient intensity to support photosynthesis. Consequently, by midsummer the hypolimnion contains a large amount of dead organic matter which has settled from the growth region in the epilimnion. Decay of this dead material exhausts the oxygen from the hypolimnetic waters and establishes a zone that is quite different chemically from the water near the surface. Between the upper and lower regions of a stratified lake is a transition zone in which the temperature decreases rapidly with depth and establishes a strong density barrier that isolates the hypolimnion from any mixing induced by wind action at the surface. Specialists have disagreed over the naming of this transitional zone. The writer follows Hutchinson (1957, p. 428, 534) in terming it the metalimnion, and in terming the horizontal plane within the metalimnion at which the rate of decrease in temperature is greatest the thermocline.

Autumnal cooling of the water near the surface increases the density of the water and induces currents which tend to deepen the epilimnion by slowly erasing the metalimnion. The process continues until the lake reaches a nearly uniform temperature. Once nearly isothermal conditions of nearly equal density have been reached, wind energy can overcome small density differences and induce mixing throughout the entire lake. This mixing phenomenon by which the chemically different water from the hypolimnion mixes with the rest of the lake is often called a turnover. When a turnover occurs rapidly in a deep lake, large volumes of foul-smelling water move into what formerly was the clean epilimnion. This movement stirs up sediment from a large part of the bottom, thereby increasing water-treatment problems where lakes or reservoirs are used as sources of water supply (Camp, 1952, p. 854).

Data collected during the cooling and turnover of Pretty Lake, LaGrange County, Ind., from August through November of 1963, define the erasure of the thermocline in a relatively small, deep lake (184 acres, 82 feet maximum depth). The temperature profiles on figures 1 and 2 illustrate the changes in the temperature pattern in Pretty Lake from its condition of maximum stratification in late July to that of complete circulation in late November. The graphs are composites of temperature measurements at 21 different locations in the lake. Figure 2, which represents data from a single vertical at the lake center, illustrates the very rapid changes during November. The curves in figures 1 and 2 are defined by measurements at 2.5-foot intervals in the vertical. Had the lake followed the typical textbook-type cooling described in the preceding paragraph, the nearly straight lines at the upper ends of the temperature profiles, which represent uniform temperature within the epilimnion, would have moved to the left instead of extending below the metalimnion (which is defined by the maximum summer stratification
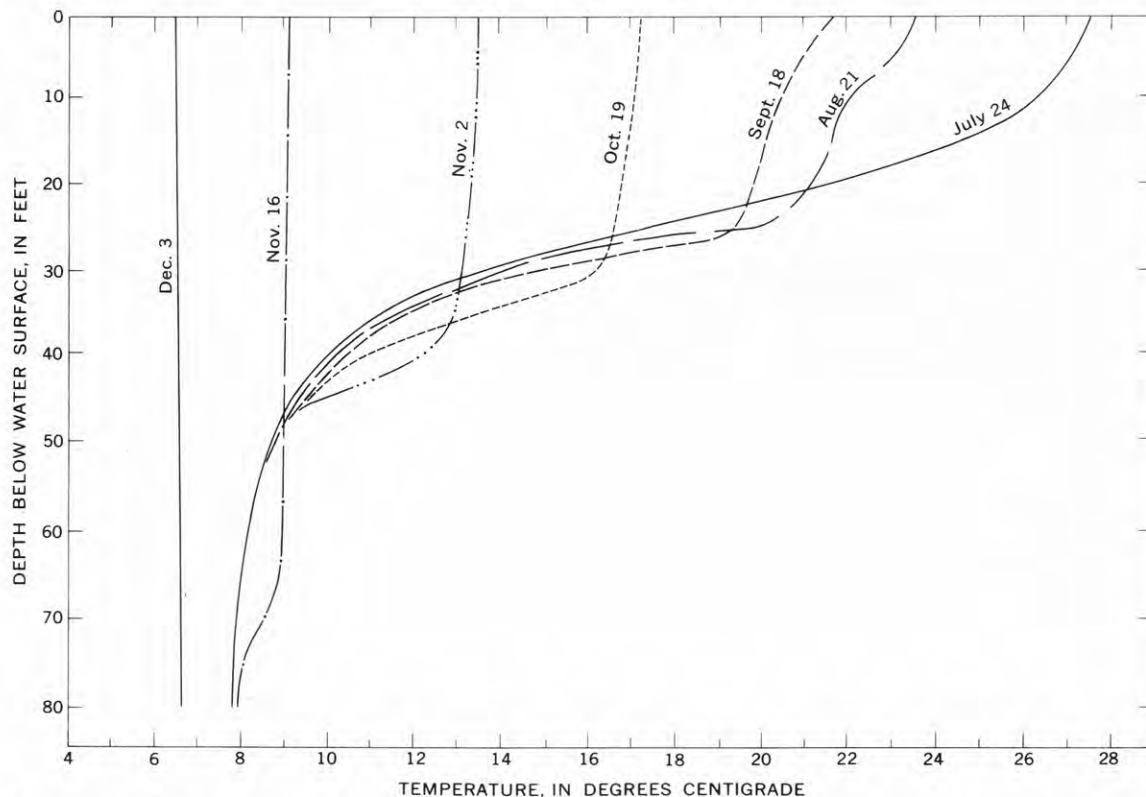
FIGURE 1.—Water-temperature profiles averaged from measurements at 21 locations on Pretty Lake during the summer and autumn of 1963.
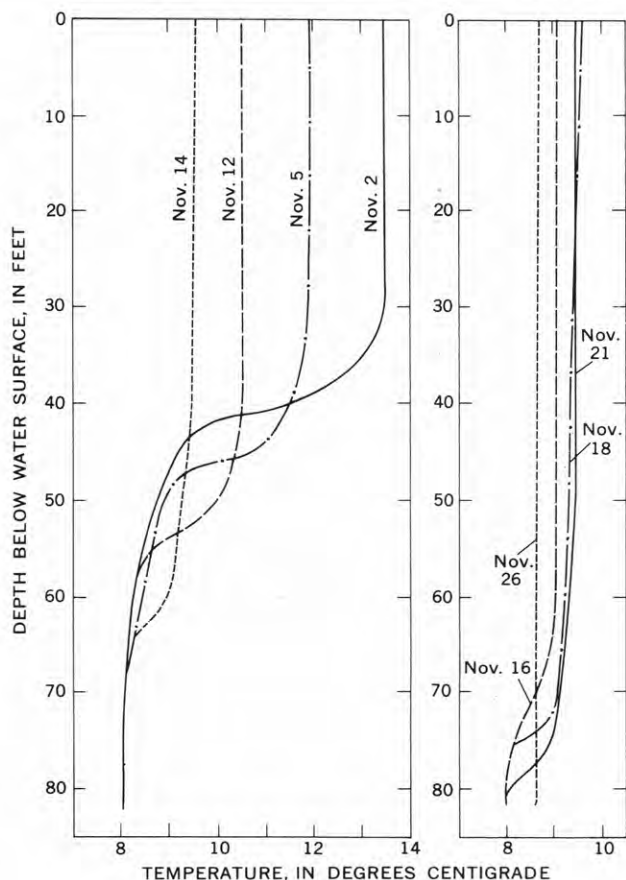
illustrated by the July 24 curve on figure 1). Under those circumstances, when the epilimnion had cooled to about 8° centigrade, conditions would have existed whereby the bottom 25 feet could have gone into circulation with the rest of the lake at one time.

Figures 1 and 2 illustrate the slow cooling of Pretty Lake during a relatively warm autumn, for which the U.S. Weather Bureau (1963) reported the temperature in nearby Fort Wayne as averaging 8.2°F above normal during October and 5.8°F above normal during November. As the lake cooled it was subjected to constant stirring by wind, which gradually broke down the density barrier of the metalimnion and extended the epilimnion deeper than the profile established at the time of maximum stratification (July 24). Rutner (1963, p. 36) has called such a process "autumnal partial circulation." In late November, when stratification had been erased completely, the temperature of the lake was still about 0.6°C warmer than the hypolimnetic minimum that existed just prior to turnover.

During the final phase of turnover in November the lowering of the thermocline occurred without epilim-

FIGURE 2.—Water-temperature profiles near the center of Pretty Lake, showing the erasure of thermal stratification during November 1963.
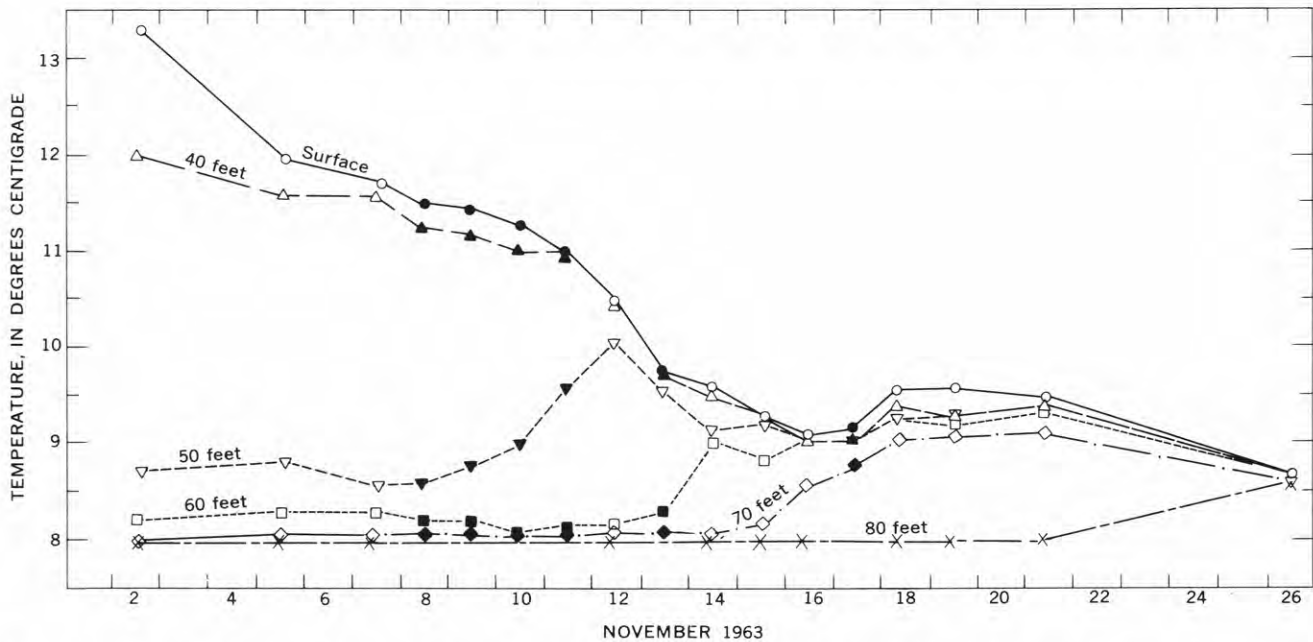
FIGURE 3.—Relation of temperature of water to depth in Pretty Lake during November 1963. Open symbols, temperatures measured with a thermistor; solid symbols, less-accurate temperatures read from a recorder chart.

netic cooling (figs. 2 and 3). Cooling rate is represented by the downward slope of the curves on figure 3. Convergence of the temperature-time curves for different depths represents the erasure of the thermocline. Upward slopes of some of the curves between November 7 and 16 denote periods when mechanical mixing and heat transfer into the metalimnion were breaking down the stratification at a rate faster than that which would have resulted from mere cooling without stirring. However, the upward slopes shown for the period November 16–18 reflect a slight warming of the entire lake during a series of warm, bright days. The breakdown of stratification between November 21 and 26 illustrates again the effect of deep mixing, which resulted in a bottom temperature that was higher after turnover than before.

The distribution of dissolved oxygen in lake water serves to define the depth of epilimnetic mixing. The zone of oxygenation is deepened as the upper metalimnion is erased and the water begins to circulate. Figure 4 shows the dissolved-oxygen concentration in Pretty Lake during the period of turnover. Comparison of the time plots of temperature and dissolved oxygen (figs. 3 and 4) reveals that the time of oxygenation of the water at a particular depth corresponds to the time of erasure of the thermal barrier. For example, on November 13, when the temperature at the 60-foot depth reached the temperature of the epilimnion, the zero oxygen curve on figure 4 crossed the 60-foot depth ordinate.
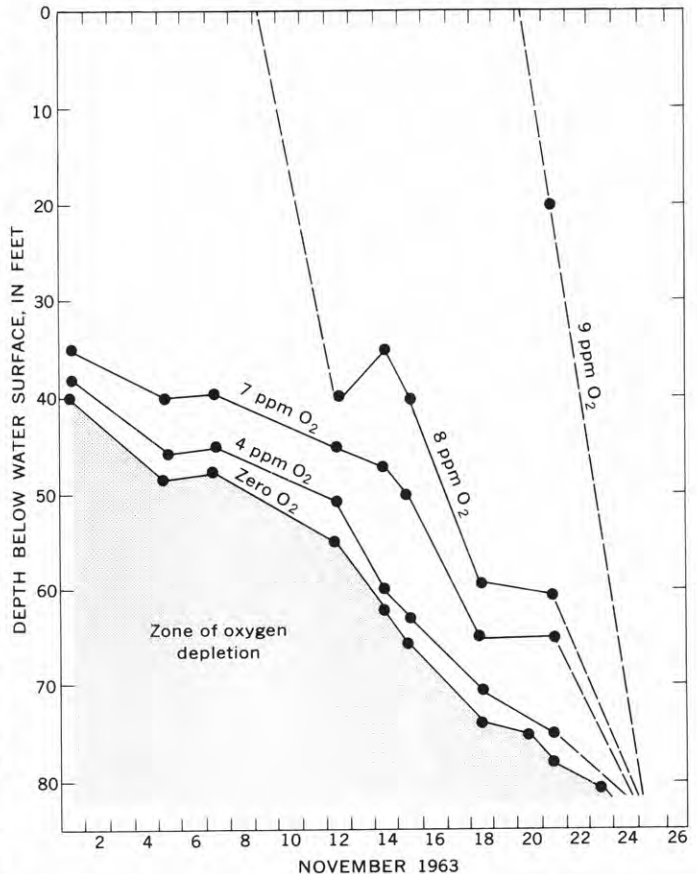
FIGURE 4.—Relation of oxygen concentration to depth in Pretty Lake during November 1963. Dashed segments of profiles inferred in part from data, not shown, for other days.

REFERENCES

Camp, T. R., 1952, Water supplies, *in* Davis, C. V., Handbook of applied hydraulics, 2d ed.: New York, McGraw Hill, p. 847–879.

Hutchinson, G. E., 1957, A treatise on limnology, v. 1: New York, John Wiley and Sons, 1015 p.

Rutner, Franz, 1963, Fundamentals of limnology, 3d ed.: Toronto, University of Toronto Press, 295 p.

U. S. Weather Bureau, 1963, Local climatological data, Fort Wayne, Indiana, Oct., Nov., 1963: U.S. Weather Bur.

A MIOCENE(?) AQUIFER IN THE PARKER-BLYTHE-CIBOLA AREA, ARIZONA AND CALIFORNIA

By D. G. METZGER, Yuma, Ariz.

Abstract.—A fanglomerate which is a potentially important aquifer has been identified in outcrops and in wells near Parker, Blythe, and Cibola, in the Colorado River valley in California and Arizona. The fanglomerate, believed to be of Miocene age, is buried beneath Pliocene(?) estuarine deposits, and beneath younger deposits of the Colorado River, at most places where it is known. It is hydraulically separated from surficial river de-deposits by clay beds in the estuarine deposits, and the water level in several wells stands above the water table. The water is suitable chemically for irrigation, although its fluoride content makes it unsuitable for domestic water supply.

A fanglomerate aquifer of potential economic significance has been defined broadly by geologic mapping and test drilling in the Parker-Blythe-Cibola area, along the Colorado River in Arizona and California (fig. 1). Several wells near Parker, Ariz., have obtained water from this aquifer for many years, but not until the present study was the aquifer differentiated from much younger deposits of the Colorado River and shown to be present at many widely separated places in the area. The fanglomerate deposit is exposed extensively near Cibola and near Parker. It is believed to extend beneath most of the valley of the Colorado River from Parker south to Cibola.

The fanglomerate is composed chiefly of cemented gravel composed of angular to subrounded and poorly sorted pebbles, and some fine-grained material, that are thought to have come from a nearby source. In exposures near Parker it locally contains thin flows of basalt. The composition of the fanglomerate is similar to that of sediments in the present-day washes. Its color depends on the predominant rock type represented by its constituent pebbles—gray where they are from the basement rocks, and brown or reddish brown where they came from volcanic rocks or older Tertiary sedimentary rocks. Because it was deposited on an irregular surface having considerable local relief, the

FIGURE 1.—Index map of Parker-Blythe-Cibola area, Arizona and California, showing outlines of mountain masses, and selected wells.

fanglomerate ranges widely in thickness. About 2,100 feet of "conglomerate" (probably the fanglomerate) was penetrated in an oil test in Milpitas Wash (well B, fig. 1). Bedding surfaces in the fanglomerate dip from the mountains toward the basins. South of Cibola the beds dip as steeply as 17°W., into the basin; but half a mile farther west they dip only 2°W. Near the site of test well LCRP 22, between Cibola and Blythe (fig. 2), the upper surface of the fanglomerate is believed to have an average westward dip of about 2°.

The fanglomerate overlies several different types of rocks—basement complex, volcanic rocks, and sedimentary rocks of Tertiary age—all of which show evidence of deformation prior to deposition of the fanglomerate.

Unconformably overlying the fanglomerate are fossiliferous deposits of Pliocene(?) age. These are believed to be of estuarine origin because they contain brackish-water fossils (Metzger, 1964, p. 15) and are thought to have been laid down during the time of deposition of the Imperial Formation (Durham and Allison, 1960, p. 61–62). MacNeil (1965) assigns the Imperial Formation to the late Miocene or early Pliocene. (No fossils have been found in the fanglomerate, but it is tentatively assigned a Miocene(?) age because of the age of the overlying deposits.) The estuarine sedimentary rocks consist of a basal limestone overlain by interbedded clay, silt, and fine sand, and a thin shore deposit of algal limestone. Their composite thickness, based on surface and subsurface data south of Parker, is about 900 feet. Most of this 900-foot thickness consists of the clay, silt, and fine sand. The basal limestone ranges from as much as 7 feet in thickness, near Parker, to 70 to 100 feet near Cibola; and the algal limestone is only a few feet thick.

The estuarine deposits rather effectively separate the fanglomerate, hydraulically, from the surficial deposits of the Colorado River. The estuarine sand transmits water readily (although its permeability is small relative to that of the river deposits); but the clay, which not only is relatively impermeable but also makes up as much as 50 percent of the estuarine section, effectively retards the vertical flow of water between the fanglomerate and the Colorado River deposits. Thus, in some wells which tap the fanglomerate the water level stands above the local water table.

The yields of wells in the fanglomerate probably are closely related to the degree of cementation of the deposit. In U.S. Geological Survey test well LCRP 15, 2 miles east of Parker, the top of the fanglomerate is 275 feet below land surface; the bottom had not been reached when drilling stopped at 520 feet. The beds are well cemented from 275 to 399 feet, from 465 to 481 feet, and from 493 to 520 feet. By dividing the coefficient of transmissibility (determined from pumping tests) by the length of the perforated interval, the average coefficient of permeability is computed to be about 80 gallons per day per square foot. Because most of the water probably came from a less cemented interval from 399 to 465 feet, the permeability for this part of the perforated interval may be 2 or 3 times the computed value.

Values for the specific capacities of wells which tap the fanglomerate (see accompanying table) range from as little as 0.01 to as much as 20 gallons per minute per foot of drawdown. Most of the wells that have produced from this aquifer are near Parker. Four of them are city of Parker well 5 and U.S. Geological Survey test wells LCRP 15, LCRP 20, and LCRP 21 (see table). The other wells are perforated not only in the fanglomerate but also in both the estuarine sedimentary rocks and the Colorado River deposits. Only three other wells in the Parker-Blythe-Cibola area have produced water from this aquifer: test well LCRP 22, well A, and well C.

Positive artesian head (that is, the water level stands above the local water table) has been found in several wells perforated in the fanglomerate: 1 foot in LCRP 15
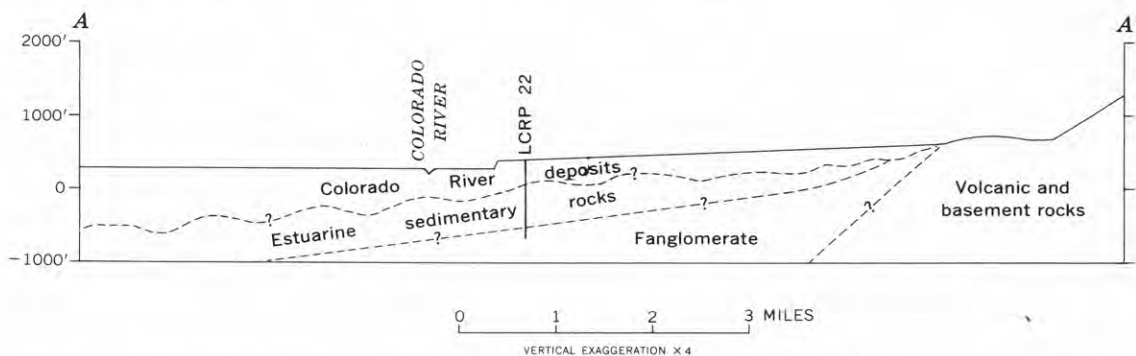
FIGURE 2.—Diagrammatic section A–A' through U.S. Geological Survey test well LCRP 22, showing inferred subsurface conditions in the south-central part of the Parker-Blythe-Cibola area, Arizona and California. Location of section is shown on figure 1.

Data for selected wells drilled into the fanglomerate

Well No. [1]	Legal description	Perforated interval in fanglomerate (feet below land surface)	Specific capacity (gpm/ft)
Arizona			
LCRP 15___	SE¼SE¼ sec. 5, T. 9 N., R. 19 W.	285–520	15
LCRP 20___	NE¼NW¼ sec. 29, T. 8 N., R. 20 W.	(2)	[3] 0. 3
LCRP 21___	NW¼NW¼ sec. 5, T. 8 N., R. 19 W.	635–745	12
LCRP 22___	NW¼NW¼ sec 16, T. 2 N., R. 22 W.	820–985	7
City of Parker 5.	NW¼SE¼ sec. 1, T. 9 N., R. 20 W.	190–400	7
A_____	NW¼NE¼ sec. 28, T. 1 N., R. 23 W.	800–1, 000	[4] 20
California			
B [5]_____	SW¼NE¼ sec. 6, T. 11 S., R. 21 E.		
C_____	SE¼NW¼ sec. 5, T. 11 S., R. 21 E.	Open hole__	0. 01

[1] See figure 1 for location.
[2] Not perforated before this report was written.
[3] Estimated from bailer test.
[4] Reported.
[5] Oil test.

2 miles east of Parker; 4 feet in LCRP 20, 9 miles southwest of Parker; and 42 feet in LCRP 22, 6 miles southeast of Blythe. Well A, a new irrigation well north of Cibola, is reported to have little or no positive artesian head, an anomaly that cannot be explained with available data.

The few analyses of water samples available from the Parker area indicate usable water for irrigation and a range in content of dissolved solids from about 600 to 1,000 parts per million. Analysis of a water sample from LCRP 22 indicated a total dissolved-solids content of 4,190 ppm. Well A is reported to have yielded water containing 1,800 ppm total dissolved solids. High concentrations of fluoride have been found in all samples of water known to come from the fanglomerate. The observed values of fluoride, 2.4 to 6.8 ppm, are significantly above the 1.5-ppm limit recommended by the U.S. Public Health Service for domestic water supplies.

Many more data must be collected before the true potential of the fanglomerate as an aquifer in the Parker-Blythe-Cibola area is known. Nevertheless, test-drilling results suggest that the deposit is widespread, of appreciable thickness, and sufficiently permeable to have the potential of a significant aquifer. Because the fanglomerate is overlain by estuarine sediments that restrict the vertical movement of water, the fanglomerate is separated, hydraulically, from the deposits of the Colorado River throughout most of the area, and in some wells which tap the fanglomerate the water level stands above the local water table. Near Parker, the water in the fanglomerate is suitable for irrigation, although its fluoride content makes it unsuitable for a domestic water supply.

REFERENCES

Durham, J. W., and Allison, E. C., 1960, The geologic history of Baja California and its marine faunas: Systematic Zoology, v. 9, no. 2, p. 47–91.

Metzger, D. G., 1964, Progress report on geohydrologic investigations in the Parker-Blythe-Cibola and Needles areas, _in_ Investigation of the water resources of the Lower Colorado River area: U.S. Geol. Survey open-file report.

MacNeil, F. S., 1965, Evolution and distribution of the genus _Mya_ and Tertiary migrations of Mollusca: U.S. Geol. Survey Prof. Paper 483–G.

USE OF SPECIFIC CONDUCTANCE TO DISTINGUISH
TWO BASE-FLOW COMPONENTS IN ECONFINA CREEK, FLORIDA

By L. G. TOLER, Ocala, Fla.

Work done in cooperation with the Florida Geological Survey

Abstract.—The base flow of Econfina Creek in northwestern Florida is provided by ground-water discharge from surficial deposits of sand and from limestone of the artesian Floridan aquifer. After computation of the proportion of the base flow provided by each aquifer, by use of average values of the specific conductance of spring water and stream water, the discharge from each aquifer was calculated by applying these proportions to the stream-discharge data. The discharge of the artesian springs varies directly with the levels of lakes, in the basin of a nearby stream, which are believed in part to recharge the Floridan aquifer.

The base flow of Econfina Creek, in northwestern Florida, is provided by discharge from two aquifers. Part of the base flow is derived from the limestone of the Floridan aquifer, which yields water through artesian springs located along a reach of several miles about midway in the basin (fig. 1). Artesian-spring water enters the creek directly from the streambed, from the base of rock bluffs, and from several short tributary channels. The largest springs are located in the vicinity of the boundary between Washington and Bay Counties. This artesian water contains from 50 to 68 parts per million of dissolved solids. The remainder of the base flow, which seeps from the virtually insoluble surficial sands that blanket the basin, contains from 10 to 20 ppm of dissolved solids.

The concentration of dissolved solids in a mixture of water from both aquifers depends on the proportions of water contributed by each, and these proportions can be calculated if the concentrations of dissolved solids in water from each aquifer and in the mixture (the stream) are known. These proportions and the discharge data for the stream can then be used to determine the flow from each aquifer.

The following equation, adapted from Hem (1959, p. 230–232), was used in this study:

$$Q_s = \frac{K_b - K_c}{K_s - K_c} Q_b,$$

where

Q_s = discharge of artesian springs in the Floridan aquifer,

Q_b = discharge of stream (Econfina Creek),

K_b = dissolved-solids concentrations in stream water,

K_c = dissolved-solids concentration in seepage from surficial sands, and

K_s = dissolved-solids concentration in artesian-spring water.

The difference between Q_b and Q_s is the volume of seepage from the surficial sands.

Any convenient measure of dissolved solids may be used in the above equation if the measurement made on the mixture is linear with respect to the proportions of each type of water. The specific electrical conductance of a water, a measure of its capacity to conduct an electrical current, is a good indicator of the concentration of dissolved solids in the water; although pure water is a poor conductor the addition of dissolved material to the water increases its conductivity markedly. Because the measurement is simple to make, specific conductance is widely used in geochemical studies of water.

An additional consideration favoring use of specific conductance in the present study was the availability of previous measurements of specific conductance of stream water. Samples of water from both aquifers were collected and mixed in the laboratory. The values for specific conductance of the mixtures, in all proportions tested, when plotted on a graph fit the straight line that connects the points which represent water from each aquifer alone. This shows that for
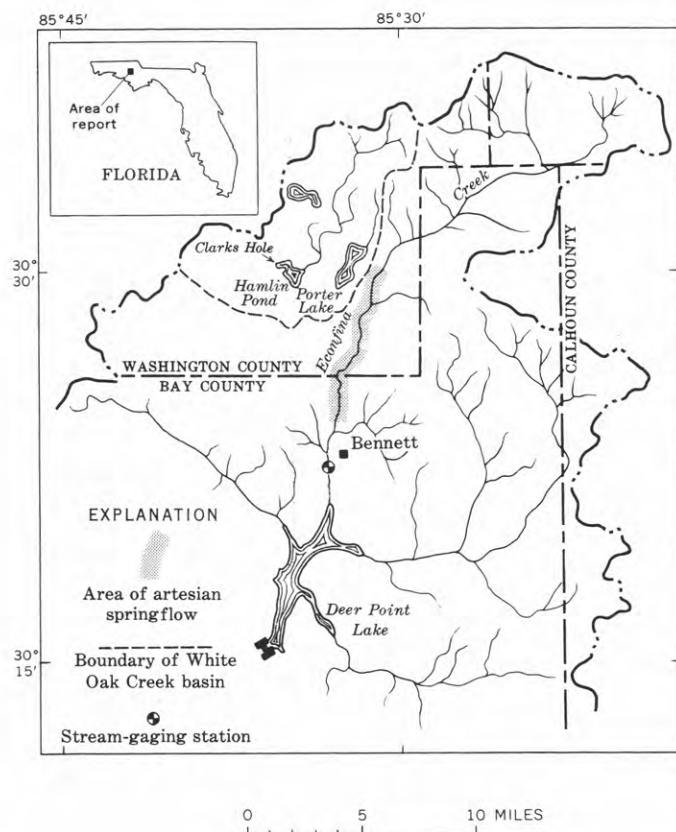
FIGURE 1.—Map showing location of the upper part of the Econfina Creek basin (heavy dashed and dotted line), Florida, and the included White Oak Creek basin. The basins have a common northwestern boundary.

the mixed water, specific conductance is a valid parameter for use in the preceding equation.

The specific conductance (K_b), in micromhos, of the water at the stream-gaging station near Bennett, Fla. (fig. 1) has been measured daily since April 1962, and gage-height readings were made at the time of collection of each daily water sample. Although continuous flow records are available for the station, stage measurements were made at the time of sampling to insure correspondence of the specific-conductance and discharge values. Discharge (Q_b) was obtained from a stage-discharge table available for the station. An average specific conductance of 114 micromhos for artesian spring water (K_s) was determined from periodic specific-conductance measurements on water samples from 4 springs, from measurements on daily samples collected from 2 springs for 1 year, and from discharge data for some of the springs. An average specific conductance of 20 micromhos for nonartesian base flow in Econfina Creek (K_c) was determined, over a period of 6 months, from measurements of specific conductance of stream water upstream from the reach characterized by inflow from artesian springs. These average values were used in all the computations.

Calculations were made for each day and were averaged for periods of stable flow in Econfina Creek. The computed flow of artesian springs ranged from 274 to 373 cubic feet per second during the period April 1962 to February 1964. The computed discharge amounted to about 70 to 75 percent of the base flow of Econfina Creek at Bennett.

Study of lake levels in the nearby White Oak Creek basin (fig. 2) offers a means of checking the validity of the specific-conductance method of determining the relative proportions of the base-flow components of Econfina Creek. Changes in the discharge of the artesian springs
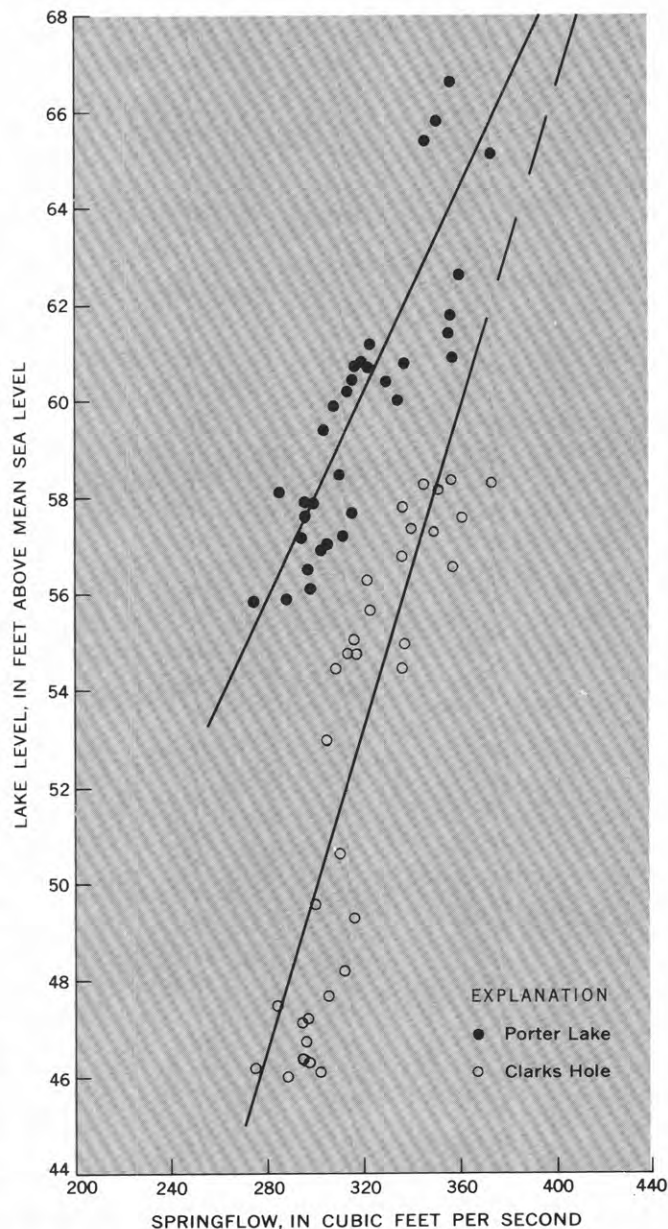
FIGURE 2.—Relation of springflow along Econfina Creek (computed with the use of measurements of specific conductance) to lake levels in White Oak Creek basin.

must be related in large part to changes in the elevation of the piezometric surface of the Floridan aquifer. Such changes in the level of the piezometric surface are commonly measured in observation wells, but records from observation wells in this area are available for only a small part of the period for which spring-discharge values were computed. However, because lakes which occupy karst depressions in the nearby White Oak Creek basin are connected hydraulically with the Floridan aquifer and serve as conduits for recharge of the aquifer, changes in the lake levels represent changes in elevation of the piezometric surface and may be used in determining relative changes in the artesian-spring component of the base flow of Econfina Creek. The higher the lake level is, the greater is the flow of the artesian springs.

Figure 2 is a plot of the flow (computed by the specific-conductance method) of the artesian-spring component of the base flow of Econfina Creek versus the stage of Porter Lake and Clarks Hole in the White Oak Creek basin. The good linear fit shown by the graphs indicates a close relation between lake level and artesian springflow and helps validate the specific-conductance method of computing artesian-spring discharge to Econfina Creek. It also substantiates the interpretation, already established on other grounds, of the hydraulic connection of Econfina Creek and the Floridan aquifer, and it offers a means of predicting changes in base flow of the creek from changes in piezometric levels.

REFERENCE

Hem, J. D., 1959, Study and interpretation of the chemical characteristics of natural water: U.S. Geol. Survey Water-Supply Paper 1473, 269 p.

RELATION BETWEEN CHEMICAL QUALITY AND WATER DISCHARGE IN SPRING CREEK, SOUTHWESTERN GEORGIA

By L. G. TOLER, Ocala, Fla.

Abstract.—A cyclical relation between water discharge and the concentration of dissolved solids has been found in Spring Creek, in southwestern Georgia. The concentration is higher during the falling stage than it was for the same values of discharge during the rising stage of the same flood, and the loop traced by a graph of discharge versus concentration follows a clockwise trend. This form of cyclical change is attributed to the greater influence of ground-water discharge on the chemical character of the stream water during the falling stage. The greater influence of ground-water discharge is believed to result from an increase in ground-water flow to streams in an area where ground-water levels respond rapidly to rainfall and where good hydraulic connection exists between the aquifer and the streams.

An inverse relation between water discharge and the concentration of dissolved solids in the water is common in streams. Direct surface runoff, which provides the greater part of the discharge during flood stages, dilutes the stream water; on the other hand the concentration of dissolved solids is relatively high during low-water stages when most of the flow is provided by ground-water discharge. Hendrickson and Krieger (1960), in a study of records for several streams in Kentucky, found a cyclical pattern of variation in which measured concentrations of dissolved solids are greater during a period of increasing discharge (rising stage) than at the same discharge rates during a period of decreasing discharge (falling stage). This paper describes a cyclical relation between water discharge and concentration in Spring Creek, in southwestern Georgia, where concentrations are greater during the falling stage than they had been at the same values of discharge during the rising stage.

Spring Creek, a tributary of the Flint River (fig. 1), drains 485 square miles above the gaging station near

Iron City, Ga. The drainage area of the creek is underlain almost everywhere by the Ocala Limestone of late Eocene age. This study is based on the following types
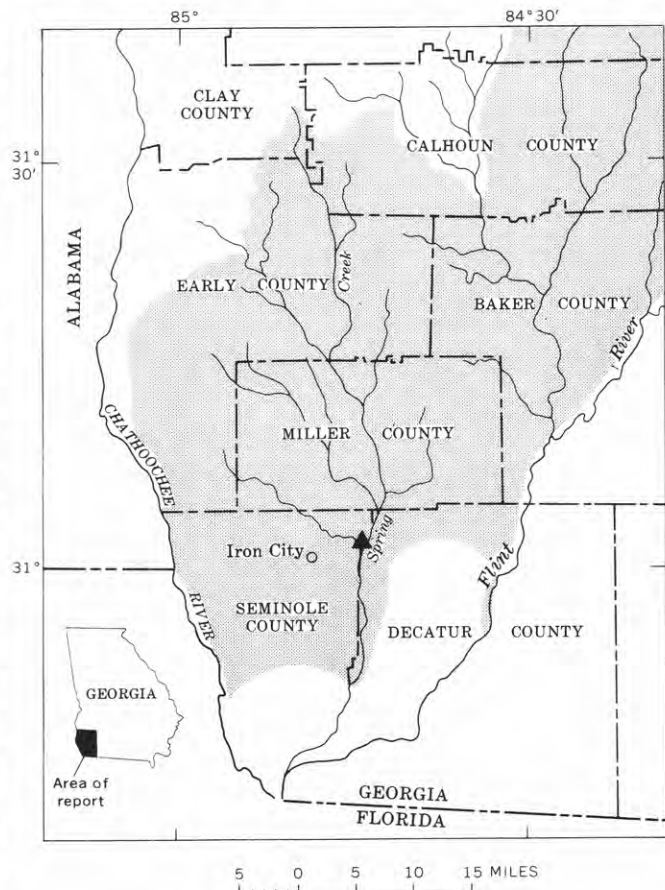
FIGURE 1.—Map of Spring Creek basin, Georgia. Sampling site (gaging station) near Iron City, Ga., shown by triangle, outcrop area of Ocala Limestone by pattern.

of samples and data obtained at the gaging station: daily water samples, later composited for analysis, collected during the period from October 1959 to September 1961; a continuous record of specific electrical conductance from October 1961 to September 1962; and long-term continuous discharge records.

The composition and concentration of dissolved solids in Spring Creek at low flow are similar to those in water

FIGURE 3.—Relation between specific conductance and water discharge in Spring Creek from October 1959 to September 1960.

in the Ocala Limestone in the area (Wait, 1960). Calcium and bicarbonate are the principal mineral constituents. Figure 2 illustrates by means of hydrographs the concentrations of calcium, bicarbonate, and dissolved solids, and the water discharge, from October 1959 to September 1960. The general inverse relation of discharge and chemical quality is well shown. The concentration of dissolved solids is lower, because of dilution at high discharge than at low discharge. The decrease in concentration is not proportional to the dilution, however, and the total amount of dissolved solids is much higher at high discharge than at low discharge.

Figure 3 shows the general relation between water discharge and concentration of dissolved solids in Spring Creek near Iron City, Ga. Concentration of dissolved solids may be expressed in terms of specific conductance because it is the ions in solution that cause water to conduct electricity. For the water in Spring Creek, specific conductance (in micromhos) is numerically proportional to dissolved solids (in parts per million) by a factor of 0.56.

Base flow at the gaging station generally ranges from about 600 cubic feet per second to slightly less than

FIGURE 2.—Hydrographs showing water discharge and chemical quality of Spring Creek, from October 1959 to September 1960.
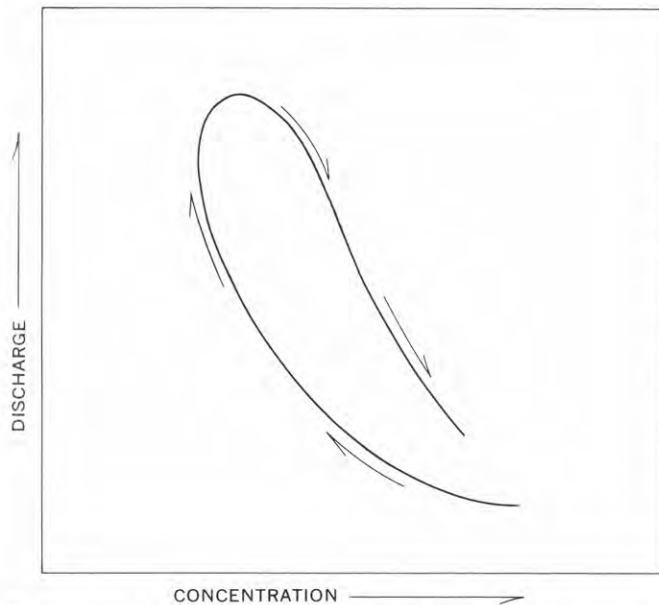
FIGURE 4.—Idealized cyclic variation between water discharge and concentration of dissolved solids in Spring Creek.

100 cfs, depending on the lengths of droughts. The wide scatter of points within this range on figure 3 is attributed to the cyclic variation between discharge and dissolved solids described in this paper, and to lateral shifts of successive cyclic paths that reflect different lengths of droughts.

Hem (1959, p. 188–192) discusses the relation between discharge and the concentration of dissolved solids in streams, and from study of several western streams suggests reasons why a clear-cut relation may not be found: lack of homogeneity in the river water at the sampling point, deviation of individual samples from the average concentration for the day (the value used in computation), derivation of the runoff from different source areas, sampling of water in the front of a flood wave that was in transit in the channel before the rise, and solution of salt previously deposited in the channel as a result of evaporation. None of these possible factors is important in Spring Creek near Iron City. Conductance profiles across the stream showed the water to be homogeneous; one year's record of continuous conductance assured reliable daily averages and gave results similar to those for daily samples; the source area is underlain by one major rock type; the slow rise of the creek and the fact that minimum conductance is reached before peak discharge suggest that water in the flood wave is well mixed with water that was in the channel before the flood; and solution of salts by the first water of a flood would be expected to cause a cycle opposite in direction to that shown for Spring Creek.

The basic cyclic relation for Spring Creek is shown on figure 4. When the discharge increases from that

which characterized base flow, the concentration of dissolved solids decreases—rapidly at first, then at a slower rate—until a minimum concentration is reached near, but commonly just before, peak discharge. After the peak has been passed the concentration of dissolved solids increases with decreasing discharge, but it is higher for a given value of discharge than it was for the same discharge on the rising stage. The loop thus formed is clockwise, as is shown on figure 4, in contrast to the counterclockwise cycle found by Hendrickson and Krieger (1960) in several streams in Kentucky.

The discharge-concentration relations for several rises and declines in discharge of Spring Creek are shown on figures 5, 6, and 7. Figure 5 represents the cyclic relation during a flood that follows a period of low base flow. Figure 6 shows how the relation varies after extended periods of rainfall and high base flow. With discharges of several thousand cubic feet per second (fig. 7), the cyclic relation is poorly defined or not present. The dependence of concentration on the phase of the cycle and on previous discharge history may be inferred from figure 8, which shows hydrographs of discharge and dissolved load. The dissolved load of a stream is a function of the concentration of dissolved solids and of the water discharge. (For Spring Creek the product of the factor 0.001509, of the discharge in cubic feet per second, and of the specific conductance in micromhos, is dissolved load in tons per day.) Dissolved load is thus quantitatively dependent on discharge, and the hydrographs on figure 8 are not com-
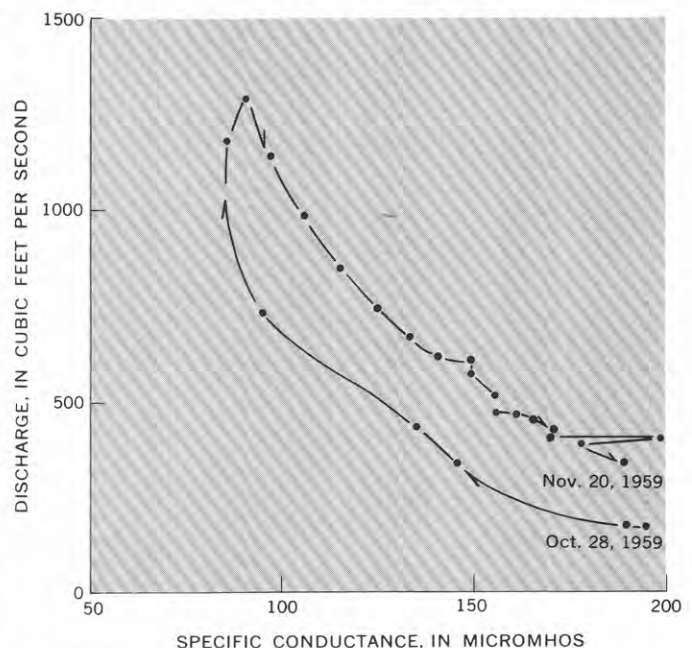
FIGURE 5.—Relation between water discharge and specific conductance in Spring Creek during and after a single flood, following an extended period of low base flow.
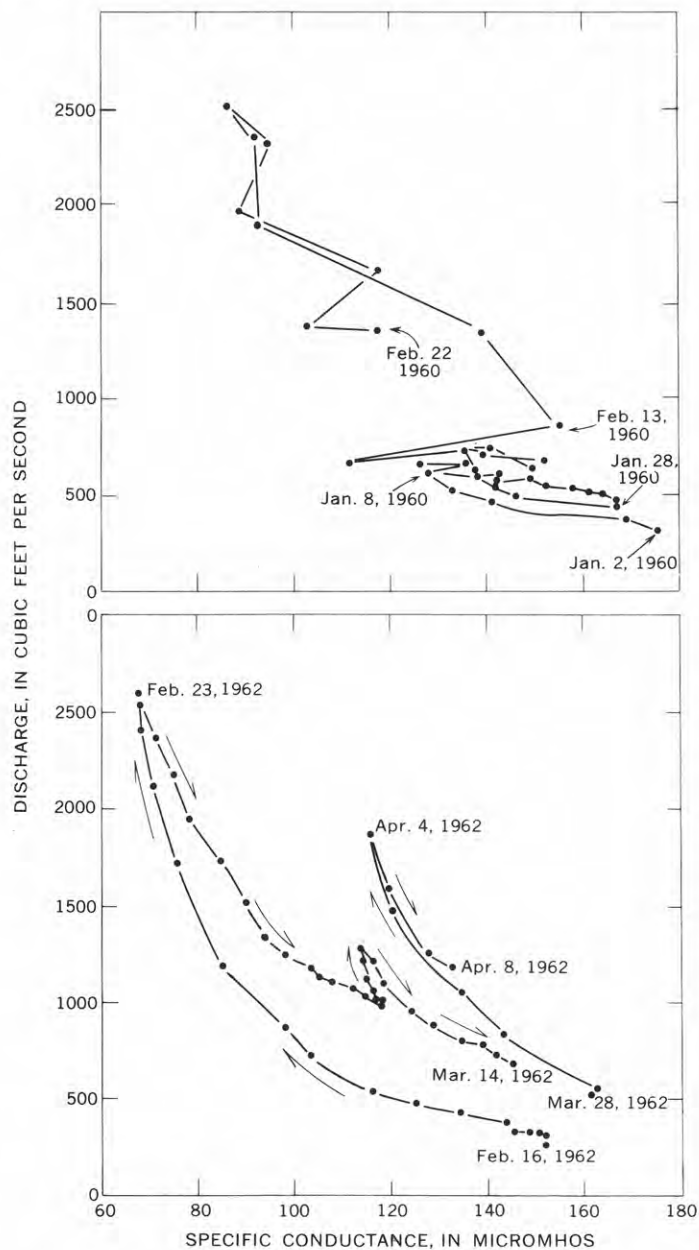
FIGURE 6.—Relation between water discharge and specific conductance in Spring Creek during and after repeated floods and following periods of moderate base flow, in 1960 (above) and in 1962 (below).

pletely independent. However, the relative heights of the graphs, at each of several times, show how the concentration of dissolved solids changed. Low flow prevailed during October and November 1961, and only moderate flow occurred thereafter until mid-February 1962. Rainfall in February, March, and April caused higher discharge. The dissolved load
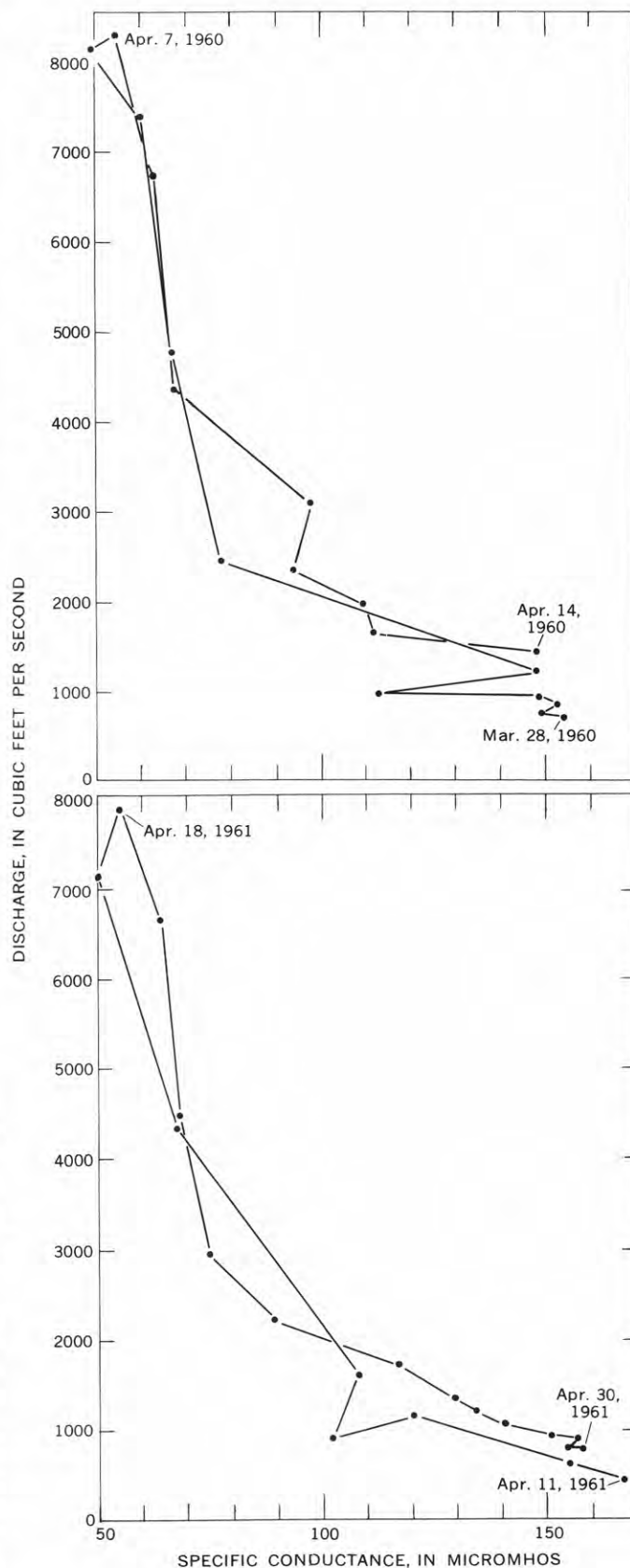
FIGURE 7.—Relation between water discharge and specific conductance in Spring Creek during periods of high discharge and following periods of relatively high base flow, in 1960 (above) and in 1961 (below).
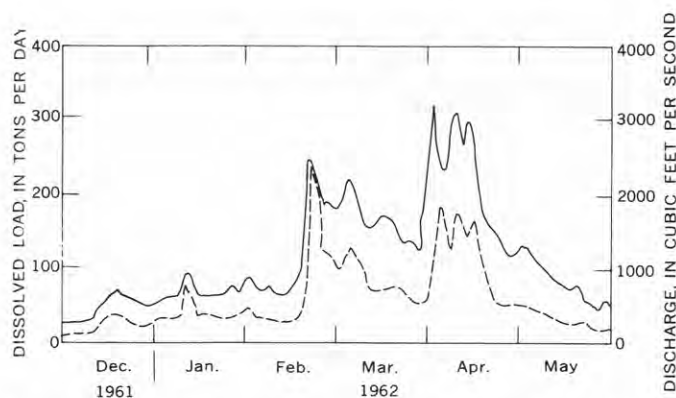
FIGURE 8.—Discharge (solid line) and dissolved-load (dashed line) hydrographs for Spring Creek.

increased rapidly with increasing discharge, but afterward declined at a rate lower than that of the discharge; this process was repeated through several high-discharge periods, and the concentration of dissolved solids remained relatively high during and after the falling stage of the flood in late February. Because the load is a function only of discharge and concentration, the hydrographs on figure 8 show clearly the changes in concentration during successive storm events. The cyclic relation for part of this period is shown on figure 6. The graphs on figure 8 also illustrate why part of the scatter of points on figure 3 is related to the difference in length of droughts.

The forms of the idealized cyclical graph (fig. 4) and of some observed fluctuations (fig. 5 and the lower graphs of fig. 6), seem consistent with changes in the relation between water discharge and concentration of dissolved solids which would be expected on theoretical grounds in a region where ground-water levels respond rapidly to rainfall infiltration and where good hydraulic connection exists between the ground water and the streams. Ground water may continue to enter the stream during part of the rising stage, but does so at a decreasing rate because the stream stage rises faster than ground-water levels in the area. By the time the flood crest has been reached, ground-water levels in the region have risen in response to the rainfall, and those levels near the stream have risen as a result of the movement of stream water into bank storage. After the flood crest has passed the locality under consideration, water moves from the ground into the stream, and in larger amounts than for the same stream stage during the rise. Part of this water had moved from the stream into the ground during the flood, but part of it (an increasing part as time progresses) was ground water before the flood and has a relatively high concentration

of dissolved solids. Therefore, the concentration of dissolved solids in the stream water can be expected to be higher during the falling stage than it was at corresponding discharge values on the rising stage. Departures from the idealized relation observed during periods of very high discharge are thought to show the effect of large quantities of stream water which move into bank storage at very high stages and then back into the stream during the falling stage. In high flood crests, little original ground water is involved in either rising or falling stages, so ground water has little effect on the concentration of dissolved solids in the stream water and the cyclical change is linear rather than of loop form.

As is noted above, the progression of the cyclical relation found in several Kentucky streams by Hendrickson and Krieger (1960) is counterclockwise. They (1960, p. 67–68) attribute the relatively high specific conductance of the stream water during the rising stage largely to the transport of relatively soluble material into the stream. They suggest that this soluble material had collected in the soil as a result of the evapotranspiration of shallow ground water and of the weathering of sulfide minerals near the land surface. They believe that the cyclical relation observed in Kentucky is counterclockwise because of the effect of the high concentration of dissolved solids in the early runoff from the land surface.

The cyclic relation of concentration and discharge in Spring Creek, which follows a clockwise path opposite that found in the Kentucky streams, is thought to be controlled largely by the amount of ground-water flow to the creek. The limestone underlying the drainage area absorbs much of the rainfall on the area, and potential surface runoff is decreased correspondingly. The slow rise and fall shown by the discharge hydrograph, and the high base flows following periods of high discharge, suggest that ground water provides much of the stream discharge. At extremely high discharge, however, surface runoff is much more effective in controlling water chemistry, and the cyclic relation is less obvious than during periods of low stream discharge.

REFERENCES

Hem, J. D., 1959, Study and interpretation of the chemical characteristics of natural water: U.S. Geol. Survey Water-Supply Paper 1473, 269 p.

Hendrickson, G. E., and Krieger, R. A., 1960, Relationship of chemical quality of water to stream discharge in Kentucky: Internat. Geol. Cong., 21st, Copenhagen, 1960, Rept., pt. 1, Geochemical cycles, p. 66–75.

Wait, R. C., 1960, Source and quality of ground water in southwestern Georgia: Georgia Geol. Survey Inf. Circ. 18, 74 p.

A PORTABLE SAMPLER FOR COLLECTING WATER SAMPLES FROM SPECIFIC ZONES IN UNCASED OR SCREENED WELLS

By RODNEY N. CHERRY, Ocala, Fla.

Abstract.—This paper describes a water sampler for use in uncased or screened wells which tap more than one water-bearing zone. It consists of two inflatable packers, and of a submersible pump which removes water from the section of the well isolated by the packers. Auxiliary instruments can be used to measure temperature, specific conductance, or other characteristics of the water in the isolated interval during pumping. The sampler is easily handled and is readily moved from one position to another and reset without removing it from the well.

Many wells penetrate two or more water-bearing zones. In bedrock, these zones commonly are fractures or other openings at different levels in the wall of the uncased part of the hole. In unconsolidated material they are likely to be relatively permeable parts of the section which have been screened and which are separated from one another by blank casing. In many places these distinct zones contain water under different head and having different chemical and physical characteristics. At one extreme these differences are small and for practical purposes insignificant; at the other they are large and have an important effect on use of the water. Water pumped from such wells is likely to be a mixture, in proportions which are variable and depend on several factors, as it is derived from two or more water-bearing zones. In parts of Florida usable ground water occurs in zones which lie between zones that yield nonusable water. Effective development of the water resources of such areas requires chemical analyses of representative water samples. This paper describes a sampler developed to obtain such samples.

In early stages of design the sampler was planned in collaboration with Vance C. Kennedy, of the U.S. Geological Survey.

DESCRIPTION

The Casee sampler (fig. 1) collects a pumped sample of water from a specific zone in an uncased or multi-screened well. Minor modification of the sampler permits remote measurement of several chemical and physical characteristics of the water in the zone being sampled. The sampler can be used in wells with diameters of 8 to 16 inches, inclusive, which do not contain pump pipes or other obstructions. It is suspended on a cable from an A-frame, and is raised and lowered by an electric motor that is powered by a 110-volt a-c portable generator. This generator also runs the electric pump which is part of the sampler.

The sampler consists of two inflatable packers or boots—one mounted above the submersible pump and the other below it. When the boots are inflated the zone between them is isolated from the remainder of the well, and water can be pumped from this isolated zone. The capacity of the pump is about 15 gallons per minute. The spacing of the boots can be varied by using different lengths of connecting pipe between them. The minimum spacing of the boots is 5 feet (length of pump). The boots are inflated by pumping water into them, from the well, through an electrically controlled valve; they are deflated by pumping the water out of them through another electrically controlled valve. Advantages of this sampler over other packer-type samplers are its portability, the ease with which it can be repositioned without removing it from the well, and the fact that it is relatively inexpensive.

Instruments to measure temperature, specific conductance, or other chemical or physical characteristics of the water in the well can be placed in the space between the boots. Experience has shown that continuous measurement of specific conductance, in this way, is very useful in determining the proper time to collect the water samples. It is desirable to pump from the well a volume of water equal to at least 3 times the capacity of the discharge line and isolated section before collecting samples for analysis, in order to ensure the collection of representative samples.
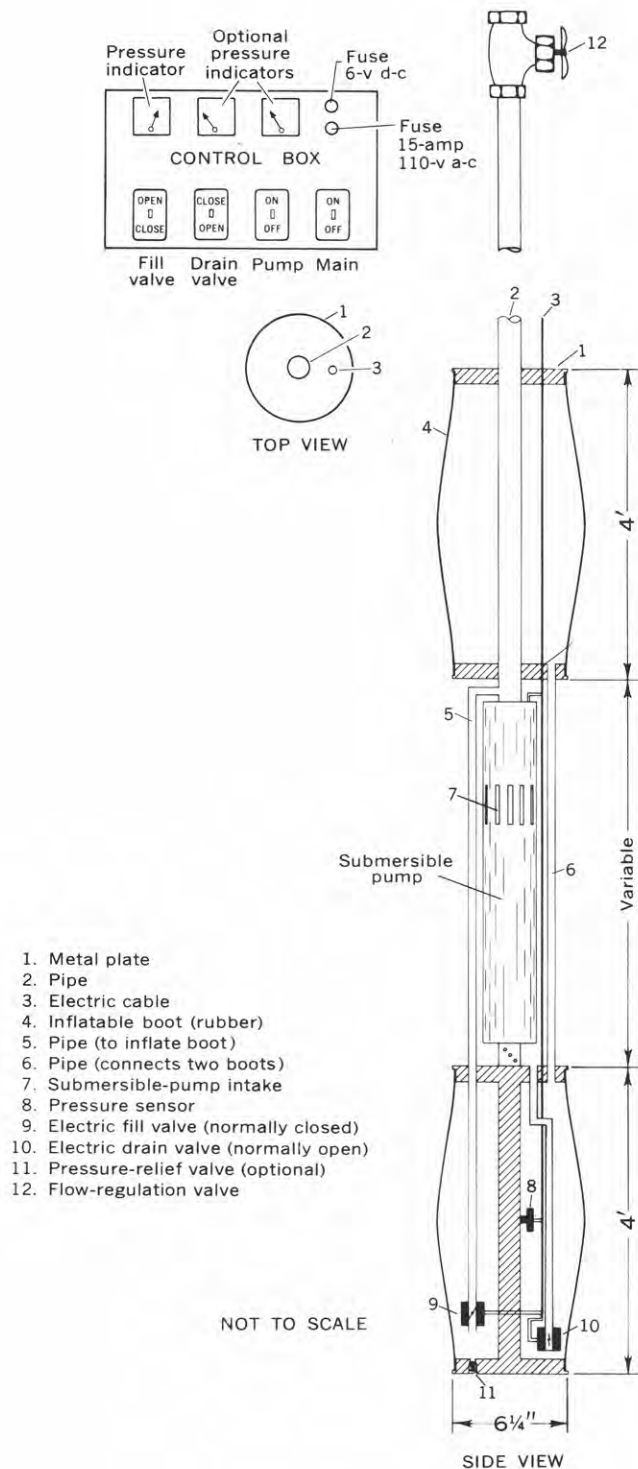
FIGURE 1.—The Casee sampler.

1. Metal plate
2. Pipe
3. Electric cable
4. Inflatable boot (rubber)
5. Pipe (to inflate boot)
6. Pipe (connects two boots)
7. Submersible-pump intake
8. Pressure sensor
9. Electric fill valve (normally closed)
10. Electric drain valve (normally open)
11. Pressure-relief valve (optional)
12. Flow-regulation valve

TESTS

During trials of the sampler the tests described below were made to determine the effectiveness of the packers or boots in isolating the section of well to be sampled.

Test 1.—A 6-foot section of relatively impermeable limestone penetrated by a well was sealed off by lowering the sampler into the well and inflating it. Discharge ceased after 90 seconds, and on a repeat test only 45 seconds elapsed before flow ceased. Leakage around the boots evidently was insignificant, for otherwise pumping would not have ceased entirely.

Test 2.—The sampler was lowered into the cased portion of the well about 120 feet below the water level and inflated. No water could be pumped from the isolated section of the well.

Test 3.—The sampler was positioned at a depth of 600 feet in a 1,100-foot well in limestone which is cased to 450 feet. The water level in the well above the sampler rose 5 feet after inflation of the packers, despite pumping at a rate of about 0.5 gallon per minute. The section of the well between 450 and 600 feet is believed to have been losing water to the deeper part of the well by downward flow, under nonpumping conditions, with a decline of water analogous to drawdown caused by pumping. The rise of the water level above the pumping section during pumping, attributed to cessation of downward flow from above 600 feet, clearly demonstrates the effectiveness of the packers.

Test 4.—Samples of water were collected at different levels from a well to determine whether there were

INSTRUCTIONS FOR OPERATING INFLATABLE BOOT SHOWN IN FIGURE 1

To inflate boots:
1. Close flow-regulation valve (12).
2. Open fill valve (9), which is normally closed.
3. Close drain valve (10), which is normally open.
4. Start pump.
    Water is pumped from well through valve (9), filling the lower boot. The water then passes through pipe (6), filling the upper boot; water is forced into the boot until the pressure inside is 15 lbs per sq in greater than the pressure outside, and the fill valve (9) is then closed. The pressure is measured electrically (8) and is read on a meter at the control box (above). Other pressure-measuring devices (optional) may be used below the sampler and inside the pump section.

To pump sample:
1. Inflate boots.
2. Close fill valve (9).
3. Open flow-regulation valve (12).

To deflate boots:
1. Open flow-regulation valve (12).
2. Close fill valve (9).
3. Open drain valve (10).
4. Activation of pump will generally reduce the deflation time.

differences in mineralization of the water. The analyses in the accompanying table show such differences and indicate, in part, an increase in mineralization of the water with depth.

It is helpful to make a caliper log (a graph showing the diameter of the well versus depth) before putting the sampler into the well, in order to avoid setting the sampler opposite a large opening that would permit leakage around one or both packers. Observation of the time required for inflation of the packers (normally not more than 30 seconds) shows whether inflation proceeded normally; and continuous or frequent measurements of specific conductance between the packers and of the water level above the sampler provide a check on the effectiveness of the seal attained.

Analyses of water collected with the Casee sampler from four isolated intervals in a well tapping limestone

[Constituents reported in parts per million]

	Analysis A (sampler at 730–736 ft)	Analysis B (sampler at 740–746 ft)	Analysis C (sampler at 770–776 ft)	Analysis D (sampler at 789–795 ft)
SiO_2	15	14	14	13
Ca	184	168	268	701
Mg	37	37	76	387
Na	245	230	565	3,260
K	4.6	4.4	8.0	88
HCO_3	220	220	148	215
SO_4	184	178	356	1,180
Cl	500	460	1,180	6,270
F	.2	.2	.2	.4
NO_3	6.1	6.8	8.9	34
Hardness	610	570	980	3,340
$K \times 10^6$ micromhos	1,900	2,010	3,880	15,600

SUBJECT INDEX

———

[For major headings such as "Economic geology," "Geophysics," "Paleontology," see under State names or refer to table of contents]

C217

AUTHOR INDEX